RUTHENIUM COMPLEXES FOR THE TREATMENT OF PROTOZOAN DISEASES OF MEDICAL AND VETERINARY IMPORTANCE

Inaugural dissertation
of the Faculty of Science,
University of Bern

presented by

Oksana Desiatkina

from Ukraine

Supervisor of the doctoral thesis:
Prof. Dr. Julien Furrer

University of Bern

RUTHENIUM COMPLEXES FOR THE TREATMENT OF PROTOZOAN DISEASES OF MEDICAL AND VETERINARY IMPORTANCE

Inaugural dissertation
of the Faculty of Science,
University of Bern

presented by

Oksana Desiatkina

from Ukraine

Supervisor of the doctoral thesis:
Prof. Dr. Julien Furrer
University of Bern

Accepted by the Faculty of Science.

Bern, 26.11.2021

The Dean
Prof. Dr. Zoltan Balogh

Table of Contents

Acknowledgements

First, I thank Prof. Julien Furrer for giving me the opportunity to work at the Department of Chemistry, Biochemistry and Pharmaceutical Sciences (DCBP), University of Bern, NMR group, on this very interesting interdisciplinary project, for supervising and supporting my research work during the four years of my PhD.

I am grateful to Prof. Paul Dyson (Institute of Chemical Sciences and Engineering, EPFL) for agreeing to evaluate my PhD dissertation and to Prof. Jean-Louis Reymond (DCBP, University of Bern) for being a chair of my defense committee.

Furthermore, I would like to thank Dr. Emilia Păunescu for her invaluable support and supervision. She supported me in acquiring new technical competencies, led me through the research process, helped with preparation, writing, and correction of articles, various materials for conferences and this very thesis. I cannot be grateful enough for her care, kindness, patience, and generous advice.

I also want to thank to all NMR group members with which I have collaborated during my PhD thesis. Special thanks to the numerous students with which I shared a part of the laboratory work on this project during these four years as MSc. Valentin Studer, MSc. Timo Felder, MSc. Martin Möshing, MSc. Serena Johns and BSc. Isabelle Holzer. I thank them for their support, shared knowledge, and hard work, and for the great atmosphere in the lab during these years.

A world of gratitude goes to all the scientists that have collaborated and contributed to this interdisciplinary project. Special thanks to Prof. Andrew Hemphill and his team from the Vetsuisse Faculty (Institute of Parasitology, University of Bern), especially to Dr. Ghalia Boubaker, Dr. Nicoleta Anghel and Dr. Yosra Amdouni, not only for all their support and hard work on the antiparasitic activity and toxicity assessment of the compounds synthesized in this study, but also for their disponibility and interesting scientific discussions.

I am also grateful to the group of Prof. Christoph Kempf and his group from the Department for BioMedical Research (University of Bern), and especially to Dr. Nico Ruprecht, MSc. Audrey Galé and Martin Hungerbühler which generously evaluated the anticancer activity of numerous compounds issued from my research and conducting confocal microscopy studies on fluorescent compounds at Microscopy Imaging Center, University of Bern.

I acknowledge the X-ray crystal structure determination service unit of the DCBP (University of Bern) for measuring, solving, refining and summarizing the structures of the compounds and special thanks to Dr. Michal Andrzejewski and Dr. Jürg Hauser.

A big thank you also to the DCBP Mass Spectrometry and Protein Analyses Services for all their support in performing the mass spectrometry and elemental analyses of the numerous compounds synthesized during my PhD research project.

Last but not least I want to express my gratitude to my family and friends, particularly to my husband and my parents for always being there for me and with me. Their constant support and confidence through these challenging four years were priceless.

Abstract

The auxotrophic parasite *Toxoplasma gondii* is a cause of toxoplasmosis. It affects all warm-blooded species, and around one third of the world human population is affected.

The Current medication consists in combination treatments based on pyrimethamine with sulfadiazine. Drugs clinically used to treat toxoplasmosis are not specific, being mainly developed for other diseases, have important side effects, and only effective during the acute stage of infection but they do not eradicate bradyzoite tissue cysts. In consequence, the development of new effective anti-*Toxoplasma* medications, exhibiting also improved tolerability, is of great importance.

Trithiolato-bridged dinuclear ruthenium(II)-arene compounds demonstrated interesting antiparasitic efficacy against *Toxoplasma gondii*, *Neospora caninum* and *Trypanosoma brucei*. Very little is known about their cellular targets and potential mode of action.

It was hypothesized that improved *in vivo* properties and a better knowledge of their exact cellular targets and mode of action can be obtained using the 'conjugate approach' consisting in anchoring judiciously chosen bioactive molecules onto the diruthenium core.

This thesis was focused on the synthesis and biological activity evaluation of various hybrid molecules in which fluorophores, metabolites and drugs were appended on the trithiolato-bridged dinuclear ruthenium(II)-arene moiety. The aims of this approach were: (i) to investigate the cellular targets/mode of action by tracing fluorophore-tagged compounds inside cells/parasites, (ii) to improve the cellular uptake of the complexes by conjugating metabolites necessary for the parasites growth, exploiting the parasite auxotrophies and metabolic peculiarities in Trojan horse strategy, and (iii) to obtain compounds with increased antiparasitic efficacy by coupling with a drug relevant to the treatment of toxoplasmosis.

Five libraries of dyads based on the diruthenium moiety were synthesized and fully characterized. Where applicable (conjugates with fluorophores), photophysical properties were also measured.

The new conjugates and representative intermediates were investigated to assess the impact of compound exposure upon *T. gondii* β-gal tachyzoites grown in HFF (human foreskin fibroblasts) and noninfected HFF. For each series the influence of the nature of the anchored organic fragment, the type and length of the linking unit were evaluated. The most active and selective compounds were also submitted to dose-response studies. Seven

compounds with IC_{50} values in nanomolar range displayed promising activity and selectivity. For some compounds TEM (transmission electron microscopy) and confocal microscopy tests were also performed. The TEM images suggest that the parasite's mitochondrion is the preferred targets of the compounds and, importantly, that the host's mitochondrion (HFF) is not affected.

Overall a library of 93 trithiolato-bridged dinuclear ruthenium(II)-arene complexes decorated with different organic substituents were developed. 7 compounds with interesting cytotoxicity/selectivity profile were identified and can be submitted for further *in vivo* studies.

Introduction

Toxoplasmosis

Epidemiology

Toxoplasmosis is one of the most widespread infection in humans and warm-blooded animals. Around 30% of the human population are chronically infected.[1] Toxoplasmosis was found in all parts of the world except Antarctic, but the seroprevalence is highly inhomogeneous (10-80%) and depends on the climate, economic, quality of water, cultural, social, dietary, and hygiene habits. The incidence is higher in countries with warm humid climate, in populations with poor-hygiene conditions, especially those with limited access to pure water, in developing countries and countries with low socioeconomic level.[2] Known areas with higher prevalence are in Eastern and Central Europe, tropical part of Africa, South America, South-East Asia and Middle East (Figure 1).[3]

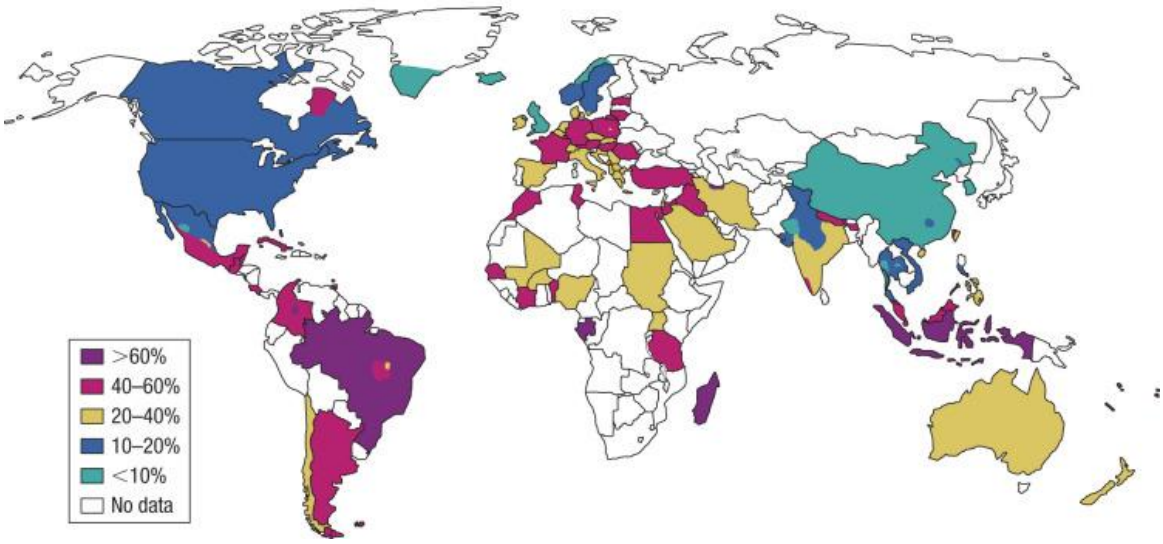

Figure 1. Global status of *T. gondii* seroprevalence in 2009 (figure taken from ref [4] with permission from Elsevier).

Currently 11 types of *Toxoplasma gondii* are known, with previously recognized types I, II and III more prevalent in Europe, North America and Africa. The other 8 types were only recently recognized and 4 of them are only found in South America.[5, 6]

The parasite

Toxoplasmosis is a zoonotic disease caused by the auxotrophic protozoan parasite

Toxoplasma gondii, an obligate intracellular parasite that can affect all warm-blooded animals. *T. gondii* belongs to the phylum Apicomplexa, subclass coccidia.[1] Three stages are observed during parasite development: sporozoites, tachyzoites and bradyzoites.[1, 2, 7] Felines are known as definitive host in which sexual reproduction and oocyst formation takes place. Oocysts containing sporozoites are formed in cat's small intestine and then are shed in feces for up to 3 weeks upon acute infection.[1, 8] After oocysts shed in environment, they sporulate and become infectious after 1-21 days.[1, 4] When ingested by intermediate host oocysts transform into tachyzoites which then rapidly multiply in the host cells leading to acute infection. Tachyzoites are mainly located in skeletal and heart muscles, CNS (central nervous system) tissues, eyes and placenta.[1] After 3-6 weeks, bradyzoites (slowly dividing parasite stage) persist in tissue cysts and can stay in this form lifelong in immunocompetent host. If the host become immunocompromised bradyzoites can reactivate and transform into tachyzoites.[1, 4]

Transmission

There are three ways of transmission of toxoplasmosis: fecal-oral (foodborne/waterborne), congenital and *via* organ transplant/blood transfusion (Figure 2).[4]

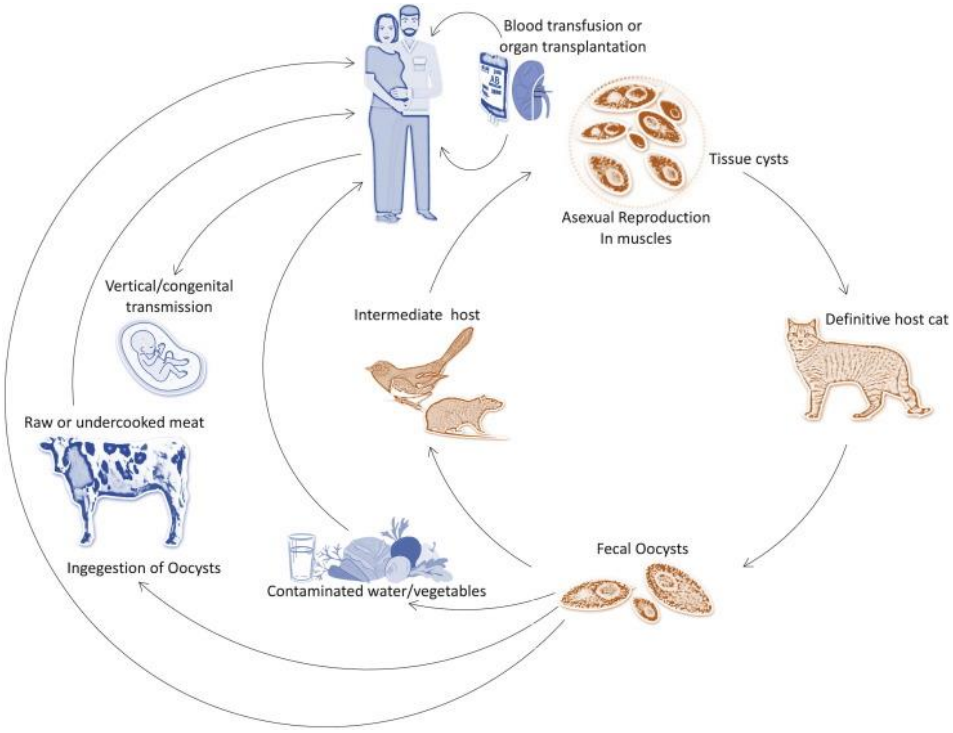

Figure 2. Life cycle of *T. gondii* (figure taken from ref.[9] under the Creative Commons CC-BY-NC-ND license).

The main way of transmission is due to eating or drinking contaminated food and water containing oocysts from feline feces. Cats eat infected pray and parasites spread in their bodies and can continue their sexual cycle, leading to oocyst formation. Oocysts can survive in seawater and therefore lead to infection in sea mammals and contaminated fish.[10, 11] It is also possible to ingest oocysts from the ground after gardening or cleaning the cat litter box.[4]

Another major way of infection is congenital (from mother to fetus), as parasites are able to cross the placenta,[12] this way of transmission being prevalent if women got infected first time during pregnancy. Other ways are due to reactivation of chronical infection in previously immunocompetent mother who became immunocompromised during gestation or infection with more virulent strain of *T. gondii*.[13] Having an acute toxoplasmosis in pregnancy is associated with reduced length of gestation and stillbirth.[13] The congenital transmission rate depends on the stage of the pregnancy.[5, 12] The time of infection is also affecting probability and severity of complications such as hydrocephaly, fetus malformation, preterm birth or ocular toxoplasmosis.

Currently there is no commercial anti- *Toxoplasma* vaccine for humans and there is only one approved vaccine for sheep (Toxovax®). The development of vaccines for humans, cats and livestock is ongoing.[14]

Symptoms

In immunocompetent persons (including pregnant women[13]) toxoplasmosis is mainly asymptomatic. Only 10-20% of infected people usually have mild influenza-like symptoms (fever, asthenia, enlarged lymphadenopathy) which are typically resolving themselves in a few weeks.[1, 4, 5] At this stage tachyzoites are cleared from the host and transform into bradyzoites and the disease become chronical.[5]

However, in immunocompromised patients' toxoplasmosis might be life-threatening and happens mainly due to reactivation of a chronical infection. It is usually affecting CNS in form of toxoplasmic encephalitis, which includes seizures, cerebellar signs, mental status changes, sensory abnormalities, movement disorders, focal motor deficits etc.[1, 4]

In fetus toxoplasmosis may be observed during ultrasound in form of intracranial calcifications and ventricular dilatation.[13] It is also possible to observe hepatic enlargement, ascites and increased placental thickness.[1] None of the abovementioned symptoms are specific and further laboratory investigations are needed.[13]

Symptoms and severity of toxoplasmosis in newborns depends on the time of infection acquisition. The babies born with congenital toxoplasmosis are usually asymptomatic. In other cases, symptoms may include intracranial calcifications, peripheral or macular retinochoroiditis, hydrocephalus, blindness or other ocular disorder, strabismus, epilepsy, microcephaly, psychomotor or mental retardation, anemia and petechia due to thrombocytopenia.[1, 4, 13]

Toxoplasmosis is associated with development of schizophrenia, Alzheimer's disease, cancer, epilepsy, bipolar disorder, obsessive-compulsive disorder, depression.[8, 15, 16] It is also linked to behavioral changes such as increased risk-taking behavior, difficulty concentration, overall reduction of mental and physical health.[8, 15, 16]

Treatments

The treatment of toxoplasmosis depends on the patient's immunity condition and symptoms. For immunocompetent patients who are not pregnant and have only mild symptoms, no treatment is usually needed. However, when symptoms are persistent, severe and/or make patient uncomfortable, a treatment must be prescribed. The current gold standard treatment is a combination of pyrimethamine and sulfadiazine (Figure 3) associated with folinic acid to minimize hematologic toxicity.[1, 4, 5, 17] Other options are combinations of pyrimethamine with clindamycin or trimethoprim with sulfamethoxazole (Figure 3). Atovaquone (Figure 3) can also be used either alone or in combination with pyrimethamine.[5, 17]

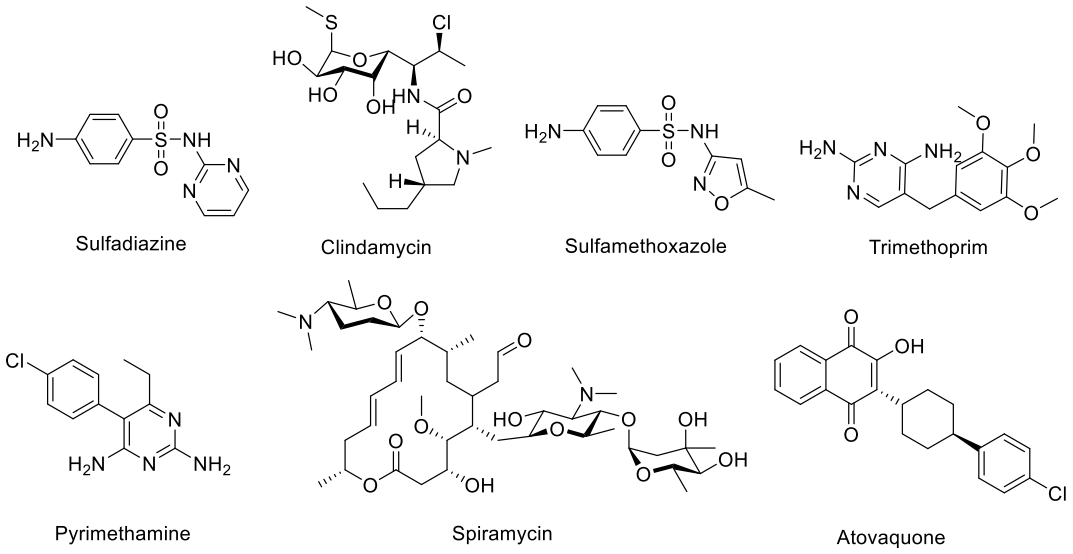

Figure 3. Structures of the drugs currently used for the treatment of toxoplasmosis.

However, none of the drugs used in clinical treatment eradicate tissue cysts and are only effective against tachyzoites.[4, 17] Atovaquone shows only limited *in vitro* activity against bradyzoites.[4]

For immunocompromised patients, except basic treatment for acute disease, maintenance treatment is usually required. Special treatment regimens apply to immunocompromised patients and infected pregnant women, the therapy being influenced by various factors as for example the cause of low immunity (HIV, transplant recipients etc.), the pregnancy stage, the drug tolerability and availability.

Metal-based compounds as potential treatments for toxoplasmosis

The main treatments of toxoplasmosis are combinations of pyrimethamine with sulfadiazine, clindamycin or atovaquone, trimethoprim with sulfamethoxazole and spiramycin. All these drugs were primary developed for other diseases (pyrimethamine and atovaquone as antimalarial agents, sulfadiazine, clindamycin and spiramycin as antibacterial agents) and repurposed for use against toxoplasmosis.[18] Nevertheless, all these medications have important side-effects and do not eradicate tissue cysts. There is also a growing incidence of reported drug resistant strains of *T. gondii* found in clinical cases.[19] In consequence, the identification of new anti-*Toxoplasma* drugs presenting increased efficacy and tolerability is of great importance.

To reach this goal, various drug discovery alternatives have been envisioned: (i) the development of new organic drugs aimed at targeting a precise organelle, enzyme or proteins, (ii) modification of natural products and (iii) high throughput screening of currently available drugs with the main idea of drug repurposing.[20]

Recent findings suggest that transition metal complexes can be considered as antiparasitic therapeutics, and several metal complexes with interesting anti-*Toxoplasma* activity were identified (Figure 4) [21-30].

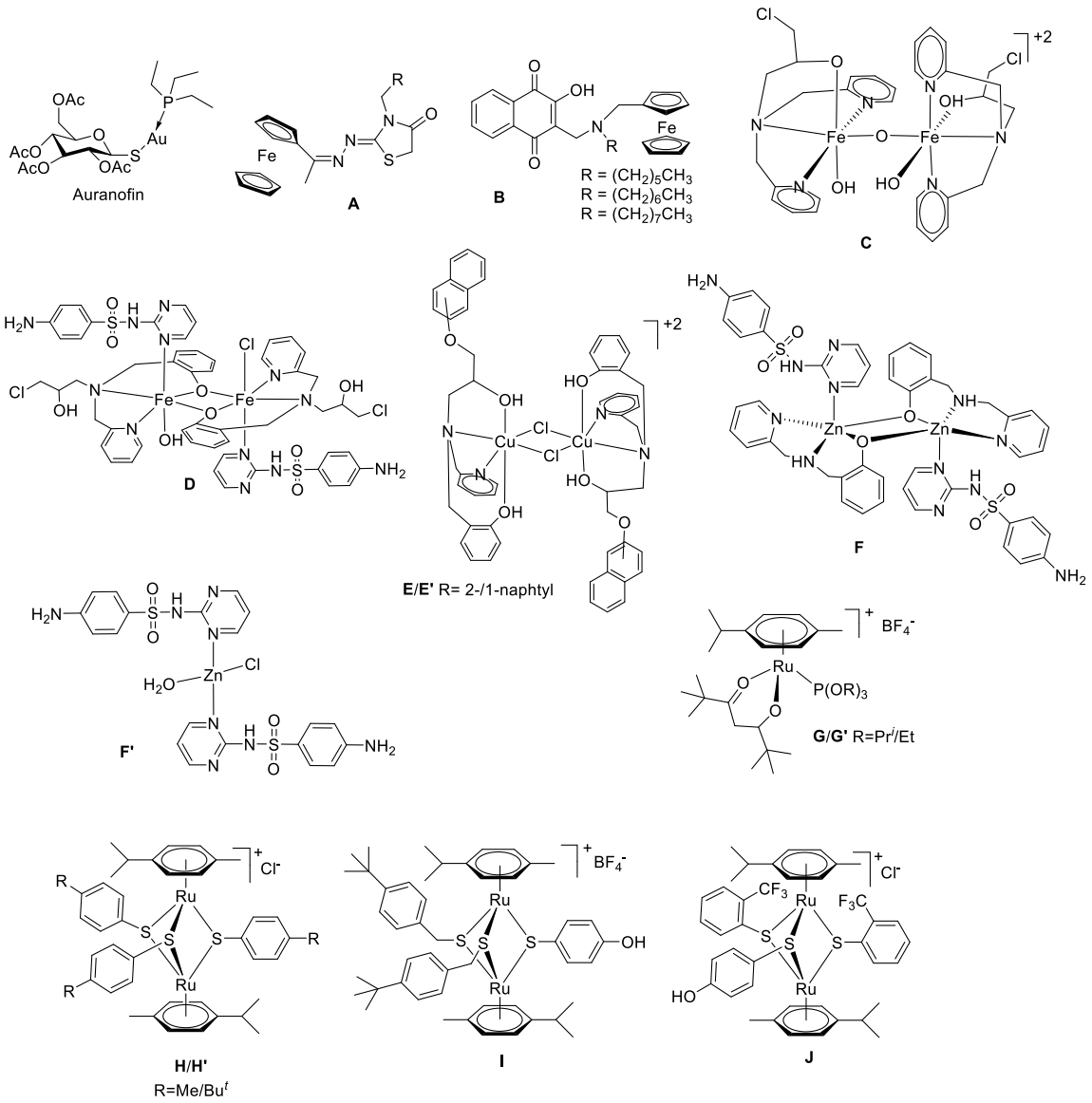

Figure 4. Metal complexes exhibiting antiparasitic activity against *T. gondii*.

One example is auranofin (Figure 4) an approved drug for use in treatment of rheumatoid arthritis. This gold complex has shown high antiparasitic activity against *T. gondii* with low IC_{50} (half maximal inhibitory concentration) values of 0.28 μM (as compared to IC_{50} values of 0.402 μM for pyrimethamine and 26.05 μM for sulfadiazine[31]), maximum inhibition of parasites growth of 82% (80% for sulfadiazine and pyrimethamine combination) and TD_{50} (the median toxic dose at which toxicity occurs in 50% of cases) of 8.21 μM for human foreskin fibroblasts (HFF, host cells) which is 29 fold higher than IC_{50}.[21]

Since the discovery of ferroquine as a potent drug against *Plasmodium falciparum*, causing malaria[32] the use of the ferrocene scaffold has become extremely popular in drug

development. A series of ferrocene-containing complexes with thiazolidinone derivatives was reported (Figure 4, **A**). Among 11 iron containing complexes, 9 were more active than the reference drug sulfadiazine, with IC_{50} values of 5-24 μM.[22] From a series of 14 ferrocenic atovaquone derivatives, 3 compounds (Figure 4, **B**) showed important antiparasitic effect on PLK and ATO *T. gondii* strains (IC_{50} in the nanomolar range) and no inhibition of host cells (HFF).[23]

The anti-*Toxoplasma* activity of various dinuclear iron and copper compounds like **C**, **D**, **E** and **E'** (Figure 4) was evaluated. Complex **C** exhibited a promising IC_{50} of 3.6 μM and do not affect host cells even when applied at 200 μM.[24] Compound **D** containing sulfadiazine showed improved IC_{50} of 1.66 μM against *T. gondii* whereas sulfadiazine had IC_{50} of only 5.30 μM.[25] Although copper complexes **E** and **E'** presented high cytotoxicity against parasite (IC_{50} of 3.54 and 0.78 μM respectively), their selectivity was lower compared to that of iron complexes **C** and **D**.[26]

Two zinc complexes with sulfadiazine **F** and **F'** (Figure 4) were effective against parasite at concentrations lower than 5 μM, did not affect host cells viability, and also induced the conversion of tachyzoites to bradyzoites.[27]

An exploratory screening of ruthenium(II)-arene complexes for antiproliferative activity against *T. gondii* and *N. caninum* revealed that complexes **G** and **G'** (Figure 4) completely inhibited parasites proliferation with IC_{50} values of 18.7 and 41.1 nM against *T. gondii*, respectively.[28] These promising results led to investigation of the antiparasitic activity of a series of trithiolato-bridged dinuclear ruthenium(II)-arene complexes.[29] From a library of 18 diruthenium compounds tested against *T. gondii*, compounds **H**, **H'** and **I** (Figure 4) were not only very active (IC_{50} values of 34, 62 and 1.2 nM, respectively) but also very selective (compounds **H** and **H'** being non-toxic and compound **I** having an IC_{50} of 5.129 μM on host cells HFF).[29] Following these results, complexes **H**, **H'** and **I** were submitted to *in vivo* tests in the neosporosis mouse model, where they exhibited only limited efficacy.[33]

Furthermore, a SAR study of trithiolato-bridged diruthenium complexes was recently performed.[30] This study challenged the influence of substituents present on different positions of the bridge thiols. Among the 54 tested trithiolato diruthenium complexes, compound **J** (Figure 4), was identified as the most promising with an IC_{50} value of 0.071 μM against *T. gondii* and toxic to host cells only at concentrations 35 times higher than its IC_{50}, and without affecting immune cells viability and proliferation when applied at concentration close to its IC_{50} (0.1 μM).[30] It is envisioned that this compound will be

subjected to others tests (stability, *in vivo* tests in mouse model, distribution in organs) in upcoming studies.

Trithiolato-bridged dinuclear ruthenium(II)-arene complexes – state of art

Since the discovery of symmetric trithiolato-bridged dinuclear ruthenium(II)-arene complexes (general formula $[(\eta^6\text{-arene})_2Ru_2(\mu_2\text{-SR})_3]^+$) in 1992 [34, 35] a plethora of compounds were synthesized.[36-43]

Following the promising anti-cancer activity of ruthenium(III) complexes such as KP-1339 (sodium *trans*-[tetrachloridobis(1*H*-indazole)ruthenate(III)])[44-46] and NAMI-A (imidazolium [*trans*-[tetrachlorido(*S*-dimethylsulfoxide)-(1*H*-imidazole)ruthenate(III)])[45, 47] and ruthenium(II) complexes like RAPTA-C ([Ru(II)(η^6-*p*-$MeC_6H_4Pr^i$)Cl_2(PTA)], PTA = 1,3,5-triaza-7-phosphoadamantane)[48-50] and RM175 ([Ru(II)(η^6-biphenyl)Cl(en)]PF_6, en = 1,2-ethylenediamine)[46, 51, 52] symmetric trithiolato-bridged ruthenium(II)-arene complexes were subjected to multiple anti-cancer studies *in vitro*.[37, 38, 40-42]

In the study performed by Gras *et al.*, 8 symmetric trithiolato-bridged dinuclear ruthenium(II)-arene complexes bearing thiophenol or 4-hydroxythiophenol as bridged thiols and two types of functionalized diene-arenes (Figure 5, **K**) as well as $[(\eta^6\text{-}C_6H_6)_2Ru_2(\mu_2\text{-SPh})_3]^+$, $[(\eta^6\text{-}p\text{-}MeC_6H_4Pr^i)_2Ru_2(\mu_2\text{-SPh})_3]^+$, $[(\eta^6\text{-}C_6Me_6)_2Ru_2(\mu_2\text{-SPh})_3]^+$ and $[(\eta^6\text{-}p\text{-}MeC_6H_4Pr^i)_2Ru_2(\mu_2\text{-S-}p\text{-}C_6H_4Me)_3]^+$ were tested *in vitro* against A2780 human ovarian cancer cell-line and its cisplatin resistant variant A2780cisR. All complexes were toxic with a broad range of IC_{50}s (0.08-132 μM) against both cell lines. Complexes with thiophenol were more cytotoxic than those with *p*-hydroxythiophenol. The type of arene moiety affected IC_{50} values although there was no clear/linear correlation to the lipophilicity or the size of the substituents.[37]

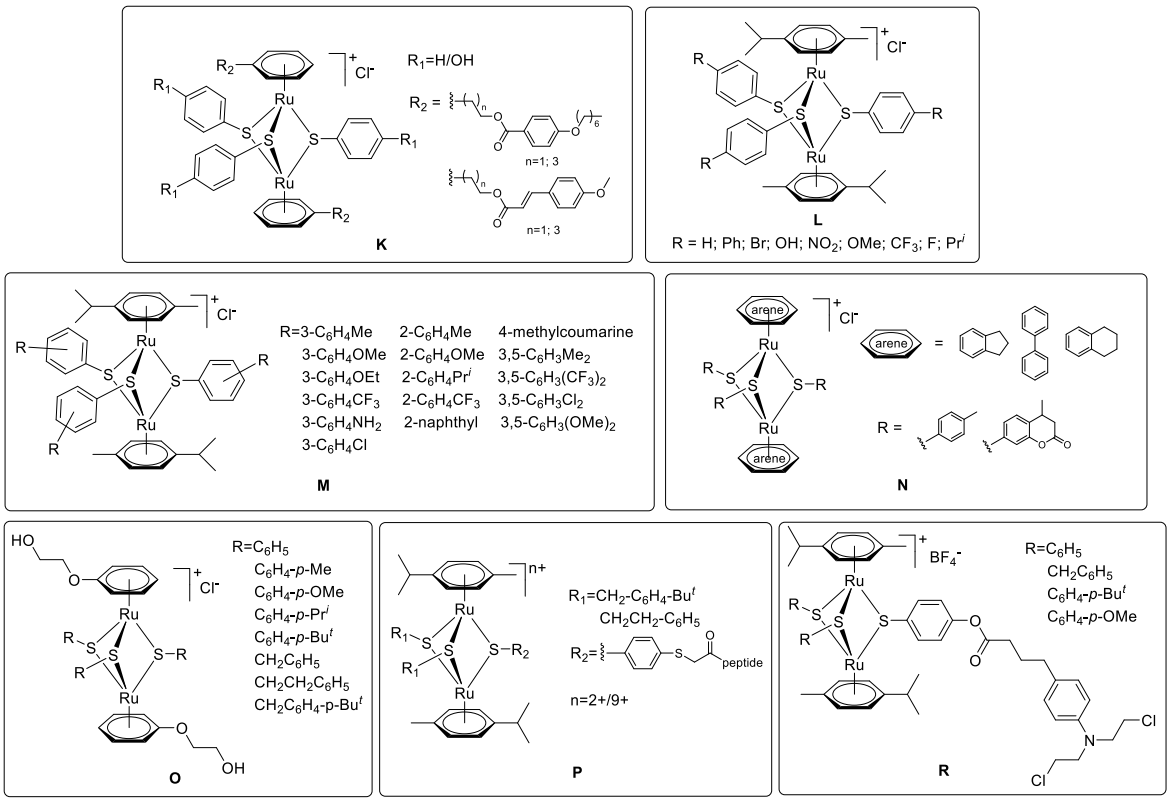

Figure 5. Structures of trithiolato-bridged dinuclear ruthenium(II)-arene complexes.

The influence of the thiols on the cytotoxicity was also investigated. 11 complexes with general formula $[(\eta^6\text{-}p\text{-}MeC_6H_4Pr^i)_2Ru_2(\mu_2\text{-}SC_6H_4\text{-}p\text{-}R)_3]$ where R = H; Me; Ph; Br; OH; NO_2; OMe; CF_3; F; Pr^i or Bu^t (Figure 5, **L** and Figure 4, **H**/**H'**), were reported and tested against A2780 and A2780cisR cancer cell lines. All complexes (except for nitro derivative) were extremely cytotoxic, with IC_{50}s in nanomolar range against both cell lines. Including the most active (IC_{50} = 0.03 μM for both A2780 and A2780cisR) compound of the series – **H'** (Figure 4).[38] A follow-up study added 16 more symmetric diruthenium complexes (Figure 5, **M**) to the family. Conjugates were tested against A2780 and A2780cisR cell lines and showed high cytotoxicity similar to the previous series.[40]

Another study was performed, with the aim of investigating the effect of different arenes on the *in vitro* cytotoxicity, in which a series of 8 water soluble diruthenium complexes was developed with $C_6H_5OCH_2CH_2OH$ as arene and different bridged thiols (Figure 5, **O**). Complexes were tested against A2780, A2780cisR and HEK293 cell lines. Conjugates bearing Pr^i and Bu^t groups showed the lowest IC_{50} values of 0.4 and 0.3 μM respectively, against A2780 cell line. Remarkably Bu^t complex showed not only high cytotoxicity against both types of cancer cells, but also interesting selectivity towards them, with IC_{50} for HEK293 cells being 7.6-fold higher. This improvement of selectivity might

be associated with the hydrophilicity of the arene.[42]

In the same line of thoughts, one more series of diruthenium complexes with various arenes (indane, biphenyl or 1,2,3,4-tetrahydronaphtalene, with 4-methilthiophenol or 7-mercapto-4-methylcoumarin as thiol ligands) was created. (Figure 5, **N**). Interestingly, the influence of the arene was far less pronounced than the influence of thiols, complexes containing 7-mercapto-4-methylcoumarin being up to 800 times less active than their analogues bearing 4-methilthiophenol.[41]

In line with other studies, it appeared that charge of the complex, Hammett and Taft constants, and lipophilicity of the thiol ligands affect toxicity, which led to the development of a first series of so-called mixed ruthenium complexes with two different types of bridge thiols with general formula $[(\eta^6\text{-}p\text{-}MeC_6H_4Pr^i)_2Ru_2(\mu_2\text{-}SR^1)_2(\mu_2\text{-}SR^2)]^+$ in 2013.[53] 18 new complexes were reported and their cytotoxicity against A2780 and A2780cisR ovarian cancer cell lines was assessed. As their symmetric counterparts, mixed trithiolato-bridged diruthenium complexes exhibited high cytotoxicity (in nanomolar range) against both cell lines. Complex with $R^1 = CH_2Ph$ and $R^2 = p\text{-}C_6H_4Bu^t$ had the highest IC_{50} value of 47.8 and 42.9 nm against cisplatin sensitive and cisplatin resistant cell lines respectively.[53]

One of the strategies used for modulating/improving biological activity of metal-based complexes is an attachment of functional molecule (e.g., metabolites, drugs, peptides etc.) onto a metal-based scaffold.[54-59]

6 complexes functionalized with several linear and cyclic peptides were developed (Figure 5, **P**). Coupling of peptides on the diruthenium core led to highly increased water solubility, but have decreased its efficacy against ovarian cancer cells (A2780 and A2780cisR).[60]

A conjugate diruthenium complex – anticancer drug was also experimented: the anticancer drug chlorambucil was attached onto several mixed ruthenium complexes (Figure 5, **R**). Four complexes along with 4 diruthenium intermediates were further tested against A2780, A2780cisR ovarian cancer cell lines, conjugates with chlorambucil were also tested against HEK293 and RF24 (immortalized human endothelial cells) cell lines. Although the IC_{50} values of the functionalized conjugates were higher than those of the starting trithiolato complexes, they were still in nanomolar range. Interestingly, the new conjugates also appeared to be very selective towards cancer cells.[61]

The most recent study was focused on synthesis and biological activity of conjugates containing two or three trithiolato-bridged ruthenium(II)-arene units. With these compounds, the influence of size, flexibility, and charge on the *in vitro* toxicity and

selectivity against human ovarian cancer cell lines A2780 and 2780cisR, human lung adenocarcinoma A24 and (D-)A24cisPt8.0 wild type and cisplatin resistant, respectively, HEK293 cells as well as *T. gondii* grown in HFF and HFF alone were investigated. Although all compounds were more toxic than cisplatin in all cancerous cell lines, they were also cytotoxic to non-cancerous cells.[62]

Apart from cancer cells, *T. gondii* and *N. caninum*, trithiolato-bridged dinuclear ruthenium(II)-arene complexes were also tested against *Trypanosoma brucei*. The complexes $[(\eta^6\text{-}p\text{-}MeC_6H_4Pr^i)_2Ru_2(\mu_2\text{-}SC_6H_4\text{-}R)_3]$ where R = *p*-CF_3; *o*-Pr^i; *m*-NH2; *m,m*-Me; *m*-Cl; *m,m*- CF_3; *o*-Me; and $[(\eta^6\text{-}p\text{-}MeC_6H_4Pr^i)_2Ru_2(\mu_2\text{-}SC_6H_4\text{-}R^1)_2(\mu_2\text{-}SC_6H_4\text{-}R^2)]$ where R^1 = *p*-OMe or *p*-Bu^t and R^2 = *p*-OH were assessed against *T. brucei* bloodstream forms and HFF. As observed against *T. gondii*, all complexes were extremely toxic and very selective to the parasite with IC_{50} values in nanomolar range.[63]

So far, the mode of action and exact cellular targets of trithiolato-bridged diruthenium complexes remain unknown and poorly understood. However, a recent work showed that complexes **H** and **H'** are targeting mitochondria in ovarian cancer cells (A2780) by using inductively coupled plasma mass spectrometry (ICP-MS), suggesting that mitochondrion is likely the preferred target of these cationic ruthenium compounds. Transmission electron microscopy performed on the *T. brucei* and *N. caninum* treated with trithiolato-bridged ruthenium(II)-arene complexes indeed showed ultrastructural alterations in mitochondria in both parasites.[33, 63]

Nevertheless, the exact target(s) in mitochondrion remains unknown: a chemical binding and adducts between trithiolato-bridged diruthenium complexes and potential cellular targets could not be evidenced: previous studies have shown that only weak interactions between a model trithiolato-bridged diruthenium complex with different proteins (transferrin, human serum albumin, cytochrome c, human serum albumin, myoglobin and ubiquitin) exist, and no interactions with model biomolecules (amino acids (except cysteine), nucleotides, glucose) could be evidenced.[64] Intriguingly, diruthenium complexes were shown to oxidize cysteine and glutathione, but no correlation with their *in vitro* activity and the catalytic activity was found.[33, 38, 65]. Thus, direct interactions between complexes and the mitochondrion components are questionable, as the way complexes are entering cells and their exact localization within the mitochondrion is still largely unknown. Hence further investigation of subcellular localization of trithiolato-bridged ruthenium(II)-arene complexes within cells is required.

Aims

Considering the importance of finding an effective and selective treatment for toxoplasmosis and latest progress in development of trithiolato-bridged dinuclear ruthenium(II)-arene complexes against parasites, the aim of this project is development of new series of trithiolato-bridged dinuclear ruthenium(II)-arene complexes bearing different organic substituents (fluorophores, metabolites, antiparasitic drugs) on one (or more) of the 'bridges'.

This project consists of three main parts:

1) Series of compounds with fluorophores.

The mode of action of this type of ruthenium complexes inside the cell/parasites remains largely unknown its investigation for better understanding and more effective modification of the complexes for further drug development is of great importance. One of the methods that allows the tracing of compound upon application is through confocal fluorescence microscopy of fluorophore-labelled conjugates. Hence, anchoring the fluorophore to a bioactive ruthenium complex will allow us to trace the fate of the molecule inside the parasite.

2) Complexes with metabolites.

In this part the focus was on improving the selectivity of trithiolato-bridged dinuclear ruthenium(II)-arene complexes against the *Toxoplasma gondii* by attaching different metabolites (purines, fatty acids, isoprenoids etc.) to the ruthenium core. *T. gondii* needs to scavenge metabolites from the host cells in order to survive, therefore the uptake of compound containing those metabolites using Trojan horse strategy should be more likely.

3) Complexes with drugs.

Using the combination of active molecules for treatment of diseases is a known strategy. It is also widely used in treatment of toxoplasmosis. In this part of the study, we aimed to develop a series of complexes bearing antibacterial and/or antiparasitic drugs (metronidazole, dapsone, sulfamethoxazole, sulfadiazine, ciprofloxacin, menadione, atovaquone analogues) in order to achieve synergetic effect and to enhance the activity of the complex.

Chapter 1 – Trithiolato-Bridged Ruthenium(II)-Arene Complexes Bearing a Fluorescent Tag

1.1. Coumarin-Tagged Dinuclear Trithiolato-Bridged Ruthenium(II)-Arene Complexes[1]

Abstract

The synthesis, characterization, photophysical and biological properties against *T. gondii* of 13 new conjugates coumarin-di-ruthenium(II)-arene complexes are presented. For all conjugates organometallic unit: coumarin an almost complete loss of fluorescence efficacy was observed. However, the nature of the fluorophore, the type of bonding, the presence and length of a linker between the coumarin dye and the ruthenium(II) moiety, and the number of dye units did influence their biological properties. The *in vitro* activity against a transgenic *T. gondii* strain grown in human foreskin fibroblasts (HFF) leads to IC_{50} values for *T. gondii* β-gal ranged from 105 nM to 735 nM. Of note, 9 compounds displayed lower IC_{50} than the standard drug pyrimethamine. One compound applied at its IC_{50} did not affect B cell proliferation but had an impact on T cell proliferation in murine splenocyte cultures. TEM of *T. gondii* β-gal infected HFF showed that treatment predominantly affected the parasites' mitochondrion.

1.1.1. Introduction

The use of ruthenium complexes as potential chemotherapeutics is an active area of research for almost two decades.[45, 66, 67] Developed initially as a potential alternative to platinum based anticancer drugs,[46, 68] ruthenium(II)-arene complexes were also considered for other pharmacological properties, particularly as antiparasitic,[28, 69-75] and antibacterial compounds.[76-79] A special class of ruthenium(II)-arene complexes is constituted by symmetric[38, 40] and 'mixed'[53] cationic trithiolato-bridged dinuclear ruthenium(II)-arene complexes (general formula $[(\eta^6\text{-arene})_2Ru_2(\mu_2\text{-SR})_3]^+$ and $[(\eta^6\text{-arene})_2Ru_2(\mu_2\text{-SR}^1)_2(\mu_2\text{-SR}^2)]^+$, respectively). The high cytotoxicity against human cancer

[1] This chapter was published as Coumarin-Tagged Dinuclear Trithiolato-Bridged Ruthenium (II)·Arene Complexes: Photophysical Properties and Antiparasitic Activity, *ChemBioChem*, **2020**, 21, 2818-2835. https://doi.org/10.1002/cbic.202000174. This article is licensed under a Creative Commons Attribution International License (CC BY 4.0). Supplementary information can be found in the chapter *Supporting information 1.1*.

cells shown by this type of compounds and, more interestingly, their apparent ability to circumvent platinum-drug resistance,[64] encouraged the development of several libraries of complexes containing this scaffold as potential biological active compounds. For example, IC_{50} values as low as 30 nM against A2780 (human ovarian cancer) cells and also against their cisplatin-resistant variant A2780cisR were measured for compounds **1.1.B** and **1.1.C** (Figure 1.1.1), while the less lipophilic complex **1.1.A** exhibited lower cytotoxicity (IC_{50} of 130 nM and 80 nM on A2780 and A2780cisR, respectively).

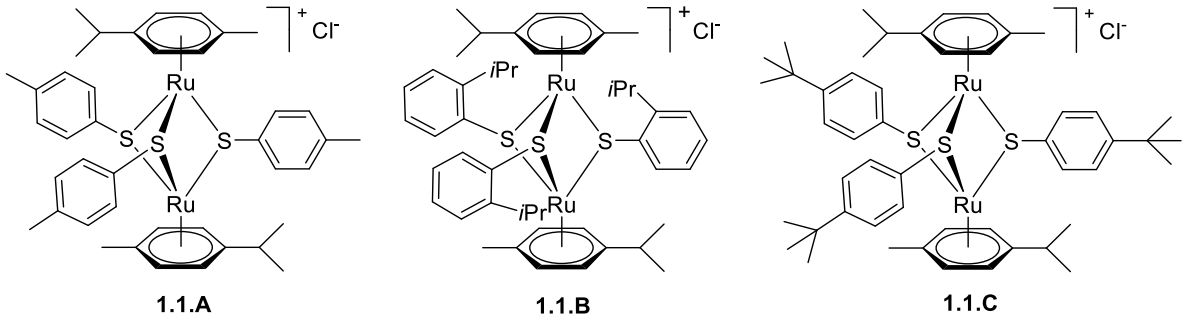

Figure 1.1.1. Structure of cationic trithiolato diruthenium(II)-arene complexes presenting high cytotoxicity against cancer cells and efficacy against various parasites.

The mechanisms by which these trithiolato dinuclear ruthenium complexes exert their cytotoxicity are still not clearly determined. Due to their lipophilic nature, these trithiolato dinuclear ruthenium complexes are only sparingly soluble in water. In contrast, the diruthenium trithiolato moiety is stable, does neither hydrolyze nor interact with biomolecules such as amino acids (other than cysteine), nucleotides, or glucose.[64] This inertness towards hydrolysis and ligand substitution can be attributed to the lack of the typical very labile Ru(II)-Cl bonds or carboxylate ligands that are present in many other Ru(II)-arene complexes. Nevertheless, weak binding to various proteins (human serum albumin, (HsA), transferrin (Tf), cytochrome c (Cyt c), ubiquitin (Ub), and myoglobin (Mb)) was demonstrated, albeit through hydrogen bonds and π-π interactions and not through covalent bonds.[64] Interestingly, catalytic oxidation of bio-relevant reducing agents including cysteine (Cys) and glutathione (GSH) to form cystine and GSSG, respectively, was demonstrated.[65] Although no correlation between the *in vitro* cytotoxicity and the catalytic activity on the oxidation reaction of glutathione could be observed,[38, 65] it is nevertheless considered that this process can be at least partially responsible for the decreased cancer cell survival.

Recently, inductively coupled plasma mass spectrometry (ICP-MS) showed that

complexes **1.1.A** and **1.1.C** specifically target the mitochondrion in A2780 (human ovarian cancer) cells, with up to 97% of the Ru content being found in the mitochondrial fraction.[33] Complex **1.1.C** was taken up by A2780 cells more efficiently than **1.1.A**, which parallels with the respective lipophilicity of the two compounds.

Lately, trithiolato diruthenium compounds were reported to exhibit interesting antiparasitic properties against *Toxoplasma gondii*,[29] *Neospora caninum*[33] and *Trypanosoma brucei*.[63] Thus, complex **1.1.A** presents an IC_{50} value of 34 nM against the apicomplexan parasite *Toxoplasma gondii* cultured in HFF (human foreskin fibroblast) monolayers,[29] while compound **1.1.B** exhibits an IC_{50} of 4 nM against *Trypanosoma brucei* bloodstream forms.[63] Viability of non-infected HFF cells treated with 2.5 µM of complex **1.1.A** was decreased to 63%, however complex **1.1.B** did not affect the vitality when applied at the same concentration.[29] In *Toxoplasma, Neospora* and in *Trypanosoma,* TEM (transmission electron microscopy) demonstrated that trithiolato diruthenium compounds affected the structural integrity of the mitochondrion after few hours of treatment, and led to a more pronounced destruction of tachyzoites at later timepoints.[29] In *T. brucei,* these compounds altered the mitochondrial membrane potential, while other organelles and structural elements of the parasites remained largely unaffected.[63]

The intracellular fate of these trithiolato dinuclear ruthenium complexes, and how they exert anticancer and antiparasitic effects, are unknown, and thus investigating their cellular traffic and possible mechanisms of action has become a priority. *In vitro*/*in vivo* tracking of organometallic drugs using traceable compounds represents a promising approach.[80, 81] Various conjugates obtained by anchoring an imaging probe to the biologically active metal-organic moiety were shown to facilitate the intracellular tracing of the metal-based drugs. [82-84] However, the modification of a drug with a fluorophore tag can strongly influence its physico-chemical properties, and thus activity and behavior. It was already shown that anchoring different fluorophores (coumarin, BODIPY, porphyrin) on the same therapeutic organometallic moiety influences cellular internalization and accumulation.[82-84] Thus, the optimization of the conjugate structure (the organometallic drug onto which the fluorophore probe is already anchored/tethered) should be considered from the beginning.

Microscopy studies of BODIPY,[83, 85] coumarin[86] and naphthalimide[87]-tagged ruthenium conjugates demonstrated that these conjugates could be applied for investigating the subcellular localization of half-sandwich ruthenium(II)-arene complexes.

Due to their good photophysical properties, chemical stability, and ease of synthetic modifications, coumarin derivatives represent an important class of fluorescent probes for biological imaging.[88, 89] Additionally, compounds presenting a coumarin scaffold display broad pharmacological activities and their potential as anticancer agents has received a lot of interest.[90-94]

In the particular case of traceable organometallic drugs, two strategies can be considered: (i) direct coordination of the (coumarin) fluorophore to the metal center[95, 96] or (ii) anchoring of the dye to more elaborated ligands.[86, 97, 98] The nature of the metal center as well as the type of the ligand can strongly affect the photophysical properties of the hybrid molecule. Some data on the development of trackable anticancer agents based on metal complexes were recently reviewed.[80, 99] Conjugates combining metalorganic units with covalently linked coumarins have been shown to be versatile tools for imaging in the case of various fluorophore-tagged platinum,[97, 98, 100] ruthenium,[86] gold[82, 100, 101] or iridium[102] complexes. Some examples of coumarin modified organometallic compounds are presented in Figure 1.1.2.

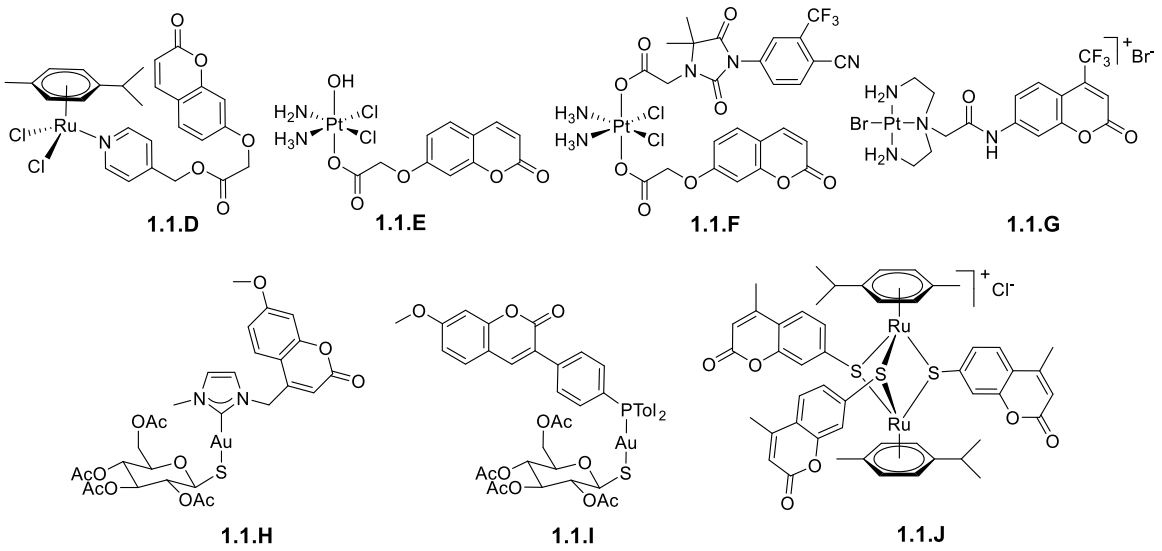

Figure 1.1.2. Structure of various organometallic moiety-coumarin conjugates.

Coumarin-tagged ruthenium(II)-arene complex **1.1.D** was shown to be useful for bioimaging.[86] Laser scanning confocal microscope (LSCM) showed that compound **1.1.D** was internalized by HCT-116 cells (human colorectal cancer, IC_{50} = 66 μM), causing intracellular fluorescence after 3 h of incubation when applied at 30 μM. The process occurred in a concentration-dependent manner. Similar results were obtained with Pt(IV)

conjugate **1.1.E**,[98] which was considered as potential tracking agent due to the presence of a coumarin moiety. Nevertheless, neither for conjugate **1.1.D** or **1.1.E** the physical properties (in terms of fluorescence quantum yield Φ_F) were reported.

Compound **1.1.F** is a three-in-one hybrid containing both an androgen receptor (AR) binding ligand and a coumarin unit connected to a Pt(IV) moiety.[100] The fluorescence quantum yield of **1.1.F** was weaker than that of the respective coumarin ligand (Φ_F = 0.072 *vs* 0.32). **1.1.F** was effectively internalized and visualized by LSCM in LNCaP (AR+) cells (androgen-sensitive human prostate adenocarcinoma cells overexpressing androgen receptor) after 4 h of incubation when applied at 20 μM. Derivative **1.1.G**, a Pt(II) complex of a coumarin modified diethylenetriamine, was developed as a selective probe, fluorescent agent and inorganic medicinal agent.[97] However, the fluorescence intensity of the coumarin moiety was reduced by 90% in this conjugate, thus no microscopy studies on cellular uptake were reported. Several gold(I) complexes bearing coumarin units were described. [82, 101, 103] For example gold(I) carbene complex **1.1.H** displayed poor photophysical properties (fluorescence quantum yield, Φ_F = 2%), the fluorescence quenching being attributed to a photoinduced electron transfer between the coumarin and the carbene.[101] Nevertheless fluorescence confocal microscopy demonstrated the uptake of **1.1.H** in the nuclei of A2780 (human ovarian cancer) cells (IC_{50} = 12 μM) at a concentration of 50 μM. In contrast, gold(I) phosphine complex **1.1.I** showed interesting photophysical properties (Φ_F = 83%), and two-photon fluorescence microscopy of MDA-MB-231 (human breast adenocarcinoma) cells showed this compounds to accumulate at the plasma membrane as small aggregates.[82] Interestingly, reports on coumarin trithiolato decorated compounds such as **1.1.J** [40, 41] focused only on the anticancer activity of the compounds and not on their photophysical properties.

The easy synthesis of symmetric and mixed trithiolato dinuclear ruthenium complexes presenting functional groups that further allow ‘chemistry on the complex’ opens the possibility to prepare various conjugates with the molecules of interest e.g. fluorophores, drugs or biomolecules (amino acids, fatty acids, polyamines, carbohydrates). Hybrid molecules with anticancer-drug chlorambucil[61] and short peptides[60] were already reported as potential strategy to enhance the anticancer activity.

In this study we report the design and synthesis of a library of new trithiolato-bridged dinuclear ruthenium(II)-arene organometallic conjugates in which coumarin fluorophore moieties were anchored as pendant arms on the bridge thiol(s). A systematic assessment of the influence of various structural features of the conjugates (nature of the

fluorophore, type of bonding (ester *vs* amide), presence and length of a linker between the coumarin dye and the binuclear ruthenium(II) moiety, number of dye units) upon the photophysical and biological properties was performed. All compounds of interest (coumarin-labelled conjugates, non-modified thiolato-bridged dinuclear ruthenium(II)-arene complexes and free dyes) were evaluated with respect to their activity against the transgenic strain *T. gondii* β-gal grown in HFF host cells. In addition, the cytotoxicity in non-infected HFF was assessed. For selected compounds, the potential to impair immunity was assessed using B and T cell proliferation assays, and TEM was carried out to evaluate structural alterations in treated parasites.

1.1.2. Results and Discussion

1.1.2.1. Synthesis and characterization of the compounds

In this study, the influence of various structural features of the coumarin conjugates (nature of the fluorophore, type of bonding (ester *vs* amide), presence and length of a linker/spacer between the dye and the diruthenium moiety, number of the fluorophore units) upon the photophysical and biological properties was evaluated.

Coumarin derivatives present a wide structural diversity due to the different substitution possibilities within their basic motif that contains a benzene ring fused to an *α*-pyrone. Analogues substituted with electron-donating groups in position 7 such as 7-methoxy and 7-diethylamino coumarins are frequently used fluorophores. The two coumarin dyes considered for this study, namely 7-(diethylamino)-2-oxo-2*H*-chromene-3-carboxylic acid (**Dye1-CO_2H**) and 11-oxo-2,3,6,7-tetrahydro-1*H*,5*H*,11*H*-pyrano[2,3-*f*]pyrido[3,2,1-*ij*]quinoline-10-carboxylic acid (also known as butterfly coumarin 343, **Dye2-CO_2H**) present easy derivatizable carboxylic group. The use of these particular fluorophores is justified by their good quantum yields, appropriate absorption/emission wavelengths (different emission colors), lipophilicity, lack of net ionic charge, photostability, and relatively small size.[88, 89] It is well known that the photophysical properties of the coumarin derivatives can be tuned with small changes in the substituents and their position.[104] If these two coumarins present very similar structure, previous reports associated the blockage of the free rotation of the C-N bond in **Dye2-CO_2H**, which constrains the nitrogen lone pair to a maximal interaction with the aromatic rings, with an improvement of the photophysical properties compared to **Dye1-CO_2H**.[105, 106] Nevertheless, if this interaction results in higher quantum yield in aqueous solution for **Dye2-CO_2H** than the diethylamino-coumarin **Dye1-CO_2H**, the coumarin substituent is

more bulky and hydrophobic.

A SAR study[30] performed on a library of trithiolato-bridged dinuclear ruthenium(II)-arene compounds showed that the nature of the substituents in the *para* position of the other two thiol ligands influence the biological properties of the complexes. Some of the compounds were developed also in an analogue series in which the bulky hydrophobic Bu^t substituents were replaced by hydrophobic polar CF_3 groups, in order to determine the role of this type of structural modifications upon the biological activity of the conjugates.

The first series of compounds were functionalized with one coumarin unit anchored to one of the bridged thiols, providing a ratio metal-organic moiety: dye of 1:1. To access this type of analogues, the previously reported[30] dinuclear trithiolato ruthenium(II)-arene intermediates, bearing one hydroxy **1.1.2a/b**, amino **1.1.3a/b** and carboxylic acid group **1.1.4a/b**, were prepared starting from the ruthenium dimer ($[Ru(\eta^6\text{-}p\text{-}MeC_6H_4Pr^i)Cl]_2Cl_2$) in two synthetic steps (Scheme 1.1.1).[53] The obtainment of this type of mixed trithiolato complexes is facilitated by the easy synthesis of the dinuclear dithiolato intermediates **1.1.1a/b** which were isolated in high yields. In the case of the carboxylate functionalized trithiolato complexes **1.1.4a/b** a mixture of CH_2Cl_2/acetone (10:1 (v/v) was used as solvent to avoid esterification side reaction catalyzed by the chlorhydric acid resulted during the reaction).

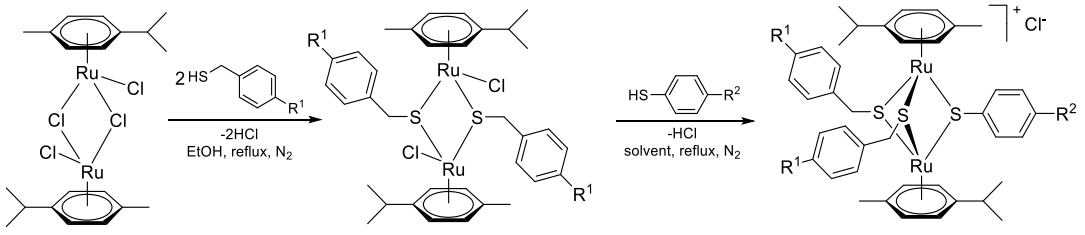

Scheme 1.1.1. Synthesis of the dinuclear dithiolato **1.1.1a/b** and OH, NH_2, CH_2CO_2H functionalized trithiolato ruthenium(II)-arene intermediates **1.1.2a/b**, **1.1.3a/b** and **1.1.4a/b**.

If intermediates **1.1.2a/b** and **1.1.3a/b** could be directly coupled with the two dyes considered **Dye1-CO_2H** and **Dye2-CO_2H** *via* ester and, respectively, amide bonds (Scheme 1.1.3), the carboxylate functionalized trithiolato complexes **1.1.4a/b** offer the possibility to introduce linkers of variable length between the organometallic moiety and the dye. To this end, the linker modified coumarins **1.1.8**, **1.1.9** and **1.1.10** were synthesized

in two steps staring from the corresponding coumarins (**Dye1-CO_2H** or **Dye1-CO_2H**) and the appropriate monoprotected diamine (Scheme 1.1.2).

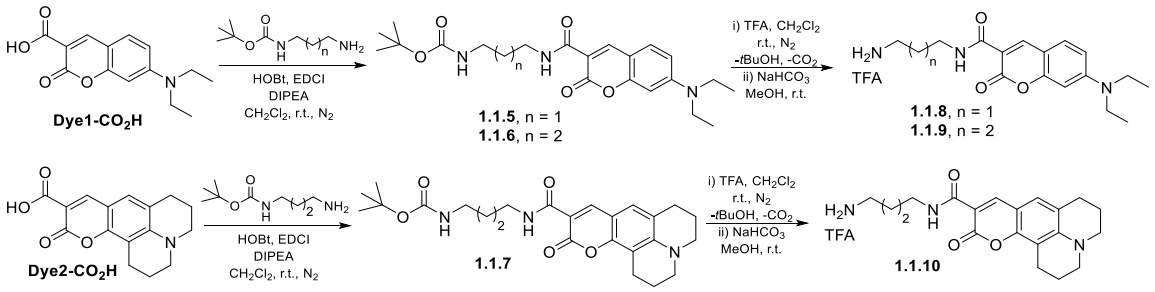

Scheme 1.1.2. Synthesis of the coumarin precursors containing an amino spacer **1.1.8**, **1.1.9** and **1.1.10**.

The coupling reactions of **1.1.2a/b** and **1.1.3a/b** with fluorophores **Dye1-CO_2H** and **Dye2-CO_2H** afforded the ester **1.1.11**, **1.1.12a/b** and amide **1.1.13**, **1.1.14a/b** conjugates in medium to good yields (65-99%) (Scheme 1.1.3). The coumarin hybrids **1.1.15**, **1.1.16a/b** and **1.1.17a/b** containing an amino spacer were obtained in reasonable yields (12-69%) by reacting the carboxylate functionalized trithiolato complexes **1.1.4a/b** with the judiciously functionalized fluorophores **1.1.8**, **1.1.9** and **1.1.10** (Scheme 1.1.4). The esterification reactions were realized using 1-ethyl-3-(3-dimethylaminopropyl)carbodiimide (EDCI) as coupling agent and 4-dimethylaminopyridine (DMAP) as catalyst. For the amide bond formation, the coupling reactions were conducted in the presence of HOBt (1-hydroxybenzotriazole) and EDCI as coupling agents and DIPEA (*N*,*N*-diisopropylethylamine) as basic catalyst. As previously reported in other conjugation reactions run on the trithiolato diruthenium complexes, the organometallic scaffold is stable to ligand exchange in the reaction conditions used.[60, 61]

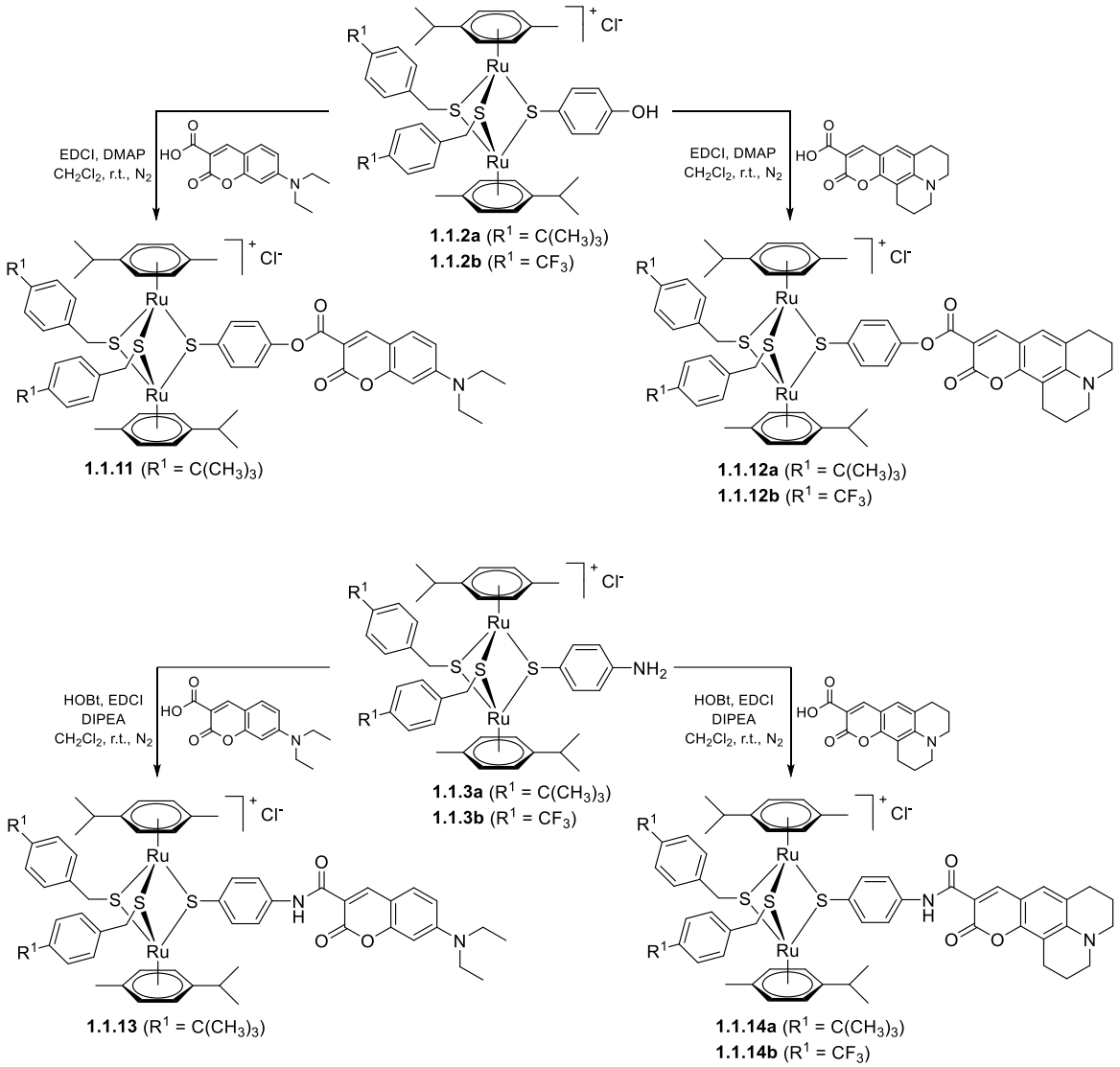

Scheme 1.1.3. Synthesis of the coumarin-based ester **1.1.11**, **1.1.12a/b** (top) and amide **1.1.13**, **1.1.14a/b** (bottom) conjugates.

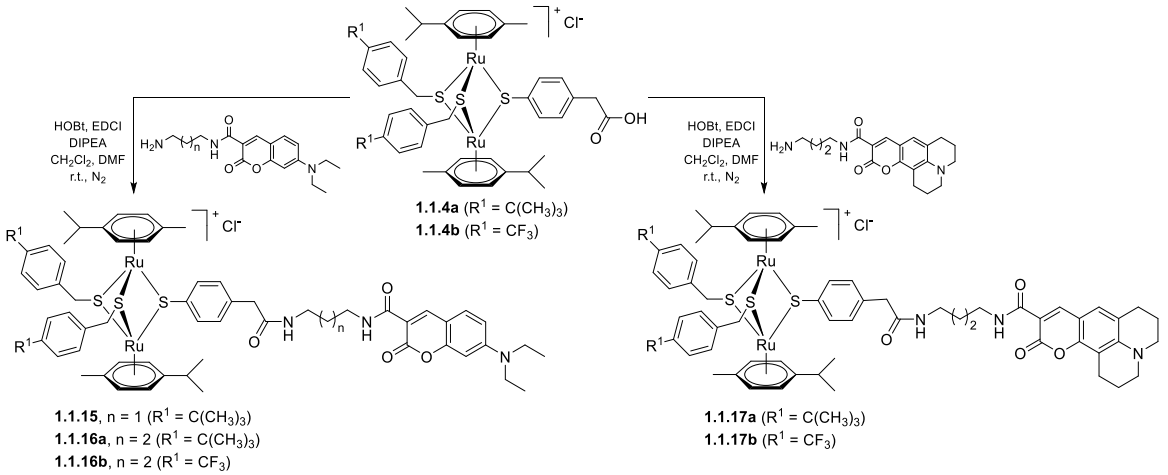

Scheme 1.1.4. Synthesis of the coumarin conjugates **1.1.15**, **1.1.16a/b** and **1.1.17a/b** containing an amino spacer.

A second family of conjugates with organometallic unit: fluorophore (dye) ratios of 1:2 and 1:3 was also synthesized (Scheme 1.1.5) and their photophysical and biological properties were evaluated.

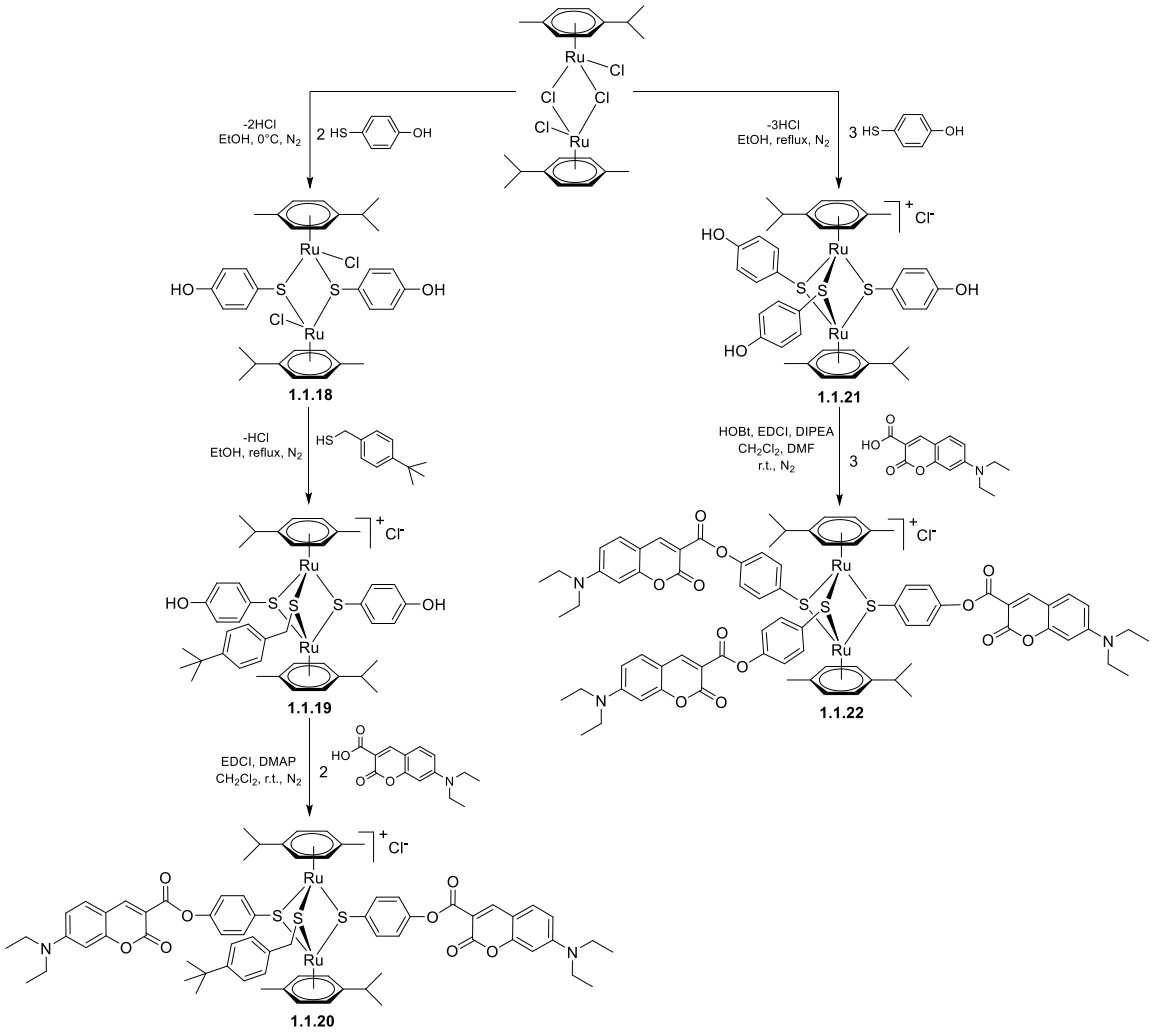

Scheme 1.1.5. Synthesis of conjugates **1.1.20** and **1.1.22** bearing two and, respectively, three fluorophore units.

Conjugate **1.1.20** functionalized with two coumarin units was synthesized in three steps starting from ($[Ru(\eta^6\text{-}p\text{-}MeC_6H_4Pr^i)Cl]_2Cl_2$). If the synthesis of the dithiolato intermediates **1.1.1a**/**b**, obtained by the complexation of less active benzylic thiols, could be easily controlled by the judicious use of the reagents ratio, the use of more reactive aromatic thiol of 4-mercaptophenol led to complex mixture of the desired dithiolato product **1.1.18**, accompanied by trithiolato and monothiolato complexes, as well as unreacted ruthenium dimer. Nevertheless, the next two steps: (i) complexation of a third thiol with the obtainment of mixed trithiolato compound **1.1.19** bearing two hydroxy groups, and (ii)

subsequent esterification reaction with **Dye1-CO$_2$H** leading to di-coumarin conjugate **1.1.20** proceed smoothly, with isolated yields of 96% and 75%, respectively (Scheme 1.1.5).

The tri-substituted conjugate **1.1.22** was obtained in two steps, the synthesis of the symmetric trihydroxy intermediate **1.1.21** (previously reported[36]) followed by the anchoring of three coumarin dye units, and was isolated in good yield (61%).

All compounds were characterized by ^{1}H, ^{19}F (when appropriate), and ^{13}C NMR spectroscopy, mass spectrometry, and elemental analysis (see *Supporting information 1.1* for full details).

For example, the ^{1}H NMR spectra of hydroxy **1.1.2a** and amine **1.1.3a** intermediates differ from those of the respective ester and amide conjugates **1.1.11**/**12a** and **1.1.13**/**1.1.14a**. After anchoring the coumarin unit *via* an ester bond, for **1.1.11** and **1.1.12a** the two protons in the α position to the ligand C-O are observed at slightly lower frequencies, by ca. $\Delta\delta_H \approx 0.05$ ppm, while the protons in the β position with respect to the C-O bond are shifted towards higher frequencies $\Delta\delta_H \approx 0.32$ ppm. In the ^{13}C NMR spectra of esters **1.1.11** and **1.1.12a** the corresponding C atoms α to the ligand C-O are observed at higher frequencies than in hydroxy intermediate **1.1.2a**, $\Delta\delta_C \approx 5.6$ ppm. Following esterification, a strong effect is observed on the ligand C-O, which is shifted to lower frequencies with $\Delta\delta_C \approx 8.6$ ppm compared to C-OH **1.1.2a**. In the case of amides **1.1.13** and **1.1.14a**, the signal corresponding to the two protons in the α position to the ligand C-NH are strongly shifted to higher frequencies, by ca. $\Delta\delta_H \approx 0.96$ ppm, while a similar but less important effect of only $\Delta\delta_H \approx 0.25$ ppm is observed in the case of the corresponding protons in the β position with respect to the C-NH. The ^{13}C NMR spectra of amides **1.1.13** and **1.1.14a** shows the C atoms α to the ligand C-NH at higher frequencies than in amine **1.1.3a** with $\Delta\delta_C \approx 4.8$ ppm. After amide bond formation, the signal corresponding to the ligand C-NH is strongly shifted to lower frequencies with $\Delta\delta_C \approx 9.6$ ppm compared to the respective signal/peak C-NH$_2$ in compound **1.1.3a**. Less important shifts are observed in the ^{1}H NMR spectra of amides **1.1.15**, **1.1.16a** and **1.1.17a** compared to acid intermediate **1.1.3a** for the corresponding protons α to the ligand C-CH$_2$CONH due to the presence of the methylene spacer.

Interesting, in the ^{1}H NMR spectra of the di-hydroxy intermediate **1.1.19** and of the di-ester **1.1.20**, two sets of signals/peaks corresponding to the two 4-mercaptophenolic ligands are observed, indicating that they are not equivalent in the NMR time scale measurement. Electrospray ionization mass spectrometry (ESI-MS) corroborated the

spectroscopic data. The spectra of the dithiolato intermediates contain a parent ion peak attributable to the $[M\text{-}Cl]^+$ ion, formed after the loss of one of the labile chlorine ligands. The ESI-MS of the cationic trithiolato complexes exhibit a strong peak corresponding to $[M\text{-}Cl]^+$ ion.

The compounds containing the trithiolato scaffold (intermediates as well as conjugates) are stable towards ligand exchange in highly complexing solvent as DMSO-d_6 even after elongated storage at 0°C (see Figures S1.1.2−S1.1.4 for the spectra corresponding to the compounds **1.1.2a-1.1.4a** and **1.1.11-1.1.17a**, *Supporting Information 1.1*). This is essential to validate the biological tests for which compounds are used as stock solutions in DMSO.

The solid state structure of symmetric intermediate **1.1.21** containing three free hydroxy groups was established by single crystal X-ray diffraction analysis (Figure 1.1.3), confirming the expected molecular structure.

1.1.2.2. X-ray crystallography

The crystal structure of the symmetric complex **1.1.21** was established in the solid state by single-crystal X-ray diffraction (ORTEP representations shown in Figure 1.1.3), confirming the expected structure. Selected bond lengths and angles are presented in Table S1.1.2. Data collection and refinement parameters are given in Table S1.1.1.

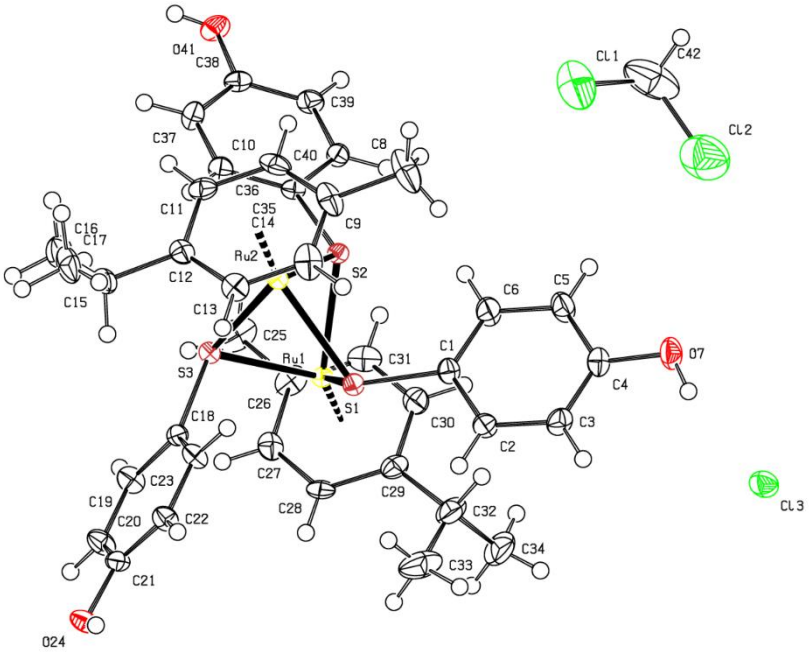

Figure 1.1.3. ORTEP representation of complex **1.1.21** (thermal ellipsoids are 50% equiprobability envelopes, and H atoms are spheres of arbitrary diameter; the asymmetric unit contains also one CH_2Cl_2 molecule).

The Ru_2S_3 unit forms a trigonal-bipyramidal framework; no metal–metal bond are present, the corresponding Ru(1)-Ru(2) distance being 3.341 Å. In the cation, the values of Ru–S bonds as well as the Ru–S–Ru angles (Table S1.1.2) are similar to those found in other symmetric *p*-cymene derivatives reported previously.[40]

In the network of **1.1.21** a complex interplay of H-bonding interactions involving the chlorine anions and the three OH groups of the complex in observed (Table S1.1.3). Each Cl^- ion interacts with the OH groups from three different cationic complexes. A dimeric organization is saw, which is mediated by four H-bonding interactions: two chlorine anions bridge two diruthenium units at the level of their respective two hydroxy groups (Figure S1.1.1). The remaining hydroxy group of each of the symmetric diruthenium complexes is involved in H-bonding interactions with another Cl^- ion. Thus, all three hydroxy groups of the symmetric trithiolato di-nuclear ruthenium(II)-arene complex **1.1.21** are involved in intermolecular H-bonding interactions, two of them interact with two chlorine anions and lead to the formation of a dimer with another diruthenium unit, while the third OH group interacts *via* H-bonds with other Cl^- anion present. In network these intermolecular H-bonding interactions lead to further arrangements e.g. with the formation of cycles involving up to four cationic complexes.

1.1.2.3. Photophysical Characterization

The photophysical properties of coumarin containing compounds investigated in this study, namely the starting **Dye1-CO_2H** and **Dye2-CO_2H**, coumarin-based amino intermediates **1.1.5-1.1.7**, and ester and amide conjugates with the trithiolato ruthenium(II)-*p*-cymene scaffold **1.1.11-1.1.17a/b**, **1.1.20** and **1.1.22**, were studied in $CHCl_3$ and EtOH at r.t. and are summarized in Tables 1.1.1 and S1.1.4. No solvatochromism was observed. The absorption and emission spectra of representative compounds for 10 μM solutions in $CHCl_3$ and/or EtOH are comparatively presented in Figures 1.1.4-1.1.5 and S1.1.5-S1.1.7.

Table 1.1.1. Photophysical data of compounds **1.1.5-1.1.17a/b**, **1.1.20** and **1.1.22** in $CHCl_3$ at r.t.

Compound	λ_{max}^{abs} (nm)	ε ($M^{-1}cm^{-1}$)	λ_{max}^{em} (nm)	$\Delta\lambda$ (nm)	Φ_F (%)
rhodamine 6G [a]	533	62696.6	557	24	75[a]
Dye1-CO_2H	431	43074.2	458	27	184
Dye2-CO_2H	449	47372.9	474	25	158
1.1.5	418.5	42971.9	449	30.5	186
1.1.6	417.5	47042.6	448	30.5	175
1.1.7	433.5	41504.7	463	29.5	170
1.1.11	431, 245	57147.6, 64027.8	455	24	4
1.1.12a	448, 245.5	59950.3, 64535.9	472	24	1
1.1.12b	447, 247.5	57647.7, 63481.4	474	27	0.4
1.1.13	439.5, 246	73039.4,68176.6	458	18.5	0.3
1.1.14a	456, 245.5	68769.4, 62124.7	478	22	2
1.1.14b	454.5, 248	57340.8, 72892.3	480	25.5	2
1.1.15	418.5, 245.5	37245.8, 63190.6	454	35.5	3
1.1.16a	417, 245.5	39772.3, 65900.6	449	32	3
1.1.16b	417, 248	50370.3, 34021.4	449	32	2
1.1.17a	433.5, 245.5	36532.7, 64378.6	462	28.5	3
1.1.17b	433.5, 248	46995.0, 32315.8	465	31.5	3
1.1.20	431.5, 248.5	105690.0, 57402.0	457	25.5	0.3
1.1.22	432, 246	136190.0, 55390,8	459	27	0.4

[a]Values taken from ref. [107]

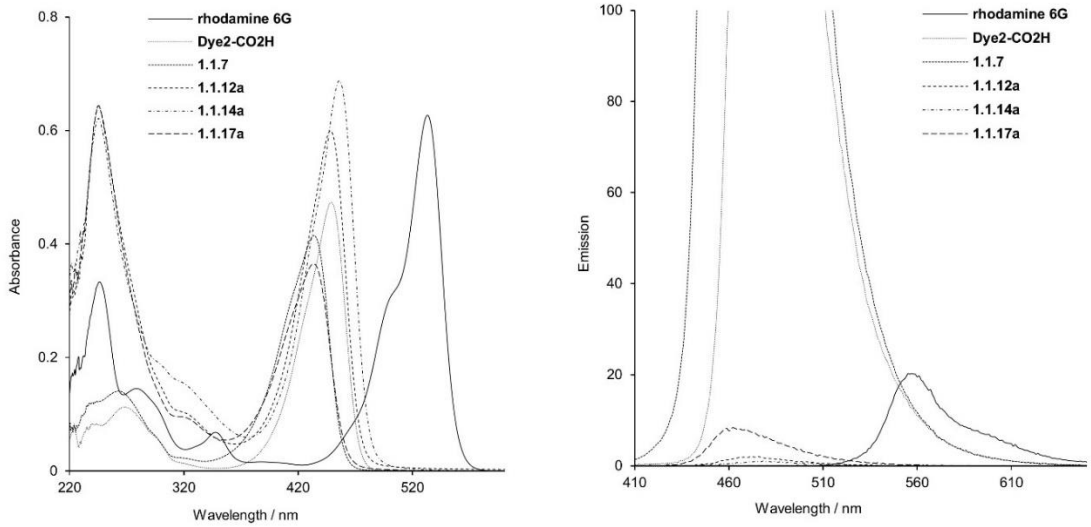

Figure 1.1.4. UV-Vis absorption (left) and emission spectra (right) of rhodamine 6G, **Dye2-CO_2H**, intermediate **1.1.7** and the corresponding ester **1.1.12a** and amide **1.1.14a**, **1.1.17a** conjugates, at 10 μM in $CHCl_3$.

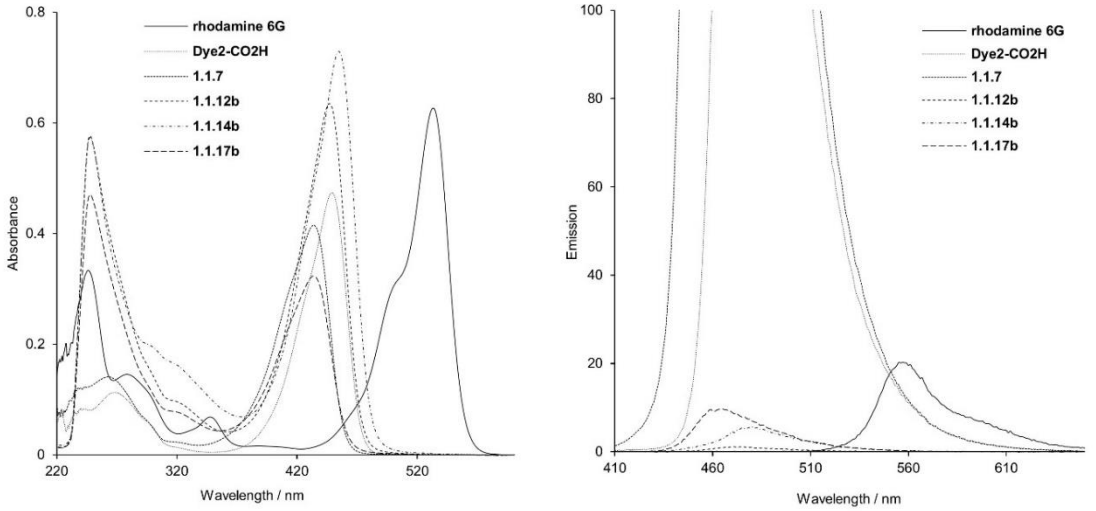

Figure 1.1.5. UV-Vis absorption (left) and emission spectra (right) of rhodamine 6G, **Dye2-CO_2H**, intermediate **1.1.7** and the corresponding ester **1.1.12b** and amide **1.1.14b**, **1.1.17b** conjugates, at 10 μM in $CHCl_3$.

The absorption spectra of all diruthenium unit: coumarin conjugates **1.1.11**-**1.1.17a/b**, **1.1.20** and **1.1.22** present a similar profile (Figures 1.1.4-1.1.5 and S1.1.5-S1.1.7). In both solvents, strong peaks corresponding to the coumarin fragment are observed in the 410-460 nm region. The signals in the 200-300 nm range, associated to the trithiolato di-nuclear ruthenium(II)-arene moiety, are better resolved in the spectra measured in $CHCl_3$ compared to those in EtOH. For **1.1.11** and **1.1.12a**/**b**, the direct attachment of the trithiolato diruthenium moiety to coumarins *via* ester bonds induced no shifts of the absorption peaks, while in case of amides **1.1.13** and **1.1.14a**/**b** a slight

bathochromic shift (Δλ ca. 10 nm) was observed. In contrast, the presence of the di-amino linker in conjugates **1.1.15**-**1.1.17a**/**b** led to a slender hypsochromic shift (Δλ ~ 12-16 nm).

When excited at 405 nm, all coumarin-containing compounds **1.1.5-1.1.17a/b**, **1.1.20** and **1.1.22** emit in the blue range (450–490 nm). The emission spectra of conjugates **1.1.11-1.1.17a/b**, presenting a 1:1 ratio organometallic unit: coumarin, show similar profiles (Figures 1.1.4-1.1.5 and S1.1.5-S1.1.7) with almost complete fluorescence quenching, only slightly less pronounced for solutions in $CHCl_3$ compared to those in EtOH. This loss of fluorescence efficacy was independent of the nature of coumarin (**Dye1-CO$_2$H** or **Dye2-CO$_2$H**), the type of bond (ester or amide) or presence of a di-amino linker between the two moieties. From this compound library, the highest calculated fluorescence quantum yields remain very modest (Φ_F = ca. 3%). Of note, similar but less pronounced quenching effects were observed in other organometallic coumarin-based conjugates.[80, 86, 97]

For all coumarin conjugates (**1.1.11-1.1.17a/b**, **1.1.20** and **1.1.22**) a small bathochromic shift of the fluorescence maximum is observed in EtOH compared to $CHCl_3$ (Δλ ca. 10 nm). The dramatic fluorescence intensity change depending on the presence, or not, of the trithiolato diruthenium unit could be valorized to monitor the stability of the conjugates towards hydrolysis and their behavior *in vitro*. Further structural optimization (as for example the introduction of longer or more rigid spacers between the diruthenium and fluorophore moieties) is required in order for this type of conjugates to be used also as trackable theranostics for the trithiolato di-nuclear ruthenium(II)-arene fragment.

In the case of conjugates **1.1.20** and **1.1.22** with organometallic moiety: dye ratios of 1:2 and, respectively, of 1:3, a proportional increase was observed for the coumarin absorbance signal (maximum at λ = 431-432 nm), which parallels the number of the attached dye units. No significant effect was observed for the emission signal at 457-459 nm, corresponding to the trithiolato diruthenium(II)-arene unit/moiety.

Coumarin intermediates **1.1.5**-**1.1.10** and conjugates bearing di-amino linkers **1.1.15**-**1.1.17a**/**b** present slightly larger Stokes shifts compared to free **Dye1-CO$_2$H** and **Dye2-CO$_2$H** and other hybrid molecule**s**. Calculated Stokes shifts values range between 22-36 nm for experiments performed using solutions in $CHCl_3$, and in 31-49 nm interval when EtOH was used as solvent.

In both solvents, $CHCl_3$ and EtOH, a linear dependence of the absorbance and emission intensity with concentration was determined (data not shown). This is observed even in the case of the conjugate **1.1.22** bearing three **Dye1-CO$_2$H** units (spectra of **1.1.22**

at various concentrations in $CHCl_3$ are summarized in Figure 1.1.6 and Figure S1.1.7).

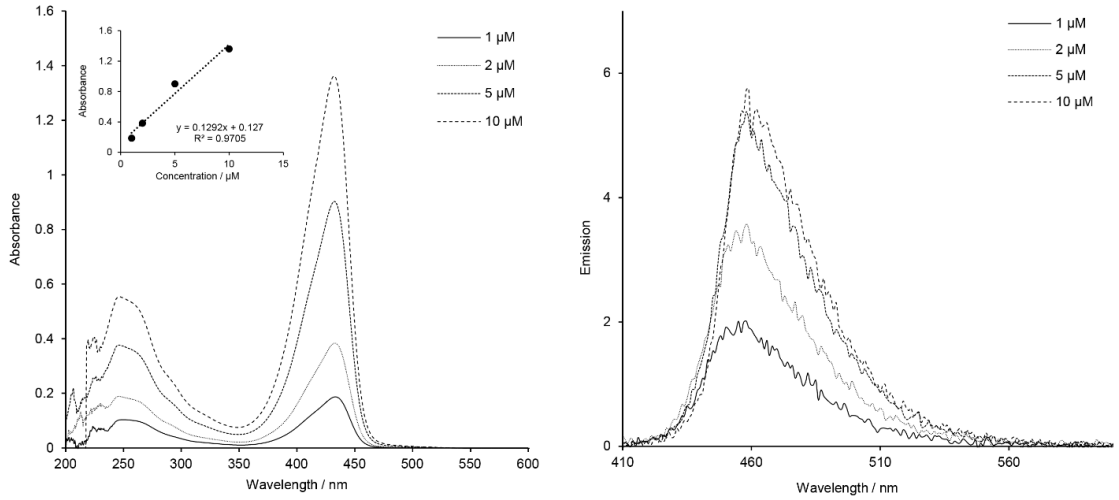

Figure 1.1.6. UV-Vis absorption (left) and emission spectra (right) of tri-coumarin ester conjugate **1.1.22** at various concentrations in $CHCl_3$.

1.1.2.4. Photostability

As the fluorescence intensity dramatically drops upon the addition of the trithiolato diruthenium unit (coumarin-ruthenium conjugates **1.1.11-1.1.17a/b**, **1.1.20** and **1.1.22** compared to free **Dye1-CO_2H** and **Dye2-CO_2H**), we used this difference to monitor the stability of the hybrid molecules. To verify the compounds' bleaching sensitivity but also stability at r.t. under air, in the presence of a polar solvent that can induce solvolysis, 10 µM **s**olutions of **1.1.12b**, **1.1.14b**, **1.1.16b**, **1.1.17b**, **1.1.20** and **1.1.22** in EtOH were maintained under indoor light for an extended time period. Absorption and emission spectra were monitored after 24 h, 48 h and one-week of light exposure, the measurements being made in the same conditions as previously described. Absorption spectra of all compounds remained unchanged after 48 h. After one week of light exposure a minor decrease of intensity can be observed for the absorbance signal in the 350-480 nm range, corresponding to the coumarin fragment.

In the emission spectra, notable changes were observed only for ester conjugates **1.1.12b**, **1.1.20**, and **1.1.22** (data not shown). A similar effect was noticed for the amide conjugates **1.1.14b** and **1.1.17b** (Figure 1.1.7), but only after one week of light exposure, while no spectral changes were observed for amide **1.1.16b**. This increase of the emission signal can be attributed to a partial solvolysis of the ester or amide bonds present on the conjugates with the release of the respective coumarin dyes. Nevertheless, considering the

time scale, and seen the very high fluorescence efficacy of **Dye1-CO_2H**, **Dye2-CO_2H** and corresponding coumarin intermediates **1.1.5-1.1.10** compared to the emission of the conjugates (fluorescence almost entirely quenched in the hybrid molecule), we can conclude that the coumarin-organometallic conjugates present high stability in the conditions used for this experiment.

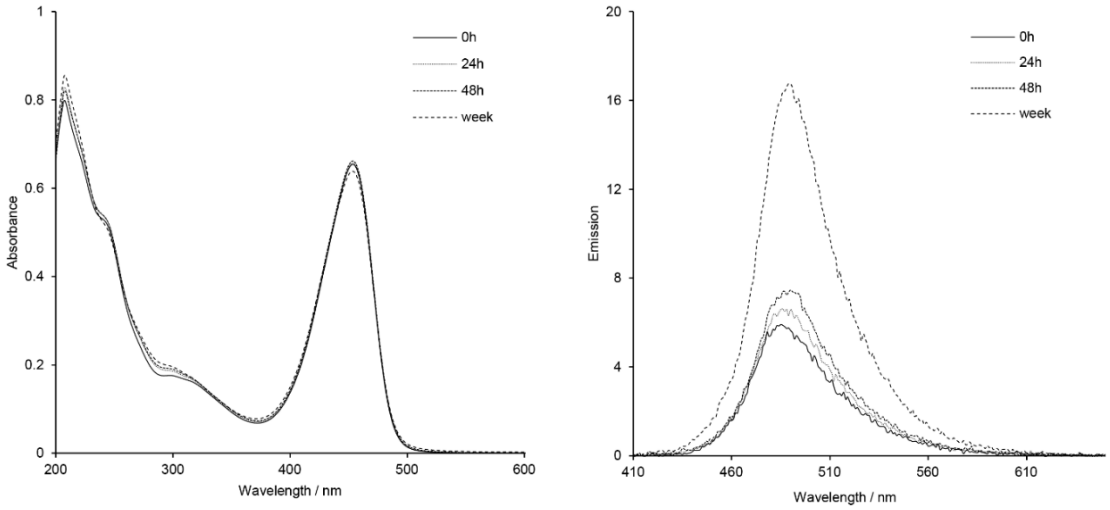

Figure 1.1.7. UV-Vis absorption (left) and emission spectra (right) of trithiolato ruthenium(II)-*p*-cymene complex **1.1.14b** after 0 h, 24 h, 48 h, and one week (168 h) of exposure to indoor light at 10 µM in EtOH.

1.1.2.5. Biological activity of the coumarin conjugates against Toxoplasma gondii

Toxoplasmosis, one of the most common global zoonotic diseases, is caused by the protozoan parasite *Toxoplasma gondii*.[108] This parasite can infect virtually all warm-blooded animals on the planet and has very high zoonotic potential. Up to one third of the human population is infected with *T. gondii*, but only a small fraction of infected individuals exhibits clinical signs. The economic impact of *T. gondii* is enormous, in that it causes severe losses in a wide range of wild and domestic animals, including most animals used in food production. In general, *T. gondii* infestation remains without clinical symptoms in immune competent individuals, and no treatment is required. However, in humans, infection has been linked to neuropsychiatric disease, and upon immunosuppression, or primary infection during pregnancy, *T. gondii* can cause toxoplasmosis, a life-threatening disease affecting both humans but also animals, which can lead to severe pathology including fetal malformation and abortion.[109] Current standard treatment options for toxoplasmosis include macrolide antibiotics and sulfonamides,[17] which inhibit protein biosynthesis and intermediary metabolism in the

apicoplast, a prokaryote-like organelle that is unique to apicomplexans.[110] However, these treatments are often characterized by adverse side effects and do not act in a parasiticidal manner. The development of novel treatment options that specifically target the parasite is therefore of prime importance.

The compounds presented in this study were screened for biological activity *in vitro* against *T. gondii* β-gal, a transgenic strain that constitutively expresses β-galactosidase, which is grown in HFF (human foreskin fibroblast) monolayers. In addition, the effects on non-infected HFF host cells were assessed. For the primary screening, cell cultures were exposed during 3 days to 1 µM and 0.1 µM of each compound (including non-modified thiolato-bridged dinuclear ruthenium(II)-arene complexes **1.1.2a/b**, **1.1.3a/b**, **1.1.4a/b**, coumarin-labeled conjugates **1.1.11**-**1.1.17a/b**, **1.1.20** and **1.1.22**, free dyes **Dye1-CO_2H** and **Dye2-CO_2H**, and corresponding coumarin-based intermediates). The viability of HFF cultures following drug treatments was measured by alamarBlue assay, and the proliferation of *T. gondii* was quantified by measuring β-galactosidase activity. The results of this primary screening are presented as percentage in relation to untreated control cultures in Table S1.1.5 (*Supporting information 1.1*). The results obtained at concentration of 0.1 µM and 1 µM of tested compound for *T. gondii* and HFF are presented in Figure 1.1.8, in relation to controls (CTR), namely HFF treated with 0.1% DMSO exhibiting 100% viability, and *T. gondii* β-gal tachyzoites treated with 0.1% DMSO showing 100% proliferation.

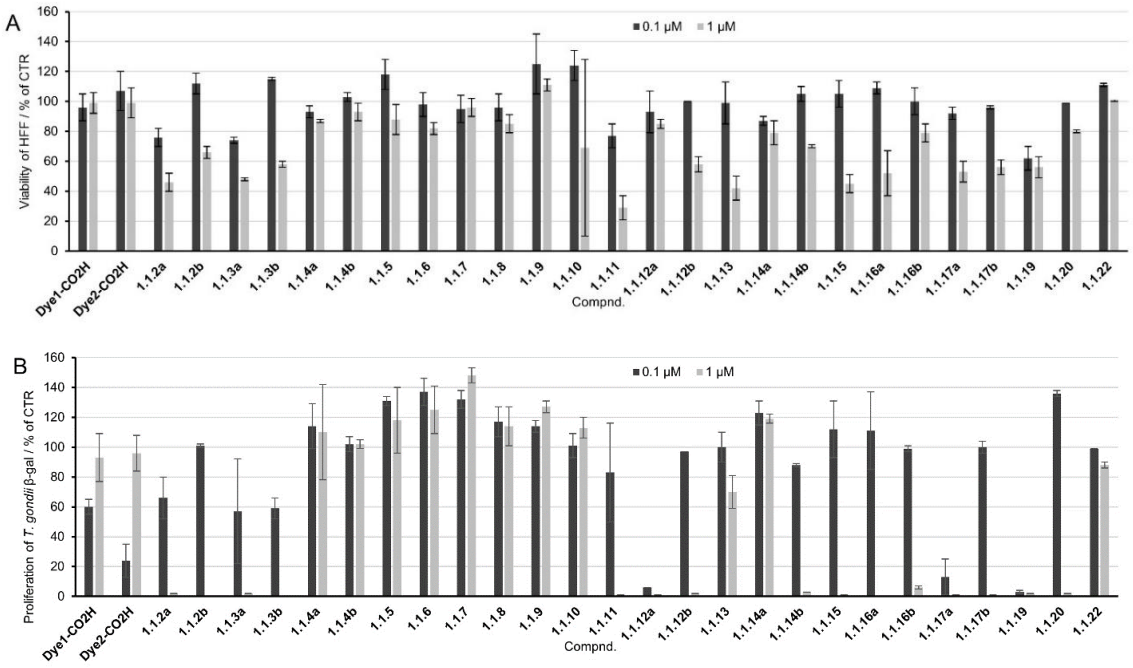

Figure 1.1.8. *In vitro* activities of compounds at 0.1 µM and 1 µM on HFF viability (A) and *T. gondii* β-gal tachyzoites proliferation (B), in relation to treatments with 0.1% DMSO. For each assay, standard deviations were calculated from triplicates.

No clear structure-activity relationship could be identified. The observed activity/cytotoxicity appeared to be the result of an interplay of various structural parameters that influence the cellular internalization and further interactions with biomolecules. The trithiolato dinuclear derivatives are mono-cationic complexes with a substantial molecular weight (> 950 g/mol). Anchoring of hydrophobic coumarin analogues as pendant arms on one of the thiol ligands, and the nature of the substituents present on the other two thiols, influence the physico-chemical properties of the molecule.

Compounds **1.1.2a**/**1.1.2b** and **1.1.3a**/**1.1.3b** bearing one hydroxy or amino group presented considerable activity against *T. gondii* β-gal at 1 µM, but also impaired HFF cell viability. The same was observed in the case of dihydroxy compound **1.1.19**. Acid functionalized trithiolato complexes **1.1.4a** and **1.1.4b** did not affect the viability of HFF monolayers, but did also not affect tachyzoite proliferation at 1 µM. None of the coumarin-based intermediates **1.1.5**-**1.1.10** (Table S1.1.5 and Figure S1.1.8 in *Supporting information 1.1*) impacted on HFF viability or *T. gondii* β-gal proliferation.

The nature of the substituents on the other two thiol ligands, hydrophobic-bulky *tert*-butyl *versus* hydrophobic-polar trifluoromethyl, had a considerable influence in the case of the hydroxyl derivatives **1.1.2a**/**1.1.2b** compared to the amino analogues **1.1.3a**/**1.1.3b**. This structural feature (Bu^t *vs* CF_3) appeared to affect the activities of the

ester compounds **1.1.12a**/**1.1.12b** and the amide compounds **1.1.14a**/**1.1.14b** in which the coumarin is directly connected to the thiol ligand. In some cases (**1.1.11** *vs* **1.1.13**, **1.1.12a** *vs* **1.1.14a**,), the amide conjugates exhibited lower antiparasitic activity compared to the esters for the same coumarin substituent.

Dye1-CO_2H -functionalized compounds **1.1.13**, **1.1.15**, and **1.1.16a** presented a similar cytotoxicity profile for HFF at 0.1 µM and 1 µM. The introduction of the linker augmented the measured activity against the parasite. For compounds bearing **Dye2-CO_2H** moieties, the introduction of a linker between the diruthenium scaffold and the coumarin led to a substantially increased antiparasitic activity in the case of Bu^t analogue **1.1.17a** compared to **1.1.14a**; however, a similar effect was not observed for CF_3 analogues **1.1.17b** and **1.1.14b**. Compounds **1.1.13**, **1.1.14a** and **1.1.22** are only poorly active against *T. gondii* β-gal at 1 µM, and the last two compounds did not notably affect HFF cell viability. In the series of **Dye1-CO_2H** functionalized ester compounds **1.1.11**, **1.1.20** and **1.1.22** no noteworthy correlation between the number of coumarin units and the measured biological activity was observed. At 1 µM, **1.1.11** displayed substantial HFF toxicity, while **1.1.20** and **1.1.22** did not. As shown in Figure 1.1.8, **Dye1-CO_2H** and **Dye2-CO_2H** did not affect viability of HFF when applied at 0.1 µM or 1 µM. However, proliferation of *T. gondii* relative to the rate of β-galactosidase activity, was decreased following treatment with 0.1 µM of **Dye1-CO_2H** (53%) and **Dye2-CO_2H** (69%; Table S1.1.5). These results may suggest that *in vitro* anti-*Toxoplasma* activity of these coumarin dyes may be lost due to solubility issues.

Based on this preliminary screening, 13 compounds were selected for determination of the IC_{50} values against *T. gondii* β-gal. These were compounds that, when applied at 1 µM, allowed viability values for HFF at 45% or more, while they also inhibited *T. gondii* proliferation by 94% or more. The results are shown in Table 1.1.2 and Figure S1.1.8, and the respective dose-response curves are shown in Figure S1.1.9.

Table 1.1.2. IC_{50} values (μM) against *T. gondii* β-gal tachyzoite proliferation and effects on HFF viability at 2.5 μM, for selected compounds and pyrimethamine (as positive control).

Compound	IC_{50} (μM)	[LS; LI] [a]	SE [b]	HFF viability at 2.5 μM (%)[c]	SD [d]
1.1.2a	0.117	[0.098; 0.139]	0.0510	56	6
1.1.2b	0.336	[0.323; 0.35]	0.0088	72	6
1.1.3a	0.153	[0.127; 0.185]	0.0488	51	5
1.1.3b	0.135	[0.105; 0.174]	0.0562	53	4
1.1.12a	0.105	[0.099; 0.111]	0.0230	58	4
1.1.12b	0.298	[0.292; 0.305]	0.0051	28	1
1.1.14b	0.391	[0.351; 0.437]	0.0236	71	5
1.1.16a	0.127	[0.170; 0.095]	0.129	4	1
1.1.16b	0.735	[0.467; 1.156]	0.1155	73	7
1.1.17a	0.243	[0.190; 0.311]	0.0905	25	5
1.1.17b	0.203	[0.113; 0.366]	0.1459	54	7
1.1.19	0.115	[0.098; 0.135]	0.0447	2	4
1.1.20	0.377	[0.36; 0.39]	0.0137	71	4
Pyrimethamine	0.326	[0.288; 0.396]	0.0518	99	6

[a] Values at 95% confidence interval (CI); LS (limit superior) and LI (limit inferior) are the upper limit and the lower limit of the CI, respectively. [b] The standard error (SE) of the estimate represents the average distance that the observed values fall from the regression line (*T. gondii* β-gal). [c] Control HFF treated only with 0.25% DMSO exhibited 100% viability. [d] The standard deviation of the mean of six replicate experiments (HFF).

The most active compound against *T. gondii* β-gal was **1.1.12a**, with an IC_{50} value of 0.105 μM. This compound was not toxic at 1 μM, but when applied at 2.5 μM it reduced HFF viability to 58%. Higher levels of HFF viability impairment were noted for compounds **1.1.12b**, **1.1.17a** and especially **1.1.19** (98% reduction in HFF viability). The difference in antiparasitic activity between compounds **1.1.12a** and **1.1.12b** (IC_{50} values of 0.105 μM and 0.298 μM, respectively) highlights the importance of the physico-chemical properties of the substituents present on the other thiol ligands, Bu^t *vs* CF_3. As shown in Table 1.1.2, unmodified hydroxy compound **1.1.2a** and amino compounds **1.1.3a** and **1.1.3b**, also presented considerable antiparasitic activities (IC50 values of 0.117 μM, 0.153 μM and 0.135 μM, respectively), furthermore, their impact on HFF viability at

2.5 µM was less pronounced compared to **1.1.17a** and **1.1.19**.

Three selected compounds (**1.1.2a**, **1.1.3a** and **1.1.12a**), applied at their respective IC_{50} against *T. gondii*, were further assessed with respect to their potential to interfere in splenocyte proliferation *in vitro.* Isolated murine splenocytes from healthy mice were stimulated with Concanavalin A (ConA) to induce T cell proliferation or with bacterial lipopolysaccharide (LPS) to induce B cell proliferation, either in the presence or absence of tested compounds **1.1.2a, 1.1.3a** and **1.1.12a**. Measurements of proliferation were done using an assay that quantifies the incorporation of 5-bromo-2'-deoxy-uridine (BrdU) into the DNA of replicating cells. As seen in Figure 1.1.9, **1.1.3a** and **1.1.12a** significantly interfered in T cell proliferative responses, which resulted in a reduction of BrdU incorporation by 25% and 31%, respectively, while **1.1.2a** did not affect T cell proliferation. Compounds **1.1.2a** and **1.1.3a** significantly impacted the proliferation of B cell (only 48% and 68% BrdU incorporation, respectively, compared to the control), whereas **1.1.12a** did not exhibit significant proliferation inhibition of antibody producing cells. Thus, **1.1.3a** affected both B and T cell proliferation, while **1.1.2a** and **1.1.12a** impaired the proliferative capacity of only one type of immune cells; B cells for **1.1.2a** (humoral immunity) and T cells for **1.1.12a** (cellular immunity).

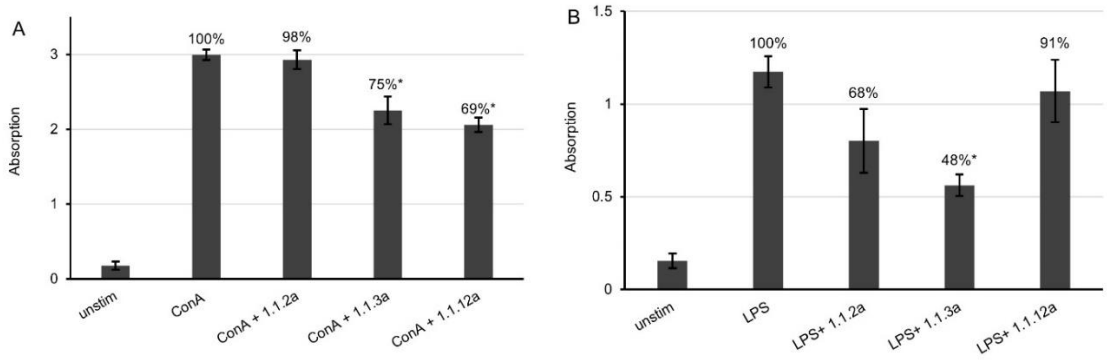

Figure 1.1.9. Inhibitory effect of selected compounds **1.1.2a**, **1.1.3a** and **1.1.12a** ConA- (A) and LPS-induced (B) proliferative activity of mouse splenocytes. Bars represent standard deviation from the mean of four replicates. A 100% of proliferation is attributed to controls (ConA and LPS); values are percentage proliferation compared to control (*) $p < 0.01$ in relation to controls (ConA or LPS).

A reduction in the capacity of T and B cells to respond to external signals by proliferative responses could also indicate a potential risk of impaired immunity. However, a reduction in cellular proliferation does not automatically imply a reduced metabolic activity or reduction in cellular viability. Thus, in addition to proliferative responses of B

and T cells upon LPS and ConA stimulation, we also assessed the effects of **1.1.2a**, **1.1.3a** and **1.1.12a** on the viability of splenocytes employing the alamarBlue assay, which allows, similar to what we have tested in HFF, to quantify metabolic activity (Figure 1.1.10). Measurements taken each hour during the first 5 h after adding the substrate resazurin showed that none of the compounds impaired the metabolic activity of ConA stimulated T cells, but compounds **1.1.2a** and **1.1.3a** significantly impaired the viability of B cells upon stimulation with LPS. **1.1.12a** did not show any interference in metabolic activity of neither B nor T cells. The lack of viability impairment of splenocytes due to exposure with **1.1.12a** observed here indicates that this compound is a promising drug candidate for future *in vivo* studies in the mouse model, to combat *T. gondii* infection without impairing the cellular and humoral immune response.

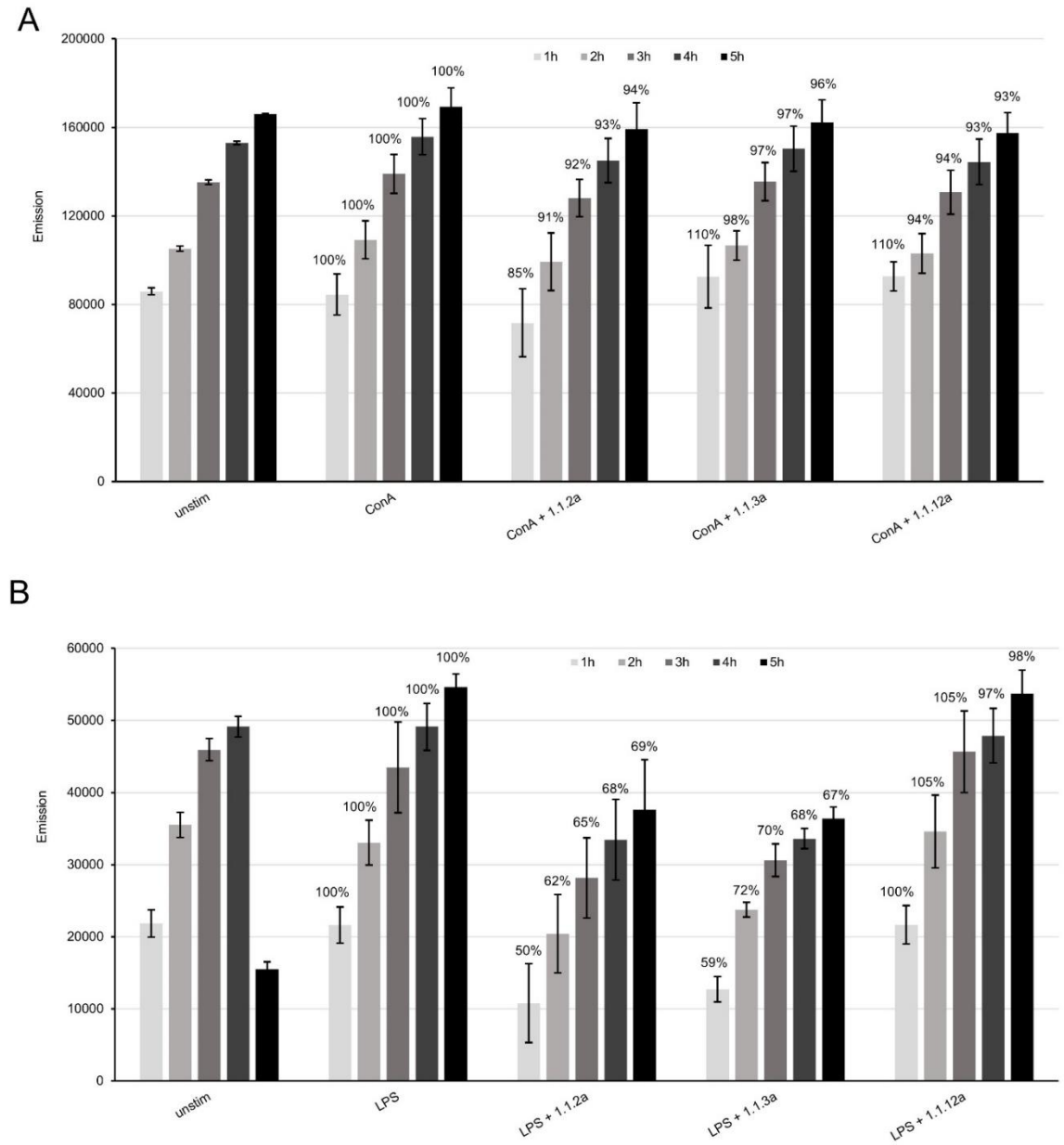

Figure 1.1.10. Determination of cytotoxic effects of **1.1.2a**, **1.1.3a** and **1.1.12a** in ConA- (A) and LPS (B) induced splenocytes by alamarBlue assay. Bars represent the mean emission of 4 replicates ± standard deviation. In both experiments and for each time point a 100% of metabolic activity was attributed to the control sample (splenocytes induced with ConA or LPS), then the percentage of metabolic activity in relation to the controls was calculated and is indicated in the graph for each sample. Significance with $p < 0.001$ was observed between LPS and LPS + **1.1.2a**, and LPS + **1.1.3a** for all five time points.

The ultrastructural changes induced by compounds **1.1.12a** (IC_{50} of 0.105 μM against *T. gondii*, HFF viability of 58% at 2.5 μM) and **1.1.17a** (IC_{50} of 0.243 μM against *T. gondii*, HFF viability of 24% at 2.5 μM) were further studied by TEM. HFF monolayers were infected with *T. gondii* β-gal tachyzoites and after 24 h drug treatments (500 nM of each compound, a concentration that did not notably affect the host cell) were initiated.

Samples were fixed and processed after 6 h, 24 h and 48 h. Non-treated control cultures are shown in Figure 1.1.11 A-C. A shows a sample fixed after 6 h post-invasion, B and C have been fixed after 36 h and 60 h post-invasion, respectively, and the increase in number of parasites illustrates the proliferation that takes place within the host cell. Once invaded, *T. gondii* tachyzoites are localized within a parasitophorous vacuole (PV), surrounded by a parasitophorous vacuole membrane (PVM), which is essentially host cell surface membrane-derived and modified by the parasite following invasion. The mitochondrion exhibits a characteristic electron dense matrix containing numerous cristae. Tachyzoites treated with 500 nM **1.1.12a** are shown in Figure 1.1.12. At 6 h after initiation of treatment, parasites do not exhibit massive alterations, however, PVs usually contained only 1-3 tachyzoites. The PVM was still clearly discernible, and the secretory organelles such as rhoptries, micronemes, and dense granules, as well as the mitochondria remained largely unaltered (Figure 1.1.12 A-B). At 24 h, first ultrastructural changes were noted within the mitochondrial matrix, which started to lose its characteristic electron-dense matrix. These mitochondrial alterations became progressively more pronounced at 24 h (Figure 1.1.12 D and E) and 48 h (Figure 1.1.12 F, G), resulting in tachyzoites that were completely devoid of a mitochondrion, but exhibited large, seemingly empty, vacuoles instead. While it is not clear whether these effects were reversible, it is conceivable that this extensive vacuolization would eventually lead to parasite death. Similar results were seen for **1.1.17a**, (Figure S1.1.10), although the effects after 24 h and 48 h were slightly less pronounced. Overall, these findings mirror previously reported structural alterations induced by ruthenium complexes reported in *T. gondii*, *N. caninum* and in *T. brucei*, and in the latter it was recently shown that active complexes strongly impaired the mitochondrial membrane potential,[29, 33, 63] which indicates that ruthenium complexes interfere in the energy metabolism of these parasites. However, while oxidative phosphorylation resulting in the generation of ATP is the major function of mitochondria, these organelles are also involved in other crucial processes, including cell cycle regulation, t-RNA- and protein-import, mitochondrial protein translation, alternative oxidase, acetate production for cytosolic and mitochondrial fatty acid biosynthesis, amino acid metabolism and calcium homeostasis, and they are involved in the steps leading to programmed cell death. How, and to what extent, these compounds actually target mitochondrial functions, or whether other targets are also involved, remains to be elucidated.

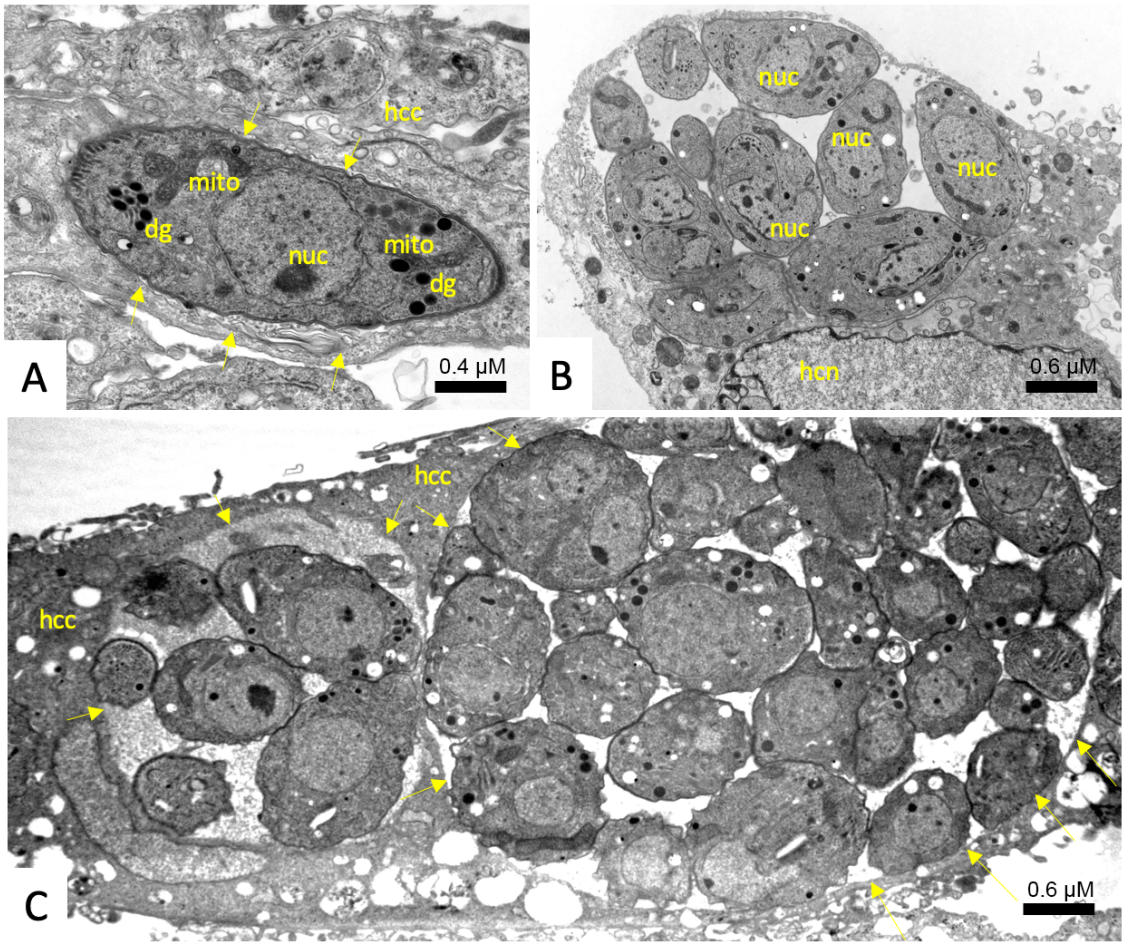

Figure 1.1.11. TEM of untreated *T. gondii*-β-gal tachyzoites fixed at 6 h (A), 24 h (B) and 48 h (C) post infection. A shows a single tachyzoite, located within a parasitophorous vacuole that is delineated by a parasitophorous vacuole membrane (arrows). B Proliferation of tachyzoites takes place within the vacuole, which occupies a substantial part of the host cell cytoplasm. C shows two neighboring parasitophorous vacuoles, delineated by arrows, located within a HFF host cell, both containing numerous newly formed tachyzoites. Note the mitochondrion (mito) with an electron dense matrix in A; nuc = tachyzoite nucleus, dg = dense granule, hcc = host cell cytoplasm; hcn = host cell nucleus.

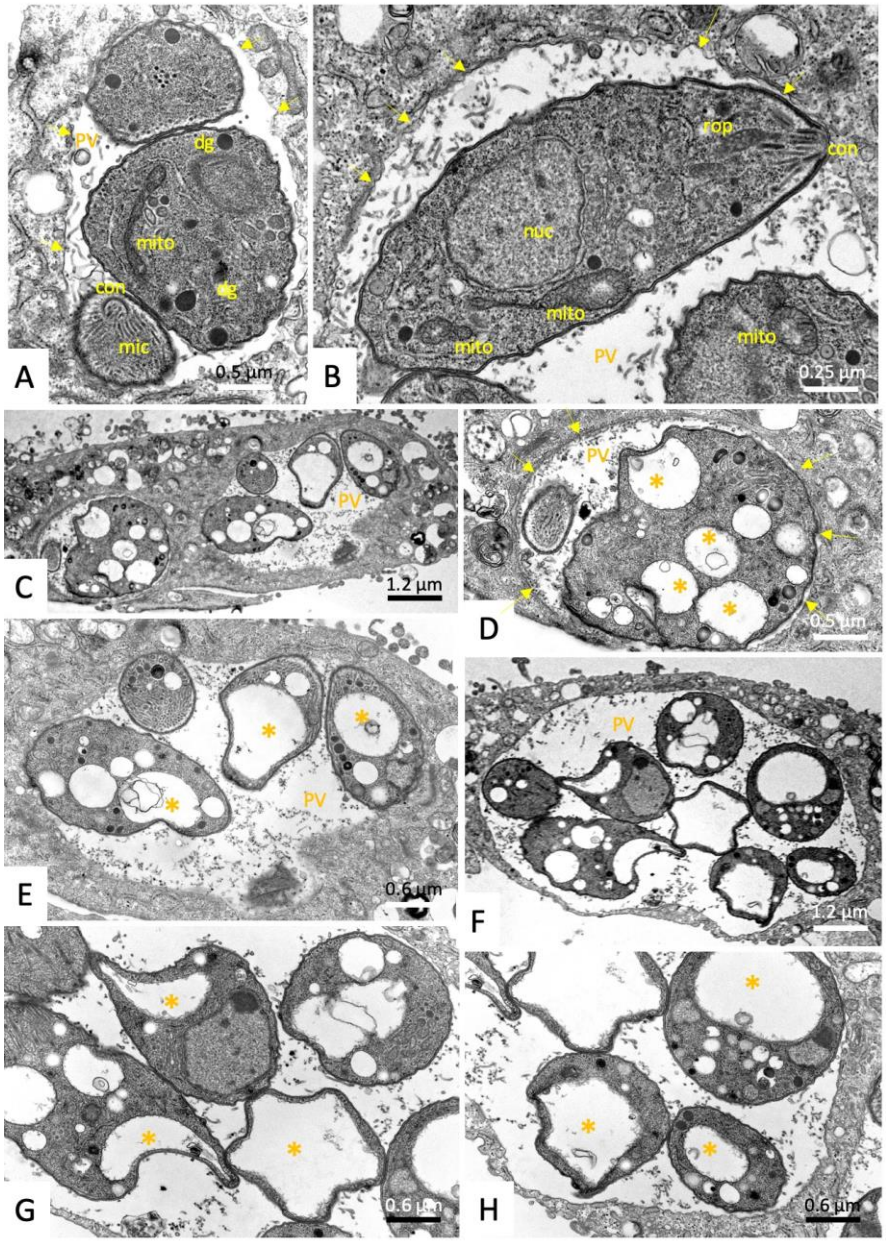

Figure 1.1.12. TEM of *T. gondii*-β-gal tachyzoites treated with 500 nM of **1.1.12a** during (6 h (A, B), 24 h (C-E) and 48 h (F-H). No alterations (A) or only very slight changes in the electron dense mitochondrial matrix (mito in B) are detected after 6 h. C-E show that alterations were much more pronounced after 24 h of treatment, C is a low magnification overview, D and E represent distinct parts of C shown at higher magnification. F is a low magnification view of a parasitophorous vacuole of tachyzoites treated for 48 h, G and H represent respective high magnifications. Note the increased vacuolization (marked with *) and the absence of any mitochondrial matrix after 24-48 h of treatment. PV = parasitophorous vacuole; mito = mitochondrion; nuc = nucleus, con = conoid; rop = rhoptries; dg = dense granule; mic = microneme; arrows point towards the parasitophorous vacuole membrane.

In order to assess the potential use of the new conjugates coumarin-diruthenium unit as cellular trackable probes fluorescence microscopy assays were performed of HFF cells treated with either 20 µM **Dye2-CO_2H** or 20 µM of **1.1.12a**, both counterstained with

an antibody directed against tubulin and NucRed, a fluorescent nuclear label (see results and experimental in *Supporting information 1.1*). However, while anti-tubulin readily stained the cytoskeleton of HFF and NucRed indicated the nucleus, no labeling could be observed with neither **Dye2-CO_2H** nor **1.1.12a**. In order to obtain trithiolato di-nuclear ruthenium conjugates suitable to be used as theranostics, the attachment of other fluorophores should be considered.

1.1.3. Conclusions

A library of 13 new trithiolato-bridged dinuclear ruthenium(II)-arene organometallic conjugates in which coumarin moieties were anchored to the bridged thiol(s), have been designed and synthesized.

Irrespective to the structural variations considered, for all conjugates organometallic unit: coumarin an almost complete loss of fluorescence efficacy was observed. However, the nature of the fluorophore, the type of bonding, the presence and length of a linker between the coumarin dye and the dinuclear ruthenium(II) moiety, and the number of dye units did influence the biological properties of these compounds. These modifications also affect the toxicity of these compounds against human fibroblasts, and impact the activity against the apicomplexan parasite *T. gondii*, grown in these cells *in vitro.* For selected compounds (**1.1.2a**, **1.1.3a** and **1.1.12a**), applied at their *T. gondii*-IC_{50}, the effect on the proliferative responses of splenocytes upon ConA (for T cell) and LPS (for B cell) stimulation was investigated, and the influence on the viability/metabolic activity of B and T cells *in vitro* was assessed. With IC_{50} values ranging from 105 nM to 735 nM, and seen that 9 compounds displayed lower IC_{50} than the standard drug pyrimethamine, suggest that these class of compounds is promising. In particular, compound **1.1.12a** did not affect the metabolic activity of B or T cells *in vitro*, is therefore not expected to impair immunity, and thus represents a promising compound for future *in vivo* assessment in toxoplasmosis mouse models.

1.1.4. Experimental section

1.1.4.1. General

The chemistry experimental part, with full description of experimental procedures and characterization data for all compounds, is presented in the *Supporting information 1.1*.

1.1.4.2. Crystal-Structure Determination

A crystal of $C_{39}H_{45}Cl_3O_3Ru_2S_3$ was mounted in air at ambient conditions. All measurements were made on a *RIGAKU Synergy S* area-detector diffractometer[111] using mirror optics monochromated Cu *K*α radiation (λ = 1.54184 Å).[112] The unit cell constants and an orientation matrix for data collection were obtained from a least-squares refinement of the setting angles of reflections in the range 6.266°<2θ< 155.814°. A total of 4310 frames were collected using ω scans, with 0.05 seconds exposure time, a rotation angle of 0.5° per frame, a crystal-detector distance of 31.0 mm, at T = 173(2) K.

Data reduction was performed using the *CrysAlisPro*[111] program. The intensities were corrected for Lorentz and polarization effects, and an absorption correction based on the multi-scan method using SCALE3 ABSPACK in *CrysAlisPro*[111] was applied. Data collection and refinement parameters are given in Table S1.1.1.

The structure was solved by direct methods using *SHELXT*[113], which revealed the positions of all non-hydrogen atoms of the title compound. All non-hydrogen atoms were refined anisotropically. H-atoms were assigned in geometrically calculated positions and refined using a riding model where each H-atom was assigned a fixed isotropic displacement parameter with a value equal to 1.5Ueq of its parent atom (for methyl groups).

Refinement of the structure was carried out on F^2 using full-matrix least-squares procedures, which minimized the function $\Sigma w(F_o^2 - F_c^2)^2$. The weighting scheme was based on counting statistics and included a factor to downweight the intense reflections. All calculations were performed using the *SHELXL-2014/7*[114] program in OLEX2.[115]

1.1.4.3. Photophysical Measurements

UV-Visible spectra were recorded on a Thermo Scientific Evolution 201 UV-Vis spectrophotometer.

Fluorescence emission spectra were measured on an Agilent Cary Eclipse fluorescence spectrophotometer.

The UV-Vis absorption spectra of compounds **1.1.5-1.1.17a/b**, **1.1.20** and **1.1.22** were recorded in the range 200-1100 nm at r.t. using solutions of 1, 2, 5 and 10 μM in $CHCl_3$ and in EtOH. Emission spectra were recorded in the range 405-650 nm after excitation at 405 nm (excitation and emission filters: auto, excitation and emission slit = 2.5 nm), using 1, 2, 5 and 10 μM solutions in $CHCl_3$ and in EtOH. All the experiments were studied at r.t., the solvent absorption was deducted as background.

1.1.4.4. Determination of Quantum Yields

Relative quantum yields for solutions in $CHCl_3$ and EtOH at r.t. were calculated by a relative method using equation (**1**) and rhodamine 6G (Φ_F = 0.75 in $CHCl_3$, Φ_F = 0.94 in EtOH) as standard.[107, 116] The absorption of rhodamine 6G was adjusted to the same value (abs < 1) as that of fluorescent molecules. Excitation was chosen at 405 nm; the emission spectra were corrected and integrated for the area under the emission curve.

$$\Phi_F(x) = \frac{A_s}{A_x} \times \frac{F_x}{F_s} \times \left(\frac{n_x}{n_s}\right)^2 \times \Phi_F(s) \quad (\mathbf{1})$$

where *A* is the absorbance at the excitation wavelength, *F* is the integration of emission intensity, *n* is the refractive index of the solvents (at 20°C) used in measurements (n = 1.446 for $CHCl_3$, n = 1.3611 for EtOH), and the subscripts *s* and *x* represent standard and unknown respectively.

$$\Delta\lambda = \lambda_{max}^{em} - \lambda_{max}^{abs} \quad (\mathbf{2})$$

Stokes shifts were calculated using equation (**2**) as the difference between the values of maxima of the intense bands in the fluorescence and absorption spectra

1.1.4.5. Experimental biology

In vitro culture of parasites and host cells

If not stated otherwise, all tissue culture media were purchased from Gibco-BRL (Zurich, Switzerland), and biochemical reagents were from Sigma (St. Louis, MO). Human foreskin fibroblasts (HFF) were maintained in DMEM-medium containing 10% fetal calf serum (FCS) (Gibco-BRL, Zürich, Switzerland) and antibiotics as described earlier.[28] *T. gondii* β-gal (transgenic *T. gondii* RH expressing the β-galactosidase gene from *E. coli*[117] were maintained in HFF cells, and were isolated and separated from their host cells as described.[28]

In vitro assessment of drug efficacy

To study the effects of compounds against *T. gondii* tachyzoites *in vitro*, 1 mM stock solutions of complexes were prepared in DMSO, and stored at -20°C. For assessment of drug efficacy against *T. gondii* tachyzoites, parasites were isolated and assays were performed using HFF as host cells as previously described.[28] In short, 5×10^3 HFF cells per well were grown to confluence in a 96 well plate in phenol-red free culture medium at 37°C with 5% CO_2. Cultures were infected with freshly isolated *T. gondii* β-gal tachyzoites (1 x 10^3 per well) and drugs were added concomitantly with infection. Initial assessments

of drug efficacy were done by exposing parasite cultures to 0.1 and 1 µM of each compound for a period of three days, or 0.1 % DMSO was added as a control. For IC_{50} determinations, compounds were added at 6 concentrations: 0.03 µM, 0.06 µM, 0.12 µM, 0.25 µM, 0.5 µM, and 1 µM. After three days of incubation at 37°C, 5% CO_2, medium was removed, and cell cultures were permeabilized using 90 µL PBS containing 0.05% Triton-X-100. After addition of 10 µL of 5 mM chlorophenol red-β-D-galactopyranoside (CPRG; Roche Diagnostics, Rotkreuz, Switzerland) dissolved in PBS, the absorption shift was measured at 570 nm wavelength at various time points on a VersaMax multiplate reader (Bucher Biotec, Basel, Switzerland). For the initial screening at 0.1 and 1 µM, the activity, measured as the release of chlorophenol red over time, was calculated as percentage from DMSO control, which represented 100% of *T. gondii* β-gal growth. For the IC_{50} assays, the activity measured as the release of chlorophenol red over time was proportional to the number of live parasites down to 50 per well as determined in pilot assays. IC_{50} values were calculated after the logit-log-transformation of relative growth and subsequent regression analysis. All calculations were performed using the corresponding software tool contained in the Excel software package (Microsoft, Seattle, WA).

Cytotoxicity assays on non-infected confluent HFF were performed also in 96 well plates by exposing HFF to a concentration range of 0.1 µM, 1 µM and 2.5 µM of each compound, and assessment of the viability by alamarBlue assay as described.[118]

Isolation of murine splenocytes

Female BALB/c mice were purchased from Charles River Laboratories (Sulzfeld, Germany) and were maintained in a common room under controlled temperature and a 14 h dark/10 h light cycle according to the standards set up by the animal welfare legislation of the Swiss Veterinary Office. The experimental protocol was approved by the Commission for Animal Experimentation of the Canton of Bern, Switzerland (Animal license No. BE101/17). Mice were euthanized using isoflurane and CO_2, and spleens were aseptically removed from euthanized mice. Single-cell suspension was prepared by gently mincing spleen tissue and passing it through sterile 40 µm cell-strainer. Erythrocytes were depleted from cell suspension using RBC Lysis Buffer (Invitrogen, Thermo Fisher Scientific) for 5 min. Viability of isolated cells was determined using Trypan Blue dye exclusion test, and preparations were only used when >99% of viable cell were counted.in a Neubauer hemocytometer. The spleen cell preparation containing T cells, dendritic cells, B cells and macrophages, was then suspended in RPMI 1640 medium including 10% FCS, 0.05 mM

2-mercaptoethanol, 2 mM L-glutamine, and 100 U of penicillin plus 50 mg of streptomycin per mL. Cell suspensions were distributed in polystyrene 96 well flat bottom sterile plastic plates (Greiner Bio-One; HuberLab) at 2×10^5 cells/100 µL/well.

Splenocyte proliferation assay

Isolated primary splenocytes were either left unstimulated or were stimulated with Concanavalin A (ConA, 5 µg/mL), lipopolysaccharide (LPS, 10 µg/mL), ConA plus compound or LPS plus compound. Compounds **1.1.2a**, **1.1.3a** and **1.1.12a** were added at their respective IC_{50} value. Experiments were performed in quadruplicate wells, 200 µL/well, and cultures were maintained in a 37°C humidified chamber containing 5% CO_2 for a total incubation period of 72 h. Proliferative responses of splenocytes were measured using a 5-bromo-20-deoxy-uridine (BrdU) cell proliferation kit (QIA58, Merck Millipore). Briefly, BrdU label was added to the cultures 18 h prior the end of the incubation period. Incorporated BrdU into the newly synthetized DNA was measured by ELISA using anti-BrdU monoclonal antibody. Immediately after stopping the reaction, the absorbance was measured at 450/540 nm, in an EnSpire multilabel reader (Perkin Elmer, Waltham). Data are presented as mean ± standard deviation (SD) for the indicated numbers. Data comparisons between groups were examined using a student's t-test (significant when $p < 0.01$).

Determination of cytotoxic effects in splenocytes

To determine whether compounds **1.1.2a**, **1.1.3a** and **1.1.12a** exhibit an effect on the metabolism of ConA- and LPS- induced splenocytes, the alamarBlue assay was performed. Isolated splenocytes were seeded in 96-well plates at a density of 1×10^6 cells/mL with a final volume of 100 µL/well. Cells were either left unstimulated or stimulated with ConA (5 µg/mL), LPS (10 µg/mL), ConA plus compound or LPS plus compound. Each compound was tested at its IC_{50} against *T. gondii* β-gal, in quadruplicate wells at a volume of 200 µl/well. Cultures were maintained in a 37°C humidified chamber containing 5% CO_2 for a total incubation period of 72 h. Resazurin (0.1 mg/mL) was added, and the fluorescence intensity was measured at 530 nm excitation wavelength and a 590 nm emission wavelength using an EnSpire multilabel reader (Perkin Elmer). Measurements were done at different time points T = 0 h, 1 h, 2 h, 3 h, 4 h and 5 h. Differences were calculated by subtracting T0 values from each time point. Data are presented as mean of emission ± standard deviation (SD) for the indicated numbers. Data comparisons between

groups were examined using a student's t-test (significant when $p < 0.001$).

1.1.4.6. Transmission electron microscopy (TEM)

HFF ($5x10^5$ per inoculum) grown to confluence in T-25 tissue culture flasks were infected with 10^5 *T. gondii* Me49 tachyzoites, and 500 nM of **1.1.12a** or **1.1.17a** were added at 24 h post-infection. After 6 h, 24 h or 48 h, cells were harvested using a cell scraper, and they were placed into the primary fixation solution (2.5 % glutaraldehyde in 100 mM sodium cacodylate buffer pH 7.3) for 2 h. Specimens were then washed 2 times in cacodylate buffer and were post-fixed in 2% OsO_4 in cacodylate buffer for 2 h, followed by washing in water, pre-staining in saturated uranyl acetate solution, and step wise dehydration in ethanol. They were then embedded in Epon 812-resin, and processed for TEM as described.[29] Specimens were viewed on a CM12 transmission electron microscope operating at 80 kV.

1.2. BODIPY-Tagged Dinuclear Trithiolato-Bridged Ruthenium(II)-Arene Complexes[2]

Abstract

The synthesis, photophysical properties and antiparasitic efficacy of a series of 15 new conjugates BODIPY-trithiolato-bridged dinuclear ruthenium(II)-arene complexes are reported (BODIPY = 4,4-difluoro-4-bora-3a,4a-diaza-*s*-indacene fluorescent markers). The influence of the bond type (amide *vs* ester), as well as that of the length of the linker between the dye unit and the diruthenium(II) complex moiety, upon the fluorescence and the biological activity were evaluated. In spite of an important quenching effect observed after appending the BODIPYs on the organometallic unit, the significant fluorescence quantum yield shown by these dyads in solution makes them potential candidates for cellular imaging.

The compounds were assessed for activity against *Toxoplasma gondii* RH strain tachyzoites expressing β-galactosidase (*T. gondii* β-gal) grown in human foreskin fibroblast (HFF) monolayers and toxicity in non-infected HFF host cells, while further dose-response assays were made on selected derivatives. The results of the first screening showed that both the size of the connector between the organometallic unit and the fluorophore, as well as of the type of bond strongly impact the biological activity, with ester conjugates being generally more efficient in inhibiting parasite proliferation but also affecting to a higher extent host cells viability. The conjugates exhibit similar IC_{50} values on *T. gondii* β-gal to that of the standard drug pyrimethamine, but they exert a stronger toxicity on HFF when applied to 2.5 µM. From this library of dyads, ester **1.2.20** and amide **1.2.28** BODIPY hybrids present better antiparasitic efficacy/cytotoxicity balance.

Aiming to more insight into the mode of action of this type of conjugates, their potential targets and cellular localization, compounds **1.2.21** and **1.2.27** were submitted to TEM (Transmission Electron Microscopy) and derivatives **1.2.10** and **1.2.20** to fluorescence microscopy tests. TEM assays demonstrated structural alterations in the parasite mitochondrion after treatments with the diruthenium conjugates. If no specific

[2] This chapter is a draft with title *Synthesis, Spectral Properties and Biological Evaluation of New Conjugates BODIPY – Dinuclear Trithiolato-Bridged Ruthenium(II)-Arene Complexes*, which is going to be submitted for publication. (Published as: Synthesis, Photophysical Properties and Biological Evaluation of New Conjugates BODIPY: Dinuclear Trithiolato-Bridged Ruthenium(II)-Arene Complexes, *ChemBioChem*, 2022, 23, e202200536, https://doi.org/10.1002/cbic.202200536. © 2022Wiley-VCHGmbH. Reproduced with permission). Supplementary information can be found in the chapter *Supporting information 1.2.*

organelle localization of the BODIPY conjugate **1.2.20** could be identified, however the compound does not appear to accumulate in the nucleus. The cellular fluorescence intensity of conjugate **1.2.20** is higher compared to that of the respective BODIPY dye **1.2.10**, although the later exhibits significantly higher fluorescence quantum yield, which might indicate a higher cellular internalization and/or a 'fixation'/accumulation of the diruthenium compound.

If the interest of these series of conjugates as antiparasitic therapeutic agents seems limited, however the compounds demonstrate potential as fluorescent probes for understanding the intracellular trafficking of trithiolato-bridged dinuclear Ru(II)-arene complexes *in vitro*, and further studies are necessary.

1.2.1. Introduction

Cationic trithiolato-bridged dinuclear ruthenium(II)-arene complexes (general formula for symmetric $[(\eta^6\text{-arene})_2Ru_2(\mu_2\text{-}SR)_3]^+$, and mixed complexes $[(\eta^6\text{-arene})_2Ru_2(\mu_2\text{-}SR^1)_2(\mu_2\text{-}SR^2)]^+$) are highly cytotoxic against human cancer cells (low micromolar range IC_{50} values (half maximal inhibitory concentration))[64] and present interesting antiparasitic efficacy against *Toxoplasma gondii*[29], *Neospora caninum*[33] and *Trypanosoma brucei*[63]. Aiming for the design and development of more efficient compounds, it became compulsory to have a better understanding of their mechanism of action and to identify potential biological targets. Yet little is known about the traffic and fate of these complexes in cells and how this relates to their anticancer or antiparasitic effect. TEM (Transmission Electron Microscopy) of *T. gondii* as well as of *T. brucei* treated with various trithiolato-bridged dinuclear ruthenium(II)-arene compounds had identified the parasites mitochondrion as a potential target[29, 63].

Various methods can be used as support for the identification of the cellular localization of metal-based bioactive compounds as for example ICP-MS (inductively coupled plasma mass spectrometry) or confocal fluorescence microscopy of complexes that are fluorescent *per se* or that are tagged with fluorescent dyes.[119] The method generally used to investigate cell uptake, subcellular distribution, and specific accumulation of metallodrugs remains ICP-MS, which relies on cellular fractioning and subsequent metal assay. Although well-established and sensitive, this method does not allow dynamic process investigations.[120] A promising strategy allowing to tackle this issue is the development of trackable therapeutic agents as fluorophore-labelled conjugates of the metal-based drugs. The following advantages are expected: information on uptake,

localization, and specific accumulation within cells could be acquired with the use of fluorescence microscopy instrumentation. These experiments could be carried out simultaneously with the fluorescent compound, and colocalization by fluorescence microscopy would provide precious information on the behaviour of the metallodrug candidate in a dynamic fashion. This technique (metallodrug derivatives with fluorescence imaging capabilities) was already successfully exploited in the case of other metal-organic compounds presenting anticancer properties[83, 121, 122] as cisplatin[123, 124].

In the past decade, half-sandwich Ru(II) organometallic complexes have received considerable interest as anticancer agents[125]. In the quest of compounds presenting both therapeutic and imaging properties/trackable therapeutic agents, the Ru(II)-arene moiety was coupled with various organic fluorophores/optical probes like anthracene[126], pyrene[127], naphthalimide[87], coumarin[86, 128], rhodamine[129], BODIPYs[83], or porphyrin[130]. For various dyes, despite the good commercial availability and relatively simple chemistry for their attachment to metal complexes, their photophysical properties are not always suitable for bioimaging purposes. Moreover, after coupling the metal-drug with the fluorophore, the emission of the final complexes could be quenched either through a photoinduced electron transfer or by de-excitation of the triplet excited state[128]. Various studies have shown that heavy metals can quench the fluorescence by enhancing non-radiative decay channels. For example, previously developed trithiolato-bridged diruthenium conjugates tagged with the coumarin fluorophores[131] showed interesting anti-*Toxoplasma* properties, but also almost complete fluorescence quenching.

Among the rich library of potential fluorescent dyes currently available, BODIPYs (boron dipyrromethene, 4,4-difluoro-4-bora-3*a*,4*a*-diaza-*s*-indacene) are between the most attractive. Their optical properties can be tuned/modulated *via* chemical modifications[132], and generally, they are highly soluble in common organic solvents with characteristics mostly independent of solvent polarity, and are chemically inert (stable in physiological pH-range, only decomposing in strong acidic and basic conditions[133, 134]). BODIPYs display, high photostability, small Stokes shifts, high fluorescence quantum yields, neutral charge, and sharp absorption and emission bands[135-137]. Since BODIPY derivatives are also non toxic[138, 139], they are especially useful for cell imaging studies and as biological probes[135, 140].

Other properties of the BODIPY fluorophores were also exploited – as the generation of singlet oxygen on light activation for photodynamic therapy / photo cytotoxicity singlet oxygen as the reactive oxygen species (ROS)[124, 141-143].

Interestingly, BODIPY analogues have been used for the study of lipid metabolism in parasites as *Toxoplasma gondii*[144-148].

If BODIPY derivatives showed generally reduced activity in cellular experiments, nevertheless the presence of the fluorophore may significantly alter the physicochemical properties and can influence the mode of action of the conjugates, modifying/redirecting their intracellular localization. Thus, it is not always clear whether the tagged derivatives are an appropriate model for studying the cellular behaviour of the metal-based drugs. For instance, reported platinum-fluorophore complexes have not reported significant nuclear localization[149],[150]. For example, various platinum complexes presenting BODIPY fluorophores appended on ligands exhibited preferential mitochondrial distribution/accumulation[141, 142, 151].

Several examples of biologically active metal-based compounds tethered with BODIPY dyes have been reported in the literature to date[152] and this type of complexes were recently reviewed[81, 119, 153]. Various platinum[123, 141], ruthenium[83], osmium[83], iridium[154], gold[155], titanium[156] and copper[157] complexes with BODIPY appendices at the level of the ligands have been identified as potential bioactive trackable fluorescent agents/probes. Some examples of different metallodrugs tethered with BODIPY dyes and their reported physico-chemical properties are presented in Figure 1.2.1.

The clinically used platinum(II) drugs cisplatin, carboplatin, and oxaliplatin have been extensively studied in the laboratory setting, sometimes by generating fluorophore-tagged analogues for imaging. An interesting case is that of the BODIPY (1,3,5,7-tetramethyl-8-(4-pyridyl)-4,4′-difluoroboradiazaindacene) labelled platinum compound **1.2.A**[158] (Figure 1) which showed high cellular proliferation inhibition against various cancer cell lines. The complexation of the platinum led to fluorescence quantum yield decrease, which was ascribed to the oxidative photoinduced electron transfer (PET) from the excited core of BODIPY to the pyridyl group[159, 160]. The subcellular localization of compound **1.2.A** and its corresponding BODIPY ligand in cancer cells was studied using confocal laser scanning microscopy. However, neither the platinum complex nor the ligand were observed in the nuclei, and the fluorescence intensity of the complex was higher than that of the ligand, paralleling a significantly enhanced cellular uptake of the complex *vs* the free ligand. **1.2.A** showed a distinct mitochondrial distribution in cancer cells, which was confirmed by monitoring colocalization with MitoTracker Red (mitochondria-specific dye) and its cellular uptake is sensitive to the mitochondrial membrane potential.

Similarly, confocal microscopy of the monofunctional platinum(II) complex **1.2.B** (*cis*-[Pt(NH_3)$_2$(L)Cl](NO_3), where L is an imidazole base conjugated to 4,4-difluoro-4-bora-3a,4a-diaza-s-indacene (BODIPY)) also showed significant mitochondrial localization of the complex[124].

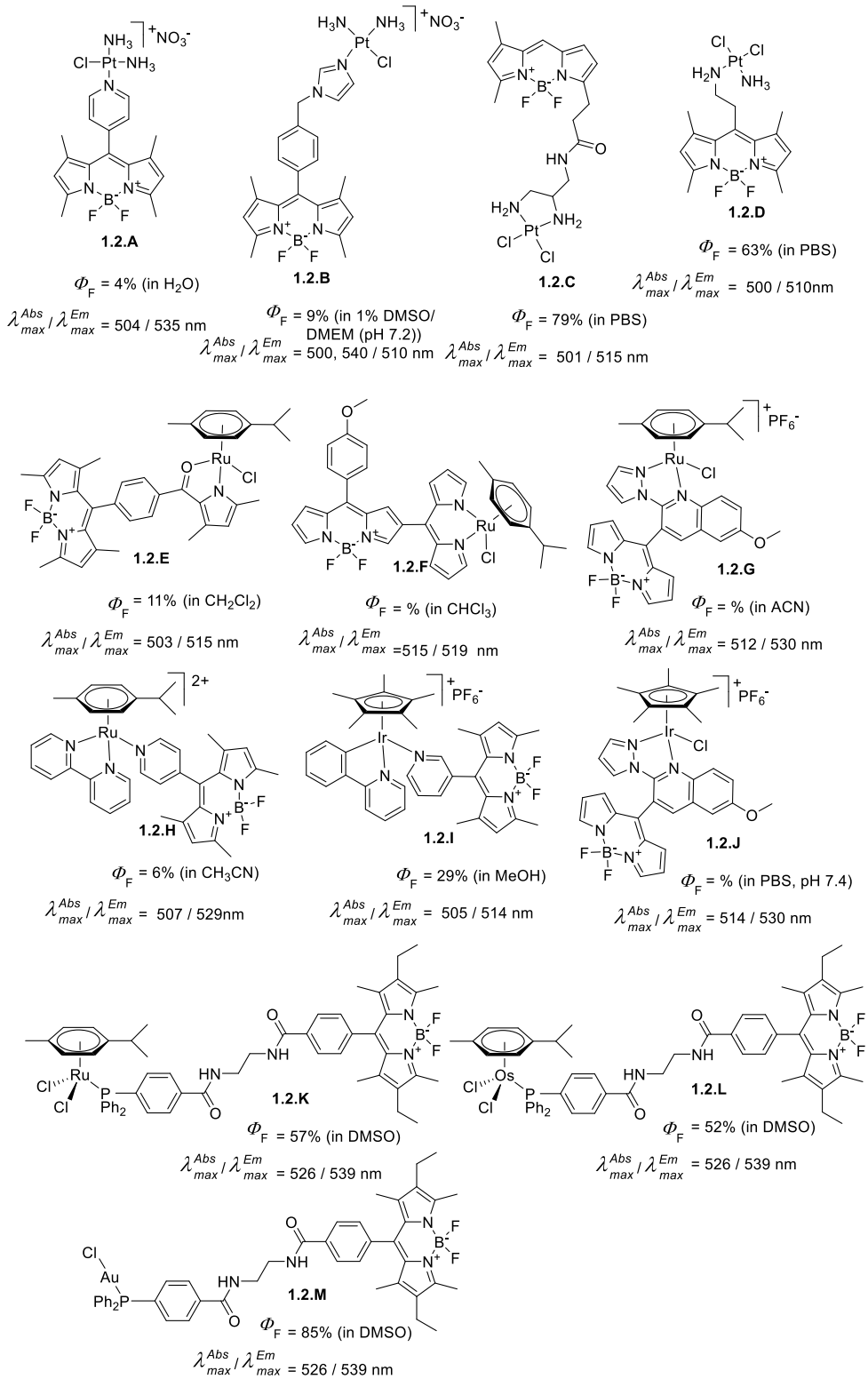

Figure 1.2.1. Structure and physico-chemical properties of reported metal-complex - BODIPY conjugates.

4,4-Difluoro-5,7-dimethyl-4-bora-3a,4a-daiza-*s*-indacene (BODIPY) was conjugated to various Pt(II) complexes to generate derivatives like **1.2.C**[123, 151] and **1.2.D**[151] with robust *in vivo* fluorescence and retained DNA-damaging and cytotoxic properties. Some compounds were successfully applied to image pharmacokinetics and tumour uptake in a xenograft cancer mouse model[151]. The *in vitro* cellular uptake and distribution of compounds **1.2.C** and **1.2.D** was characterized. For **1.2.C** microscopy revealed a predominately cytosolic/perinuclear localization, with nuclear distribution at higher concentrations[123]. Similarly, **1.2.D** localized in the cytoplasm near the nucleus[151].

Both the nature of the ligand and that of the coordinated metal centre can strongly influence the photophysical properties of the conjugates. Along with platinum-based BODIPY complexes[124, 151, 158], half-sandwich ruthenium, iridium, or rhodium BODIPY conjugates have been studied for mitochondrial imaging experiments.[85]

A N,O-based BODIPY ligand was used to develop highly fluorescent and photostable Ru(II), Rh(III), and Ir(III) metal complexes as **1.2.E**[85] in Figure 1.2.1. The compounds exhibited negligible cytotoxicity at a concentration used for imaging purposes. The live cell imaging capabilities of the complexes were investigated *via* confocal microscopy, revealing that the compounds localized specifically in the mitochondria. Coordination to the metal centre led to fluorescence quenching, and some variations of the quantum yields were observed with increase in solvent polarity.

The quantum yield of BODIPY complex **1.2.F** was almost comparable to that of the corresponding BODIPY ligand[161] which indicated that the presence of heavy Ru(II) ions did not significantly quench the fluorescence of the BODIPY unit in this compound. However, absorption and fluorescence studies of compound **1.2.F** and its corresponding ligand indicated that the presence of the Ru(II)-dipyrrin moiety at the b-position of BODIPY alters the electronic properties of the BODIPY unit significantly.

Incorporation of arene Ru(II) units at a suitable position within BODIPY chromophores may improve water solubility of the dyes and also facilitate an inter-system-crossing (ISC) process which in turn increases the reactive oxygen species (ROS) generation ability. Moreover, PDT performances of the photosensitizers could be enhanced *via* a potential synergistic effect, by a combination of the cytotoxic arene ruthenium moiety

with the fluorescent BODIPY chromophores in the same molecule. Thus a series of ruthenium(II)-arene complexes bearing BODIPY functionalized ligands as for examples as for example **1.2.G** [Ru(η^6-*p*-cymene)(L2)Cl]PF_6 involving 5-[6-methoxy-2-(1*H*-pyrazol-1-yl)quinoline]-BODIPY (L) as ligand[162] behave as a potential 'theranostic' agent, exhibiting high photo-cytotoxicity under visible light on cancer cells, while being less toxic in the dark. **1.2.G** preferentially accumulated in the cancer cells lysosome.

BODIPY–Ru(II) arene dyads as **1.2.H** in Figure 1.2.1 were also shown to effectively enable photo-inactivation against cancer cells[152, 163]. The photochemical properties of the BODIPY-containing Ru(II)-arene complex **1.2.H** [(η^6-*p*-cymene)Ru(bpy)(py-BODIPY)]$(PF_6)_2$, where *p*-cymene is $MeC_6H_4Pr^i$, bpy is 2,2′-bipyridine and py-BODIPY is a 4,4-difluoro-4-bora-3a,4a-diaza-*s*-indacene dye containing a pyridine group at the 8-position, were investigated[152]. If the Ru(II)-arene unit coordination was followed by an important fluorescence quenching, complex **1.2.H** showed however strong luminescence centred at 538 nm in CH_3CN, which should originate from the fluorescence of the coordinated-BODIPY ligand.

Another interesting case is that of **1.2.I**, a cyclometalated half-sandwich iridium(III) complex with the general formula [(η^5-Cp*)Ir(ppy)L]PF6 where η^5-Cp* = pentamethylcyclopentadienyl and ppy = 2-phenyl-pyridine as C∧N-chelating ligand and L = 3-pyridyl-BODIPY (BODIPY = 4,4-difluoro-4-bora-3a,4a-diaza-s-indacene dye containing a 3-pyridylgroup at the *meso* position) (Figure 1.2.1)[164]. The introduction of the pyridyl-BODIPY ligand increased the lipophilicity of the complex and slowed down the hydrolysis rate, which in turn increased the cytotoxicity of the metallodrug candidate. The photophysical properties of the dyad were investigated and compared to the pyridyl-BODIPY precursor. Complex **1.2.I** exhibited a typical fluorescence emission band, identical to the free *meso*-pyridyl-BODIPY ligand, and in spite of a partial quenching noticed upon complexation of the organometallic entity, **1.2.I** showed a rather high quantum yield. This effect was explained by intramolecular photoinduced electron transfer (PET) from *meso*-pyridyl-BODIPY to the [(*p*-cym)Ru(N∧N)] moiety[152, 163]. Cell uptake of the dyad **1.2.I** and corresponding BODIPY ligand was monitored by living cell fluorescence imaging. Fluorescence emission was detected indistinctly in most cells exposed to **1.2.I** and 3-pyridyl-BODIPY as large diffuse zones and small bright spots in the cytoplasm. The experiment gave strong evidence that both compounds were membrane permeant and accumulated in cells. The amount of **1.2.I** accumulated in cells is higher than the amount of the corresponding ligand N3-py-BODIPY. Cell internalization was very

rapid and energy-dependent transport processes might be involved in cell uptake of compound **1.2.I**.

The same ligand as in ruthenium(II) complex **1.2.G** (a pyrazole-appended quinoline-based 4,4-difluoro-4-bora-3a,4adiaza-s-indacene, L) has been used for the preparation of iridium(III) complex **1.2.J** [(η^5-C_5Me_5)Ir(L)Cl]PF_6[165]. Complex **1.2.J** exhibited medium cytotoxicity towards cancer cells and showed a preference for accumulation in cell membranes without reaching the nuclei. Moreover, in this case apparently solely the BODIPY moiety determined the cellular uptake.

One interesting example is that of a BODIPY–phosphane ligand which proved to be a versatile tool for imaging organometallic complexes[83], and led to a new family of theranostics, featuring ruthenium, osmium and gold. The compounds' cytotoxicity was tested on cancer cells, and their cell uptake was followed by fluorescence microscopy *in vitro*. The fluorescence was not affected upon coordination to Au(I) (complex **1.2.M**, Figure 1.2.1) but was moderately quenched in the Ru(II) and Os(II) cases (complexes **1.2.K** and **1.2.L**, respectively, Figure 1.2.1), which are prone to photoinduced electron transfer[166], as well as to promote BODIPY phosphorescence[167]. Nonetheless, **1.2.K** and **1.2.L**'s quantum yields remain relatively high to consider their potential use as fluorescent probes. The detection of the BODIPY-phosphane complexes **1.2.K**-**1.2.M** and of the corresponding ligand in living cells by fluorescence microscopy was also performed. The in vitro imaging showed that the compounds rapidly bind to the biological membranes, with no clear specificity. Moreover, no difference was noted between the BODIPY–phosphane ligand and its metal derivatives implying that the uptake and distribution properties of the compounds are mainly determined by the BODIPY moiety. The staining and fluorescence properties were shown to be independent of the active transport mechanisms.

Previous studies have shown that trithiolato-bridged compounds are highly stable and prone to further derivatisation using 'chemistry on the complex'. Conjugates can be obtained by anchoring the molecule of interest on one of the bridge thiols, a strategy that proved successful in previous studies. Thus, various conjugates with peptides[60], the anticancer drug chlorambucil[61], the coumarin fluorophore[131] were recently synthesized and assessed for their anticancer or antiparasitic properties.

This study challenged the obtainment of new conjugates BODIPY (borondipyrromethene)-trithiolato-bridged diruthenium(II)-arene units as potential metallodrug antiparasitic tracking agents. The fluorophore should be tethered to the metal

framework while retaining the structural-activity requirements of the organometallic moiety.

Aiming not only to identify compounds that can be used as fluorescent 'tracers' but also to understand the parameters that can influence the photophysical properties as well as the cytotoxicity/antiparasitic activity of this type of dyads, different structural elements as: i) the type of the bond between the two units (ester *vs* amide), ii) the length of the linker, and iii) the nature of the BODIPY dye (with an aliphatic or an aromatic substituent in *meso*-position), were varied. The photophysical properties of the new conjugates as well as those of the corresponding free dyes were studied. The antiparasitic activity of the compounds was assessed against the apicomplexan parasite *T. gondii* and the cytotoxicity of the compounds was determined on HFF. Representative derivatives were also submitted to TEM and confocal microscopy studies to gain more insight on the compounds' potential targets and intracellular localization.

1.2.2. Results and Discussion

1.2.2.1. Chemistry

Three mixed trithiolato diruthenium(II)-arene derivatives bearing functionalizable groups like OH (**1.2.2**), NH_2 (**1.2.3**) and CO_2H (**1.2.4**) (same as **1.1.2a**, **1.1.3a** and **1.1.4a** respectively) were synthesized following previously reported protocols[30, 62, 131]. A two-step procedure was employed (Scheme 1.2.1). The symmetric dithiolato intermediate **1.2.1** (same as **1.1.1a**) was obtained by the reaction of the ruthenium dimer [Ru(η^6-*p*-$MeC_6H_4Pr^i$)Cl]$_2$Cl$_2$[168] with two equivalents of 4-*tert*-butylbenzenemethanethiol and was isolated in good yield (91%). In a second step, a third bridge thiol was introduced between the two Ru(II)-arene units following previously described procedures[53, 131]. Thus, complexes **1.2.2** and **1.2.3** were synthesized by reacting dithiolato intermediate **1.2.1** with 4-mercaptophenol and respectively 4-aminobenzenethiol in refluxing EtOH. For the obtainment of carboxy analogue **1.2.4** using 2-(4-mercaptophenyl)acetic acid as the third thiol, a mixture of CH_2Cl_2/$(CH_3)_2CO$ was used as solvent to avoid the esterification side reaction catalysed by the HCl produced in the reaction.

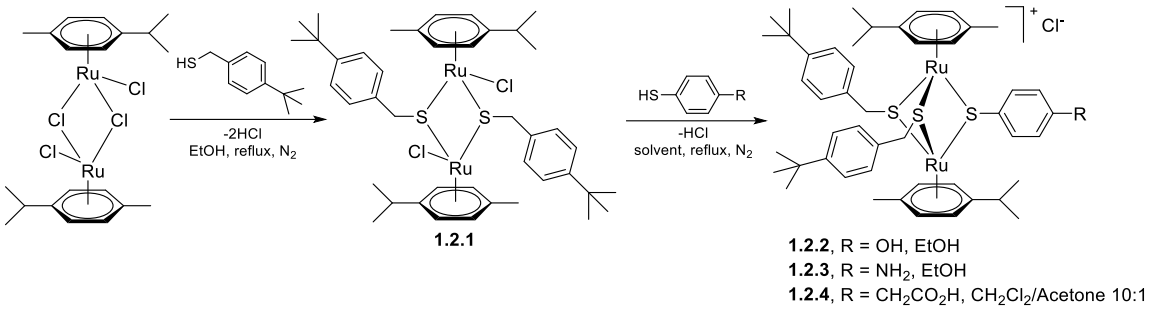

Scheme 1.2.1. Synthesis of the dinuclear dithiolato **1.2.1** and OH, NH_2, CH_2CO_2H functionalized trithiolato ruthenium(II)-arene intermediates **1.2.2**, **1.2.3** and **1.2.4**.

The synthetic approaches to the borondipyrromethene core are based on chemistry well known from porphyrin research[169]. A first library of carboxy-functionalized *meso*-BODIPY compounds **1.2.8**-**1.2.10** was synthesized[170-173] presenting chains of various length between the fluorophore and the CO_2H group. The fluorophores were obtained by the condensation of 3-ethyl-2,4-dimethylpyrrole with four commercially available acid chlorides as acylium equivalent: methyl 4-chloro-4-oxobutyrate, methyl 6-chloro-6-oxohexanoate, methyl 8-chloro-8-oxooctanoate and methyl 10-chloro-10-oxodecanoate) (Scheme 1.2.2)[170]. The intermediate acylpyrroles were not isolated, and application of an excess of base (DIPEA, *N*,*N*-diisopropylethylamine) and boron trifluoride etherate ($BF_3 \cdot Et_2O$) yielded the methyl protected BODIPY dyes **1.2.5**-**1.2.8** (32-52%)[170]. In a second step the esters **1.2.5**-**1.2.8** were hydrolysed in basic conditions (KOH in Pr^i-OH) leading to the isolation of the BODIPY carboxy analogues in **1.2.9**-**1.2.12** in medium yield (45-quant.%, Scheme 1.2.2)[171-173].

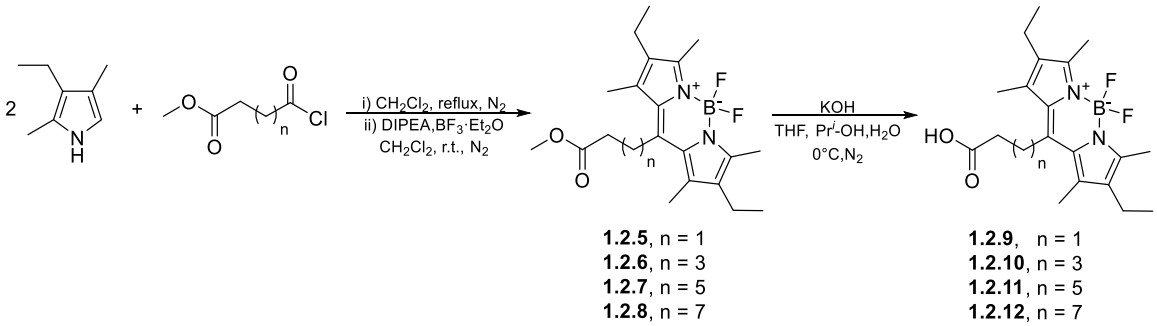

Scheme 1.2.2. Synthesis of the BODIPY precursors containing a carboxy group **1.2.9**-**1.2.12**.

Carboxy fluorophores **1.2.9**-**1.2.12** were then reacted with the diruthenium hydroxy and amine derivatives **1.2.2** and **1.2.3** leading to the obtainment of the ester derivatives **1.2.19**-**1.2.22**, and respectively, amide dyads **1.2.23**-**1.2.26** (Scheme 1.2.3).

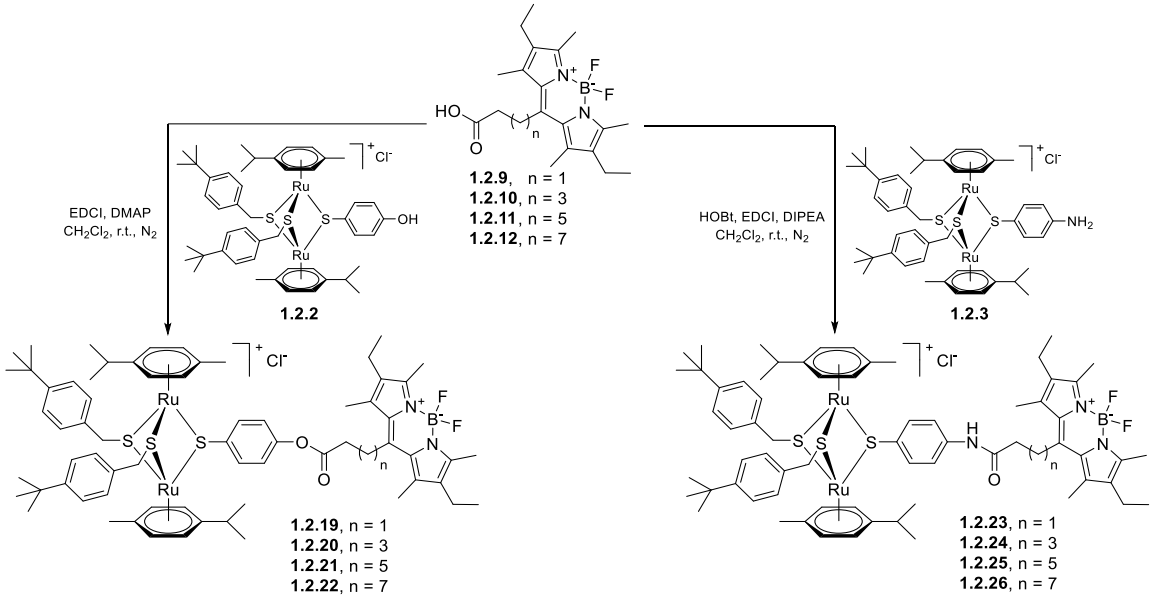

Scheme 1.2.3. Synthesis of the ester **1.2.19**-**1.2.22** (left) and amide **1.2.23**-**1.2.26** (right) conjugates BODIPY-dinuclear trithiolato ruthenium(II)-arene complexes containing alkyl spacers of various lengths.

In the first case, EDCI (*N*-(3-dimethylaminopropyl)-*N′*-ethylcarbodiimide hydrochloride) was used as coupling agents and DMAP (*N*,*N*-dimethylpyridin-4-amine) as base[174] and the esters dyads **1.2.19**-**1.2.22** were isolated in 12-93 % yield. In the parallel series of amide analogues, the reaction took place in the presence of EDCI and HOBt (1-hydroxybenzotriazole) as coupling agents and of DIPEA as basic catalyst[175], and the conjugates **1.2.23**-**1.2.26** were isolated with 22-74% yield.

Assessing the influence of the functional group present on the fluorophore upon the photophysical properties of the BODIPY-trithiolato-diruthenium conjugates was also aimed. The type of bonding between the two units was maintained as ester or amide, but the diruthenium arene **1.2.5** functionalized with a carboxy group was used as reagent. One hydroxy (**1.2.14**) and two amino-functionalized (**1.2.17** and **1.2.18**) *meso*-substituted BODIPY compounds with short alkyl spacers were synthesized following the reactions presented in Scheme 1.2.4.

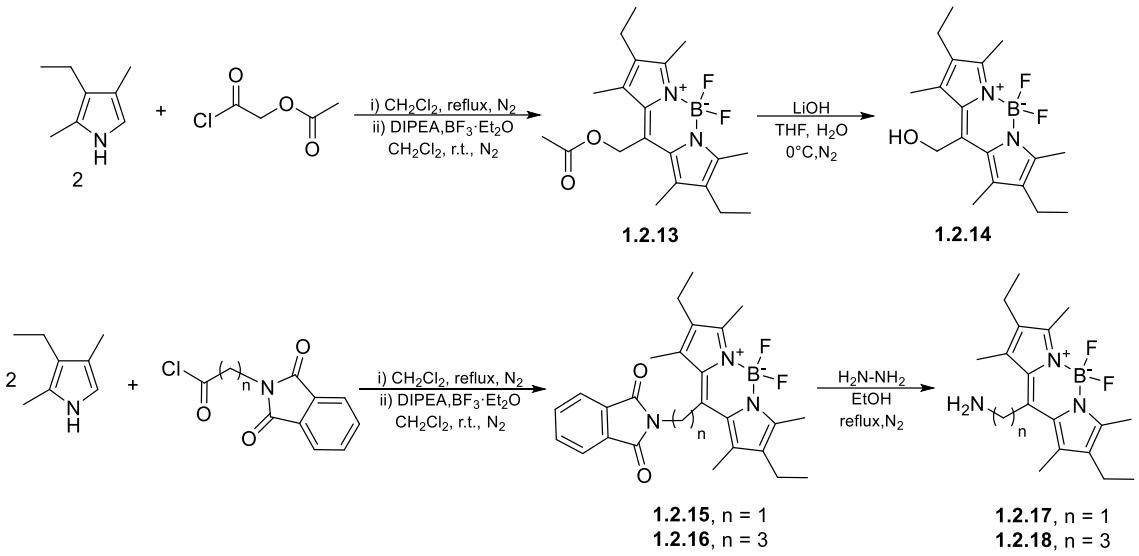

Scheme 1.2.4. Synthesis of the BODIPY intermediates containing a hydroxy group **1.2.14** (top) and an amino group **1.2.17** and **1.2.18** (bottom).

Hydroxy BODIPY compound **1.2.14** was obtained following a two-step procedure presented in Scheme 1.2.4 (top) using reported protocols[170]. In the first step, acetyl protected intermediate **1.2.13** was obtained by the reaction of 3-ethyl-2,4-dimethylpyrrole with commercially available 2-chloro-2-oxoethyl acetate as acylium equivalent. Addition of an excess of base (DIPEA) to the intermediate acylpyrrole formed *in situ*, followed by application of boron trifluoride etherate ($BF_3{\cdot}Et_2O$) yielded the BODIPY dye **1.2.13** (35%). Ester hydrolysis in basic conditions (LiOH) released the hydroxy BODIPY **1.2.14**, isolated in 43% yield.

The amino BODIPY analogues **1.2.17** and **1.2.18** were obtained following the reaction pathway presented in Scheme 1.2.4 (bottom) using previously described procedures[176, 177]. First, 3-ethyl-2,4-dimethylpyrrole was reacted with amino phthalimide protected derivatives 1,3-dioxo-2-isoindolineacetyl chloride and 1,3-dioxo-2-isoindolinebutanoyl chloride as acylium equivalents, leading to intermediates **1.2.15** and **1.2.16** isolated with 44 and 26% yield, respectively. In a second step the phthalimide group in compounds **1.2.15** and **1.2.16** was deprotected using hydrazine in refluxing EtOH[176], and the BODIPY amino alkyl derivatives **1.2.17** and **1.2.18** were isolated in 25 and 18% yield. The BODIPY hydroxy **1.2.14** and the amino **1.2.17** and **1.2.18** derivatives were further reacted with diruthenium complex **1.2.4** functionalized with a carboxy group on one of the bridge thiols, using the reaction conditions presented in Scheme 1.2.5.

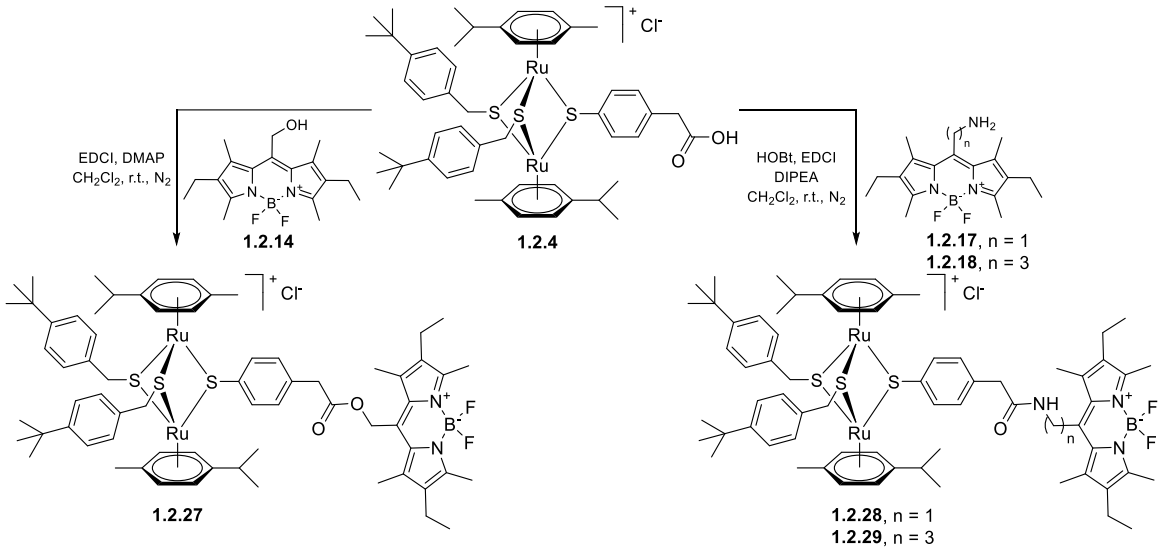

Scheme 1.2.5. Synthesis of the ester (left) and amide (right) conjugates BODIPY-dinuclear trithiolato ruthenium(II)-arene complexes **1.2.27**, **1.2.28** and **1.2.29** containing short alkyl spacers.

Ester conjugate **1.2.27** was obtained using EDCI as coupling agent and DMAP as base and was isolated in 35% yield. Amide dyads **1.2.28** and **1.2.29** were obtained in the presence of EDCI and HOBt as coupling agents and DIPEA as base and were isolated both in 52% yield.

Aiming for improved photophysical properties, the use of structurally different BODIPY dyes was also considered[137]. Derivatives presenting an additional aromatic unit in the *meso*-position were largely studied and represent and interesting option[119, 178, 179].

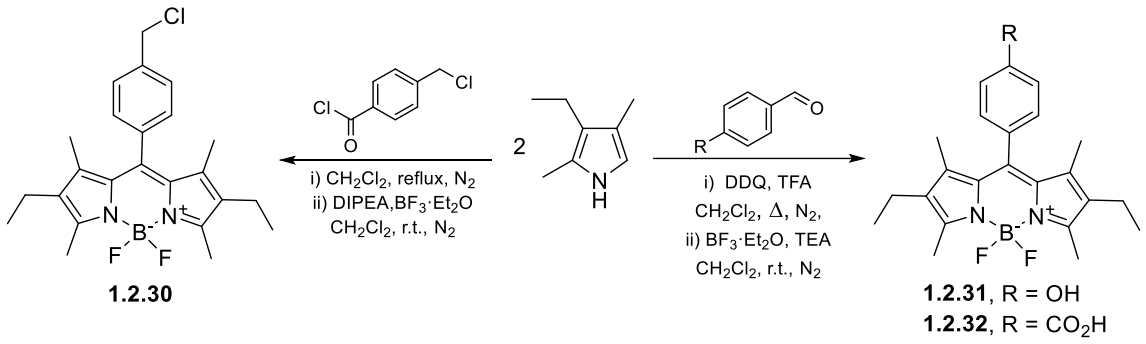

Scheme 1.2.6. Synthesis of the *meso*-arene BODIPY dyes **1.2.30**, **1.2.31** and **1.2.32** functionalized with chloromethylene, hydroxy and carboxy groups, respectively.

BODIPY derivative **1.2.30**, presenting a chlorine atom in benzylic position, was synthesized by reacting 3-ethyl-2,4-dimethylpyrrole with 4-(chloromethyl)benzoyl chloride as acylium equivalent. Addition of an excess of base (DIPEA) to the intermediate

acylpyrrole formed *in situ*, followed by application of boron trifluoride etherate ($BF_3 \cdot Et_2O$) led to the BODIPY dye **1.2.30** isolated in 85% yield.

The catalysed condensation of pyrrole derivatives with aromatic aldehydes, followed by oxidation and complexation is a largely used method for the obtainment of *meso*-aryl BODIPY fluorophores,[180, 181] which led to abundant use of the *meso* aryl group as a synthetic handle for the introduction of various functional groups.[179] The acid (TFA, trifluoroacetic acid) catalysed condensation of 4-hydroxybenzaldehyde and 4-carboxybenzaldehyde with 3-ethyl-2,4-dimethylpyrrole (Scheme 1.2.6) afforded corresponding dipyrromethane intermediates which were not isolated, but were further oxidated with DDQ (2,3-dichloro-5,6-dicyano-*p*-benzoquinone) to yield dipyrrin structures. The dipyrrins were further subjecting to base (TEA, triethylamine) and boron trifluoride etherate ($BF_3 \cdot Et_2O$) affording the boron difluoride complexes **1.2.31** and **1.2.32** in medium yield of 28 and 25%, respectively (Scheme 1.2.6).

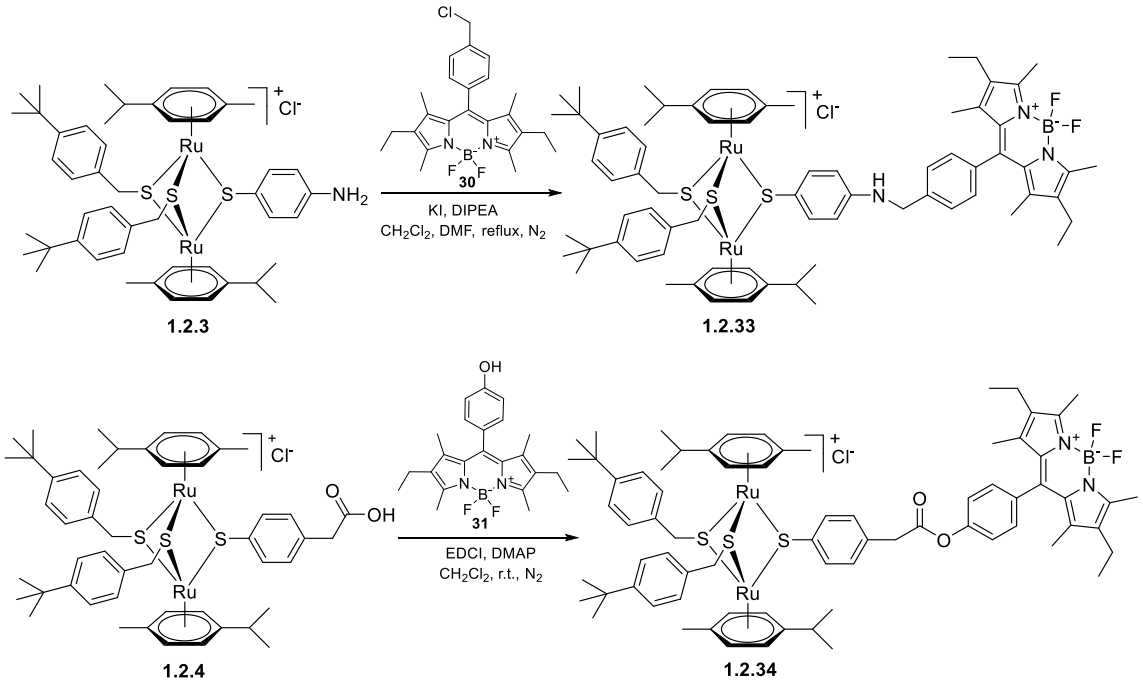

Scheme 1.2.7. Synthesis of the amine (top) and ester (bottom) conjugates BODIPY-dinuclear trithiolato ruthenium(II)-arene conjugates **1.2.33** and **1.2.34** containing aryl handles.

Nucleophilic substitution of the chlorine atom in intermediate **1.2.30** with the diruthenium amino derivative **1.2.3** in the presence of KI as activator, in basic conditions (DIPEA) (Scheme 1.2.7), allowed the obtainment of the BODIPY amino conjugate **1.2.33** isolated in 50% yield.

Hydroxy functionalized BODIPY derivative **1.2.31** was further reacted with diruthenium carboxy compound **1.2.4** using EDCI as coupling agent and DMAP as basic catalyst, to obtain ester conjugate **1.2.34** isolated in 30% yield.

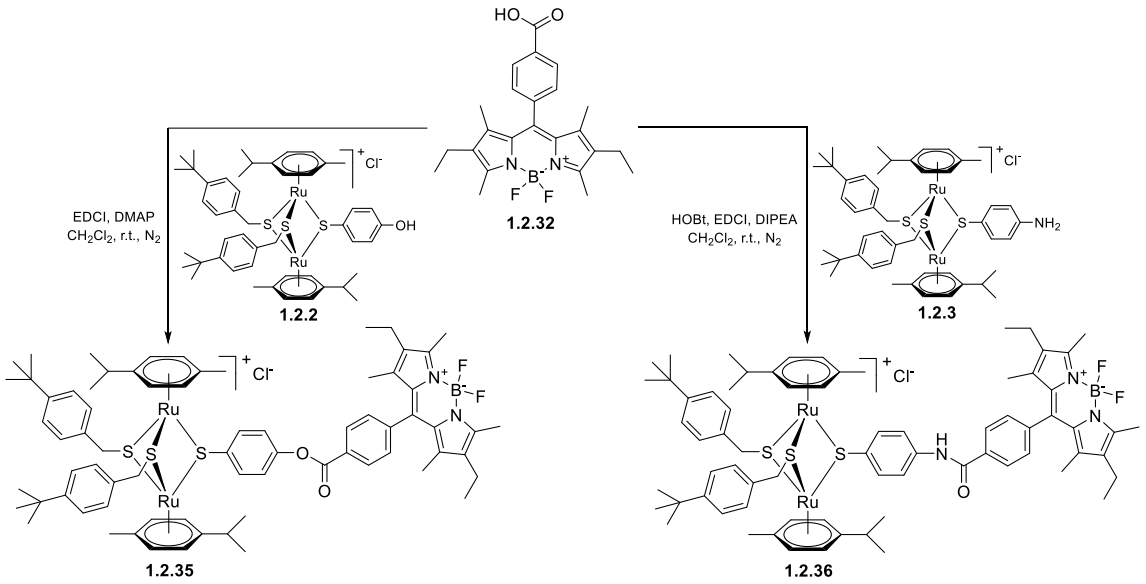

Scheme 1.2.8. Synthesis of the ester (left) and amide (right) dyads BODIPY-dinuclear trithiolato ruthenium(II)-arene complexes **1.2.35** and **1.2.36** containing aryl connectors.

Carboxy *meso*-aryl BODIPY dye **1.2.32** was reacted with the diruthenium hydroxy and amine intermediates **1.2.2** and **1.2.3** leading to the obtainment of the ester **1.2.35** and, respectively, amide **1.2.36** conjugates (Scheme 1.2.8). In the first case, the reaction was run in the presence of EDCI as coupling agent and DMAP as basic catalyst and the ester dyad **1.2.35** was isolated in 25% yield. The synthesis of the amide analogue **1.2.36** took place in the presence of EDCI and HOBt as coupling agents and of DIPEA as basic catalyst, and the conjugate was isolated with 56% yield.

All compounds were fully characterized by ^{1}H, ^{13}C and, where suitable, ^{19}F and ^{11}B nuclear magnetic resonance (NMR) spectroscopy, high resolution electrospray ionization mass spectrometry (HR ESI-MS) and elemental analysis (see the Experimental Section Chemistry in *Supporting Information 1.2.* for full details). Mass spectrometry corroborated the spectroscopic data with the trithiolato diruthenium conjugates **1.2.19**-**1.2.29** and **1.2.33**-**1.2.36** exhibiting molecular ion peaks corresponding to $[M\text{-}Cl]^{+}$ ions.

For the assessment of the biological activity, the compounds were prepared as stock solutions in dimethylsulfoxide (DMSO), a solvent in which the compounds present very good solubility. Similarly to previous reports[30, 62, 131], ^{1}H-NMR spectra of conjugates

1.2.2-1.2.4, **1.2.15-1.2.21** dissolved in DMSO-d_6, recorded at 25°C 5 min and more than 1 month after sample preparation showed no visible changes (see Figures S1.2.5-S1.2.7 in the *Supporting Information 1.2.*), demonstrating very good stability of the compounds in this highly complexing solvent.

1.2.2.2. X-ray Crystallography

The crystal structures of intermediates **1.2.16** and **1.2.30** were established in the solid state by single-crystal X-ray diffraction (ORTEP representation are shown in Figure 1.2.2, see *Supporting Information 1.2* for full experimental details and more related information), confirming the expected structure. Data collection and refinement parameters are given in Table S1.2.1, while selected structural parameters are presented in Table 1.2.2.

Slow evaporation of solutions of **1.2.16** and, respectively, **1.2.30** in $CHCl_3$ afforded pink-violet single crystals suitable for X-ray diffraction. The crystallographic data revealed that **1.2.16** crystallizes in the triclinic system, space group P-1, while **1.2.30** crystallizes in the monoclinic system, space group $P2_1/n$. In both structures, the central six-membered ring of the BODIPY moiety is almost coplanar with the adjacent pyrrole rings, with a π-electron delocalization in the BODIPY core, as often observed for this class of fluorophores[182-185]. The two B–N distances are similar, indicating the expected delocalization of the positive charge. For N1–C1 and N2–C9 the measured bond lengths indicate a pronounced double bond character.

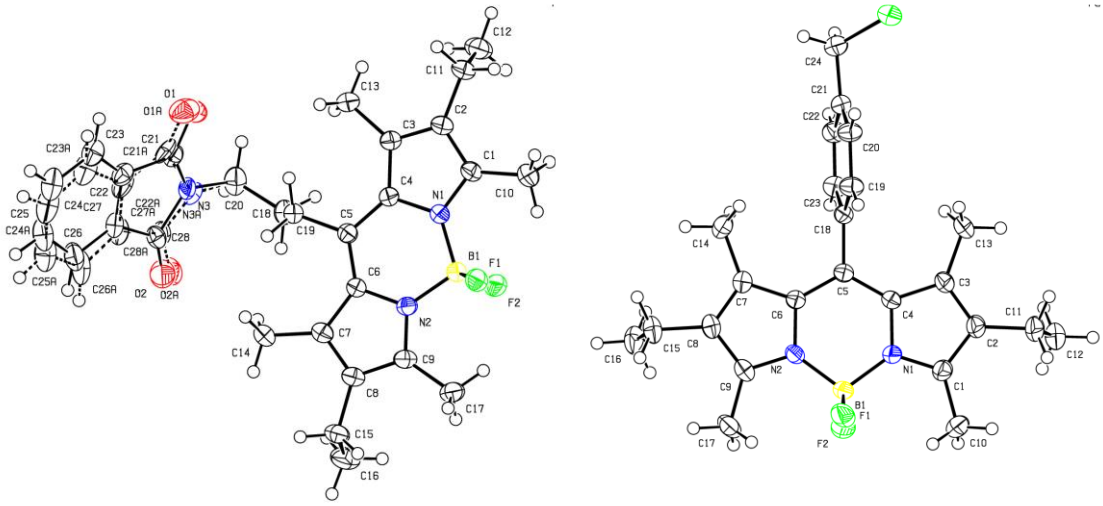

1.2.16 **1.2.30**

Figure 1.2.2. ORTEP representation of BODIPY intermediates **1.2.16** (**OD67-18**) and **1.2.30 (OD13-19)** (thermals ellipsoids are shown with 50% probability).

Table 1.2.1. Selected structural parameters for the crystal structures of **1.2.16** (**OD 67-18**)**(19JF004C2)** and **1.2.30** (**OD13-19**)**(19JF004C2)**.

Compound	**B–N (Å)**	**B–F (Å)**	**N-C(CH_3) (Å)**	**N–B–N (°)**	**F–B–F (°)**
1.2.16	N_1-B_1 1.5396(18) N_2-B_1 1.5399(18)	F_1-B_1 1.3947(17) F_2-B_1 1.3918(17)	N_1-C_1 1.3534(16) N_2-C_9 1.3456(16)	N_1-B_1-N_2 107.11(11)	F_2-B_1-F_1 108.47(11)
1.2.30	N_1-B_1 1.5472(19) N_2-B_1 1.543(2)	F_1-B_1 1.391(2) F_2-B_1 1.385(2)	N_1-C_1 1.3471(19) N_2-C_9 1.3505(18)	N_2-B_1-N1 106.87(11)	F_2-B_1-F_1 109.64(13)

1.2.2.3. Photophysical Properties

The basic photophysical properties of the compounds investigated in this study, namely the BODIPY intermediates **1.2.5-1.2.18** and **1.2.30-1.2.32**, and ester and amide conjugates BODIPY - trithiolato ruthenium(II)-arene complexes **1.2.19-1.2.29** and **1.2.33-1.2.36** are summarized in Table 1.2.2. The absorption and emission spectra of compounds **1.2.7**, **1.2.11**, **1.2.21**, **1.2.25**, **1.2.32**, **1.2.35** and **1.2.36** 10 μM solution in $CHCl_3$ are comparatively shown in Figures 1.2.3-1.2.5.

Table 1.2.2. Photophysical properties of compounds **1.2.5-1.2.36** in $CHCl_3$.

Compnd.	λ_{max}^{Abs} **(nm)**	ε **($M^{-1}cm^{-1}$)**	λ_{max}^{Em} **(nm)**	$\Delta\lambda$ **(nm)**	Φ_F **(%)**
Rhodamine 6G*	532.5	60832.8	557	24.5	75*
1.2.5	527	62440.3	543	16	79
1.2.6	524	57593.2	538	14	82
1.2.7	523	71699.1	538	15	87
1.2.8	522.5	53674.9	537	14.5	84
1.2.9	526.5	35884.7	540	13.5	77
1.2.10	523.5	24534.4	536	12.5	92
1.2.11	523	55178.2	536	13	83
1.2.12	522.5	51363.4	537	14.5	86
1.2.13	549	36932.2	569	20	72
1.2.14	544.5	55663.2	565	20.5	64
1.2.15	546, 309.5	8045.19	554	8	14
1.2.16	525	46390.0	539	14	64
1.2.17	534	56442.9	551	17	78
1.2.18	527.5	43566.5	542	14.5	63
1.2.19	529, 245	56519.5, 63901.6	543	14	11
1.2.20	524, 244.5	63619.5, 63006.0	539	15	17
1.2.21	523, 244.5	62739.9, 69086.4	538	15	14
1.2.22	522.5, 247	68351.7, 70393.6	538	15.5	18
1.2.23	524.5, 245.5	59063.5, 69777.7	540	15.5	12
1.2.24	521.5, 245	64531.5, 73078.6	536	14.5	12
1.2.25	521.5, 245	58855.7, 67572.0	536	14.5	14
1.2.26	521.5, 247.5	66142.7, 74163.7	536	14.5	18
1.2.27	536, 247.5	1598.3, 4660.3	552	16	10
1.2.28	539, 244.5	50505.5, 67274.0	556	17	5
1.2.29	521.5, 247.5	64983.9, 68330.6	537	15.5	6
1.2.30	527.5	56484.9	544	16.5	63
1.2.31	525.5	59696.8	541	15.5	74
1.2.32	528.5	48019.8	547	18.5	40
1.2.33	526.5, 247.5	65652.2, 74004.7	545	18.5	6
1.2.34	527.5, 247.5	64733.1, 67122.7	545	17.5	15
1.2.35	529.5, 247.5	38450.4, 62860.5	548	18.5	17
1.2.36	527, 247.5	60159.8, 71312.0	544	17	19

*Values taken from ref.[107]

The BODIPY ester intermediates **1.2.5-1.2.8**, in which the polar functionalizable group is separated from the dye moiety by aliphatic chains of different lengths, exhibit typical absorption and emission bands between 522-527 nm and 537-543 nm respectively, with high quantum yields (Φ_F = 77-87%). Slight hypsochromic shifts in both absorption and emission spectra can be observed after deprotection to acids **1.2.9**-**1.2.12**, with minor changes in quantum yields. Interestingly, the length of the linker chain affects both

absorption and emission wavelength, with shorter chains leading to more important bathochromic shifts. For example, compounds **1.2.13-1.2.18** absorb at 525-549 nm and emit at 539-569 nm, and exhibit quantum yields considerably lover (Φ_F = 63-78%) compared to intermediates with longer chain. Compound **1.2.15** shows extremely low quantum yield of 14%, probably due to the presence of the phthalimide group in the near vicinity to the BODIPY unit. Phenyl-*meso* compounds **1.2.30**-**1.2.32** absorb at 525-528 nm and emit at 541-547 nm. Changing the nature of the *meso* substituent from aliphatic to aromatic does not affect neither absorption nor emission of BODIPYs, but the quantum yields are significantly lower (Φ_F = 40-74%).

As shown in Figures 1.2.3-1.2.5, upon illumination at 450 nm the conjugates **1.2.19**-**1.2.29** and **1.2.33**-**1.2.36** emitted at 500-570 nm (green area) due to BODIPY chromophores. Absorption spectra of all conjugates (**1.2.19**-**1.2.29** and **1.2.33**-**1.2.36**) are similar (Figure 1.2.3-1.2.5) and correspond well to a merge of the absorption spectra of the two units (diruthenium intermediates and BODIPY dyes), with strong peaks at 200-300 nm and 450-570 nm regions. The introduction of the diruthenium moiety does not influence the absorption of the dye unit, but however it leads to an important quenching of the fluorescence irrespective to the nature of functionalizable polar group anchored on the BODIPY dye or the type of bond connecting the two units (ester *vs* amide). The less important quenching effect was observed in the case of conjugates with BODIPY dyes with aromatic rings in *meso* position (**1.2.34**-**1.2.36**) probably due to a more rigid structure. No direct correlation between the intensity of the quenching and length of the linking chain or the type of connecting bond was observed.

With the exception of compounds **1.2.11**, **1.2.12** and **1.2.22**, the other BODIPY intermediates and conjugates present rather comparable Stokes' shifts values between 13-16 nm (Table 1.2.2) similar to other reported compounds[179].

A similar but less pronounced quenching effect was observed in the case of other previously reported conjugates BODIPY – Ru(II)-arene complexes[83],[49], considered a result of the fact that this type of compounds are prone to photoinduced electron transfer[166], and that they can promote phosphorescence of the BODIPY unit[167].

A series of trithiolato-bridged dinuclear ruthenium(II)-arene coumarin analogues exhibited almost complete fluorescence quenching and could not be exploited for compounds intracellular visualization[131].

Nevertheless, in spite of the observed quenching effect, the significant emission shown by the BODIPY-diruthenium complex conjugates **1.2.18**, **1.2.22**, **1.2.26**, **1.2.35** and **1.2.36** in solution makes them potential candidates for use as tracking agents.

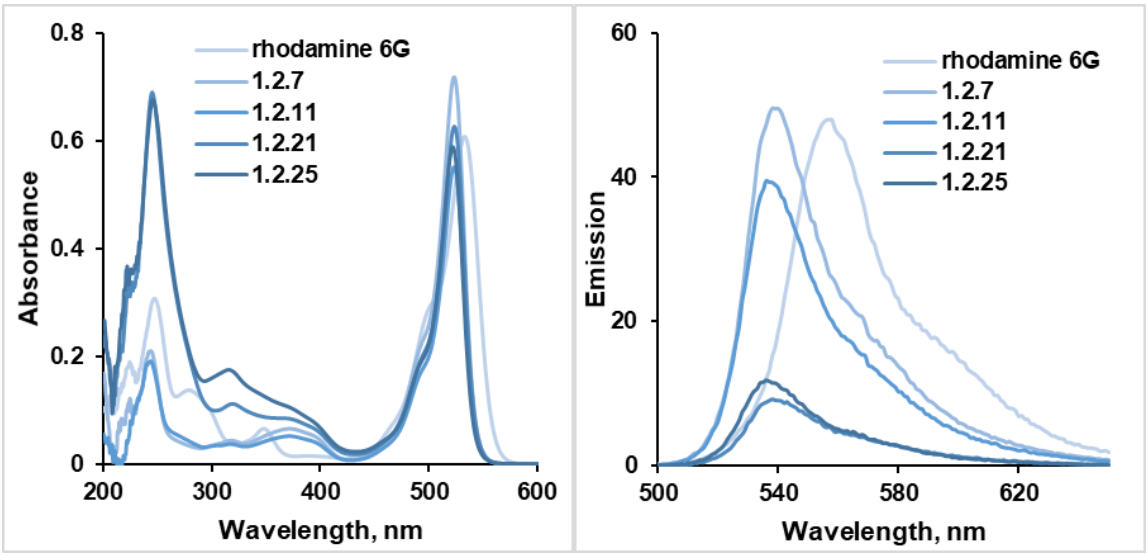

Figure 1.2.3. UV-Vis absorption (left) and emission spectra (right) of rhodamine 6G, BODIPY intermediates **1.2.5**, **1.2.11** and the corresponding ester **1.2.21** and amide **1.2.25** conjugates BODIPY - trithiolato ruthenium(II)-arene complex, at 10 µM in $CHCl_3$.

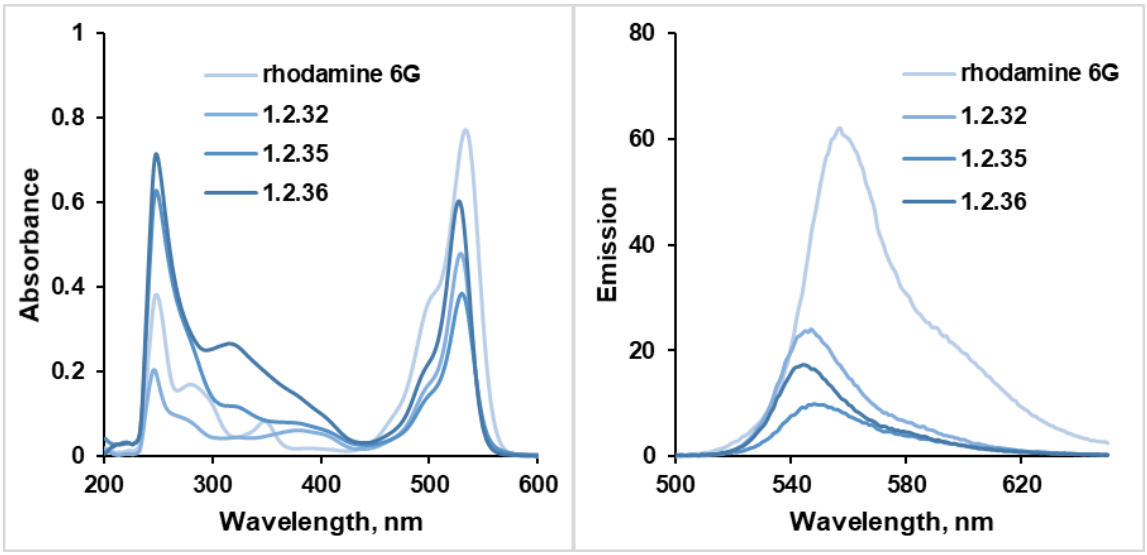

Figure 1.2.4. UV-Vis absorption (left) and emission spectra (right) of rhodamine 6G, BODIPY intermediate **1.2.32** and the corresponding ester **1.2.35** and amide **1.2.36** conjugates BODIPY - trithiolato ruthenium(II)-arene complex at 10 µM in $CHCl_3$.

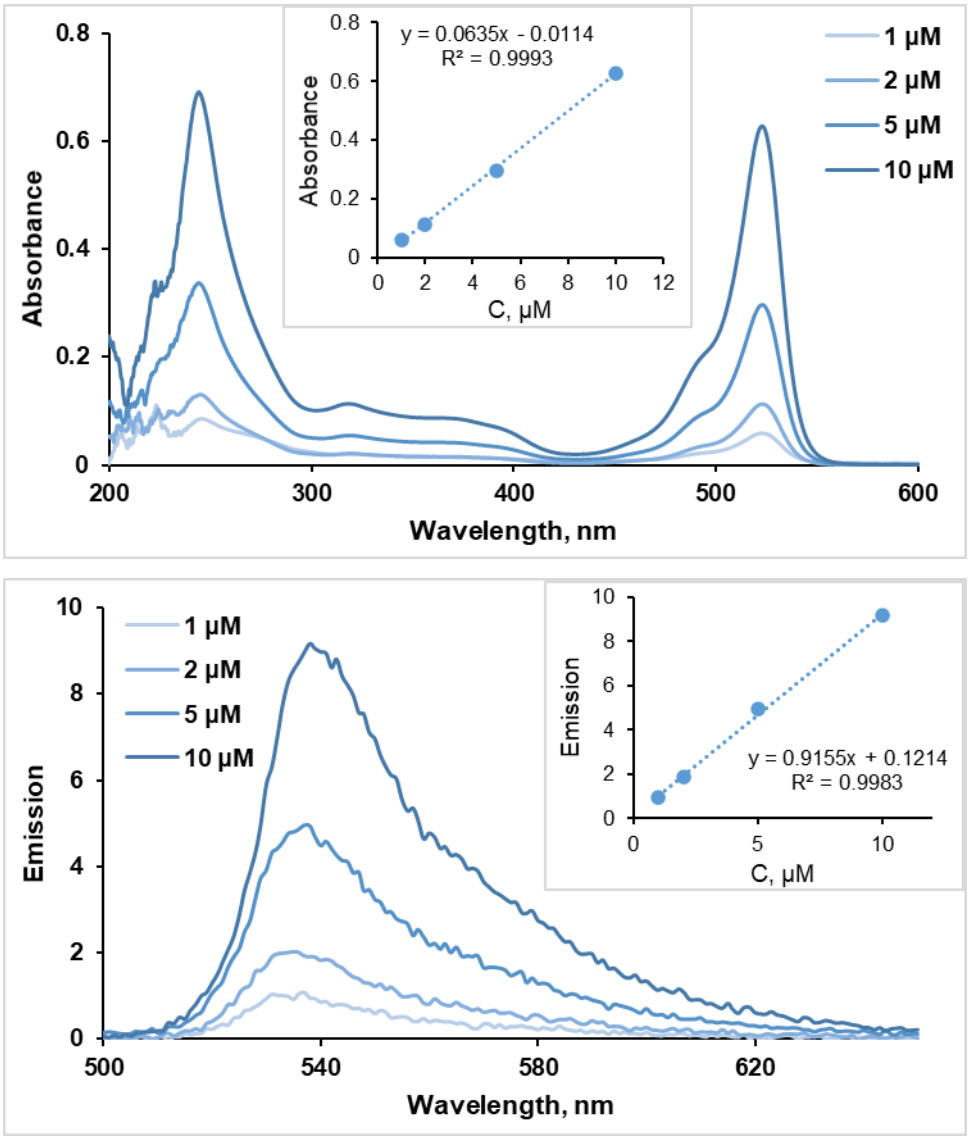

Figure 1.2.5. UV-Vis absorption (top) and emission spectra (bottom) of ester conjugate **1.2.21** BODIPY - trithiolato ruthenium(II)-arene complexes at various concentrations in $CHCl_3$.

1.2.2.4. In vitro antiparasitic activity

The compounds presented in this study were assessed for biological activity *in vitro* against *T. gondii* β-gal, a transgenic strain that constitutively expresses β-galactosidase, which is grown in HFF (human foreskin fibroblast) monolayers. In addition, the effects on non-infected HFF host cells were also screened. For a primary screening, cell cultures were exposed during 72 h to 1 and 0.1 µM of each compound of interest BODIPY-labelled conjugates **1.2.19-1.2.29** and **1.2.33-1.2.36**, free BODIPY dyes and their respective intermediates **1.2.5-1.2.18** and **1.2.30-1.2.32**. The non-modified trithiolato-bridged dinuclear ruthenium(II)-arene complexes **1.2.2-1.2.4** have been evaluated previously against *T. gondii* β-gal under similar conditions[30, 62, 131], and the corresponding values

were introduced in Table 1.2.3 and Figure 1.2.6 for comparison. The viability of HFF cultures following compound treatments was measured by alamarBlue assay, and the proliferation of *T. gondii* was quantified by measuring β-galactosidase activity. The results of this primary screening are presented as percentage in relation to untreated control cultures in Tables 1.2.3 and S1.2.1. The results obtained at concentration of 0.1 and 1 µM of tested compound for *T. gondii* and HFF are presented in Figures 1.2.6 and S1.2.1, in relation to controls (CTR), namely HFF treated with 0.1% DMSO exhibiting 100% viability, and *T. gondii* β-gal tachyzoites treated with 0.1% DMSO showing 100% proliferation.

Table 1.2.3. Primary efficacy/cytotoxicity screening of diruthenium compounds in non-infected HFF cultures and *T. gondii* β-gal tachyzoites cultured in HFFs. The compounds selected for determination of IC_{50} values against *T. gondii* β-gal are tagged with *. [a]Data for compounds **1.2.2**-**1.2.4** were previously reported [131].

Compound	HFF viability (%)		*T. gondii* β-gal growth (%)	
	0.1 µM	**1 µM**	**0.1 µM**	**1 µM**
1.2.2[a]	76 ± 6	46 ± 6	66 ± 14	2 ± 0
1.2.3[a]	74 ± 2	48 ± 1	57 ± 1	2 ± 0
1.2.4[a]	93 ± 4	87 ± 1	114 ± 15	110 ± 32
1.2.19	86 ± 11	49 ± 18	44 ± 0	2 ± 0
1.2.20	84 ± 8	60 ± 17	83 ± 0	2 ± 0
1.2.21	87 ± 6	73 ± 13	17 ± 1	5 ± 1
1.2.22	126 ± 6	90 ± 2	34 ± 0	46 ± 0
1.2.23	100 ± 0	71 ± 14	77 ± 3	151 ± 111
1.2.24	94 ± 3	80 ± 8	112 ± 20	231 ± 21
1.2.25	81 ± 27	78 ± 16	57 ± 14	286 ± 58
1.2.26	115 ± 7	104 ± 0	86 ± 15	99 ± 16
1.2.27	122 ±21	117 ± 19	10 ± 0	12 ± 3
1.2.28	183 ± 10	69 ± 20	82 ± 26	5 ± 1
1.2.29	153 ± 7	153 ± 8	104 ±1	121 ± 7
1.2.33	109 ± 3	101 ± 4	87 ± 1	40 ± 1
1.2.34	126 ± 4	129 ± 3	62 ±1	140 ± 1
1.2.35	110 ± 4	108 ± 2	85 ±4	28 ±2
1.2.36	129 ± 4	133 ± 3	93 ±4	128 ± 3

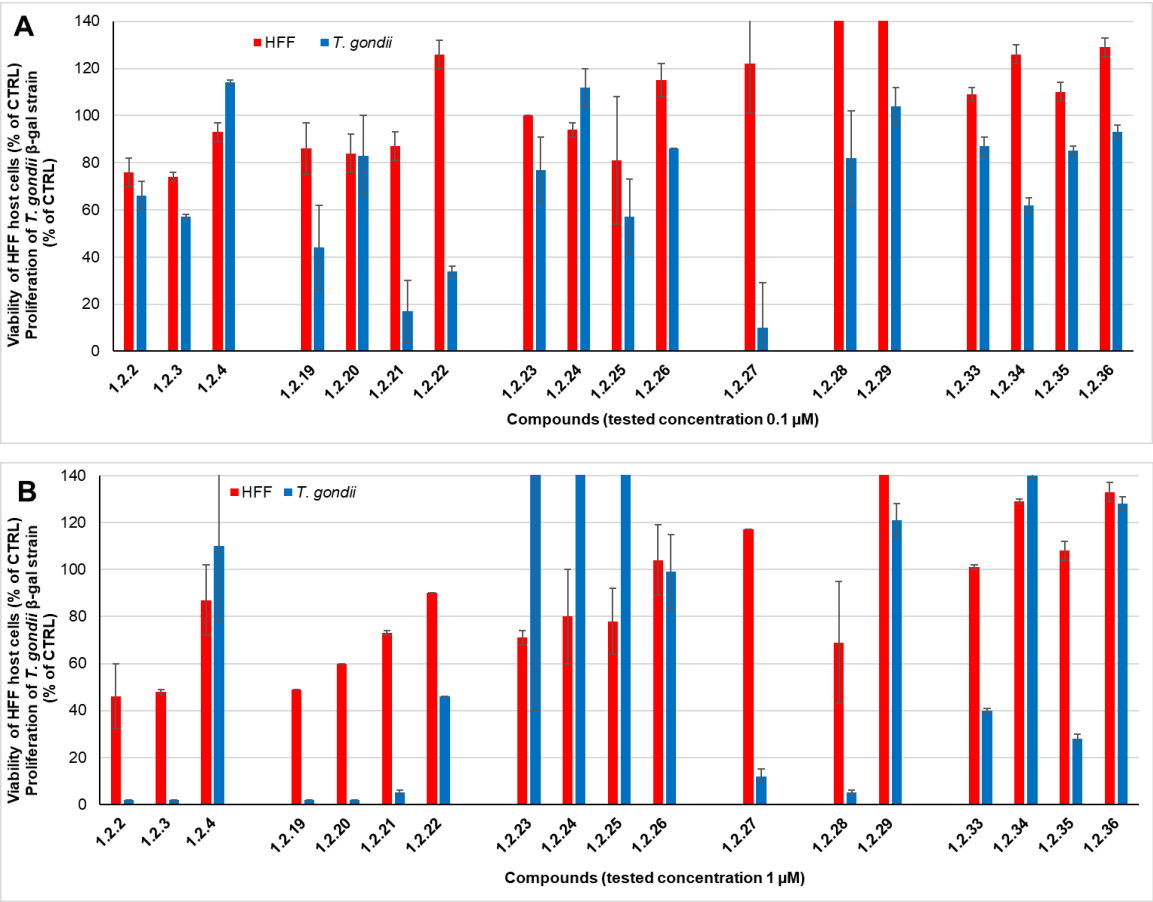

Figure 1.2.6. Clustered column chart showing the *in vitro* activities at 0.1(A) and 1(B) µM of the trithiolato diruthenium compounds on HFF viability and *T. gondii β-gal* proliferation. Non-infected HFF monolayers treated only with 0.1% DMSO exhibited 100% viability and 100% proliferation was attributed to *T. gondii* β-gal tachyzoites treated with 0.1% DMSO only. For each assay, standard deviations were calculated from triplicates and are displayed on the graph. Data for compounds **1.2.2**-**1.2.4** were previously reported[131].

The biological activities of the hydroxy, amino and carboxy diruthenium compounds **1.2.2**-**1.2.4** were discussed before. While **1.2.4** has very limited effect on both HFF viability and parasite proliferation at both tested concentrations, **1.2.2** and **1.2.3** almost completely abolished parasite proliferation at 1 µM, but are also toxic to the host cells at this concentration.

Both esters **1.2.19**-**1.2.22** and the corresponding amide analogues **1.2.23**-**1.2.25** exert a medium to low toxicity to HFF when applied at 1 µM, the effect being more pronounced for ester derivatives and for compounds with shorter linkers between the two units (almost linear dependence). Ester derivatives are also significantly more efficient in inhibiting *T. gondii* β-gal proliferation as compared to the respective amides especially at 1 µM, even if the values need to be considered with caution considering the effect of the compounds on host cell viability at the same concentration. Esters **1.2.19** and **1.2.20** with

shorter connectors between the diruthenium and the BODIPY unit share similar toxicity/activity profile with the corresponding organometallic hydroxy intermediate **1.2.2**, which is not the case for the amide conjugates **1.2.23**-**1.2.26** and the diruthenium amino intermediate **1.2.3**.

Also, for the small series of compounds **1.2.27**, **1.2.28** and **1.2.29**, both the nature of the bond between the two units and the length of the connector strongly influences the biological activity. Ester **1.2.27** did not affect host cells viability while structurally related amide **1.2.27** presented medium toxicity when applied at 1 µM, while both compounds inhibited parasite proliferation when applied at the highest concentration. Similar to the corresponding diruthenium carboxy intermediate **1.2.4**, amide **1.2.29** exhibited neither cytotoxicity nor antiparasitic effect at the tested concentrations.

Conjugates **1.2.33**-**1.2.36**, in which the fluorophore presents an aryl group in the *meso*-position, do not affect the HFF viability at the tested concentrations, and exhibit only poor efficacy in inhibiting parasite proliferation even at 1 µM.

Table 1.2.4. Half-maximal inhibitory concentration (IC_{50}) values (µM) on *T. gondii* β-gal for eight selected compounds and pyrimethamine (used as standard), and their effect at 2.5 µM on HFF viability.

Compound	*T. gondii* β-gal			HFF	
	IC_{50} (µM)	**[LS; LI][b]**	**SE[c]**	**viability at 2.5 µM (%)[d]**	**SD[e]**
Pyrimethamine[a]	0.326	[0.396; 0.288]	0.051	99	6
1.2.2[a]	0.117	[0.139; 0.098]	0.144	56	3
1.2.3[a]	0.153	[0.185; 0.127]	0.138	51	2
1.2.4[a]	0.181	[1.482; 0.273]	2.700	99	2
1.2.19	0.384	[0.435; 0.339]	0.138	60	1
1.2.20	0.389	[0.506; 0.299]	0.214	68	1
1.2.21	0.335	[0.348; 0.322]	0.051	60	1
1.2.27	0.542	[0.843; 0.349]	0.569	56	5
1.2.28	0.358	[0.427; 0.301]	0.209	69	4

[a]Data for pyrimethamine, **1.2.2**, **1.2.3** and **1.2.4** were previously reported[131]. [b]Values at 95% confidence interval (CI); LS is the upper limit of CI and LI is the lower limit of CI. [c]The standard error of the regression (SE), represents the average distance that the observed values fall from the regression line. [d]Control HFF cells treated only with 0.25 % DMSO exhibited 100% viability. [e]The standard deviation of the mean (3 replicate experiments).

The conjugates present rather poor antiparasitic activity (IC_{50} values (Table 1.2.4) on *T. gondii* in the range 0.335-0.542 µM) compared to previously reported diruthenium complexes[29, 30] or hybrid molecules in which the diruthenium moiety was functionalized with other fluorophores like coumarin derivatives[131] or antimicrobial drugs[186] assessed in similar conditions. This proves crucial importance of the nature of

the organic fragment appended on the organometallic scaffold for the overall biological activity of the conjugates. If the antiparasitic activity of the conjugates (in terms of IC_{50} values on *T. gondii*) remains close to that of the standard drug pyrimethamine (IC_{50} = 0.326 µM), they exert a stronger toxicity on the host cells when applied to 2.5 µM. With the exception of conjugate **1.2.27** (which in spite of the promising results obtained in the primary screening exhibited the lowest IC_{50} value), the conjugates that were submitted to dose-response tests show rather similar IC_{50} values and inhibition of the HFF viability. Ester **1.2.20** and amide **1.2.28** exhibit better antiparasitic efficacy/cytotoxicity balance.

If the compounds remain of interest as potential fluorescent sondes for cellular compartments (cells and eventual parasites), their interest as antiparasitic therapeutic agents seems limited.

In order to have more insight into the mode of action of this type of conjugates and their intracellular localization and behavior, selected compounds were submitted to further TEM and fluorescence microscopy tests.

1.2.2.5 Transmission electron microscopy

The ultrastructural changes induced by compounds **1.2.21** and **1.2.27** were further studied by TEM. HFF monolayers were infected with *T. gondii* β-gal tachyzoites and after 24 h drug treatments (500 nM of each compound, a concentration that did not notably affect the host cell) were initiated (Figures 1.2.8 and 1.2.9). Samples were fixed and processed after 24 h. Non-treated control cultures are shown in Figure 1.2.7.

At 24 h, ultrastructural changes were noted within the mitochondrial matrix, which started to lose its characteristic electron-dense matrix. These mitochondrial alterations were however less pronounced compared to similar modifications induced by coumarin-trithiolato diruthenium conjugates[131] or by other complexes with no organic molecule appended on one of the bridge thiols[29].

Structurally diverse mitochondria-targeting anticancer metal complexes[187] have been studied and various structures can be used for the bioimaging of this organelle[188].

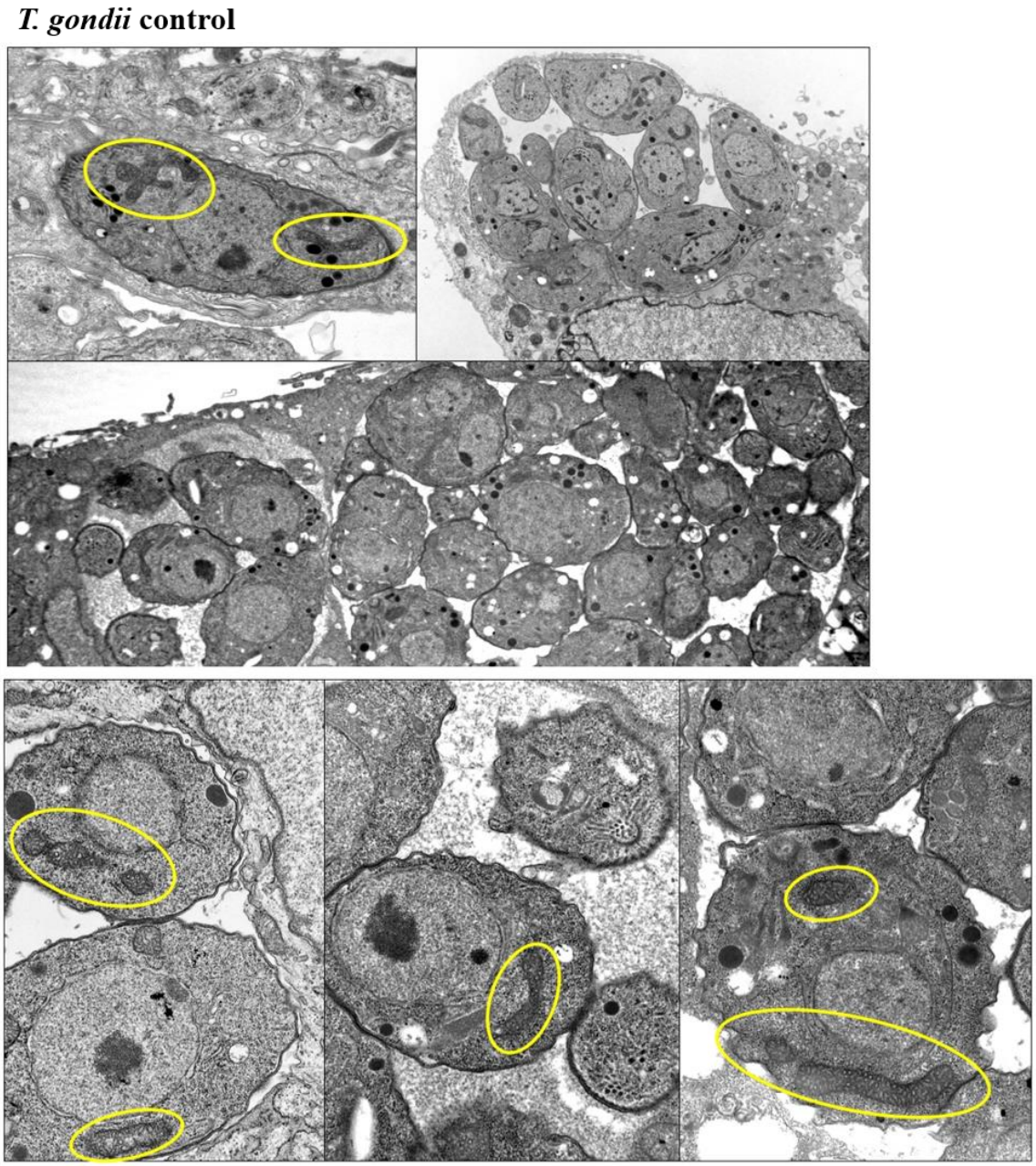

Figure 1.2.7. TEM of *T. gondii* β-gal tachyzoites fixed at 24 h post infection.

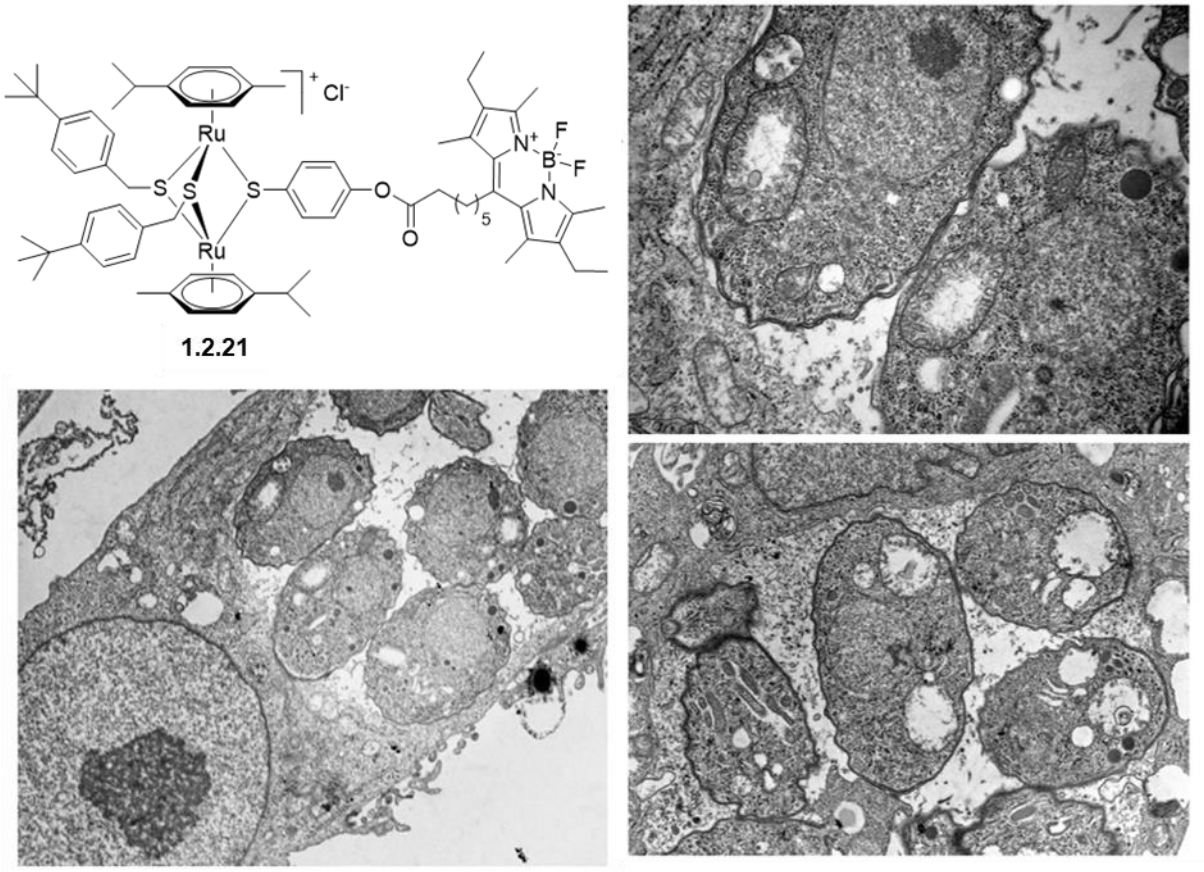

Figure 1.2.8. TEM of *T. gondii* β-gal tachyzoites treated with 500 nM of **1.2.21**, 24 h after treatment initiation.

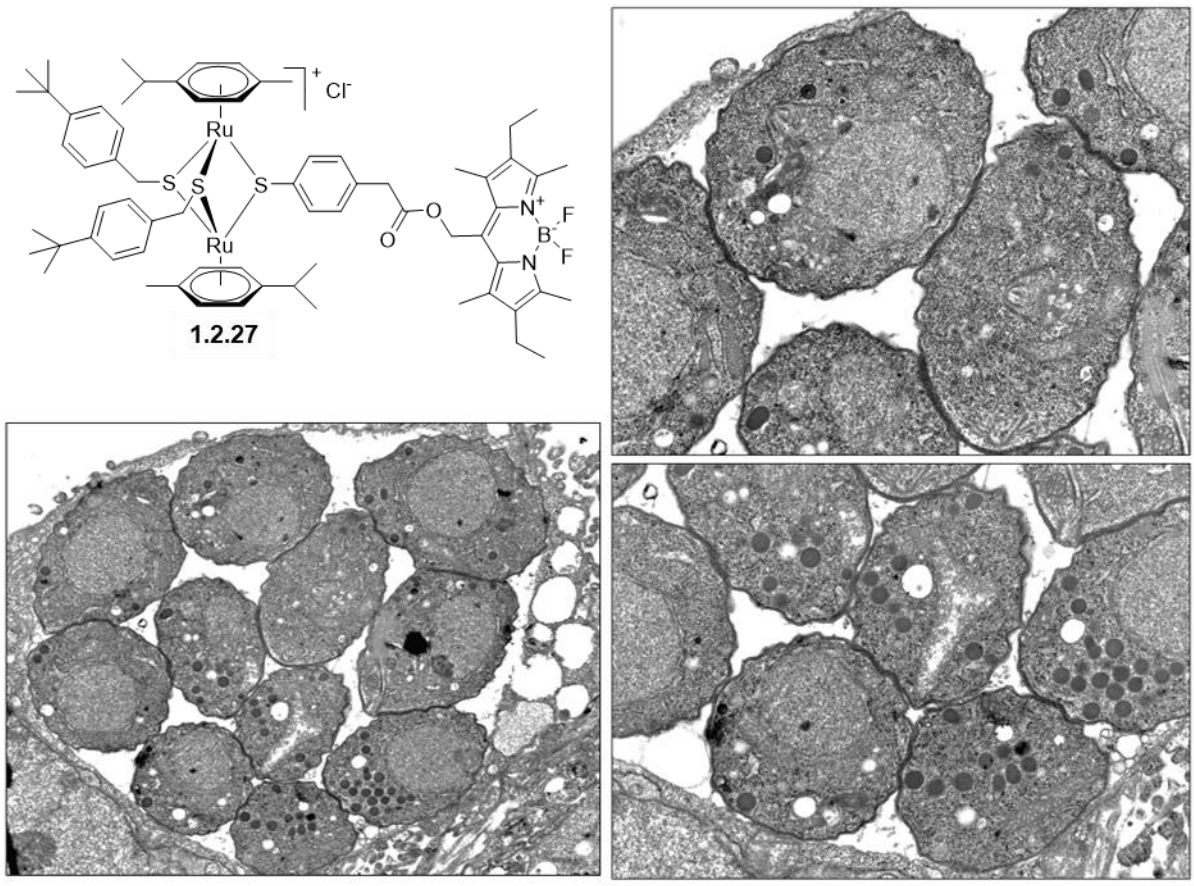

Figure 1.2.9. TEM of *T. gondii* β-gal tachyzoites treated with 500 nM of **1.2.27**, 24 h after treatment initiation.

1.2.2.6. Fluorescence microscopy

In order to assess the potential use of the new conjugates coumarin-diruthenium unit as cellular trackable probes and to identify possible key targets, fluorescence microscopy assays (Figure 1.2.10) were performed on HFF cells treated with either 20 μM carboxy BODIPY dye **1.2.10** or 20 μM of the corresponding BODIPY-diruthenium conjugate **1.2.20**, both counter-stained with Tubulin Tracker™ Deep Red (dye providing deep-red/far-red fluorescence when polymerized tubulin in live cells) and DAPI (4′,6-diamidino-2-phenylindole), a blue-fluorescent nuclear-DNA stain. The tubulin dye readily stained the cytoskeleton of HFF and DAPI indicated the nucleus.

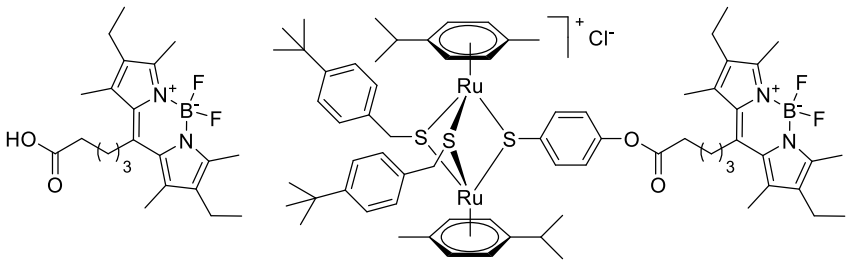

1.2.10 1.2.20

Compound	Tubulin	DAPI	BODIPY	Merged
1.2.10	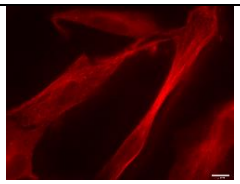	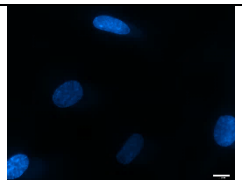	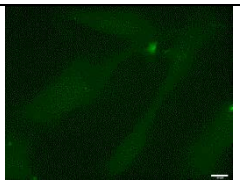	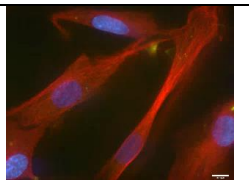
1.2.20	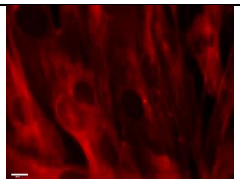	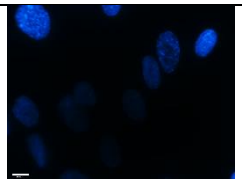	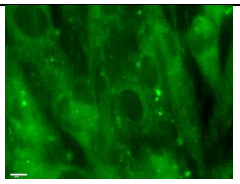	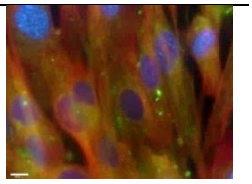

Figure 1.2.10. Fluorescence microscopy of HFF treated with 20 µM of BODIPY dye **1.2.10**, corresponding diruthenium conjugate **1.2.20** or 0.5% DMSO, for 1 h at 37°C. Cells were also stained with Tubulin Tracker™ Deep Red and DAPI stains.

If both tested compounds were cell internalized, no organelle localized labelling could be observed with neither **1.2.10** nor **1.2.20**. However, compounds **1.2.10** nor **1.2.20** do not appear to be localized in the nucleus (no co-localization with the DNA-stain DAPI), in spite the cationic nature of the diruthenium conjugate which can interact with anionic molecules as the DNA. Interestingly, the fluorescence intensity of the conjugate **1.2.20** inside cells appears to be higher compared to that of the simple dye **1.2.10**, although the latest exhibits significantly higher fluorescence quantum yield. This might indicate a better internalization and/or a 'fixation'/retention of the diruthenium compound. A similar effect was reported for other hybrids metal complex-BODIPY dye[158]. An explanation for the enhanced cellular uptake is that the positively charged diruthenium units facilitate the cellular uptake of conjugate **1.2.20**, because positive charges can promote/facilitate internalization[158]. If the compounds are indeed binding to polymerized tubulin, they can inhibit cell division and possibly other functions utilizing polymerized tubulin.

Considering the compounds good fluorescence in intracellular environment, their potential use as imaging tools should be further assessed in other experimental settings.

1.2.3. Conclusions

To address our challenge, namely, to obtain antiparasitic metallodrugs that can also be used as fluorescent tracking agents, a series of 15 new conjugates BODIPY-trithiolato-bridged dinuclear ruthenium arene complexes have been synthesized and fully characterized. The influence of the type of connection (amide *vs* ester) as well as that of the length of the linker between the two units BODIPY-dinuclear ruthenium complex moiety upon the photophysical and biological properties of the dyads were evaluated.

The assessment of spectral properties of the dyads confirms their potential application as probes for fluorescence imaging in spite of an important fluorescence quenching which accompany the BODIPY connection to the diruthenium unit. However, a certain caution should be considered seen that the conjugates exhibit lower antiparasitic activity compared to previously reported diruthenium complexes, and thus the cellular pharmacology of the conjugates can deviate from that of non-modified diruthenium complexes.

The structural variations considered as type of the connecting bond, length of the linker, presence of an additional aromatic ring in BODIPY-*meso* position had limited effect on the conjugates' fluorescence, but a significant impact on the compounds' toxicity and antiparasitic properties. For example, the ester conjugates exhibited noteworthy/substantially higher toxicity on the host cells compared to the corresponding amide analogues.

TEM indicated the parasite mitochondrion as a potential target but the effect was nevertheless reduced compared to that of previously reported trithiolato-bridged dinuclear ruthenium(II)-arene compounds.

First confocal microscopy assays performed on HFF cells revealed that the conjugates are internalized and exhibit strong fluorescence in the intracellular environment. A co-localization with the Tubulin Tracker™ Deep Red stain was observed while no co-localization with the nucleus DAPI stain was detected, indicating that while the dyads readily stained the cytoskeleton they do not accumulate in the nucleus. Interestingly, the intracellular fluorescence intensity was higher for the conjugate compared to that of the free BODIPY dye.

The compounds show good fluorescence in intracellular environment and their potential use as imaging tools deserves further attention.

1.2.4. Experimental part

1.2.4.1. Chemistry

The chemistry experimental part, with full description of experimental procedures and characterization data for all compounds, as well as the data corresponding to the crystal structures determination are presented in the *Supporting information 1.2*.

1.2.4.2. Photophysical measurements

1.2.4.2.1. Instruments and methods

UV-Visible spectra were recorded on a Thermo Scientific Evolution 201 UV-Vis spectrophotometer, and the fluorescence emission spectra were recorded on an Agilent Cary Eclipse fluorescence spectrophotometer.

The UV-Vis absorption spectra of compounds **1.2.5-1.2.36** were recorded in the 200-1100 nm range at r.t. using 1, 2, 5 and 10 μM solutions in $CHCl_3$. Emission spectra were recorded in the 450-650 nm range after excitation at 450 nm at r.t. using the same solutions (1, 2, 5 and 10 μM solutions in $CHCl_3$).

1.2.4.2.2. Determination of quantum yields

Relative quantum yields in $CHCl_3$ at r.t. were calculated using equation (**1**) and rhodamine 6G (Φ_F = 0.75 in $CHCl_3$) as standard[107].

$$\Phi_F(x) = \frac{A_s}{A_x} \times \frac{F_x}{F_s} \times \left(\frac{n_x}{n_s}\right)^2 \times \Phi_F(s) \quad (\mathbf{1})$$

where *A* is the absorbance at the excitation wavelength, *F* is the area under the emission curve, *n* is the refractive index of the solvent (at 20°C) used in measurements (n = 1.446 for $CHCl_3$), and the subscripts *s* and *x* represent standard and unknown respectively.

Stokes shifts were calculated using equation (**2**) as the difference between the values of maxima of the intense bands in the fluorescence and absorption spectra:

$$\Delta\lambda = \lambda_{max}^{em} - \lambda_{max}^{abs} \quad (\mathbf{2})$$

1.2.4.3. Biological activity evaluation

1.2.4.3.1. In vitro activity assessment against T. gondii tachyzoites and HFF

All tissue culture media were purchased from Gibco-BRL, and biochemical agents from Sigma-Aldrich. Human foreskin fibroblasts (HFF) were purchased from ATCC, maintained in DMEM (Dulbecco's Modified Eagle's Medium) supplemented with 10% fetal calf serum (FCS, Gibco-BRL, Waltham, MA, USA) and antibiotics as previously

described[28]. Transgenic *T. gondii* β-gal samples (expressing the β-galactosidase gene from *Escherichia coli*) were kindly provided by Prof. David Sibley (Washington University, St. Louis, MO, USA) and were maintained, isolated, and prepared for new infections as shown before[28, 117].

All the compounds were prepared as 1 mM stock solutions from powder in dimethyl sulfoxide (DMSO, Sigma, St. Louis, MO, USA). For in vitro activity and cytotoxicity assays, HFF were seeded at 5×10^3/well and allowed to grow to confluence in phenol-red free culture medium at 37 °C and 5% CO_2. Transgenic *T. gondii* β-gal tachyzoites were isolated and prepared for infection as described[28]. *T. gondii* tachyzoites were released from host cells, and HFF monolayers were infected with freshly isolated parasites (1×10^3/well), and compounds were added concomitantly with infection. In the primary screening, HFF monolayers infected with *T. gondii* β-gal received 0.1 and 1 μM of each compound, or the corresponding concentration of DMSO (0.01 or 0.1% respectively) as controls and incubated for 72 h at 37˚C/5% CO_2 as previously described[62].

For the next step, IC_{50} measurements for *T. gondii* β-gal were performed. The selected compounds were added concomitantly with infection in 8 serial concentrations 0.007, 0.01, 0.03, 0.06, 0.12, 0.25, 0.5, and 1 μM. After a period of 72 h of culture at 37 °C/5% CO_2, the culture medium was aspirated, and cells were permeabilized by adding 90 μL PBS (phosphate-buffered saline) with 0.05% Triton X-100. After the addition of 10 μL 5 mM chlorophenolred-β-D-galactopyranoside (CPRG; Roche Diagnostics, Rotkreuz, Switzerland) in PBS, the absorption shift was measured at 570 nm wavelength at various time points using an EnSpire® multimode plate reader (PerkinElmer, Inc., Waltham, MA, USA).

For the primary screening at 0.1 and 1 μM, activity was measured as the release of chlorophenol red over time, was calculated as a percentage from the respective DMSO control, which represented 100% of *T. gondii* β-gal growth. For the IC_{50} assays, the activity measured as the release of chlorophenol red over time was proportional to the number of live parasites down to 50 per well as determined in pilot assays. IC_{50} values were calculated after the logit-log-transformation of relative growth and subsequent regression analysis.

All calculations were performed using the corresponding software tool contained in the Excel software package (Microsoft, Redmond, WA, USA). Cytotoxicity assays using uninfected confluent HFF host cells were performed by the alamarBlue assay as previously reported[118]. Confluent HFF monolayers in 96 well-plates were exposed to 0.1, 1 and 2.5 μM of each compound. Non-treated HFF as well as DMSO controls (0.01%, 0.1% and

0.25%) were included. After 72 h of incubation at 37 °C/5% CO_2, the medium was removed, and plates were washed once with PBS. 200 µL of Resazurin (1:200 dilution in PBS) were added to each well. Plates were measured at excitation wavelength 530 nm and emission wavelength 590 nM at the EnSpire® multimode plate reader (PerkinElmer, Inc.). Fluorescence was measured at different time points. Relative fluorescence units were calculated from time points with linear increases.

1.2.4.4. Transmission electron microscopy (TEM)

HFF ($5x10^5$ per inoculum) grown to confluence in T-25 tissue culture flasks were infected with 10^5 *T. gondii* Me49 tachyzoites, and 500 nM of **1.2.21** or **1.2.27** were added at 24 h post-infection. After 6, 24 or 48 h, cells were harvested using a cell scraper, and they were placed into the primary fixation solution (2.5 % glutaraldehyde in 100 mM sodium cacodylate buffer pH 7.3) for 2 h. Specimens were then washed 2 times in cacodylate buffer and were post-fixed in 2% OsO_4 in cacodylate buffer for 2 h, followed by washing in water, pre-staining in saturated uranyl acetate solution, and step wise dehydration in ethanol. They were then embedded in Epon 812-resin and processed for TEM as described[29]. Specimens were viewed on a CM12 transmission electron microscope operating at 80 kV.

1.2.4.5. Fluorescence microscopy

Glass cover slips of 12 mm in diameter were placed in 24-well culture plate and sterilized by UV for 40 min. HFF in DMEM supplemented with 10% heat-inactivated, sterile, filtered FCS and 2% antibiotics (penicillin streptomycin) were seeded at 2×10^4 cells/mL and plates were allowed to grow for 3 days at 37 °C with 5% CO_2. Culture medium was removed and replaced with fresh medium (1 mL/well) containing (i) 0.5%DMSO, (ii) 20 µM of BODIPY dye **1.2.10** or (iii) 20 µM of ester conjugate **1.2.20** and were then incubated for 1 h at 37°C / 5% CO_2. Subsequently the medium was discarded, coverslips were washed 3 times with sterile PBS, fixed with 2% paraformaldehyde (PFA) in PBS for 20 min, permeabilized (0.2 % Triton X-100 in PBS) for 5 min, and unspecific binding sites were blocked in blocking solution (3% BSA, 0.2% NaAcid in PBS) for 2 h at r.t.. Glass coverslips were then incubated for 30 min with Tubulin Tracker™ Deep Red and DAPI reagents at 37°C. Fluorescence microscopy was performed with a Nikon Eclipse E800 digital confocal fluorescence microscope. Images were acquired and processed with Openlab 5.5.2 software.

Chapter 2 – Trithiolato-Bridged Ruthenium(II)-Arene Complexes Bearing Metabolites

2.1. Nucleic base-Tagged Dinuclear Trithiolato-Bridged Ruthenium(II)-Arene Complexes[3]

Abstract

'Chemistry on the complex' is a powerful tool for the development of new libraries of organometallic compounds. For the obtainment of novel conjugates based on the trithiolato-bridged dinuclear ruthenium(II)-arene scaffold using a CuAAC (copper catalyzed azide-alkyne cycloaddition) synthetic approach were synthesized. Functionalized alkyne- and azide-diruthenium intermediates were coupled *via* click reactions to nucleobase derivatives and other small molecules bearing the corresponding complementary unit. In total 37 compounds (diruthenium conjugates and corresponding intermediates) were assessed in a primary screening for *in vitro* activity against transgenic *Toxoplasma gondii* tachyzoites constitutively expressing β-galactosidase (*T. gondii* β-gal) at 0.1 and 1 µM. In parallel the cytotoxicity in non-infected host cells (human foreskin fibroblasts, HFF) was determined by alamarBlue assay. 25 compounds that strongly impaired parasite proliferation with little effect on HFF viability were further subjected to *T. gondii* β-gal dose-response studies (half maximal inhibitory concentration (IC_{50}) determination) and their toxicity for HFF was assessed at 2.5 µM. These sequential tests led to the identification of two promising compounds for further development: an adenine ester conjugate **2.1.14** and a click conjugate with an hydroxymethylene substituent **2.1.36**. Both exhibit low IC_{50} values on *T. gondii* β-gal (0.059 and 0.111 µM, respectively) lower than the IC_{50} = 0.326 µM measured for the standard drug pyrimethamine, and have a good selectivity, as they are weakly toxic to HFF when applied at 2.5 µM.

2.1.1. Introduction

Toxoplasma gondii, the most prevalent of all protozoan infections in man, is an opportunistic human pathogen, which chronically infects about 30% of humans worldwide,

[3] This chapter is a draft with title *Synthesis and Antiparasitic Activity of New Nucleic Base-tethered Trithiolato-bridged Dinuclear Ruthenium(II)-Arene Compounds*, which is going to be submitted for publication. (Published as: New Nucleic Base-Tethered Trithiolato-Bridged Dinuclear Ruthenium(II)-Arene Compounds: Synthesis and Antiparasitic Activity, *Molecules*, 2022, 27, 8173. https://doi.org/10.3390/molecules27238173. This article is licensed under a Creative Commons Attribution International License (CC BY 4.0)). Supplementary information can be found in the chapter *Supporting information 2.1*.

as well as domestic and wild animals causing an important health, social and economic blight[189, 190]. In most cases, infection remains asymptomatic or causes unspecific, influenza-like symptoms initially. Chronic infection is mostly lifelong, largely persists within the central nervous system, and has long been considered to be without any consequences in otherwise healthy individuals[191]. *T. gondii* infection can be life-threatening in immunocompromised hosts, and when contracted by seronegative pregnant women, it may cause abortion. Transplacental infection in new-borns is bound to result in severe neurological damage and ocular toxoplasmosis[192]. *T. gondii* is affecting livestock, most notably sheep, where it can cause abortion and birth of weak offspring that can transmit the parasite to the next generation[190, 193].

Current management of toxoplasmosis relies on conventional chemotherapy, which is confronted to important shortcomings related to reduced tolerance and overall potency, poor efficacy to the latent stage of the parasite, as well as drug resistance[194, 195]. Prevailing treatments are based on combination therapy comprising sulfonamides and pyrimethamine or other antibiotics[196]. Additional treatments against acute toxoplasmosis include other agents that interfere in folate synthesis such as dapsone, but also protein synthesis inhibitors (e.g., clindamycin, azithromycin, clarithromycin, erythromycin, spiramycin), and inhibitors of apicoplast division such as doxycycline and minocycline[192]. Overall, most treatments are unspecific, have adverse side effects, and resistance formation has been recognized as a serious constraint. Toxoplasmosis poses an unmet and challenging need for treatment, and novel options are required[20, 194]. To address these difficulties a range of approaches are used to identify new agents including (i) extending the usefulness of existing drugs by generating new formulations with varying strengths/combinations/dosing regimens, (ii) *de novo* drug discovery, and (iii) drug repurposing[197-199].

T. gondii is an obligate intracellular pathogen that can invade and replicate in any nucleated mammalian cell, the parasite being in stringent dependence on specific host cell resources[200]. *T. gondii* lacks many genes encoding the entire metabolic pathways, but has evolved efficient strategies to acquire essential metabolites from mammalian cells[201]. For survival, the parasite is auxotrophic for numerous nutrients and has acquired salvage mechanisms to import the essential compounds that it cannot synthesize, as for example, various metabolites including polyamines, cholesterol, purine derivatives and isoprenoids[201]. Targeting the specific metabolic defects of the parasite based on its auxotrophic nature (e.g., starving the parasite by nutrient depletion or disrupting the salvage

pathways) constitutes a source of therapeutic exploration[201]. Due to the large phylogenic separation between the mammalian host and *T. gondii*, parasite transporters and enzymes responsible for the uptake and metabolism of nutrients may constitute potential targets for chemotherapy[201]. The use of parasitic protozoa cell cycle as potential chemotherapeutic source was already explored[202-204]. Various approaches can be considered: (i) using specific inhibitors of transporters/enzymes involved in the salvage pathway[201]; (ii) developing 'subversive' substate analogues that are metabolized to toxic molecules[201]; (iii) using the parasite nutrient 'appetite' and needs associated to its accelerated growth to increase the internalization of other molecules through a metabolite-drug conjugate in a Trojan Horse like strategy. Anchoring various nutrients/metabolites to a compound that is toxic to the parasite, is a foreseen method based on the ability of *T. gondii* to sequester and scavenge this type of hybrid molecules.

The rational design of an antiparasitic drug is usually based on biochemical and physiological differences between pathogens and mammalian host, some of the most striking distinctions being found in purine metabolism[205, 206], with the respective parasite and mammalian enzymes involved in these metabolic pathways showing discrepancies in substrate specificity[204, 207, 208]. Targeting the *T. gondii* purine salvage pathways represents a potential pharmacological strategy[201, 207, 209] and several studies already explored this approach[210-217]. However, this approach was not widely explored due to the apprehension that compounds targeting parasite metabolic pathway can also be toxic to the host[204].

T. gondii is a purine auxotroph unable of *de novo* biosynthesis of purine nucleic bases and relies on their uptake from the host cell to meet its nutritional requirements[201, 218-221]. The parasite purines are adenine, guanine, xanthine and hypoxanthine[218]. These nucleobases are not only essential building blocks for nucleic acids synthesis but are also required for the obtainment of other metabolites and proteins, as well as in reactions necessitating energy[218].

Some of the *T. gondii* metabolites, like amino acids, fatty acids, lipoate, pyrimidine derivatives, and folate, are not only scavenged from the host but also endogenously produced by the parasite[201]. If the parasite is a strict auxotrophic organism for purines, it scavenges but also synthesizes pyrimidine nucleobases and nucleosides[201, 222-225].

If numerous purine analogues were developed for therapeutic purposes, most of these compounds have been synthesized and evaluated regarding their effects for the treatment of cancer and viral infections[226-228]. Purine based compounds have only

sparingly been tested as antiparasitic drugs *in vitro*[229]. Among the obstacles confronting preclinical and clinical tests of purine analogues as potential antiparasitic agents, prevails the dread from limited selectivity and host toxicity. However, the feasibility of using purine analogues, which perturbs nucleotide metabolism as potential antiparasitic agents, was previously demonstrated[207] and several subversive purine analogues and inhibitors have shown efficacy against *T. gondii*[230, 231].

The research of novel organometallic compounds for biological applications has received a lot of interest in the past decades[232-234]. If initially most of the bioactive metalorganic compounds were conceived as alternatives to anticancer platinum-based drugs[235-237], other pharmacological properties, particularly antimicrobial[238-243], and antiparasitic[20, 70-72, 244, 245] activities, further encouraged studies in this domain. Ruthenium(II)-arene complexes have shown particularly interesting efficacy/selectivity profile in the fight against various parasites[28, 69, 246, 247]. Combining two or more multifunctionalities into a hybrid structure is a popular strategy in the design of new therapeutic agents. Prior approaches aiming to improve targeting and anticancer activity of metal-based compounds (e.g., platinum[58, 248] and ruthenium[248] complexes), revealed significant benefits after their modification with metabolites[249].

Nucleobases constitute one of the most important core structures in drug discovery seen that they interfere with the nucleic acid synthesis processes. The effectiveness of this class of molecules in treating cancer and various viral infections is well established[226-228]. The incorporation of metal complexes into nucleobases, nucleosides and nucleotides provided compounds with a wide range of applications. Special attention was given to the use of this type of derivatives as biological markers (in nuclear medicine and bioimaging) or building blocks for supramolecular assemblies[250-253]. Other applications focused on their use as potential therapeutic agents with emphasis on their use as anticancer agents[251, 252]. An important effort was invested in the development of various metallocene-DNA/RNA nucleobase conjugates[252, 254-256] and research was further extended to other organometallic derivatives[257-260]. Some examples are presented in Figure 2.1.1.

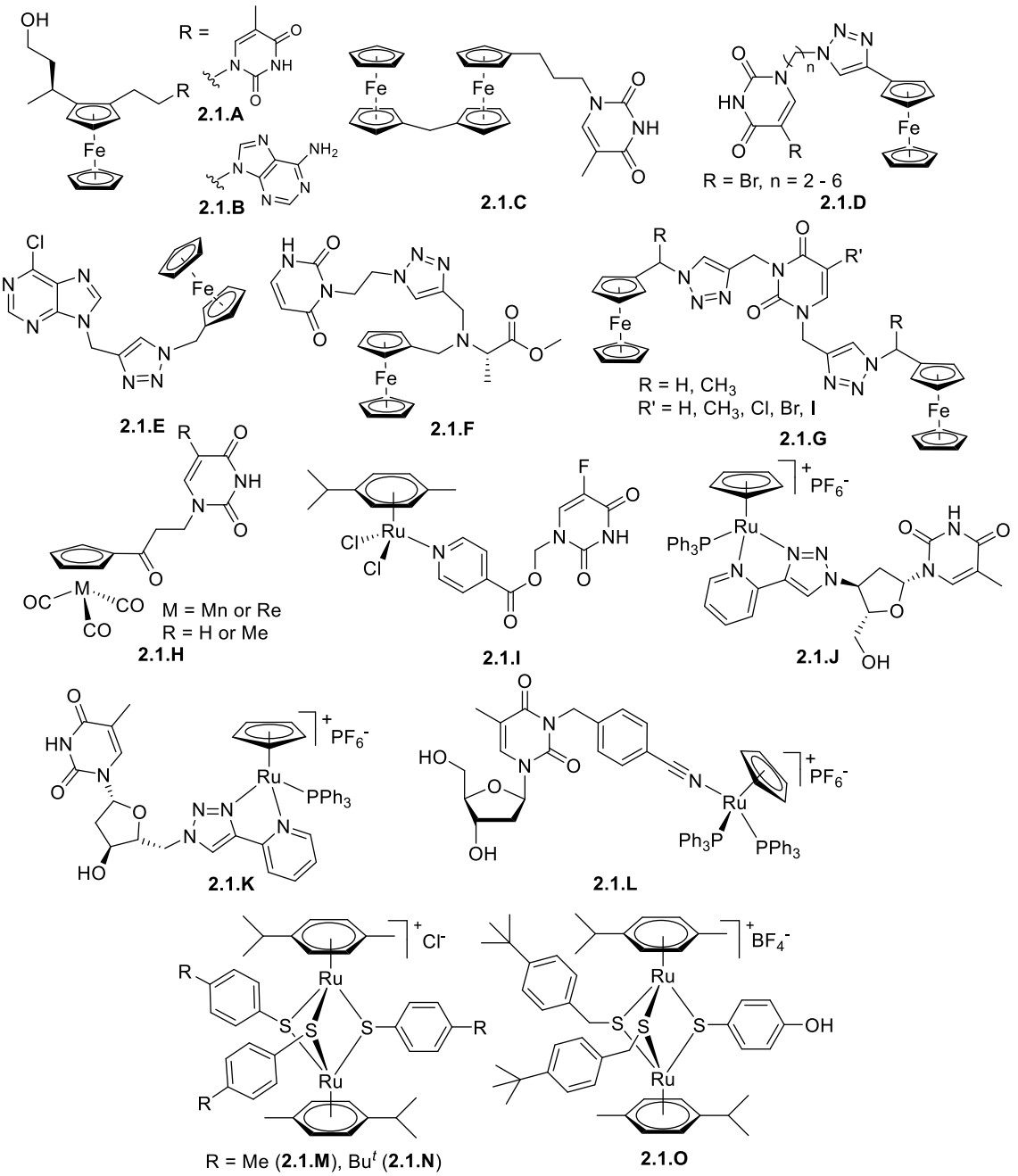

Figure 2.1.1. Structures of various conjugates metal complex - nucleobase/nucleoside (**2.1.A**-**2.1.L**), and of symmetric (**2.1.M**, **2.1.N**) and mixed (**2.1.O)** trithiolato-bridged ruthenium(II)-arene complexes active on *T. gondii.*

For example, nucleosides organometallic analogues in which the five-membered sugar ring was entirely replaced by a cyclopentadienyl (Cp) unit in ferrocene presented promising anticancer activity (**2.1.A** and **2.1.B**, Figure 2.1.1)[261, 262]. Thymine **2.1.A** and adenine **2.1.B** derivatives containing both a hydroxy alkyl linker and a nucleobase exhibited micro- and submicromolar activities against various cancer cell lines, while they proved to be poorly toxic to nontumorigenic human cell cultures[261].

From a series of mono-, di-, and tri-nuclear metallocene-uracil derivatives, compound **2.1.C**, presented promising *in vitro* anticancer activity[263].

Copper-catalysed azide-alkyne [3 + 2] cycloaddition (CuAAC) was used to prepare a series of uracil-ferrocene conjugates (as **2.1.D**) as potential antitubercular agents [264]; an improvement in activity for compounds presenting a bromo-substituent on the uracil along with moderate chain lengths (n = 2–6) was observed.

Compound **2.1.E**, the *N*9 isomer of 6-chloropurine containing a ferrocenylmethylene unit, was also obtained using a CuAAC reaction. **2.1.E** not only exerted potent cytotoxic effect on cancer cells but also showed favourable *in vitro* physicochemical and pharmacological properties including high solubility, moderate permeability and good metabolic stability in human liver microsomes[265].

Derivative **2.1.F**, a ferrocene - L-alanine ester - uracil conjugate obtained using click reaction, displayed weak antifungal activity against the yeast strain of *Candida guilliermondii* (IBA 155)[255].

2.1.G-like compounds, bis-ferrocene conjugates bridged by 1,2,3-triazole linkers to 5-substituted uracil, showed pronounced and selective cytostatic activities on various cancer cells with mitochondria as molecular target [266].

Cymantrene and cyrhetrene uracil and thymine conjugates as **2.1.H**, showed promising antitrypanosomal activity against *Trypanosoma brucei* and were non-toxic to human myeloid leukaemia HL-60 cells[267].

Ruthenium(III) complexes linked to nucleobases or nucleoside units were also reported[268] and more complex nucleolipidic structures were designed to overcome the delivery barrier of the organometallic nucleoside drugs[269]. Also, various ruthenium(II) complexes containing 6-methyl-2-thiouracil[270, 271] or 5-fluorouracil (5-FU)[272] were evaluated for their antiproliferative activity on cancer cells.

Half-sandwich ruthenium(II)-arene compounds containing 5-fluorouracil (5-FU) units anchored on pyridine leg ligands were reported (as **2.1.I**, Figure 2.1.1)[273, 274]; the cytotoxicity of **2.1.I** against BEL-7402 human hepatocarcinoma cells was moderately improved, indicating a synergistic action of the two units.

The activity of the organometallic-nucleobase or nucleoside conjugates can be strongly influenced by the way in which the two units are connected. For example, ruthenium(II)–arene complexes presenting as leg ligands water-soluble 3,5,6-bicyclophosphite ligands based on glucose modified with uracil, 5-FU or thymine were non-toxic on the tested cancer cells[275]. Contrary, thymidine-ruthenium conjugates **2.1.J**

and **2.1.K** with the general formula [(η^5-C_5H_5)Ru(N–N)PPh_3][PF_6] in which the ribose moiety was appropriately modified for ruthenium N–N chelation, presented interesting cytotoxic effects on HCT116 human colon cancer cells, with the cellular uptake independent of nucleoside transporters mediation[276].

2.1.L-like ruthenium-nucleoside conjugates with the general formula [(η^5-C_5H_5)Ru(PP)L][PF_6] (PP = dppe (1,2-bis(diphenylphosphino)ethane), $2PPh_3$ and L = 3-*N*-(*p*-cyanobenzyl)thymidine derivative ligand) showed remarkable stability in aqueous media and high cytotoxicity in HCT116 colon cancer cells with the cellular uptake independent of nucleoside transporters[257].

Among the metal-based anticancer compounds explored in the last 40 years, ruthenium complexes emerged as one of the most encouraging classes[46, 277]. Trithiolato-bridged dinuclear ruthenium(II)-arene complexes (e.g., compounds **2.1.M**-**2.1.O** in Figure 2.1.1) represent a particular class of ruthenium(II)-arene compounds with a structure based on two half-sandwich ruthenium(II)-arene units bridged by three thiols, the Ru_2S_3 unit forming a trigonal-bipyramidal framework. Two different types of complexes can be distinguished, namely 'symmetric' in which the three thiols are identic (**2.1.M**, **2.1.N** in Figure 2.1.1), and 'mixed' bearing at least one different thiol (**2.1.O**, Figure 2.1.1). These compounds are very active against cancer cells but not very selective[64], and recent studies showed that they also exhibit interesting antiparasitic properties against *Toxoplasma* gondii, *Neospora caninum* and *Trypanosoma brucei*[29, 33, 63]. For example, on *T. gondii*[29] and *N. caninum*[33] complexes **2.1.M**, **2.1.N** and **2.1.O** (Figure 2.1.1) presented not only high antiparasitic activity but also interesting selectivity profile. On both parasites complex **2.1.O** showed very low IC_{50} values of 1.2 nM for *T. gondii* and, respectively, of 1 nM on *N. caninum*[29, 33].

Identifying easy and efficient ways to access new organometallic compounds libraries has received a lot of attention. The post-functionalization of organometallic compounds, also called ‘chemistry on the complex’, can be used to develop new types of ruthenium conjugates in a convenient manner and can be extended to larger series of derivatives[278-280]. If this modular strategy allows to introduce the variability in a late synthetic stage[281], it requires high stability of the metal-ligand precursor withstanding synthetic reaction conditions used for post-coordination chemistry[280].

The easy synthesis and scale-up of mixed trithiolato dinuclear ruthenium complexes as well as their outstanding chemical inertness make this scaffold a good substrate for post-functionalization. Conjugates with short peptides[60], coumarins[131] or anticancer and

antimicrobial drugs[61, 186], have been reported as an approach to improve water solubility, or to enhance the anticancer or antiparasitic activity. Amide or ester coupling reactions allowed easy modification of mixed trithiolato diruthenium compounds bearing hydroxy, amine and carboxylic acid groups[61, 131, 186]. Nevertheless, the use of this type of modifications proved limited in some cases[186].

The aim of this study was the synthesis of new conjugates trithiolato-bridged binuclear ruthenium(II)-arene unit - nucleic bases, aiming to exploit the parasite metabolic and peculiarities auxotrophies for an improved antiparasitic activity of the hybrid molecules. The library of nucleobases comprised adenine, uracil, cytosine, thymine and xanthine. In addition to the nature of the nucleobase, different structural variations were investigated for the hybrid molecules, as the nature of the connector between the two units.

One objective was also to identify new pathways allowing not only straightforward and efficient access to larger diruthenium conjugates libraries but also the introduction of other types of linkers. The foreseen strategy challenged the use of CuAAC reactions[282, 283] for the formation of a 1*H*-1,2,3-triazole as conjugate connector. This type of linker exhibits favourable properties, including a moderate dipole character, hydrogen-bonding capability, rigidity, and stability[284]. Azide-alkyne click reactions proved as an easy and efficient way for the post-functionalization of metal complexes[264, 278, 279, 285-293]. As click reactions require two partners, an azide and an alkyne derivative, the use of the trithiolato dinuclear ruthenium scaffold in either role can be asserted in reaction with pair molecules containing the respective complementary group. A first example of a trithiolato-diruthenium conjugate with metronidazole obtained using a CuAAC reaction was recently reported[186].

Anchoring nucleobase entities is expected to boost preferential uptake of the metal complex-metabolite (purine, pyrimidine) hybrid molecule *via* a 'Trojan horse' strategy. This can increase uptake and result in higher and more specific antiparasitic activity. To evaluate this approach, conjugates with other types of small molecules were also synthesized and tested.

The newly obtained hybrids and associated intermediates were submitted to a first *in vitro* screening, assessing the activity against a transgenic *T. gondii* strain constitutively expressing β-galactosidase (*T. gondii* β-gal) grown in human foreskin fibroblasts (HFF). In parallel the compounds cytotoxicity was evaluated in non-infected HFF by alamarBlue assay. These tests were carried out at 0.1 and 1 µM. The compounds exhibiting interesting antiparasitic activity (90% tachyzoite proliferation inhibition) and low cytotoxicity (>50%

HFF viability) at 1 µM were subjected to a second screening consisting in *T. gondii* IC_{50} (half-maximal inhibitory concentration) determination, and HFF cytotoxicity assessment at 2.5 µM.

2.1.2. Results and discussion

2.1.2.1. Chemistry

2.1.2.1.1. Synthesis of the trithiolato-bridged dinuclear ruthenium(II)-arene intermediates

The study focused on the synthesis of new conjugates in which various nucleobases were connected on the trithiolato-bridged ruthenium (II)-arene scaffold. To access the hybrid molecules, selected intermediates bearing functional groups allowing further modification, e.g., *via* ester conjugation or click chemistry, were synthesized. A key stage consisted in the synthesis of the 'mixed' trithiolato-bridged ruthenium(II)-arene intermediates **2.1.2**[131] (same as **1.1.3a**), **2.1.3**[131] (same as **1.1.4a**) and **2.1.4**[30] functionalized with one amino, carboxy or hydroxy group respectively (Scheme 1), on which compounds bearing appropriate substituents could be covalently tethered. Complexes **2.1.2**, **2.1.3** and **2.1.4** were obtained following a two-step pathway (Scheme 2.1.1) by adapting previously reported procedures[53, 131]. In the first step, precursor **2.1.1** (same as **1.1.1a**) was obtained starting from commercially available ruthenium dimer ($[Ru(\eta^6\text{-}p\text{-}MeC_6H_4Pr^i)Cl_2]_2$) and (4-(*tert*-butyl)phenyl)methanethiol as previously described[131].

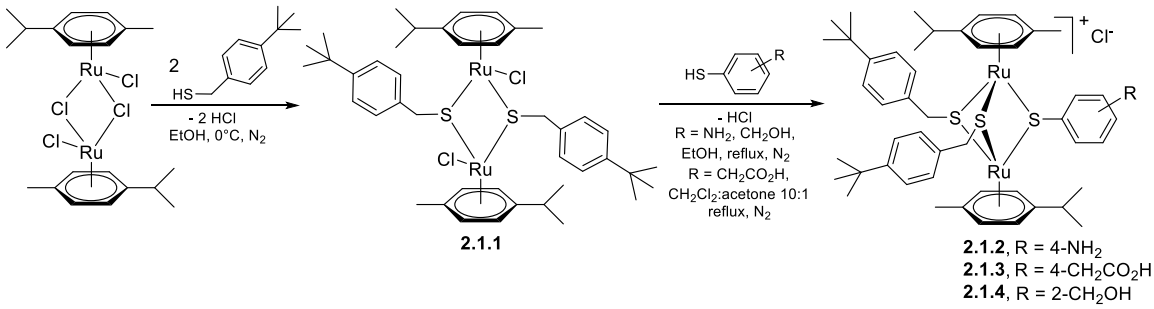

Scheme 2.1.1. Synthesis of the mixed ruthenium(II)-arene complexes **2.1.2**, **2.1.3** and **2.1.4**.

Compounds **2.1.2** and **2.1.4** were obtained by reacting **2.1.1** with excess 4-amino-benzenethiol and, respectively, (2-mercaptophenyl)methanol in refluxing EtOH as earlier reported[30, 131]. In the case of **2.1.3**[131], a mixture of CH_2Cl_2:acetone (10:1 v/v) was used as solvent in order to avoid esterification side reaction of the carboxylic group catalyzed by the hydrochloric acid resulted in the reaction.

2.1.2 and **2.1.3** were further reacted with various alkyne derivatives bearing carboxy, hydroxy and amino groups using ester or amide coupling reactions as presented in Scheme 2.1.2.

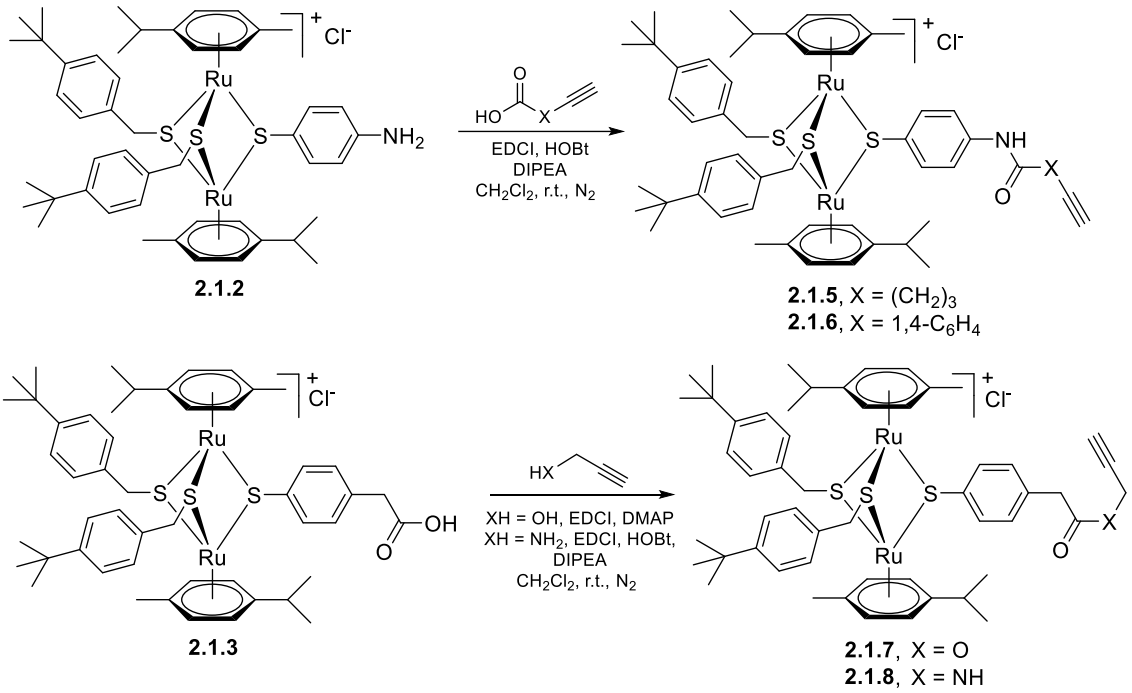

Scheme 2.1.2. Synthesis of the alkyne diruthenium derivatives **2.1.5** and **2.1.6** (top), **2.1.7** and **2.1.8** (bottom) from the amino and carboxy intermediates **2.1.2** and **2.1.3**.

Reactions of amino derivative **2.1.2** with 5-hexynoic acid and 4-ethynylbenzoic acid (Scheme 2.1.2, top) in the presence of EDCI (*N*-(3-dimethylaminopropyl)-*N*′-ethylcarbodiimide hydrochloride) and HOBt (1-hydroxybenzotriazol) as coupling agents, in basic conditions (DIPEA, *N*,*N*-diisopropylethylamine), afforded the aliphatic **2.1.5** and aromatic **2.1.6** ruthenium-alkyne compounds in 68 and 34% yield, respectively. Alkyne derivatives **2.1.7** and **2.1.8**, were obtained by reacting carboxy diruthenium compound **2.1.3** with propargyl alcohol and propargyl amine (Scheme 2.1.2, bottom). Ester **2.1.7** was obtained in the presence of EDCI as coupling agent and DMAP (4-(dimethylamino)pyridine) as basic catalyst, and amide **2.1.8** was obtained using conditions previously described for **2.1.5** and **2.1.6**. Ester **2.1.7** was isolated in medium yield (60%), and amide **2.1.8** was described previously[186].

The trithiolato diruthenium(II)-arene compounds can act also as azide partner in click reactions. Azide-functionalized dinuclear compound **2.1.9** was obtained following a two-step process starting from trithiolato hydroxy precursor **2.1.4** as presented in Scheme

2.1.3 (top). The hydroxy group of **2.1.4** was activated by mesylation with MsCl in basic conditions (TEA, triethylamine), followed by the nucleophilic substitution with azide; **2.1.9** was isolated in good yield (66%, over two steps).

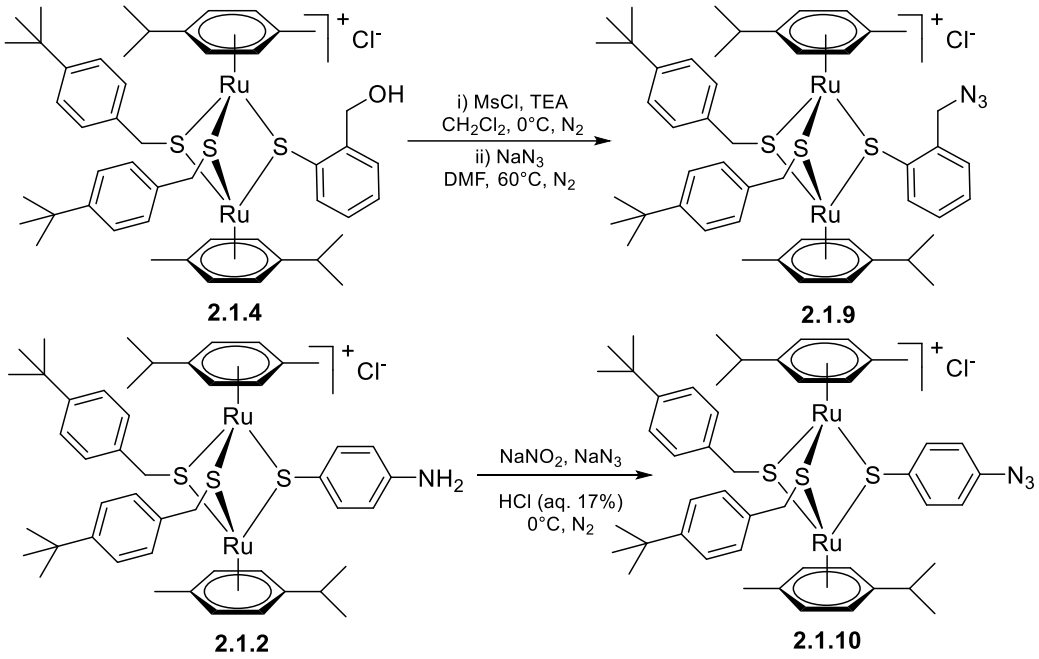

Scheme 2.1.3. Synthesis of the azide diruthenium derivatives **2.1.9** (top) and **2.1.10** (bottom).

Diruthenium azide **2.1.10** was obtained by adapting a literature procedure[294] (Scheme 2.1.3 (bottom)), starting from amino derivative **2.1.4** using the Sandmeyer reaction. First, a diazonium intermediate was prepared using $NaNO_2$ in acidic conditions (HCl), followed by a subsequent displacement with the azide nucleophile. The poor solubility of the starting amine **2.1.4** and of the intermediate diazonium salt (not isolated) led to incomplete conversion. We found that **2.1.10** was instable upon heating and in silica gel chromatographic columns, and in consequence only a small quantity of this intermediate was purified for biological evaluation tests. Nevertheless, compound **2.1.10** could be used for click reactions even if it contained traces of amine **2.1.4**. Attempts to synthesize **2.1.10** using other reported protocols[295, 296] were unsuccessful (either the azide was not obtained or the conversion was poorer).

Based on their structural features, the various nucleobase-diruthenum conjugates obtained in this study were organized in five families.

2.1.2.1.2. Synthesis of the compounds constituting family 1

The compounds of family 1 contain the nucleic base moiety directly introduced as one of the bridging thiols (Scheme 2.1.4). Reactions of the dithiolato diruthenium(II)-arene intermediate **2.1.1** with 2-thiocytosine, 4-thiouracil and 2-thioxanthine allowed the isolation of mixed trithiolato derivatives **2.1.11**, **2.1.12** and **2.1.13** in low yields of 13, 23 and 44%, respectively.

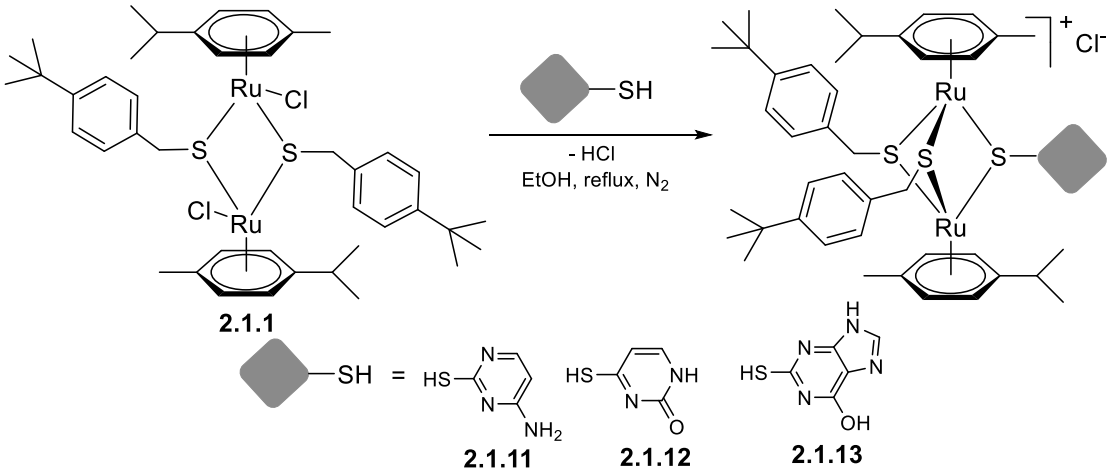

Scheme 2.1.4. Synthesis of the trithiolato diruthenium complexes **2.1.11**, **2.1.12** and **2.1.13**.

The direct introduction of nucleic base fragment on the trithiolato diruthenium scaffold using this method presented important limitations. If many nucleobase thiol derivatives are commercially available, their poor solubility in refluxing EtOH led to poor conversions and important difficulties in the recovery of the pure product in reactions run with 6-thioguanine, 8-mercaptoadenine and 2-thiobarbituric acid. **2.1.11** and **2.1.12** still contained small impurities and their biological activity was not assessed.

2.1.2.1.3. Synthesis of the compounds constituting family 2

Family 2 comprises ester conjugate **2.1.14** which was obtained by reacting carboxy intermediate **2.1.3** with 9-(2-hydroxyethyl)adenine **2.1.14A** in the presence of EDCI as coupling agent and DMAP as base, and was isolated in 43% yield (Scheme 2.1.5).

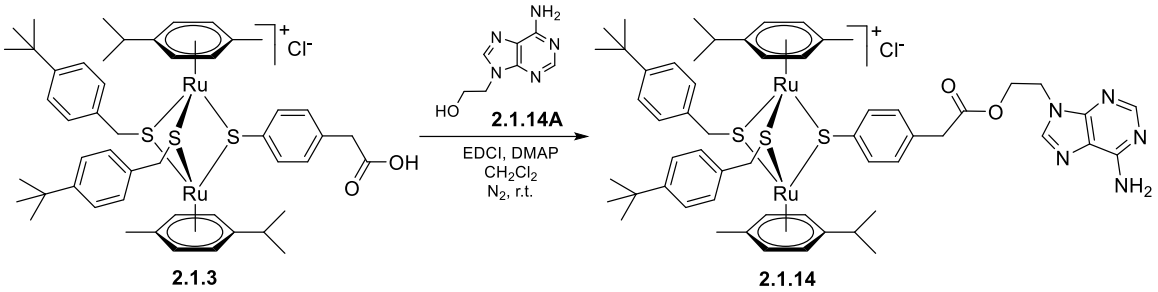

Scheme 2.1.5. Synthesis of the adenine ester conjugate **2.1.14**.

2.1.2.1.4. Synthesis of the compounds constituting family 3

The use of the click reactions[286, 297] as tool for the obtainment of new conjugates with nucleobases was challenged. First reactions were run using trithiolato azide derivatives **2.1.9** and **2.1.10** as substrates (Scheme 2.1.6). In a first step, *N*-propargyl derivatives of uracil (**2.1.15**), thymine (**2.1.16**), cytosine (**2.1.17**) and adenine (**2.1.18**) were synthesized by the nucleophilic substitution of propargylic bromide with the corresponding nucleobases in basic conditions (K_2CO_3), adapting a literature procedure[297-299] (Scheme 2.1.6). Alkyne intermediates **2.1.15**, **2.1.16**, **2.1.17** and **2.1.18** were isolated in low to medium yields (25-48% range).

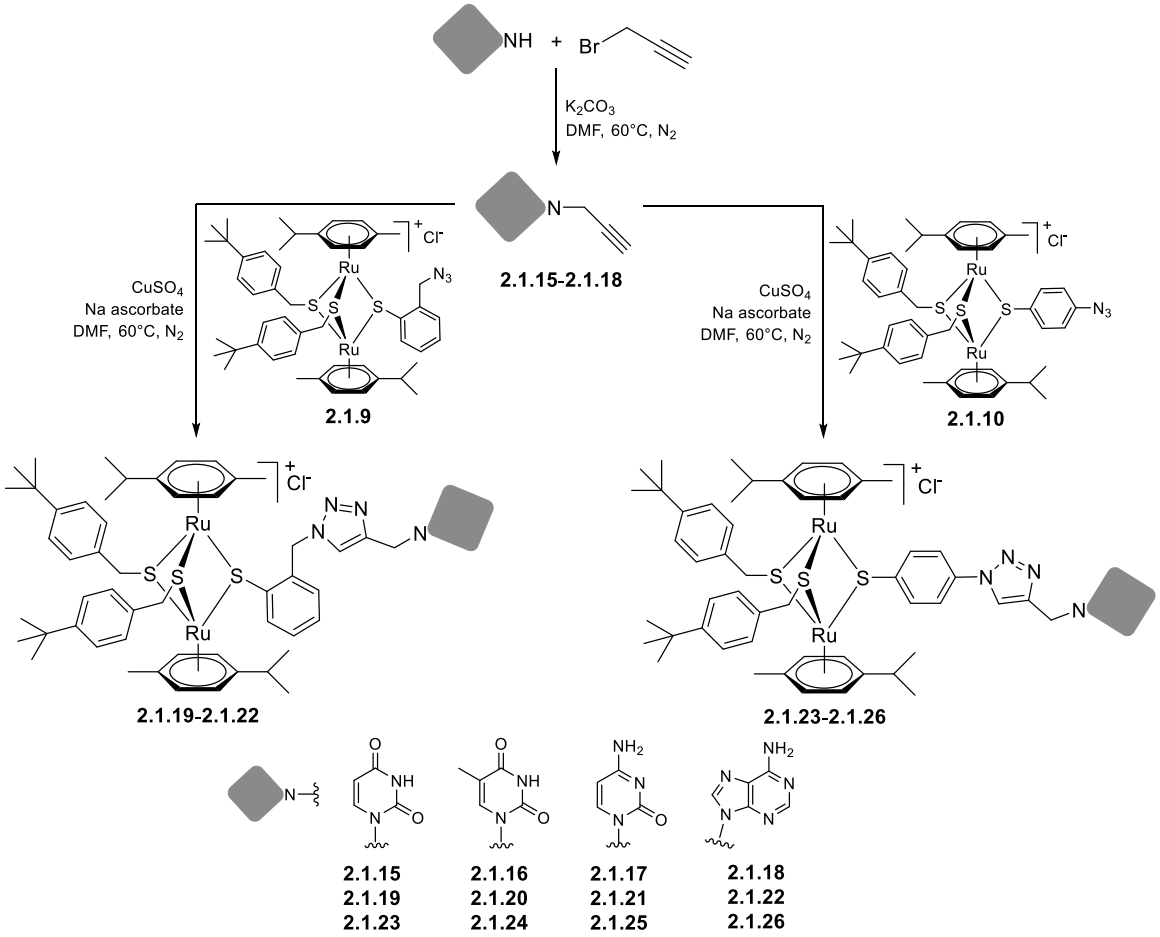

Scheme 2.1.6. Synthesis of the uracil (**2.1.15**,), thymine (**2.1.16**), cytosine (**2.1.17**) and adenine (**2.1.18**) propargyl derivatives and their CuAAC reactions with the dinuclear ruthenium(II) complexes **2.1.9** (left) and **2.1.10** (right) as azide partner, affording conjugates **2.1.19**-**2.1.22** and, respectively, **2.1.23**-**2.1.26**.

The CuAAc click reactions were made by adapting reported procedures[286, 297], in the presence of Cu_2SO_4 and sodium ascorbate as reducing agent. Performing click reactions on azide substrate **2.1.9** (Scheme 2.1.6 (left)) was expected to be challenging due to steric hindrance, especially when run with a bulky alkyne partner. Click products **2.1.19**, **2.1.20**, **2.1.21** and **2.1.22** were isolated in medium to low yields (19-48% range), the quantities of isolated products being sufficient for a first antiparasitic activity and cytotoxicity screening. Similar reaction conditions were used for the CuAAC reactions between diruthenium azide substrate **2.1.10** and nucleic base propargyl derivatives **2.1.15**, **2.1.16**, **2.1.17**, and **2.1.18** (Scheme 2.1.6 (right)). Click products **2.1.23**, **2.1.24**, **2.1.25** and **2.1.26** were isolated in low yields (17 to 30% range).

2.1.2.1.5. Synthesis of the compounds constituting family 4

The dinuclear ruthenium(II)-arene complexes can also act as alkyne partner in

CuAAc click reactions. As proof of concept, a model uracil azide **2.1.27** was synthesized. Nucleophilic substitution of the chlorine in 6-(chloromethyl)uracil with azide allowed the isolation of 6-(azidomethyl)uracil **2.1.27** (Scheme 2.1.7) in low yield (22%).

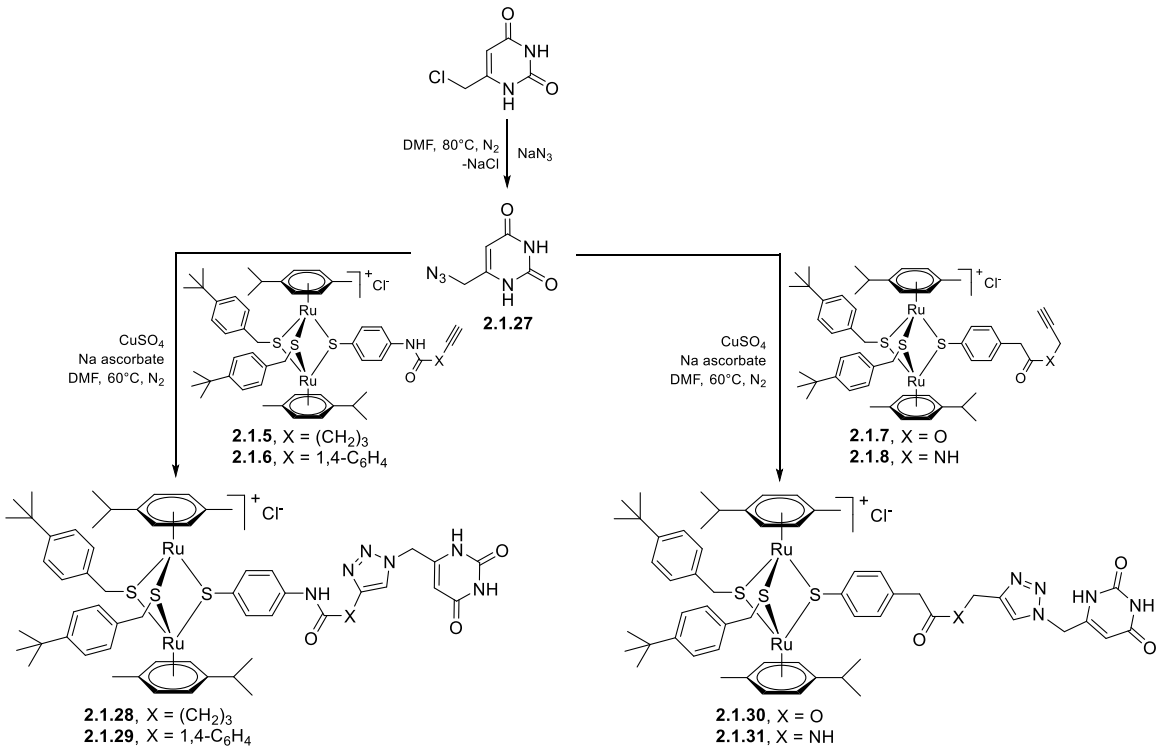

Scheme 2.1.7. Synthesis of azide uracil derivative **2.1.27** and of corresponding click conjugates **2.1.28**, **2.1.29**, **2.1.30** and **2.1.31**, using diruthenium alkyne intermediates **2.1.5**-**2.1.8**.

Uracil azide **2.1.27** was reacted with the alkyne containing diruthenium(II)-arene derivatives **2.1.5** and **2.1.6** (Scheme 2.1.7 (right)) in presence of $CuSO_4$ and sodium ascorbate[286, 297], which allowed the isolation of the corresponding click products **2.1.28** and **2.1.29** in low and medium yields of 31 and 73%, respectively. Similar conditions were applied in the reactions of **2.1.27** with alkyne derivatives **2.1.7** and **2.1.8** (Scheme 2.1.7 (left)) leading to the uracil click products **2.1.30** and **2.1.31** in low yields of 38 and 32%, respectively. Thus, the uracil azide **2.1.26** afforded the obtainment of various conjugates presenting different type of spacers (aliphatic **2.1.28** *vs* aromatic **2.1.29**), as well as ester (**2.1.30**) or amide bonds (**2.1.28**, **2.1.29**, **2.1.31**) (Scheme 2.1.7).

Adenine azide derivative **2.1.32** was synthesized in two steps starting from 9-(2-hydroxyethyl)adenine (**2.1.14A**) (Scheme 2.1.8). **2.1.32** was further coupled with the alkyne functionalized diruthenium compound **8** (Scheme 2.1.8), allowing the isolation of conjugate **2.1.33** in low yield (13%).

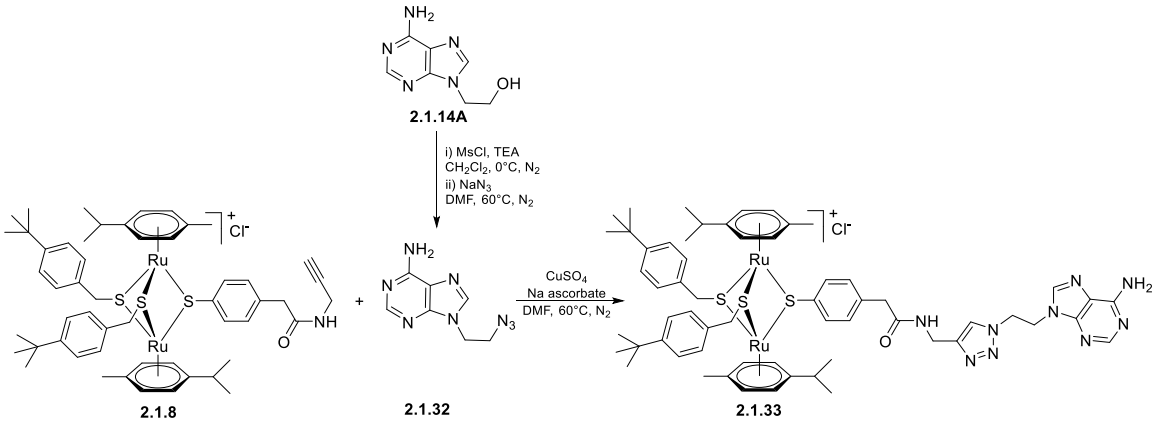

Scheme 2.1.8. Synthesis of the azide adenine derivative **2.1.32** and of the corresponding click conjugate **2.1.33**.

2.1.2.1.6. Synthesis of the compounds constituting family 5

To evaluate the importance of the nature of the substituent anchored on the diruthenium scaffold, a series of click conjugates of **2.1.9** and **2.1.10** with various substrates like ethynylbenzene and 4-ethynylbenzyl alcohol, propargyl alcohol and 2-ethynylpyridine was also synthesized (Scheme 2.1.9). The CuAAc click reactions were performed in similar conditions[286, 297]. If the phenyl derivative **2.1.34** was obtained in good yield (90%), the products with more polar substituents were isolated only in very low yields (6% for **2.1.35** and 19% for **2.1.36**).

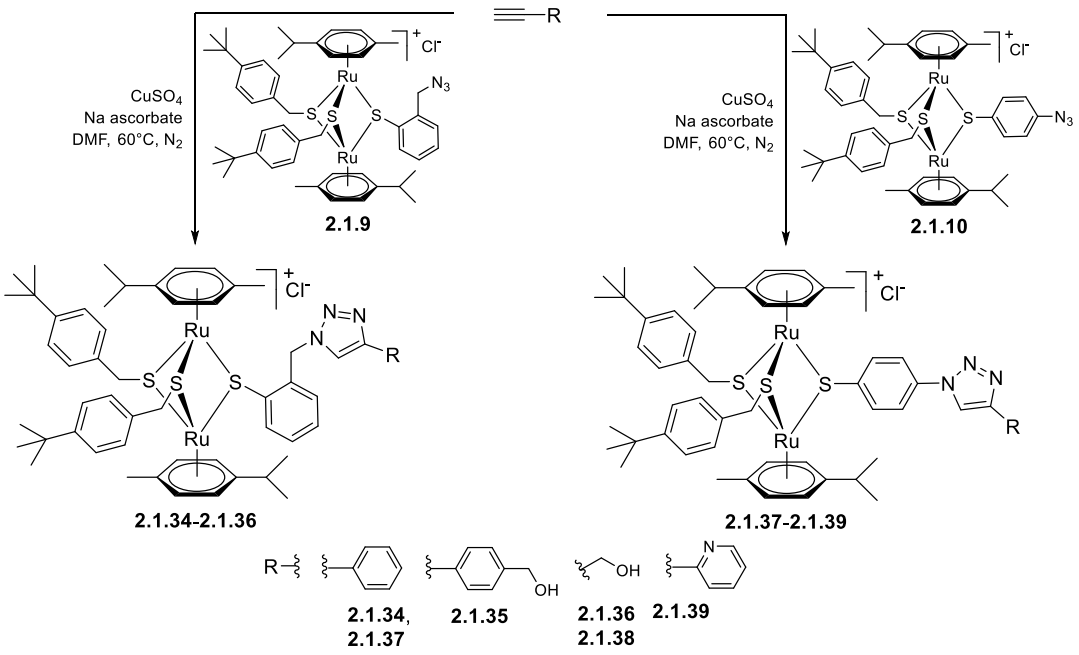

Scheme 2.1.9. CuAAC reactions of azide diruthenium derivatives **2.1.9** (left) and **2.1.10** (right) with ethynylbenzene, 4-ethynylbenzyl alcohol, propargyl alcohol and 2-ethynylpyridine.

A similar effect was observed in the reactions run using azide **2.1.10** as substrate. The phenyl click product **2.1.37** was isolated in high yield (79%), while the reactions with more polar ethynyl compounds were less performant and compounds **2.1.38** and **2.1.39** were isolated only with 26 and, respectively, 9% yield.

The compounds were fully characterized by and ^{1}H- and ^{13}C-NMR spectroscopy, ESI-MS and elemental analysis experiments (full description in *Supporting information 2.1*).

For the assessment of the biological activity, 1 mM stock solutions of all compounds were prepared in dimethylsulfoxide (DMSO), in which the compounds are well soluble and stable. ^{1}H-NMR spectra of conjugates **2.1.28**, **2.1.33** and **2.1.39** dissolved in DMSO-d_6, recorded at 25 °C 5 min and X days after sample preparation showed no visible changes (see *Supporting information 2.1.*), demonstrating very good stability of the compounds in this highly complexing solvent.

Furthermore, for evaluating the potential nucleobase-pairing H-bonding interactions of the compounds, ^{1}H-NMR measurements were performed using DMSO-d_6 solutions of uracil, thymine, cytosine and adenine conjugates **2.1.23**, **2.1.24**, **2.1.25** and **2.1.26** and corresponding pare nucleic bases (see details in *Supporting information 2.1.*). These tests confirmed the prominent stability of this type of conjugates in DMSO-d_6 and demonstrated the presence of week H-bonding interactions proved by some significant modifications of signals shape and chemical shift.

2.1.2.2. Antiparasitic activity assessment

The compounds (conjugates and respective intermediates) were subjected to a sequential biological screening. The antiparasitic activity (proliferation inhibition) was evaluated using *T. gondii* β-gal grown in HFF host cell monolayers and the cytotoxic effects were studied in non-infected HFF monolayers[29]. A first screening (Table 2.1.1 and Figure 2.1.2) of all compounds against *T. gondii* β-gal tachyzoites and HFF was carried out at 0.1 and 1 µM concentrations. In a second screening, the selected compounds (molecules that when applied at 1 µM inhibited *T. gondii*-β-gal proliferation by at least 90% and did not impair HFF viability by more than 50%) were submitted to dose response studies to determine the IC_{50} values, and potential cytotoxicity in HFF was assessed at 2.5 µM (results summarized in Table 2.1.2).

The antiparasitic activity of compounds **2.1.2**-**2.1.4** and **2.1.8** was previously reported[30, 131, 186] and the values are provided for comparison. The library of tested compounds included diruthenium intermediates **2.1.5**-**2.1.7**, **2.1.9** and **2.1.10**, thioxanthine derivative **2.1.13** (Family 1), adenine ester derivative **2.1.14** and its respective 9-(2-hydroxyethyl)adenine precursor **2.1.14A** (Family 2), nucleobase propargyl derivatives **2.1.15**-**2.1.18**, and their corresponding click conjugates **2.1.19**-**2.1.22** and **2.1.23**-**2.1.26** (Family 3), azide uracil and adenine compounds **2.1.27** and **2.1.32** and their respective conjugates **2.1.28**-**2.1.31** and **2.1.33** (Family 4), and hybrid molecules with other substituents **2.1.34**-**2.1.39** (Family 5). Compounds **2.1.11** and **2.1.12** still contained small impurities and were not suitable for bioactivity evaluation.

Table 2.1.1. Efficacy/cytotoxicity screening of compounds in non-infected HFF cultures and *T. gondii* β-gal tachyzoites cultured in HFF. Tests were realized in triplicate. The values of the compounds selected for determination of IC_{50} values against *T. gondii* β-gal are highlighted in bold.

Compound	**HFF viability (%)**		***T. gondii* β-gal growth (%)**	
	0.1 µM	**1 µM**	**0.1 µM**	**1 µM**
Ruthenium intermediates				
2.1.2[a]	**74 ± 2**	**48 ± 1**	**57 ± 1**	**2 ± 0**
2.1.3[a]	**93 ± 4**	**87 ± 1**	**114 ± 15**	**110 ± 32**
2.1.4[a]	**80 ± 1**	**69 ± 6**	**2 ± 0**	**1 ± 0**
2.1.5	**101 ± 0**	**96 ± 0**	**21 ± 2**	**0 ± 0**
2.1.6	**95 ± 1**	**49 ± 2**	**112 ± 6**	**1 ± 1**
2.1.7	**100 ± 2**	**53 ± 3**	**19 ± 1**	**0 ± 0**
2.1.8[a]	**71 ± 2**	**46 ± 6**	**52 ± 13**	**3 ± 1**
2.1.9	**96 ± 1**	**64 ± 1**	**9 ± 1**	**1 ± 0**
2.1.10	**94 ± 1**	**70 ± 1**	**10 ± 1**	**0 ± 0**
Family 1				
2.1.13	156 ± 1	102 ± 1	85 ± 2	179 ± 3
Family 2				
2.1.14A	136 ± 3	84 ± 14	75 ± 11	130 ± 2
2.1.14	**95 ± 11**	**76 ± 2**	**12 ± 1**	**1 ± 0**
Family 3				
2.1.15	107 ± 2	96 ± 2	109 ± 5	83 ± 0
2.1.16	100 ± 4	107 ± 7	354 ± 5	168 ± 6
2.1.17	96 ± 1	93 ± 1	111 ± 5	90 ± 7
2.1.18	96 ± 2	89 ± 3	117 ± 4	91 ± 6
2.1.19	**93 ± 2**	**85 ± 0**	**117 ± 7**	**7 ± 0**
2.1.20	**100 ± 2**	**71 ± 2**	**102 ± 0**	**1 ± 0**
2.1.21	**109 ± 0**	**89 ± 1**	**4 ± 0**	**0 ± 0**

Compound	HFF viability (%)		*T. gondii* β-gal growth (%)	
	0.1 µM	**1 µM**	**0.1 µM**	**1 µM**
2.1.22	**102 ± 0**	**77 ± 2**	**79 ± 3**	**1 ± 0**
2.1.23	**100 ± 1**	**76 ± 1**	**114 ± 4**	**1 ± 0**
2.1.24	**98 ± 10**	**96 ± 4**	**56 ± 15**	**0 ± 0**
2.1.25	94 ± 9	91 ± 8	82 ± 6	35 ± 7
2.1.26	**109 ± 2**	**76 ± 0**	**109 ± 6**	**0 ± 0**
Family 4				
2.1.27	**123 ± 16**	**111 ± 9**	**4 ± 0**	**3 ± 0**
2.1.28	101 ± 1	88 ± 1	97 ± 6	76 ± 5
2.1.29	101 ± 5	102 ± 1	102 ± 3	116 ± 5
2.1.30	**114 ± 0**	**112 ± 3**	**142 ± 3**	**7 ± 0**
2.1.31	99 ± 3	98 ± 6	109 ± 1	127 ± 23
2.1.32	104 ± 2	103 ± 3	103 ± 8	94 ± 2
2.1.33	84 ±6	71 ± 3	94 ± 11	83 ± 11
Family 5				
2.1.34	**96 ± 1**	**70 ± 1**	**7 ± 1**	**0 ± 0**
2.1.35	**89 ± 0**	**27 ± 1**	**1 ± 0**	**0 ± 0**
2.1.36	**115 ± 1**	**87 ± 2**	**7 ± 0**	**0 ± 0**
2.1.37	**99 ± 0**	**71 ± 0**	**13 ± 1**	**0 ± 0**
2.1.38	**104 ± 0**	**71 ± 1**	**42 ± 2**	**0 ± 0**
2.1.39	**94 ± 2**	**90 ± 1**	**14 ± 1**	**0 ± 0**

[a]Data for compounds **2.1.2**-**2.1.4** and **2.1.8** were previously reported[30, 131, 186].

From the diruthenium alkyne intermediates **2.1.5**, **2.1.6**, **2.1.7** and **2.1.8**, only derivative **2.1.5** presented reduced toxicity on HFF at 1 µM. The aromatic amide **2.1.6** and ester **2.1.7** intermediates were toxic to the host cells at 1 µM, and amide **2.1.8** affected HFF viability even at 0.1 µM. Unlike compound **2.1.6**, amide **2.1.5** exhibited an improved HFF toxicity and parasite efficacy profile compared with its amino diruthenium precursor **2.1.2**. Ester **2.1.7** and amide **2.1.8** affect more the proliferation of *T. gondii* β-gal than the carboxy precursor **2.1.3** but also exerted a stronger effect on the host cells viability.

The azide diruthenium intermediates **2.1.9** and **2.1.10** exhibited high activity against the parasite even at 0.1 µM but were toxic to HFF at 1 µM.

Within family 1, compound **2.1.13** with 2-thioxanthine as one of the bridges did not affect HFF viability but was only faintly active against the parasite at 1 µM.

The adenine ester conjugate **2.1.14** from family 2 had significantly improved antiparasitic activity compared to both its precursors **2.1.3** and **2.1.14A** (9-(2-hydroxyethyl)adenine), almost abolishing parasite growth at 1 µM, while exhibiting low HFF toxicity at the same concentration.

From the compounds of family 3, the uracil, thymine, cytosine and adenine

propargyl derivatives **2.1.15**, **2.1.16**, **2.1.17** and **2.1.18** had reduced toxicity on HFF but also low activity on *T. gondii* β-gal for both tested concentrations. The click conjugates **2.1.19-2.1.22** were all non-toxic to HFF when tested at 0.1 µM. However, thymine and adenine derivatives **2.1.20** and **2.1.22** impacted the host cell viability to a higher extent when tested at 1 µM (71 and 77%). While all four conjugates **2.1.19-2.1.22** almost abolished parasite proliferation at 1 µM, only cytosine conjugate **2.1.21** had a strong anti-antiparasitic effect at 0.1 µM. Compared to the diruthenium precursor **2.1.9**, conjugates **2.1.19-2.1.22** are less toxic on HFF at 1 µM, but with the exception of **2.1.21**, they are also less efficient against parasite proliferation at 0.1 µM.

Compounds **2.1.23-2.1.26** obtained from the azide compound **2.1.10**, did not affected HFF viability at 0.1 µM. However, uracil and adenine derivatives **2.1.23** and **2.1.26** presented a higher toxicity to the host cells at 1 µM (76% for both). Compared to its congeners, thymine functionalized compound **2.1.24** had a stronger antiparasitic effect at 0.1 µM, while cytosine derivative **2.1.25** had a low impact on parasite proliferation even at 1 µM. Nevertheless, compounds **2.1.23**, **2.1.24** and **2.1.26** bearing uracil, thymine and adenine, almost abolished parasite proliferation when applied at 1 µM. In comparison to the azide precursor **2.1.10**, nucleobase click conjugates **2.1.23-2.1.26** affected less the host cells viability at 1 µM, but were also less active on the parasite at 0.1 µM.

In Family 3, when comparing conjugates presenting the same nucleobase, cytosine derivatives **2.1.21** and **2.1.25** exhibited the most striking difference on *T. gondii* β-gal activity. While **2.1.21** almost abolished parasite proliferation when applied at 0.1 µM (4%), **2.1.25** exerted reduced antiparasitic efficacy even at 1 µM (35%). This indicates that the nature of the linker between the diruthenium scaffold and the nucleobase can strongly influence the activity.

From family 4, azidomethyl uracil derivative **2.1.27** was highly active on the parasite even at 0.1 µM, without affecting the parasite viability at 1 µM. The activity profile of **2.1.27** was in strong contrast with that of the uracil propargyl compound **2.1.15** which presented reduced efficacy against the parasite even at 1 µM. However, a certain similarity can be observed between the activity profile of **2.1.27** and that of the diruthenum azide derivatives **2.1.9** and **2.1.10**, suggesting that compounds containing azide groups could be an interesting way to follow for future development. Uracil conjugates **2.1.28-2.1.31** showed all reduced effect on HFF viability. Amide analogues **2.1.28**, **2.1.29** and **2.1.31** presented little efficacy against *T. gondii* β-gal even at 1 µM. Compound **2.1.29**, with a rigid aromatic linker, didn't exhibit antiparasitic effect at the tested concentrations, and a

similar outcome was observed for **2.1.31** presenting a short aliphatic connector. Compared to **2.1.31**, increased flexibility of the connecting side chain in **2.1.28** did not impact the effect on HFF but ameliorated the efficacy on the parasite at 1 µM. Compounds **2.1.30** and **2.1.31** containing an ester and, respectively, an amide bond in the linking unit, had little effect on the host cells at both tested concentrations as well as on the parasite at 0.1 µM. However, ester **2.1.30** presented a strong antiparasitic effect compared to amide **2.1.31** when applied at 1 µM, underlining the importance of the linker for the biological activity.

Uracil triazole conjugates **2.1.29**, **2.1.30** and **2.1.31** exerted lower toxicity to the host cells compared to respective alkyne intermediates **2.1.6**, **2.1.7** and **2.1.8**.

Relative to uracil derivative **2.1.31**, adenine functionalized compound **2.1.33** presented a slightly increased activity on the parasite but also higher toxicity on the host cells on both tested concentrations.

For compounds constituting family 5, interesting toxicity differences are observed between click compounds **2.1.34-2.1.36** obtained from the diruthenium azide intermediate **2.1.9**. Both compounds **2.1.34** and **2.1.35** containing an additional aromatic ring, and thus increased lipophilicity and rigidity, showed higher toxicity on HFF at 1 µM. Only derivative **2.1.36** with a short methylenehydroxy chain was active on the parasite while remaining non-toxic to the host cells.

Interestingly, phenyl derivative **2.1.37** presented a rather similar toxicity profile to its analogue **2.1.34** for a different mode of connection to the diruthenium moiety. However, this was not the case for derivatives **2.1.38** and **2.1.36** both presenting the same methylenehydroxy group as substituent. Compared to **2.1.36**, compound **2.1.38** exhibited an increased toxicity on HFF and a reduced efficacy on the parasite when applied at 0.1 µM. Relative to **2.1.37**, compound **2.1.39** bearing an electron deficient pyridine ring instead of a phenyl substituent, did not affect HFF viability while still presenting antiproliferative activity on the parasite. From family 5, compared to precursor diruthenium azides **2.1.9** and **2.1.10**, only click products **2.1.36** and **2.1.39** exhibited an improved toxicity profile to the host cells, while still being active on the parasite.

Analysing adenine conjugates **2.1.14**, **2.1.22**, **2.1.26** and **2.1.33**, the most promising candidate for further development is ester analogue **2.1.14**. This underlines the importance of the linking unit on the activity of the hybrid molecules.

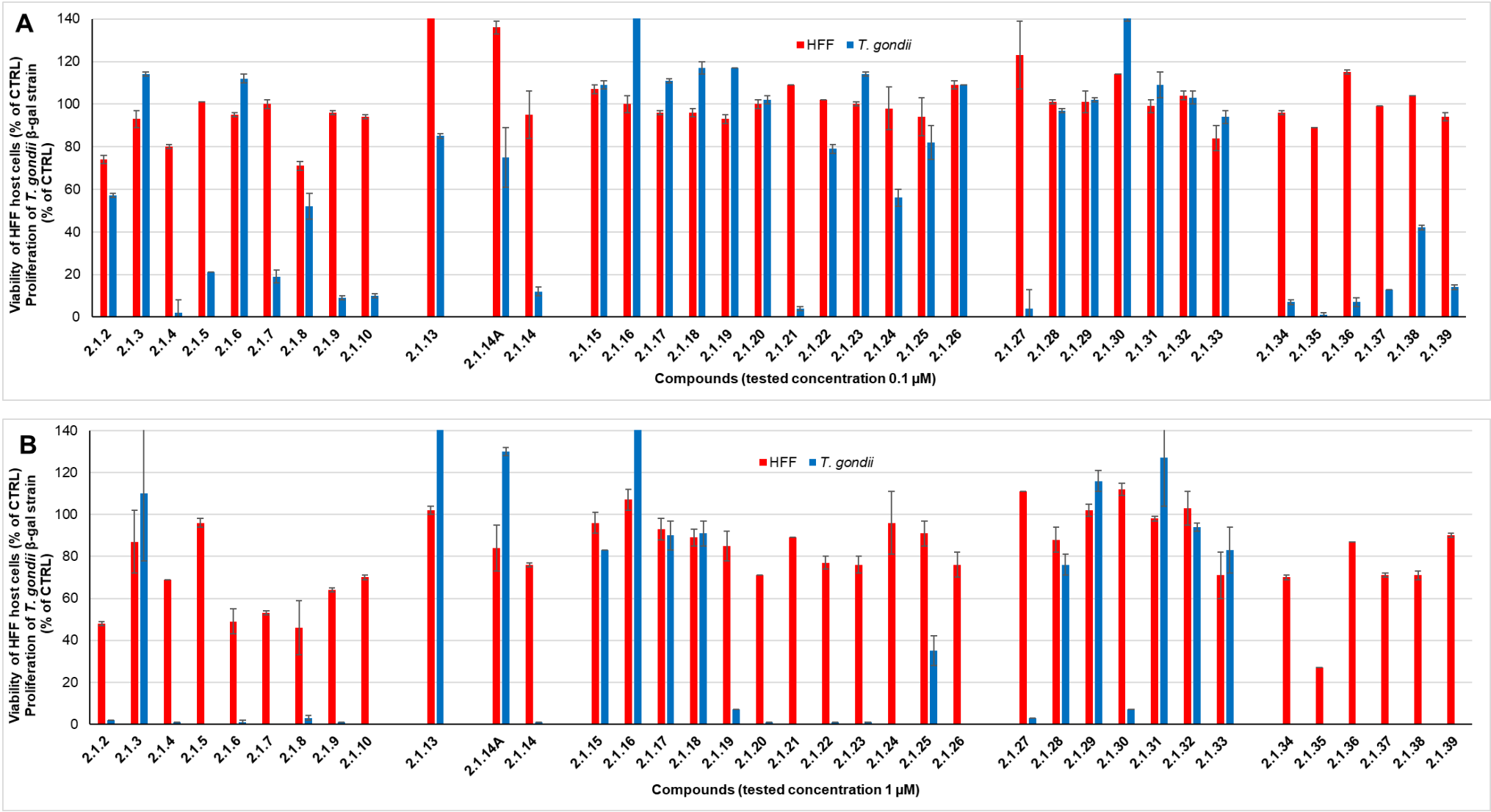

Figure 2.1.2. Clustered column chart showing the *in vitro* activities at 0.1 (A) and 1 µM (B) of the 37 tested compounds on HFF viability and *T. gondii* β-gal proliferation. Non-infected HFF monolayers treated only with 0.1% DMSO exhibited 100% viability and 100% proliferation was attributed to *T. gondii* β-gal tachyzoites treated only with 0.1% DMSO. Blue bars represent viability values of HFF, and red bars represent proliferation of *T. gondii* β-gal tachyzoites. For each assay, standard deviations were calculated from triplicates and are displayed on the graph. Data for compounds **2.1.2**-**2.1.4** were previously reported[30, 131, 186].

The uracil conjugates **2.1.19**, **2.1.23**, **2.1.28**, **2.1.29**, **2.1.30** and **2.1.31** exhibited reduced toxicity to HFF at 1 µM but also limited activity on the parasite at 0.1 µM. Compounds **2.1.19**, **2.1.23** and **2.1.30** presented anti-proliferative properties on the parasite only at 1 µM, while **2.1.28**, **2.1.29** and **2.1.31** showed reduced antiparasitic activity even at this concentration.

The data obtained after the first screening indicate that the nature of the anchored moiety (nucleobase or not), as well as that of the connector appear to strongly influence the antiparasitic activity compared to the toxicity on the host cells. 25 compounds fulfilled our selection criteria (compounds that when applied at 1 µM inhibited *T. gondii*-β-gal proliferation by at least 90% and did not impair HFF viability by more than 50%) and were submitted to a secondary screening consisting in dose response studies to determine the IC_{50} values on *T. gondii* β-gal, and toxicity in host cells assessed at 2.5 µM (Table 2.1.2).

Table 2.1.2. IC_{50} (μM) values for *T. gondii* β-gal and viability of HFFs (%) at 2.5 μM for the 25 selected compounds.

Compounds	*T. gondii* β-gal IC_{50} (μM)	[LS; LI][d]	SE[e]	HFF viability at 2.5 μM (%)[f]	SD[g]
Pyrimethamine	0.326	[0.396; 0.288]		99	6
Ruthenium intermediates					
2.1.2[a]	0.153	[0.127; 0.185]	0.138	51	5
2.1.3[a]	0.181	[1.482; 0.274]	2.700	9	2
2.1.4[b]	0.038	[0.059; 0.024]	0.324	4	1
2.1.5	0.038	[0.179; 0.134]	0.180	34	1
2.1.6	0.288	[0.348; 0.239]	0.187	17	1
2.1.7	0.289	[0.364; 0.230]	0.148	51	3
2.1.8[c]	0.042	[0.049; 0.036]	0.123	48	7
2.1.9	0.048	[0.058; 0.040]	0.139	11	1
2.1.10	0.065	[0.081; 0.052]	0.143	38	1
Family 2					
2.1.14	0.059	[0.086; 0.040]	0.224	76	3
Family 3					
2.1.19	0.598	[0.598; 0.598]	0	50	0
2.1.20	0.363	[0.371; 0.354]	0.015	39	1
2.1.21	0.046	[0.058; 0.037]	0.138	38	1
2.1.22	0.108	[0.141; 0.083]	0.188	52	1
2.1.23	0.440	[0.440; 0.440]	0	64	1
2.1.24	0.357	[0.418; 0.305]	0.158	85	4
2.1.26	0.178	[0.226; 0.140]	0.174	45	2
Family 4					
2.1.27	0.284	[0.688; 0.117]	0.701	92	2
2.1.30	0.659	[0.684; 0.635]	0.053	97	1
Family 5					
2.1.34	0.093	[0.108; 0.079]	0.110	3	0
2.1.35	0.047	[0.062; 0.037]	0.159	0	0
2.1.36	0.111	[0.135; 0.091]	0.111	77	1
2.1.37	0.096	[0.122; 0.076]	0.162	52	1
2.1.38	0.128	[0.164; 0.099]	0.167	59	1
2.1.39	0.075	[0.091; 0.061]	0.123	1	0

[a]Compound reported in ref.[131] [b]Compound reported in ref.[30] [c]Compound reported in ref.[186] [d]Values at 95% confidence interval (CI); LS is the upper limit of CI and LI is the lower limit of CI. [e]Standard error of the regression (SE), represents the average distance at which the measured values fall from the regression line. [f]Control HFF cells treated only with 0.25 % DMSO exhibited 100% viability. [g]Standard deviation of the mean (six replicate experiments).

From the diruthenium intermediates only amine **2.1.2**, propargyl ester **2.1.7** and amide **2.1.8** exhibited medium toxicity on HFF at 2.5 µM (respectively, 51, 51 and 48%). all other intermediates compounds were highly toxic on the host cells at this tested concentration. However, an interesting IC_{50} value difference was observed between ester **2.1.7** and amide **2.1.8** (0.289 *vs* 0.042 µM) for a similar effect on HFF.

Adenine ester derivative **2.1.14** from family 2 was the most promising of the series with an IC_{50} value of 0.059 µM (5 time lower than that measured for the standard drug pyrimethamine, IC_{50} = 0.326 µM), while still being weakly toxic for the host cells at 2.5 µM (a concentration 40 times higher compared to its IC_{50}).

From Family 3, only click conjugates **2.1.19**, **2.1.22**, **2.1.23** and **2.1.24** presented medium or lower toxicity on the host cells. Adenine compound **2.1.22** exhibited a promising IC_{50} value of 0.108 µM but also affect HFF viability (52%). Uracil and thymine click derivatives **2.1.23** and **2.1.24** had a lower influence on the host cells viability (64 and 85%) but presented IC_{50} values higher or comparable to pyrimethamine (0.440 and 0.357 µM).

Uracil derivatives **2.1.27** (azide intermediate) and **2.1.30** (click compound presenting an ester bond) do not affect host cells viability at 2.5 µM (92 and 97%) but exhibited also elevated IC_{50} values (0.284 and 0.659 µM). A significant difference in HFF toxicity was noticed between the diruthenium azides **2.1.9** and **2.1.10**, and uracil azide derivative **2.1.27** at 2.5 µM (11 and 38% *vs* 92%).

From the click products with other types of ethynyl derivatives (Family 5), compounds **2.1.34**, **2.1.35** and **2.1.39** were highly toxic on the HFF at 2.5 µM. The way in which the groups are linked to the diruthenium scaffold appears to be important as phenyl analogue **2.1.34** was significantly more toxic to the host cells compared to **2.1.37** (3 *vs* 52%). However, the differences between the hydroxymethylene compounds **2.1.36** and **2.1.38** were less important both in terms of IC_{50} values on *T. gondii* β-gal (0.111 *vs* 0.128 µM) and toxicity to the HFF (77 *vs* 59%).

No striking SAR (structure-activity relationships) could be identified. Both the attached unit and the connector pay an important role. The most interesting compounds identified which can be considered for further studies are adenine ester **2.1.14** and the click product with an hydroxymethylene substituent **2.1.36**.

The mechanism of action of the trithiolato diruthenium compounds is not yet completely established. This type of compounds show general low water solubility[64] and contrary to other Ru(II) complexes presenting labile chlorine or carboxylate ligands, they

do not hydrolyze and are stable in the presence of most biomolecules like amino acids and DNA. Only the oxidation of cysteine (Cys) and glutathione (GSH) to form cystine and GSSG, respectively, was observed in the presence of some compounds, but no correlation between the *in vitro* cytotoxicity and the catalytic activity on the oxidation reaction of glutathione was observed[38, 65].

Recently, inductively coupled plasma mass spectrometry (ICP-MS) experiments proved that complexes **2.1.M** and **2.1.N** (Figure 2.1.1) specifically target the mitochondrion in A2780 ovarian cancer cells[33]. Noteworthy, TEM (transmission electron microscopy) studies of various parasites (*Toxoplasma gondii*, *Neospora caninum*, *Trypanosoma brucei*) treated with dinuclear ruthenium(II) complexes revealed alterations in the mitochondrial ultrastructure pointing out this organelle as potential target[29, 33, 63].

2.1.3. Conclusions

This study was focused on the synthesis and antiparasitic activity assessment of nucleobase-tethered trithiolato-bridged dinuclear ruthenium(II)-arene compounds, aiming to exploit the parasite auxotrophies and metabolic peculiarities regarding this type of metabolites. Various types of structures and synthetic strategies were proposed and evaluated, leading to the isolation of 17 diruthenium moiety-nucleobase hybrid molecules. To assess the nucleobase-conjugate strategy, 6 derivatives presenting other type of anchored molecules were also obtained and tested. CuAAC click reactions proved a useful method for the post-functionalization of trithiolato diruthenium compounds with various substrates including nucleobase derivatives. The organometallic fragment could be used both as alkyne and azide group bearing partner and allowed the isolation of 19 new click conjugates. This strategy can be extended to develop other thiolato-bridged ruthenium(II)-arene conjugates in a more convenient manner and can eventually be used to construct larger libraries of compounds.

However, in view of the results presented in this study, targeting the parasite metabolic pathways using nucleobase conjugates of the trithiolato diruthenium derivatives does not appear as a very promising approach. In the used *in vitro* biological activity assessment, the hybrid molecules presenting nucleobase units did not necessarily performed better compared to conjugates presenting other type of substituents. However, the antiparasitic activity and the toxicity on the host cells were influenced not only by the nature of the molecule appended to the diruthenium scaffold but also by type of the connection between the two moieties.

Compounds **2.1.14**, an adenine ester conjugate, and **2.1.36**, a click product presenting an hydroxymethylene substituent, exhibited interesting IC_{50} values on *T. gondii* β-gal of 0.059 and 0.111 µM, respectively, with only medium toxicity to HFF, and these hybrid molecules deserve further investigations.

2.1.4. Experimental

2.1.4.1. Chemistry

The chemistry experimental part, with full description of experimental procedures and characterization data for all compounds, is presented in the *Supporting information 2.1*.

2.1.4.2. In vitro activity assessment against T. gondii tachyzoites and HFF

All tissue culture media were purchased from Gibco-BRL, and biochemical agents from Sigma-Aldrich. Human foreskin fibroblasts (HFF) were purchased from ATCC, maintained in DMEM (Dulbecco's Modified Eagle's Medium) supplemented with 10% fetal calf serum (FCS, Gibco-BRL, Waltham, MA, USA) and antibiotics as previously described[28]. Transgenic *T. gondii* β-gal (expressing the β-galactosidase gene from *Escherichia coli*) were kindly provided by Prof. David Sibley (Washington University, St. Louis, MO, USA) and were maintained, isolated, and prepared for new infections as shown before[28, 117]. All the compounds were prepared as 1 mM stock solutions from powder, in dimethyl sulfoxide (DMSO, Sigma, St. Louis, MO, USA). For *in vitro* activity and cytotoxicity assays, HFF were seeded at $5x10^3$/well and allowed to grow to confluence in phenol-red free culture medium at 37°C and 5% CO_2. Transgenic *T. gondii* β-gal tachyzoites were isolated and prepared for infection as described[115]. *T. gondii* tachyzoites were released from host cells, and HFF monolayers were infected with freshly isolated parasites ($1x10^3$/well), and compounds were added concomitantly with infection. In the primary screening, HFF monolayers infected with *T. gondii* β-gal received 0.1 and 1 µM of each compound, or the corresponding concentration of DMSO (0.01 or 0.1% respectively) as controls and incubated for 72 h at 37˚C/5% CO_2 as previously described[62]. For the next step, IC_{50} measurements for *T. gondii* β-gal were performed. The selected compounds were added concomitantly with infection in 8 serial concentrations 0.007, 0.01, 0.03, 0.06, 0.12, 0.25, 0.5, and 1 µM. After a period of 72 h of culture at 37°C/5% CO_2, culture medium was aspirated, and cells were permeabilized by adding 90 µL PBS (phosphate buffered saline) with 0.05% Triton X-100. After addition of 10 µL 5 mM chlorophenolred-β-D-galactopyranoside (CPRG; Roche Diagnostics, Rotkreuz,

Switzerland) in PBS, the absorption shift was measured at 570 nm wavelength at various timepoints using an EnSpire® multimode plate reader (PerkinElmer, Inc, Waltham, MA, USA). For the primary screening at 0.1 and 1 μM, activity was measured as the release of chlorophenol red over time, was calculated as percentage from the respective DMSO control, which represented 100% of *T. gondii* β-gal growth. For the IC_{50} assays, the activity measured as the release of chlorophenol red over time was proportional to the number of live parasites down to 50 per well as determined in pilot assays. IC_{50} values were calculated after the logit-log-transformation of relative growth and subsequent regression analysis. All calculations were performed using the corresponding software tool contained in the Excel software package (Microsoft, Redmond, WA, USA). Cytotoxicity assays using uninfected confluent HFF host cells were performed by the alamarBlue assay as previously reported[118]. Confluent HFF monolayers in 96 well-plates were exposed to 0.1, 1 and 2.5 μM of each compound. Non-treated HFF as well as DMSO controls (0.01%, 0.1% and 0.25%) were included. After 72 h of incubation at 37°C/5% CO_2, the medium was removed, and plates were washed once with PBS. 200 μL of Resazurin (1:200 dilution in PBS) were added to each well. Plates were measured at excitation wavelength 530 nm and emission wavelength 590 nM at the EnSpire® multimode plate reader (PerkinElmer, Inc). Fluorescence was measured at different timepoints. Relative fluorescence units were calculated from timepoints with linear increase.

2.2. Trithiolato-Bridged Ruthenium(II)-Arene Complexes Bearing Lipophilic Moiety[4]

Abstract

Trithiolato-bridged dinuclear ruthenium(II)-arene complexes were shown to be active against various protozoan parasites including *Toxoplasma gondii*. Attaching metabolites to the diruthenium scaffold could constitute a promising strategy to improve cellular uptake and targeting of the organometallic compound. Lipids, isoprenoids and lipoate represent important metabolites scavenged by *T. gondii* from the host cell but also synthesized by the parasite to support its rapid growth, and this type of molecules constitute interesting units to attach to organometallic compounds in a conjugate approach. The synthesis and anti-*Toxoplasma* activity of 26 new trithiolato-bridged ruthenium(II)-arene complexes bearing various lipophilic appendages are reported. The influence of several structural elements as the nature of the organic unit (lipoic acid, isoterpenoids, acids with saturated and unsaturated chains of various length) as well as the type of the connecting bond upon the conjugates biological properties was examined. In a primary screening, the compounds antiparasitic efficacy and cytotoxicity were assessed against transgenic *T. gondii* tachyzoites constitutively expressing β-galactosidase and on human foreskin fibroblasts (HFF) used as host cells at two concentrations (0.1 and 1 µM). In a secondary screening, 10 conjugates were submitted to dose-dependence measurements (*T. gondii* IC_{50} (half maximal inhibitory concentration) determination). No clear SAR (structure-activity relationship) could be identified. Two hybrid molecules, namely butyric and myristic esters **2.2.11a** and **2.2.14a**, exhibited high efficacy in inhibiting parasite proliferation (IC_{50} values 0.036 and 0.135 µM, respectively), while maintaining a medium-low toxicity to the parasite (HFF viability 72 and 78%, correspondingly, for compounds applied at 2.5 µM), and deserve further attention.

[4] This chapter is a draft with title *Lipophilic trithiolato-bridged dinuclear ruthenium(II)-arene conjugates*, which is going to be submitted for publication. Supplementary information can be found in the chapter *Supporting information 2.2*. (Published as: Trithiolato-bridged dinuclear ruthenium(II)-arene conjugates tethered with lipophilic units: Synthesis and *Toxoplasma gondii* antiparasitic activity *Journal of Organometallic Chemistry*, 986, 2023, 122624, https://doi.org/10.1016/j.jorganchem.2023.122624).

2.2.1. Introduction

Toxoplasma gondii is an obligate intracellular parasite belonging to the phylum Apicomplexa that infects all warm-blooded animals, including humans. Drug treatment for toxoplasmosis is not satisfactory and is threatened by resistance[17, 194, 195].

Trithiolato-bridged dinuclear ruthenium(II)-arene complexes (general formula $[(\eta^6\text{-arene})_2Ru_2(\mu_2\text{-SR})_3]^+$ symmetric and $[(\eta^6\text{-arene})_2Ru_2(\mu_2\text{-SR}^1)_2(\mu_2\text{-SR}^2)]^+$ mixed, as compounds **2.2.L1**/**2.2.L2** and **2.2.M** in Figure 2.2.1) proved to be an interesting scaffold for drug discovery. This type of compounds were shown to be not only highly cytotoxic against human cancer cells[64] but also efficient against various protozoan parasites, such as *Toxoplasma gondii*[29], *Neospora caninum*[33] and *Trypanosoma brucei*[63]. The half-maximal proliferation inhibitory concentrations (IC_{50}) of complexes **2.2.L1** (R = Me), **2.2.L2** (R = Bu^t) and **2.2.M** against *in vitro* cultured *T. gondii* tachyzoites were 34, 62 and 1 nM, respectively, and these compounds did not impair the viability of human foreskin fibroblast (HFF) host cells[29].

The auxotrophies and metabolic defects in *T. gondii* can be exploited as therapeutic approaches[201]. *T. gondii* can replicate in every nucleated host cell by orchestrating metabolic interactions to derive crucial nutrients as for example lipids[300, 301]. *T. gondii* is an avid scavenger of lipids retrieved from the host cell[302] and apicoplast fatty acid synthesis is essential for organelle biogenesis and parasite survival[303]. Fatty acids have a multitude of biological functions being used not only as important molecules for energy storage but also as building blocks of membranes. Following lipid uptake, this parasite stores excess lipids in lipid droplets. Supplemental unsaturated fatty acids (oleic, palmitoleic, linoleic) accumulate in large lipid droplets and impair parasite replication, whereas saturated fatty acids (palmitic, stearic) neither stimulate lipid droplets formation nor impact growth. Depending to its growth and survival needs, the parasite synthesizes lipids or adeptly acquires/scavenges them from the host environment[201, 304-307]. *T. gondii* reliance on host lipid resources can open new pathways to restrict parasite growth[302, 304]. The parasite uncontrolled uptake of unsaturated fatty acids and its vulnerability to lipid storage inhibition have been suggested as potential approaches to be used against the parasite[201, 302]. *T. gondii* diverts a large variety of lipid precursors from host cytoplasm and efficiently manufacture them into complex lipids. Parasite starvation can be induced upon deprivation from essential host lipids. Lipid analogues with anti-proliferative properties can be taken up by the parasites, which results in parasite membrane defects, and ultimately death.

Conjugating the trithiolato-bridged diruthenium organometallic unit with metabolites/nutrients for which the parasite shows high affinity constitutes an interesting approach aiming to the obtainment of compounds with improved properties in terms of selectivity and antiparasitic efficacy. The diruthenium complexes are highly stable and can be easily derivatized at the level of bridge thiols by complex post-functionalization[61, 62, 131, 186].

In this study, the versatility of the trithiolato diruthenium unit for modification with different lipophilic derivatives which are relevant to *T. gondii* survival and growth was challenged[201]. The metabolites and final products that are both scavenged and synthesized by *Toxoplasma* comprise lipids and isoprenoids (as farnesol and geranylgeraniol)[201]. Lipoate represents a unique case of 'auxotrophy' because this cofactor, although synthesized and taken up by the parasite, is used for separate functions according to its origin[201].

The pool of lipophilic molecules considered for the modification of the organometallic unit include lipoic acid, isoprenoinds (geraniol, farnesol and geranylgeraniol) as well as various carboxylic acids with medium and long saturated and unsaturated chains.

Conjugation with lipophilic compounds gave interesting results in the case of various organometallic compounds with potential applications as anti-cancer drugs.

The requirement for safer drugs, i.e. for compounds with larger therapeutic windows/less toxicity, has stimulated research into platinum drug delivery strategies[58, 308], such as incorporating in liposomal nanoparticles[309-312] and the development of platinum(IV) prodrugs that are reduced to active platinum(II) compounds post cell-internalization[313]. Various active Pt(II) and Pt(IV) complexes presenting lipophilic units as ligands or attached to ligands have been reported[314-319]. An example is miriplatin (**2.2.A** in Figure 2.2.1), a platinum(II) fatty acid conjugate which was approved for the treatment of hepatocellular carcinoma in Japan in 2009[320-322].

Another example is derivative **2.2.B** (Figure 2.2.1), from a series of Pt(IV) complexes bearing a hydrophobic unbranched aliphatic chain of different length. **2.2.B** exhibited not only higher activity compared to cisplatin on various cancer cell lines but also improved selectivity for cancer cells compared to normal cells, the effect being influenced by the length of the hydrophobic chains[315, 323]. Similarly, Pt(IV) compound **2.2.C** (Figure 2.2.1) bearing two units of octanoic acid as axial ligands, showed high activity against various cisplatin sensitive and resistant cell lines and enhanced

efficacy compared to less lipophilic compounds[316, 324].

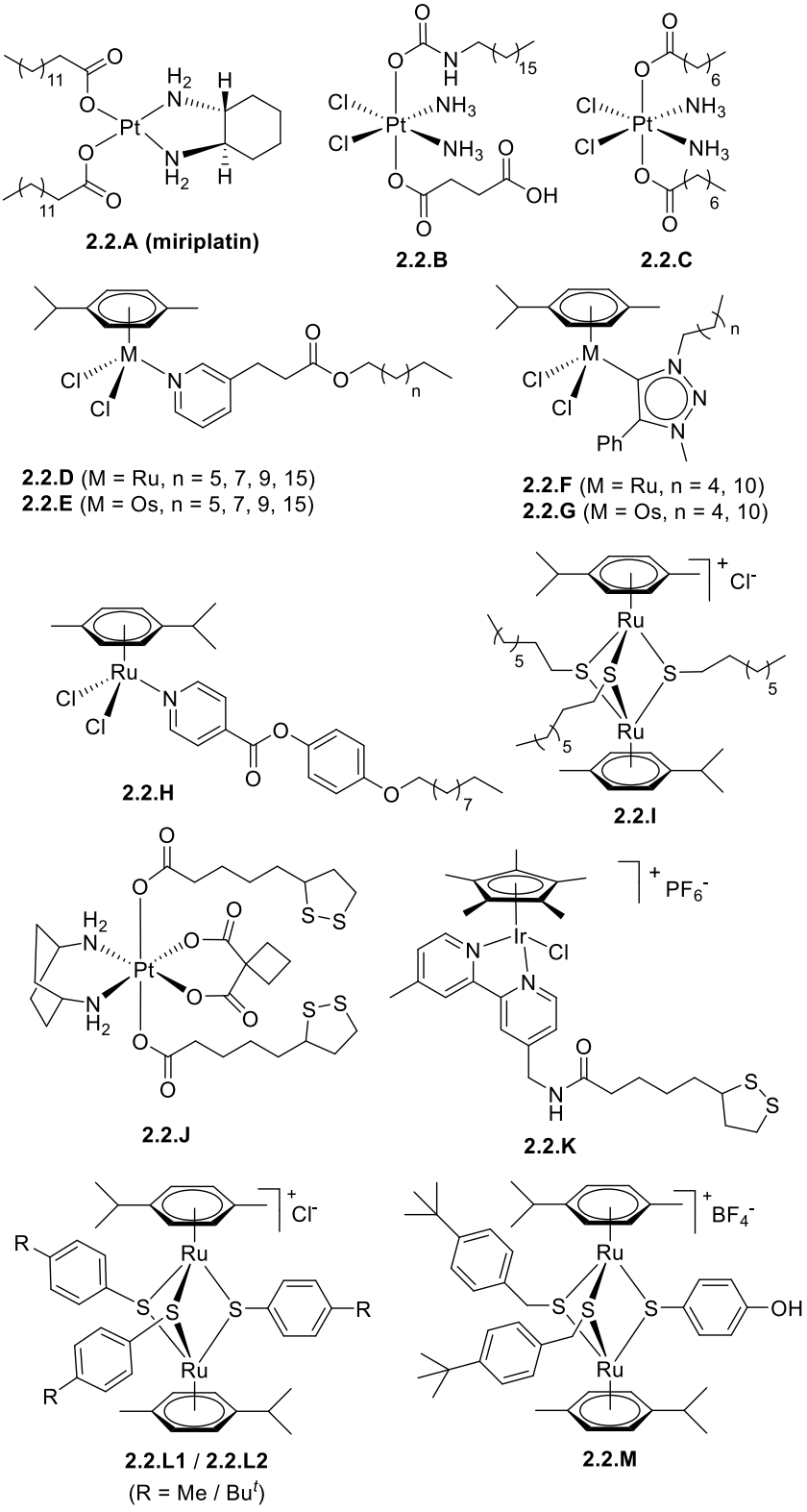

Figure 2.2.1. Structure of miriplatin (**2.2.A**), of Pt(IV) complexes with liphophilic substituents **2.2.B** and **2.2.C**, of Ru(II)- and Os(II)-arene complexes with lipophilic chains **2.2.D**-**2.2.H**, of the trithiolato dinuclear ruthenium(II)-arene complex **2.2.I** with lipophilic ligands, of Pt(IV) and Ir(III) conjugates with lipoic acid **2.2.J** and **2.2.K**, and of trithiolato dinuclear ruthenium(II)-arene complexes **2.2.L1**/**2.2.L2** and **2.2.M** exhibiting anti-*Toxoplasma* activity.

Various examples of ruthenium and osmium complexes bearing lipophilic substituents were also reported[325]. The cytotoxicity of a library of pyridine ligands modified with long alkyl chain and their corresponding complexes (**2.2.D**, Figure 2.2.1) has been assessed on a panel of cancer cell[325]. Both complexes and ligands with shorter alkyl chains (n = 5, 7), showed generally poor activity against cancerous and non-cancerous cells. The complex with n = 9 was active in some cell lines and also moderately toxic against non-tumourigenic HEK293 cells and showed increased cytotoxicity under mild hyperthermia (2 h cellular treatment at 41°C). The ruthenium complex with the longest alkyl chain (n = 15), showed general low activity at 37°C but exhibited good thermoactivity[325]. A similar lack of cytotoxicity was observed for the analogue series of osmium complexes **2.2.E** (M = Os) (Figure 2.2.1)[326]. Compounds **2.2.D** and **2.2.E** were less cytotoxic than other ruthenium and osmium(II)-arene complexes that contain hydrophobic chains, such as those with 1,2,3-triazolylidene-*N*-heterocyclic carbine ligands modified with *n*-hexyl and *n*-dodecyl aliphatic chains **2.2.F** and **2.2.G** (Figure 2.2.1) which exhibited low-micromolar IC_{50} values against a range of human cancer cell lines[327].

Likewise, complexes like **2.2.H** (Figure 2.2.1) exhibited very high cytotoxicity in both cisplatin sensitive and resistant cancer cells[328]. In this case, the efficacy in inhibiting cancer cells proliferation was considered to be due to the long-chain isonicotinic ester group seen that the analogous pyridine complex [(η^6-*p*-$MeC_6H_4Pr^i$)Ru(Py)Cl_2] was inactive under comparable conditions while the free ligand presented low IC_{50} values[328].

Trithiolato diruthenium complex **2.2.I** (Figure 2.2.1), presenting octane-1-thiols as bridges between the two Ru(II)-arene units[329], was highly cytotoxic (IC_{50} values in the nanomolar range on cisplatin sensitive and resistant cancer cells) and exhibited a slight selectivity for cancer cells over the model healthy cells.

Lipoic acid-platinum(IV) conjugate **2.2.J** (Figure 2.2.1)[330], prodrug is based on the Pt(II) complex kiteplatin with two α-lipoic acid units attached in axial positions exhibited increased activity compared to the reference kiteplatin on various cancer cell lines. However, half-sandwich Ir(III) complex **2.2.K** (Figure 2.2.1) also functionalized with α-lipoic acid on a bidentate 2,2-bipyridine leg ligand showed no cytotoxicity on various cancer cell lines, which was associated to its low lipophilicity for hard penetration into the cancer cells, easy hydrolysis, and reaction with GSH[331].

Various NAMI-A-like Ru(III) cytotoxic complexes were developed as highly functionalized lipidic structures, aimed to ensure both efficient protection against extracellular degradation and high cellular internalization of the metal[269, 332, 333].

The aims of this study were the development of a library of trithiolato-bridged ruthenium(II)-arene complexes with appended lipophilic substituents of different types (e.g., medium chain carboxylic acids, lipoic acid, isoprenoids) and the evaluation of the conjugates antiparasitic efficacy. Different structural variations as the type of connection (ester *vs.* amide), or the presence and the number of double bonds in the chains were addressed. The new diruthenium conjugates and associated intermediates, as well as the lipophilic compounds, were screened *in vitro* against *T. gondii* tachyzoites expressing β-galactosidase (*T. gondii* β-gal) grown in human foreskin fibroblasts (HFF) with complementary assessment of HFF viability using alamarBlue assay. The compounds exhibiting promising antiparasitic activity and selectivity were further subjected to dose-response (IC_{50} determination) on *T. gondii* β-gal.

2.2.2. Results and discussion

2.2.2.1. Chemistry

The synthesis of the carboxy, hydroxy and amino diruthenium intermediates **2.2.1**-**2.2.3** (Schemes 2.2.1-2.2.3), and that of the respective ethyl ester **2.2.7a** ([(η^6-*p*-$MeC_6H_4Pr^i$)$_2$$Ru_2$($\mu_2$-$SCH_2C_6H_4$-*p*-$Bu^t$)$_2$($\mu_2$-$SC_6H_4$-*p*-$CH_2CO_2Et$)]Cl), and of the acetic acid ester **2.2.10a** ([(η^6-*p*-$MeC_6H_4Pr^i$)$_2$$Ru_2$($\mu_2$-$SCH_2C_6H_4$-*p*-$Bu^t$)$_2$($\mu_2$-$SC_6H_4$-*p*-OAc)]Cl) and amide **2.2.10b** ([(η^6-*p*-$MeC_6H_4Pr^i$)$_2$$Ru_2$($\mu_2$-$SCH_2C_6H_4$-*p*-$Bu^t$)$_2$($\mu_2$-$SC_6H_4$-*p*-NHAc)]Cl) were reported previously[30, 62, 131].

The first series of ester conjugates **2.2.4a**-**2.2.6a** and **2.2.8a** were synthesized by reacting diruthenium carboxy intermediate **2.2.1** (same as **1.1.4a**) with the terpenoids geraniol (**2.2.4**), farnesol (**2.2.5**) and geranylgeraniol (**2.2.6**), and with *n*-butanol (**2.2.8**) in the presence of EDCI (*N*-(3-dimethylaminopropyl)-*N′*-ethylcarbodiimide hydrochloride) as coupling agent and DMAP (4-(dimethylamino)pyridine) as basic catalyst, the compounds being isolated in 36-61% yield (Scheme 2.2.1). Similar reaction conditions were used for the obtainment of the second series of ester conjugates **2.2.9a** and **2.2.11a**-**2.2.17a**, synthesized by the reaction of trithiolato diruthenium hydroxy derivative **2.2.2** (same as **1.1.2a**) with lipoic (**2.2.9**), butyric (**2.2.11**), hexanoic (**2.2.12**), decanoic (**2.2.13**), myristic (**2.2.14**), stearic (**2.2.15**), oleic (**2.2.16**) and elaidic (**2.2.17**) acids, respectively, the compounds being isolated in 58-88% yields (Scheme 2.2.2).

The amide derivatives **2.2.9b** and **2.2.11b**-**2.2.17b** and **2.2.18**-**2.2.20**, were obtained by the reaction of the diruthenium amino derivative **2.2.3** (same as **1.1.3a**) with lipoic (**9**), butyric (**11**), hexanoic (**2.2.12**), decanoic (**2.2.13**), myristic (**2.2.14**), stearic (**2.2.15**), oleic (**2.2.16**) and elaidic (**2.2.17**), linoleic (**2.2.18**), α-linolenic (**2.2.19**) and γ-linolenic (**2.2.20**) acids, in the presence of EDCI and HOBt (1-hydroxybenzotriazol) as coupling agents, in basic conditions (DIPEA, *N*,*N*-diisopropylethylamine) (Scheme 2.2.3). The compounds were isolated in 48-91% yields. Reactions of diruthenium hydroxy derivative **2.2.2** with the fatty acids presenting more than one double bond were also attempted but the ester conjugates could not be isolated pure due to important degradation occurred during the purification process.

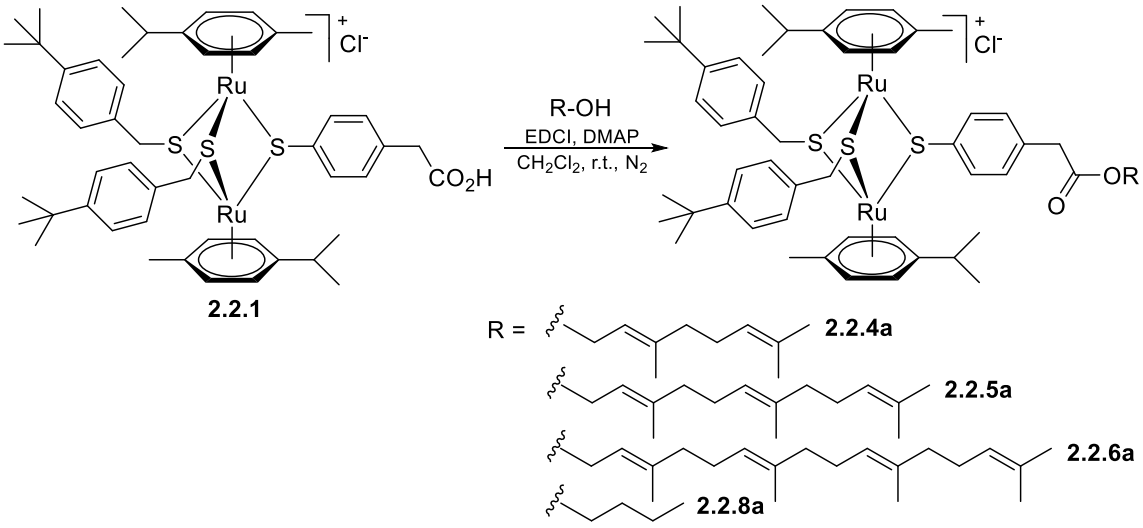

Scheme 2.2.1. Synthesis of the first series of ester derivatives **2.2.4a**-**2.2.6a** and **2.2.8a** starting from diruthenium carboxy intermediate **2.2.1**.

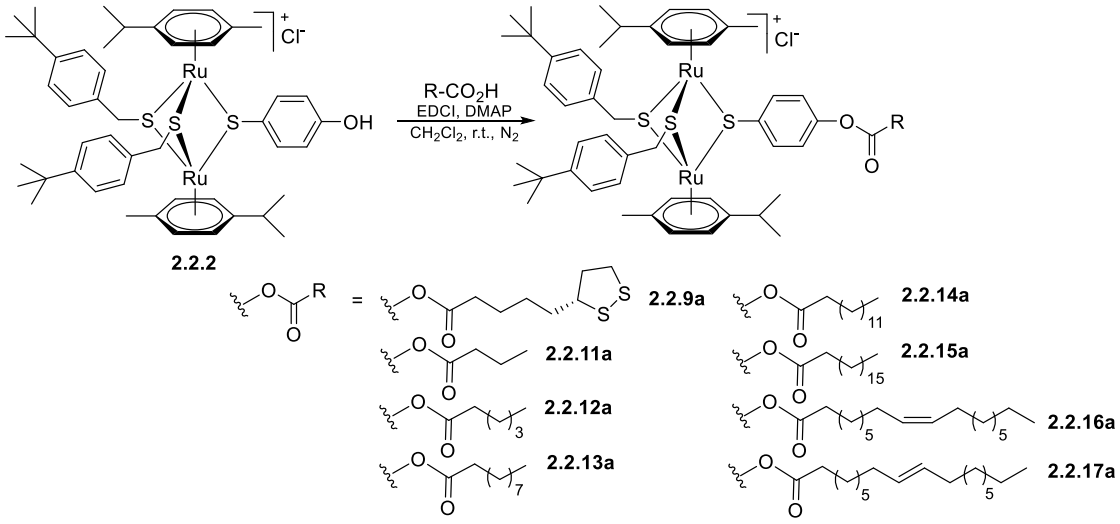

Scheme 2.2.2. Synthesis of the second series of ester derivatives **2.2.9a** and **2.2.11a**-**2.2.17a**

starting from diruthenium hydroxy intermediate **2.2.2**.

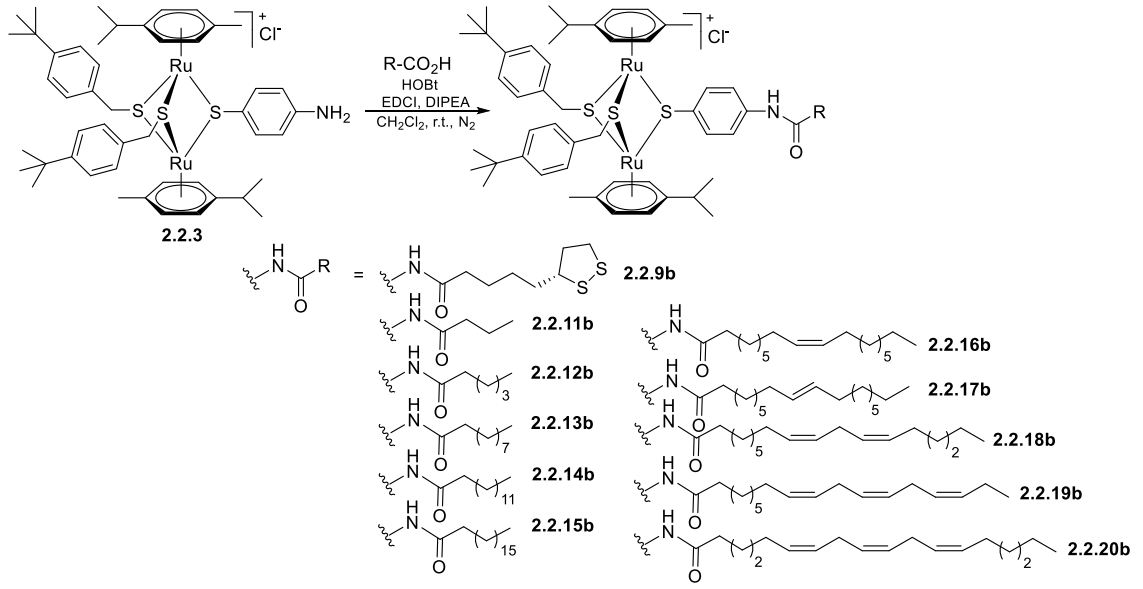

Scheme 2.2.3. Synthesis of the series of amide derivatives **2.2.9b**, **2.2.11b**-**2.2.20b** starting from diruthenium amino intermediate **2.2.3**.

2.2.2.2. In vitro activity against the apicomplexan parasite Toxoplasma gondii

The new conjugates (26 compounds), the lipophilic derivatives (15 compounds) and the representative diruthenium intermediates were investigated to assess the impact of compound exposure upon *T. gondii* β-gal tachyzoites grown in HFF (human foreskin fibroblasts) and noninfected HFF. The diruthenium intermediates **2.2.1**-**2.2.3**, the ethyl ester **2.2.7a** ([(η^6-*p*-MeC$_6$H$_4$Pr^i)$_2$Ru$_2$(μ_2-SCH$_2$C$_6$H$_4$-*p*-Bu^t)$_2$(μ_2-SC$_6$H$_4$-*p*-CH$_2$CO$_2$Et)]Cl), and the acetic acid ester **2.2.10a** ([(η^6-*p*-MeC$_6$H$_4$Pr^i)$_2$Ru$_2$(μ_2-SCH$_2$C$_6$H$_4$-*p*-Bu^t)$_2$(μ_2-SC$_6$H$_4$-*p*-OAc)]Cl) and amide **2.2.10b** ([(η^6-*p*-MeC$_6$H$_4$Pr^i)$_2$Ru$_2$(μ_2-SCH$_2$C$_6$H$_4$-*p*-Bu^t)$_2$(μ_2-SC$_6$H$_4$-*p*-NHAc)]Cl) have been evaluated previously against *T. gondii* β-gal under similar conditions[30, 62, 131], and the corresponding values were introduced in Table 2.2.1 and Figure 2.2.2 for comparison. In a primary screening, transgenic *T. gondii* tachyzoites constitutively expressing β-galactosidase (*T. gondii* β-gal) were cultured in HFF monolayers and exposed to concentrations of 1 and 0.1 µM of each compound of interest. In parallel, the cytotoxicity of these compounds was evaluated at the same concentrations in noninfected HFF. As a measure of the parasite proliferation, β-galactosidase activity was determined, while the impact on noninfected HFF was assessed using the alamarBlue assay. The results for the diruthenium intermediates **2.2.1**-**2.2.3** and the corresponding ester **2.2.4a**-**2.2.17a** and amide **2.2.9b**-**2.2.20b** conjugates are

summarized in Table 2.2.1 and Figure 2.2.2, while the data measured for the lipophilic derivatives are presented in Figure S2.2.1 and Table S2.2.1 (*Supporting information 2.2*).

Table 2.2.1. Primary efficacy/cytotoxicity screening of compounds in non-infected HFF cultures and *T. gondii* β-gal tachyzoites cultured in HFF. The compounds selected for determination of IC_{50} values against *T. gondii* β-gal are tagged with *.

Compound	HFF viability (%)		*T. gondii* β-gal growth (%)	
	0.1 µM	1 µM	0.1 µM	1 µM
Diruthenium intermediates				
2.2.1[a,*]	93 ± 4	87 ± 1	114 ± 15	110 ± 32
2.2.2[a,*]	76 ± 6	46 ± 6	66 ± 14	2 ± 0
2.2.3[a,*]	74 ± 2	48 ± 1	57 ± 1	2 ± 0
First series of ester conjugates				
2.2.4a*	109 ±1	74 ± 0	109 ± 2	23 ± 7
2.2.5a	144 ± 4	99 ± 4	80 ± 15	5 ± 0
2.2.6a	103 ± 1	73 ± 1	112 ± 3	26 ± 1
2.2.7a	50 ± 4	46 ± 11	3 ± 0	4 ± 1
2.2.8a*	33 ± 0	0 ± 0	81 ± 2	81 ± 3
Second series of ester conjugates				
2.2.9a	109 ± 3	108 ± 4	94 ± 11	2 ± 0
2.2.10a [a,*]	74 ± 2	52 ± 3	5 ± 0	2 ± 1
2.2.11a*	14 ± 0	0 ± 0	97 ± 1	94 ± 0
2.2.12a*	41 ± 1	0 ± 0	97 ± 2	95 ± 0
2.2.13a	101 ± 5	65 ± 4	212 ± 10	148 ± 12
2.2.14a*	71 ±11	59 ± 4	94 ± 3	1 ± 0
2.2.15a	97 ± 2	67 ± 4	132 ± 23	4 ± 0
2.2.16a	94 ± 3	80 ± 11	88 ± 1	4 ± 0
2.2.17a	87 ± 4	71 ± 4	109 ± 6	4 ± 0
Amide conjugates				
2.2.9b*	104 ± 15	100 ± 3	105 ± 10	23 ± 0
2.2.10b	62 ± 7	27 ± 1	4 ± 0	3 ± 1
2.2.11b*	6 ± 1	0 ± 0	95 ± 1	94 ± 0
2.2.12b*	93 ± 4	1 ± 0	98 ± 2	94 ± 1
2.2.13b	107 ± 6	75 ± 7	224 ± 1	88 ± 19
2.2.14b*	94 ± 2	71 ± 5	92 ± 1	5 ± 1
2.2.15b	98 ± 5	78 ± 4	146 ± 12	7 ± 1
2.2.16b	97 ± 8	74 ± 4	134 ± 13	9 ± 3
2.2.17b	99 ± 4	78 ± 2	127 ± 6	6 ± 0
2.2.18b	93 ± 3	77 ± 8	95 ± 65	5 ± 0
2.2.19b*	105 ±7	96 ± 2	4 ± 0	3 ± 0
2.2.20b	94 ± 1	93 ± 3	125 ± 24	120 ± 26

[a]Data for compounds **2.2.1**-**2.2.3**, **2.2.7a** and **2.2.10a**, **2.2.10b** were previously reported[30, 62, 131].

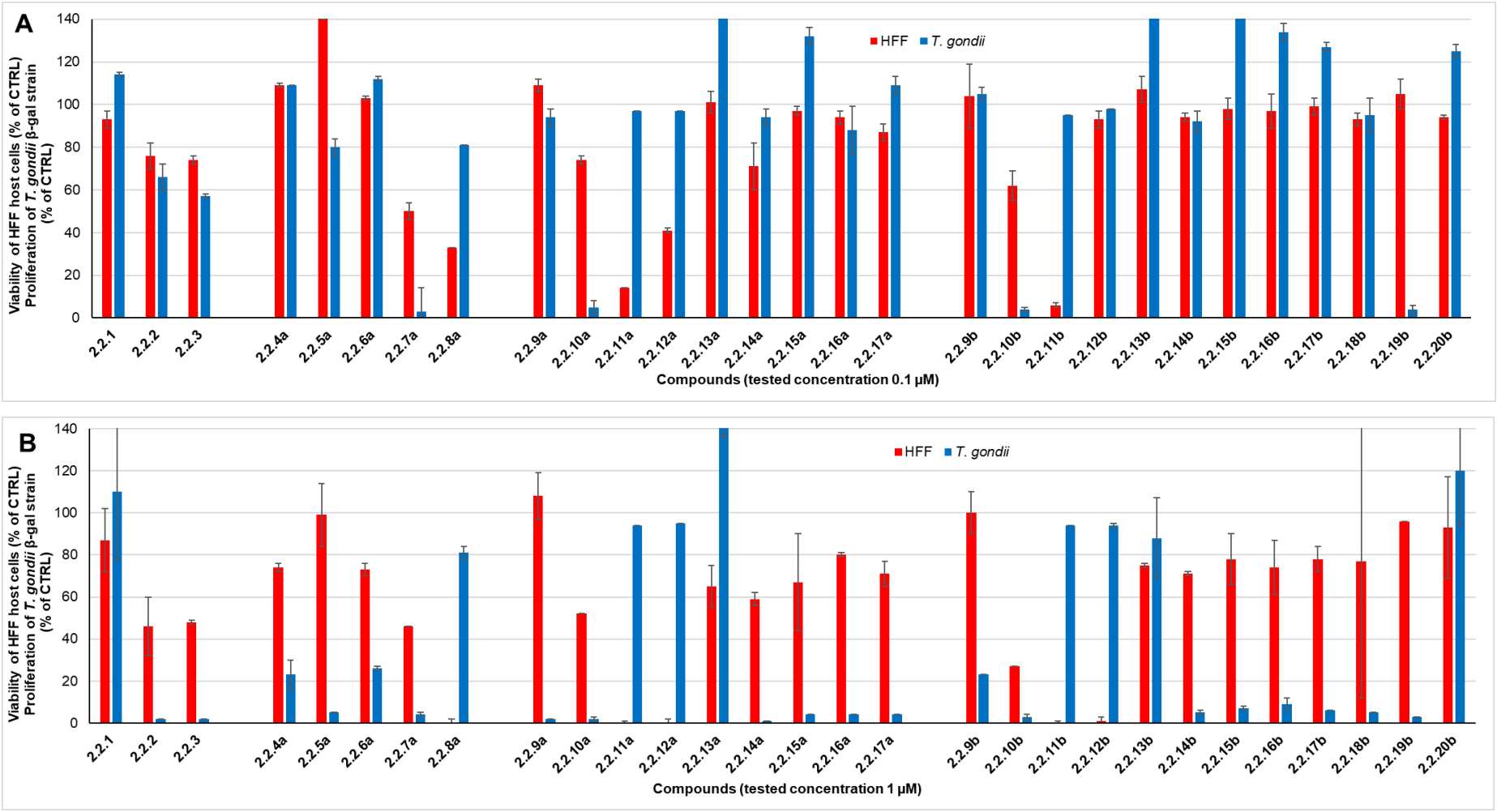

Figure 2.2.2. Clustered column chart showing the *in vitro* activities at 0.1 (A) and 1 (B) µM of the 29 diruthenium compounds on HFF viability and *T. gondii* β-gal proliferation. Non-infected HFF monolayers treated only with 0.1% DMSO exhibited 100% viability and 100% proliferation was attributed to *T. gondii* β-gal tachyzoites treated with 0.1% DMSO only. For each assay, standard deviations were calculated from triplicates. Data for compounds **2.2.1**-**2.2.3**, **2.2.7a** and **2.2.10a**, **2.2.10b** were previously reported[30, 62, 131].

From the library of tested lipophilic derivatives (Figure S2.2.1 and Table S2.2.1), only geraniol (**2.2.4**), farnesol (**2.2.5**), geranylgeraniol (**2.2.6**), and butyric (**2.2.11**), α-linolenic (**2.2.19**) and γ-linolenic (**2.2.20**) acids slightly affected the host cells viability when applied at 1 µM, the other compounds being non-toxic to HFF at the screening concentrations. From the same series, only geraniol (**2.2.4**), farnesol (**2.2.5**), *n*-butanol (**2.2.8**) and α-lipoic acid (**2.2.9**) exhibited some limited effect on the parasite proliferation.

For the conjugates, both the nature of the lipophilic appendices and that of the connection between the diruthenium moiety and the anchored unit strongly influence the measured cytotoxicity and the antiparasitic activity. The first screening revealed no straightforward SAR (structure-activity relationship), in spite of some identified tendencies.

From the first series of esters, only farnesol conjugate **2.2.5a** did not affect the HFF viability at both tested concentrations. Geraniol and geranylgeraniol conjugates **2.2.4a** and **2.2.6a** reduced the HFF viability to less than 80% when applied at 1 µM. Both ethyl and butyl esters **2.2.7a** and **2.2.8a** were cytotoxic to the host cells, the latest one abolishing the HFF growth at the highest concentration tested, and thus cannot be considered for further tests. Interestingly, farnesol conjugate **2.2.5a** is more active on *T. gondii* compared to the other terpenoid analogs **2.2.4a** and **2.2.6a**, almost abolishing parasite proliferation when applied at 1 µM. From the first series of ester derivatives, farnesol ester **2.2.5a** exhibits the best activity/cytotoxicity balance. Carboxy diruthenium intermediate **2.2.1**, neither affected the HFF viability nor the parasite growth at the tested concentrations.

From the second series of ester conjugates, only α-lipoic ester **2.2.9a** exhibited no cytotoxicity on HFF when applied at 1 µM. The length of the lipophilic chain influences the ester conjugates toxicity on HFF, but the effect is not linear. Compounds **2.2.13a** and **2.2.15a**-**2.2.17a** were moderately affecting the host cells viability (reduction to 65-80%). **2.2.10a** and **2.2.14a**, acetic and myristic esters, respectively, present similar effects on the host cells, reducing their viability even at 0.1 µM to 74 and 71%, the effect being more

pronounced when applied at 1 µM (viability reduction to 52 and 59%, respectively). Butanoic and hexanoic esters **2.2.11a** and **2.2.12a**, exhibited high cytotoxicity on HFFs even at 0.1 µM (host cells viability reduced to 14 and 41%, respectively, while they abolished host cells proliferation when applied at 1 µM. Butyric, hexanoic and decanoic esters **2.2.11a**, **2.2.12a** and **2.2.13a** had no effect on *T. gondii* growth at both tested concentrations, while derivatives with longer chains **2.2.14a-2.2.17a** exhibited antiparasitic effect only when applied at 1 µM. Compared to hydroxy diruthenium derivative **2.2.2**, acetyl derivative **2.2.10a** presents a similar cytotoxicity profile, while attachment of longer chains in ester conjugates **2.2.13a**-**2.2.17a** is associated to lesser impact on HFF viability.

Some parallelism can be observed between the esters **2.2.9a**-**2.2.17a** and the corresponding amides analogues **2.2.9b**-**2.2.17b**. Thus, α-lipoic amide **2.2.9b** was not toxic to HFF even at 1 µM, while compounds **2.2.13b**-**2.2.17b** reasonably reduced host cells viability, to a lesser extent compared to the corresponding ester derivatives. Both ester and amide conjugates with medium length appendices as butyric, hexanoic, decanoic **2.2.11a**-**2.2.13a** and **2.2.11b**-**2.2.13b** have no effect of parasite growth. Similar to esters analogues **2.2.14a-2.2.17a** but to a lesser effect, amide derivatives with longer chains **2.2.14a-2.2.17a** exhibited antiparasitic effect only at 1 µM. The presence of one double bond in the lipophilic chain of conjugates **2.2.16a**, **2.2.17a** and **2.2.16b**, **2.2.17b** derived from oleic and elaidic acids, does not bring important changes in terms of host cells toxicity or antiparasitic efficacy compared to the respective stearic acid compounds **2.2.15a** and **2.2.15b**. A similar effect is also observed in the case of linoleic amide conjugate **2.2.18b** related to **2.2.15b**. The position of the double bonds on the chains can be important as, both **2.2.19b** and **2.2.20b** are not toxic to the host cells, but while the former strongly inhibits parasite proliferation, the second exhibits no effect on *T. gondii*.

Table 2.2.2. IC_{50} values (μM) against *T. gondii* β-gal tachyzoite proliferation and effects on HFF viability at 2.5 μM, for selected compounds and pyrimethamine (as positive control). *T. gondii* proliferation and HFF viability were quantified by β-galactosidase and alamarBlue assay, respectively. Data for compounds **2.2.1**-**2.2.3** and **2.2.10a** were previously reported[30, 62, 131].

Compound	*T. gondii* β-gal			HFF	
	IC_{50} (μM)	[LS; LI][b]	SE[c]	viability at 2.5 μM (%)[d]	SD[e]
Pyrimethamine[a]	0.326	[0.396; 0.288]	0.052	99	6
Diruthenium intermediates					
2.2.1[a]	0.181	[1.482; 0.274]	2.700	99	2
2.2.2[a]	0.117	[0.139; 0.098]	0.144	56	3
2.2.3[a]	0.153	[0.185; 0.127]	0.138	51	2
First series of ester conjugates					
2.2.4a	0.173	[0.260; 0.115]	0.371	66	3
2.2.8a	0.086	[0.097; 0.076]	0.087	1	0
First series of ester conjugates					
2.2.10a[a]	0.065	[0.101; 0.042]	0.092	16	5
2.2.11a	0.036	[0.050; 0.026]	0.175	72	0
2.2.12a	0.150	[0.199; 0.113]	0.177	0	0
2.2.14a	0.135	[0.160; 0.115]	0.152	78	0
Amide conjugates					
2.2.11b	0.073	[0.098; 0.054]	0.171	0	0
2.2.12b	0.118	[0.126; 0.110]	0.055	0	0
2.2.14b	0.495	[0.502; 0.489]	0.010	90	0
2.2.19b	0.113	[0.331; 0.039]	0.732	90	2

[a]Data for pyrimethamine, **2.2.1**-**2.2.3** and **2.2.10a** were previously reported[30, 62, 131]. [b]Values at 95% confidence interval (CI); LS is the upper limit of CI and LI is the lower limit of CI. [c]The standard error of the regression (SE), represents the average distance that the observed values fall from the regression line. [d]Control HFF cells treated only with 0.25 % DMSO exhibited 100% viability. [e]The standard deviation of the mean (six replicate experiments).

The dose-response experiments (results summarized in Table 2.2.2) allowed the identification of two compounds that are interesting for further tests, namely ester conjugates of butyric and myristic acids **2.2.11a** and **2.2.14a**. These hybrids were not only

highly efficient in inhibiting *T. gondii* β-gal proliferation (IC_{50} values of 0.36 and 0.135 µM, respectively), but also exhibited only medium cytotoxicity on HFF when applied at 2.5 µM (viability of 72 and 78%, correspondingly). **2.2.11a** and **2.2.14a** presented a better antiparasitic activity/toxicity balance compared to the corresponding hydroxy diruthenium derivative **2.2.2** from which they were obtained. The tests also confirmed the importance of the nature of the bond between the two units, as the butyramide analogue **2.2.11b** strongly affected host cells viability at 2.5 µM, and myristamide **2.2.14b** exhibited reduced cytotoxicity on HFF but also reduced antiparasitic activity (IC_{50} = 0.495 µM). Other structural elements, as for example the chain length, are also very important. Thus both ester and amide conjugates **2.2.12a** and **2.2.12b** from hexanoic acid are highly toxic to HFF at 2.5 µM, compared to the respective analogues from myristic acid **2.2.12a** and **2.2.12b** which exhibited only medium or low toxicity to the host cells.

2.2.3 Conclusions

Aiming to compounds exhibiting improved antiparasitic properties/selectivity balance, the synthesis and *in vitro* evaluation of 26 new conjugates based on trithiolato-bridged ruthenium(II)–arene scaffold tethered with various lipophilic derivatives are presented. The influence of various structural elements as the nature of the lipophilic appendage and that of chemical bond between the two units was assessed. In total, 49 compounds (hybrid molecules, organic lipophilic derivatives) were submitted to a first activity screening against *T. gondii* β-gal tachyzoites cultured in HFF and cytotoxicity determination against HFF host cells, which allowed the identification of 10 interesting conjugates. The IC_{50} values against *T. gondii* and the evaluation of HFF viability after exposure to 2.5 µM led to the selection of the butyric and myristic ester conjugate **2.2.11a** and **2.2.14a** as the most promising of the proposed library.

The nature of the lipophilic pending unit and of the bond linking the two moieties greatly impacts biological activity, even if no direct structure-activity relationship could be identified and the process seems to be multifactorial dependent.

Tethering lipophilic compounds to the trithiolato diruthenium(II)-arene scaffold led to compounds exhibiting different antiparasitic efficacy/cytotoxicity profiles compared to the parent organometallic complexes, and a fine structural tuning was necessary to obtain compounds with optimal properties. From the compounds library obtained in this study, ester conjugates **2.2.11a** and **2.2.14a** from butyric and myristic acids deserve further attention.

2.2.4. Experimental

2.2.4.1. Chemistry

The chemistry experimental part, with full description of experimental procedures and characterization data for all compounds, is presented in the *Supporting information 2.2*.

2.2.4.2. In vitro activity assessment against T. gondii tachyzoites and HFF

All tissue culture media were purchased from Gibco-BRL, and biochemical agents from Sigma-Aldrich. Human foreskin fibroblasts (HFF) were purchased from ATCC, maintained in DMEM (Dulbecco's Modified Eagle's Medium) supplemented with 10% fetal calf serum (FCS, Gibco-BRL, Waltham, MA, USA) and antibiotics as previously described[28]. Transgenic *T. gondii* β-gal (expressing the β-galactosidase gene from *Escherichia coli*) were kindly provided by Prof. David Sibley (Washington University, St. Louis, MO, USA) and were maintained, isolated, and prepared for new infections as shown before[28, 117]. All the compounds were prepared as 1 mM stock solutions from powder, in dimethyl sulfoxide (DMSO, Sigma, St. Louis, MO, USA). For *in vitro* activity and cytotoxicity assays, HFF were seeded at $5x10^3$/well and allowed to grow to confluence in phenol-red free culture medium at 37°C and 5% CO_2. Transgenic *T. gondii* β-gal tachyzoites were isolated and prepared for infection as described[28]. *T. gondii* tachyzoites were released from host cells, and HFF monolayers were infected with freshly isolated parasites ($1x10^3$/well), and compounds were added concomitantly with infection.

In the primary screening, HFF monolayers infected with *T. gondii* β-gal received 0.1 and 1 μM of each compound, or the corresponding concentration of DMSO (0.01 or 0.1% respectively) as controls and incubated for 72 h at 37˚C/5% CO_2 as previously described[62]. For the next step, IC_{50} measurements for *T. gondii* β-gal were performed. The selected compounds were added concomitantly with infection in 8 serial concentrations 0.007, 0.01, 0.03, 0.06, 0.12, 0.25, 0.5, and 1 μM. After a period of 72 h of culture at 37°C/5% CO_2, culture medium was aspirated, and cells were permeabilized by adding 90 μL PBS (phosphate buffered saline) with 0.05% Triton X-100. After addition of 10 μL 5 mM chlorophenolred-β-D-galactopyranoside (CPRG; Roche Diagnostics, Rotkreuz, Switzerland) in PBS, the absorption shift was measured at 570 nm wavelength at various timepoints using an EnSpire® multimode plate reader (PerkinElmer, Inc, Waltham, MA, USA). For the primary screening at 0.1 and 1 μM, activity was measured as the release of chlorophenol red over time, was calculated as percentage from the respective DMSO control, which represented 100% of *T. gondii* β-gal growth. For the IC_{50} assays, the activity measured as the release of chlorophenol red over time was proportional to the number of live parasites down to 50 per well as determined in pilot assays. IC_{50} values were calculated after the logit-log-transformation of relative growth and subsequent regression analysis. All calculations were performed using the corresponding software tool contained in the Excel software package (Microsoft, Redmond, WA, USA). Cytotoxicity assays using uninfected confluent HFF host cells were performed by the alamarBlue assay as previously reported[118]. Confluent HFF monolayers in 96 well-plates were exposed to 0.1, 1 and 2.5 μM of each compound. Non-treated HFF as well as DMSO controls (0.01%, 0.1% and 0.25%) were included. After 72 h of incubation at 37°C/5% CO_2, the medium was removed, and plates were washed once with PBS. 200 μL of Resazurin (1:200 dilution in PBS) were added to each well. Plates were measured at excitation wavelength 530 nm and emission wavelength 590 nM at the EnSpire® multimode plate reader (PerkinElmer, Inc). Fluorescence was

measured at different timepoints. Relative fluorescence units were calculated from timepoints with linear increase.

Chapter 3 – Trithiolato-Bridged Ruthenium(II)-Arene Complexes Bearing an Organic Drug[5]

Abstract

Tethering known drugs to a metalorganic moiety is an efficient approach for modulating the anticancer, antibacterial, and antiparasitic activity of organometallic complexes. This study focused on the synthesis and evaluation of new di-ruthenium(II)arene compounds linked to several anti-microbial compounds such as dapsone, sulfamethoxazole, sulfadiazine, sulfadoxine, triclosan, metronidazole, ciprofloxacin, as well as menadione (a 1,4-naphtoquinone derivative). In a primary screen, 30 compounds (17 hybrid molecules, diruthenium intermediates and antimicrobials) were assessed for in vitro activity against transgenic *T. gondii* tachyzoites constitutively expressing β-galactosidase (*T. gondii* β-gal) at 0.1 and 1 µM. In parallel, the cytotoxicity in non-infected host cells (human foreskin fibroblasts, HFF) was determined by alamarBlue assay. When assessed at 1 µM, five compounds strongly impaired parasite proliferation by > 90%, and HFF viability was retained at 50% or more, and they were further subjected to *T. gondii* β-gal dose-response studies. Two compounds, notably **3.11** and **3.13**, amide and ester conjugates with sulfadoxine and metronidazole, exhibited low IC50 (half-maximal inhibitory concentration) values 0.063 and 0.152 µM, and low or intermediate impairment of HFF viability at 2.5 µM (83 and 64%). The nature of the anchored drug as well as that of the linking unit impacted the biological activity.

3.1. Introduction

In the last two decades, important research in the fight against cancer was focused

[5] This chapter was published as Synthesis and Antiparasitic Activity of New Conjugates—Organic Drugs Tethered to Trithiolato-Bridged Dinuclear Ruthenium(II)–Arene Complexes, *Inorganics*, **2021**, 9, 59. https://doi.org/10.3390/inorganics9080059. This article is licensed under a Creative Commons Attribution International License (CC BY 4.0). Supplementary information can be found the chapter *Supporting information 3*.

on the use of ruthenium compounds as alternatives to platinum drugs currently employed as therapeutics [334-337]. Among the prominent compounds which have opened the way for recent research in this field remain ruthenium(III) complexes **NKP-1339** (sodium *trans*-[tetrachloridobis(1*H*-indazole)ruthenate(III)]) [44-46] and **NAMI-A** (imidazolium [*trans*-[tetrachlorido(*S*-dimethylsulfoxide)-(1*H*-imidazole)ruthenate(III)]) [45, 47], as well as ruthenium(II)–arene complexes **RAPTA-C** ([Ru(II)(η^6-*p*-MeC$_6$H$_4$Pr^i)Cl$_2$(PTA)], PTA = 1,3,5-triaza-7-phosphoadamantane) [48-50] and **RM175** ([Ru(II)(η^6-biphenyl)Cl(en)]PF$_6$, en = 1,2-ethylenediamine) [46, 51, 52]. The ruthenium(II)–arene organometallic scaffold proved to be a versatile platform for the design of novel bioorganometallic agents and cationic or neutral compounds with the general structure [(η^6-arene)Ru(X)(Y)(Z)] presenting both hydrophobic and hydrophilic properties have attracted increasing attention [125]. Following the work pioneered by **RAPTA-C** and **RM175**, studies on organometallic ruthenium(II)–arene complexes are not only rapidly progressing but also particularly relevant, with a plethora of compounds presenting anticancer, antibiotic, antifungal and antiparasitic properties [71, 72, 79, 244, 338, 339]. Important research focused on hybrid structures in which the robust ruthenium(II)–arene unit is associated with the various biologically active compounds, a strategy with implications for developing of novel metal-based compounds presenting multiple targets [340].

Trithiolato-bridged dinuclear ruthenium(II)–arene complexes constitute a particular family of ruthenium(II)–arene compounds, whose structure is based on two half-sandwich units linked by three thiols forming a trigonal-bipyramidal unit (Figure 3.1). Two types of structures can be distinguished, namely symmetric complexes (Figure 3.1, **3.A** and **3.A'**) in which the three thiols are identical (general formula [(η^6-*p*-MeC$_6$H$_4$Pr^i)$_2$Ru$_2$(μ_2-SR)$_3$]X), and mixed complexes (Figure 3.1, **3.B**) bearing at least one different thiol (general formula [(η^6-*p*-MeC$_6$H$_4$Pr^i)$_2$Ru$_2$(μ_2-SR1)$_2$(μ_2-SR2)]X). These compounds have been initially developed and evaluated as catalysts [341], and subsequently as cytotoxic agents. Particularly complex **3.A'** (R = Bu^t) was highly active against *in vitro* cultured cancer cells [37, 38, 40, 53, 64], and three analogues were also tested *in vivo* [342, 343]. This

encouraged us to assess trithiolato diruthenium complexes as potential antiparasitic agents, and several derivatives were highly active against *Toxoplasma gondii* [29], *Neospora caninum* [33] and *Trypanosona brucei* [63]. The half-maximal proliferation inhibitory concentrations (IC_{50}) of complexes **3.A** (R = Me), **3.A'** (R = Bu^t) and **3.B** against *in vitro* cultured *T. gondii* tachyzoites were 34, 62 and 1 nM, respectively, and these compounds did not impair the viability of human foreskin fibroblast (HFF) host cells [29].

Toxoplasmosis is considered one of the most common parasitic diseases affecting approximately one-third of the world's population. In immunocompetent hosts, the infection is usually controlled and asymptomatic, but in immunocompromised persons, such as AIDS patients or persons undergoing immunosuppressive therapy, newly acquired reactivated toxoplasmosis can cause serious complications such as toxoplasmic encephalitis or ocular toxoplasmosis [14], and primary infection during pregnancy, can lead to abortions or fetal malformation. The current therapeutic options are suboptimal, target only the acute disease, and do not eradicate the parasite in chronic infections encysted organisms (bradyzoites) [8, 194]. Additionally, adverse side effects are frequently reported [17, 194]. Thus, safer, and more effective treatment options are needed.

Cationic trithiolato dinuclear ruthenium(II)–arene complexes represent promising scaffolds. Tethering a functional molecule (e.g., fluorophore, metabolite, drug) to a metal framework is one of the strategies used for tracking, directing, or modulating the biological activity of metal-based complexes [57-59]. In numerous cases, conjugation to organometallic moieties led to the enhanced biological activity of the parental drug [337, 344]. The trithiolato diruthenium compounds showed high stability and post-functionalization of the bridge thiols proved a useful method to introduce valuable modifications [60, 61, 131]. This approach proceeds under mild conditions and constitutes an efficient entry to conjugates with biorelevant moieties. The easy access and upscaling of certain mixed trithiolato diruthenium compounds bearing derivatizable groups (e.g., OH, SH, NH_2, CO_2H) [53, 131] (as **3.B**, Figure 3.1) allowed the development and investigation of hybrid structures functionalized with the anticancer drug chlorambucil [61], 7-amino-

coumarin fluorophores [131], and peptides [60]. This type of structure is aimed at improving the cytotoxicity against cancer cells [60, 61], the water solubility [60] and the selectivity and antiparasitic activity on *T. gondii* [131].

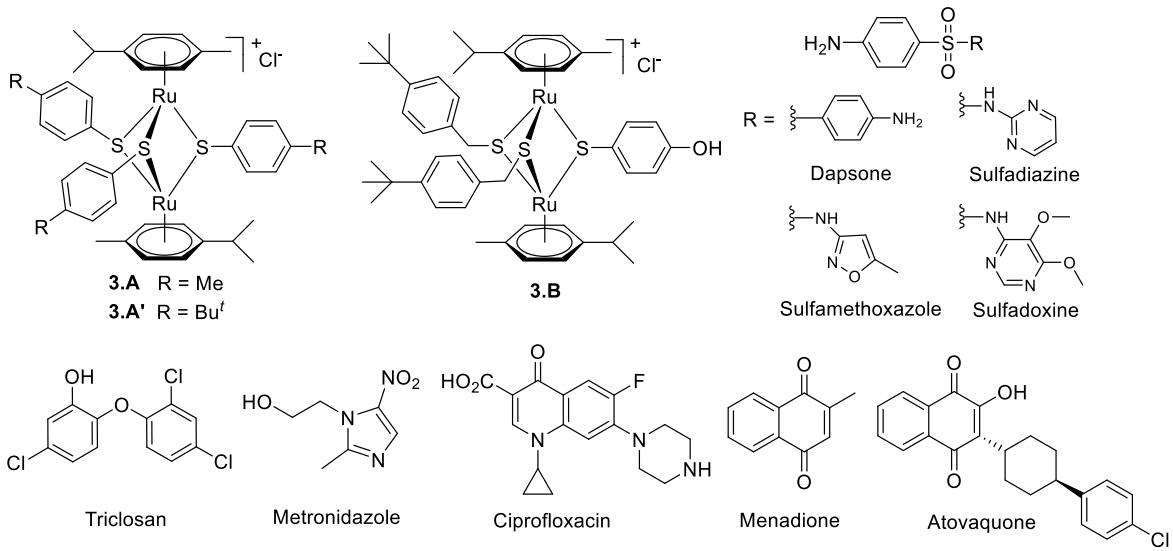

Figure 3.1. Structure of selected symmetric (**3.A**, **3.A'**) and mixed (**3.B**) trithiolato-bridged ruthenium(II)–arene complexes and of the antimicrobial drugs considered for tethering to the diruthenium unit.

In this study, a series of structurally diverse antimicrobial agents presenting also relevant anti-*Toxoplasma* activity have been selected to be conjugated to the trithiolato diruthenium core (Figure 3.1) [17, 192, 194, 199]. Ruthenium(II)–arene, as well as iridium(III)- and rhodium(III)-cyclopentadienyl are among the favored organometallic units to be tested in intramolecular combination with various drugs.

Sulfonamides (sulfa-drugs) such as sulfadiazine (4-amino-*N*-(pyrimidin-2-yl)benzenesulfonamide), sulfamethoxazole (4-amino-*N*-(5-methylisoxazol-3-yl)benzenesulfonamide), and sulfadoxine (4-amino-*N*-(5,6-dimethoxypyrimidin-4-yl)benzenesulfonamide) (Figure 3.1) are bacteriostatic agents presenting a broad-spectrum of activity against Gram-positive and Gram-negative bacteria, *Toxoplasma* and other protozoan pathogens. Drug combinations including pyrimethamine/sulfadiazine and trimethoprim/sulfamethoxazole remain among the most frequently applied treatments for

toxoplasmosis [17, 194, 195, 345, 346]. Several studies focused on combining sulfa-drugs with various half-sandwich 'piano-stool' organometallic units for biological applications [347-349] (e.g., **3.C** and **3.D** in Figure 3.2). The sulfa-drug can be directly coordinated to the organometallic unit (**3.C**) [347], or can be covalently connected to a ligand (**3.D**) [348, 349]. 'Piano-stool' half-sandwich compounds of the type [(η^6-*p*-$MeC_6H_4Pr^i$)Ru(sulfadiazine)$_2$] and [(η^5-C_5Me_5)Rh(sulfadiazine)$_2$] (where C_5Me_5 is pentamethylcyclopentadienyl) (**3.C**, Figure 3.2) were evaluated for their potential antimicrobial activity [347]. While the ruthenium complex was biologically inactive, the rhodium compound was potent against Gram-positive bacteria, *Candida albicans* and *Cryptococcus neoformans* [347].

Another example is a series of organo-ruthenium, rhodium and iridium derivatives of sulfadoxine anchored on *N*,*N*′-chelate pyridylimino quinolylimino-bidentate ligands [348] (e.g., **3.D**, Figure 3.2). Screening for *in vitro* activity against *Plasmodium falciparum* chloroquine-sensitive and -resistant strains and *Mycobacterium tuberculosis* showed the activity to be dependent on the organometallic unit, with ruthenium complexes being inactive. The rhodium and iridium compounds inhibited parasite growth with IC_{50} values in the sub- and low micromolar range, with no significant toxicity towards human embryonic kidney cells (HEK293). Moreover, sulfadoxine was not active in most of the assays, supporting the hypothesis that organometallic conjugates of drugs can beneficially affect bioactivity.

Triclosan (5-chloro-2-(2,4-dichlorophenoxy)phenol, Figure 3.1) is an antibacterial agent that was shown to inhibit the *in vitro* proliferation of *T. gondii* tachyzoites in the low nanomolar range [350, 351]. As triclosan presents poor water solubility and oral bioavailability, various studies focused on derivatives aiming at increased solubility and potency [352-354], as well as improved drug delivery and pharmacological properties against *T. gondii* [355-357].

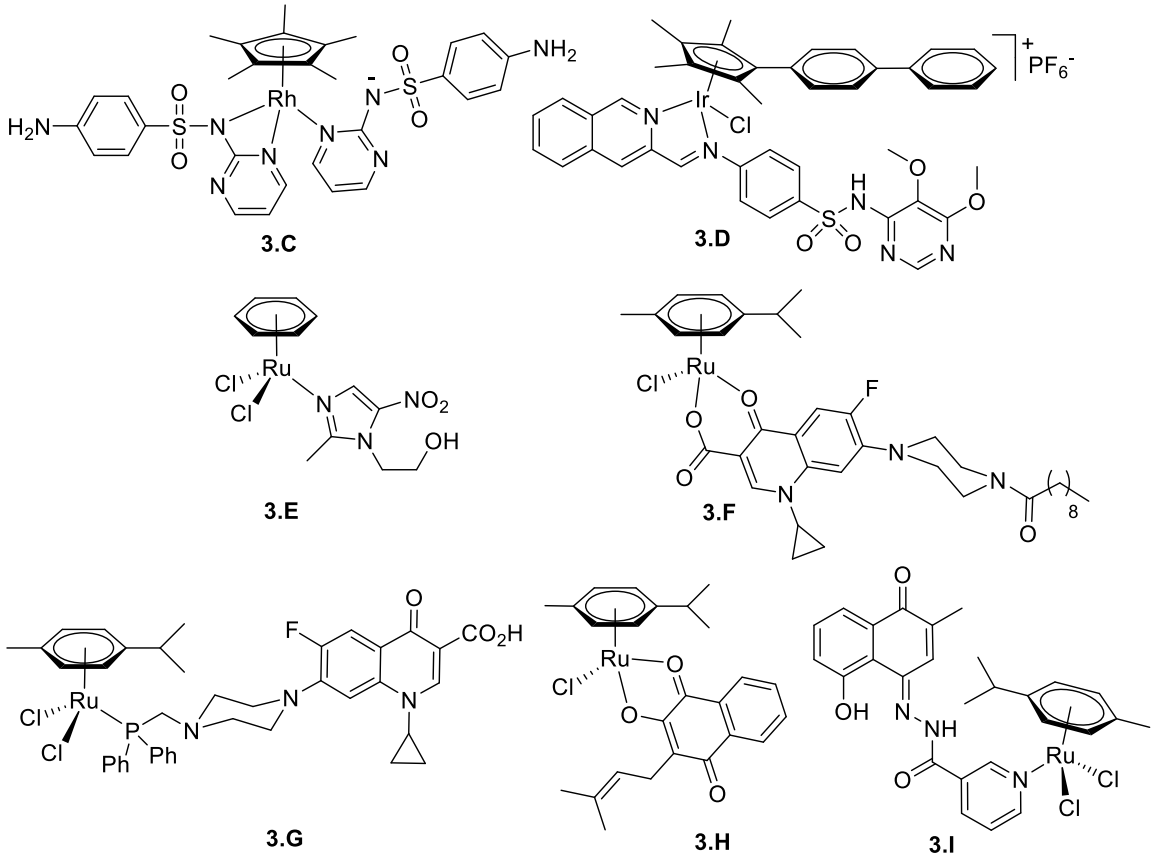

Figure 3.2. Structure of half-sandwich RhCp* sulfadiazine complex (**3.C**), IrCp*biph sulfadoxine conjugate **3.D**, ruthenium(II)–arene conjugates with metronidazole (**3.E**), ciprofloxacin (**3.F** and **3.G**), lapachol (**3.H**), and plumbagin (**3.I**).

Metronidazole (1-β-hydroxyethyl-2-methyl-5-nitroimidazole, Figure 3.1) is used to treat antibacterial and antiprotozoal infections [358, 359]. A significant reduction of brain cysts was observed in a mouse model of chronic toxoplasmosis after combined treatment with spiramycin and metronidazole [360]. The potential use of ruthenium(II)–benzene metronidazole complex **3.E** as a hypoxic cell cytotoxic agent has been assessed, revealing a higher selective toxicity for **3.E** compared to the free metronidazole [361].

Fluoroquinolones antibiotics (such as ciprofloxacin (1-cyclopropyl-6-fluoro-4-oxo-7-(piperazin-1-yl)-1,4-dihydroquinoline-3-carboxylic acid), Figure 3.1) are widely used in human and veterinary medicine. Along with other fluoroquinolones, previous reports identified promising anti-*Toxoplasma* effects upon treatments with certain ciprofloxacin derivatives [362, 363]. Ruthenium(II)–arene complexes bearing fluoroquinolone-based ligands showed interesting anticancer and antimicrobial activities (e.g., **3.F** and **3.G** in

Figure 3.2) [78, 364, 365]. The drug can be either directly coordinated to the metal (**3.F**), or covalently linked to a ligand (**3.G**). Coordinating 7-(4-(decanoyl)piperazin-1-yl)-ciprofloxacin, to the ruthenium(II)(η^6-*p*-$MeC_6H_4Pr^i$) unit in compound **3.F** [78] yielded multifunctional properties: high cytotoxicity in several cancer cell lines and moderate dose-dependent antibacterial activity in *Escherichia coli* as well as in a clinical *E. coli* isolate resistant to β-lactams. Compound **3.G**, bearing ciprofloxacin connected to an aminomethyl(diphenyl)phosphine ligand, was loaded in polymeric nanoformulations and exhibited promising cytotoxicity *in vitro* [364].

Derivatives containing the 1,4-naphtoquinone moiety, including atovaquone (2-((1*r*,4*r*)-4-(4-chlorophenyl)cyclohexyl)-3-hydroxynaphthalene-1,4-dione, Figure 3.1), buparvaquone (2-((4-(tert-butyl)cyclohexyl)methyl)-3-hydroxynaphthalene-1,4-dione) or lapachol (2-hydroxy-3-(3-methylbut-2-en-1-yl)naphthalene-1,4-dione) exhibit interesting anticancer and antiparasitic properties [366-370]. Atovaquone (Figure 3.1) is active *in vitro* against *T. gondii* tachyzoites with low nanomolar IC_{50} values and is one of the drugs currently applied to treat acute toxoplasmosis in humans [17, 194, 195]. Buparvaquone is also highly active against *T. gondii in vitro* and was shown to limit cerebral infection of dams and vertical transmission in mice infected with *T. gondii* oocysts [367]. Ruthenium(II)–arene complexes with naphtoquinone-based ligands have shown potential anticancer properties [371-375] (e.g., **3.H** and **3.I** in Figure 3.2). Ruthenium(II)–*p*-$MeC_6H_4Pr^i$ complex **3.H** with lapachol as a bidentate ligand was shown to induce apoptosis in human cancer cells in the low micromolar range by a mode of action involving oxidative stress [374]. Hydrazone-linked plumbagin ruthenium(II) conjugate **3.I** showed distinct and selective cancer cell growth inhibition, stronger DNA binding than plumbagin, and Pgp (P-glycoprotein) transporter inhibition [371].

This study aimed to synthesize new conjugates trithiolato-bridged binuclear ruthenium(II)–arene unit antimicrobial drug. The library of active organic compounds comprised sulfa-drugs (dapsone, sulfamethoxazole, sulfadiazine, sulfadoxine), triclosan, metronidazole, ciprofloxacin and menadione **(**2-methylnaphthalene-1,4-dione**)** (Figure

3.1). In addition to the nature of the antimicrobial drug, different structural variations were investigated for the hybrid molecules, as the connector between the two components (ester, amide, triazole) and the relative proportion drug unit/diruthenium moiety (i.e., 1:1 *vs.* 3:1).

The antimicrobial drugs, the newly obtained conjugates and the associated intermediates were submitted to a first *in vitro* screening, assessing the activity against a transgenic *T. gondii* strain constitutively expressing β-galactosidase (*T. gondii* β-gal) grown in human foreskin fibroblasts (HFF). In parallel, the cytotoxicity of these compounds was evaluated in noninfected HFF by the alamarBlue assay. The compounds exhibiting interesting antiparasitic activity and low cytotoxicity were subjected to *T. gondii* IC_{50} determination.

3.2. Results and Discussion

3.2.1. Chemistry

3.2.1.1. Synthesis of the Trithiolato-Bridged Diruthenium Intermediates

To access the hybrid molecules, selected diruthenium intermediates with groups allowing further modification via ester/amide conjugation or click chemistry (CuAAC, Cu(I)-catalyzed azide-alkyne cycloaddition) were synthesized (Schemes 3.1 and 3.2). The dithiolato ruthenium precursor **3.1** (same as **1.1.1a**) was synthesized by the reaction of the ruthenium dimer ($[Ru(\eta^6\text{-}p\text{-}MeC_6H_4Pr^i)Cl_2]_2$) with two equivalents of 4-(*tert*-butyl)phenyl)methanethiol (Scheme 3.1) as previously reported [131].

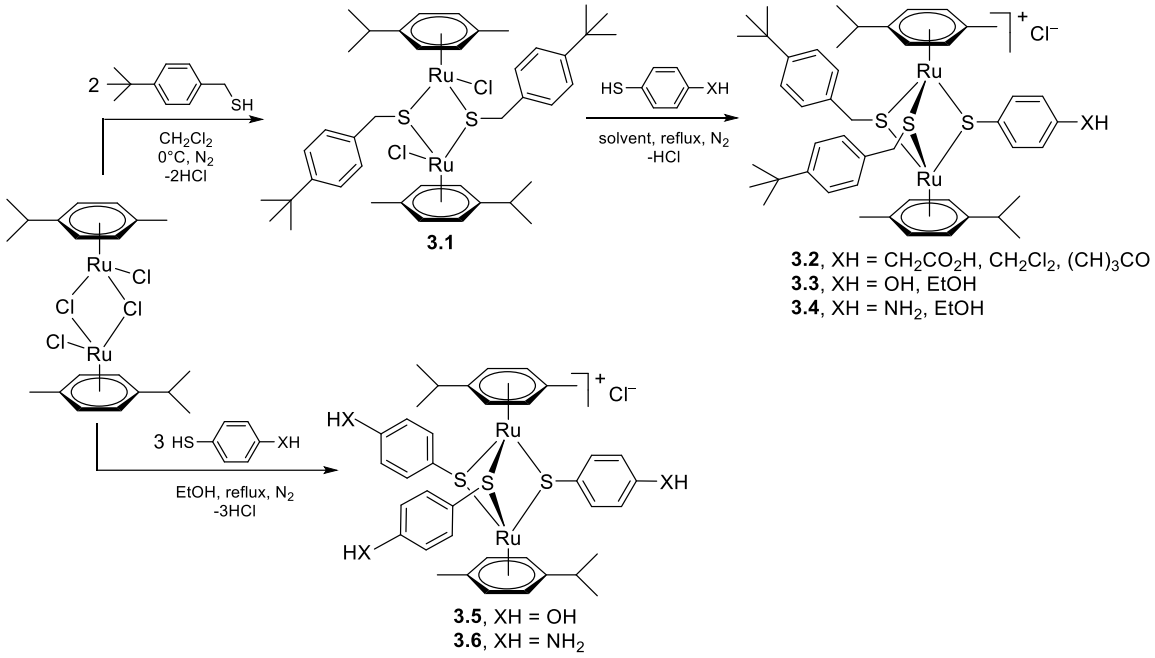

Scheme 3.1. Synthesis of the dithiolato diruthenium precursor **3.1**, of the mixed trithiolato intermediates **3.2**, **3.3**, and **3.4**, and the symmetric trithiolato intermediates **3.5** and **3.6**.

3.1 was further reacted with appropriate thiols (2-(4-mercaptophenyl)acetic acid, 4-mercaptophenol and 4-aminobenzenethiol), leading to the obtainment of mixed trithiolato diruthenium(II)–arene complexes **3.2** (same as **1.1.4a**), **3.3** (same as **1.1.2a**), and **3.4** (same as **1.1.3a**), bearing carboxy [131], hydroxy [53, 131] and, respectively, amino [131] groups (Scheme 3.1) following reported procedures.

To vary the number of drug units tethered to the diruthenium moiety, symmetric trithiolato intermediates **3.5** (same as **1.1.21**) [36, 38, 131] and **3.6** [30] bearing three hydroxy or amino groups were also synthesized following reported protocols by reacting the ruthenium dimer ($[Ru(\eta^6\text{-}p\text{-}MeC_6H_4Pr^i)Cl]_2Cl_2$) with 4-mercaptophenol and, respectively, 4-aminobenzenethiol in excess (Scheme 3.1).

In the conjugates, the nature of the linker between the diruthenium unit and the drug molecule might be very important for the stability and the biological activity of the hybrid molecule. To extend the purpose of this study, in addition to ester and amide bonds, the use of the triazole ring as a linker was also investigated.

Compound **3.7** (same as **2.1.8**), a diruthenium intermediate bearing a pending

alkyne group, was synthesized in good yield (83%) by the amide coupling of carboxy derivative **3.2** and propargyl amine by adapting a reported procedure [131] (Scheme 3.2). HOBt (1-hydroxybenzotriazol) and EDCI (*N*-(3-dimethylaminopropyl)-*N*′-ethylcarbodiimide hydrochloride) were used as coupling agents in basic conditions (DIPEA, *N*,*N*-diisopropylethylamine).

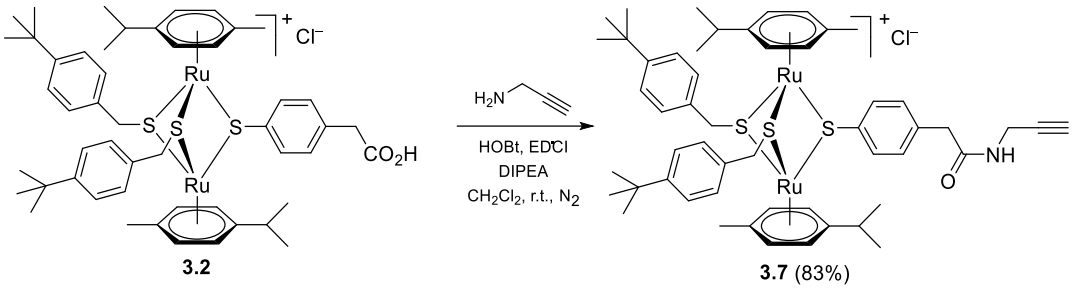

Scheme 3.2. Synthesis of the diruthenium trithiolato alkyne intermediate **3.7**.

3.2.1.2. Conjugates with Sulfa-Drugs (Dapsone, Sulfamethoxazole, Sulfadiazine, Sulfadoxine)

Conjugates **3.8**, **3.9**, **3.10** and **3.11** were obtained in modest yields (29, 24, 24 and 35%, respectively) by the amide coupling of the carboxy diruthenium intermediate **3.2** with commercially available sulfa-drugs dapsone, sulfamethoxazole, sulfadiazine and sulfadoxine in the presence of the coupling agents HOBt and EDCI, in basic conditions (DIPEA) (Scheme 3.3). The reduced solubility of the starting amines led to poor conversions and yields of isolated pure compounds.

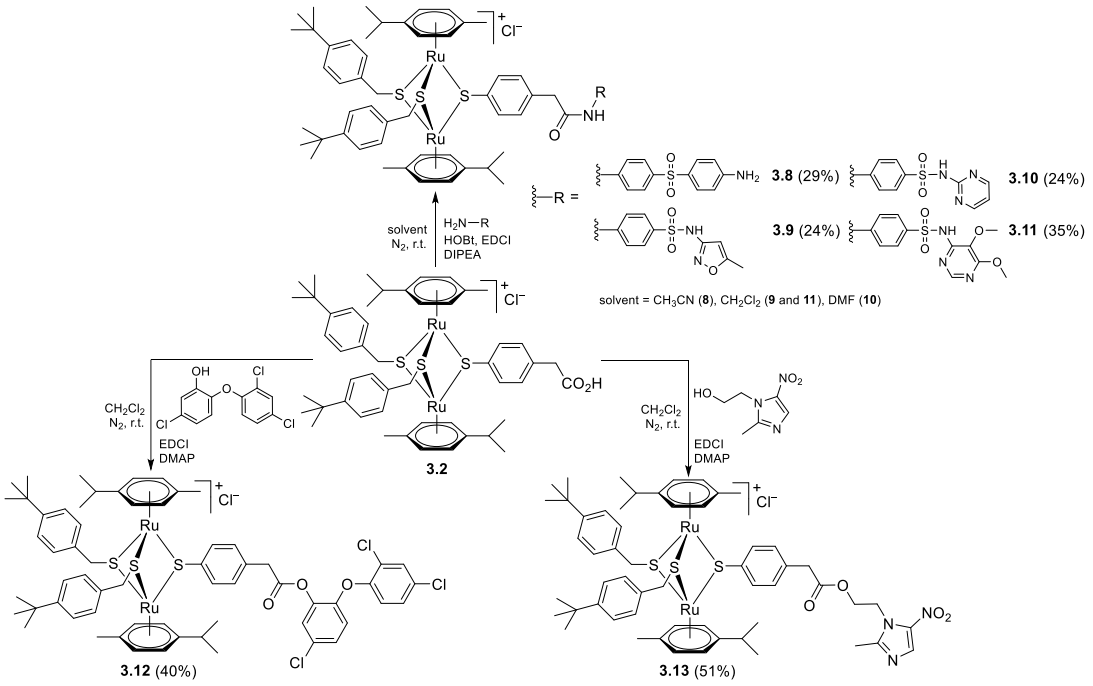

Scheme 3.3. Synthesis of the amide conjugates with the sulfa-drugs dapsone **3.8**, sulfamethoxazole **3.9**, sulfadiazine **3.10**, sulfadoxine **3.11**, and ester conjugates with triclosan **3.12** and metronidazole **3.13**.

3.2.1.3. Conjugates with Triclosan and Metronidazole

Ester conjugates with triclosan and metronidazole **3.12** and **3.13** were obtained by reacting carboxy complex **3.2** with the corresponding drugs, both containing free hydroxy groups (Scheme 3.3). Reactions were performed using EDCI as a coupling agent and DMAP (4-(dimethylamino)pyridine) as a basic catalyst, compounds **3.12** and **3.13** being isolated in medium yields of 40 and 51%.

The 'click' metronidazole conjugate **3.15** was synthesized by the 1,3-dipolar cycloaddition reaction of the alkyne diruthenium intermediate **7** with the metronidazole azide derivative **3.14** performed in the presence of $CuSO_4$ as a catalyst and sodium ascorbate as a reducing agent (Scheme 3.4), using an adapted literature procedure [286, 297]; conjugate **3.15** was isolated in 33% yield. The metronidazole azide **3.14** was synthesized in two steps (activation of the hydroxy group as mesylate followed by the nucleophilic substitution with azide). Of note, this is the first time that the 1,3-dipolar cycloaddition reaction is used for synthesizing conjugates based on the trithiolato diruthenium scaffold.

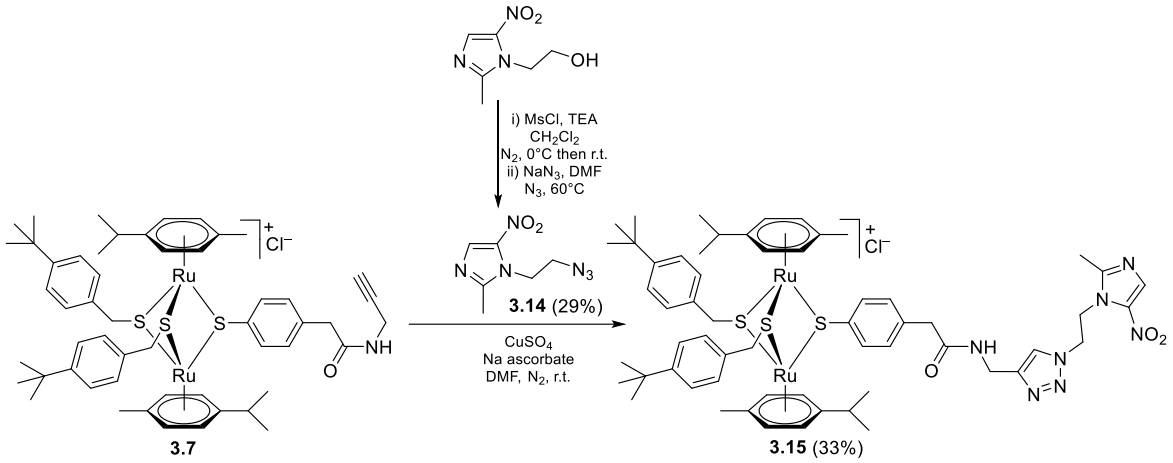

Scheme 3.4. Synthesis of metronidazole 'click' conjugate **3.15**.

3.2.1.4. Conjugates with Ciprofloxacin

For the derivatization of ciprofloxacin, two positions can be considered: the carboxy group in position 3 or the piperazine fragment in position 7 of the fluoroquinolone core [376]. To avoid possible side reactions, the protection of one of these groups was considered prior to attempt connecting this moiety to the trithiolato diruthenium unit. The piperazine fragment of ciprofloxacin was protected using Boc_2O (di-*tert*-butyl dicarbonate) in basic conditions (TEA, triethylamine) following a reported protocol [377] (Scheme 3.5), and intermediate **3.16** was isolated in quantitative yield.

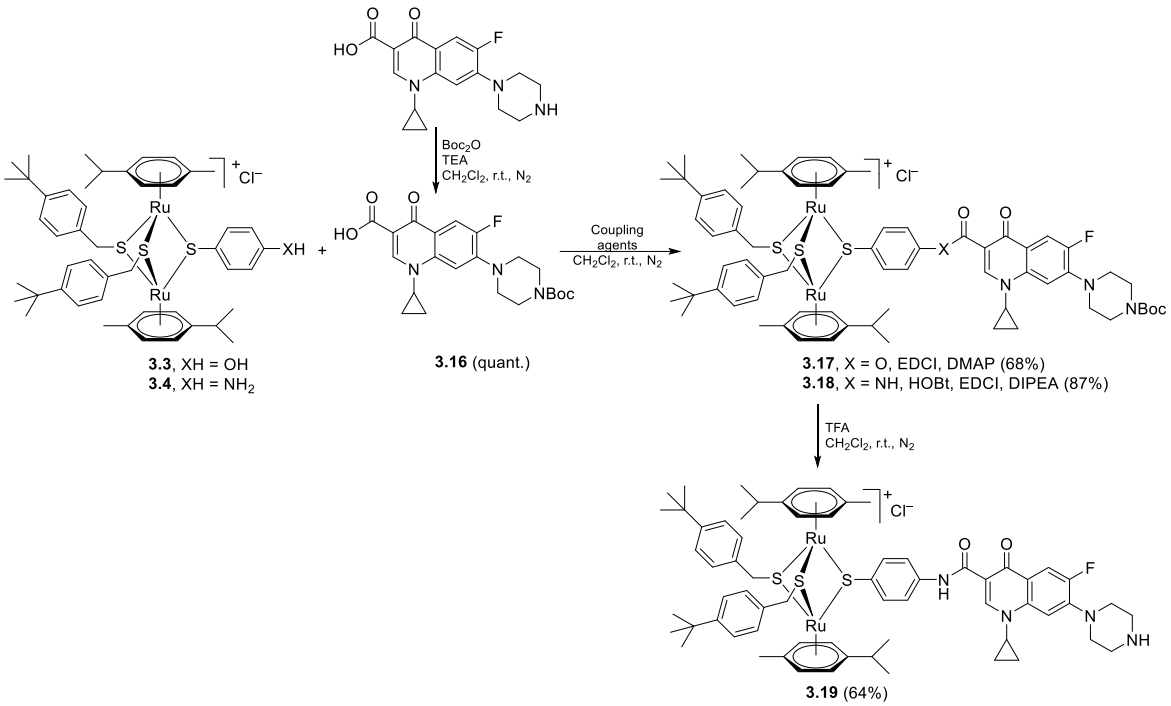

Scheme 3.5. Synthesis of the ciprofloxacin conjugates **3.17**, **3.18** and **3.19**.

The 'mixed' hydroxy and amino diruthenium complexes **3.3** and **3.4** were reacted with piperazine *N*-Boc protected ciprofloxacin **3.16** (Scheme 3.5). The esterification (conjugate **3.17**) was realized in the presence of EDCI and DMAP, while the amide coupling (conjugate **3.18**) was performed in the presence of HOBt, EDCI, and DIPEA. While the amide conjugate **3.18** was easily isolated in high yield (87%), the ester conjugate **3.17** could not be obtained in pure form, as it is prone to hydrolysis/solvolysis during purification. The *N*-Boc deprotection of **3.18** was realized in classical acidic conditions [378, 379] (TFA, trifluoroacetic acid, Scheme 3.5), allowing the isolation of compound **3.19** in 64% yield.

3.2.1.5. Conjugates with Menadione

Since atovaquone (Figure 3.1) and buparvaquone are quinone-based antimicrobial medications for the prevention and treatment of *T. gondii* [366, 367, 369] and other parasites, we have considered the development of a small library of compounds in which the 1,4-naphtoquinone motif is associated with the trithiolato diruthenium scaffold. To

validate the concept, a simpler structure based on the menadione moiety (2-methylnaphthalene-1,4-dione, Figure 3.1) was approached. First, menadione carboxy derivatives **3.20**, **3.21** and **3.22** that can be further anchored on the diruthenium unit were synthesized. This type of modification was previously used to prepare carboxy analogues of lawsone (2-hydroxynaphthalene-1,4-dione) [380-382], menadione or plumbagin (5-hydroxy-2-methylnaphthalene-1,4-dione) [383-386]. Compounds **3.20**, **3.21** and **3.22**, bearing linkers of different lengths between the 1,4-naphtoquinone moiety and the carboxylic group, were obtained from menadione and succinic, suberic and adipic acid, respectively, in the presence of $AgNO_3$ and $(NH_4)_2S_2O_3$ following literature procedures [383], and were isolated in medium yields of 70, 61 and 52%, respectively (Scheme 3.6).

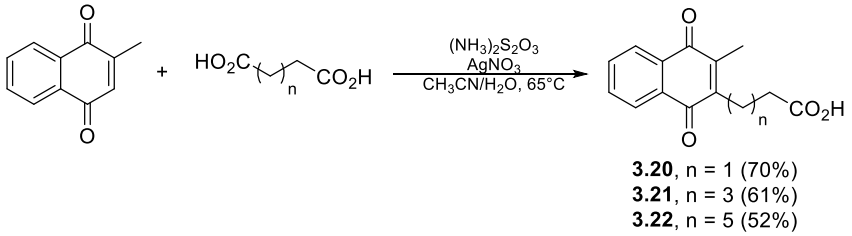

Scheme 3.6. Synthesis of carboxylic acid-functionalized 1,4-naphtoquinone derivatives **3.20**, **3.21** and **3.22**.

3.20 was further reacted with the hydroxy and amino diruthenium complexes **3.3** and **3.4** (Scheme 3.7). The esterification reaction was realized in the presence of EDCI and DMAP and important issues were encountered in the purification of conjugate **3.23** due to degradation (59%). The amide coupling was performed in the presence of HOBt, EDCI and DIPEA, and led to the isolation of **3.24** in medium yield (54%).

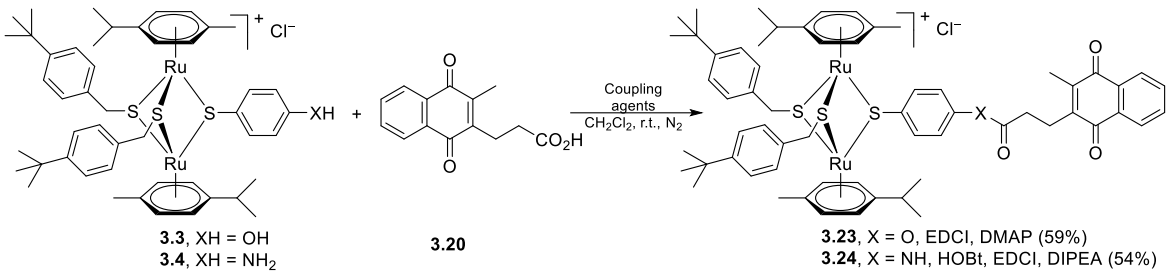

Scheme 3.7. Synthesis of 1,4-naphtoquinone ester and amide conjugates **3.23** and **3.24**.

Varying the relative proportion between the metal units and the drug fragments in this type of conjugates might lead to improved bio-efficacy [174, 387]. To increase the number of 1,4-naphtoquinone molecules anchored on the trithiolato diruthenium core, symmetric intermediates **3.5** and **3.6** bearing either three hydroxy or three amino groups were used for the ester and amide couplings with **3.20**, **3.21** and **3.22** (Scheme 3.8). The reaction of **3.5** with the carboxy 1,4-naphtoquinone derivative **3.20** in the presence of HOBt, EDCI and DIPEA, allowed only the isolation of the monosubstituted conjugate **3.25** in a low yield of 27%. At the same time, important degradation of the diruthenium substrate was observed.

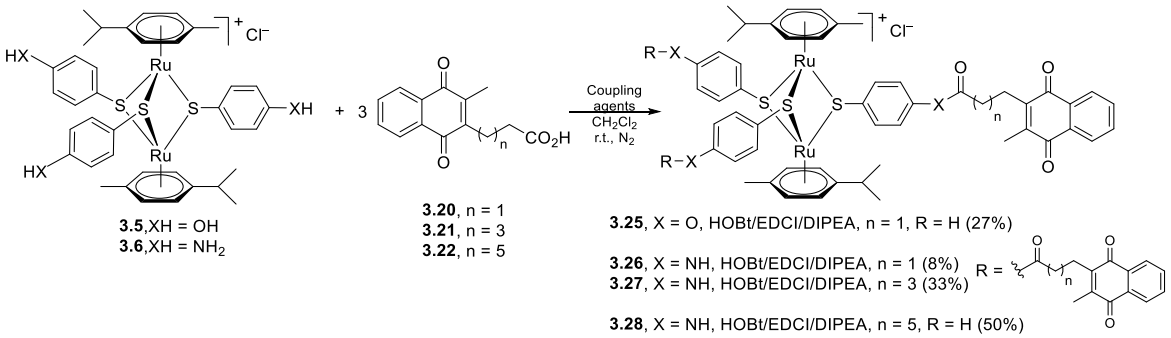

Scheme 3.8. Synthesis of 1,4-naphtoquinone conjugates **3.25**, **3.26**, **3.27** and **3.28**.

The reactions of **3.6** with the menadione carboxy derivatives **3.20** and **3.21** in the presence of HOBt, EDCI, and DIPEA led to the isolation of the tri-amide conjugates **3.26** and **3.27** with low yields of 8% and 33%, respectively (Scheme 3.8). However, the reaction of **3.6** with the 1,4-naphtoquinone analogue **3.22** performed in similar conditions led only to the monosubstituted conjugate **3.28**, isolated with a medium yield of 50%.

All compounds were analyzed and characterized by ^{1}H, ^{13}C and ^{19}F (where suitable) nuclear magnetic resonance spectroscopy (NMR), electrospray ionization mass spectrometry (ESI-MS) and elemental analysis (see Experimental part-Chemistry in the *Supporting information 3* for full details). ESI-MS corroborated the spectroscopic data with the dithiolato precursor **3.1**, the trithiolato diruthenium intermediates **3.2**–**3.7** and the conjugates **3.8**–**3.11** (sulfa-drugs), **3.12** (triclosan), **3.13** and **3.15** (metronidazole), **3.17**–**3.19** (ciprofloxacin) and **3.23**–**3.28** (menadione) exhibiting molecular ion peaks corresponding to $[M\text{-}Cl]^{+}$ ions.

For the assessment of the biological activity, the compounds were prepared as stock solutions in dimethylsulfoxide (DMSO), in which the compounds are well soluble. ^{1}H-NMR spectra of similar conjugates (with polypeptides, coumarin units or derivatives with two or three diruthenium units) dissolved in DMSO-d_6 or deuterated water, recorded at 25 °C 5 min and 28 days after sample preparation showed no visible changes, demonstrating very good stability of the compounds in this highly complexing solvent and in water. [30, 60, 62, 131]

3.2.2. X-ray Crystallography

The crystal structure of the trithiolato diruthenium sulfamethoxazole conjugate **3.9** was established in the solid state by single-crystal X-ray diffraction (an ORTEP representation is shown in Figure 3.3), confirming the expected structure. To the best of our knowledge, this is the first example of a structure containing the trithiolato-bridged diruthenium unit and an organic moiety. Data collection and refinement parameters are given in Table 3.1. Selected bond lengths and angles are presented in Table 3.2.

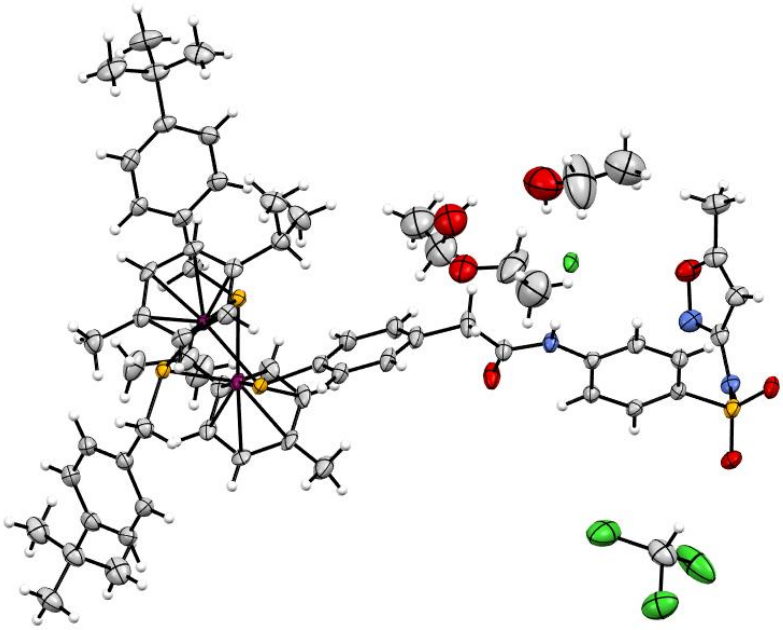

Figure 3.3. ORTEP representation of complex **3.9** (thermal ellipsoids are 50% equiprobability envelopes, and H atoms are spheres of arbitrary diameter; the asymmetric unit contains one organometallic complex, three EtOH, and one $CHCl_3$ molecule).

Table 3.1. Crystal data and structure refinement for **3.9**.

Compound	**3.9**
Formula	$C_{60}H_{74}ClN_3O_4Ru_2S_4 \cdot 3CH_3CH_2OH \cdot CHCl_3$
F.W. ($g \cdot mol^{-1}$)	1524.62
Temperature (K)	110.2(5)
Crystal system	Monoclinic
Space group	$P2_1/n$
a (Å)	14.13470(10)
b (Å)	24.4657(2)
c (Å)	20.7272(2)
α (°)	90
β (°)	100.0580(10)
γ (°)	90
V ($Å^3$)	7057.62(10)
Z	4
D_{calc} ($g \cdot cm^{-3}$)	1.435
μ (mm^{-1})	6.380
F(000)	3168.0
Crystal size (mm^3)	0.2 × 0.075 × 0.05
Θ range for data collection (°)	5.64 to 154.266
Index ranges	
h	−17/12
k	−30/30
l	−26/25
Reflns. collected	56,233
Independent reflns.	14,528 [R_{int} = 0.0442, R_{sigma} = 0.0350]
Data/restraints/parameters	14,528/2/803
GoodF^2	1.047
R1 [$I \geq 2\sigma(I)$]	0.0564
wR2	0.1597
R1 [all data]	0.0613
wR2	0.1645
Largest diff. peak/hole ($Å^{-3}$)	3.23/−1.47

Table 3.2. Comparison of key bond lengths (Å) and angles (°) of the diruthenium moiety in **3.9** and previously reported mixed complex **3.J** (Figure 3.4, data from ref. [388]).

	Complex **3.9**	Complex **3.J**
Ru-S	Ru(1)-S(1) 2.3749(10) Ru(1)-S(2) 2.3927(10) Ru(1)-S(3) 2.3973(10) Ru(2)-S(1) 2.3884(10) Ru(2)-S(2) 2.3931(11) Ru(2)-S(3) 2.3869(10)	Ru(1)-S(1) 2.3878(9) Ru(1)-S(2) 2.4023(9) Ru(1)-S(3) 2.3813(8) Ru(2)-S(1) 2.3992(9) Ru(2)-S(2) 2.3991(8) Ru(2)-S(3) 2.3882(8)
Ru-η6	Ru(1)-cent(C21-C26) Ru(2)-cent(C31-C36)	Ru(1)-cent(C1-C6) 1.708 Ru(2)-cent(C11-C16) 1.709
S-Ru-S	S(1)-Ru(2)-S(2) 76.29(4) S(1)-Ru(2)-S(3) 74.94(4) S(2)-Ru(2)-S(3) 77.32(4) S(1)-Ru(1)-S(2) 76.56(3) S(1)-Ru(1)-S(3) 75.00(4) S(2)-Ru(1)-S(3) 77.13(4)	S(1)-Ru(1)-S(2) 74.95(3) S(1)-Ru(1)-S(3) 77.72(3) S(2)-Ru(1)-S(3) 75.75(3) S(1)-Ru(2)-S(2) 74.81(3) S(1)-Ru(2)-S(3) 77.37(3) S(2)-Ru(2)-S(3) 75.68(3)
Ru-S-Ru	Ru(1)-S(1)-Ru(2) 89.45(3) Ru(1)-S(2)-Ru(2) 88.91(3) Ru(1)-S(3)-Ru(2) 88.95(4)	Ru(1)-S(1)-Ru(2) 89.27(3) Ru(1)-S(2)-Ru(2) 88.93(3) Ru(1)-S(3)-Ru(2) 89.68(3)
Ru-cent(S-S-S)-Ru	Ru(1)-cent(S1-S3)-Ru(2) 178.71	Ru(1)-cent(S1-S3)-Ru(2) 177.30
cent η6-cent(S-S-S)-cent η6	cent(C24-C29)-cent(S1-S3)-cent(C72-C77) 177.74	cent(C1-C6)-cent(S1-S3)-cent(C11-C16) 176.25

Cent—represents the centroid calculated using Mercury CCDC 4.1.2.

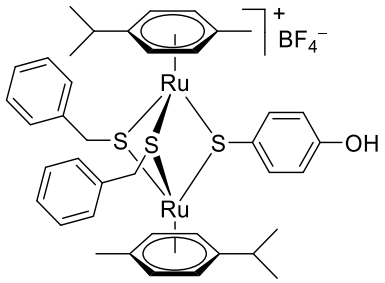

Figure 3.4. Structure of complex **3.J**, $[(\eta^6\text{-}p\text{-}MeC_6H_4Pr^i)_2Ru_2(\mu_2\text{-}SCH_2\text{-}C_6H_5)_2(\mu_2\text{-}SC_6H_4\text{-}p\text{-}OH)]BH_4$ [388].

In the network, an organization in dimers due to the presence of intermolecular H-bonding interactions between the sulfamethoxazole fragments was observed (Figure 3.5).

These interactions involve sulfonamide NH from one molecule and the carboxyamide oxygen atom of another molecule. Additional H-bonding interactions are observed between the carboxyamide NH and the Cl^- counterion. Representative bond lengths and angles for these interactions are given in Table 3.3.

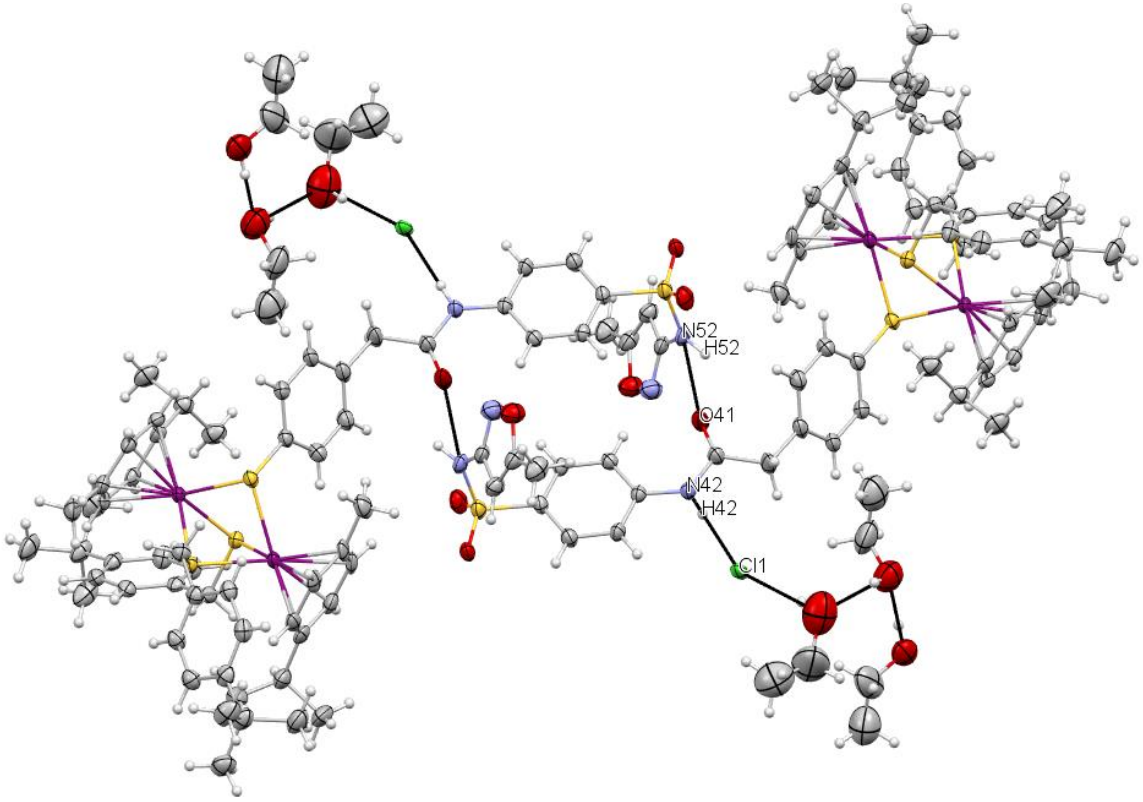

Figure 3.5. Intermolecular H-bonding interactions in the crystal of **3.9** with the formation of dimers; two H-bonds interconnect the carboxyamide C=O groups from the two diruthenium complexes to the sulfonamide NH from the other molecule. Supplementary H-bonding interactions were observed between the carboxyamide NH and the Cl^- counterion (contacts D-H···A correspond to N-H···Cl^-, N-H···O, image produced using Mercury CCDC 4.1.2, see bond parameters in Table 3.3).

Table 3.3. Intramolecular H-bonding interactions for complex **3.9**.

Compound	**Contact**	**Distance (Å)**			**Angle (°)**
	D-H···A	***D*-H**	**H···*A***	***D*···*A***	***D*-H···*A***
9	N52-H52…O41	0.860	2.162	2.786	129.22
	N42-H42…Cl1	0.859	2.407	3.254	169.15

3.2.3. Assessment of the In Vitro Activity against the Apicomplexan Parasite Toxoplasma gondii

3.2.3.1. Primary Screening

The activity against *T. gondii* tachyzoites and HFF (human foreskin fibroblasts) host cells of the new conjugates (13 compounds), of the antimicrobial drugs (8 compounds) and the representative intermediates (9 compounds) has been investigated. The trithiolato intermediates **3.2**–**3.6** have been evaluated previously against *T. gondii* β-gal under similar conditions [29, 30, 131], and the corresponding values were introduced in Table 3.4 and Figure 3.6 for comparison. Of note, complex **3.5** exhibited no activity against the parasite [29] and was therefore not included in the discussion of the results. The purity of isolated ciprofloxacin and menadione ester conjugates **3.17**, **3.23** and **3.25** was not satisfactory and, therefore, these compounds were not evaluated.

In a primary screening, transgenic *T. gondii* tachyzoites constitutively expressing β-galactosidase (*T. gondii* β-gal) were cultured in HFF monolayers and exposed to concentrations of 1 and 0.1 μM of each compound of interest. In parallel, the cytotoxicity of these compounds was evaluated at the same concentrations in noninfected HFF. As a measure of the parasite proliferation, β-galactosidase activity was determined, while the impact on noninfected HFF was assessed using the alamarBlue assay; the results are summarized in Table 3.4 and Figure 3.6.

Table 3.4. Cytotoxicity/efficacy screening of compounds in noninfected HFF cultures and *T. gondii* β-gal tachyzoites cultured in HFF. Tests were realized in triplicate. The values of the compounds selected for determination of IC_{50} values against *T. gondii* β-gal are highlighted in bold.

Compound	HFF Viability (%)		*T. gondii* β-gal Growth (%)	
	0.1 µM	**1 µM**	**0.1 µM**	**1 µM**
Ruthenium intermediates				
3.2 [a]	**91 ± 4**	**73 ± 1**	**114 ± 2**	**110 ± 2**
3.3 [a]	**76 ± 6**	**46 ± 6**	**66 ± 14**	**2 ± 0**
3.4 [a]	**74 ± 2**	**48 ± 1**	**57 ± 1**	**2 ± 0**
3.6 [a]	97 ± 4	61 ± 6	115 ± 4	85 ± 5
3.7	71 ± 2	46 ± 6	52 ± 13	3 ± 1
Conjugates with sulfa-drugs				
Dapsone	92 ± 4	103 ± 3	77 ± 4	42 ± 0
3.8	104 ± 1	91 ± 2	148 ± 2	36 ± 2
Sulfamethoxazole	93 ± 3	102 ± 5	78 ± 5	75 ± 7
3.9	90 ± 12	63 ± 7	83 ± 8	77 ± 3
Sulfadiazine	101 ± 2	33 ± 3	57 ± 5	70 ± 5
3.10	**113 ± 1**	**93 ± 2**	**72 ± 3**	**0 ± 0**
Sulfadoxine	97 ± 3	104 ± 0	111 ± 3	83 ± 2
3.11	**100 ± 3**	**100 ± 8**	**116 ± 1**	**11 ± 1**
Conjugates with triclosan and metronidazole				
Triclosan	99 ± 1	97 ± 1	80 ± 2	71 ± 2
3.12	100 ± 2	103 ± 1	76 ± 6	66 ± 12
Metronidazole	101 ± 2	100 ± 1	115 ± 8	116 ± 6
3.13	**115 ± 2**	**93 ± 1**	**101 ± 7**	**1 ± 0**
3.14	98 ± 3	97 ± 2	115 ±7	92 ± 1
3.15	**116 ± 1**	**99 ± 1**	**98 ± 2**	**1 ± 0**
Conjugates with ciprofloxacin				
Ciprofloxacin	101 ± 1	99 ± 0	82 ± 3	84 ± 3
3.18	92 ± 0	89 ± 0	94 ± 2	102 ± 1
3.19	102 ± 2	94 ± 2	68 ± 4	21 ± 3
Conjugates with menadione				
Menadione	117 ± 3	101 ± 4	103 ± 7	50 ± 2
3.20	105 ± 3	94 ± 2	101 ± 8	107 ± 3
3.21	109 ± 2	95 ± 1	86 ± 10	84 ± 5
3.22	110 ± 3	87 ± 1	83 ± 4	92 ± 1
3.24	**95 ± 1**	**92 ± 2**	**65 ± 4**	**3 ± 0**
3.26	101 ± 2	102 ± 1	89 ± 16	90 ± 7
3.27	100 ± 2	100 ± 3	164 ± 4	92 ± 3
3.28	98 ± 3	92 ± 2	71 ± 6	46 ± 1

[a] Data for compounds **3.2**–**3.6** were previously reported [29, 30, 131]. Complex **3.5** exhibited no activity against the parasite [29] (values not shown).

Diruthenium Intermediates

From the diruthenium intermediates, carboxy and tri-amino derivatives **3.2** and **3.6** had no effect on parasite proliferation, but slightly affected HFF viability at 1 µM. In contrast, hydroxy, amino and alkyne functionalized compounds **3.3**, **3.4** and **3.7** drastically reduced *T. gondii* β-gal proliferation when administered at 1 µM but were also toxic to HFF already at 0.1 µM.

Antimicrobial Drugs and Conjugates

Except for sulfadiazine and sulfamethoxazole conjugate **3.9**, all antimicrobial drugs, intermediates based on the antimicrobials, and conjugates did not affect the viability of the HFF even at the highest tested concentration (1 µM) (Table 3.4, Figure 3.6).

The poor *in vitro* anti-*Toxoplasma* activity of the selected antimicrobial drugs agrees with some previously reported data [192].

If dapsone impaired parasite proliferation even at 0.1 µM, its conjugate **3.8** inhibited *T. gondii* β-gal proliferation to 36% only when applied at 1 µM. Both sulfamethoxazole and its conjugate **3.9** exhibited only reduced effect on the parasite. However, while sulfamethoxazole had little influence on HFF viability, **3.9** displayed considerable cytotoxicity to host cells at 1 µM.

Remarkably, the sulfadiazine conjugate **3.10** was not toxic to HFF but inhibited the *T. gondii* β-gal proliferation to 72% when administrated at 0.1 µM, and completely abolished it at 1 µM. Sulfadiazine was toxic to HFF when administrated at 1 µM, but at 0.1 µM, it did not affect the HFF viability but reduced the *T. gondii* β-gal proliferation to 57%. When applied at 1 µM, sulfadoxine-conjugate **3.11** exhibited a stronger effect on the *T. gondii* β-gal proliferation compared to sulfadoxine (11 *vs*. 83%).

All sulfa-drugs were connected to the trithiolato diruthenium unit *via* similar strong carbamide bonds. With the exception of the sulfamethoxazole conjugate **3.9**, the nature of the anchored organic drug had little effect on the viability of the host cells, but in some cases, impacted the efficacy against the parasite (e.g., sulfadiazine *vs*. **3.10** and sulfadoxine *vs*. **3.11**). Compared to the trithiolato diruthenium amino analogue **3.4**, conjugates with

sulfa-drugs were all less cytotoxic to HFF.

Compared to the diruthenium carboxy intermediate **3.2**, ester conjugates with triclosan **3.12** and metronidazole **3.13** reduced parasite proliferation more efficiently at 1 µM.

Both triclosan and its ester conjugate **3.12** presented a similar reduced antiparasitic effect (at 1 µM parasite proliferation was reduced to 71 and 66%, respectively).

Although metronidazole and azide intermediate **3.14** displayed only low activity against *T. gondii* β-gal, conjugates **3.13** (ester) and **3.15** (triazole) were highly active at 1 µM and almost abolished proliferation. In this case, conjugation to the trithiolato diruthenium unit improved the antiparasitic activity without increasing host toxicity. Alkyne intermediate **3.7** was more active on the parasite than the carboxy precursor **3.2**, but also more toxic to HFF, while 'click' metronidazole conjugate **3.15** impacted less the HFF viability than **3.7**.

Compared to amino diruthenium compound **3.4**, amide conjugates with ciprofloxacin **3.18** and **3.19**, and with menadione **3.24** were less detrimental to host cell viability.

N-Boc protected ciprofloxacin conjugate **3.18** exhibited no antiparasitic activity, while the deprotected conjugate **3.19** had a stronger impact on *T. gondii* β-gal proliferation in comparison to ciprofloxacin (21 *vs*. 84% at 1 µM).

When administered at 1 µM, menadione reduced *T. gondii* β-gal proliferation to 50%, while its derivatives **3.20**, **3.21** and **3.22**, presenting different chain lengths between the 1,4-naphtoquinone unit and the carboxy group, exhibited little antiparasitic effect. Compared to menadione intermediate **3.20**, the amide conjugate **3.24** presented increased anti-*T. gondii* β-gal activity, almost abolishing parasite proliferation at 1 µM. Conjugates **3.26** and **3.27** presenting three menadione units connected via amide bonds to the trithiolato diruthenium core did not affect parasite proliferation, regardless of the linker size. A similar lack of antiparasitic effect has been previously observed in the case of a coumarin trisubstituted ester derivative [131] and might be associated with the important size of this

type of analogue. This observation is corroborated by the results obtained for the monosubstituted conjugate **3.28**, which presented increased efficacy on the parasite compared to intermediate **3.22**. The difference in antiparasitic activity between the monosubstituted derivatives **3.24** and **3.28** might be due to the nature of the other two bridging thiols and the length of the linker between the diruthenium scaffold and the menadione moiety.

The first screening allowed the identification of five conjugates, **3.10** (sulfadiazine), **3.11** (sulfadoxine), **3.13** and **3.15** (metronidazole), **3.19** (ciprofloxacin) and **3.24** (menadione) that were more active against *T. gondii* at 1 μM compared to the respective antimicrobial drug. Concomitantly, these derivatives exhibited low or intermediate impairment of HFF viability at the highest tested concentration (1 μM). The highest antiparasitic activity increase was observed in the case of the metronidazole ester and triazole conjugates **3.13** and **3.15**, which almost abolished parasite proliferation when administered at 1 μM while the antimicrobial drug was inactive at the same concentration. The most modest amelioration was observed in the case of menadione and its respective conjugate **3.24** which, at 1 μM, reduced parasite proliferation with 50 and 3%, respectively.

3.2.3.2. Secondary Screening

Based on the primary screening, conjugates **3.10**, **3.11**, **3.13**, **3.15** and **3.24** were selected for the determination of the IC_{50} values against *T. gondii* and the assessment of HFF viability after exposure to 2.5 μM. For the selection of the compounds for IC_{50} determination, two criteria had to be simultaneously satisfied: (i) *T. gondii* β-gal growth inhibition of 90% or more compared to an untreated control when the compound was applied at 1 μM, and (ii) HFF host cell viability not impaired by more than 50% for a compound applied at 1 μM. The results are summarized in Table 3.5, and dose-response curves are shown in Figure S3.1 (*Supporting information 3*).

For comparison, the results obtained for the carboxy and amino-functionalized diruthenium intermediates **3.2** and **3.4**, as well as those for pyrimethamine used as the standard, are also shown.

A

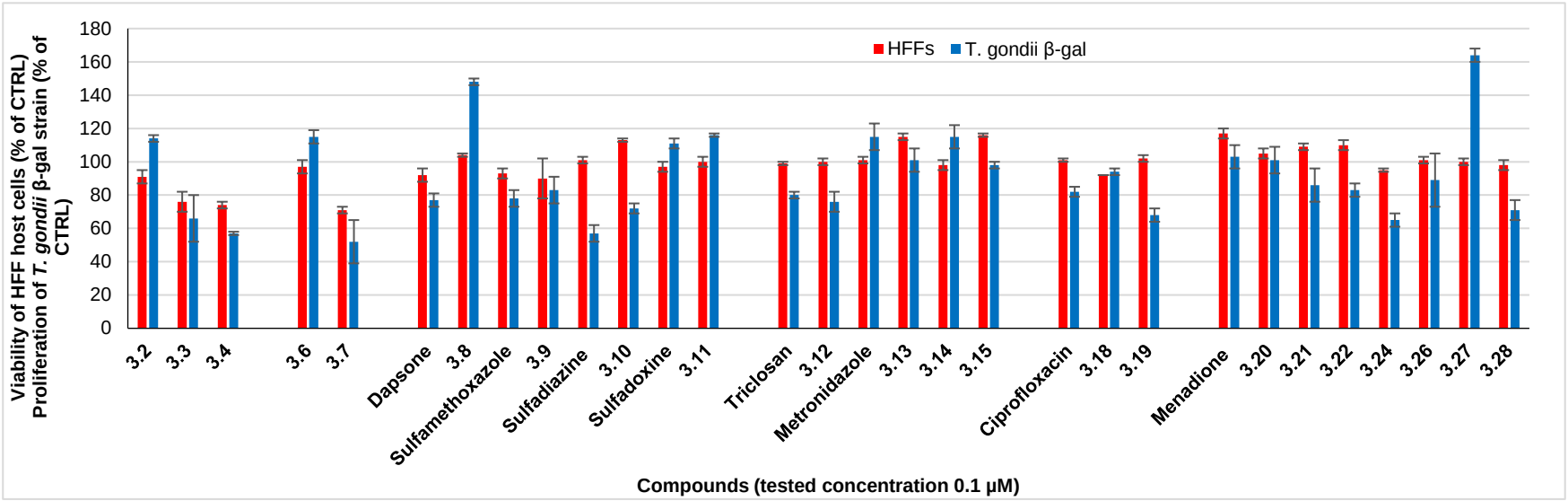
Viability of HFF host cells (% of CTRL)
Proliferation of T. gondii β-gal strain (% of CTRL)
HFFs
T. gondii β-gal
180
160
140
120
100
80
60
40
20
0
3.2
3.3
3.4
3.6
3.7
Dapsone
3.8
Sulfamethoxazole
3.9
Sulfadiazine
3.10
Sulfadoxine
3.11
Triclosan
3.12
Metronidazole
3.13
3.14
3.15
Ciprofloxacin
3.18
3.19
Menadione
3.20
3.21
3.22
3.24
3.26
3.27
3.28
Compounds (tested concentration 0.1 µM)

B

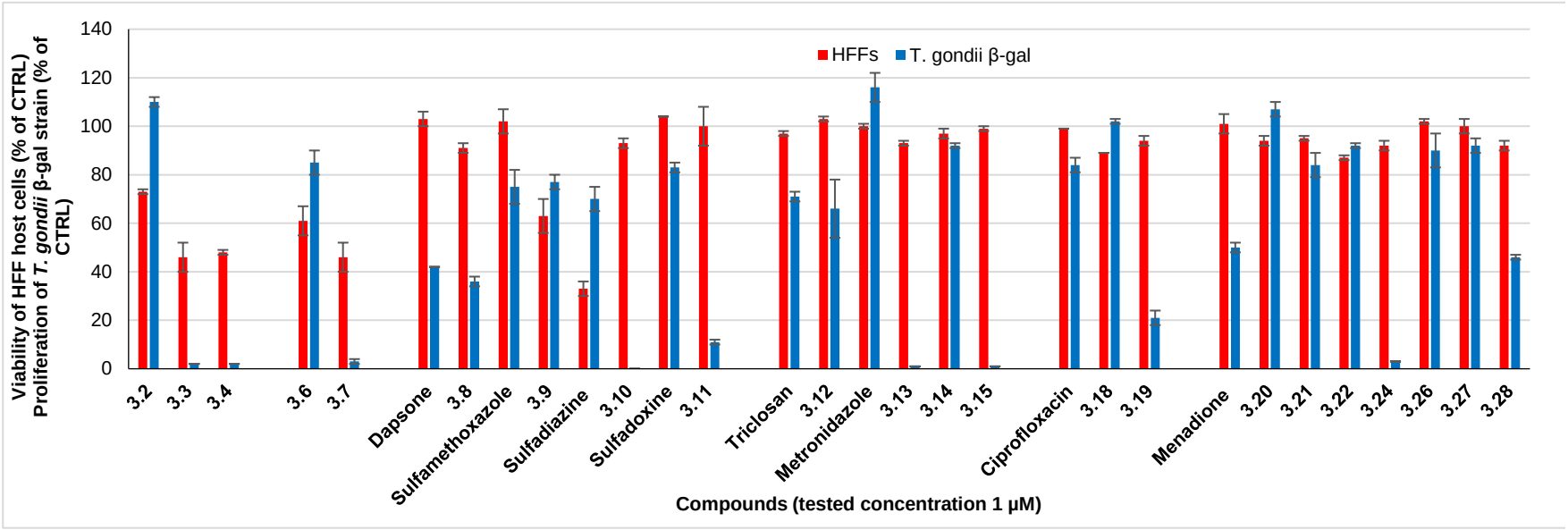

Figure 3.6. Clustered column chart showing the *in vitro* activities at 0.1 (**A**) and 1 μM (**B**) of the 30 tested compounds on HFF viability and *T. gondii* β-gal proliferation. Noninfected HFF monolayers treated only with 0.1% DMSO exhibited 100% viability and 100% proliferation was attributed to *T. gondii* β-gal tachyzoites treated only with 0.1% DMSO. Red bars represent viability values of HFF, and blue bars represent the proliferation of *T. gondii* β-gal tachyzoites. For each assay, standard deviations were calculated from triplicates and are displayed on the graph. Data for compounds **3.2**–**3.4** and **3.6** were previously reported in [29, 30, 131]. Complex **3.5** exhibited no activity against the parasite [29] (values not shown).

Table 3.5. Half-maximal inhibitory concentration (IC_{50}) values (μM) on *T. gondii* β-gal for seven selected compounds and pyrimethamine (used as standard), and their effect at 2.5 μM on HFF viability.

Compound	*T. gondii* β-gal IC_{50} (μM)	[LS; LI] [b]	SE [c]	HFF Viability at 2.5 μM (%) [d]	SD [e]
Pyrimethamine	0.326	[0.396; 0.288]	0.052	99	6
Ruthenium intermediates					
3.2 [a]	0.181	[1.482; 0.274]	0.954	99	2
3.4 [a]	0.153	[0.185; 0.127]	0.049	51	5
Conjugates with sulfa-drugs					
3.10	0.524	[0.562; 0.488]	0.069	62	1
3.11	0.063	[0.072; 0.055]	0.136	83	0
Conjugates with triclosan and metronidazole					
3.13	0.152	[0.181; 0.127]	0.175	64	3
3.15	0.500	[0.884; 0.284]	0.568	102	2
Conjugates with menadione					
3.24	0.481	[0.525; 0.441]	0.086	32	3

[a] Data for pyrimethamine, **3.2** and **3.4** were previously reported [29, 30, 131]. [b] Values at 95% confidence interval (CI); LS is the superior limit of CI and LI is the inferior limit of CI. [c] The standard error of the regression (SE), represents the average distance that the observed values fall from the regression line. [d] Control HFF cells treated only with 0.25% DMSO exhibited 100% viability. [e] The standard deviation of the mean (six replicate experiments).

The most interesting compound of the series is the sulfadoxine conjugate **3.11**, exhibiting a low IC_{50} (0.063 μM), and only slightly affecting the HFF viability at 2.5 μM (83%). Of note, the IC_{50} value of **3.11** is significantly lower than that of the corresponding carboxy diruthenium intermediate (0.181 μM) or that of pyrimethamine (0.326 μM). Interestingly, the sulfadiazine derivative **3.10** presented poor antiparasitic activity (IC_{50} 0.524 μM, more than 8 times higher compared to **3.11**), and increased toxicity to HFF (62%). These significant differences between these two conjugates underline the importance of the drug fragment for the biological activity, as both conjugates share the same diruthenium moiety and similar bonding between the two units. Sulfadoxine is interesting as this sulfonamide is used in combination with pyrimethamine in the treatment or prevention of malaria [389-392].

A significant difference was observed between the two metronidazole conjugates

3.13 and **3.15**. In comparison to **3.2**, the ester conjugate **3.13** presents a lower IC_{50} value (0.152 *vs*. 0.181 µM), but increased HFF toxicity when administered at 2.5 µM (64 *vs*. 99%). The triazole conjugate **3.15** exhibited no HFF cytotoxicity but also reduced antiparasitic activity. As both compounds were obtained from the same carboxy diruthenium analogue **3.2**, the differences are likely due to the linking units between the diruthenium moiety and metronidazole.

The amide menadione hybrid **3.24** was not only more toxic to HFF (viability at 2.5 µM, 32 *vs*. 51%) but also less active in parasite proliferation inhibition compared to the corresponding amino intermediate **3.4** (0.481 *vs*. 0.153 µM).

Overall, the results obtained for conjugates **3.10**, **3.11**, **3.13**, **3.15** and **3.24** indicate that this type of hybrid molecules, antimicrobial drug-thiolato-bridged dinuclear ruthenium(II)–arene complex, seems promising and that a fine-tuning of the biological activity can be achieved by a judicious choice of the drugs and connecting units.

The mechanism of action of these trithiolato-bridged dinuclear ruthenium(II)–arene complexes and conjugates has not been yet elucidated. In contrast to almost all other ruthenium(II)–arene complexes presenting labile chlorine or carboxylate ligands, these dinuclear ruthenium(II)–arene compounds do not hydrolyze and are stable in the presence of DNA and amino acids [64]. Oxidation of cysteine (Cys) and glutathione (GSH) to form cystine and glutathione-disulfide (GSSG), respectively, was observed in the presence of some complexes. Still, no correlation between *in vitro* cytotoxicity and the catalytic activity on the oxidation reaction of glutathione could be established [38, 65].

For some compounds, transmission electron microscopy (TEM) detected ultrastructural alterations in the matrix of the *T. gondii* mitochondria within few hours of treatment, followed by a more pronounced destruction of tachyzoites at later time points [29, 131]. Gaining more insight into the mechanisms of action of these dinuclear complexes, responsible for the observed effects on various parasites, will allow a more rational selection of drugs that could be anchored to the diruthenium scaffold (e.g., organic molecules sharing the same molecular target or that can direct the diruthenium fragment to reach a specific biomolecule or organelle).

3.3. Experimental

3.3.1. Chemistry

The experimental chemistry portion, with a full description of experimental procedures and characterization data for all compounds, is presented in the *Supporting information 3*.

3.3.2. Crystal-Structure Determination

A crystal of **3.9** ($C_{60}H_{74}ClN_3O_4Ru_2S_4 \cdot 3CH_3CH_2OH \cdot CHCl_3$) was mounted in the air at ambient conditions. All measurements were made on a *RIGAKU Synergy S* area-detector diffractometer [111] using mirror optics monochromated Cu *K*α radiation (λ = 1.54184 Å) [112]. The unit cell constants and an orientation matrix for data collection were obtained from a least-squares refinement of the setting angles of reflections in the range $2.82° < \theta < 77.133°$. A total of 2404 frames were collected using ω scans, with 0.25 s exposure time, a rotation angle of 0.5° per frame, a crystal-detector distance of 65.0 mm, at T = 110(2) K.

Data reduction was performed using the *CrysAlisPro* [111] program. The intensities were corrected for Lorentz and polarization effects, and an absorption correction based on the multiscan method using SCALE3 ABSPACK in *CrysAlisPro* [111] was applied. Data collection and refinement parameters are given in Table 3.1.

The structure was solved by direct methods using *SHELXT* [113], which revealed the positions of all non-hydrogen atoms of the title compound. All non-hydrogen atoms were refined anisotropically. H-atoms were assigned in geometrically calculated positions and refined using a riding model where each H-atom was assigned a fixed isotropic displacement parameter with a value equal to 1.2 Ueq of its parent atom (1.5 Ueq for methyl groups).

The refinement of the structure was carried out on F^2 using full-matrix least-squares procedures, which minimized the function $\Sigma w(F_o^2 - F_c^2)^2$. The weighting scheme was based on counting statistics and included a factor to down-weight the intense reflections. All calculations were performed using the *SHELXL-2014/7* [114] program in OLEX2 [115].

3.3.3. In Vitro Activity Assessment against T. gondii Tachyzoites and HFF

All tissue culture media were purchased from Gibco-BRL, and biochemical agents from Sigma-Aldrich. Human foreskin fibroblasts (HFF) were purchased from ATCC, maintained in DMEM (Dulbecco's Modified Eagle's Medium) supplemented with 10% fetal calf serum (FCS, Gibco-BRL, Waltham, MA, USA) and antibiotics as previously

described [28]. Transgenic *T. gondii* β-gal samples (expressing the β-galactosidase gene from *Escherichia coli*) were kindly provided by Prof. David Sibley (Washington University, St. Louis, MO, USA) and were maintained, isolated, and prepared for new infections as shown before [28, 117].

All the compounds were prepared as 1 mM stock solutions from powder in dimethyl sulfoxide (DMSO, Sigma, St. Louis, MO, USA). For *in vitro* activity and cytotoxicity assays, HFF were seeded at 5×10^3/well and allowed to grow to confluence in phenol-red free culture medium at 37 °C and 5% CO_2. Transgenic *T. gondii* β-gal tachyzoites were isolated and prepared for infection as described [28]. *T. gondii* tachyzoites were released from host cells, and HFF monolayers were infected with freshly isolated parasites (1×10^3/well), and compounds were added concomitantly with infection. In the primary screening, HFF monolayers infected with *T. gondii* β-gal received 0.1 and 1 μM of each compound, or the corresponding concentration of DMSO (0.01 or 0.1% respectively) as controls and incubated for 72 h at 37˚C/5% CO_2 as previously described [62].

For the next step, IC_{50} measurements for *T. gondii* β-gal were performed. The selected compounds were added concomitantly with infection in 8 serial concentrations 0.007, 0.01, 0.03, 0.06, 0.12, 0.25, 0.5, and 1 μM. After a period of 72 h of culture at 37 °C/5% CO_2, the culture medium was aspirated, and cells were permeabilized by adding 90 μL PBS (phosphate-buffered saline) with 0.05% Triton X-100. After the addition of 10 μL 5 mM chlorophenolred-β-D-galactopyranoside (CPRG; Roche Diagnostics, Rotkreuz, Switzerland) in PBS, the absorption shift was measured at 570 nm wavelength at various time points using an EnSpire® multimode plate reader (PerkinElmer, Inc., Waltham, MA, USA).

For the primary screening at 0.1 and 1 μM, activity was measured as the release of chlorophenol red over time, was calculated as a percentage from the respective DMSO control, which represented 100% of *T. gondii* β-gal growth. For the IC_{50} assays, the activity measured as the release of chlorophenol red over time was proportional to the number of live parasites down to 50 per well as determined in pilot assays. IC_{50} values were calculated after the logit-log-transformation of relative growth and subsequent regression analysis.

All calculations were performed using the corresponding software tool contained in the Excel software package (Microsoft, Redmond, WA, USA). Cytotoxicity assays using uninfected confluent HFF host cells were performed by the alamarBlue assay as previously reported [118]. Confluent HFF monolayers in 96 well-plates were exposed to 0.1, 1 and 2.5 μM of each compound. Non-treated HFF as well as DMSO controls (0.01%, 0.1% and

0.25%) were included. After 72 h of incubation at 37 °C/5% CO_2, the medium was removed, and plates were washed once with PBS. 200 µL of Resazurin (1:200 dilution in PBS) were added to each well. Plates were measured at excitation wavelength 530 nm and emission wavelength 590 nM at the EnSpire® multimode plate reader (PerkinElmer, Inc.). Fluorescence was measured at different time points. Relative fluorescence units were calculated from time points with linear increases.

3.4. Conclusions

This study has focused on the synthesis and *in vitro* evaluation of 13 new conjugates based on trithiolato-bridged ruthenium(II)–arene scaffold tethered with various antimicrobial drugs, aiming at improving the antiparasitic properties and the selectivity.

The type of chemical bond between the two units and their relative proportion was varied. In total, 30 compounds (conjugates, representative intermediates, drugs) were submitted to a first activity screening against *T. gondii* β-gal tachyzoites cultured in HFF and cytotoxicity determination against HFF host cells, which allowed the identification of five interesting conjugates. The IC_{50} values against *T. gondii* and the evaluation of HFF viability after exposure to 2.5 µM led to the selection of the sulfadoxine conjugate **3.11** as the most promising of this series of 13 conjugates.

Our study suggests that the nature of the drug and of the linker between the drug and the diruthenium(II) moiety greatly impacts biological activity. Overall, anchoring antimicrobial drugs to trithiolato diruthenium(II)–arene moieties is a promising approach for obtaining new compounds presenting different toxicity profiles than the parent organometallic complexes. The conjugates obtained in this study deserve further attention and can be evaluated for other pharmacological applications (e.g., antiproliferative activity on cancer cells or as antibacterials).

Conclusions

Protozoan parasites among which *Toxoplasma gondii*, are important threat to people and animals worldwide. Hence the development of new effective and selective medications is of great importance.

This study was focused on the synthesis of new series of trithiolato-bridged dinuclear ruthenium(II)-arene complexes and conjugates as potential anti-toxoplasma drugs with improved activity and selectivity. The nature of the anchored moieties (fluorophores, metabolites and drugs), their relative proportion, nature of the linking unit between the diruthenium core and the conjugated molecule (ester, amide, triazole) were varied. Five series of compounds with total of 18 ruthenium intermediates 29 intermediates and 93 new ruthenium complexes functionalized with organic molecules were synthesized and fully characterized. All dyads and respective intermediates were submitted to first biological *in vitro* screening on *T. gondii* β-gal grown in HFF and HFF themselves, followed with IC_{50} determination for the most active compounds against *T. gondii* β-gal with good selectivity profile towards HFF host cells.

In the first two series coumarin and BODIPY fluorescent dyes were successfully attached to the trithiolato-bridged ruthenium(II)-arene scaffold. Although fluorescence was almost completely quenched upon coupling in case of coumarin-tagged conjugates they presented interesting bioactivity. BODIPY analogues showed better physico-chemical properties, but reduced antiparasitic activity. Four complexes (**1.2.20**, **1.2.22**, **1.2.26**, and **1.2.36**) exhibited sufficient quantum yields (up to Φ_F =19%) and first confocal microscopy studies in HFF were performed.

The obtainment of nucleobase-tethered diruthenium conjugates allowed the exploit of a new synthetic approach: the use of CuAAC click reactions on the complex. This method allowed to couple nucleic bases and proved itself to be a valuable option for further derivatization of this type of diruthenium complexes. However, attachment of nucleobase onto diruthenium scaffold does not appear to be a very promising strategy for improvement of antiparasitic activity.

The series of complexes bearing lipophilic moieties confirmed that the activity of these diruthenium complexes depends strongly on the lipophilicity/hydrophilicity balance, thus no direct structure-activity relationship could be identified. The process seems to be dependent on multiple factors and a fine structural tuning is needed to obtain compounds

with improved biological properties.

Attachment of antimicrobial drugs to trithiolato-bridged ruthenium(II)–arene complexes proved itself to be a promising strategy for obtaining new conjugates with different toxicity profiles compared the parent organometallic complexes.

Among 93 newly developed dyads, compounds **1.1.12a**, **1.2.21**, **2.1.14**, **2.1.36**, **2.2.11a**, **2.2.14a** and **3.11** showed interesting activity and selectivity profile, with IC_{50} values of 0.105, 0.059, 0.111, 0.036, 0.135 and 0.063 μM respectively, with medium to low cytotoxicity towards host cells when applied at 2.5 μM, (viability of HFF 58-83%).

Overall, this study shows that attachment of different organic moieties onto trithiolato-bridged dinuclear ruthenium(II)-arene scaffold can lead to an improved *T. gondii* antiparasitic efficacy and selectivity.

The compounds developed in this work can be submitted for further biological *in vitro* activity screening against other types of parasites, bacteria, and cancer cells and *in vivo* (mouse model) tests on *T. gondii*.

Additional investigation of the cellular localization/molecular targets of complexes with fluorescent tags inside cells with confocal microscopy is required for better understanding of their mode of actions which would facilitate further structure modifications depending on the results. The exact influence of polarity and lipophilicity on the cytotoxicity could be confirmed with a thorough study of parameters such as logP, of the complexes and interactions of the best complexes from the series (**1.1.12a**, **1.2.21**, **2.1.14**, **2.1.36**, **2.2.11a**, **2.2.14a** and **3.11**) with model membranes, peptides, DNA, etc. for better understanding of influence of the substituents on the diruthenium core.

Supporting information

1.1. Coumarin-Tagged Dinuclear Trithiolato-Bridged Ruthenium(II)-Arene Complexes[6]

1.1.1. X-ray crystallography

Table S1.1.1. Crystal data and structure refinement for **1.1.21 (19JF005_M029f(21-30))**

Compound	**1.1.21 (19JF005_M029f(21-30))**
Formula	$C_{39}H_{45}Cl_3O_3Ru_2S_3$
F.W. ($g \cdot mol^{-1}$)	966.42
Temperature (K)	173.01(10)
Crystal system	monoclinic
Space group	$P2_1/c$
a (Å)	10.17797(4)
b (Å)	21.05828(9)
c (Å)	19.56601(8)
α (°)	90
β (°)	103.8437(4)
γ (°)	90
V ($Å^3$)	4071.77(3)
Z	4
D_{calc} ($g \cdot cm^{-3}$)	1.576
μ (mm^{-1})	9.537
F(000)	1960.0
Crystal size (mm^3)	0.25 × 0.15 × 0.1
Radiation	CuKα (λ = 1.54184)
2Θ range for data collection (°)	6.266 to 155.814
Index ranges	
h	-12 / 12
k	-26 / 24
l	-24 / 24
Reflns. collected	64148
Independent reflns.	8560 [R_{int} = 0.0727, R_{sigma} = 0.0347]
Data/restraints/parameters	8560/0/460
GoodF^2	1.037
R1 [I>=2σ (I)]	0.0383
wR_2	0.0993
R1 [all data]	0.0398
wR_2	0.1006
Largest diff. peak/hole ($Å^{-3}$)	0.95 and -1.55 e

[6] This chapter was published as Coumarin-Tagged Dinuclear Trithiolato-Bridged Ruthenium (II)·Arene Complexes: Photophysical Properties and Antiparasitic Activity, *ChemBioChem*, **2020**, 21, 2818-2835. https://doi.org/10.1002/cbic.202000174. This article is licensed under a Creative Commons Attribution International License (CC BY 4.0)

Table S1.1.2. Comparison of key bond lengths (Å) and angles (°) of **1.1.21** (**19JF005_M029f(21-30)**).	
	19JF005_M029f(21-30)
Ru-S	Ru(1)-S(1) 2.4091(7) Ru(1)-S(2) 2.3834(7) Ru(1)-S(3) 2.4006(7) Ru(2)-S(1) 2.4182(7) Ru(2)-S(2) 2.3688(7) Ru(2)-S(3) 2.4117(7)
Ru-*η*6	Ru(1)-cent(C26-C31) 1.691 Ru(2)-cent(C9-C14) 1.699
S-Ru-S	S(1)-Ru(1)-S(2) 76.18(2) S(1)-Ru(1)-S(3) 76.00(2) S(2)-Ru(1)-S(3) 78.38(2) S(1)-Ru(2)-S(2) 76.27(2) S(1)-Ru(2)-S(3) 75.62(2) S(2)-Ru(2)-S(3) 78.44(2)
Ru-S-Ru	Ru(1)-S(1)-Ru(2) 87.59(2) Ru(1)-S(2)-Ru(2) 89.34(2) Ru(1)-S(3)-Ru(2) 87.93(2)
Ru-cent(S-S-S)-Ru	Ru(1)-cent(S1-S3)-Ru(2) 176.46
cent *η*6-cent(S-S-S)-cent *η*6	cent(C26-C31)-cent(S1-S3)-cent(C9-C14) 175.83

Table S1.1.3. Intramolecular H-bonding interactions for complex **1.1.21** (**19JF005_M029f(21-30)**).					
Compnd.	**Contact**	**Distance (Å)**			**Angle (°)**
	D-H···A	***D*-H**	**H···*A***	***D*···*A***	***D*-H···*A***
21 **19JF005_M029f(21-30)**	O24-H24…Cl3	0.820	2.325	3.144	177.62
	O7-H7…Cl3	0.820	2.239	3.032	162.66
	O41-H41…Cl3	0.820	2.325	3.102	158.19

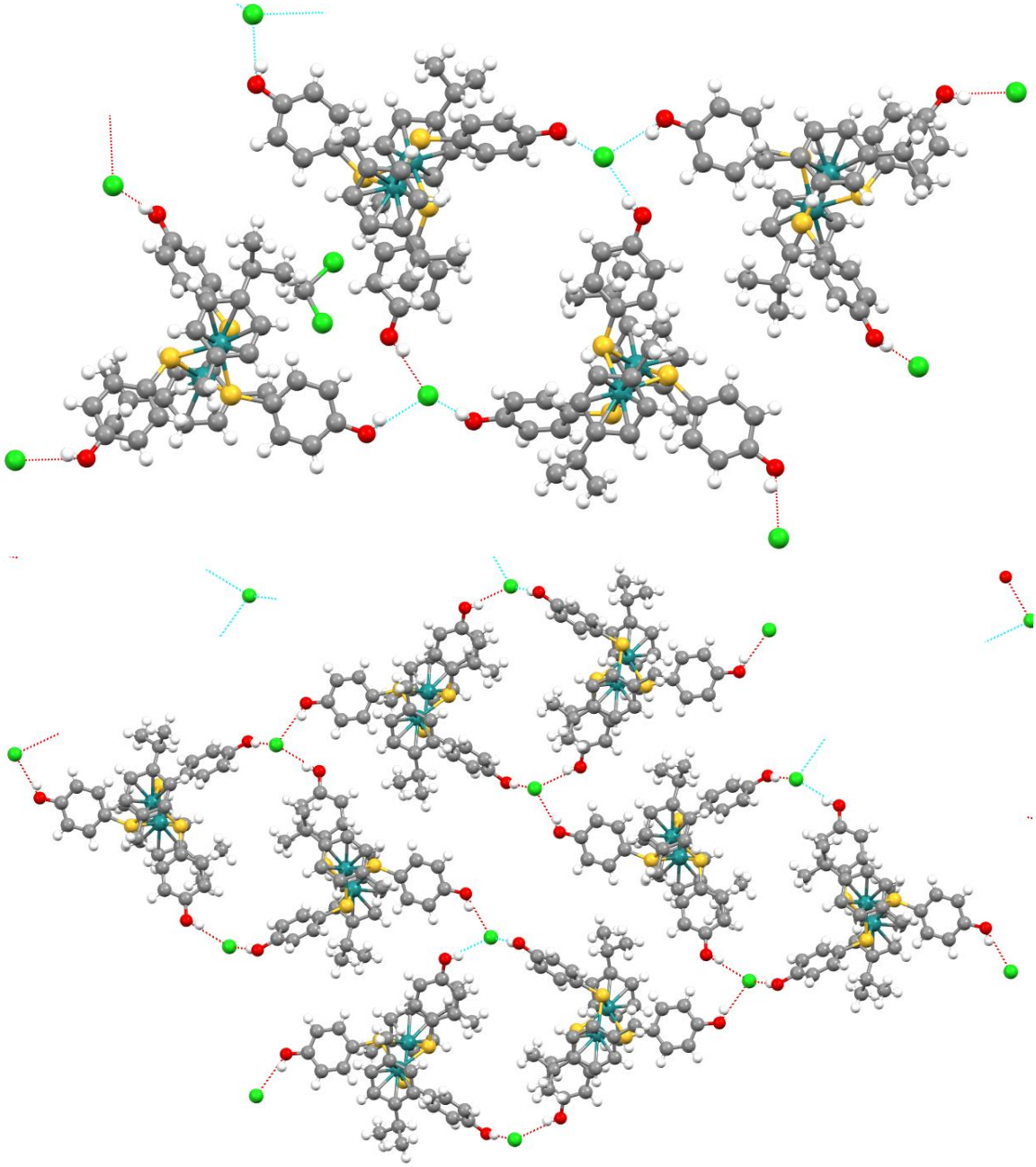

Figure S1.1.1. Intermolecular H-bonding interactions in the crystal of **1.1.21 (19JF005_M029f(21-30))** with the formation of dimers; four H-bonds interconnect four hydroxy groups from two di-ruthenium complexes via two chorine anion bridges, (contacts D-H···A correspond to O-H···Cl^-, image produced using Mercury CCDC 4.1.2, see bond parameters in Table 1.1.2).

1.1.2. Stability in DMSO-d_6

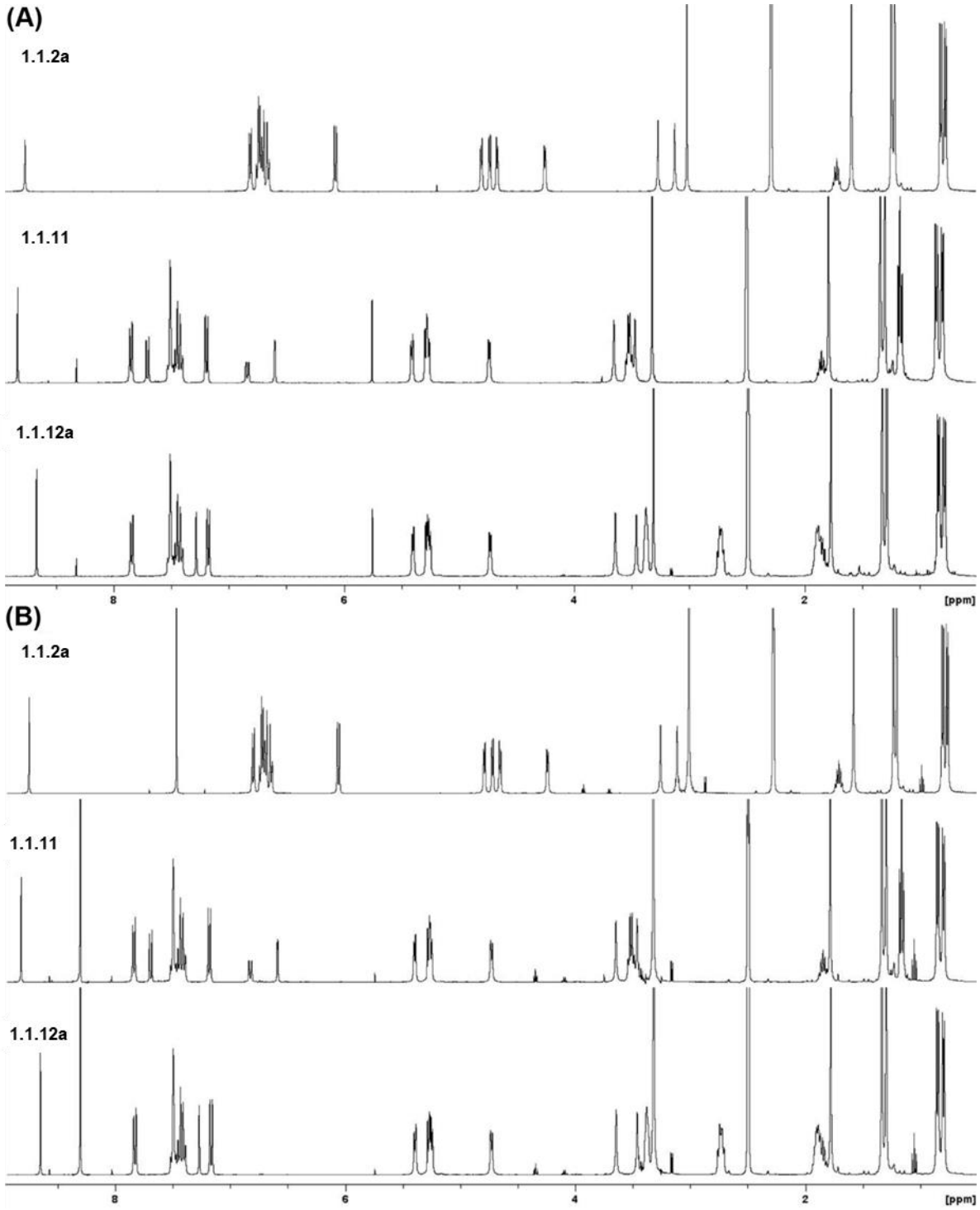

Figure S1.1.2. ^{1}H NMR Spectra of **1.1.2a**, **1.1.11** and **1.1.12a** recorded in DMSO-d_6 at 25°C; (A) recorded 5 min after sample preparation, and (B) sample after > 365 days storage at 0-5°C in the dark.

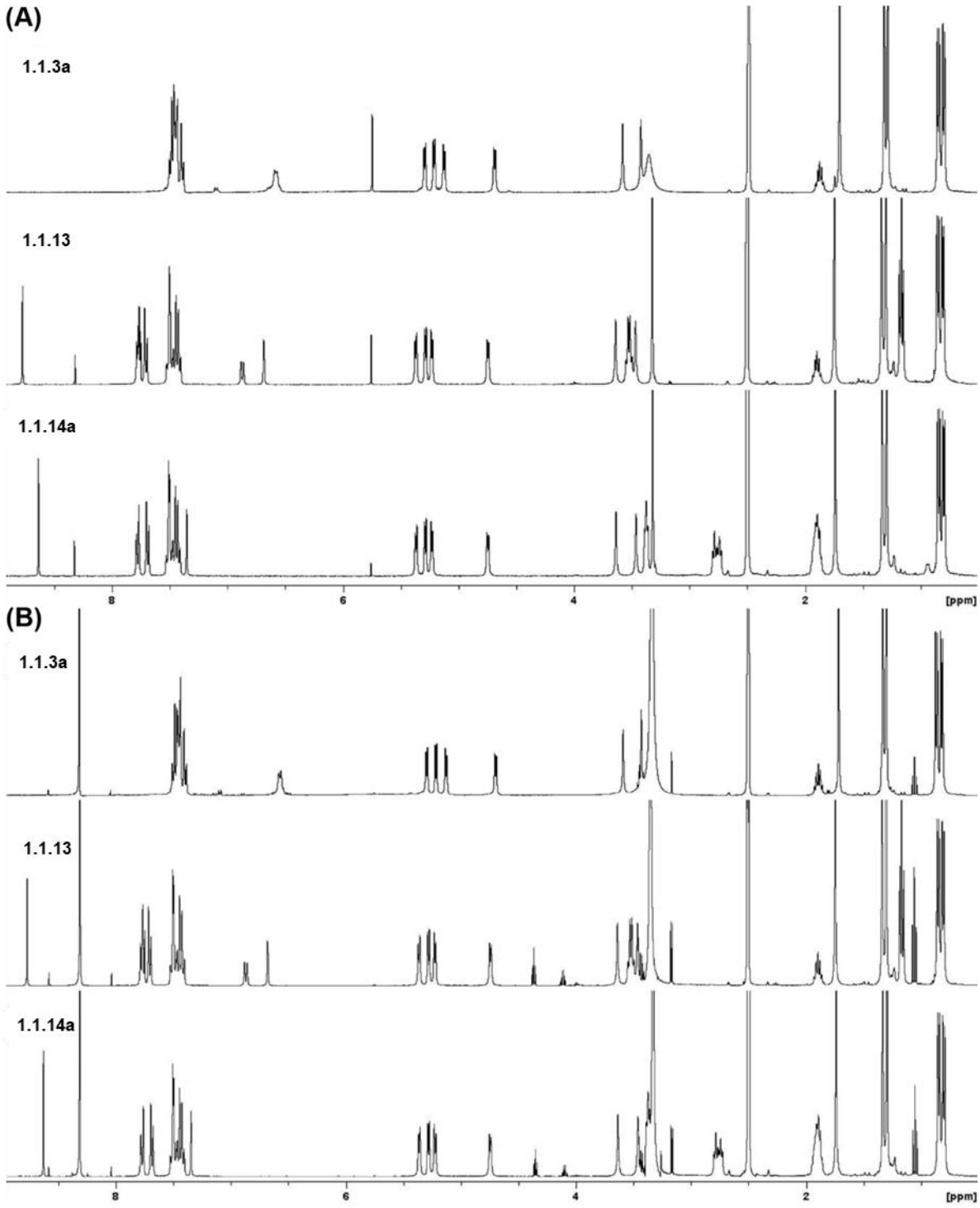

Figure S1.1.3. ^{1}H NMR spectra of **1.1.3a**, **1.1.13** and **1.1.14a** recorded in DMSO-d_6 at 25°C; (A) recorded 5 min after sample preparation, and (B) sample after > 365 days storage at 0-5°C in the dark.

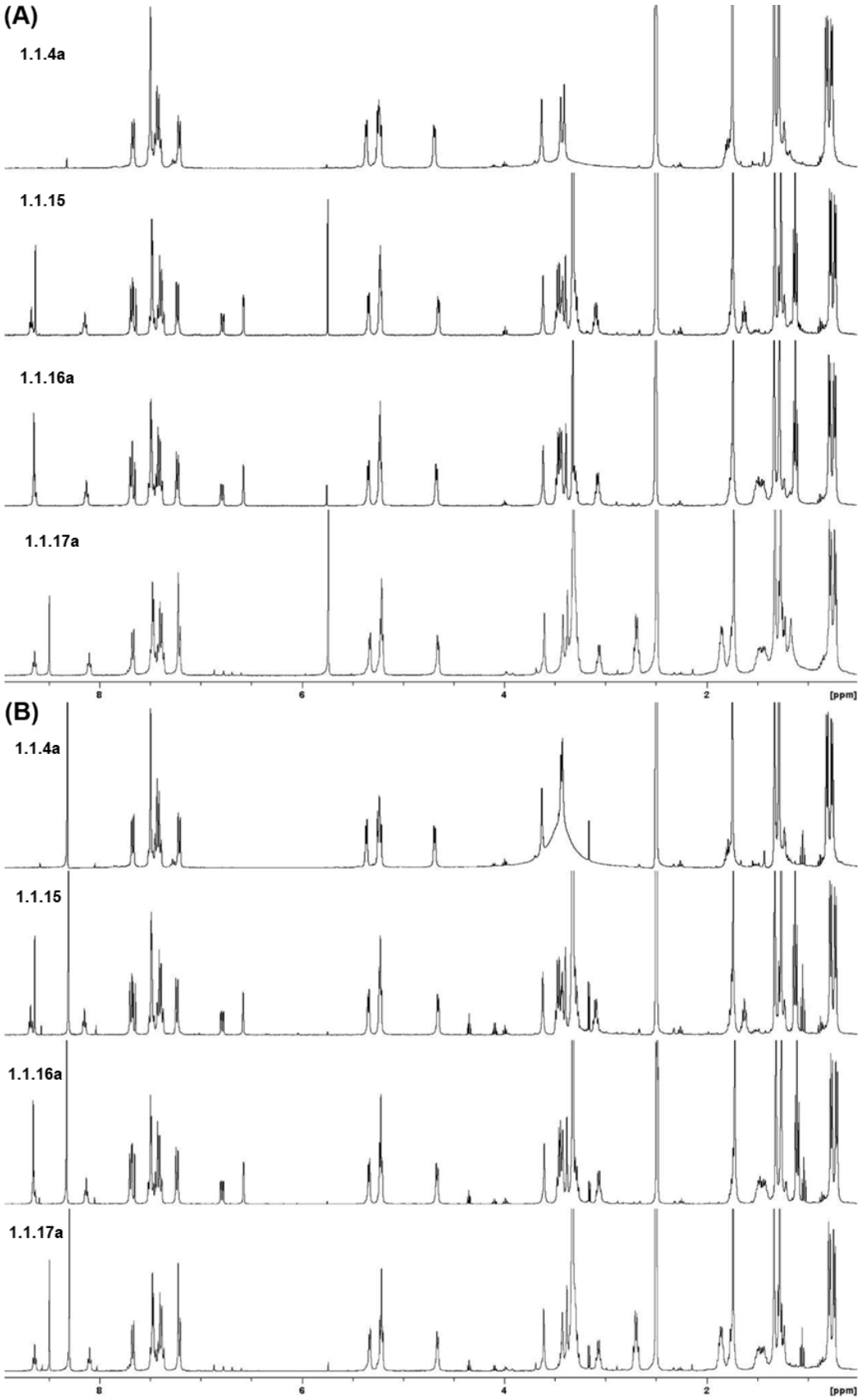

Figure S1.1.4. ^{1}H NMR spectra of **1.1.4a**, **1.1.15**, **1.1.16a** and **1.1.17a** recorded in DMSO-d_6 at 25°C; (A) recorded 5 min after sample preparation, and (B) sample after > 365 days storage at 0-5°C in the dark.

1.1.3 Photophysical Characterization

Table S1.1.4. Photophysical data of compounds **1.1.5-1.1.17a/b**, **1.1.20** and **1.1.22** in EtOH at r.t..

Compound	λ_{max}^{abs} (nm)	ε ($M^{-1}cm^{-1}$)	λ_{max}^{em} (nm)	$\Delta\lambda$ (nm)	Φ_F (%)
rhodamine 6G*	529.5	91583.4	555	25.5	94*
Dye1-CO_2H	423.5	33814.8	457	33.5	13
Dye2-CO_2H	445	30558.6	486	41	140
1.1.5	417.5	43561.9	464	46.5	12
1.1.6	417.5	42765.0	466	48.5	12
1.1.7	435.5	34320.6	480	44.5	130
1.1.8	420.5	15501.3	468	47.5	11
1.1.9	419.5	24175.6	466	46.5	11
1.1.10	437	45453.2	480	43	124
1.1.11	426.5	53185.9	458	31.5	0.2
1.1.12a	445	55210.5	481	36	1.7
1.1.12b	445.5	59061.7	480	34.5	0.6
1.1.13	436	66782.6	-	-	0
1.1.14a	453.5	64679.7	489	35.5	0.4
1.1.14b	453.5	65408.8	485	31.5	1.9
1.1.15	418.5	36376.6	459	40.5	0.8
1.1.16a	418.5	39905.5	459	40.5	0.9
1.1.16b	418.5	32988.9	460	41.5	1.0
1.1.17a	436	32712.9	479	43	1.8
1.1.17b	436.5	29334.5	479	42.5	2.4
1.1.20	428	97373.8	466	38	0.06
1.1.22	428.5	146466.0	465	36.5	0.1

*Values taken from ref.[116]

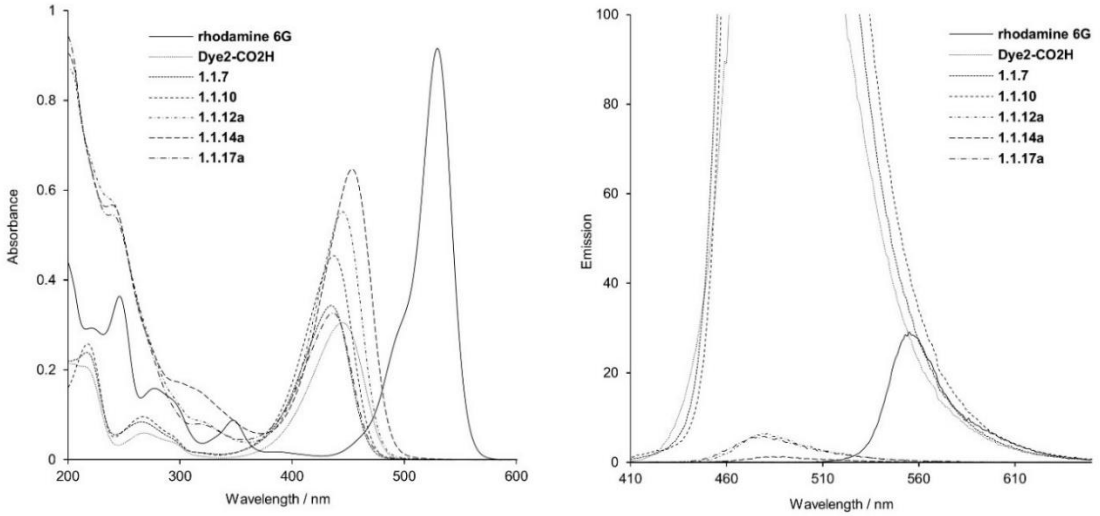

Figure S1.1.5. UV-Vis absorption (left) and emission spectra (right) of rhodamine 6G, **Dye2-CO_2H**, intermediate **1.1.7**, **1.1.10** and the corresponding ester **1.1.12a** and amide **1.1.14a**, **1.1.17a** conjugates, at 10 µM in EtOH.

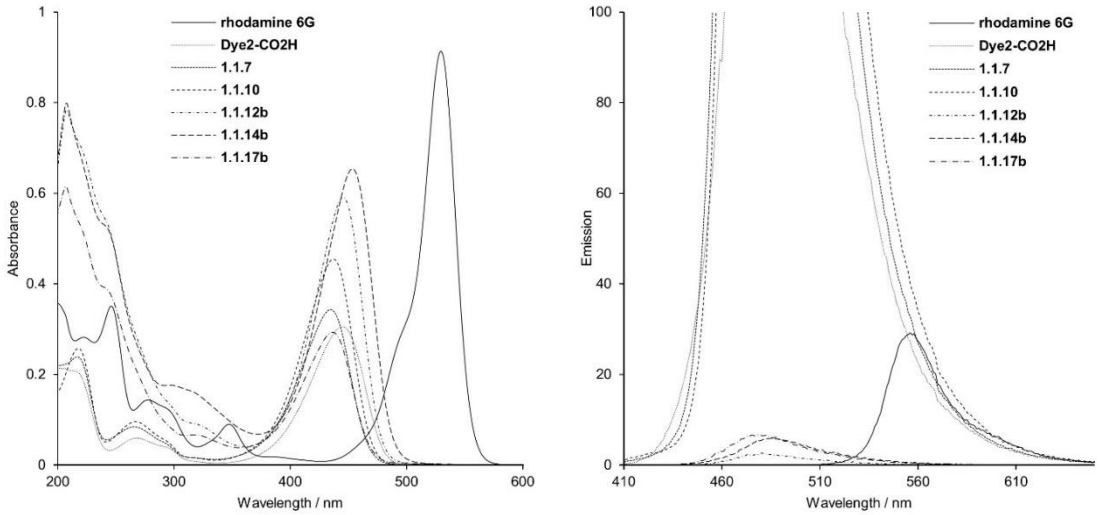

Figure S1.1.6. UV-Vis absorption (left) and emission spectra (right) of rhodamine 6G, **Dye2-CO_2H**, intermediate **1.1.7**, **1.1.10** and the corresponding ester **1.1.12b** and amide **1.1.14b**, **1.1.17b** conjugates, at 10 µM in EtOH.

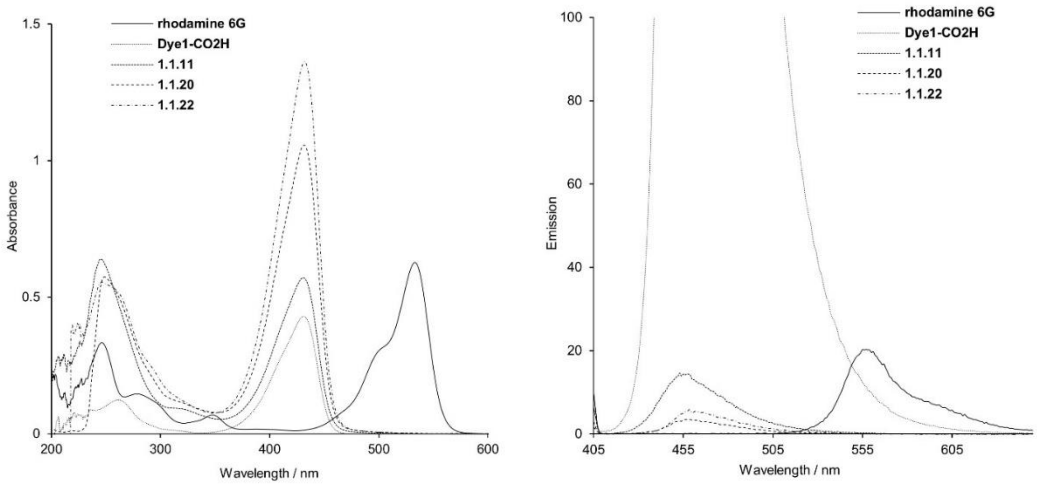

Figure S1.1.7. UV-Vis absorption (left) and emission spectra (right) of rhodamine 6G, **Dye1-CO_2H** and ester conjugates **1.1.11**, **1.1.20**, **1.1.22**, at 10 μM in EtOH.

1.1.4. Biological activity

Table S1.1.5. Primary efficacy/cytotoxicity screening of the non-modified trithiolato di-ruthenium compounds and corresponding coumarin conjugates. Those compounds selected for determination of IC_{50} values against *T. gondii* β-gal are marked with a *. Symmetric trihydroxy thiolato-bridged dinuclear ruthenium(II)-arene compound **1.1.21** was evaluated previously.[29, 36]

Compound	HFF viability (%)		*T. gondii* β-gal proliferation (%)	
	0.1 µM	**1 µM**	**0.1 µM**	**1 µM**
Dye1-CO_2H	103 ± 1	105 ±1	53 ± 12	118 ± 6
Dye2-CO_2H	106 ± 1	105 ± 0	69 ± 11	92 ± 6
1.1.2a*	76 ± 6	46 ± 6	66 ± 14	2 ± 0
1.1.2b*	112 ± 7	66 ± 4	101 ± 1	0 ± 0
1.1.3a*	74 ± 2	48 ± 1	57 ± 1	2 ± 0
1.1.3b*	115 ± 1	58 ± 2	59 ± 7	0 ± 0
1.1.4a	93 ± 4	87 ± 1	114 ± 15	110 ± 32
1.1.4b	103 ± 3	93 ± 6	102 ± 5	102 ± 3
1.1.5	118 ± 10	88 ± 10	131 ± 3	118 ± 22
1.1.6	98 ± 8	82 ± 4	137 ± 9	125 ± 16
1.1.7	95 ± 9	96 ± 6	132 ± 6	148 ± 5
1.1.8	96 ± 9	85 ± 6	117 ± 10	114 ± 13
1.1.9	125 ± 20	111 ± 4	114 ± 4	127 ± 4
1.1.10	124 ± 5	69 ± 9	101 ± 8	113 ± 7
1.1.12a*	93 ± 14	85 ± 3	6 ± 0	1 ± 0
1.1.12b*	100 ± 0	58 ± 5	97 ± 0	2 ± 0
1.1.13	99 ± 14	42 ± 8	100 ± 10	70 ± 11
1.1.14a	87 ± 3	79 ± 8	123 ± 8	119 ± 3
1.1.14b*	105 ± 5	70 ± 1	88 ± 1	3 ± 0
1.1.15	105 ± 9	45 ± 6	112 ± 19	1 ± 0
1.1.16a*	109 ± 4	52 ± 15	111 ± 26	0 ± 0
1.1.16b*	100 ± 9	79 ± 6	99 ± 2	6 ± 1
1.1.17a*	92 ± 4	53 ± 7	13 ± 12	1 ± 0
1.1.17b*	96 ± 1	56 ± 5	100 ± 4	1 ± 0
1.1.19*	62 ± 8	56 ± 7	3 ± 1	2 ± 0
1.1.20*	99 ± 0	80 ± 1	136 ± 2	2 ±0
1.1.22	111 ± 1	101 ± 1	99 ±0	88 ±2

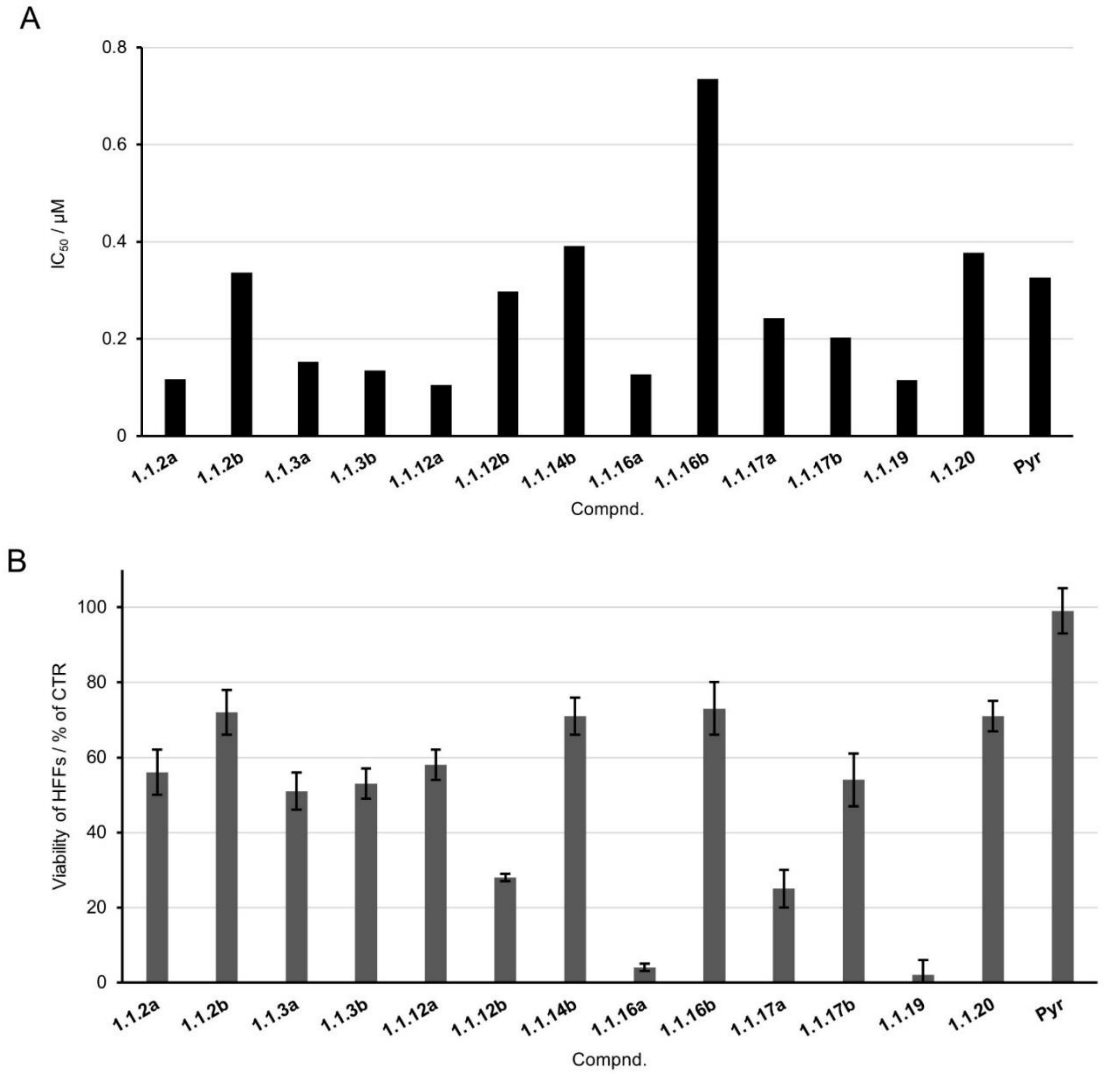

Figure S1.1.8. IC_{50} values on *T. gondii* β-gal (A) and HFF viability at 2.5 µM (B) determined for selected trithiolato-bridged dinuclear ruthenium(II)-arene complexes and pyrimethamine. *T. gondii* β-gal proliferation and HFF viability were quantified by β-galactosidase and alamarBlue assay, respectively.

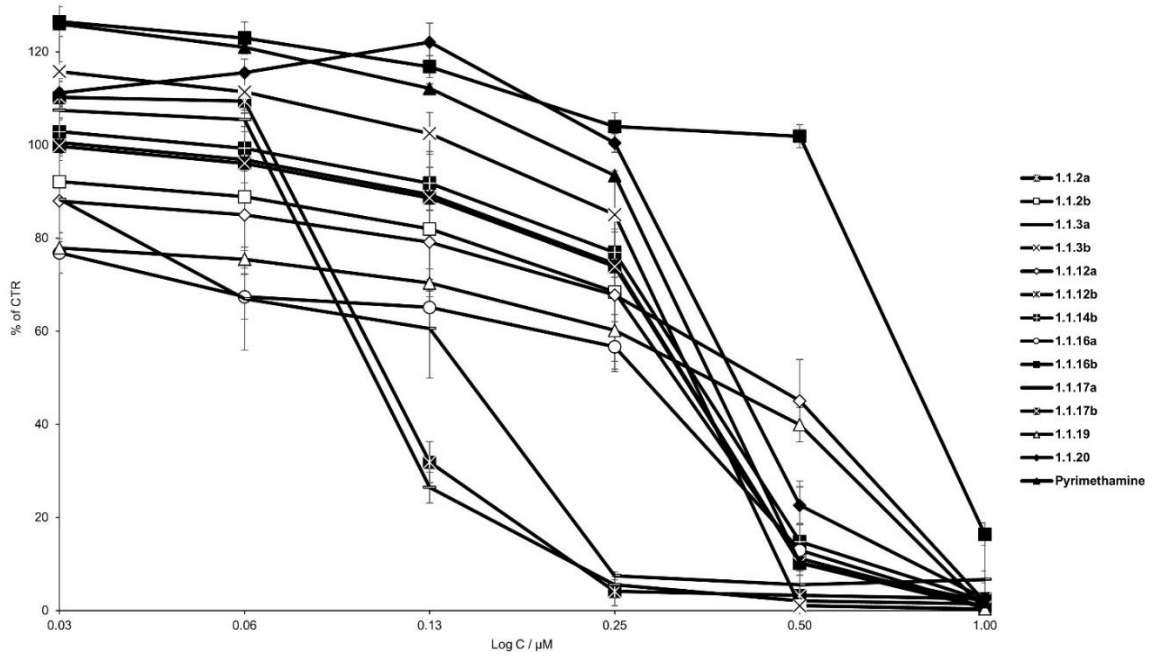

Figure S1.1.9. Dose response curves for the selected compounds for which the IC_{50} against *T. gondii* β-gal was determined. Bars represent standard deviations. Six concentrations between 1 µM and 0.0312 µM were tested, each in six replicate wells.

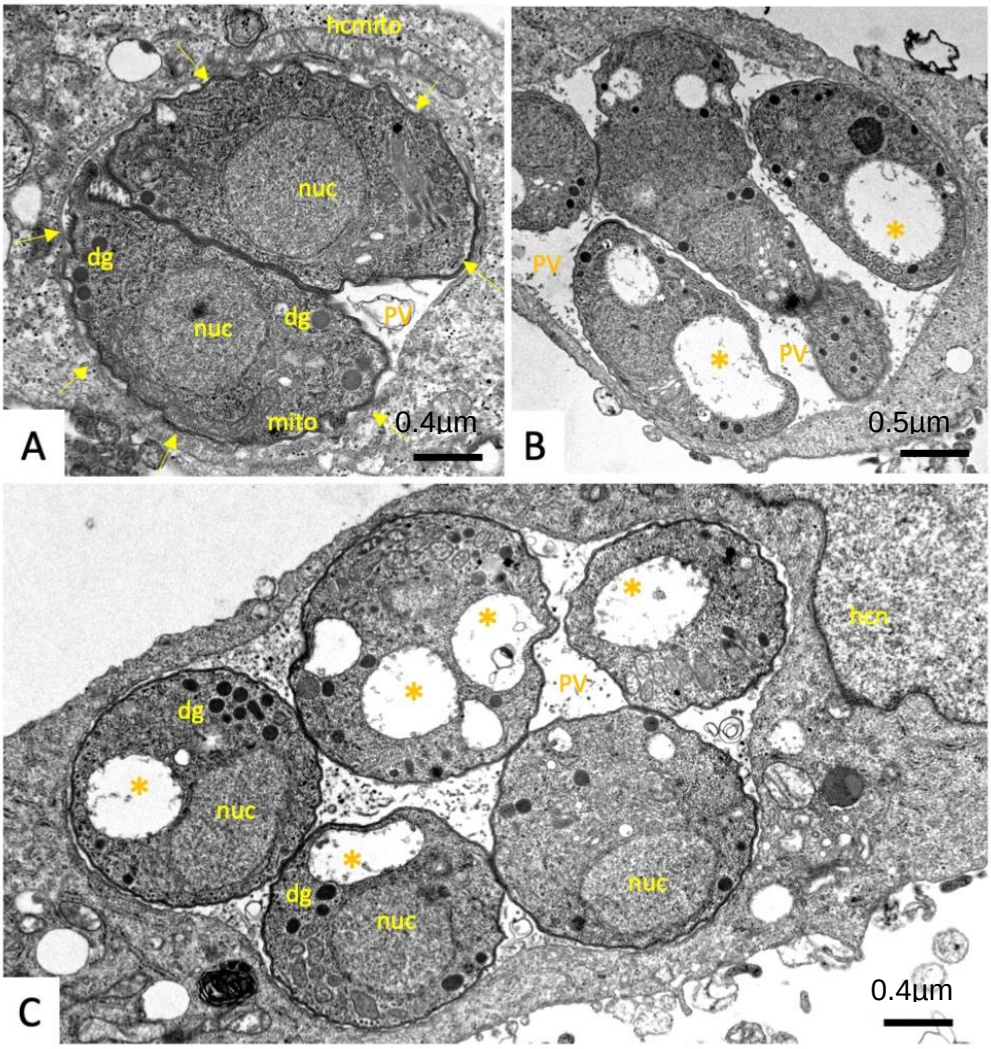

Figure S1.1.10. TEM of *T. gondii* ME49 tachyzoites treated with 500 nM of **1.1.17a** after 6 h (A), 24 h (B) and 48 h (C) after initiation of treatment. No effects are detected at 6 h, but clear vacuolization (marked with *) and a lack discernible mitochondria are seen at 24 to 48 h of treatment. Nuc = nucleus, hcmito = host cell mitochondrium; dg = dense granule; PV = parasitophorous vacuole; arrows point towards the parasitophorous vacuole membrane.

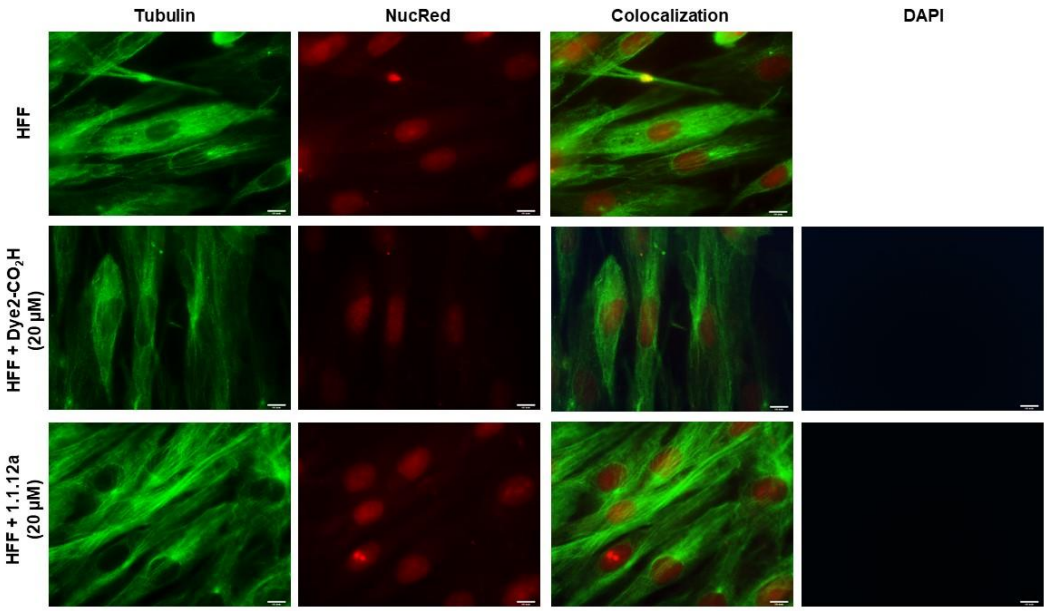

Figure S1.1.11. Fluorescence microscopy of HFF treated with 20 µM of **Dye2-CO_2H**, **1.1.12a** or 0.5% DMSO, for 1 h at 37°C. **Dye2-CO_2H**, and compound **1.1.12a** were visualized with the DAPI filter (excitation wavelength 461 nm). Cells were also stained with clone B-5-1-2 (monoclonal mouse anti-tubulin/anti-mouse fluorescein isothiocyanate, FITC) and NucRed reagent.

1.1.5. Experimental

Chemistry[7]

General

$RuCl_3 \cdot 3H_2O$ was obtained from Fluorochem, and all other chemicals were purchased from Aldrich, Alfa Aesar, Acros, ABCR, or TCI Chemicals and used without further purification. Amberlyst® A21 free base was purchased from Aldrich and washed with MeOH before use. Reactions were performed under an inert atmosphere of N_2 using Schlenk techniques with dry solvents preserved on molecular sieves dried (Acros Organics). The dimer $[Ru(\eta^6\text{-}p\text{-cymene})Cl]_2Cl_2$ was prepared and purified according to literature procedures.[168] ^1H (400.13 MHz) and ^{13}C (100.62 MHz) NMR spectra were recorded on a Bruker Avance II 400 spectrometer at 298 K. ^{19}F (282.40 MHz) spectra were recorded on a Bruker Avance III 300 spectrometer at 298 K. The chemical shifts are reported in parts per million (ppm) and referenced to residual solvent peaks[393] ($CDCl_3$, ^1H δ 7.26, $^{13}C\{^1H\}$ δ 77.16 ppm; MeOD-d_4, ^1H δ 3.31, $^{13}C\{^1H\}$ δ 49.00 ppm, DMSO-d_6, ^1H δ 2.50, $^{13}C\{^1H\}$ δ 39.52 ppm) and coupling constants (J) are reported in hertz (Hz). High resolution electrospray ionization mass spectra (HRESI-MS) were carried out by the Mass Spectrometry and Protein Analyses Services at DCB and were obtained on a LTQ Orbitrap XL ESI (Thermo) operated in positive ion mode. Thermal elemental analyses were carried out by the Mass Spectrometry and Protein Analyses Services at DCB and were obtained on a Flash 2000 Organic Elemental Analyzer (Thermo Scientific). Reactions were monitored by TLC using Macherey-Nagel TLC silica gel coated aluminium sheets Alugram® Xtra SIL G/UV_{254} and visualized with UV at 254 nm and 366 nm (coumarin functionalized compounds). Preparative TLC purifications were performed using Macherey-Nagel TLC silica gel glass pre-coated TCL plates SIL G-25 UV_{254}, and silica extracts were filtered on Macherey-Nagel disposable syringe filters Chromafil® Xtra PTFE-20-25 (pore size 0.20 µm). Compounds were purified by column flash chromatography on silica gel

[7] Only syntheses of compounds obtained by the author of this thesis are presented.

Sigma-Aldrich (60 Å, 230-400 mesh) using the elution systems indicated.

Abbreviations:
DIPEA - *N*,*N*-Diisopropylethylamine
DMAP - 4-(Dimethylamino)-pyridine
DMF - Dimethylformamide
Dye1-CO_2H - 7-(diethylamino)-2-oxo-2*H*-chromene-3-carboxylic acid
Dye2-CO_2H - 11-oxo-2,3,6,7-tetrahydro-1*H*,5*H*,11*H*-pyrano[2,3-*f*]pyrido[3,2,1-*ij*]quinoline-10-carboxylic acid (coumarin 343)
EDCI - *N*-(3-Dimethylaminopropyl)-*N'*-ethylcarbodiimide hydrochloride
EtOAc – Ethyl acetate
Hex – n-Hexane
HOBt·H_2O - 1-Hydroxybenzotriazole hydrate
TEA – Triethylamine

For the description of the NMR spectra: *Ar* – arene, *Coum* – coumarin.

Synthesis and characterization
The dithiolato intermediates **1.1.1a** and **1.1.1b** were prepared and purified by adapting previously reported procedure.[394]
Synthesis of [(η^6-p-$MeC_6H_4Pr^i$)$_2$$Ru_2$($\mu_2$-S-$CH_2$-p-$C_6H_4Bu^t$)$Cl_2$] (1.1.1a)
To a solution of dimer ([Ru(η^6-*p*-$MeC_6H_4Pr^i$)Cl]$_2$$Cl_2$) (3.00 g, 4.899 mmol, 1 equiv) in EtOH (300 mL) at 0°C under inert atmosphere (N_2) was added dropwise a solution of 4-*tert*-butyl-benzene-methanethiol (1.767 g, 9.797 mmol, 2 equiv) in EtOH (10 mL). The reaction mixture was stirred at 0°C for further 4 h and then concentrated at 40°C under reduced pressure to small volume. The product was precipitated with Et_2O (100 mL), and then the solid was washed with Et_2O (3 x 50 mL) and dried to afford **1.1.1a** as an orange solid (4.03 g, 4.475 mmol, yield 91%).
R_f (CH_2Cl_2/CH_3OH 9.5:0.5) = 0.434;
^{1}H-NMR ($CDCl_3$) δ_H, ppm: 7.49 (4H, d, 4xCH_2-(*Ar*)C-CH-C*H*-C-C(CH_3)$_3$, $^3J_{H,H}$ = 8.1 Hz), 7.32 (4H, d, 4xCH_2-(*Ar*)C-C*H*-CH-C-C(CH_3)$_3$, $^3J_{H,H}$ = 8.1 Hz), 4.93 (2H, m, 2xCH_3-(*Ar*)C-CH-C*H*-C), 4.80 (4H, m, 2xCH_3-(*Ar*)C-CH-C*H*-C, 2xCH_3-(*Ar*)C-C*H*-CH-C), 4.11 (2H, d, 2xS-C*H*$_2$-(*Ar*)C-CH-CH-C-C(CH_3)$_3$, $^2J_{H,H}$ = 11.3 Hz), 3.88 (2H, m, 2xCH_3-(*Ar*)C-C*H*-CH-C), 3.32 (2H, d, 2xS-C*H*$_2$-(*Ar*)C-CH-CH-C-C(CH_3)$_3$, $^2J_{H,H}$ = 11.3 Hz), 2.82 (2H, sept, 2x(*Ar*)C-CH-CH-C-C*H*(CH_3)$_2$, $^3J_{H,H}$ = 6.8 Hz), 1.90 (6H, s, 2xC*H*$_3$-(*Ar*)C-CH-CH-C), 1.33 (18H, s, 2xS-CH_2-(*Ar*)C-CH-CH-C-C(C*H*$_3$)$_3$), 1.11-1.25 (12H, m, 2x(*Ar*)C-CH-CH-C-CH(C*H*$_3$)$_2$);
^{13}C-NMR ($CDCl_3$) δ_C, ppm: 150.1 (2C, 2xS-CH_2-(*Ar*)C-CH-CH-*C*-C(CH_3)$_3$), 137.9 (2C, 2xS-CH_2-(*Ar*)*C*-CH-CH-C-C(CH_3)$_3$), 130.3 (4C, 4xS-CH_2-(*Ar*)C-*C*H-CH-C-C(CH_3)$_3$), 124.6 (4C, 4xS-CH_2-(*Ar*)C-CH-*C*H-C-C(CH_3)$_3$), 105.9 (2C, 2xCH_3-(*Ar*)C-CH-CH-*C*), 97.3 (2C, 2xCH_3-(*Ar*)*C*-CH-CH-C), 85.4 (2C, 2xCH_3-(*Ar*)C-*C*H-CH-C), 84.1 (2C, 2xCH_3-(*Ar*)C-CH-*C*H-C), 83.0 (2C, 2xCH_3-(*Ar*)C-*C*H-CH-C), 79.5 (2C, 2xCH_3-(*Ar*)C-CH-*C*H-C), 36.6 (2C, 2xS-*C*H_2-(*Ar*)C-CH-CH-C-C(CH_3)$_3$), 34.7 (2C, 2xS-CH_2-(*Ar*)C-CH-CH-C-*C*(CH_3)$_3$), 31.6 (6C, 2xS-CH_2-(*Ar*)C-CH-CH-C-C(*C*H_3)$_3$), 30.0 (2C, 2x(*Ar*)CH-CH-C-*C*H(CH_3)$_2$), 23.4 (2C, (*Ar*)CH-CH-C-CH(*C*H_3)$_2$), 21.6 (2C, (*Ar*)CH-CH-C-CH(*C*H_3)$_2$), 18.8 (2C, 2x*C*H_3-(*Ar*)C-CH-CH);
HRMS (ESI(+)): *m/z* calcd for $C_{42}H_{58}ClRu_2S_2^+$: 865.1750 $[M-Cl]^+$; found: 865.1779 (the isotopic pattern corresponds well to the calculated one).

The mixed trithiolato ruthenium(II)-arene complexes **1.1.2a/b**, **1.1.3a/b** and **1.1.4a/b** were prepared and purified by adapting a formerly published protocol.[53]

Synthesis of [(η^6-*p*-MeC$_6$H$_4$Pr^i)$_2$Ru$_2$(SCH$_2$-*p*-C$_6$H$_4$Bu^t)$_2$(SC$_6$H$_4$-*p*-OH)]Cl (1.1.2a)

To a solution of **1.1.1a** (1.290 g, 1.433 mmol, 1 equiv) in refluxing EtOH (150 mL) was added dropwise a solution of 4-hydroxy-benzenethiol (0.542 g, 4.300 mmol, 3 equiv) in EtOH (20 mL). The reaction mixture was further heated at reflux under inert atmosphere (N_2) for 24 h. The reaction evolution was verified by TLC and then the reaction mixture was concentrated to dryness under reduced pressure.

Purification by column chromatography using CH_2Cl_2/CH_3OH mixture afforded **1.1.2a** as an orange solid (1.353 g, 1.366 mmol, yield 95%).

***R*$_f$** (CH_2Cl_2/CH_3OH 10:1) = 0.467;

^{1}H-NMR ($CDCl_3$) δ_H, ppm: 10.36 (1H, s, OH), 7.38-7.48 (10H, m, 2xS-(*Ar*)C-C*H*-CH-C-OH, 4xCH_2-(*Ar*)C-C*H*-CH-C-C(CH_3)$_3$, 4xCH_2-(*Ar*)C-CH-C*H*-C-C(CH_3)$_3$), 7.24 (2H, m, 2xS-(*Ar*)C-CH-C*H*-C-OH, $^3J_{H,H}$ = 8.7 Hz), 4.98 (2H, d, 2xCH_3-(*Ar*)C-CH-C*H*-C, $^3J_{H,H}$ = 5.8 Hz), 4.88 (2H, d, 2xCH_3-(*Ar*)C-CH-C*H*-C, $^3J_{H,H}$ = 5.8 Hz), 4.70 (2H, d, 2xCH_3-(*Ar*)C-C*H*-CH-C, $^3J_{H,H}$ = 5.7 Hz), 4.58 (2H, d, 2xCH_3-(*Ar*)C-C*H*-CH-C, $^3J_{H,H}$ = 5.8 Hz), 3.54 (2H, s, S-C*H*$_2$-(*Ar*)C-CH-CH-C-C(CH_3)$_3$), 3.36 (2H, s, S-C*H*$_2$-(*Ar*)C-CH-CH-C-C(CH_3)$_3$), 1.97 (2H, sept, 2x(*Ar*)C-CH-CH-C-C*H*(CH_3)$_2$, $^3J_{H,H}$ = 6.9 Hz), 1.69 (6H, s, 2xC*H*$_3$-(*Ar*)C-CH-CH-C), 1.36 (9H, s, S-CH_2-(*Ar*)C-CH-CH-C-C(C*H*$_3$)$_3$), 1.34 (9H, s, S-CH_2-(*Ar*)C-CH-CH-C-C(C*H*$_3$)$_3$), 0.97 (6H, d, (*Ar*)C-CH-CH-C-CH(C*H*$_3$)$_2$, $^3J_{H,H}$ = 6.9 Hz), 0.93 (6H, d, (*Ar*)C-CH-CH-C-CH(C*H*$_3$)$_2$, $^3J_{H,H}$ = 6.9 Hz);

^{13}C-NMR ($CDCl_3$) δ_C, ppm: 160.1 (1C, S-(*Ar*)C-CH-CH-*C*-OH), 151.9, 151.8 (2C, 2xS-CH_2-(*Ar*)C-CH-CH-*C*-C(CH_3)$_3$), 137.0, 136.7 (2C, 2xS-CH_2-(*Ar*)*C*-CH-CH-C-C(CH_3)$_3$), 133.4 (2C, 2xS-(*Ar*)C-*C*H-CH-C-OH), 129.3, 129.1 (4C, 4xS-CH_2-(*Ar*)C-*C*H-CH-C-C(CH_3)$_3$), 125.7, 125.6 (4C, 4xS-CH_2-(*Ar*)C-CH-*C*H-C-C(CH_3)$_3$), 124.1 (1C, S-(*Ar*)*C*-CH-CH-C-OH), 117.3 (2C, 2xS-(*Ar*)C-CH-*C*H-C-OH), 107.5 (2C, 2xCH_3-(*Ar*)C-CH-CH-*C*), 100.2 (2C, 2xCH_3-(*Ar*)*C*-CH-CH-C), 84.1 (2C, 2xCH_3-(*Ar*)C-CH-*C*H-C),83.6 (2C, 2xCH_3-(*Ar*)C-*C*H-CH-C), 83.5 (2C, 2xCH_3-(*Ar*)C-CH-*C*H-C), 82.2 (2C, 2xCH_3-(*Ar*)C-*C*H-CH-C), 39.9 (1C, S-*C*H_2-(*Ar*)C-CH-CH-C-C(CH_3)$_3$), 39.2 (1C, S-*C*H_2-(*Ar*)C-CH-CH-C-C(CH_3)$_3$), 34.91 (1C, S-CH_2-(*Ar*)C-CH-CH-C-*C*(CH_3)$_3$), 34.88 (1C, S-CH_2-(*Ar*)C-CH-CH-C-*C*(CH_3)$_3$), 31.55 (3C, S-CH_2-(*Ar*)C-CH-CH-C-C(*C*H_3)$_3$), 31.54 (3C, S-CH_2-(*Ar*)C-CH-CH-C-C(*C*H_3)$_3$), 31.0 (2C, 2x(*Ar*)CH-CH-C-*C*H(CH_3)$_2$), 23.2 (2C, (*Ar*)CH-CH-C-CH(*C*H_3)$_2$), 22.9 (2C, (*Ar*)CH-CH-C-CH(*C*H_3)$_2$), 18.1 (2C, 2x*C*H_3-(*Ar*)C-CH-CH);

HRMS (ESI(+)): *m/z* calcd for $C_{48}H_{63}ORu_2S_3^+$: 955.2123 $[M\text{-}Cl]^+$; found: 955.2102 (the isotopic pattern corresponds well to the calculated one);

Elemental analysis: calcd (%) for $C_{48}H_{63}ClORu_2S_3 \cdot 2CH_3OH$: C 56.98, H 6.79; found C 56.91, H 6.78.

Synthesis of [(η^6-*p*-MeC$_6$H$_4$Pr^i)$_2$Ru$_2$(μ_2-SCH$_2$C$_6$H$_4$-p-Bu^t)$_2$(μ_2-SC$_6$H$_4$-*p*-NH$_2$)]Cl (1.1.3a)

To as solution of **1.1.1a** (2.00 g, 2.221 mmol, 1 equiv) in refluxing EtOH (140 mL) was added dropwise a solution of 4-amino-benzenethiol (0.809 g, 6.663 mmol, 3 equiv) in EtOH (10 mL). The reaction mixture was further heated at reflux under inert atmosphere (N_2) for 24 h. The reaction evolution was verified by TLC and then the reaction mixture was concentrated to dryness under reduced pressure. Purification by column chromatography using CH_2Cl_2/CH_3OH 10:1 mixture afforded **1.1.3a** as an orange solid (2.10 g, 2.126 mmol, yield 96%).

***R*$_f$** (CH_2Cl_2/CH_3OH 10:1) = 0.518;

^{1}H-NMR ($CDCl_3$) δ_H, ppm: 7.39-7.52 (10H, m, 2xS-(*Ar*)C-C*H*-CH-C-NH_2, 4xCH_2-(*Ar*)C-C*H*-CH-C-C(CH_3)$_3$, 4xCH_2-(*Ar*)C-CH-C*H*-C-C(CH_3)$_3$), 6.75 (2H, m, 2xS-(*Ar*)C-CH-C*H*-C-NH_2, $^3J_{H,H}$ = 8.5 Hz), 5.01 (2H, d, 2xCH_3-(*Ar*)C-CH-C*H*-C, $^3J_{H,H}$ = 5.6 Hz), 4.90 (2H, d, 2xCH_3-(*Ar*)C-CH-C*H*-C, $^3J_{H,H}$ = 5.7 Hz), 4.74 (2H, d, 2xCH_3-(*Ar*)C-C*H*-CH-C, $^3J_{H,H}$ = 5.7 Hz), 4.58 (2H, d, 2xCH_3-(*Ar*)C-C*H*-CH-C, $^3J_{H,H}$ = 5.8 Hz), 3.54 (2H, s, S-C*H*$_2$-(*Ar*)C-CH-CH-C-C(CH_3)$_3$), 3.37 (2H, s, S-C*H*$_2$-(*Ar*)C-CH-CH-C-C(CH_3)$_3$), 1.97 (2H, sept, 2x(*Ar*)C-CH-CH-C-C*H*(CH_3)$_2$,

$^{3}J_{H,H}$ = 6.9 Hz), 1.71 (6H, s, 2xC$\underline{H_3}$-(*Ar*)C-CH-CH-C), 1.36 (9H, s, S-CH$_2$-(*Ar*)C-CH-CH-C-C(C$\underline{H_3}$)$_3$), 1.34 (9H, s, S-CH$_2$-(*Ar*)C-CH-CH-C-C(C$\underline{H_3}$)$_3$), 0.98 (6H, d, (*Ar*)C-CH-CH-C-CH(C$\underline{H_3}$)$_2$, $^{3}J_{H,H}$ = 6.9 Hz), 0.93 (6H, d, (*Ar*)C-CH-CH-C-CH(C$\underline{H_3}$)$_2$, $^{3}J_{H,H}$ = 6.9 Hz);

^{13}C-NMR (CDCl$_3$) δ_C, ppm: 151.85, 151.77 (2C, 2xS-CH$_2$-(*Ar*)C-CH-CH-$\underline{C}$-C(CH$_3$)$_3$), 148.8 (1C, S-(*Ar*)C-CH-CH-$\underline{C}$-NH$_2$), 137.0, 136.8 (2C, 2xS-CH$_2$-(*Ar*)$\underline{C}$-CH-CH-C-C(CH$_3$)$_3$), 133.6 (2C, 2xS-(*Ar*)C-$\underline{C}$H-CH-C-NH$_2$), 129.3, 129.1 (4C, 4xS-CH$_2$-(*Ar*)C-$\underline{C}$H-CH-C-C(CH$_3$)$_3$), 125.7, 125.5 (4C, 4xS-CH$_2$-(*Ar*)C-CH-$\underline{C}$H-C-C(CH$_3$)$_3$), 122.9 (1C, S-(*Ar*)$\underline{C}$-CH-CH-C-NH$_2$), 115.6 (2C, 2xS-(*Ar*)C-CH-$\underline{C}$H-C-NH$_2$), 107.3 (2C, 2xCH$_3$-(*Ar*)C-CH-CH-$\underline{C}$), 100.2 (2C, 2xCH$_3$-(*Ar*)$\underline{C}$-CH-CH-C), 84.1 (2C, 2xCH$_3$-(*Ar*)C-CH-$\underline{C}$H-C), 83.64 (2C, 2xCH$_3$-(*Ar*)C-$\underline{C}$H-CH-C), 83.56 (2C, 2xCH$_3$-(*Ar*)C-CH-$\underline{C}$H-C), 82.2 (2C, 2xCH$_3$-(*Ar*)C-$\underline{C}$H-CH-C), 39.9 (1C, S-$\underline{C}$H$_2$-(*Ar*)C-CH-CH-C-C(CH$_3$)$_3$), 39.2 (1C, S-$\underline{C}$H$_2$-(*Ar*)C-CH-CH-C-C(CH$_3$)$_3$), 34.91 (1C, S-CH$_2$-(*Ar*)C-CH-CH-C-$\underline{C}$(CH$_3$)$_3$), 34.88 (1C, S-CH$_2$-(*Ar*)C-CH-CH-C-$\underline{C}$(CH$_3$)$_3$), 31.6 (6C, 2xS-CH$_2$-(*Ar*)C-CH-CH-C-C($\underline{C}$H$_3$)$_3$), 31.0 (2C, 2x(*Ar*)CH-CH-C-$\underline{C}$H(CH$_3$)$_2$), 23.2 (2C, (*Ar*)CH-CH-C-CH($\underline{C}$H$_3$)$_2$), 22.9 (2C, (*Ar*)CH-CH-C-CH($\underline{C}$H$_3$)$_2$), 18.2 (2C, 2x$\underline{C}$H$_3$-(*Ar*)C-CH-CH);

HRMS (ESI(+)): *m/z* calcd for $C_{48}H_{64}NRu_2S_3^+$: 954.2282 [M-Cl]$^+$; found: 954.2291 (the isotopic pattern corresponds well to the calculated one);

Elemental analysis: calcd (%) for $C_{48}H_{64}ClNRu_2S_3 \cdot 3.5CH_3OH$: C 56.18, H 7.14, N 1.27; found C 56.17, H 7.33, N 1.19.

Synthesis of [(η^6-*p*-MeC$_6$H$_4$Pr^i)$_2$Ru$_2$(μ_2-SCH$_2$C$_6$H$_4$-*p*-Bu^t)$_2$(μ_2-SC$_6$H$_4$-*p*-CH$_2$CO$_2$H)]Cl (1.1.4a)

To a solution of **1.1.1a** (2.500 g, 2.778 mmol, 1 equiv) in refluxing CH_2Cl_2 (200 mL) was added dropwise under inert atmosphere (N_2) a solution of 4-mercaptophenylacetic acid (0.934 g, 5.555 mmol, 2 equiv) in acetone (20 mL). The reaction mixture was further heated at reflux under inert atmosphere (N_2) for 24 h. The reaction evolution was verified by TLC and then the reaction mixture was concentrated to dryness under reduced pressure. Purification by column chromatography using CH_2Cl_2/CH_3OH mixture as eluent afforded **1.1.4a** as an orange solid (2.693 g, 2.610 mmol, yield 94%).

***R*$_f$** (CH_2Cl_2/CH_3OH 10:1) = 0.364;

^{1}H-NMR (CDCl$_3$) δ_H, ppm: 7.62 (2H, d, 2xS-(*Ar*)C-CH-C$\underline{H}$-C-CH$_2$-CO$_2$H, $^{3}J_{H,H}$ = 7.8 Hz), 7.38-7.52 (10H, m, 2xS-(*Ar*)C-C$\underline{H}$-CH-C-CH$_2$-CO$_2$H, 4xCH$_2$-(*Ar*)C-C$\underline{H}$-CH-C-C(CH$_3$)$_3$, 4xCH$_2$-(*Ar*)C-CH-C$\underline{H}$-C-C(CH$_3$)$_3$), 5.02 (2H, d, 2xCH$_3$-(*Ar*)C-CH-C$\underline{H}$-C, $^{3}J_{H,H}$ = 5.5 Hz), 4.89 (2H, d, 2xCH$_3$-(*Ar*)C-CH-C$\underline{H}$-C, $^{3}J_{H,H}$ = 5.6 Hz), 4.80 (2H, d, 2xCH$_3$-(*Ar*)C-C$\underline{H}$-CH-C, $^{3}J_{H,H}$ = 4.8 Hz), 4.58 (2H, d, 2xCH$_3$-(*Ar*)C-C$\underline{H}$-CH-C, $^{3}J_{H,H}$ = 5.6 Hz), 3.93 (2H, s, S-(*Ar*)C-CH-CH-C-C$\underline{H_2}$-CO$_2$H), 3.57 (2H, s, S-C$\underline{H_2}$-(*Ar*)C-CH-CH-C-C(CH$_3$)$_3$), 3.36 (2H, s, S-C$\underline{H_2}$-(*Ar*)C-CH-CH-C-C(CH$_3$)$_3$), 1.90 (2H, sept, 2x(*Ar*)C-CH-CH-C-C$\underline{H}$(CH$_3$)$_2$, $^{3}J_{H,H}$ = 6.8 Hz), 1.69 (6H, s, 2xC$\underline{H_3}$-(*Ar*)C-CH-CH-C), 1.35 (9H, s, S-CH$_2$-(*Ar*)C-CH-CH-C-C(C$\underline{H_3}$)$_3$), 1.32 (9H, s, S-CH$_2$-(*Ar*)C-CH-CH-C-C(C$\underline{H_3}$)$_3$), 0.94 (6H, d, (*Ar*)C-CH-CH-C-CH(C$\underline{H_3}$)$_2$, $^{3}J_{H,H}$ = 6.8 Hz), 0.89 (6H, d, (*Ar*)C-CH-CH-C-CH(C$\underline{H_3}$)$_2$, $^{3}J_{H,H}$ = 6.8 Hz);

^{13}C-NMR (CDCl$_3$) δ_C, ppm: 173.9 (1C, S-(*Ar*)C-CH-CH-C-CH$_2$-$\underline{C}$O$_2$H), 151.91, 151.86 (2C, 2xS-CH$_2$-(*Ar*)C-CH-CH-$\underline{C}$-C(CH$_3$)$_3$), 137.1 (1C, S-(*Ar*)C-CH-CH-$\underline{C}$-CH$_2$-CO$_2$H), 136.8, 136.6 (2C, 2xS-CH$_2$-(*Ar*)$\underline{C}$-CH-CH-C-C(CH$_3$)$_3$), 135.1 (1C, S-(*Ar*)$\underline{C}$-CH-CH-C-CH$_2$-CO$_2$H), 132.3 (2C, 2xS-(*Ar*)C-CH-$\underline{C}$H-C-CH$_2$-CO$_2$H), 130.8 (2C, 2xS-(*Ar*)C-$\underline{C}$H-CH-C-CH$_2$-CO$_2$H), 129.4, 129.1 (4C, 4xS-CH$_2$-(*Ar*)C-$\underline{C}$H-CH-C-C(CH$_3$)$_3$), 125.7, 125.6 (4C, 4xS-CH$_2$-(*Ar*)C-CH-$\underline{C}$H-C-C(CH$_3$)$_3$), 107.4 (2C, 2xCH$_3$-(*Ar*)C-CH-CH-$\underline{C}$), 100.7 (2C, 2xCH$_3$-(*Ar*)$\underline{C}$-CH-CH-C), 83.92 (2C, 2xCH$_3$-(*Ar*)C-CH-$\underline{C}$H-C), 83.86 (2C, 2xCH$_3$-(*Ar*)C-CH-$\underline{C}$H-C), 83.6 (2C, 2xCH$_3$-(*Ar*)C-$\underline{C}$H-CH-C), 82.4 (2C, 2xCH$_3$-(*Ar*)C-$\underline{C}$H-CH-C), 42.3 (1C, S-(*Ar*)C-CH-CH-C-$\underline{C}$H$_2$-CO$_2$H), 40.0 (1C, S-$\underline{C}$H$_2$-(*Ar*)C-CH-CH-C-C(CH$_3$)$_3$), 39.4 (1C, S-$\underline{C}$H$_2$-(*Ar*)C-CH-CH-C-C(CH$_3$)$_3$), 34.91 (1C, S-CH$_2$-(*Ar*)C-CH-CH-C-$\underline{C}$(CH$_3$)$_3$), 34.88 (1C, S-CH$_2$-(*Ar*)C-CH-CH-C-$\underline{C}$(CH$_3$)$_3$), 31.6 (6C, 2xS-CH$_2$-(*Ar*)C-CH-CH-

C-C(<u>C</u>H$_3$)$_3$), 31.0 (2C, 2x(*Ar*)CH-CH-C-<u>C</u>H(CH$_3$)$_2$), 23.2 (2C, (*Ar*)CH-CH-C-CH(<u>C</u>H$_3$)$_2$), 22.8 (2C, (*Ar*)CH-CH-C-CH(<u>C</u>H$_3$)$_2$), 18.2 (2C, 2x<u>C</u>H$_3$-(*Ar*)C-CH-CH);
HRMS (ESI(+)): *m/z* calcd for $C_{50}H_{65}O_2Ru_2S_3^+$: 997.2228 [M-Cl]$^+$; found: 997.2227 (the isotopic pattern corresponds well to the calculated one);
Elemental analysis: calcd (%) for $C_{50}H_{65}ClO_2Ru_2S_3 \cdot 2.5CH_2Cl_2 \cdot CH_3OH$: C 50.35, H 5.84; found C 50.31; H 5.86.

Synthesis of [(η^6-*p*-MeC$_6$H$_4$Pr^i)$_2$Ru$_2$(SCH$_2$C$_6$H$_4$Bu^t)$_2$(SC$_6$H$_4$-*p*-OR)]Cl (R = 11-oxo-2,3,6,7-tetrahydro-1*H*,5*H*,11*H*-pyrano[2,3-*f*]pyrido[3,2,1-*ij*]quinoline-10-carboxylate) (1.1.12a)
To a solution of **Dye2-CO$_2$H** (0.072 g, 0.253 mmol, 1.25 equiv) in dry CH_2Cl_2 (100 mL) were added successively EDCI (0.050 g, 0.263 mmol, 1.30 equiv), **1.1.2a** (0.200 g, 0.202 mmol, 1 equiv), and DMAP (0.030 g, 0.242 mmol, 0.20 equiv). The reaction mixture was stirred at room temperature for 24 h, the reaction evolution was verified by ^{1}H NMR ($CDCl_3$) and TLC and then the mixture was concentrated to dryness under reduced pressure. Purification by flash column chromatography using a CH_2Cl_2/MeOH mixture as eluent afforded the product as an orange solid (0.195 g, 0.155 mmol, yield 77%).
***R*$_f$** (CH_2Cl_2/MeOH 10:1) = 295;
^{1}H-NMR ($CDCl_3$) δ_H, ppm: 8.54 (1H, s, (*Coum*)O-C-C-C-<u>H</u>-C-(C=O)), 7.78 (2H, d, 2xS-(*Ar*)C-C<u>H</u>-CH-C-O, $^3J_{H,H}$ = 8.7 Hz), 7.38-7.48 (8H, m, 4xCH$_2$-(*Ar*)C-C<u>H</u>-CH-C-C(CH$_3$)$_3$, 4xCH$_2$-(*Ar*)C-CH-C<u>H</u>-C-C(CH$_3$)$_3$), 7.18 (2H, d, 2xS-(*Ar*)C-CH-C<u>H</u>-C-O, $^3J_{H,H}$ = 8.7 Hz), 7.03 (1H, s, (*Coum*)O-C-C-C<u>H</u>-C-CH$_2$), 5.10 (2H, d, 2xCH$_3$-(*Ar*)C-CH-C<u>H</u>-C, $^3J_{H,H}$ = 5.8 Hz), 5.00 (2H, d, 2xCH$_3$-(*Ar*)C-CH-C<u>H</u>-C, $^3J_{H,H}$ = 5.8 Hz), 4.87 (2H, d, 2xCH$_3$-(*Ar*)C-C<u>H</u>-CH-C, $^3J_{H,H}$ = 5.8 Hz), 4.65 (2H, d, 2xCH$_3$-(*Ar*)C-C<u>H</u>-CH-C, $^3J_{H,H}$ = 5.8 Hz), 3.60 (2H, s, S-C<u>H$_2$</u>-(*Ar*)C-CH-CH-C-C(CH$_3$)$_3$), 3.42 (2H, s, S-C<u>H$_2$</u>-(*Ar*)C-CH-CH-C-C(CH$_3$)$_3$), 3.37 (2H, t, (*Coum*)O-C-C-CH-C-(CH$_2$)$_2$-C<u>H$_2$</u>-N, $^3J_{H,H}$ = 5.7 Hz), 3.36 (2H, t, (*Coum*)O-C-C-(CH$_2$)$_2$-C<u>H$_2$</u>-N), $^3J_{H,H}$ = 5.6 Hz), 2.89 (2H, t, (*Coum*)O-C-C-CH-C-C<u>H$_2$</u>-(CH$_2$)$_2$-N, $^3J_{H,H}$ = 6.3 Hz), 2.78 (2H, t, (*Coum*)O-C-C-C<u>H$_2$</u>-(CH$_2$)$_2$-N, $^3J_{H,H}$ = 6.2 Hz), 1.93-2.01 (4H, m, (*Coum*)O-C-C-CH-C-CH$_2$-C<u>H$_2$</u>-CH$_2$-N, (*Coum*)O-C-C-CH$_2$-C<u>H$_2$</u>-CH$_2$-N), 1.94 (2H, sept, 2x(*Ar*)C-CH-CH-C-C<u>H</u>(CH$_3$)$_2$, $^3J_{H,H}$ = 6.9 Hz), 1.76 (6H, s, 2xC<u>H$_3$</u>-(*Ar*)C-CH-CH-C), 1.36 (9H, s, S-CH$_2$-(*Ar*)C-CH-CH-C-C(C<u>H$_3$</u>)$_3$), 1.33 (9H, s, S-CH$_2$-(*Ar*)C-CH-CH-C-C(C<u>H$_3$</u>)$_3$), 0.97 (6H, d, (*Ar*)C-CH-CH-C-CH(C<u>H$_3$</u>)$_2$, $^3J_{H,H}$ = 6.9 Hz), 0.91 (6H, d, (*Ar*)C-CH-CH-C-CH(C<u>H$_3$</u>)$_2$, $^3J_{H,H}$ = 6.9 Hz);
^{13}C-NMR ($CDCl_3$) δ_C, ppm: 162.5 (1C, S-(*Ar*)C-CH-CH-C-O-(<u>C</u>=O)), 158.8 (1C, (*Coum*)O-C-C-CH-C-(<u>C</u>=O)), 154.0 (1C, (*Coum*)O-<u>C</u>-C-CH-C-(C=O)), 151.9, 151.8 (2C, 2xS-CH$_2$-(*Ar*)C-CH-CH-<u>C</u>-C(CH$_3$)$_3$), 151.6 (1C, (*Ar*)<u>C</u>-N-CH$_2$-CH$_2$), 150.3 (1C, (*Coum*)O-C-C-<u>C</u>H-C-(C=O)), 149.5 (1C, S-(*Ar*)C-CH-CH-<u>C</u>-O-C(C=O)), 136.8, 136.7 (2C, 2xS-CH$_2$-(*Ar*)<u>C</u>-CH-CH-C-C(CH$_3$)$_3$), 134.7 (1C, S-(*Ar*)<u>C</u>-CH-CH-C-O-(C=O)), 133.5 (2C, 2xS-(*Ar*)C-<u>C</u>H-CH-C-O-(C=O)), 129.4, 129.2 (4C, 4xS-CH$_2$-(*Ar*)C-<u>C</u>H-CH-C-C(CH$_3$)$_3$), 127.7 (1C, (*Coum*)O-C-C-<u>C</u>H-C-(CH$_2$)$_3$-N), 125.7, 125.6 (4C, 4xS-CH$_2$-(*Ar*)C-CH-<u>C</u>H-C-C(CH$_3$)$_3$), 122.9 (2C, 2xS-(*Ar*)C-CH-C<u>H</u>-C-O-(C=O))), 119.8 (1C, (*Coum*)O-C-<u>C</u>-(CH$_2$)$_3$-N), 107.8 (1C, (*Coum*)O-C-C-CH-<u>C</u>-(C=O)-O), 107.5 (2C, 2xCH$_3$-(*Ar*)C-CH-CH-<u>C</u>), 105.9 (1C, (*Coum*)O-C-<u>C</u>-CH-C-(C=O)-O), 105.2 (1C, (*Coum*)O-C-C-CH-<u>C</u>-(CH$_2$)$_3$-N), 100.5 (2C, 2xCH$_3$-(*Ar*)<u>C</u>-CH-CH-C), 84.0 (2C, 2xCH$_3$-(*Ar*)C-CH-C<u>H</u>-C), 83.92 (2C, 2xCH$_3$-(*Ar*)C-CH-<u>C</u>H-C), 83.89 (2C, 2xCH$_3$-(*Ar*)C-<u>C</u>H-CH-C), 82.5 (2C, 2xCH$_3$-(*Ar*)C-<u>C</u>H-CH-C), 50.6 (1C, (*Coum*)O-C-C-CH-C-(CH$_2$)$_2$-<u>C</u>H$_2$-N), 50.1 (1C, (*Coum*)O-C-C-(CH$_2$)$_2$-<u>C</u>H$_2$-N), 40.1 (1C, S-<u>C</u>H$_2$-(*Ar*)C-CH-CH-C-C(CH$_3$)$_3$), 39.6 (1C, S-<u>C</u>H$_2$-(*Ar*)C-CH-CH-C-C(CH$_3$)$_3$), 34.93 (1C, S-CH$_2$-(*Ar*)C-CH-CH-C-<u>C</u>(CH$_3$)$_3$), 34.89 (1C, S-CH$_2$-(*Ar*)C-CH-CH-C-<u>C</u>(CH$_3$)$_3$), 31.56 (3C, S-CH$_2$-(*Ar*)C-CH-CH-C-C(<u>C</u>H$_3$)$_3$), 31.54 (3C, S-CH$_2$-(*Ar*)C-CH-CH-C-C(<u>C</u>H$_3$)$_3$), 31.0 (2C, 2x(*Ar*)CH-CH-C-<u>C</u>H(CH$_3$)$_2$), 27.5 (1C, (*Coum*)O-C-C-CH-C-<u>C</u>H$_2$-(CH$_2$)$_2$-N), 23.2 (2C, (*Ar*)CH-CH-C-CH(<u>C</u>H$_3$)$_2$), 22.8 (2C, (*Ar*)CH-CH-C-CH(<u>C</u>H$_3$)$_2$), 21.1 (1C, (*Coum*)O-C-

C-CH-C-CH_2-<u>C</u>H_2-CH_2-N), 20.23 (1C, (*Coum*)O-C-C-CH_2-<u>C</u>H_2-CH_2-N), 20.19 (1C, (*Coum*)O-C-C-<u>C</u>H_2-$(CH_2)_2$-N), 18.3 (2C, 2x<u>C</u>H_3-(*Ar*)C-CH-CH);

HRMS (ESI(+)): *m*/*z* calcd for $C_{64}H_{76}NO_4Ru_2S_3^+$: 1222.3018 $[M\text{-}Cl]^+$; found: 1222.3010 (the isotopic pattern corresponds well to the calculated one);

Elemental analysis: calcd (%) for $C_{64}H_{76}ClNO_4Ru_2S_3 \cdot 0.5CH_2Cl_2 \cdot CH_3OH$: C 59.08, H 6.13, N 1.05; found: C 59.14, H 6.04, N 0.97.

Synthesis of [(η^6-*p*-$MeC_6H_4Pr^i$)$_2$$Ru_2$($SCH_2C_6H_4Bu^t$)$_2$($SC_6H_4$-*p*-$CH_2CO_2NH(CH_2)_3NHR$)]Cl (R = 7-(diethylamino)-2-oxo-2*H*-chromene-3-carboxylate) (1.1.15)

To a solution of **1.1.4a** (0.250 g, 0.242 mmol, 1 equiv), in dry CH_2Cl_2 (50 mL) were added successively EDCI (0.139 g, 0.726 mmol, 3 equiv), HOBt·H_2O (0.081 g, 0.581 mmol, 2.4 equiv) and DIPEA (0.2 mL, 1.210 mmol, 5 equiv). After 10 min was added **1.1.8** (0.230 g, 0.726 mmol, 3 equiv). The reaction mixture was stirred at room temperature for 72 h, the reaction evolution was verified by ^{1}H NMR ($CDCl_3$) and TLC and then the mixture was concentrated to dryness under reduced pressure. Purification by flash column chromatography using a CH_2Cl_2/MeOH mixture as eluent afforded the product as an orange solid (0.120 g, 0.090 mmol, yield 37%).

***R*$_f$** (CH_2Cl_2/MeOH 10:1) = 0.537;

^{1}H-NMR ($CDCl_3$) δ_H, ppm: 8.88 (1H, t br, S-(*Ar*)C-CH-CH-C-CH_2-(C=O)-N<u>*H*</u>, $^3J_{H,H}$ = 5.9 Hz), 8.65 (1H, s, (*Coum*)O-C-C-C<u>*H*</u>-C-(C=O)), 8.51 (1H, t br, NH-$(CH_2)_2$-CH_2-N<u>*H*</u>-(C=O)-C(*Coum*), $^3J_{H,H}$ = 5.7 Hz), 7.63 (2H, d, 2xS-(*Ar*)C-CH-C<u>*H*</u>-C-CH_2-(C=O)-NH, $^3J_{H,H}$ = 8.2 Hz), 7.51 (2H, d, 2xS-(*Ar*)C-C<u>*H*</u>-CH-C-CH_2-(C=O)-NH, $^3J_{H,H}$ = 8.2 Hz), 7.38-7.49 (9H, m, 4xCH_2-(*Ar*)C-C<u>*H*</u>-CH-C-C$(CH_3)_3$, 4xCH_2-(*Ar*)C-CH-C<u>*H*</u>-C-C$(CH_3)_3$, (*Coum*)O-C-C-C<u>*H*</u>-CH-C-N$(CH_2$-$CH_3)_2$), 6.62 (1H, dd, (*Coum*)O-C-C-CH-C<u>*H*</u>-C-N$(CH_2$-$CH_3)_2$, $^3J_{H,H}$ = 9.0 Hz, $^4J_{H,H}$ = 2.4 Hz), 6.45 (1H, d, (*Coum*)O-C-C<u>*H*</u>-C-N$(CH_2$-$CH_3)_2$, $^4J_{H,H}$ = 2.3 Hz), 5.02 (2H, d, 2xCH_3-(*Ar*)C-CH-C<u>*H*</u>-C, $^3J_{H,H}$ = 5.8 Hz), 4.90 (2H, d, 2xCH_3-(*Ar*)C-CH-C<u>*H*</u>-C, $^3J_{H,H}$ = 5.8 Hz), 4.80 (2H, d, 2xCH_3-(*Ar*)C-C<u>*H*</u>-CH-C, $^3J_{H,H}$ = 5.7 Hz), 4.59 (2H, d, 2xCH_3-(*Ar*)C-C<u>*H*</u>-CH-C, $^3J_{H,H}$ = 5.7 Hz), 3.72 (2H, s, S-(*Ar*)C-CH-CH-C-C<u>*H*$_2$</u>-(C=O)-NH), 3.57 (2H, s, S-C<u>*H*$_2$</u>-(*Ar*)C-CH-CH-C-C$(CH_3)_3$), 3.38-3.48 (2H, m, NH-C<u>*H*$_2$</u>-$(CH_2)_2$-NH-(C=O)-C(*Coum*)), 3.42 (4H, qvart, N(C<u>*H*$_2$</u>-$CH_3)_2$, $^3J_{H,H}$ = 7.1 Hz), 3.37 (2H, s, S-C<u>*H*$_2$</u>-(*Ar*)C-CH-CH-C-C$(CH_3)_3$), 3.31 (2H, qvart, NH-$(CH_2)_2$-C<u>*H*$_2$</u>-NH-(C=O)-C(*Coum*), $^3J_{H,H}$ = 6.3 Hz), 1.92 (2H, sept, 2x(*Ar*)C-CH-CH-C-C<u>*H*</u>$(CH_3)_2$, $^3J_{H,H}$ = 6.9 Hz), 1.83 (2H, qvin, NH-CH_2-C<u>*H*$_2$</u>-CH_2-NH, $^3J_{H,H}$ = 6.6 Hz), 1.68 (6H, s, 2xC<u>*H*$_3$</u>-(*Ar*)C-CH-CH-C), 1.35 (9H, s, S-CH_2-(*Ar*)C-CH-CH-C-C(C<u>*H*$_3$</u>)$_3$), 1.32 (9H, s, S-CH_2-(*Ar*)C-CH-CH-C-C(C<u>*H*$_3$</u>)$_3$), 1.21 (6H, t, N(CH_2-C<u>*H*$_3$</u>)$_2$, $^3J_{H,H}$ = 7.1 Hz), 0.94 (6H, d, (*Ar*)C-CH-CH-C-CH(C<u>*H*$_3$</u>)$_2$, $^3J_{H,H}$ = 6.9 Hz), 0.89 (6H, d, (*Ar*)C-CH-CH-C-CH(C<u>*H*$_3$</u>)$_2$, $^3J_{H,H}$ = 6.9 Hz);

^{13}C-NMR ($CDCl_3$) δ_C, ppm: 171.4 (1C, S-(*Ar*)C-CH-CH-C-CH_2-(<u>C</u>=O)-NH), 163.6 (1C, (*Coum*)O-C-C-CH-C-(<u>C</u>=O)-NH), 162.6 (1C, (*Coum*)O-C-C-CH-C-(<u>C</u>=O)-O), 157.7 (1C, (*Coum*)O-<u>C</u>-C-CH-C-(C=O)), 152.6 (1C, (*Ar*)<u>C</u>-N(CH_2-CH_3), 151.94, 151.87 (2C, 2xS-CH_2-(*Ar*)C-CH-CH-<u>C</u>-C$(CH_3)_3$), 148.0 (1C, (*Coum*)O-C-C-<u>C</u>H-C-(C=O)), 138.6 (1C, S-(*Ar*)C-CH-CH-<u>C</u>-CH_2-(C=O)-NH), 136.8, 136.6 (2C, 2xS-CH_2-(*Ar*)<u>C</u>-CH-CH-C-C$(CH_3)_3$), 135.0 (1C, S-(*Ar*)<u>C</u>-CH-CH-C-CH_2-(C=O)-NH), 132.4 (2C, 2xS-(*Ar*)C-CH-<u>C</u>H-C-CH_2-(C=O)-NH), 131.2 (1C, (*Coum*)O-C-C-<u>C</u>H-CH-C-N$(CH_2$-$CH_3)_2$), 130.5 (2C, 2xS-(*Ar*)C-<u>C</u>H-CH-C-CH_2-(C=O)-NH), 129.4, 129.1 (4C, 4xS-CH_2-(*Ar*)C-<u>C</u>H-CH-C-C$(CH_3)_3$), 125.7, 125.6 (4C, 4xS-CH_2-(*Ar*)C-CH-<u>C</u>H-C-C$(CH_3)_3$), 110.6 (1C, (*Coum*)O-C-<u>C</u>-CH-C-(C=O)), 110.0 (1C, (*Coum*)O-C-C-CH-<u>C</u>H-C-N(CH_2-CH_3), 108.5 (1C, (*Coum*)O-C-C-CH-<u>C</u>-(C=O)), 107.4 (2C, 2xCH_3-(*Ar*)C-CH-CH-<u>C</u>), 100.5 (2C, 2xCH_3-(*Ar*)<u>C</u>-CH-CH-C), 96.7 (1C, (*Coum*)O-C-<u>C</u>H-C-N$(CH_2CH_3)_2$), 84.0 (2C, 2xCH_3-(*Ar*)C-CH-<u>C</u>H-C), 83.76 (2C, 2xCH_3-(*Ar*)C-CH-<u>C</u>H-C), 83.72 (2C, 2xCH_3-(*Ar*)C-<u>C</u>H-C*H*-C), 82.4 (2C, 2xCH_3-(*Ar*)C-<u>C</u>H-CH-C), 45.2 (2C, N(<u>C</u>H_2-$CH_3)_2$), 43.3 (1C, S-(*Ar*)C-CH-CH-C-<u>C</u>H_2-(C=O)-NH), 40.0 (1C, S-<u>C</u>H_2-(*Ar*)C-CH-CH-C-C$(CH_3)_3$), 39.4 (1C, S-<u>C</u>H_2-(*Ar*)C-CH-CH-C-

$C(CH_3)_3$), 37.2 (1C, NH-$\underline{C}H_2$-$(CH_2)_2$-NH-(C=O)-C(*Coum*)), 36.8 (1C, NH-$(CH_2)_2$-$\underline{C}H_2$-NH-(C=O)-C(*Coum*)), 34.92 (1C, S-CH_2-(*Ar*)C-CH-CH-C-$\underline{C}(CH_3)_3$), 34.88 (1C, S-CH_2-(*Ar*)C-CH-CH-C-$\underline{C}(CH_3)_3$), 31.55 (3C, S-CH_2-(*Ar*)C-CH-CH-C-C($\underline{C}H_3)_3$), 31.53 (3C, S-CH_2-(*Ar*)C-CH-CH-C-C($\underline{C}H_3)_3$), 31.0 (2C, 2x(*Ar*)CH-CH-C-$\underline{C}H(CH_3)_2$), 29.8 (1C, NH-CH_2-$\underline{C}H_2$-CH_2-NH-(C=O)-C(*Coum*)), 23.2 (2C, (*Ar*)CH-CH-C-CH($\underline{C}H_3)_2$), 22.8 (2C, (*Ar*)CH-CH-C-CH($\underline{C}H_3)_2$), 18.2 (2C, 2x$\underline{C}H_3$-(*Ar*)C-CH-CH), 12.6 (2C, N(CH_2-$\underline{C}H_3)_2$);

HRMS (ESI(+)): *m*/*z* calcd for $C_{67}H_{86}N3O_4Ru_2S_3^+$: 1296.3862 $[M-Cl]^+$; found: 1296.3842 (the isotopic pattern corresponds well to the calculated one);

Elemental analysis: calcd (%) for $C_{67}H_{86}ClN_3O_4Ru_2S_3 \cdot 2CH_3OH$: C 59.40, H 6.79, N 3.01; found C 59.45, H 7.28, N 3.01.

Synthesis of [(η^6-*p*-$MeC_6H_4Pr^i$)$_2$$Ru_2$($SCH_2C_6H_4Bu^t$)$_2$($SC_6H_4$-*p*-$CH_2CO_2NH(CH_2)_4NHR$)]Cl (R = 7-(diethylamino)-2-oxo-2*H*-chromene-3-carboxylate) (1.1.16a)

To a solution of **1.1.4a** (0.250 g, 0.242 mmol, 1 equiv), in dry CH_2Cl_2 (50 mL) were added successively EDCI (0.139 g, 0.726 mmol, 3 equiv), HOBt·H_2O (0.081 g, 0.581 mmol, 2.4 equiv) and DIPEA (0.2 mL, 1.210 mmol, 5 equiv). After 10 min was added **1.1.9** (0.241 g, 0.726 mmol, 3 equiv). The reaction mixture was stirred at room temperature for 72 h, the reaction evolution was verified by ^{1}H NMR ($CDCl_3$) and TLC and then the mixture was concentrated to dryness under reduced pressure. Purification by flash column chromatography using a CH_2Cl_2/MeOH mixture as eluent afforded the product as an orange solid (0.143 g, 0.106 mmol, yield 44%).

R_f (CH_2Cl_2/MeOH 10:1) = 0.500;

^{1}H-NMR ($CDCl_3$) δ_H, ppm: 8.75 (1H, t br, S-(*Ar*)C-CH-CH-C-CH_2-(C=O)-N$\underline{H}$, $^3J_{H,H}$ = 5.6 Hz), 8.67 (1H, s, (*Coum*)O-C-C-C$\underline{H}$-C-(C=O)), 8.63 (1H, t br, (*Coum*)O-C-C-CH-C-(C=O)-N$\underline{H}$, $^3J_{H,H}$ = 6.3 Hz), 7.61 (2H, d, 2xS-(*Ar*)C-CH-C$\underline{H}$-C-CH_2-(C=O)-NH, $^3J_{H,H}$ = 8.2 Hz), 7.54 (2H, d, 2xS-(*Ar*)C-C$\underline{H}$-CH-C-CH_2-(C=O)-NH, $^3J_{H,H}$ = 8.2 Hz), 7.38-7.48 (9H, m, 4xCH_2-(*Ar*)C-C$\underline{H}$-CH-C-$C(CH_3)_3$, 4xCH_2-(*Ar*)C-CH-C$\underline{H}$-C-$C(CH_3)_3$, (*Coum*)O-C-C-C$\underline{H}$-CH-C-N(CH_2-$CH_3)_2$), 6.61 (1H, dd, (*Coum*)O-C-C-CH-C$\underline{H}$-C-N(CH_2-$CH_3)_2$, $^3J_{H,H}$ = 9.0 Hz, $^4J_{H,H}$ = 2.4 Hz), 6.44 (1H, d, (*Coum*)O-C-C$\underline{H}$-C-N(CH_2-$CH_3)_2$, $^4J_{H,H}$ = 2.1 Hz), 5.01 (2H, d, 2xCH_3-(*Ar*)C-CH-C$\underline{H}$-C, $^3J_{H,H}$ = 5.7 Hz), 4.89 (2H, d, 2xCH_3-(*Ar*)C-CH-C$\underline{H}$-C, $^3J_{H,H}$ = 5.8 Hz), 4.80 (2H, d, 2xCH_3-(*Ar*)C-C$\underline{H}$-CH-C, $^3J_{H,H}$ = 5.7 Hz), 4.58 (2H, d, 2xCH_3-(*Ar*)C-C$\underline{H}$-CH-C, $^3J_{H,H}$ = 5.8 Hz), 3.75 (2H, s, S-(*Ar*)C-CH-CH-C-C$\underline{H_2}$-(C=O)-NH), 3.56 (2H, s, S-C$\underline{H_2}$-(*Ar*)C-CH-CH-C-$C(CH_3)_3$), 3.42 (6H, qvart, N(C$\underline{H_2}$-$CH_3)_2$, NH-$(CH_2)_3$-C$\underline{H_2}$-NH-(C=O)-C(*Coum*), $^3J_{H,H}$ = 7.0 Hz), 3.36 (2H, s, S-C$\underline{H_2}$-(*Ar*)C-CH-CH-C-$C(CH_3)_3$), 3.28 (2H, qvart, NH-C$\underline{H_2}$-$(CH_2)_3$-NH-(C=O)-C(*Coum*), $^3J_{H,H}$ = 5.7 Hz), 1.92 (2H, sept, 2x(*Ar*)C-CH-CH-C-C$\underline{H}(CH_3)_2$, $^3J_{H,H}$ = 6.9 Hz), 1.68 (6H, s, 2xC$\underline{H_3}$-(*Ar*)C-CH-CH-C), 1.59-1.72 (4H, m, NH-CH_2-C$\underline{H_2}$-$(CH_2)_2$-NH-(C=O)-C(*Coum*), NH-$(CH_2)_2$-C$\underline{H_2}$-CH_2-NH-(C=O)-C(*Coum*), 1.36 (9H, s, S-CH_2-(*Ar*)C-CH-CH-C-C(C$\underline{H_3}$)$_3$), 1.32 (9H, s, S-CH_2-(*Ar*)C-CH-CH-C-C(C$\underline{H_3}$)$_3$), 1.20 (6H, t, N(CH_2-C$\underline{H_3}$)$_2$, $^3J_{H,H}$ = 7.1 Hz), 0.94 (6H, d, (*Ar*)C-CH-CH-C-CH(C$\underline{H_3}$)$_2$, $^3J_{H,H}$ = 6.9 Hz), 0.89 (6H, d, (*Ar*)C-CH-CH-C-CH(C$\underline{H_3}$)$_2$, $^3J_{H,H}$ = 6.9 Hz);

^{13}C-NMR ($CDCl_3$) δ_C, ppm: 171.4 (1C, S-(*Ar*)C-CH-CH-C-CH_2-(C=O)-NH), 163.1 (1C, (*Coum*)O-C-C-CH-C-(C=O)-NH), 162.7 (1C, (*Coum*)O-C-C-CH-C-(C=O)-O), 157.7 (1C, (*Coum*)O-C-C-CH-C-(C=O)), 152.5 (1C, (*Ar*)C-N(CH_2-CH_3), 151.93, 151.88 (2C, 2xS-CH_2-(*Ar*)C-CH-CH-C-$C(CH_3)_3$), 148.0 (1C, (*Coum*)O-C-C-CH-C-(C=O)), 138.6 (1C, S-(*Ar*)C-CH-CH-C-CH_2-(C=O)-NH), 136.8, 136.6 (2C, 2xS-CH_2-(*Ar*)C-CH-CH-C-$C(CH_3)_3$), 134.7 (1C, S-(*Ar*)C-CH-CH-C-CH_2-(C=O)-NH), 132.3 (2C, 2xS-(*Ar*)C-CH-CH-C-CH_2-(C=O)-NH), 131.2 (1C, (*Coum*)O-C-C-CH-CH-C-N(CH_2-$CH_3)_2$), 130.6 (2C, 2xS-(*Ar*)C-CH-CH-C-CH_2-(C=O)-NH), 129.3, 129.1 (4C, 4xS-CH_2-(*Ar*)C-CH-CH-C-$C(CH_3)_3$), 125.7, 125.6 (4C, 4xS-CH_2-(*Ar*)C-CH-CH-C-$C(CH_3)_3$), 110.6 (1C, (*Coum*)O-C-C-CH-C-(C=O)), 110.0 (1C, (*Coum*)O-C-C-CH-CH-C-N(CH_2CH_3), 108.5 (1C, (*Coum*)O-C-C-CH-C-(C=O)), 107.4 (2C, 2xCH_3-(*Ar*)C-CH-CH-C), 100.5

(2C, 2xCH_3-(*Ar*)*C*-CH-CH-C), 96.6 (1C, (*Coum*)O-C-*C*H-C-N(CH_2-CH_3)$_2$), 83.9 (2C, 2xCH_3-(*Ar*)C-CH-*C*H-C), 83.8 (2C, 2xCH_3-(*Ar*)C-*C*H-CH-C), 83.7 (2C, 2xCH_3-(*Ar*)C-CH-*C*H-C), 82.4 (2C, 2xCH_3-(*Ar*)C-*C*H-CH-C), 45.2 (2C, N(*C*H_2-CH_3)$_2$), 43.1 (1C, S-(*Ar*)C-CH-CH-C-*C*H_2-(C=O)-NH), 40.0 (1C, S-*C*H_2-(*Ar*)C-CH-CH-C-C(CH_3)$_3$), 39.6 (1C, NH-*C*H_2-(CH_2)$_3$-NH-(C=O)-C(*Coum*)), 39.34 (1C, S-*C*H_2-(*Ar*)C-CH-CH-C-C(CH_3)$_3$), 39.27 (1C, NH-(CH_2)$_3$-*C*H_2-NH-(C=O)-C(*Coum*)), 34.90 (1C, S-CH_2-(*Ar*)C-CH-CH-C-*C*(CH_3)$_3$), 34.87 (1C, S-CH_2-(*Ar*)C-CH-CH-C-*C*(CH_3)$_3$), 31.53 (3C, S-CH_2-(*Ar*)C-CH-CH-C-C(*C*H_3)$_3$), 31.52 (3C, S-CH_2-(*Ar*)C-CH-CH-C-C(*C*H_3)$_3$), 31.0 (2C, 2x(*Ar*)CH-CH-C-*C*H(CH_3)$_2$), 27.3 (1C, NH-(CH_2)$_2$-*C*H_2-CH_2-NH-(C=O)-C(*Coum*)), 27.0 (1C, NH-CH_2-*C*H_2-(CH_2)$_2$-NH-(C=O)-C(*Coum*)), 23.1 (2C, (*Ar*)CH-CH-C-CH(*C*H_3)$_2$), 22.8 (2C, (*Ar*)CH-CH-C-CH(*C*H_3)$_2$), 18.1 (2C, 2x*C*H_3-(*Ar*)C-CH-CH), 12.5 (2C, N(CH_2-*C*H_3)$_2$);

HRMS (ESI(+)): *m*/*z* calcd for $C_{67}H_{86}N3O_4Ru_2S_3^+$: 1310.4018 $[M-Cl]^+$; found: 1310.3981 (the isotopic pattern corresponds well to the calculated pattern);

Elemental analysis: calcd (%) for $C_{68}H_{88}ClN_3O_4Ru_2S_3 \cdot 2CH_3OH$: C 59.66, H 6.87, N 2.98, found C 59.63, H 7.57, N 2.96.

Synthesis of [(η^6-*p*-$MeC_6H_4Pr^i$)$_2$$Ru_2$($SCH_2C_6H_4Bu^t$)$_2$($SC_6H_4$-*p*-$CH_2CO_2NH(CH_2)_4NHR$)]Cl (R = 11-oxo-2,3,6,7-tetrahydro-1*H*,5*H*,11*H*-pyrano[2,3-*f*]pyrido[3,2,1-*ij*]quinoline-10-carboxylate) (1.1.17a)

To a solution of **1.1.4a** (0.250 g, 0.242 mmol, 1 equiv), in dry CH_2Cl_2 (50 mL) were added successively EDCI (0.139 g, 0.726 mmol, 3 equiv), HOBt·H_2O (0.081 g, 0.581 mmol, 2.4 equiv) and DIPEA (0.2 mL, 1.210 mmol, 5 equiv). After 10 min was added **1.1.10** (0.258 g, 0.726 mmol, 3 equiv). The reaction mixture was stirred at room temperature for 72 h, the reaction evolution was verified by ^{1}H NMR ($CDCl_3$) and TLC and then the mixture was concentrated to dryness under reduced pressure. Purification by flash column chromatography using a CH_2Cl_2/MeOH mixture as eluent afforded the product as an orange solid (0.230 g, 0.168 mmol, yield 69%).

R_f (CH_2Cl_2/MeOH 10:1) = 0.491;

^{1}H-NMR ($CDCl_3$) δ_H, ppm: 8.83 (1H, t br, S-(*Ar*)C-CH-CH-C-CH_2-(C=O)-N*H*, $^3J_{H,H}$ = 5.8 Hz), 8.62-8.70 (1H, m br, O-C-C-CH-C-(C=O)-N*H*), 8.59 (1H, s, (*Coum*)O-C-C-C*H*-C-(C=O)), 7.62 (2H, d, 2xS-(*Ar*)C-CH-C*H*-C-CH_2-(C=O)-NH, $^3J_{H,H}$ = 8.2 Hz), 7.57 (2H, d, 2xS-(*Ar*)C-C*H*-CH-C-CH_2-(C=O)-NH, $^3J_{H,H}$ = 8.2 Hz), 7.38-7.50 (8H, m, 4xCH_2-(*Ar*)C-C*H*-CH-C-C(CH_3)$_3$, 4xCH_2-(*Ar*)C-CH-C*H*-C-C(CH_3)$_3$), 6.97 (1H, s, (*Coum*)O-C-C-C*H*-C-CH_2), 5.02 (2H, d, 2xCH_3-(*Ar*)C-CH-C*H*-C, $^3J_{H,H}$ = 5.7 Hz), 4.90 (2H, d, 2xCH_3-(*Ar*)C-CH-C*H*-C, $^3J_{H,H}$ = 5.8 Hz), 4.80 (2H, d, 2xCH_3-(*Ar*)C-C*H*-CH-C, $^3J_{H,H}$ = 5.7 Hz), 4.59 (2H, d, 2xCH_3-(*Ar*)C-C*H*-CH-C, $^3J_{H,H}$ = 5.8 Hz), 3.76 (2H, s, S-(*Ar*)C-CH-CH-C-C*H*$_2$-(C=O)-NH), 3.57 (2H, s, S-C*H*$_2$-(*Ar*)C-CH-CH-C-C(CH_3)$_3$), 3.40-3.45 (2H, qvart br, NH-(CH_2)$_3$-C*H*$_2$-NH-(C=O)-C(*Coum*), $^3J_{H,H}$ = 5.4 Hz), 3.37 (2H, s, S-C*H*$_2$-(*Ar*)C-CH-CH-C-C(CH_3)$_3$), 3.28-3.32 (6H, m, (*Coum*)O-C-C-CH-C-(CH_2)$_2$-C*H*$_2$-N, (*Coum*)O-C-C-(CH_2)$_2$-C*H*$_2$-N, NH-C*H*$_2$-(CH_2)$_3$-NH-(C=O)-C(*Coum*), $^3J_{H,H}$ = 5.6 Hz), 2.84 (2H, t, (*Coum*)O-C-C-CH-C-C*H*$_2$-(CH_2)$_2$-N, $^3J_{H,H}$ = 6.4 Hz), 2.74 (2H, t, (*Coum*)O-C-C-C*H*$_2$-(CH_2)$_2$-N, $^3J_{H,H}$ = 6.2 Hz), 1.90-2.01 (4H, m, (*Coum*)O-C-C-CH-C-CH_2-C*H*$_2$-CH_2-N, (*Coum*)O-C-C-CH_2-C*H*$_2$-CH_2-N), 1.93 (2H, sept, 2x(*Ar*)C-CH-CH-C-C*H*(CH_3)$_2$, $^3J_{H,H}$ = 6.9 Hz), 1.68 (6H, s, 2xC*H*$_3$-(*Ar*)C-CH-CH-C), 1.59-1.75 (4H, m, C(*Coum*)-(C=O)-NH-CH_2-C*H*$_2$-(CH_2)$_2$-NH_2, C(*Coum*)-(C=O)-NH-(CH_2)$_2$-C*H*$_2$-CH_2-NH_2), 1.37 (9H, s, S-CH_2-(*Ar*)C-CH-CH-C-C(C*H*$_3$)$_3$), 1.33 (9H, s, S-CH_2-(*Ar*)C-CH-CH-C-C(C*H*$_3$)$_3$), 0.94 (6H, d, (*Ar*)C-CH-CH-C-CH(C*H*$_3$)$_2$, $^3J_{H,H}$ = 6.9 Hz), 0.90 (6H, d, (*Ar*)C-CH-CH-C-CH(C*H*$_3$)$_2$, $^3J_{H,H}$ = 6.9 Hz);

^{13}C-NMR ($CDCl_3$) δ_C, ppm: 171.5 (1C, S-(*Ar*)C-CH-CH-C-CH_2-(*C*=O)-NH), 163.6 (1C, (*Coum*)O-C-C-CH-C-(*C*=O)-NH), 163.0 (1C, (*Coum*)O-C-C-CH-C-(*C*=O)), 152.7 (1C, (*Coum*)O-*C*-C-CH-C-(C=O)), 151.96, 151.92 (2C, 2xS-CH_2-(*Ar*)C-CH-CH-*C*-C(CH_3)$_3$), 148.1 (2C,

(*Coum*)O-C-C-<u>C</u>H-C-(C=O)), (*Ar*)<u>C</u>-N-CH_2-CH_2), 138.7 (1C, S-(*Ar*)C-CH-CH-<u>C</u>-CH_2-(C=O)-NH), 136.8, 136.6 (2C, 2xS-CH_2-(*Ar*)<u>C</u>-CH-CH-C-C$(CH_3)_3$), 134.7 (1C, S-(*Ar*)<u>C</u>-CH-CH-C-CH_2-(C=O)-NH), 132.4 (2C, 2xS-(*Ar*)C-<u>C</u>H-CH-C-CH_2-(C=O)-NH), 130.6 (2C, 2xS-(*Ar*)C-CH-<u>C</u>H-C-CH_2-(C=O)-NH), 129.4, 129.1 (4C, 4xS-CH_2-(*Ar*)C-<u>C</u>H-CH-C-C$(CH_3)_3$), 127.1 (1C, (*Coum*)O-C-C-<u>C</u>H-C-$(CH_2)_3$-N), 125.7, 125.6 (4C, 4xS-CH_2-(*Ar*)C-CH-<u>C</u>H-C-C$(CH_3)_3$), 119.6 (1C, (*Coum*)O-C-<u>C</u>-$(CH_2)_3$-N), 109.4 (1C, (*Coum*)O-C-C-CH-<u>C</u>-(C=O)-NH), 108.4 (1C, (*Coum*)O-C-<u>C</u>-CH-C-(C=O)-NH), 107.4 (2C, 2xCH_3-(*Ar*)C-CH-CH-<u>C</u>), 105.7 (1C, (*Coum*)O-C-C-CH-<u>C</u>-$(CH_2)_3$-N), 100.5 (2C, 2xCH_3-(*Ar*)<u>C</u>-CH-CH-C), 84.0 (2C, 2xCH_3-(*Ar*)C-CH-<u>C</u>H-C), 83.76 (2C, 2xCH_3-(*Ar*)C-CH-<u>C</u>H-C), 83.73 (2C, 2xCH_3-(*Ar*)C-<u>C</u>H-CH-C, 82.4 (2C, 2xCH_3-(*Ar*)C-<u>C</u>H-CH-C), 50.4 (1C, (*Coum*)O-C-C-CH-C-$(CH_2)_2$-<u>C</u>H_2-N), 49.9 (1C, (*Coum*)O-C-C-$(CH_2)_2$-<u>C</u>H_2-N), 43.2 (1C, S-(*Ar*)C-CH-CH-C-<u>C</u>H_2-(C=O)-NH), 40.0 (1C, S-<u>C</u>H_2-(*Ar*)C-CH-CH-C-C$(CH_3)_3$), 39.5 (1C, NH-$(CH_2)_3$-<u>C</u>H_2-NH-(C=O)-C(*Coum*)), 39.4 (1C, S-<u>C</u>H_2-(*Ar*)C-CH-CH-C-C$(CH_3)_3$), 39.3 (1C, NH-<u>C</u>H_2-$(CH_2)_3$-NH-(C=O)-C(*Coum*)), 34.94 (1C, S-CH_2-(*Ar*)C-CH-CH-C-<u>C</u>$(CH_3)_3$), 34.90 (1C, S-CH_2-(*Ar*)C-CH-CH-C-<u>C</u>$(CH_3)_3$), 31.6 (6C, 2xS-CH_2-(*Ar*)C-CH-CH-C-C(<u>C</u>$H_3)_3$), 31.0 (2C, 2x(*Ar*)CH-CH-C-<u>C</u>H$(CH_3)_2$), 27.6 (1C, (*Coum*)O-C-C-CH-C-<u>C</u>H_2-$(CH_2)_2$-N), 27.4 (1C, NH-$(CH_2)_2$-<u>C</u>H_2-CH_2-NH-(C=O)-C(*Coum*)), 27.0 (1C, NH-CH_2-<u>C</u>H_2-$(CH_2)_2$-NH-(C=O)-C(*Coum*)), 23.2 (2C, (*Ar*)CH-CH-C-CH(<u>C</u>$H_3)_2$), 22.9 (2C, (*Ar*)CH-CH-C-CH(<u>C</u>$H_3)_2$), 21.3 (1C, (*Coum*)O-C-C-CH-C-CH_2-<u>C</u>H_2-CH_2-N), 20.4 (1C, (*Coum*)O-C-C-CH_2-<u>C</u>H_2-CH_2-N), 20.3 (1C, (*Coum*)O-C-C-<u>C</u>H_2-$(CH_2)_2$-N), 18.2 (2C, 2x<u>C</u>H_3-(*Ar*)C-CH-CH);

HRMS (ESI(+)): *m*/*z* calcd for $C_{70}H_{88}N_3O_4Ru_2S_3^+$: 1334.4018 $[M\text{-}Cl]^+$, and for $C_{70}H_{89}N_3O_4Ru_2S_3^{+2}$: 667.7046 $[M\text{-}Cl+H]^{+2}$; found: 1334.3999, 667.2009 (the isotopic pattern corresponds well to the calculated one);

Elemental analysis: calcd (%) for $C_{70}H_{88}ClN_3O_4Ru_2S_3 \cdot 0.5CH_3OH$: C 61.13, H 6.55, N 3.03; found C 61.14, H 7.24, N 2.73.

Synthesis of [(η^6-*p*-$MeC_6H_4Pr^i$)$_2$Ru$_2$(μ_2-$SCH_2C_6H_4$-*p*-Bu^t)(μ_2-SC_6H_4-*p*-O-R)$_2$]Cl (R = 7-(diethylamino)-2-oxo-2*H*-chromene-3-carboxylate) (1.1.20)

To a solution of **Dye2-CO_2H** (0.139 g, 0.505 mmol, 2.5 equiv) in dry CH_2Cl_2 (50 mL) was added EDCI (0.097 g, 0.505 mmol, 2.5 equiv) After 10 min were added successively **1.1.19** (0.200 g, 0.202 mmol, 1 equiv) and DMAP (0.015 g, 0.121 mmol, 0.6 equiv). The reaction mixture was stirred at room temperature for 24 h, the reaction evolution was verified by ^{1}H NMR ($CDCl_3$) and TLC and then the mixture was concentrated to dryness under reduced pressure. Purification by flash column chromatography using a CH_2Cl_2/MeOH mixture as eluent afforded **1.1.20** as an orange solid (0.215 g, 0.151 mmol, yield 75%).

***R*$_f$** (CH_2Cl_2/CH_3OH 10:1) = 0.429;

^{1}H-NMR ($CDCl_3$) δ_H, ppm: 8.70 (1H, s, (*Coum*)O-C-C-C<u>H</u>-C-(C=O)), 8.66 (1H, s, (*Coum*)O-C-C-C<u>H</u>-C-(C=O)), 7.95 (2H, d, 2xS-(*Ar*)C-CH-C<u>H</u>-C-O, $^3J_{H,H}$ = 8.3 Hz), 7.80 (2H, d, 2xS-(*Ar*)C-CH-C<u>H</u>-C-O, $^3J_{H,H}$ = 8.3 Hz), 7.50 (1H, d, (*Coum*)O-C-C-C<u>H</u>-CH-C-N$(CH_2$-$CH_3)_2$, $^3J_{H,H}$ = 6.8 Hz), 7.48 (1H, d, (*Coum*)O-C-C-C<u>H</u>-CH-C-N$(CH_2$-$CH_3)_2$, $^3J_{H,H}$ = 6.8 Hz), 7.42-7.47 (4H, m, 2xS-CH_2-(*Ar*)C-CH-C<u>H</u>-C-C$(CH_3)_3$, 2xS-CH_2-(*Ar*)C-C<u>H</u>-CH-C-C$(CH_3)_3$), 7.27 (2H, d, 2xS-(*Ar*)C-C<u>H</u>-CH-C-O, $^3J_{H,H}$ = 8.3 Hz), 7.21 (2H, d, 2xS-(*Ar*)C-C<u>H</u>-CH-C-O, $^3J_{H,H}$ = 8.3 Hz), 6.67 (2H, dd, 2xO-C-C-CH-C<u>H</u>-C-N$(CH_2$-$CH_3)_2$, $^3J_{H,H}$ = 9.0 Hz), 6.49 (2H, m, 2x(*Coum*)O-C-C<u>H</u>-C-N$(CH_2$-$CH_3)_2$), 5.12 (4H, m, 2xCH_3-(*Ar*)C-CH-C<u>H</u>-C, 2xCH_3-(*Ar*)C-C<u>H</u>-CH-C), 5.07 (2H, d, 2xCH_3-(*Ar*)C-CH-C<u>H</u>-C, $^3J_{H,H}$ = 5.7 Hz), 4.93 (2H, d, 2xCH_3-(*Ar*)C-C<u>H</u>-CH-C, $^3J_{H,H}$ = 5.7 Hz), 3.62 (2H, s, S-C<u>H_2</u>-(*Ar*)C-CH-CH-C-C$(CH_3)_3$), 3.48 (8H, qvart, 2xN(C<u>H_2</u>-$CH_3)_2$, $^3J_{H,H}$ = 7.0 Hz), 1.92 (2H, sept, 2x(*Ar*)-C-CH-CH-C-C<u>H</u>$(CH_3)_2$, $^3J_{H,H}$ = 6.4 Hz), 1.72 (6H, s, 2xC<u>H_3</u>-(*Ar*)C-CH-CH-C), 1.34 (9H, s, S-CH_2-(*Ar*)C-CH-CH-C-C(C<u>H_3</u>)$_3$), 1.26 (12H, t, 2xN$(CH_2$-C<u>H_3</u>$)_2$, $^3J_{H,H}$ = 7.0 Hz), 0.92 (12H, d, 2x(*Ar*)C-CH-CH-C-CH(C<u>H_3</u>$)_2$, $^3J_{H,H}$ = 6.4 Hz);

^{13}C-NMR ($CDCl_3$) δ_C, ppm: 162.28, 162.25 (2C, 2xS-(*Ar*)-C-CH-CH-C-O-(*C*=O)), 159.01, 158.99 (2C, 2x(*Coum*)O-*C*-C-CH-C-(C=O)), 158.4, 158.3 (2C, 2x(*Coum*)O-C-C-CH-C-(*C*=O)), 153.72, 153.69 (2C, 2x(*Ar*)-*C*-N(CH_2-CH_3)$_2$), 151.9 (1C, S-CH_2-(*Ar*)C-CH-CH-*C*-C(CH_3)$_3$), 151.6, 151.3 (2C, 2xS-(*Ar*)C-CH-CH-*C*-O-(C=O)), 150.7, 150.6 (2C, 2x(*Coum*)O-C-C-*C*H-C-(C=O)), 136.7 (1C, S-CH_2-(*Ar*)*C*-CH-CH-C-C(CH_3)$_3$), 135.7, 134.9 (2C, 2xS-(*Ar*)*C*-CH-CH-C-O-(C=O)), 133.7, 133.5 (4C, 4xS-(*Ar*)C-CH-*C*H-C-O-(C=O)), 131.96, 131.91 (2C, 2x(*Coum*)O-C-C-*C*H-CH-C-N(CH_2-CH_3)$_2$), 129.5 (2C, 2xS-CH_2-(*Ar*)C-*C*H-CH-C-C(CH_3)$_3$), 125.7 (2C, 2xS-CH_2-(*Ar*)C-CH-*C*H-C-C(CH_3)$_3$), 123.0, 122.8 (4C, 4xS-(*Ar*)-C-*C*H-CH-C-O-(C=O)), 110.2 (2C, 2x(*Coum*)O-C-C-CH-*C*H-C-N(CH_2-CH_3)$_2$), 107.99, 107.95 (2C, 2x(*Coum*)O-C-*C*-CH-C-(C=O)), 107.8 (2C, 2xCH_3-(*Ar*)C-CH-CH-*C*), 106.9, 106.8 (2C, 2x(*Coum*)O-C-C-CH-*C*-(C=O)), 100.3 (2C, 2xCH_3-(*Ar*)*C*-CH-CH-C), 96.8 (2C, 2x(*Coum*)O-C-*C*H-C-N(CH_2-CH_3)$_2$), 84.9 (2C, 2xCH_3-(*Ar*)C-CH-*C*H-C), 85.57 (2C, 2xCH_3-(*Ar*)C-*C*H-CH-C), 85.53 (2C, 2xCH_3-(*Ar*)C-CH-*C*H-C), 82.9 (2C, 2xCH_3-(*Ar*)C-*C*H-CH-C), 45.4 (4C, 2xN(*C*H_2-CH_3)$_2$), 38.9 (1C, S-*C*H_2-(*Ar*)C-CH-CH-C-C(CH_3)$_3$), 34.9 (1C, S-CH_2-(*Ar*)C-CH-CH-C-*C*(CH_3)$_3$), 31.5 (3C, S-CH_2-(*Ar*)C-CH-CH-C-C(*C*H_3)$_3$), 29.8 (2C, 2x(*Ar*)C-CH-CH-C-*C*H(CH_3)$_2$), 22.8 (2C, (*Ar*)C-CH-CH-C-CH(*C*H_3)$_2$), 22.6 (2C, (*Ar*)C-CH-CH-C-CH(*C*H_3)$_2$), 18.1 (2C, 2x*C*H_3-(*Ar*)C-CH-CH), 12.6 (4C, 2xN(CH_2-*C*H_3)$_2$);
HRMS (ESI(+)): *m/z* calcd for $C_{71}H_{79}N_2O_8Ru_2S_3^+$: 1387.3080 $[M\text{-}Cl]^+$, and for $C_{71}H_{79}N_2NaO_8Ru_2S_3^{+2}$: 705.1486 $[M\text{-}Cl+Na]^{+2}$; found 1387.3135, 705.1511 (the isotopic pattern corresponds well to the calculated one);
Elemental analysis: calcd (%) for $C_{71}H_{79}ClN_2O_8Ru_2S_3 \cdot 0.25CH_2Cl_2 \cdot CH_3OH \cdot 0.25H_2O$: C 58.64, H 5.72, N 1.89; found C 58.61, H 5.75, N 4.19.

Biology

(Immuno-)Fluorescence microscopy

Glass cover slips of 12 mm in diameter were placed in 24-well culture plate and sterilized by UV for 40 min. HFF in DMEM supplemented with 10% heat-inactivated, sterile, filtered FCS and 2% antibiotics (penicillin streptomycin) were seeded at 2×10^4 cells/mL and plates were allowed to grow for 3 days at 37°C with 5% CO_2. Culture medium was removed and replaced with fresh medium (1 mL/well) containing (i) 0.5%DMSO, (ii) 20 μM of **Dye2-CO_2H** or (iii) 20 μM of **1.1.12a**, and were then incubated for 1 h at 37°C / 5% CO_2. Subsequently the medium was discarded, coverslips were washed 3 times with sterile PBS, fixed with 2% paraformaldehyde (PFA) in PBS for 20 min, permeabilized (0.2 % Triton X-100 in PBS) for 5 min, and unspecific binding sites were blocked in blocking solution (3% BSA, 0.2% NaAcid in PBS) for 2 h at RT. Glass coverslips were then incubated for 30 min in monoclonal mouse anti-tubulin (clone B-5-1-2, Sigma) diluted 1:500 in PBS / 0.3% BSA. After washing with PBS, the secondary antibody conjugate (anti-mouse fluorescein isothiocyanate, FITC, Sigma) was applied at a dilution of 1:300 in PBS / 0.3% BSA. Cells were then stained with NucRed reagent (2 drops/mL) for 30 min at 37°C. Fluorescence microscopy was performed with a Nikon Eclipse E800 digital confocal fluorescence microscope. Images were acquired and processed with Openlab 5.5.2 software.

1.2. BODIPY-Tagged Dinuclear Trithiolato-Bridged Ruthenium(II)-Arene Complexes[8]

1.2.1. Antiparasitic activity screening

Table S1.2.1. Primary efficacy/cytotoxicity screening of BODIPY compounds in non-infected HFF cultures and *T. gondii* β-gal tachyzoites cultured in HFFs.

Compounds	HFF viability (%)		*T. gondii* β-gal growth (%)	
	0.1 µM	**1 µM**	**0.1 µM**	**1 µM**
1.2.5	103 ± 3	100 ± 3	153 ± 10	89 ± 0
1.2.6	59 ± 22	46 ± 8	126 ± 0	643 ± 0
1.2.7	116 ± 5	105 ± 1	141 ± 3	103 ± 13
1.2.8	107 ± 3	103 ±2	135 ± 7	119 ± 2
1.2.9	98 ± 5	81 ± 1	42 ± 0	130 ± 0
1.2.10	97 ± 4	93 ± 5	42 ± 0	95 ± 0
1.2.11	113 ± 7	81 ± 1	87 ± 13	141 ± 2
1.2.12	118 ± 3	94 ± 4	136 ± 6	130 ± 4
1.2.13	57 ± 11	73 ± 5	173 ± 0	681 ± 0
1.2.14	74 ± 5	84 ± 5	218 ± 0	466 ± 0
1.2.15	63 ± 13	64 ± 5	52 ± 0	516 ± 0
1.2.16	126 ± 4	129 ± 3	107 ± 0	169 ± 5
1.2.17	107 ± 3	93 ± 2	80 ± 2	86 ± 2
1.2.18	129 ± 4	133 ± 3	129 ± 0	138 ± 0
1.2.30	105 ± 3	85 ± 1	164 ± 2	287 ± 6
1.2.31	97 ± 3	105 ± 2	182 ± 4	325 ± 5
1.2.32	97 ± 1	102 ± 1	109 ± 1	107 ± 1

[8] This chapter is a draft with title *Synthesis, Spectral Properties and Biological Evaluation of New Conjugates BODIPY – Dinuclear Trithiolato-Bridged Ruthenium(II)-Arene Complexes*, which is going to be submitted for publication.

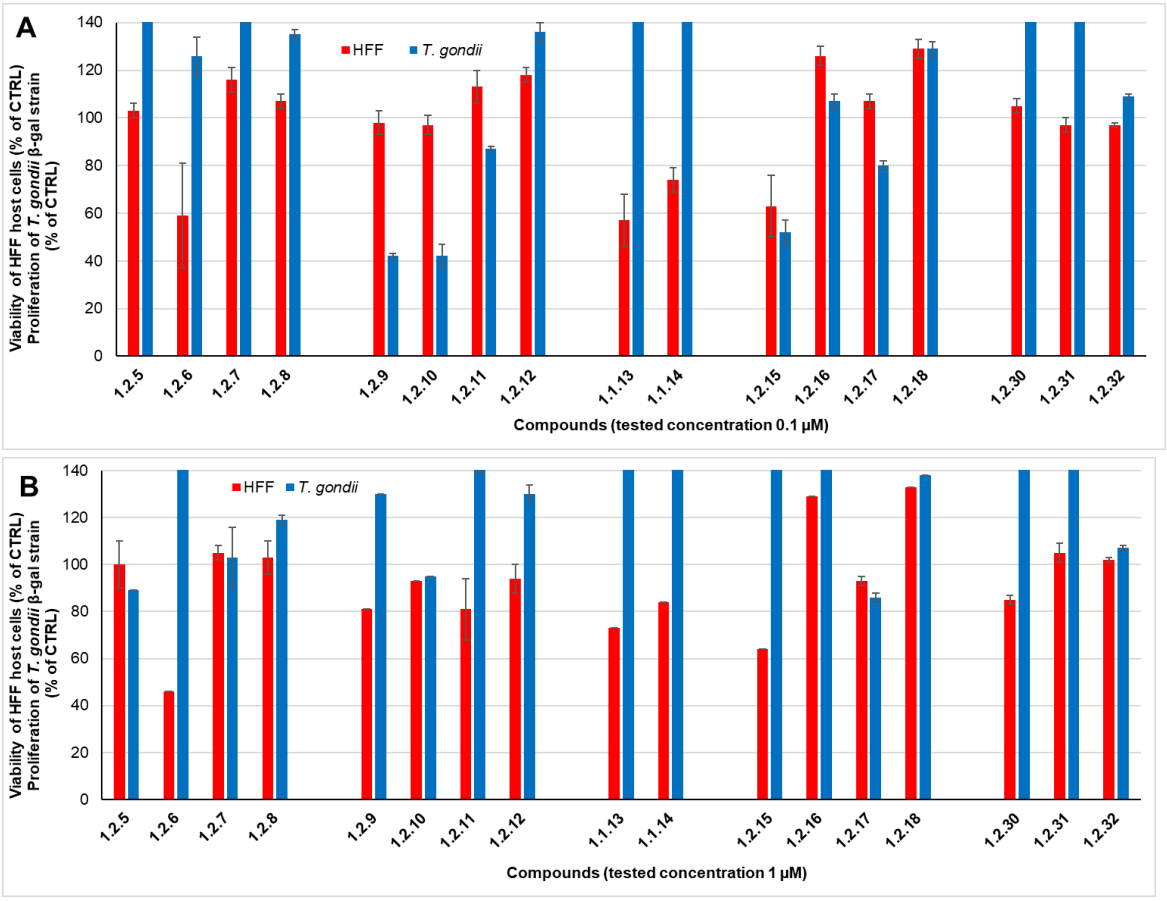

Figure S1.2.1. Clustered column chart showing the *in vitro* activities at 0.1 (A) and 1 (B) µM of the BODIPY compounds on HFF viability and *T. gondii* β-gal proliferation. Non-infected HFF monolayers treated only with 0.1% DMSO exhibited 100% viability and 100% proliferation was attributed to *T. gondii* β-gal tachyzoites treated with 0.1% DMSO only. For each assay, standard deviations were calculated from triplicates and are displayed on the graph.

1.2.2. X-ray crystallography

All measurements were made on a *RIGAKU Synergy S* area-detector diffractometer[1] using mirror optics monochromated Cu *K*α radiation (λ = 1.54184 Å). The crystals of **1.2.16** ($C_{28}H_{32}BF_2N_3O_2$) and **1.2.30** ($C_{24}H_{28}BClF_2N_2$) were mounted in air at ambient conditions.

For **1.2.16** the unit cell constants and an orientation matrix for data collection were obtained from a least-squares refinement of the setting angles of reflections in the range $3.6° < \theta < 76.3°$. A total of 5808 frames were collected using ω scans, with 0.48 and 1.93 s exposure time, a rotation angle of 0.5° per frame, a crystal-detector distance of 34.0 mm, at T = 173(2) K.

In the case of **1.2.30** the unit cell constants and an orientation matrix for data collection were obtained from a least-squares refinement of the setting angles of reflections in the range $4.1° < \theta < 76.9°$. A total of 4848 frames were collected using ω scans, with 1.6 and 6.2 s exposure time, a rotation angle of 0.5° per frame, a crystal-detector distance of 34.0 mm, at T = 173(2) K.

Data reduction was performed using the *CrysAlisPro*[111] program. The intensities were corrected for Lorentz and polarization effects, and a numerical absorption correction

based on gaussian integration over a multifaceted crystal model was applied. Data collection and refinement parameters for both **1.2.16** and **1.2.30** are given in Table S1.2.2.

The structures were solved by direct methods using *SHELXT*[113], which revealed the positions of all non-hydrogen atoms of the compounds. The non-hydrogen atoms were refined anisotropically. All H-atoms were placed in geometrically calculated positions and refined using a riding model where each H-atom was assigned a fixed isotropic displacement parameter with a value equal to $1.2U_{eq}$ of its parent atom ($1.5U_{eq}$ for the methyl groups).

In the case of **1.2.30** the isoindoline group is disordered about two sites. Its ADP's were restrained with the SHELX SIMU and RIGU instructions.

Refinement of the structures was carried out on F^2 using full-matrix least-squares procedures, which minimized the function $\Sigma w(F_o^2 - F_c^2)^2$. The weighting scheme was based on counting statistics and included a factor to downweight the intense reflections. All calculations were performed using the *SHELXL-2014/7*[114] program in OLEX2[115].

Table S1.2.2. Crystal data and structure refinement for **1.2.16** (**OD67-18**)**(19 JF004C2)** and for **1.2.30** (**OD13-19**) **(19JF004C2)**.

Compound	**1.2.16 (OD67-18) (19JF004C2)**	**1.2.30 (OD13-19) (19JF003)**
Empirical formula	$C_{28}H_{32}BF_2N_3O_2$	$C_{24}H_{28}BClF_2N_2$
Formula weight	491.37	428.74
Temperature (K)	173.01(10)	173.01(10)
Crystal system	triclinic	monoclinic
Space group	P-1	$P2_1/n$
a (Å)	9.5256(5)	11.50910(10)
b (Å)	11.5677(5)	9.24230(10)
c (Å)	12.8518(2)	20.75700(10)
α (°)	103.146(3)	90
β (°)	93.535(3)	98.8770(10)
γ (°)	113.543(5)	90
Volume ($Å^3$)	1245.65(9)	2181.49(3)
Z	2	4
ρ_{calc} (g/cm^3)	1.310	1.305
μ (mm^{-1})	0.755	1.797
F(000)	520.0	904.0
Crystal size (mm^3)	0.134 × 0.094 × 0.037	0.364 × 0.055 × 0.037
Radiation	Cu*K*α (λ = 1.54184)	Cu*K*α (λ = 1.54184)
2Θ range for data collection (°)	7.168 to 154.706	8.288 to 154.414
Index ranges	$-11 \le h \le 8$ $-14 \le k \le 14$ $-15 \le l \le 16$	$-14 \le h \le 14$ $-11 \le k \le 8$ $-26 \le l \le 26$
Reflections collected	23464	34706
Independent reflections	5110 [R_{int} = 0.0561, R_σ = 0.0364]	4557 [R_{int} = 0.0433, R_σ = 0.0199]
Data/restraints/parameters	5110/540/438	4557/0/277
Goodness-of-fit on F^2	1.070	1.048
Final R indexes [$I \ge 2\sigma$ (I)]	R_1 = 0.0446 wR_2 = 0.1228	R_1 = 0.0420 wR_2 = 0.1166
Final R indexes [all data]	R_1 = 0.0518 wR_2 = 0.1282	R_1 = 0.0446 wR_2 = 0.1187
Largest diff. peak/hole (e $Å^{-3}$)	0.27/-0.28	0.34/-0.37

In the crystal packing of **1.2.16**, the molecules are organized in dimeric head-to-tail units (Figure S1.2.2) with the BODIPY moieties parallel and close in space. These dimers further dictate network packing in zipper like antisense chains (Figure S1.2.2).

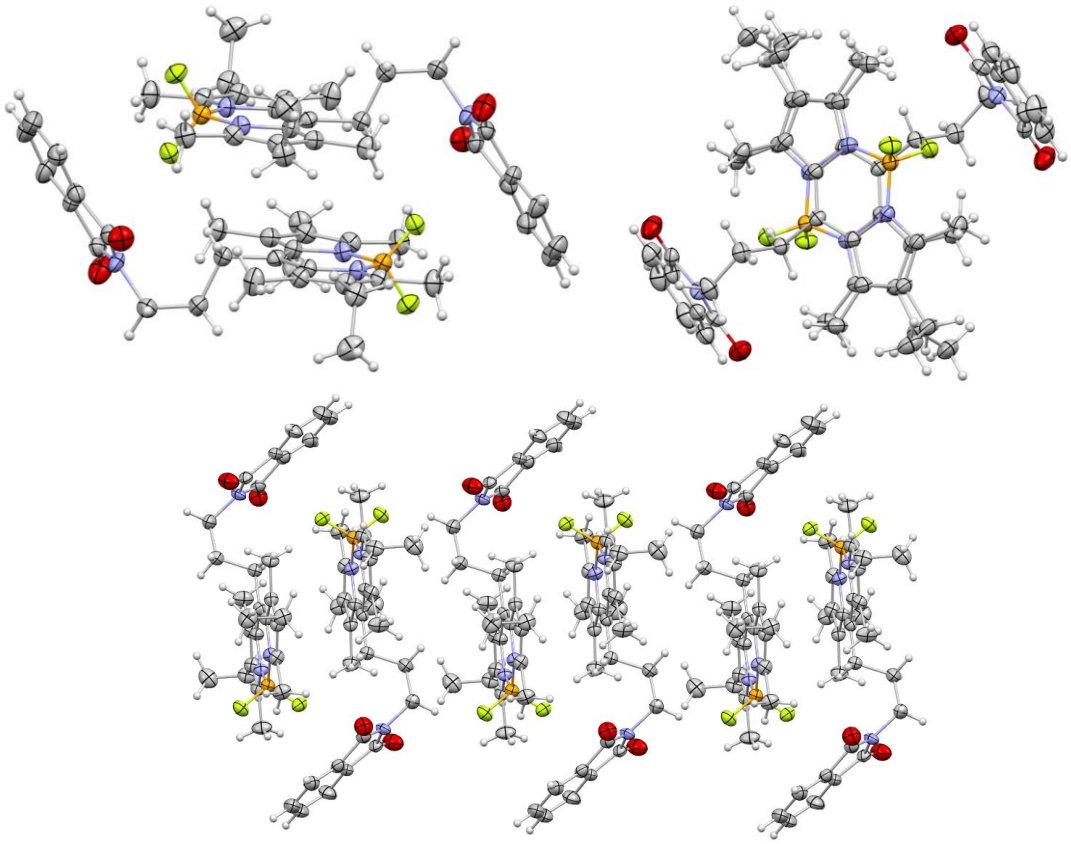

Figure S1.2.2. Packing in the crystal of **1.2.16** (images produced using Mercury CCDC 2021.2.0).

In the crystal packing of **1.2.30**, the molecules are also organized in dimeric head-to-tail units (Figures S1.2.3 and S1.2.4) but in this case the BODIPY moieties are neither parallel or close in space. In the dimers, the BODIPY of one molecule is in the neighborhood of the *meso*-aryl substituent on the other molecule, and an intermolecular H-π interaction between one H atom (H20) of the *meso*-aryl group and one of the pyrrole rings of a neighboring BODIPY molecule (distance H20 – centroid (C9C8C7C6N2 2.734 Å), Figure S1.2.4).

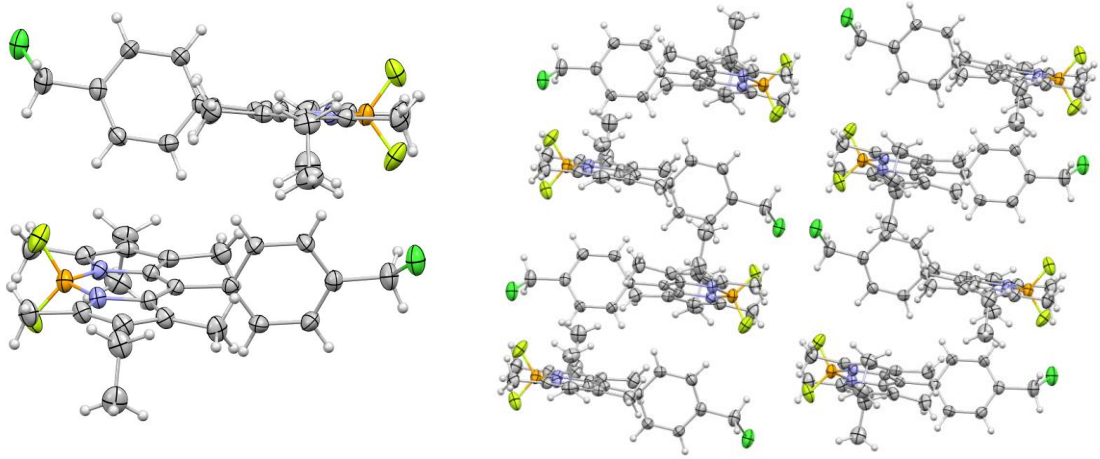

Figure S1.2.3. Packing in the crystal of **1.2.30** (images produced using Mercury CCDC 2021.2.0).

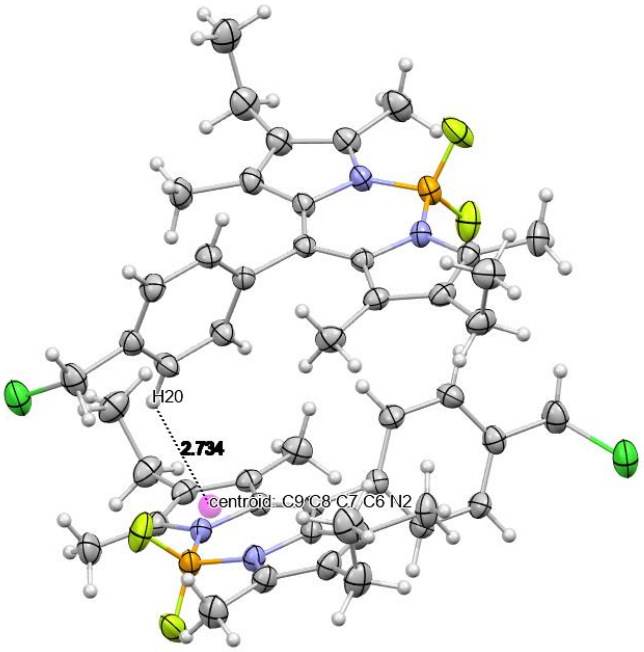

Figure S1.2.4. Intermolecular H-π interaction in the crystal of **1.2.30** (distance between the H atom and the centroid of the pyrrole unit is 2.734 Å, image produced using Mercury CCDC 2021.2.0).

1.2.3. Experimental

Chemistry[9]

General

Chemical reagents were purchased from commercial sources (Aldrich, AlfaAesar, AcrosOrganics, and TCI Chemicals) and used without further purification. The ruthenium dimer [Ru(η^6-*p*-$MeC_6H_4Pr^i$)Cl_2]$_2$ was prepared and purified according to a literature procedure[168].

The reactions were performed in dry CH_2Cl_2 (Acros Organics), collected and used under inert atmosphere (N_2), using conventional Schlenk techniques. The reactions evolution has been monitored by ^{1}H NMR ($CDCl_3$) and TLC using Merck TLC Silicagel coated aluminum sheets 60 F_{254}, using UV lamp at 254 nm for visualization, and using CH_2Cl_2/CH_3OH and EtOAc/Hex mixtures as eluent systems. Purifications were carried out by column chromatography on Silicagel (40-63 μm) using appropriate CH_2Cl_2/MeOH or EtOAc/Hex mixtures in gradient as eluent. ^{1}H (400.13 MHz), ^{13}C (100.62 MHz), spectra were recorded on a Bruker Avance II 400 spectrometer at 298 K. ^{19}F (282.40 MHz) and ^{11}B (96.29 MHz) NMR spectra were recorded on a Bruker Avance III 300 spectrometer at 298 K. The chemical shifts are reported in parts per million (ppm) and referenced to deuterated solvent residual peaks ($CDCl_3$: ^{1}H δ 7.26, ^{13}C{^{1}H} δ 77.16 ppm, MeOH: ^{1}H δ 3.31, ^{13}C{^{1}H} δ 49.00 ppm)[393] and coupling constants (*J*) are reported in Hertz (Hz). High Resolution Electrospray Ionization mass spectra (HR ESI-MS) were carried out by the Mass Spectrometry and Protein Analyses Services at DCB and were obtained on a LTQ Orbitrap XL ESI (Thermo) operated in positive-ion mode. Elemental analyses were carried out by the Mass Spectrometry and Protein Analyses Services at DCB and were obtained on a Flash 2000 Organic Elemental Analyzer (Thermo Scientific).

[9] Only syntheses of compounds obtained by the author of this thesis are presented.

Abbreviations:
$BF_3{\cdot}Et_2O$ - Boron trifluoride diethyl etherate
DDQ - 2,3-Dichloro-5,6-dicyano-*p*-benzoquinone
DIPEA - *N,N*-Diisopropylethylamine
DMAP- 4-(Dimethylamino)pyridine
DMF – dimethylformamide
EDCI -*N*-(3-Dimethylaminopropyl)-*N′*-ethylcarbodiimide hydrochloride
EtOAc - Ethyl acetate
Hex - *n*-Hexane
$HOBt{\cdot}H_2O$ -1-Hydroxybenzotriazole hydrate
TEA – Triethylamine
THF – Tetrahydrofuran
TFA – Trifluoroacetic acid.
For the NMR spectra; *Ar* – arene, *BPy* – BODIPY.

Synthesis of trithiolato dinuclear ruthenium(II)-arene intermediates 1.2.1-1.2.4
Compounds **1.2.1** ([(η^6-*p*-$MeC_6H_4Pr^i$)Ru(μ_2-$SCH_2C_6H_4$-*p*-Bu^t)Cl]$_2$), **1.2.2** ([(η^6-*p*-$MeC_6H_4Pr^i$)$_2$Ru$_2$(μ_2-$SCH_2C_6H_4$-*p*-Bu^t)$_2$(μ_2-SC_6H_4-*p*-OH)]Cl), **1.2.3** ([(η^6-*p*-$MeC_6H_4Pr^i$)$_2$Ru$_2$(μ_2-$SCH_2C_6H_4$-p-Bu^t)$_2$(μ_2-SC_6H_4-*p*-NH_2)]Cl), and **1.2.4** ([(η^6-*p*-$MeC_6H_4Pr^i$)$_2$Ru$_2$(μ_2-$SCH_2C_6H_4$-*p*-Bu^t)$_2$(μ_2-SC_6H_4-*p*-CH_2CO_2H)]Cl) have been recently reported[30, 53, 131, 394].

Synthesis of the carboxy BODIPY derivatives 1.2.9-1.2.12.
The BODIPY ester precursors were prepared and purified by adapting a literature procedure[170].

Synthesis of 4,4-difluoro-8-(3-methoxy-3-oxopropan-1-yl)-1,3,5,7-tetramethyl-2,6-diethyl-4-bora-3a,4a-diaza-*s*-indacene (1.2.5)
To a solution of 3-ethyl-2,4-dimethylpyrrole (0.600 g, 4.675 mmol, 2 equiv.) in dry CH_2Cl_2 (20 mL) at reflux under inert atmosphere (N_2) was added dropwise a solution of methyl 4-chloro-4-oxobutyrate (0.435 g, 2.805 mmol, 1.2 equiv.) in dry CH_2Cl_2 (10 mL). The reaction mixture was refluxed for further 3 h, then allowed to cool down to r.t.. DIPEA (1.7 mL, 9.350 mmol, 4 equiv.) was added and after 30 min, $BF_3{\cdot}Et_2O$ (soln. ca. 48% BF_3 in Et_2O, 1.15 mL, 9.350 mmol, 4 equiv.) was added dropwise, and after another 30 min the reaction mixture was concentrated under reduced pressure to dryness and purified by column chromatography using EtOAc/Hex to afford **1.2.5** as a pink solid (0.321 g, 0.824 mmol, yield 35%).
^{1}H-NMR ($CDCl_3$) δ_H, ppm: 3.74 (3H, s, C$\underline{H_3}$O-(C=O)-CH_2), 3.33-3.37 (2H, m, CH_3O-(C=O)-C$\underline{H_2}$-CH_2), 2.58-2.63 (2H, m, CH_3O-(C=O)-CH_2-C$\underline{H_2}$), 2.49 (6H, s, 2xBF_2-N-C-C$\underline{H_3}$), 2.40 (4H, qvart, 2xBF_2-N-C-C-C$\underline{H_2}$-CH_3, $^3J_{H,H}$ = 7.6 Hz), 2.35 (6H, s, 2xBF_2-N-C-C-C$\underline{H_3}$), 1.04 (6H, t, 2xBF_2-N-C-C-CH_2-C$\underline{H_3}$, $^3J_{H,H}$ = 7.6 Hz).
^{13}C-NMR ($CDCl_3$) δ_C, ppm: 172.5 (1C, CH_3O-($\underline{C}$=O)-CH_2), 153.1 (2C, 2xBF_2-N-$\underline{C}$-CH_3), 141.7 (2C, 2xBF_2-N-$\underline{C}$-C-CH_3), 135.8 (2C, 2xBF_2-N-C-$\underline{C}$-CH_3), 133.1 (2C, 2xBF_2-N-C-$\underline{C}$-CH_2-CH_3), 130.8 (1C, CH_3O-(C=O)-$(CH_2)_2$-$\underline{C}$), 52.2 (1C, $\underline{C}H_3$O-(C=O)-CH_2), 35.4 (1C, CH_3O-(C=O)-CH_2-$\underline{C}H_2$-CH_2), 23.8 (1C, CH_3O-(C=O)-$\underline{C}H_2$-CH_2-CH_2), 17.3 (2C, 2xBF_2-N-C-C-$\underline{C}H_2$-CH_3), 14.9 (2C, 2xBF_2-N-C-C-CH_2-$\underline{C}H_3$), 13.5 (2C, 2xBF_2-N-C-C-$\underline{C}H_3$), 12.6 (2C, t, 2xBF_2-N-C-$\underline{C}H_3$, $^3J_{C,B}$ = 3 Hz).
^{19}F-NMR ($CDCl_3$) δ_C, ppm: -145.97 (2F, m, B$\underline{F_2}$).
^{11}B-NMR ($CDCl_3$) δ_C, ppm: 0.59 (1B, t, $\underline{B}F_2$, $^1J_{B,F}$ = 32.719 Hz).
R_f (Hex/EtOAc 9:1 (v/v)) = 0.214.
ESI-MS(+): *m/z* found 371.2293 $[M-F]^+$, calcd. for $C_{21}H_{29}BFN_2O_2^+$ 371.2301.

Elemental analysis (%): calcd. for $C_{21}H_{29}BF_2N_2O_2 \cdot 0.25EtOAc$ C 64.09, H 7.58, N 6.79; found C 64.09, H 7.81, N 6.72.

Synthesis of 4,4-difluoro-8-(5-methoxy-5-oxopentan-1-yl)-1,3,5,7-tetramethyl-2,6-diethyl-4-bora-3a,4a-diaza-*s*-indacene (1.2.6)

To a solution of 3-ethyl-2,4-dimethylpyrrole (0.500 g, 3.896 mmol, 2 equiv.) in dry CH_2Cl_2 (20 mL) at reflux under inert atmosphere (N_2) was added dropwise a solution of methyl 6-chloro-6-oxohexanoate (0.431 g, 2.338 mmol, 1.2 equiv.) in dry CH_2Cl_2 (10 mL). The reaction mixture was refluxed for further 2 h, then allowed to cool down to r.t.. DIPEA (1.5 mL, 7.792 mmol, 4 equiv.) was added and after 15 min, $BF_3 \cdot Et_2O$ (soln. ca. 48% BF_3 in Et_2O, 1.00 mL, 7.792 mmol, 4 equiv.) was added dropwise and after another 15 min the reaction mixture was concentrated under reduced pressure to dryness and purified by column chromatography using EtOAc/Hex to afford **1.2.6** as a pink solid (0.423 g, 1.011 mmol, yield 52%).

^{1}H-NMR ($CDCl_3$) δ_H, ppm: 3.67 (3H, s, $C\underline{H_3}O$-(C=O)-CH_2), 2.98-3.03 (2H, m, CH_3O-(C=O)-$(CH_2)_3$-$C\underline{H_2}$), 2.49 (6H, s, 2xBF_2-N-C-$C\underline{H_3}$), 2.37-2.43 (6H, m, CH_3O-(C=O)-$C\underline{H_2}$-$(CH_2)_3$, 2xBF_2-N-C-C-$C\underline{H_2}$-CH_3, $^3J_{H,H}$ = 7.5 Hz), 2.33 (6H, s, 2xBF_2-N-C-C-C$\underline{H_3}$), 1.83 (2H, qvint, CH_3O-(C=O)-CH_2-$C\underline{H_2}$-$(CH_2)_2$), 1.62-1.71 (2H, m, CH_3O-(C=O)-$(CH_2)_2$-$C\underline{H_2}$-CH_2, $^3J_{H,H}$ = 7.4 Hz), 1.04 (6H, t, 2xBF_2-N-C-C-CH_2-$C\underline{H_3}$, $^3J_{H,H}$ = 7.5 Hz).

^{13}C-NMR ($CDCl_3$) δ_C, ppm: 173.7 (1C, CH_3O-($\underline{C}$=O)-CH_2), 152.4 (2C, 2xBF_2-N-$\underline{C}$-CH_3), 144.2 (2C, 2xBF_2-N-$\underline{C}$-C-CH_3), 135.8 (2C, 2xBF_2-N-C-$\underline{C}$-CH_3), 132.8 (2C, 2xBF_2-N-C-$\underline{C}$-CH_2-CH_3), 131.1 (1C, CH_3O-(C=O)-$(CH_2)_4$-$\underline{C}$), 51.8 (1C, $\underline{C}H_3O$-(C=O)-CH_2), 33.8 (1C, CH_3O-(C=O)-$\underline{C}H_2$-$(CH_2)_3$), 31.3 (1C, CH_3O-(C=O)-$(CH_2)_2$-$\underline{C}H_2$-CH_2), 28.3 (1C, CH_3O-(C=O)-$(CH_2)_3$-$\underline{C}H_2$), 5.4 (1C, CH_3O-(C=O)-CH_2-$\underline{C}H_2$-$(CH_2)_2$), 17.3 (2C, 2xBF_2-N-C-C-$\underline{C}H_2$-CH_3), 15.0 (2C, 2xBF_2-N-C-C-CH_2-$\underline{C}H_3$), 13.4 (2C, 2xBF_2-N-C-C-$\underline{C}H_3$), 12.6 (2C, t, 2xBF_2-N-C-$\underline{C}H_3$, $^3J_{C,B}$ = 3 Hz).

^{19}F-NMR ($CDCl_3$) δ_C, ppm: (-145.84)-(-146.22) (2F, m,B$\underline{F_2}$).

^{11}B-NMR ($CDCl_3$) δ_C, ppm: 0.60 (1B, t, $\underline{B}F_2$, $^1J_{B,F}$ = 32.8 Hz).

R_f (Hex/EtOAc 9:1 (v/v)) = 0.188.

ESI-MS(+):*m/z* found 399.2619 $[M-F]^+$, 418.2603 $[M]^+$, 441.2499 $[M+Na]^+$, calcd. for $C_{23}H_{33}BFN_2O_2^+$ 399.2614, for $C_{23}H_{33}BF_2N_2O_2$ 418.2603 and for $C_{23}H_{33}BF_2N_2O_2Na^+$ 441.2495.

Elemental analysis (%): calcd. for $C_{23}H_{33}BF_2N_2O_2 \cdot 0.1CH_3OH$ C 65.82, H 7.99, N 6.65; found C 65.83, H 8.18, N 6.53.

Synthesis of 4,4-difluoro-8-(7-methoxy-7-oxoheptan-1-yl)-1,3,5,7-tetramethyl-2,6-diethyl-4-bora-3a,4a-diaza-*s*-indacene (1.2.7)

To a solution of 3-ethyl-2,4-dimethylpyrrole (0.600 g, 4.675 mmol, 2 equiv.) in dry CH_2Cl_2 (20 mL) at reflux, under inert atmosphere (N_2) was added dropwise a solution of methyl 8-chloro-8-oxooctanoate (0.604 g, 2.805 mmol, 1.2 equiv.) in dry CH_2Cl_2 (10 mL). The reaction mixture was refluxed for further 3 h, then allowed to cool to r.t.. DIPEA (1.7 mL, 9.350 mmol, 4 equiv.) was added and after 30 min, $BF_3 \cdot Et_2O$ (soln. ca. 48% BF_3 in Et_2O, 0.920 mL, 4.872 mmol, 4 equiv.) was added dropwise. After another 30 min the reaction mixture was concentrated to dryness under reduced pressure and purification by column chromatography using EtOAc/Hex mixture afforded **1.2.7** as a pink solid (0.456 g, 1.022 mmol, yield 45%).

^{1}H-NMR ($CDCl_3$) δ_H, ppm: 3.67 (3H, s, $C\underline{H_3}O$-(C=O)-CH_2), 2.95-2-99 (2H, m, CH_3O-(C=O)-$C\underline{H_2}$-$(CH_2)_5$), 2.49 (6H, s, 2xBF_2-N-C-$C\underline{H_3}$), 2.39 (4H, qvart, 2xBF_2-N-C-C-$C\underline{H_2}$-CH_3, $^3J_{H,H}$ = 7.6 Hz), 2.32 (6H, s, 2xBF_2-N-C-C-C$\underline{H_3}$), 2.32 (2H, t, CH_3O-(C=O)-$(CH_2)_5$-$C\underline{H_2}$, $^3J_{H,H}$ = 7.5 Hz), 1.66 (2H, qvint, CH_3O-(C=O)-$(CH_2)_4$-$C\underline{H_2}$-CH_2, $^3J_{H,H}$ = 7.5 Hz), 1.60-1.65 (2H, m, CH_3O-(C=O)-CH_2-$C\underline{H_2}$-$(CH_2)_4$), 1.51 (2H, qvint, CH_3O-(C=O)-$(CH_2)_2$-$C\underline{H_2}$-$(CH_2)_3$, $^3J_{H,H}$ = 6.9 Hz), 1.36-1.45 (2H, m, CH_3O-(C=O)-$(CH_2)_3$-$C\underline{H_2}$-$(CH_2)_2$), 1.04 (6H, t, 2xBF_2-N-C-C-CH_2-$C\underline{H_3}$, $^3J_{H,H}$ = 7.6 Hz).

^{13}C-NMR ($CDCl_3$) δ_C, ppm: 174.2 (1C, CH_3O-(<u>*C*</u>=O)-CH_2), 152.2 (2C, 2xBF_2-N-<u>*C*</u>-CH_3), 144.8 (2C, 2xBF_2-N-<u>*C*</u>-C-CH_3), 135.7 (2C, 2xBF_2-N-C-<u>*C*</u>-CH_3), 132.7 (2C, 2xBF_2-N-C-<u>*C*</u>-CH_2-CH_3), 131.1 (1C, CH_3O-(C=O)-$(CH_2)_6$-<u>*C*</u>), 51.6 (1C, <u>*C*</u>H_3O-(C=O)-CH_2), 34.1 (1C, CH_3O-(C=O)-$(CH_2)_5$-<u>*C*</u>H_2), 31.8 (1C, CH_3O-(C=O)-CH_2-<u>*C*</u>H_2-$(CH_2)_4$), 30.1 (1C, CH_3O-(C=O)-$(CH_2)_2$-<u>*C*</u>H_2-$(CH_2)_3$), 29.1 (1C, CH_3O-(C=O)-$(CH_2)_3$-<u>*C*</u>H_2-$(CH_2)_2$), 28.6 (1C, CH_3O-(C=O)-<u>*C*</u>H_2-$(CH_2)_5$), 25.0 (1C, CH_3O-(C=O)-$(CH_2)_4$-<u>*C*</u>H_2-CH_2), 17.3 (2C, 2xBF_2-N-C-C-<u>*C*</u>H_2-CH_3), 14.3 (2C, 2xBF_2-N-C-C-CH_2-<u>*C*</u>H_3), 13.5 (2C, 2xBF_2-N-C-C-<u>*C*</u>H_3), 12.5 (2C, t, 2xBF_2-N-C-<u>*C*</u>H_3, $^3J_{C,B}$ = 3 Hz).
^{19}F-NMR ($CDCl_3$) δ_C, ppm: -146.03 (2F, dd, B<u>*F*</u>$_2$, $^1J_{B,F}$ = 30.9 Hz, $^2J_{F,F}$ = 34.3 Hz).
^{11}B-NMR ($CDCl_3$) δ_C, ppm: 0.61 (1B, t, <u>*B*</u>F_2, $^1J_{B,F}$ = 32.8 Hz).
R_f (Hex/EtOAc 9:1) = 0.223.
ESI-MS(+):*m/z* found 426.2849 $[M\text{-}F\text{-}H]^+$, 431.2670 $[M\text{-}CH_3]^+$, 446.2900 $[M]^+$, 469.2799 $[M+Na]^+$, calcd. for $C_{25}H_{36}BFN_2O_2^+$ 426.2848, $C_{24}H_{34}BF_2N_2O_2^+$ 431.2676, $C_{25}H_{37}BF_2N_2O_2^+$ 446.2911, $C_{25}H_{37}BF_2N_2NaO^+$ 469.2808.
Elemental analysis (%): calcd. for $C_{25}H_{37}BF_2N_2O_2$ C 67.27, H 8.36, N 6.28; found C 67.47, H 8.57, N 6.28.

Synthesis of 4,4-difluoro-8-(9-methoxy-9-oxononan-1-yl)-1,3,5,7-tetramethyl-2,6-diethyl-4-bora-3a,4a-diaza-*s*-indacene (1.2.8)
To a solution of 3-ethyl-2,4-dimethylpyrrole (1.826 g, 14.229 mmol, 2 equiv.) in dry CH_2Cl_2 (20 mL) at reflux under inert atmosphere (N_2) was added dropwise a solution of methyl 10-chloro-10-oxodecanoate (2.066 g, 8.537 mmol, 1.2 equiv.) in dry CH_2Cl_2 (10 mL). The reaction mixture was refluxed for further 4 h, then allowed to cool to r.t. DIPEA (5 mL, 28.458 mmol, 4 equiv.) was added and after 1 h, $BF_3{\cdot}Et_2O$ (soln. ca. 48% BF_3 in Et_2O, 3.5 mL, 28.458 mmol, 4 equiv.) was added dropwise. After another 1 h the reaction mixture was concentrated to dryness under reduced pressure and purification by column chromatography using EtOAc/Hex mixture afforded **1.2.8** as a pink solid (1.0739 g, 2.263 mmol, yield 32%).
^{1}H-NMR ($CDCl_3$) δ_H, ppm: 3.66 (3H, s, C<u>*H*</u>$_3$O-(C=O)-CH_2), 2.94-2.99 (2H, m, CH_3O-(C=O)-$(CH_2)_7$-C<u>*H*</u>$_2$-(*BPy*)C), 2.49 (6H, s, 2xBF_2-N-C-C<u>*H*</u>$_3$), 2.39 (4H, 2xBF_2-N-C-C-C<u>*H*</u>$_2$-CH_3, $^3J_{H,H}$ = 7.6 Hz), 2.32 (6H, s, 2xBF_2-N-C-C-C<u>*H*</u>$_3$), 2.27-2.36 (2H, m, CH_3O-(C=O)-C<u>*H*</u>$_2$-$(CH_2)_3$-(*BPy*)C), 1.55-1.67 (4H, m, CH_3O-(C=O)-CH_2-C<u>*H*</u>$_2$-$(CH_2)_6$-(*BPy*)C, CH_3O-(C=O)-$(CH_2)_6$-C<u>*H*</u>$_2$-CH_2-(*BPy*)C), 1.44-1.53 (2H, qvint, CH_3O-(C=O)-$(CH_2)_2$-C<u>*H*</u>$_2$-$(CH_2)_5$-(*BPy*)C, $^3J_{H,H}$ = 7.1 Hz), .28-1.41 (6H, m, CH_3O-(C=O)-$(CH_2)_3$-C<u>*H*</u>$_2$-$(CH_2)_4$-(*BPy*)C, CH_3O-(C=O)-$(CH_2)_4$-C<u>*H*</u>$_2$-$(CH_2)_3$-(*BPy*)C, CH_3O-(C=O)-$(CH_2)_5$-C<u>*H*</u>$_2$-$(CH_2)_2$-(*BPy*)C), 1.04 (6H, t, 2xBF_2-N-C-C-CH_2-C<u>*H*</u>$_3$, $^3J_{H,H}$ = 7.6 Hz).
^{13}C-NMR ($CDCl_3$) δ_C, ppm: 174.4 (1C, CH_3O-(<u>*C*</u>=O)-CH_2), 152.1 (2C, 2xBF_2-N-<u>*C*</u>-CH_3), 145.0 (2C, 2xBF_2-N-<u>*C*</u>-C-CH_3), 135.8 (2C, 2xBF_2-N-C-<u>*C*</u>-CH_3), 132.6 (2C, 2xBF_2-N-C-<u>*C*</u>-CH_2-CH_3), 131.1 (1C, CH_3O-(C=O)-$(CH_2)_8$-(*BPy*)<u>*C*</u>), 51.6 (1C, <u>*C*</u>H_3O-(C=O)-CH_2), 34.2 (1C, CH_3O-(C=O)-<u>*C*</u>H_2-$(CH_2)_7$-(*BPy*)C), 31.9 (1C, CH_3O-(C=O)-$(CH_2)_6$-<u>*C*</u>H_2-CH_2-(*BPy*)C), 30.4 (1C, CH_3O-(C=O)-$(CH_2)_2$-<u>*C*</u>H_2-$(CH_2)_5$-(*BPy*)C), 29.38 (1C, CH_3O-(C=O)-$(CH_2)_3$-<u>*C*</u>H_2-$(CH_2)_4$-(*BPy*)C), 29.35 (1C, CH_3O-(C=O)-$(CH_2)_4$-<u>*C*</u>H_2-$(CH_2)_3$-(*BPy*)C), 29.2 (1C, CH_3O-(C=O)-$(CH_2)_5$-<u>*C*</u>H_2-$(CH_2)_2$-(*BPy*)C), 28.7 (1C, CH_3O-(C=O)-$(CH_2)_7$-<u>*C*</u>H_2-(*BPy*)C), 25.0 (1C, CH_3O-(C=O)-CH_2-<u>*C*</u>H_2-$(CH_2)_6$-(*BPy*)C), 17.3 (2C, 2xBF_2-N-C-C-<u>*C*</u>H_2-CH_3), 15.0 (2C, 2xBF_2-N-C-C-CH_2-<u>*C*</u>H_3), 13.5 (2C, 2xBF_2-N-C-C-<u>*C*</u>H_3), 12.5 (2C, t, 2xBF_2-N-C-<u>*C*</u>H_3, $^3J_{C,B}$ = 3 Hz).
^{19}F-NMR ($CDCl_3$) δ_C, ppm:(-145.86)-(-146.21) (2F, m,B<u>*F*</u>$_2$, $^1J_{F,B}$ = 30.6 Hz).
^{11}B-NMR ($CDCl_3$) δ_C, ppm:0.62 (1B, t, <u>*B*</u>F_2, $^1J_{B,F}$ = 32.8 Hz).
R_f (Hex/EtOAc 9:1) = 0.400.
ESI-MS(+): *m/z* found 455.3237 $[M\text{-}F]^+$, calcd. for $C_{27}H_{41}BFN_2O_2^+$ 455.3240.
Elemental analysis (%): calcd. for $C_{27}H_{41}BF_2N_2O_2$ C 68.35, H 8.71, N 5.90; found C 68.20, H 8.96, N 5.49.

The carboxy BODIPY derivatives **1.2.9**-**1.2.12** were prepared and purified by adapting literature procedures[171-173].

Synthesis of 4,4-difluoro-8-(2-carboxyethan-1-yl)-1,3,5,7-tetramethyl-2,6-diethyl-4-bora-3a,4a-diaza-*s*-indacene (1.2.9)

To a solution of **1.2.5** (0.812 g, 2.081 mmol, 1 equiv.) in THF (10 mL) at 0°C and under inert atmosphere (N_2) was added solution of aqueous 0.1 N KOH/Pr^{i}OH 2:5 (v/v) (116 mL, 3.330 mmol KOH, 1.6 equiv.). After 2 h, the reaction evolution was verified by TLC (CH_2Cl_2/CH_3OH 10:0.5 (v/v)), the reaction mixture was neutralized by dropwise addition of 0.1 N aqueous HCl and concentrated to dryness. The residue was solubilized in EtOAc (50 mL), and the organic solution was dried over anhydrous Na_2SO_4, filtered and concentrated to dryness. Purification by column chromatography using CH_2Cl_2/CH_3OH afforded **1.2.9** as a pink solid (0.356 g, 0.946 mmol, yield 45%).

^{1}H-NMR (MeOD-*d*$_4$) δ_C, ppm: 3.36-3.41 (2H, m, HO-(C=O)-C$\underline{H_2}$-CH_2), 2.50-2.55 (2H, m, HO-(C=O)-CH_2-C$\underline{H_2}$), 2.44 (4H, qvart, 2xBF_2-N-C-C-C$\underline{H_2}$-CH_3, $^3J_{H,H}$ = 7.5 Hz), 2.43 (6H, s, 2xBF_2-N-C-C$\underline{H_3}$), 2.42 (6H, s, 2xBF_2-N-C-C-C$\underline{H_3}$), 1.06 (6H, t, 2xBF_2-N-C-C-CH_2-C$\underline{H_3}$, $^3J_{H,H}$ = 7.5 Hz).

^{13}C-NMR (MeOD-*d*$_4$) δ_C, ppm: 181.0 (1C, HO-($\underline{C}$=O)-CH_2), 153.4 (2C, 2xBF_2-N-$\underline{C}$-CH_3), 145.3 (2C, 2xBF_2-N-$\underline{C}$-C-CH_3), 137.3 (2C, 2xBF_2-N-C-$\underline{C}$-CH_3), 134.0 (2C, 2xBF_2-N-C-$\underline{C}$-CH_2-CH_3), 132.0 (1C, HO-(C=O)-$(CH_2)_2$-$\underline{C}$), 38.7 (1C, HO-(C=O)-CH_2-C$\underline{H_2}$), 25.7 (1C, HO-(C=O)-$\underline{C}H_2$-CH_2), 17.9 (2C, 2xBF_2-N-C-C-$\underline{C}H_2$-CH_3), 15.2 (2C, 2xBF_2-N-C-C-CH_2-$\underline{C}H_3$), 13.7 (2C, 2xBF_2-N-C-C-$\underline{C}H_3$), 12.5 (2C, m, 2xBF_2-N-C-$\underline{C}H_3$).

^{19}F-NMR (MeOD-*d*$_4$) δ_C, ppm: -146.54 (2F, dd, B$\underline{F_2}$, $^1J_{B,F}$ = 24.7/31.3 Hz, $^2J_{F,F}$ = 34.5 Hz).

^{11}B-NMR (MeOD-*d*$_4$) δ_C, ppm: 0.54 (1B, t, $\underline{B}F_2$, $^1J_{B,F}$ = 32.1 Hz).

R_f (CH_2Cl_2/CH_3OH 10:1) = 0.611.

ESI-MS(+): *m/z* found 357.2165 $[M-F]^+$, 376.2148 $[M]^+$, 415.1698 $[M+K]^+$, calcd. for $C_{20}H_{27}BFN_2O_2^+$ 357.2144, $C_{20}H_{27}BF_2N_2O_2^+$ 376.2134 and $C_{20}H_{27}BF_2KN_2O_2^+$ 415.1765.

Elemental analysis (%): calcd. for $C_{20}H_{27}BF_2N_2O_2 \cdot 4.2CH_2Cl_2 \cdot 8H_2O$ C 33.14, H 5.91, N 3.19; found C 33.15, H 5.95, N 3.70.

Synthesis of 4,4-difluoro-8-(4-carboxybutan-1-yl)-1,3,5,7-tetramethyl-2,6-diethyl-4-bora-3a,4a-diaza-*s*-indacene (1.2.10)

To a solution of **1.2.6** (0.306 g, 0.732 mmol, 1equiv.) in THF (10 mL) at 0°C and under inert atmosphere (N_2) was added solution of aqueous 0.1 N KOH-Pr^{i}OH 2:5 (v/v) (53 mL, 1.464 mmol KOH, 2 equiv.). After 2 h and the reaction evolution was verified by TLC (CH_2Cl_2/CH_3OH 10:0.5 (v/v)), the reaction mixture was neutralized by dropwise addition of 0.1 N aqueous HCl and evaporated to dryness. The residue was solubilized in EtOAc (20 mL), and the organic solution was dried over anhydrous Na_2SO_4, filtered and concentrated to dryness under reduced pressure. Purification by column chromatography using CH_2Cl_2/CH_3OH afforded **1.2.10** as a pink solid (0.144 g, 0.355 mmol, yield 49%).

^{1}H-NMR ($CDCl_3$) δ_C, ppm: 2.92-2.97 (2H, m, HO-(C=O)-$(CH_2)_3$-C$\underline{H_2}$), 2.40 (6H, s, 2xBF_2-N-C-C$\underline{H_3}$), 2.31 (4H, qvart, 2xBF_2-N-C-C-C$\underline{H_2}$-CH_3, $^3J_{H,H}$ = 7.5 Hz), 2.27 (6H, s, 2xBF_2-N-C-C-C$\underline{H_3}$), 2.24-2.29 (2H, m, HO-(C=O)-C$\underline{H_2}$-$(CH_2)_3$), 1.73 (2H, qvint, HO-(C=O)-CH_2-C$\underline{H_2}$-$(CH_2)_2$), $^3J_{H,H}$ = 7.4 Hz), 1.53-1.64 (2H, m, HO-(C=O)-$(CH_2)_2$-C$\underline{H_2}$-CH_2), 0.96 (6H, t, 2xBF_2-N-C-C-CH_2-C$\underline{H_3}$, $^3J_{H,H}$ = 7.5 Hz).

^{13}C-NMR ($CDCl_3$) δ_C, ppm: 180.9 (1C, HO-($\underline{C}$=O)-CH_2), 152.1 (2C, 2xBF_2-N-$\underline{C}$-CH_3), 144.5 (2C, 2xBF_2-N-$\underline{C}$-C-CH_3), 135.8 (2C, 2xBF_2-N-C-$\underline{C}$-CH_3), 132.7 (2C, 2xBF_2-N-C-$\underline{C}$-CH_2-CH_3), 130.9 (1C, HO-(C=O)-$(CH_2)_4$-$\underline{C}$), 35.7 (1C, HO-(C=O)-$\underline{C}H_2$-$(CH_2)_3$), 31.5 (1C, HO-(C=O)-$(CH_2)_2$-$\underline{C}H_2$-

CH_2), 28.2 (1C, HO-(C=O)-$(CH_2)_3$-C$\underline{H_2}$), 26.0 (1C, HO-(C=O)-CH_2-$\underline{C}H_2$-$(CH_2)_2$), 17.1 (2C, 2xBF_2-N-C-C-$\underline{C}H_2$-CH_3), 14.7 (2C, 2xBF_2-N-C-C-CH_2-$\underline{C}H_3$), 13.3 (2C, 2xBF_2-N-C-C-$\underline{C}H_3$), 12.3 (2C, m, 2xBF_2-N-C-$\underline{C}H_3$).

^{19}F-NMR (MeOD-*d*$_4$) δ_C, ppm:(-145.80)-(-146.09) (2F, m, B$\underline{F_2}$).

^{11}B-NMR (MeOD-*d*$_4$) δ_C, ppm: 0.55 (1B, t, $\underline{B}F_2$, $^1J_{B,F}$ = 32.2 Hz).

ESI-MS(+): *m/z* found 385.2450 $[M-F]^+$, 404.2430 $[M]^+$, 427.2327 $[M+Na]^+$, 443.1978 $[M+K]^+$, calcd. for $C_{22}H_{31}BFN_2O_2^+$ 385.2463, $C_{22}H_{31}BF_2N_2O_2$ 404.2447, $C_{22}H_{31}BF_2N_2NaO_2^+$ 427.2344 and $C_{22}H_{31}BF_2KN_2O_2^+$ 443.2084.

Elemental analysis (%): calcd. for $C_{22}H_{31}BF_2N_2O_2 \cdot 37.5H_2O$ C 24.47, H 9.89, N 2.59; found C 24.57, H 9.51, N 2.53.

Synthesis of 4,4-difluoro-8-(6-carboxyhexan-1-yl)-1,3,5,7-tetramethyl-2,6-diethyl-4-bora-3a,4a-diaza-*s*-indacene (1.2.11)

To a solution of **1.2.7** (0.229 g, 0.513 mmol, 1 equiv.) in THF (10 mL) at 0°C under inert atmosphere (N_2) was added solution of aqueous 0.1 N KOH-Pr^{i}OH 2:5 (v/v) (28 mL, 0.821 mmol KOH, 1.6 equiv.). After 2h, and the reaction evolution was verified by TLC (CH_2Cl_2/CH_3OH 10:0.5 (v/v)), then the reaction mixture was neutralized by dropwise addition of 0.1 N aqueous HCl and was evaporated to dryness. The residue was solubilized in EtOAc (20 mL), and the organic solution was dried over anhydrous Na_2SO_4, filtered and concentrated to dryness under reduced pressure. Purification by column chromatography using CH_2Cl_2/CH_3OH afforded **1.2.11** as a pink solid (0.101 g, 0.234 mmol, yield 45%).

^{1}H-NMR (MeOD-*d*$_4$) δ_H, ppm: 3.02-3.06 (2H, m, HO-(C=O)-C$\underline{H_2}$-$(CH_2)_5$), 2.45 (4H, qvart, 2xBF_2-N-C-C-C$\underline{H_2}$-CH_3, $^3J_{H,H}$ = 7.6 Hz), 2.43 (6H, s, 2xBF_2-N-C-C$\underline{H_3}$), 2.37 (6H, s, 2xBF_2-N-C-C-C$\underline{H_3}$), 2.31 (2H, t, HO-(C=O)-$(CH_2)_5$-C$\underline{H_2}$, $^3J_{H,H}$ = 7.3 Hz), 1.65 (2H, qvint, HO-(C=O)-$(CH_2)_4$-C$\underline{H_2}$-CH_2, $^3J_{H,H}$ = 7.3 Hz), 1.63 (2H, qvint, HO-(C=O)-CH_2-C$\underline{H_2}$-$(CH_2)_4$, $^3J_{H,H}$ = 7.5 Hz), 1.56 (2H, qvint, HO-(C=O)-$(CH_2)_2$-C$\underline{H_2}$-$(CH_2)_3$, $^3J_{H,H}$ = 7.4 Hz), 1.41-1.51 (2H, m, HO-(C=O)-$(CH_2)_3$-C$\underline{H_2}$-$(CH_2)_2$), 1.06 (6H, t, 2xBF_2-N-C-C-CH_2-C$\underline{H_3}$, $^3J_{H,H}$ = 7.6 Hz).

^{13}C-NMR (MeOD-*d*$_4$) δ_C, ppm: 177.5 (1C, HO-($\underline{C}$=O)-CH_2), 153.0 (2C, 2xBF_2-N-$\underline{C}$-CH_3), 146.7 (2C, 2xBF_2-N-$\underline{C}$-C-CH_3), 137.3 (2C, 2xBF_2-N-C-$\underline{C}$-CH_3), 133.8 (2C, 2xBF_2-N-C-$\underline{C}$-CH_2-CH_3), 132.1 (1C, HO-(C=O)-$(CH_2)_6$-$\underline{C}$), 34.8 (1C, HO-(C=O)-$(CH_2)_5$-CH_2), 32.9 (1C, HO-(C=O)-CH_2-$\underline{C}H_2$-$(CH_2)_4$), 30.9 (1C, HO-(C=O)-$(CH_2)_2$-$\underline{C}H_2$-$(CH_2)_3$), 29.9 (1C, HO-(C=O)-$(CH_2)_3$-$\underline{C}H_2$-$(CH_2)_2$), 29.4 (1C, HO-(C=O)-$\underline{C}H_2$-$(CH_2)_5$), 26.0 (1C, HO-(C=O)-$(CH_2)_4$-$\underline{C}H_2$-CH_2), 17.9 (2C, 2xBF_2-N-C-C-$\underline{C}H_2$-CH_3), 15.2 (2C, 2xBF_2-N-C-C-CH_2-$\underline{C}H_3$), 13.6 (2C, 2xBF_2-N-C-C-$\underline{C}H_3$), 12.4 (2C, t, 2xBF_2-N-C-$\underline{C}H_3$, $^3J_{C,B}$ = 3 Hz).

^{19}F-NMR (MeOD-*d*$_4$) δ_C, ppm: -146.55 (2F, dd, B$\underline{F_2}$, $^1J_{B,F}$ = 25.0/31.6 Hz, $^2J_{F,F}$ = 34.6 Hz).

^{11}B-NMR (MeOD-*d*$_4$) δ_C, ppm: 0.56 (1B, t, $\underline{B}F_2$, $^1J_{B,F}$ = 32.2 Hz).

R$_f$ (CH_2Cl_2/CH_3OH 10:1) = 0.694.

ESI-MS(+): *m/z* found 413.2785 $[M-F]^+$, 432.2766 $[M]^+$, 455.2656 $[M+Na]^+$, calcd. for $C_{24}H_{35}BFN_2O_2^+$ 413.2770, for $C_{24}H_{35}BF_2N_2O_2^+$ 432.2754 and for $C_{24}H_{35}BF_2N_2NaO_2^+$ 455.2652.

Elemental analysis (%): calcd. for $C_{24}H_{35}BF_2N_2O_2 \cdot 0.2CH_2Cl_2 \cdot 0.8CH_3OH$ C 63.22, H 8.19, N 5.90; found C 63.30, H 8.21, N 5.97.

Synthesis of 4,4-difluoro-8-(8-carboxyoctan-1-yl)-1,3,5,7-tetramethyl-2,6-diethyl-4-bora-3a,4a-diaza-*s*-indacene (1.2.12)

To a solution of **1.2.8** (1.000 g, 2.1077 mmol, 1 equiv.) in THF (30 mL) at 0°C under inert atmosphere (N_2) was added solution of aqueous 0.1 N KOH-Pr^{i}OH 2:5 (v/v) (119 mL, 3.372 mmol KOH, 1.6 equiv.). After 24h and the reaction evolution was verified by TLC (CH_2Cl_2/CH_3OH 10:0.5 (v/v)), then the reaction mixture was neutralized by dropwise addition of 0.1 N aqueous HCl

and evaporated to dryness. The residue was solubilized in EtOAc (50 mL), and the organic solution was dried over anhydrous Na_2SO_4, filtered and concentrated to dryness under reduced pressure. Purification by column chromatography using CH_2Cl_2/CH_3OH mixture afforded **1.2.12** as a pink solid (1.3113 g, 2.848 mmol, quant.).

^{1}H-NMR ($CDCl_3$) δ_H, ppm: 2.93-2.97 (2H, m, HO-(C=O)-$(CH_2)_7$-C$\underline{H_2}$-(*BPy*)C), 2.47 (6H, s, 2xBF_2-N-C-C$\underline{H_3}$), 2.38 (4H, 2xBF_2-N-C-C-C$\underline{H_2}$-CH_3, $^3J_{H,H}$ = 7.6 Hz), 2.30 (6H, s, 2xBF_2-N-C-C-C$\underline{H_3}$), 2.28-2.34 (2H, m, HO-(C=O)-C$\underline{H_2}$-$(CH_2)_3$-(*BPy*)C), 1.55-1.66 (4H, m, HO-(C=O)-CH_2-C$\underline{H_2}$-$(CH_2)_6$-(*BPy*)C, CH_3O-(C=O)-$(CH_2)_6$-C$\underline{H_2}$-CH_2-(*BPy*)C), 1.41-1.51 (2H, m, HO-(C=O)-$(CH_2)_2$-C$\underline{H_2}$-$(CH_2)_5$-(*BPy*)C, $^3J_{H,H}$ = 6.4 Hz), 1.24-1.38 (6H, m, HO-(C=O)-$(CH_2)_3$-C$\underline{H_2}$-$(CH_2)_4$-(*BPy*)C, HO-(C=O)-$(CH_2)_4$-C$\underline{H_2}$-$(CH_2)_3$-(*BPy*)C, HO-(C=O)-$(CH_2)_5$-C$\underline{H_2}$-$(CH_2)_2$-(*BPy*)C), 1.02 (6H, t, 2xBF_2-N-C-C-CH_2-C$\underline{H_3}$, $^3J_{H,H}$ = 7.6 Hz).

^{13}C-NMR ($CDCl_3$) δ_C, ppm: 174.2 (1C, HO-(C$\underline{}$=O)-CH_2), 152.2 (2C, 2xBF_2-N-C$\underline{}$-CH_3), 144.9 (2C, 2xBF_2-N-C$\underline{}$-C-CH_3), 135.7 (2C, 2xBF_2-N-C-C$\underline{}$-CH_3), 132.7 (2C, 2xBF_2-N-C-C$\underline{}$-CH_2-CH_3), 131.0 (1C, HO-(C=O)-$(CH_2)_8$-(*BPy*)C$\underline{}$), 34.7 (1C, HO-(C=O)-C$\underline{}$$H_2$-$(CH_2)_7$-(*BPy*)C), 32.0 (1C, HO-(C=O)-$(CH_2)_6$-C$\underline{}$$H_2$-$CH_2$-(*BPy*)C), 30.4 (1C, HO-(C=O)-$(CH_2)_2$-C$\underline{}$$H_2$-$(CH_2)_5$-(*BPy*)C), 29.3 (2C, HO-(C=O)-$(CH_2)_3$-C$\underline{}$$H_2$-$(CH_2)_4$-(*BPy*)C, HO-(C=O)-$(CH_2)_4$-C$\underline{}$$H_2$-$(CH_2)_3$-(*BPy*)C), 29.2 (1C, HO-(C=O)-$(CH_2)_5$-C$\underline{}$$H_2$-$(CH_2)_2$-(*BPy*)C), 28.6 (1C, HO-(C=O)-$(CH_2)_7$-C$\underline{}$$H_2$-(*BPy*)C), 25.0 (1C, HO-(C=O)-CH_2-C$\underline{}$$H_2$-$(CH_2)_6$-(*BPy*)C), 17.3 (2C, 2xBF_2-N-C-C-C$\underline{}$$H_2$-$CH_3$), 15.0 (2C, 2xB$F_2$-N-C-C-$CH_2$-C$\underline{}$$H_3$), 13.4 (2C, 2xB$F_2$-N-C-C-C$\underline{}$$H_3$), 12.5 (2C, t, 2xB$F_2$-N-C-C$\underline{}$$H_3$, $^3J_{C,B}$ = 2 Hz).

^{19}F-NMR ($CDCl_3$) δ_C, ppm:(-145.86)-(-146.21) (2F, m, B$\underline{F_2}$, $^1J_{F,B}$ = 30.6 Hz).

^{11}B-NMR ($CDCl_3$) δ_C, ppm:0.62 (1B, t, B$\underline{}$$F_2$, $^1J_{B,F}$ = 32.8 Hz).

R_f (CH_2Cl_2/CH_3OH 10:1) = 0.533.

ESI-MS(+): *m/z* found 441.3070 $[M-F]^+$, 460.3051 $[M]^+$, 499.2598 $[M+K]^+$, calcd. for $C_{26}H_{39}BFN_2O_2^+$ 441.3083, for $C_{26}H_{39}BF_2N_2O_2^+$ 460.3067 and for $C_{26}H_{39}BF_2N_2KO_2^+$ 499.2704.

Elemental analysis (%): calcd. for $C_{26}H_{39}BF_2N_3O_2 \cdot 2CH_3OH \cdot 0.25CH_2Cl_2$ C 62.18, H 8.77, N 5.13; found C 62.09, H 8.35, N 5.07.

Synthesis of the BODIPY derivatives containing a hydroxy group 1.2.14 and an amino group 1.2.17 and 1.2.18.

Synthesis of 4,4-difluoro-8-((acetoxymethyl)-1,3,5,7-tetramethyl-2,6-diethyl-4-bora-3a,4a-diaza-*s*-indacene (1.2.13)

To a solution of 3-ethyl-2,4-dimethylpyrrole (0.800 g, 6.234 mmol, 2 equiv.) in dry CH_2Cl_2 (20 mL) at reflux under inert atmosphere (N_2) was added dropwise a solution of 2-chloro-2-oxoethyl acetate (0.527 g, 3.740 mmol, 1.2 equiv.) in dry CH_2Cl_2 (10 mL). The reaction mixture was refluxed for further 3 h, then allowed to cool down to r.t.. DIPEA (2.25 mL, 12.468 mmol, 4 equiv.) was added to the reaction mixture and after 30 min, $BF_3 \cdot Et_2O$ (soln. ca. 48% BF_3 in Et_2O, 1.5 mL, 12.468 mmol, 4 equiv.) was added dropwise and after another 30 min the reaction mixture was concentrated to dryness and purification by column chromatography using EtOAc/Hex mixture afforded **1.2.13** as a pink solid (0.413 g, 1.098 mmol, yield 35%).

^{1}H-NMR ($CDCl_3$) δ_H, ppm: 2.50 (6H, s, 2xBF_2-N-C-C$\underline{H_3}$), 2.38 (4H, qvart, 2xBF_2-N-C-C-C$\underline{H_2}$-CH_3, $^3J_{H,H}$ = 7.6 Hz), 2.25 (6H, s, 2xBF_2-N-C-C-C$\underline{H_3}$), 2.13 (3H, s, C$\underline{H_3}$-(C=O)-O-CH_2), 1.25 (3H, s, CH_3-(C=O)-O-C$\underline{H_2}$), 1.04 (6H, t, 2xBF_2-N-C-C-CH_2-C$\underline{H_3}$, $^3J_{H,H}$ = 7.6 Hz).

^{13}C-NMR ($CDCl_3$) δ_C, ppm: 170.8 (1C, CH_3-(C$\underline{}$=O)-O-CH_2), 155.2 (2C, 2xBF_2-N-C$\underline{}$-CH_3), 136.7 (2C, 2xBF_2-N-C-C$\underline{}$-CH_3), 133.7 (2C, 2xBF_2-N-C-C$\underline{}$-CH_2-CH_3), 132.4 (2C, 2xBF_2-N-C$\underline{}$-C-CH_3), 131.7 (1C, CH_3-(C=O)-O-CH_2-C$\underline{}$), 29.8 (1C, CH_3-(C=O)-O-C$\underline{H_2}$), 20.7 (1C, C$\underline{}$$H_3$-(C=O)-O-$CH_2$), 17.3 (2C, 2xB$F_2$-N-C-C-C$\underline{}$$H_2$-$CH_3$), 14.8 (2C, 2xB$F_2$-N-C-C-$CH_2$-C$\underline{}$$H_3$), 12.8 (2C, m, 2xB$F_2$-N-C-C$\underline{}$$H_3$), 12.7 (2C, 2xB$F_2$-N-C-C-C$\underline{}$$H_3$).

^{19}F-NMR ($CDCl_3$) δ_C, ppm: -145.74 (2F, dd, B$\underline{F_2}$, $^1J_{B,F}$ = 32.6 Hz, $^2J_{F,F}$ = 33.1 Hz).
^{11}B-NMR ($CDCl_3$) δ_C, ppm: 0.59 (1B, t, $\underline{B}F_2$, $^1J_{B,F}$= 32.6 Hz).
R_f (Hex/EtOAc 9:1) = 0.241.
ESI-MS(+):*m/z* found 357.2150 $[M-F]^+$, 377.2212 $[M+H]^+$, 399.2030 $[M+Na]^+$, calcd. for $C_{20}H_{27}BFN_2O_2^+$ 357.2144, for $C_{20}H_{28}BF_2N_2O_2^+$ 377.2206 and for $C_{20}H_{27}BF_2N_2NaO_2^+$ 399.2026.
Elemental analysis (%): calcd. for $C_{20}H_{27}BF_2N_2O_2 \cdot 0.35$EtOAc C 63.14, H 7.38, N 6.88; found C 63.11, H 7.43, N 6.88.

Synthesis of 4,4-difluoro-8-(hydroxymethyl)-1,3,5,7-tetramethyl-2,6-diethyl-4-bora-3a,4a-diaza-*s*-indacene (1.2.14)
The BODIPY alcohol derivative **1.2.14** was prepared and purified by adapting a literature procedure[170]. To a solution of ester **1.2.13** (0.400 g, 1.063 mmol, 1 equiv.) in THF (22 mL) at r.t. under inert atmosphere (N_2) was added a solution of $LiOH \cdot H_2O$ (0.134 g. 3.189 mmol, 3 equiv.) in H_2O (22 mL). The reaction mixture was stirred for further 6 h and then the reaction mixture was extracted with EtOAc (3x100 mL). The combined organic layers were washed successively with saturated NH_4Cl aq. solution (3x100 mL) and brine (1×100 mL), dried over anhydrous Na_2SO_4, filtered and concentrated to dryness. Purification by column chromatography using EtOAc/Hex afforded **1.2.14** as a pink solid (0.153 g, 0.457 mmol, yield 43%).
^{1}H-NMR ($CDCl_3$) δ_H, ppm: 4.93 (3H, d, HO-C$\underline{H_2}$-C, $^3J_{H,H}$ = 5.4 Hz), 2.49 (6H, s, 2xBF_2-N-C-C$\underline{H_3}$), 2.42 (6H, s, 2xBF_2-N-C-C-C$\underline{H_3}$), 2.40 (4H, qvart, 2xBF_2-N-C-C-C$\underline{H_2}$-CH_3, $^3J_{H,H}$ = 7.6 Hz), 1.05 (6H, t, 2xBF_2-N-C-C-CH_2-C$\underline{H_3}$, $^3J_{H,H}$ = 7.6 Hz).
^{13}C-NMR ($CDCl_3$) δ_C, ppm: 154.8 (2C, 2xBF_2-N-$\underline{C}$-CH_3), 136.6 (2C, 2xBF_2-N-C-$\underline{C}$-CH_3), 136.5 (1C, HO-CH_2-$\underline{C}$), 133.5 (2C, 2xBF_2-N-C-$\underline{C}$-CH_2-CH_3), 131.7 (2C, 2xBF_2-N-$\underline{C}$-C-CH_3), 56.4 (1C, HO-C$\underline{H_2}$-C), 17.3 (2C, 2xBF_2-N-C-C-$\underline{C}H_2$-CH_3), 14.9 (2C, 2xBF_2-N-C-C-CH_2-$\underline{C}H_3$), 12.8 (4C, m, 2xBF_2-N-C-$\underline{C}$H3, 2xBF2-N-C-C-$\underline{C}H_3$).
^{19}F-NMR ($CDCl_3$) δ_C, ppm: -145.97 (2F, dd, B$\underline{F_2}$, $^1J_{B,F}$ = 32.8 Hz, $^2J_{F,F}$ = 33.5 Hz).
^{11}B-NMR ($CDCl_3$) δ_C, ppm: 0.60 (1B, t, $\underline{B}F_2$, $^1J_{B,F}$ = 32.7 Hz).
R_f (EtOAc/Hex 9:1) = 0.089.
ESI-MS(-):*m/z* found 333.1974 $[M-H]^-$, calcd. for $C_{18}H_{24}BF_2N_2O^-$ 333.1950.
ESI-MS(+):*m/z* foundfor 315.2036 $[M-F]^+$, 334.2021 $[M]^+$, 337.2339 $[M-F+Na]^+$, 357.1912 $[M+Na]^+$, calcd. for $C_{18}H_{25}BFN_2O^+$ 315.2038, for $C_{18}H_{25}BF_2N_2O^+$ 334.2023, for $C_{18}H_{25}BFN_2NaO^+$ 338.1936, and for $C_{18}H_{25}BF_2N_2NaO^+$ 357.1920.
Elemental analysis (%): calcd. for $C_{18}H_{25}BF_2N_2O \cdot 0.25Hex\cdot 0.25$EtOAc C 65.18, H 8.14, N 7.42; foundC 65.25, H 8.14, N, 7.40.

Synthesis of 4,4-difluoro-8-(2-methylene-1,3-dioxoisoindolin)-1,3,5,7-tetramethyl-2,6-diethyl-4-bora-3a,4a-diaza-*s*-indacene (1.2.15)
The BODIPY phthalimide intermediate **1.2.15** was prepared and purified by adapting a literature procedure[176].
To a solution of 3-ethyl-2,4-dimethylpyrrole (0.600 g, 4.675 mmol, 2 equiv.) in dry CH_2Cl_2 (20 mL) at reflux under inert atmosphere (N_2) was added dropwise a solution of 1,3-dioxo-2-isoindolineacetyl chloride (0.653 g, 2.805 mmol, 1.2 equiv.) in dry CH_2Cl_2 (10 mL). The reaction mixture was refluxed for further 3 h, then allowed to cool to r.t., DIPEA (1.7 mL, 9.350 mmol, 4 equiv.) was added and after 30 min, $BF_3 \cdot Et_2O$ (soln. ca. 48% $BF_3 \cdot Et_2O$, 1.15 mL, 9.350 mmol, 4 equiv.) was added dropwise. After another 30 min the reaction mixture was concentrated to dryness and purification by column chromatography using EtOAc/Hex mixture afforded **1.2.15** as a pink solid (0.478 g, 1.032 mmol, yield 44%).
^{1}H-NMR ($CDCl_3$) δ_H, ppm: 7.87-7.90 (4H, m, CH-C$\underline{H}$-C-(C=O)-N-CH_2-C), 7.72-7.74 (4H, m,

C*H*-CH-C-(C=O)-N-CH_2-C), 4.84 (3H, s, PhtN-CH_2-C), 2.39 (4H, qvart, 2xBF_2-N-C-C-CH_2-CH_3, $^3J_{H,H}$ = 7.6 Hz), 2.37 (6H, s, 2xBF_2-N-C-CH_3), 2.16 (6H, s, 2xBF_2-N-C-C-CH_3), 1.05 (6H, t, 2xBF_2-N-C-C-CH_2-CH_3, $^3J_{H,H}$ = 7.6 Hz).

^{13}C-NMR ($CDCl_3$) δ_C, ppm: 179.6 (2C, (*C*=O)-N-(*C*=O)), 134.1 (2C, 2xN-(C=O)-(*Ar*)C-CH-C*H*), 132.5 (2C, 2xN-(C=O)-(*Ar*)*C*-CH-CH), 123.6 (2C, 2xN-(C=O)-(*Ar*)C-*C*H-CH), 168.3 (2C, 2xBF_2-N-*C*-CH_3), 134.5 (2C, 2xBF_2-N-C-*C*-CH_3), 134.4 (1C, PhtN-CH_2-*C*), 133.3 (2C, 2xBF_2-N-C-*C*-CH_2-CH_3), 132.5 (2C, 2xBF_2-N-*C*-C-CH_3), 44.7 (1C, PhtN-CH_2-C), 17.3 (2C, 2xBF_2-N-C-C-*C*H_2-CH_3), 15.5 (2C, 2xBF_2-N-C-C-CH_2-*C*H_3), 12.2 (2C, m, 2xBF_2-N-C-*C*H_3), 11.6 (2C, m, 2xBF_2-N-C-C-*C*H_3).

^{19}F-NMR ($CDCl_3$) δ_C, ppm: -145.74 (2F, dd, B*F*$_2$, $^1J_{B,F}$ = 31.7 Hz, $^2J_{F,F}$ = 34.1 Hz).

^{11}B-NMR ($CDCl_3$) δ_C, ppm: 0.68 (1B, t, *B*F_2, $^1J_{B,F}$ = 32.1 Hz).

R_f (Hex/EtOAc 9:1) = 0.089.

ESI-MS(+): *m/z* found 333.1203 $[M\text{-Pht}]^+$, 463.2229 $[M]^+$, calcd. for $C_{18}H_{26}BF_2N_3^+$ 333.2182 and for $C_{26}H_{28}BF_2N_3O_2$ 463.2243.

Elemental analysis (%): calcd. for $C_{26}H_{28}BF_2N_3O_2 \cdot 0.48CH_2Cl_2$ C 63.09, H 5.79, N 8.34; found C 63.04, H 5.33, N, 7.94.

Synthesis of 4,4-difluoro-8-(3-(1,3-dioxoisoindolin-2-yl)propan-1-yl)-1,3,5,7-tetramethyl-2,6-diethyl-4-bora-3a,4a-diaza-*s*-indacene (1.2.16)

To a solution of 3-ethyl-2,4-dimethylpyrrole (0.807 g, 6.292 mmol, 2 equiv.) in dry CH_2Cl_2 (20 mL) at reflux under inert atmosphere (N_2) was added dropwise a solution of 1,3-dioxo-2-isoindolinebutanoyl chloride (0.950 g, 3.775 mmol, 1.2 equiv.) in dry CH_2Cl_2 (10 mL). The reaction mixture was refluxed for further 3.5 h, then allowed to cool down to r.t.. DIPEA (2.2 mL, 12.583 mmol, 4 equiv.) was added and after 30 min, $BF_3 \cdot Et_2O$ (soln. ca. 48% BF_3 in Et_2O, 1.5 mL, 12.583 mmol, 4 equiv.) was added dropwise and after another 30 min the reaction mixture was concentrated to dryness and purification by column chromatography using EtOAc/Hex mixture afforded **1.2.16** as a pink solid (0.409 g, 0.834 mmol, yield 26%).

^{1}H-NMR ($CDCl_3$) δ_H, ppm: 7.85-7.88 (2H, m, CH-C*H*-C-(C=O)-N-CH_2-C), 7.73-7.75 (2H, m, C*H*-CH-C-(C=O)-N-CH_2-C), 3.86 (2H, t, PhtN-CH_2-$(CH_2)_2$-C), 3.06 (2H, m, PhtN-$(CH_2)_2$-CH_2-C), 2.47 (6H, s, 2xBF_2-N-C-CH_3), 2.38 (4H, qvart, 2xBF_2-N-C-C-CH_2-CH_3, $^3J_{H,H}$ = 7.6 Hz), 2.32 (6H, s, 2xBF_2-N-C-C-CH_3), 2.00 (3H, s, PhtN-CH_2-CH_2-CH_2-C), 1.03 (6H, t, 2xBF_2-N-C-C-CH_2-CH_3, $^3J_{H,H}$ = 7.6 Hz).

^{13}C-NMR ($CDCl_3$) δ_C, ppm: 168.4 (2C, (*C*=O)-N-(*C*=O)), 152.7 (2C, 2xBF_2-N-*C*-CH_3), 142.8 (2C, 2xN-(C=O)-(*Ar*)*C*-CH-CH), 135.7 (2C, 2xBF_2-N-C-*C*-CH_3), 134.3 (2C, 2xN-(C=O)-(*Ar*)C-CH-C*H*), 132.9 (2C, 2xBF_2-N-*C*-C-CH_3), 132.1 (2C, 2xBF_2-N-C-*C*-CH_2-CH_3), 131.0 (1C, 2xBF_2-N-C-*C*-CH_2-CH_2-CH_2-PhtN), 123.5 (2C, 2xN-(C=O)-(*Ar*)C-*C*H-CH), 37.9 (1C, PhtN-*C*H_2-$(CH_2)_2$-C), 30.4 (1C, PhtN-CH_2-*C*H_2-CH_2-C), 26.0 (1C, PhtN-$(CH_2)_2$-*C*H_2-C), 17.3 (2C, 2xBF_2-N-C-C-*C*H_2-CH_3), 14.9 (2C, 2xBF_2-N-C-C-CH_2-*C*H_3), 13.4 (2C, 2xBF_2-N-C-C-*C*H_3), 12.6 (2C, 2xBF_2-N-C-*C*H_3).

^{19}F-NMR ($CDCl_3$) δ_C, ppm: -146.00 (2F, dd, B*F*$_2$, $^1J_{B,F}$ = 32.0 Hz, $^2J_{F,F}$ = 33.6 Hz).

^{11}B-NMR ($CDCl_3$) δ_C, ppm: 0.68 (1B, t, *B*F_2, $^1J_{B,F}$ = 32.1 Hz).

R_f (Hex/EtOAc 9:1) = 0.297.

ESI-MS(+):*m/z* found 472.2555 $[M\text{-F}]^+$, 514.2436 $[M+Na]^+$, calcd. for $C_{28}H_{32}BFN_3O_2^+$ 472.2566 and $C_{28}H_{32}BF_2N_3NaO_2^+$ 514.2448.

Elemental analysis (%): calcd. for $C_{28}H_{32}BF_2N_3O_2$ C 68.44, H 6.56, N 8.55; found C 68.45, H 6.62, N 8.36.

Synthesis of 4,4-difluoro-8-(methanamine)-1,3,5,7-tetramethyl-2,6-diethyl-4-bora-3a,4a-diaza-*s*-indacene (1.2.17)

The amino BODIPY derivative **1.2.17**was prepared and purified by adapting literature procedures[176, 177]. To a solution of **1.2.15** (0.592 g, 1.278 mmol, 1 equiv.) in EtOH/dry CH_2Cl_2 (40 mL, 1:1 (v/v)), was added hydrazine hydrate (0.124 mL, 2.556 mmol, 2 equiv.) and the mixture was stirred at reflux under inert atmosphere (N_2) for 4 h. The reaction mixture was cooled to r.t., the white precipitate formed during the reaction was removed by filtration, and the filtrate was concentrated under reduced pressure to dryness. Purification by column chromatography using CH_2Cl_2/CH_3OH afforded **1.2.17** as a pink solid (0.105 g, 0.315. mmol, yield 25%).

^{1}H-NMR ($CDCl_3$) δ_H, ppm: 4.14 (2H, s, H_2N-C$\underline{H_2}$-C), 2.50 (6H, s, 2xBF_2-N-C-C$\underline{H_3}$), 2.41 (6H, s, 2xBF_2-N-C-C-C$\underline{H_3}$), 2.40 (4H, qvart, 2xBF_2-N-C-C-C$\underline{H_2}$-CH_3, $^3J_{H,H}$ = 7.6 Hz), 1.05 (6H, t, 2xBF_2-N-C-C-CH_2-C$\underline{H_3}$, $^3J_{H,H}$ = 7.6 Hz).

^{13}C-NMR ($CDCl_3$) δ_C, ppm: 153.7 (2C, 2xBF_2-N-$\underline{C}$-CH_3), 142.0 (2C, 2xBF_2-N-C-$\underline{C}$-CH_3), 135.8 (1C, H_2H-CH_2-$\underline{C}$), 133.2 (2C, 2xBF_2-N-C-$\underline{C}$-CH_2-CH_3), 130.9 (2C, 2xBF_2-N-$\underline{C}$-C-CH_3), 37.8 (1C, H_2N-C$\underline{H_2}$-C), 17.3 (2C, 2xBF_2-N-C-C-$\underline{C}$$H_2$-$CH_3$), 14.9 (2C, 2x$BF_2$-N-C-C-$CH_2$-$\underline{C}$$H_3$), 13.1 (2C, 2xBF2-N-C-C-$\underline{C}$$H_3$), 12.7 (2C, t, 2x$BF_2$-N-C-$\underline{C}$$H_3$, $^2J_{C,B}$ = 3 Hz).

^{19}F-NMR ($CDCl_3$) δ_C, ppm: -146.05 (2F, dd, B$\underline{F_2}$, $^1J_{B,F}$ = 32.7 Hz, $^2J_{F,F}$ = 33.4 Hz).

^{11}B-NMR ($CDCl_3$) δ_C, ppm: 0.60 (1B, t, $\underline{B}F_2$, $^1J_{B,F}$ = 32.8 Hz).

R_f(CH_2Cl_2/CH_3OH 10:1) = 0.741.

ESI-MS(+):*m/z* found 314.2194 $[M-F]^+$, 334.2256 $[M+H]^+$, 356.2073 $[M+Na]^+$, 667.4441 $[2M+H]^+$, 689.4260 $[2M+Na]^+$ and 1000.6645 $[3M+H]^+$, calcd. for $C_{18}H_{26}BFN_3^+$ 314.2198, for $C_{18}H_{27}BF_2N_3^+$ 334.2261, for $C_{18}H_{26}BF_2N_3Na^+$ 356.2080, for $C_{36}H_{53}B_2F_4N_6^+$ 667.4448, for $C_{36}H_{52}B_2F_4N_6Na^+$689.4268, and for $C_{54}H_{79}B_3F_6N_9^+$ 1000.6636.

Elemental analysis (%): calcd. for $C_{18}H_{26}BF_2N_3$·0.2EtOAc C 64.36, H 7.93, N 11.98; found C 64.46, H 8.10, N 11.81.

Synthesis of 4,4-difluoro-8-(3-aminopropan-1-yl)-1,3,5,7-tetramethyl-2,6-diethyl-4-bora-3a,4a-diaza-*s*-indacene (1.2.18)

The BODIPY amino intermediate was prepared and purified by adapting literature procedures[176, 177]. To a solution of **1.2.16** (0.350 g, 0.712 mmol, 1 equiv.) in EtOH/dry CH_2Cl_2 (20/20 ml) was added hydrazine hydrate (0.200 mL, 3.560 mmol, 5 equiv.) and the mixture was stirred at reflux under inert atmosphere (N_2) for 24 h. The reaction mixture was cooled down to r.t., the white precipitate formed during the reaction was removed by filtration, and the filtrate was concentrated under reduced pressure to dryness. Purification by column chromatography using CH_2Cl_2/CH_3OH mixture afforded **1.2.18** as a pink solid (0.090 g, 0.249 mmol, yield 35%).

^{1}H-NMR ($CDCl_3$) δ_H, ppm: 3.07 (2H, t, H_2N-C$\underline{H_2}$-$(CH_2)_2$-C, $^3J_{H,H}$ = 7.1 Hz), 3.00 (2H, t, H_2N-$(CH_2)_2$-C$\underline{H_2}$-C, $^3J_{H,H}$ = 6.9 Hz), 2.46 (6H, s, 2xBF_2-N-C-C$\underline{H_3}$), 2.34 (4H, qvart, 2xBF_2-N-C-C-C$\underline{H_2}$-CH_3, $^3J_{H,H}$ = 7.6 Hz), 2.30 (6H, s, 2xBF_2-N-C-C-C$\underline{H_3}$), 2.05 (2H, m, H_2N -CH_2-C$\underline{H_2}$-CH_2-C), 1.00 (6H, t, 2xBF_2-N-C-C-CH_2-C$\underline{H_3}$, $^3J_{H,H}$ = 7.4 Hz).

^{13}C-NMR ($CDCl_3$) δ_C, ppm: 153.1 (2C, 2xBF_2-N-$\underline{C}$-CH_3), 141.5 (2C, 2xBF_2-N-C-$\underline{C}$-CH_3), 135.8 (1C, H_2H-CH_2-$\underline{C}$), 133.2 (2C, 2xBF_2-N-C-$\underline{C}$-CH_2-CH_3), 130.9 (2C, 2xBF_2-N-$\underline{C}$-C-CH_3), 40.0 (2C, H_2N-$\underline{C}$$H_2$-$(CH_2)_2$-C), 29.4 (2C, H_2N -CH_2-$\underline{C}$$H_2$-$CH_2$-C), 25.4 (2C, H_2N -$(CH_2)_2$-$\underline{C}$$H_2$-C), 17.3 (2C, 2x$BF_2$-N-C-C-$\underline{C}$$H_2$-$CH_3$), 14.9 (2C, 2x$BF_2$-N-C-C-$CH_2$-$\underline{C}$$H_3$), 13.7 (2C, 2xBF2-N-C-C-$\underline{C}$$H_3$), 12.6 (2C, 2x$BF_2$-N-C-$\underline{C}$$H_3$).

^{19}F-NMR ($CDCl_3$) δ_C, ppm: (-145.25)-(-145.93) (2F, m,B$\underline{F_2}$).

^{11}B-NMR ($CDCl_3$) δ_C, ppm: 0.56 (1B, s, $\underline{B}F_2$).

R_f (CH_2Cl_2/CH_3OH 10:1) = 0.133.

ESI-MS(+):*m/z* found 342.2517 $[M-F]^+$, 362.2581 $[M+H]^+$, calcd. for $C_{20}H_{30}BFN_3^+$ 342.2511 and

for $C_{20}H_{31}BF_2N_3^+$ 362.2574.
Elemental analysis (%): calcd. for $C_{20}H_{30}BF_2N_3 \cdot CH_2Cl_2$ C 56.53, H 7.23, N 9.42; found C 56.61, H 7.29, N 9.47.

Synthesis of the ester and amide conjugates BODIPY – dinuclear trithiolato ruthenium(II)-p-cymene complexes 1.2.19-1.2.22 and 1.2.23-1.2.26.

The ester conjugates BODIPY – dinuclear trithiolato ruthenium(II)-*p*-cymene complexes were prepared and purified by adapting a literature procedure[174].
Synthesis of [(η^6-*p*-$MeC_6H_4Pr^i$)$_2$Ru$_2$(μ_2-$SCH_2C_6H_4$-*p*-Bu^t)$_2$(μ_2-SC_6H_4-*p*-O-(CO)R)]Cl (R = 4,4-difluoro-8-(2-ethan-1-yl)-1,3,5,7-tetramethyl-2,6-diethyl-4-bora-3a,4a-diaza-*s*-indacene) (1.2.19)
To a solution of **1.2.9** (0.099 g, 0.263 mmol, 1.3 equiv.) in dry CH_2Cl_2 (20 mL) at r.t. under inert atmosphere (N_2) were added successively EDCI (0.058 g, 0.303 mmol, 1.5 equiv.), **1.2.2** (0.200 g, 0.202 mmol, 1 equiv.) and DMAP (0.007 g, 0.061 mmol, 0.3 equiv.). The reaction mixture was stirred at r.t. under inert atmosphere (N_2) for further 72 h and the reaction evolution was verified by TLC (CH_2Cl_2/CH_3OH 10:1 (v/v)). The reaction mixture was concentrated to dryness under reduced pressure and purification by column chromatography using CH_2Cl_2/CH_3OH mixture afforded **1.2.19** as a pink-orange solid (0.033 g, 0.024 mmol, yield 12%).
^{1}H-NMR ($CDCl_3$) δ_H, ppm: 7.85 (2H, d, 2xS-(*Ar*)C-C*H*-CH-C-O, $^3J_{H,H}$ = 8.6 Hz), 7.42-7.50 (8H, m, , 4xCH_2-(*Ar*)C-C*H*-CH-C-C(CH_3)$_3$, 4xCH_2-(*Ar*)C-CH-C*H*-C-C(CH_3)$_3$), 7.08 (2H, d, 2xS-(*Ar*)C-CH-C*H*-C-O, $^3J_{H,H}$ = 8.6 Hz), 5.30 (2H, d, 2xCH_3-(*Ar*)C-CH-C*H*-C, $^3J_{H,H}$ = 5.8 Hz), 5.05 (2H, d, 2xCH_3-(*Ar*)C-C*H*-CH-C, $^3J_{H,H}$ = 5.8 Hz), 4.98 (2H, d, 2xCH_3-(*Ar*)C-CH-C*H*-C, $^3J_{H,H}$ = 5.8 Hz), 4.64 (2H, d, 2xCH_3-(*Ar*)C-C*H*-CH-C, $^3J_{H,H}$ = 5.8 Hz), 3.62 (2H, s, C*H$_2$*-(*Ar*)C-CH-CH-C-C(CH_3)$_3$), 3.47-3.52 (2H, m, O-(C=O)-C*H$_2$*-CH_2), 3.46 (2H, s, C*H$_2$*-(*Ar*)C-CH-CH-C-C(CH_3)$_3$), 2.86-2.90 (2H, m, O-(C=O)-CH_2-C*H$_2$*), 2.52 (6H, s, 2xBF_2-N-C-C*H$_3$*), 2.43 (6H, s, 2xBF_2-N-C-C-C*H$_3$*), 2.42 (4H, qvart, 2xBF_2-N-C-C-C*H$_2$*-CH_3, $^3J_{H,H}$ = 7.5 Hz), 1.92 (2H, sept, 2x(*Ar*)C-CH-CH-C-C*H*(CH_3)$_2$, $^3J_{H,H}$ = 6.9 Hz), 1.77 (6H, s, 2xC*H$_3$*-(*Ar*)C-CH-CH-C), 1.37 (9H, s, S-CH_2-(*Ar*)C-CH-CH-C-C(C*H$_3$*)$_3$), 1.33 (9H, s, S-CH_2-(*Ar*)C-CH-CH-C-C(C*H$_3$*)$_3$), 1.07 (6H, t, 2xBF_2-N-C-C-CH_2-C*H$_3$*, $^3J_{H,H}$ = 7.5 Hz), 0.96 (6H, d, (*Ar*)C-CH-CH-C-CH(C*H$_3$*)$_2$, $^3J_{H,H}$ = 6.9 Hz), 0.91 (6H, d, (*Ar*)C-CH-CH-C-CH(C*H$_3$*)$_2$, $^3J_{H,H}$ = 6.9 Hz).
^{13}C-NMR ($CDCl_3$) δ_C, ppm: 170.3 (1C, O-(*C*=O)-CH_2), 153.4 (2C, 2xBF_2-N-*C*-CH_3), 151.9, 151.8 (2C, 2xS-CH_2-(*Ar*)C-CH-CH-*C*-C(CH_3)$_3$), 150.9 (1C, S-(*Ar*)C-CH-CH-*C*-O), 141.1 (2C, 2xBF_2-N-*C*-C-CH_3), 136.9, 136.8 (2C, 2xS-CH_2-(*Ar*)*C*-CH-CH-C-C(CH_3)$_3$), 135.8 (2C, 2xBF_2-N-C-*C*-CH_3), 135.6 (1C, S-(*Ar*)*C*-CH-CH-C-O), 133.9 (2C, 2xS-(*Ar*)C-*C*H-CH-C-O), 133.3 (2C, 2xBF_2-N-C-*C*-CH_2-CH_3), 130.9 (1C, O-(C=O)-(CH_2)$_2$-*C*), 129.4, 129.3 (2C, 2xS-CH_2-(*Ar*)C-*C*H-CH-C-C(CH_3)$_3$), 125.7, 125.5 (2C, 2xS-CH_2-(*Ar*)C-CH-*C*H-C-C(CH_3)$_3$), 122.4 (2C, 2xS-(*Ar*)C-CH-*C*H-C-O), 107.2 (2C, 2xCH_3-(*Ar*)C-CH-CH-*C*), 100.7 (2C, 2xCH_3-(*Ar*)*C*-CH-CH-C), 84.3 (1C, CH_3-(*Ar*)C-CH-*C*H-C), 83.91 (1C, CH_3-(*Ar*)C-*C*H-CH-C), 83.86 (1C, CH_3-(*Ar*)C-CH-*C*H-C), 82.7 (1C, CH_3-(*Ar*)C-*C*H-CH-C), 40.2 (1C, S-*C*H_2-(*Ar*)C-CH-CH-C-C(CH_3)$_3$), 39.7 (1C, S-*C*H_2-(*Ar*)C-CH-CH-C-C(CH_3)$_3$), 35.7 (1C, O-(C=O)-CH_2-C*H$_2$*), 34.94 (1C, S-CH_2-(*Ar*)C-CH-CH-C-*C*(CH_3)$_3$), 34.88 (1C, S-CH_2-(*Ar*)C-CH-CH-C-*C*(CH_3)$_3$), 31.57 (3C, S-CH_2-(*Ar*)C-CH-CH-C-C(*C*H_3)$_3$), 31.55 (3C, S-CH_2-(*Ar*)C-CH-CH-C-C(*C*H_3)$_3$), 31.0 (2C, 2x(*Ar*)CH-CH-C-*C*H(CH_3)$_2$), 23.7 (1C, O-(C=O)-*C*H_2-CH_2), 23.2 (2C, (*Ar*)CH-CH-C-CH(*C*H_3)$_2$), 22.8 (2C, (*Ar*)CH-CH-C-CH(*C*H_3)$_2$), 18.3 (2C, 2x*C*H_3-(*Ar*)C-CH-CH), 17.3 (2C, 2xBF_2-N-C-C-*C*H_2-CH_3), 15.0 (2C, 2xBF_2-N-C-C-CH_2-*C*H_3), 13.7 (2C, 2xBF_2-N-C-C-*C*H_3), 12.7 (2C, m, 2xBF_2-N-C-*C*H_3).
^{19}F-NMR ($CDCl_3$) δ_C, ppm: -145.89 (2F, dt, B*F$_2$*, $^1J_{B,F}$ = 32.1 Hz, $^2J_{F,F}$ = 64.6 Hz).
^{11}B-NMR ($CDCl_3$) δ_C, ppm: 0.62 (1B, t, *B*F_2, $^1J_{B,F}$ = 32.3 Hz).

R_f (CH_2Cl_2/CH_3OH 10:1) = 0.537.
ESI-MS(+):*m/z* found 1313.4180 $[M\text{-}Cl]^+$, calcd. for $C_{68}H_{88}BF_2N_2O_2Ru_2S_3^+$ 1313.4151.
Elemental analysis (%): calcd. for $C_{68}H_{88}BClF_2N_2O_2Ru_2S_3 \cdot 2H_2O \cdot CH_3OH$ C 58.52, H 6.83, N 1.98; found C 58.51, H 6.95, N 1.95.

Synthesis of [(η^6-*p*-$MeC_6H_4Pr^i$)$_2$$Ru_2$($\mu_2$-$SCH_2C_6H_4$-*p*-$Bu^t$)$_2$($\mu_2$-$SC_6H_4$-*p*-O-(CO)R)]Cl (R = 4,4-difluoro-8-(4-butan-1-yl)-1,3,5,7-tetramethyl-2,6-diethyl-4-bora-3a,4a-diaza-*s*-indacene) (1.2.20)
To a solution of **1.2.10** (0.082 g, 0.202 mmol, 1 equiv.) in dry CH_2Cl_2 (20 mL) at r.t. under inert atmosphere (N_2) were added successively EDCI (0.049 g, 0.253 mmol, 1.25 equiv.), **1.2.2** (0.200 g, 0.202 mmol, 1 equiv.) and DMAP (0.006 g, 0.051 mmol, 0.25 equiv.). The reaction mixture was stirred at r.t. under inert atmosphere (N_2) for further 72 h and the reaction evolution was verified by TLC (CH_2Cl_2/CH_3OH 10:1 (v/v)). The reaction mixture was concentrated to dryness under reduced pressure and purification by column chromatography using CH_2Cl_2/CH_3OH afforded **1.2.20** as an orange-pink solid (0.054 g, 0.039 mmol, yield 19%).
^{1}H-NMR ($CDCl_3$) δ_H, ppm: 7.80 (2H, d, 2xS-(*Ar*)C-C*H*-CH-C-O, $^3J_{H,H}$ = 8.6 Hz), 7.42-7.49 (8H, m, 4xCH_2-(*Ar*)C-C*H*-CH-C-C(CH_3)$_3$, 4xCH_2-(*Ar*)C-CH-C*H*-C-C(CH_3)$_3$), 7.04 (2H, d, 2xS-(*Ar*)C-CH-C*H*-C-OH, $^3J_{H,H}$ = 8.6 Hz), 5.16 (2H, d, 2xCH_3-(*Ar*)C-CH-C*H*-C, $^3J_{H,H}$ = 5.8 Hz), 5.03 (2H, d, 2xCH_3-(*Ar*)C-C*H*-CH-C, $^3J_{H,H}$ = 5.8 Hz), 4.96 (2H, d, 2xCH_3-(*Ar*)C-CH-C*H*-C, $^3J_{H,H}$ = 5.8 Hz), 4.58 (2H, d, 2xCH_3-(*Ar*)C-C*H*-CH-C, $^3J_{H,H}$ = 5.8 Hz), 3.62 (2H, s, C*H*$_2$-(*Ar*)C-CH-CH-C-C(CH_3)$_3$), 3.45 (2H, s, C*H*$_2$-(*Ar*)C-CH-CH-C-C(CH_3)$_3$), 3.06-3.10 (2H, m, O-(C=O)-C*H*$_2$-(CH_2)$_3$), 2.68 (2H, t, O-(C=O)-(CH_2)$_3$-C*H*$_2$, $^3J_{H,H}$ = 7.2 Hz), 2.50 (6H, s, 2xBF_2-N-C-C*H*$_3$), 2.41 (4H, qvart, 2xBF_2-N-C-C-C*H*$_2$-CH_3, $^3J_{H,H}$ = 7.5 Hz), 2.37 (6H, s, 2xBF_2-N-C-C-C*H*$_3$), 1.94 (2H, qvint, O-(C=O)-(CH_2)$_2$-C*H*$_2$-CH_2, $^3J_{H,H}$ = 7.6 Hz), 1.88 (2H, sept, 2x(*Ar*)C-CH-CH-C-C*H*(CH_3)$_2$, $^3J_{H,H}$ = 6.9 Hz), 1.72-1.84 (2H, m, O-(C=O)-CH_2-C*H*$_2$-(CH_2)$_2$), 1.78 (6H, s, 2xC*H*$_3$-(*Ar*)C-CH-CH-C), 1.37 (9H, s, S-CH_2-(*Ar*)C-CH-CH-C-C(C*H*$_3$)$_3$), 1.33 (9H, s, S-CH_2-(*Ar*)C-CH-CH-C-C(C*H*$_3$)$_3$), 1.05 (6H, t, 2xBF_2-N-C-C-CH_2-C*H*$_3$, $^3J_{H,H}$ = 7.5 Hz), 0.95 (6H, d, (*Ar*)C-CH-CH-C-CH(C*H*$_3$)$_2$, $^3J_{H,H}$ = 6.9 Hz), 0.89 (6H, d, (*Ar*)C-CH-CH-C-CH(C*H*$_3$)$_2$, $^3J_{H,H}$ = 6.9 Hz).
^{13}C-NMR ($CDCl_3$) δ_C, ppm: 171.5 (1C, O-(*C*=O)-CH_2), 152.5 (2C, 2xBF_2-N-*C*-CH_3), 151.9, 151.8 (2C, 2xS-CH_2-(*Ar*)C-CH-CH-*C*-C(CH_3)$_3$), 151.0 (1C, S-(*Ar*)C-CH-CH-*C*-O), 144.0 (2C, 2xBF_2-N-*C*-C-CH_3), 136.84, 136.79 (2C, 2xS-CH_2-(*Ar*)*C*-CH-CH-C-C(CH_3)$_3$), 135.8 (2C, 2xBF_2-N-C-*C*-CH_3), 135.2 (1C, S-(*Ar*)*C*-CH-CH-C-O), 133.8 (2C, 2xS-(*Ar*)C-*C*H-CH-C-O), 132.8 (2C, 2xBF_2-N-C-*C*-CH_2-CH_3), 131.0 (1C, O-(C=O)-(CH_2)$_4$-*C*), 129.4, 129.3 (2C, 2xS-CH_2-(*Ar*)C-*C*H-CH-C-C(CH_3)$_3$), 125.7, 125.5 (2C, 2xS-CH_2-(*Ar*)C-CH-*C*H-C-C(CH_3)$_3$), 122.4 (2C, 2xS-(*Ar*)C-CH-*C*H-C-O), 107.1 (2C, 2xCH_3-(*Ar*)C-CH-CH-*C*), 100.7 (2C, 2xCH_3-(*Ar*)*C*-CH-CH-C), 84.5 (1C, CH_3-(*Ar*)C-CH-*C*H-C), 83.8 (1C, CH_3-(*Ar*)C-*C*H-CH-C), 83.7 (1C, CH_3-(*Ar*)C-CH-*C*H-C), 82.7 (1C, CH_3-(*Ar*)C-*C*H-CH-C), 40.2 (1C, S-*C*H_2-(*Ar*)C-CH-CH-C-C(CH_3)$_3$), 39.7 (1C, S-*C*H_2-(*Ar*)C-CH-CH-C-C(CH_3)$_3$), 34.94 (1C, S-CH_2-(*Ar*)C-CH-CH-C-*C*(CH_3)$_3$), 34.88 (1C, S-CH_2-(*Ar*)C-CH-CH-C-*C*(CH_3)$_3$), 34.1 (1C, O-(C=O)-(CH_2)$_3$-C*H*$_2$), 31.57 (3C, S-CH_2-(*Ar*)C-CH-CH-C-C(*C*H_3)$_3$), 31.55 (3C, S-CH_2-(*Ar*)C-CH-CH-C-C(*C*H_3)$_3$), 31.4 (1C, O-(C=O)-CH_2-*C*H_2-(CH_2)$_2$), 31.0 (2C, 2x(*Ar*)CH-CH-C-*C*H(CH_3)$_2$), 28.3 (1C, O-(C=O)-*C*H_2-(CH_2)$_3$), 25.2 (1C, O-(C=O)-(CH_2)$_2$-*C*H_2-CH_2), 23.3 (2C, (*Ar*)CH-CH-C-CH(*C*H_3)$_2$), 22.7 (2C, (*Ar*)CH-CH-C-CH(*C*H_3)$_2$), 18.3 (2C, 2x*C*H_3-(*Ar*)C-CH-CH), 17.3 (2C, 2xBF_2-N-C-C-*C*H_2-CH_3), 15.0 (2C, 2xBF_2-N-C-C-CH_2-*C*H_3), 13.6 (2C, 2xBF_2-N-C-C-*C*H_3), 12.6 (2C, m, 2xBF_2-N-C-*C*H_3).
^{19}F-NMR ($CDCl_3$) δ_C, ppm: -145.99 (2F, m, B*F*$_2$).
^{11}B-NMR ($CDCl_3$) δ_C, ppm: 0.63 (1B, t, *B*F_2, $^1J_{B,F}$ = 32.5 Hz).
R_f (CH_2Cl_2/CH_3OH 10:1) = 0.500.
ESI-MS(+):*m/z* found 1341.446 $[M\text{-}Cl]^+$, calcd. for $C_{70}H_{92}BF_2N_2O_2Ru_2S_3^+$ 1341.4464.

Elemental analysis (%): calcd. for $C_{70}H_{92}BClF_2N_2O_2Ru_2S_3 \cdot 1.5H_2O$ C 59.92, H 6.82, N 2.00; found C 59.93, H 6.83, N 2.32.

Synthesis of [(η^6-*p*-$MeC_6H_4Pr^i$)$_2$$Ru_2$($\mu_2$-$SCH_2C_6H_4$-*p*-$Bu^t$)$_2$($\mu_2$-$SC_6H_4$-*p*-O-(CO)R)]Cl (R = 4,4-difluoro-8-(6-hexan-1-yl)-1,3,5,7-tetramethyl-2,6-diethyl-4-bora-3a,4a-diaza-*s*-indacene) (1.2.21)

To a solution of **1.2.11** (0.098 g, 0.227 mmol, 1.3 equiv.) in dry CH_2Cl_2 (20 mL) at r.t. under inert atmosphere (N_2) were added successively EDCI (0.050 g, 0.263 mmol, 1.5 equiv.), **1.2.2** (0.173 g, 0.174 mmol, 1 equiv.) and DMAP (0.006 g, 0.052 mmol, 0.3 equiv.). The reaction mixture was stirred at r.t. under inert atmosphere (N_2) for further 72 h and the reaction evolution was verified by TLC (CH_2Cl_2/CH_3OH 10:1 (v/v)). The reaction mixture was concentrated to dryness under reduced pressure and purification by column chromatography using CH_2Cl_2/CH_3OH afforded **1.2.21** as an orange-pink solid (0.227 g, 0.162 mmol, yield 93%).

^{1}H-NMR ($CDCl_3$) δ_H, ppm: 7.89 (2H, d, 2xS-(*Ar*)C-C*H*-CH-C-O, $^3J_{H,H}$ = 8.6 Hz), 7.41-7.49 (8H, m, 4xCH_2-(*Ar*)C-C*H*-CH-C-C(CH_3)$_3$, 4xCH_2-(*Ar*)C-CH-C*H*-C-C(CH_3)$_3$), 7.04 (2H, d, 2xS-(*Ar*)C-CH-C*H*-C-O, $^3J_{H,H}$ = 8.6 Hz), 5.14 (2H, d, 2xCH_3-(*Ar*)C-CH-C*H*-C, $^3J_{H,H}$ = 5.8 Hz), 5.01 (2H, d, 2xCH_3-(*Ar*)C-C*H*-CH-C, $^3J_{H,H}$ = 5.8 Hz), 4.93 (2H, d, 2xCH_3-(*Ar*)C-CH-C*H*-C, $^3J_{H,H}$ = 5.8 Hz), 4.62 (2H, d, 2xCH_3-(*Ar*)C-C*H*-CH-C, $^3J_{H,H}$ = 5.8 Hz), 3.61 (2H, s, C*H*$_2$-(*Ar*)C-CH-CH-C-C(CH_3)$_3$), 3.43 (2H, s, C*H*$_2$-(*Ar*)C-CH-CH-C-C(CH_3)$_3$), 2.99-3.03 (2H, m, O-(C=O)-C*H*$_2$-(CH_2)$_5$), 2.59 (2H, t, O-(C=O)-(CH_2)$_5$-C*H*$_2$, $^3J_{H,H}$ = 7.5 Hz), 2.49 (6H, s, 2xBF_2-N-C-C*H*$_3$), 2.40 (4H, qvart, 2xBF_2-N-C-C-C*H*$_2$-CH_3, $^3J_{H,H}$ = 7.5 Hz), 2.34 (6H, s, 2xBF_2-N-C-C-C*H*$_3$), 1.89 (2H, sept, 2x(*Ar*)C-CH-CH-C-C*H*(CH_3)$_2$, $^3J_{H,H}$ = 6.8 Hz), 1.73-1.84 (2H, m, O-(C=O)-(CH_2)$_4$-C*H*$_2$-CH_2), 1.76 (6H, s, 2xC*H*$_3$-(*Ar*)C-CH-CH-C), 1.63-1.71 (2H, m, O-(C=O)-CH_2-C*H*$_2$-(CH_2)$_4$), 1.53-1.63 (2H, m, O-(C=O)-(CH_2)$_2$-C*H*$_2$-(CH_2)$_3$), 1.46-1.54 (2H, m, O-(C=O)-(CH_2)$_3$-C*H*$_2$-(CH_2)$_2$), 1.36 (9H, s, S-CH_2-(*Ar*)C-CH-CH-C-C(C*H*$_3$)$_3$), 1.32 (9H, s, S-CH_2-(*Ar*)C-CH-CH-C-C(C*H*$_3$)$_3$), 1.04 (6H, t, 2xBF_2-N-C-C-CH_2-C*H*$_3$, $^3J_{H,H}$ = 7.5 Hz), 0.94 (6H, d, (*Ar*)C-CH-CH-C-CH(C*H*$_3$)$_2$, $^3J_{H,H}$ = 6.9 Hz), 0.89 (6H, d, (*Ar*)C-CH-CH-C-CH(C*H*$_3$)$_2$, $^3J_{H,H}$ = 6.9 Hz).

^{13}C-NMR ($CDCl_3$) δ_C, ppm: 171.9 (1C, O-(*C*=O)-CH_2), 152.2 (2C, 2xBF_2-N-*C*-CH_3), 151.9, 151.8 (2C, 2xS-CH_2-(*Ar*)C-CH-CH-*C*-C(CH_3)$_3$), 151.2 (1C, S-(*Ar*)C-CH-CH-*C*-O), 144.8 (2C, 2xBF_2-N-*C*-C-CH_3), 136.80, 136.76 (2C, 2xS-CH_2-(*Ar*)*C*-CH-CH-C-C(CH_3)$_3$), 135.8 (2C, 2xBF_2-N-C-*C*-CH_3), 135.1 (1C, S-(*Ar*)*C*-CH-CH-C-O), 133.7 (2C, 2xS-(*Ar*)C-*C*H-CH-C-O), 132.7 (2C, 2xBF_2-N-C-*C*-CH_2-CH_3), 131.1 (1C, O-(C=O)-(CH_2)$_6$-*C*), 129.4, 129.2 (2C, 2xS-CH_2-(*Ar*)C-*C*H-CH-C-C(CH_3)$_3$), 125.7, 125.5 (2C, 2xS-CH_2-(*Ar*)C-CH-*C*H-C-C(CH_3)$_3$), 122.5 (2C, 2xS-(*Ar*)C-CH-*C*H-C-O), 107.2 (2C, 2xCH_3-(*Ar*)C-CH-CH-*C*), 100.7 (2C, 2xCH_3-(*Ar*)*C*-CH-CH-C), 84.3 (1C, CH_3-(*Ar*)C-CH-*C*H-C), 83.8 (2C, CH_3-(*Ar*)C-CH-*C*H-C, CH_3-(*Ar*)C-*C*H-CH-C), 82.7 (1C, CH_3-(*Ar*)C-*C*H-CH-C), 40.2 (1C, S-*C*H_2-(*Ar*)C-CH-CH-C-C(CH_3)$_3$), 39.7 (1C, S-*C*H_2-(*Ar*)C-CH-CH-C-C(CH_3)$_3$), 34.93 (1C, S-CH_2-(*Ar*)C-CH-CH-C-*C*(CH_3)$_3$), 34.87 (1C, S-CH_2-(*Ar*)C-CH-CH-C-*C*(CH_3)$_3$), 34.4 (1C, O-(C=O)-(CH_2)$_5$-*C*H_2), 31.56 (3C, S-CH_2-(*Ar*)C-CH-CH-C-C(*C*H_3)$_3$), 31.54 (3C, S-CH_2-(*Ar*)C-CH-CH-C-C(*C*H_3)$_3$), 31.9 (1C, O-(C=O)-CH_2-*C*H_2-(CH_2)$_4$), 31.0 (2C, 2x(*Ar*)CH-CH-C-*C*H(CH_3)$_2$), 30.1 (1C, O-(C=O)-(CH_2)$_2$-*C*H_2-(CH_2)$_3$), 29.1 (1C, O-(C=O)-(CH_2)$_3$-*C*H_2-(CH_2)$_2$), 28.6 (1C, O-(C=O)-*C*H_2-(CH_2)$_5$), 24.9 (1C, O-(C=O)-(CH_2)$_4$-*C*H_2-CH_2), 23.2 (2C, (*Ar*)CH-CH-C-CH(*C*H_3)$_2$), 22.7 (2C, (*Ar*)CH-CH-C-CH(*C*H_3)$_2$), 18.3 (2C, 2x*C*H_3-(*Ar*)C-CH-CH), 17.3 (2C, 2xBF_2-N-C-C-*C*H_2-CH_3), 15.0 (2C, 2xBF_2-N-C-C-CH_2-*C*H_3), 13.6 (2C, 2xBF_2-N-C-C-*C*H_3), 12.5 (2C, t, 2xBF_2-N-C-*C*H_3, $^3J_{C,B}$ = 3 Hz).

^{19}F-NMR ($CDCl_3$) δ_C, ppm: -145.96 (2F, m,B*F*$_2$).

^{11}B-NMR ($CDCl_3$) δ_C, ppm: 0.62 (1B, t, *B*F_2, $^1J_{B,F}$ = 32.2 Hz).

R_f (CH_2Cl_2/CH_3OH 10:1) = 0.398.

ESI-MS(+): *m/z* found 1369.4884 $[M\text{-}Cl]^+$, calcd. for $C_{72}H_{96}BF_2N_2O_2Ru_2S_3^+$ 1369.4777.

Elemental analysis (%): calcd. for $C_{72}H_{96}BClF_2N_2O_2Ru_2S_3 \cdot 2.2H_2O \cdot 0.5CH_2Cl_2$ C 58.59, H 6.88, N 1.88; found C 58.61, H 6.88, N 1.91.

Synthesis of [(η^6-*p*-MeC$_6$H$_4$Pr^i)$_2$Ru$_2$(μ_2-SCH$_2$C$_6$H$_4$-*p*-Bu^t)$_2$(μ_2-SC$_6$H$_4$-*p*-O-(CO)R)]Cl (R = 4,4-difluoro-8-(8-octan-1-yl)-1,3,5,7-tetramethyl-2,6-diethyl-4-bora-3a,4a-diaza-*s*-indacene) (1.2.22)

To a solution of **1.2.12** (0.121 g, 0.263 mmol, 1.3 equiv.) in dry CH_2Cl_2 (20 mL) at r.t. under inert atmosphere (N_2) were added successively EDCI (0.058 g, 0.303 mmol, 1.5 equiv.), **1.2.2** (0.200 g, 0.202 mmol, 1 equiv.) and DMAP (0.007 g, 0.061 mmol, 0.25 equiv.). The reaction mixture was stirred at r.t. under inert atmosphere (N_2) for further 72 h and the reaction evolution was verified by TLC (CH_2Cl_2/CH_3OH 10:1 (v/v)). The reaction mixture was concentrated to dryness under reduced pressure and purification by column chromatography using CH_2Cl_2/CH_3OH mixture afforded **1.2.22** as an orange-pink solid (0.143 g, 0.100 mmol, yield 50%).

^{1}H-NMR ($CDCl_3$) δ_H, ppm: 7.80 (2H, d, 2xS-(*Ar*)C-C*H*-CH-C-O, $^3J_{H,H}$ = 8.6 Hz), 7.41-7.49 (8H, m, 4xCH_2-(*Ar*)C-C*H*-CH-C-C(CH_3)$_3$, 4xCH_2-(*Ar*)C-CH-C*H*-C-C(CH_3)$_3$), 7.05 (2H, d, 2xS-(*Ar*)C-CH-C*H*-C-O, $^3J_{H,H}$ = 8.6 Hz), 5.15 (2H, d, 2xCH_3-(*Ar*)C-CH-C*H*-C, $^3J_{H,H}$ = 5.8 Hz), 5.03 (2H, d, 2xCH_3-(*Ar*)C-C*H*-CH-C, $^3J_{H,H}$ = 5.8 Hz), 4.94 (2H, d, 2xCH_3-(*Ar*)C-CH-C*H*-C, $^3J_{H,H}$ = 5.8 Hz), 4.63 (2H, d, 2xCH_3-(*Ar*)C-C*H*-CH-C, $^3J_{H,H}$ = 5.8 Hz), 3.61 (2H, s, C*H*$_2$-(*Ar*)C-CH-CH-C-C(CH_3)$_3$), 3.45 (2H, s, C*H*$_2$-(*Ar*)C-CH-CH-C-C(CH_3)$_3$), 2.99-3.03 (2H, m, O-(C=O)-C*H*$_2$-(CH_2)$_5$), 2.58 (2H, t, O-(C=O)-(CH_2)$_7$-C*H*$_2$, $^3J_{H,H}$ = 7.5 Hz), 2.49 (6H, s, 2xBF_2-N-C-C-C*H*$_3$), 2.40 (4H, qvart, 2xBF_2-N-C-C-C*H*$_2$-CH_3, $^3J_{H,H}$ = 7.5 Hz), 2.34 (6H, s, 2xBF_2-N-C-C-C*H*$_3$), 1.90 (2H, sept, 2x(*Ar*)C-CH-CH-C-C*H*(CH_3)$_2$, $^3J_{H,H}$ = 6.8 Hz), 1.73-1.84 (2H, m, O-(C=O)-(CH_2)$_4$-C*H*$_2$-CH_2), 1.76 (6H, s, 2xC*H*$_3$-(*Ar*)C-CH-CH-C), 1.63-1.71 (2H, m, O-(C=O)-CH_2-C*H*$_2$-(CH_2)$_4$), 1.67 (6H, s, 2xC*H*$_3$-(*Ar*)C-CH-CH-C), 1.53-1.63 (2H, m, O-(C=O)-(CH_2)$_2$-C*H*$_2$-(CH_2)$_3$), 1.46-1.54 (2H, m, O-(C=O)-(CH_2)$_3$-C*H*$_2$-(CH_2)$_2$), 1.36 (9H, s, S-CH_2-(*Ar*)C-CH-CH-C-C(C*H*$_3$)$_3$), 1.33 (9H, s, S-CH_2-(*Ar*)C-CH-CH-C-C(C*H*$_3$)$_3$), 1.04 (6H, t, 2xBF_2-N-C-C-CH_2-C*H*$_3$, $^3J_{H,H}$ = 7.5 Hz), 0.94 (6H, d, (*Ar*)C-CH-CH-C-CH(C*H*$_3$)$_2$, $^3J_{H,H}$ = 6.8 Hz), 0.89 (6H, d, (*Ar*)C-CH-CH-C-CH(C*H*$_3$)$_2$, $^3J_{H,H}$ = 6.8 Hz).

^{13}C-NMR ($CDCl_3$) δ_C, ppm: 172.1 (1C, O-(*C*=O)-CH_2), 152.1 (2C, 2xBF_2-N-*C*-CH_3), 151.9 (2C, 2xS-CH_2-(*Ar*)C-CH-CH-*C*-C(CH_3)$_3$), 151.8 (1C, S-(*Ar*)C-CH-CH-*C*-O), 151.2 (2C, 2xBF_2-N-*C*-CH_3), 145.1 (2C, 2xBF_2-N-*C*-C-CH_3), 136.87, 136.81 (2C, 2xS-CH_2-(*Ar*)*C*-CH-CH-C-C(CH_3)$_3$), 135.8 (2C, 2xBF_2-N-C-*C*-CH_3), 135.1 (1C, S-(*Ar*)*C*-CH-CH-C-O), 133.7 (2C, 2xS-(*Ar*)C-*C*H-CH-C-O), 132.7 (2C, 2xBF_2-N-C-*C*-CH_2-CH_3), 131.1 (1C, O-(C=O)-(CH_2)$_6$-*C*), 129.4, 129.3 (2C, 2xS-CH_2-(*Ar*)C-*C*H-CH-C-C(CH_3)$_3$), 125.7, 125.5 (2C, 2xS-CH_2-(*Ar*)C-CH-*C*H-C-C(CH_3)$_3$), 122.5 (2C, 2xS-(*Ar*)C-CH-*C*H-C-O), 107.2 (2C, 2xCH_3-(*Ar*)C-CH-CH-*C*), 100.7 (2C, 2xCH_3-(*Ar*)*C*-CH-CH-C), 84.3 (1C, CH_3-(*Ar*)C-CH-*C*H-C), 83.8 (2C, CH_3-(*Ar*)C-CH-*C*H-C, CH_3-(*Ar*)C-*C*H-CH-C), 82.7 (1C, CH_3-(*Ar*)C-*C*H-CH-C), 40.2 (1C, S-*C*H_2-(*Ar*)C-CH-CH-C-C(CH_3)$_3$), 39.7 (1C, S-*C*H_2-(*Ar*)C-CH-CH-C-C(CH_3)$_3$), 34.93 (1C, S-CH_2-(*Ar*)C-CH-CH-C-*C*(CH_3)$_3$), 34.88 (1C, S-CH_2-(*Ar*)C-CH-CH-C-*C*(CH_3)$_3$), 34.5 (1C, O-(C=O)-(CH_2)$_5$-*C*H_2), 32.0 (3C, S-CH_2-(*Ar*)C-CH-CH-C-C(*C*H_3)$_3$), 31.58 (3C, S-CH_2-(*Ar*)C-CH-CH-C-C(*C*H_3)$_3$), 31.55 (1C, O-(C=O)-CH_2-*C*H_2-(CH_2)$_4$), 31.0 (2C, 2x(*Ar*)CH-CH-C-*C*H(CH_3)$_2$), 30.4 (1C, O-(C=O)-(CH_2)$_2$-*C*H_2-(CH_2)$_3$), 29.8 (1C, O-(C=O)-(CH_2)$_5$-*C*H_2-(CH_2)$_2$), 29.5 (1C, O-(C=O)-(CH_2)$_6$-*C*H_2-CH_2), 29.4 (1C, O-(C=O)-(CH_2)$_7$-*C*H_2), 29.2 (1C, O-(C=O)-(CH_2)$_3$-*C*H_2-(CH_2)$_2$), 28.7 (1C, O-(C=O)-*C*H_2-(CH_2)$_5$), 24.9 (1C, O-(C=O)-(CH_2)$_4$-*C*H_2-CH_2), 23.2 (2C, (*Ar*)CH-CH-C-CH(*C*H_3)$_2$), 22.7 (2C, (*Ar*)CH-CH-C-CH(*C*H_3)$_2$), 18.3 (2C, 2x*C*H_3-(*Ar*)C-CH-CH), 17.3 (2C, 2xBF_2-N-C-C-*C*H_2-CH_3), 15.0 (2C, 2xBF_2-N-C-C-CH_2-*C*H_3), 13.5 (2C, 2xBF_2-N-C-C-*C*H_3), 12.5 (2C, t, 2xBF_2-N-C-*C*H_3, $^3J_{C,B}$ = 3 Hz).

^{19}F-NMR ($CDCl_3$) δ_C, ppm: -146.00 (2F, m,B*F*$_2$).

^{11}B-NMR ($CDCl_3$) δ_C, ppm: 0.63 (1B, t, *B*F_2, $^1J_{B,F}$ = 32.4 Hz).

R_f (CH_2Cl_2/CH_3OH 10:1) = 0.305.

ESI-MS(+):*m/z* found 1397.5085 $[M-Cl]^+$, calcd. for $C_{74}H_{100}BF_2N_2O_2Ru_2S_3^+$ 1397.5090.
Elemental analysis (%): calcd. for $C_{74}H_{100}BClF_2N_2O_2Ru_2S_3 \cdot 0.25CH_2Cl_2 \cdot CH_3OH$ C 60.84, H 7.09, N 1.89; found C 60.91, H 7.09, N 1.80.

The amide conjugates BODIPY – dinuclear trithiolato ruthenium(II)-*p*-cymene complexes were prepared by adapting a literature procedure[175].

Synthesis of [(η^6-*p*-$MeC_6H_4Pr^i$)$_2$Ru$_2$(μ_2-$SCH_2C_6H_4$-*p*-Bu^t)$_2$(μ_2-SC_6H_4-*p*-NH-(CO)R)]Cl (R = 4,4-difluoro-8-(2-ethan-1-yl)-1,3,5,7-tetramethyl-2,6-diethyl-4-bora-3a,4a-diaza-*s*-indacene) (1.2.23)

To a solution of **1.2.9** (0.099 g, 0.263 mmol, 1.3 equiv.) in dry CH_2Cl_2 (20 mL) at r.t. under inert atmosphere (N_2) were added HOBt·H_2O (0.067 g, 0.485 mmol, 2.4 equiv.) and DIPEA (0.1mL, 0.505 mmol, 2.5 equiv.). After 15 min have been added successively EDCI (0.116 g, 0.606 mmol, 3 equiv.), **1.2.3** (0.200 g, 0.202 mmol, 1 equiv.) and DIPEA (0.1 mL, 0.505 mmol, 2.5 equiv.). The reaction mixture was stirred at r.t. under inert atmosphere (N_2) for further 72 h and the reaction evolution was verified by TLC (CH_2Cl_2/CH_3OH 10:1 (v/v)). The reaction mixture was concentrated to dryness and purification by column chromatography using CH_2Cl_2/CH_3OH afforded **1.2.23** as an orange-pink solid (0.202 g, 0.150 mmol, yield 74%).

^{1}H-NMR ($CDCl_3$) δ_H, ppm: 11.71 (1H, s, (Ar)C-N*H*-(C=O)), 8.24 (2H, d, 2xS-(*Ar*)C-CH-C*H*-C-NH, $^3J_{H,H}$ = 8.5 Hz), 7.59 (2H, d, 2xS-(*Ar*)C-C*H*-CH-C-NH, $^3J_{H,H}$ = 8.5 Hz), 7.39-7.52 (8H, m, 4xCH_2-(*Ar*)C-C*H*-CH-C-C(CH_3)$_3$, 4xCH_2-(*Ar*)C-CH-C*H*-C-C(CH_3)$_3$), 4.99 (2H, d, 2xCH_3-(*Ar*)C-CH-C*H*-C, $^3J_{H,H}$ = 5.7 Hz), 4.88 (2H, d, 2xCH_3-(*Ar*)C-C*H*-CH-C, $^3J_{H,H}$ = 5.7 Hz), 4.67 (2H, d, 2xCH_3-(*Ar*)C-CH-C*H*-C, $^3J_{H,H}$ = 5.7 Hz), 4.62 (2H, d, 2xCH_3-(*Ar*)C-C*H*-CH-C, $^3J_{H,H}$ = 5.7 Hz), 3.55 (2H, s, C*H*$_2$-(*Ar*)C-CH-CH-C-C(CH_3)$_3$), 3.46-3.50 (2H, m, NH-(C=O)-C*H*$_2$-CH_2), 3.36 (2H, s, C*H*$_2$-(*Ar*)C-CH-CH-C-C(CH_3)$_3$), 3.07-3.11 (2H, m, NH-(C=O)-CH_2-C*H*$_2$), 2.50 (6H, s, 2xBF_2-N-C-C*H*$_3$), 2.49 (6H, s, 2xBF_2-N-C-C-C*H*$_3$), 2.39 (4H, qvart, 2xBF_2-N-C-C-C*H*$_2$-CH_3, $^3J_{H,H}$ = 7.5 Hz), 2.03 (2H, sept, 2x(*Ar*)C-CH-CH-C-C*H*(CH_3)$_2$, $^3J_{H,H}$ = 6.9 Hz), 1.66 (6H, s, 2xC*H*$_3$-(*Ar*)C-CH-CH-C), 1.38 (9H, s, S-CH_2-(*Ar*)C-CH-CH-C-C(C*H*$_3$)$_3$), 1.36 (9H, s, S-CH_2-(*Ar*)C-CH-CH-C-C(C*H*$_3$)$_3$), 1.05 (6H, t, 2xBF_2-N-C-C-CH_2-C*H*$_3$, $^3J_{H,H}$ = 7.5 Hz), 1.01 (6H, d, 2x(*Ar*)C-CH-CH-C-CH(C*H*$_3$)$_2$, $^3J_{H,H}$ = 6.9 Hz), 0.96 (6H, d, 2x(*Ar*)C-CH-CH-C-CH(C*H*$_3$)$_2$, $^3J_{H,H}$ = 6.9 Hz).

^{13}C-NMR ($CDCl_3$) δ_C, ppm: 171.8 (1C, NH-(*C*=O)-CH_2), 152.2 (2C, 2xBF_2-N-*C*-CH_3), 152.1 (2C, 2xS-CH_2-(*Ar*)C-CH-CH-*C*-C(CH_3)$_3$), 143.7 (2C, 2xBF_2-N-*C*-C-CH_3), 141.5 (1C, S-(*Ar*)*C*-CH-CH-C-NH), 136.9, 136.7 (2C, 2xS-CH_2-(*Ar*)*C*-CH-CH-C-C(CH_3)$_3$), 136.5 (2C, 2xBF_2-N-C-*C*-CH_3), 132.7 (2C, 2xS-(*Ar*)C-*C*H-CH-C-NH), 132.6 (2C, 2xBF_2-N-C-*C*-CH_2-CH_3), 131.3 (1C, NH-(C=O)-(CH_2)$_2$-*C*), 129.5 (1C, S-(*Ar*)C-CH-CH-*C*-NH), 129.3, 129.1 (2C, 2xS-CH_2-(*Ar*)C-*C*H-CH-C-C(CH_3)$_3$), 125.73, 125.69 (2C, 2xS-CH_2-(*Ar*)C-CH-*C*H-C-C(CH_3)$_3$), 120.8 (2C, 2xS-(*Ar*)C-CH-*C*H-C-NH), 107.9 (2C, 2xCH_3-(*Ar*)C-CH-CH-*C*), 100.1 (2C, 2xCH_3-(*Ar*)*C*-CH-CH-C), 84.5 (1C, CH_3-(*Ar*)C-CH-*C*H-C), 84.0 (1C, CH_3-(*Ar*)C-*C*H-CH-C), 83.0 (1C, CH_3-(*Ar*)C-CH-*C*H-C), 82.2 (1C, CH_3-(*Ar*)C-*C*H-CH-C), 39.9 (1C, S-*C*H_2-(*Ar*)C-CH-CH-C-C(CH_3)$_3$), 39.2 (1C, S-*C*H_2-(*Ar*)C-CH-CH-C-C(CH_3)$_3$), 37.3 (1C,NH-(C=O)-CH_2-C*H*$_2$), 34.96 (1C, S-CH_2-(*Ar*)C-CH-CH-C-*C*(CH_3)$_3$), 34.94 (1C, S-CH_2-(*Ar*)C-CH-CH-C-*C*(CH_3)$_3$), 31.57, 31.55 (6C, 2xS-CH_2-(*Ar*)C-CH-CH-C-C(*C*H_3)$_3$), 31.2 (2C, 2x(*Ar*)CH-CH-C-*C*H(CH_3)$_2$), 24.3 (1C, NH-(C=O)-*C*H_2-CH_2), 23.1 (4C, 2x(*Ar*)CH-CH-C-CH(*C*H_3)$_2$), 18.1 (2C, 2x*C*H_3-(*Ar*)C-CH-CH), 17.4 (2C, 2xBF_2-N-C-C-*C*H_2-CH_3), 15.0 (2C, 2xBF_2-N-C-C-CH_2-*C*H_3), 14.0 (2C, 2xBF_2-N-C-C-*C*H_3), 12.6 (2C, m, 2xBF_2-N-C-*C*H_3).

^{19}F-NMR ($CDCl_3$) δ_C, ppm: -145.55, -146.04 (2F, m,B*F*$_2$).

^{11}B-NMR ($CDCl_3$) δ_C, ppm: 0.67 (1B, t, *B*F_2, $^1J_{B,F}$ = 31.5 Hz).

R_f (CH_2Cl_2/CH_3OH 10:1) = 0.611.

ESI-MS(+):*m/z* found 1312.4344 $[M-Cl]^+$, calcd. for $C_{68}H_{89}BF_2N_3ORu_2S_3^+$ 1312.4310.

Elemental analysis (%): calcd. for $C_{68}H_{89}BClF_2N_3ORu_2S_3 \cdot 0.35CH_2Cl_2 \cdot CH_3OH$ C 59.12, H 6.70, N 2.98; found C 59.13, H 6.76, N 2.99.

Synthesis of[(η^6-*p*-$MeC_6H_4Pr^i$)$_2$$Ru_2$($\mu_2$-$SCH_2C_6H_4$-*p*-$Bu^t$)$_2$($\mu_2$-$SC_6H_4$-*p*-NH-(CO)R)]Cl (R = 4,4-difluoro-8-(4-butan-1-yl)-1,3,5,7-tetramethyl-2,6-diethyl-4-bora-3a,4a-diaza-*s*-indacene) (1.2.24)

To a solution of **1.2.10** (0.082 g, 0.202 mmol, 1 equiv.) in dry CH_2Cl_2 (20 mL) at r.t., under inert atmosphere (N_2) were added HOBt·H_2O (0.067 g, 0.485 mmol, 2.4 equiv.) and DIPEA (0.1 mL, 0.505 mmol, 2.5 equiv.). After 15 min have been added successively EDCI (0.116 g, 0.606 mmol, 3 equiv.), **1.2.3** (0.200 g, 0.202 mmol, 1 equiv.) and DIPEA (0.1 mL, 0.505 mmol, 2.5 equiv.). The reaction mixture was stirred at r.t. under inert atmosphere (N_2) for further 72 h and the reaction evolution was verified by TLC (CH_2Cl_2/CH_3OH 10:1 (v/v)). The reaction mixture was concentrated to dryness under reduced pressure and purification by column chromatography using CH_2Cl_2/CH_3OH mixture afforded **1.2.24** as a pink-orange solid (0.085 g, 0.062 mmol, yield 31%).

^{1}H-NMR ($CDCl_3$) δ_H, ppm: 8.45 (2H, d, 2xS-(*Ar*)C-CH-C*H*-C-NH, $^3J_{H,H}$ = 8.7 Hz), 7.56 (2H, d, 2xS-(*Ar*)C-CH-C*H*-C-NH, $^3J_{H,H}$ = 8.7 Hz), 7.39-7.52 (8H, m, 4xCH_2-(*Ar*)C-C*H*-CH-C-C(CH_3)$_3$, 4xCH_2-(*Ar*)C-CH-C*H*-C-C(CH_3)$_3$), 4.97 (2H, d, 2xCH_3-(*Ar*)C-CH-C*H*-C, $^3J_{H,H}$ = 5.7 Hz), 4.87 (2H, d, 2xCH_3-(*Ar*)C-C*H*-CH-C, $^3J_{H,H}$ = 5.7 Hz), 4.68 (2H, d, 2xCH_3-(*Ar*)C-CH-C*H*-C, $^3J_{H,H}$ = 5.7 Hz), 4.61 (2H, d, 2xCH_3-(*Ar*)C-C*H*-CH-C, $^3J_{H,H}$ = 5.7 Hz), 3.54 (2H, s, C*H*$_2$-(*Ar*)C-CH-CH-C-C(CH_3)$_3$), 3.35 (2H, s, C*H*$_2$-(*Ar*)C-CH-CH-C-C(CH_3)$_3$), 3.05-3.09 (2H, m, NH-(C=O)-C*H*$_2$-(CH_2)$_3$), 2.84 (2H, t, NH-(C=O)-(CH_2)$_3$-C*H*$_2$, $^3J_{H,H}$ = 7.3 Hz), 2.48 (6H, s, 2xBF_2-N-C-C*H*$_3$), 2.40 (6H, s, 2xBF_2-N-C-C-C*H*$_3$), 2.39 (4H, qvart, 2xBF_2-N-C-C-C*H*$_2$-CH_3, $^3J_{H,H}$ = 7.5 Hz), 2.00 (2H, sept, 2x(*Ar*)C-CH-CH-C-C*H*(CH_3)$_2$, $^3J_{H,H}$ = 6.9 Hz), 1.99 (2H, qvint, NH-(C=O)-(CH_2)$_2$-C*H*$_2$-CH_2, $^3J_{H,H}$ = 7.3 Hz), 1.72-1.84 (2H, m, NH-(C=O)-CH_2-C*H*$_2$-(CH_2)$_2$), 1.66 (6H, s, 2xC*H*$_3$-(*Ar*)C-CH-CH-C), 1.37 (9H, s, S-CH_2-(*Ar*)C-CH-CH-C-C(C*H*$_3$)$_3$), 1.35 (9H, s, S-CH_2-(*Ar*)C-CH-CH-C-C(C*H*$_3$)$_3$), 1.04 (6H, t, 2xBF_2-N-C-C-CH_2-C*H*$_3$, $^3J_{H,H}$ = 7.5 Hz), 0.99 (6H, d, 2x(*Ar*)C-CH-CH-C-CH(C*H*$_3$)$_2$, $^3J_{H,H}$ = 6.9 Hz), 0.94 (6H, d, 2x(*Ar*)C-CH-CH-C-CH(C*H*$_3$)$_2$, $^3J_{H,H}$ = 6.9 Hz).

^{13}C-NMR ($CDCl_3$) δ_C, ppm: 173.6 (1C, NH-(*C*=O)-CH_2), 152.2 (2C, 2xS-CH_2-(*Ar*)C-CH-CH-*C*-C(CH_3)$_3$), 151.9 (2C, 2xBF_2-N-*C*-CH_3), 145.5 (2C, 2xBF_2-N-*C*-C-CH_3), 141.9 (1C, S-(*Ar*)*C*-CH-CH-C-NH), 137.0 (2C, 2xBF_2-N-C-*C*-CH_3), 136.6 (2C, 2xS-CH_2-(*Ar*)*C*-CH-CH-C-C(CH_3)$_3$), 132.8 (2C, 2xS-(*Ar*)C-*C*H-CH-C-NH), 132.6 (2C, 2xBF_2-N-C-*C*-CH_2-CH_3), 131.3 (1C, NH-(C=O)-(CH_2)$_4$-*C*), 129.4, 129.2 (2C, 2xS-CH_2-(*Ar*)C-*C*H-CH-C-C(CH_3)$_3$), 129.1 (1C, S-(*Ar*)C-CH-CH-*C*-NH), 125.83, 125.79 (2C, 2xS-CH_2-(*Ar*)C-CH-*C*H-C-C(CH_3)$_3$), 120.6 (2C, 2xS-(*Ar*)C-CH-*C*H-C-NH), 108.0 (2C, 2xCH_3-(*Ar*)C-CH-CH-*C*), 100.2 (2C, 2xCH_3-(*Ar*)*C*-CH-CH-C), 84.5 (1C, CH_3-(*Ar*)C-CH-*C*H-C), 84.0 (1C, CH_3-(*Ar*)C-*C*H-CH-C), 83.3 (1C, CH_3-(*Ar*)C-CH-*C*H-C), 82.3 (1C, CH_3-(*Ar*)C-*C*H-CH-C), 40.0 (1C, S-*C*H_2-(*Ar*)C-CH-CH-C-C(CH_3)$_3$), 39.3 (1C, S-*C*H_2-(*Ar*)C-CH-CH-C-C(CH_3)$_3$), 37.0 (1C, NH-(C=O)-(CH_2)$_3$-C*H*$_2$), 35.06 (1C, S-CH_2-(*Ar*)C-CH-CH-C-*C*(CH_3)$_3$), 35.03 (1C, S-CH_2-(*Ar*)C-CH-CH-C-*C*(CH_3)$_3$), 31.67, 31.65 (6C, 2xS-CH_2-(*Ar*)C-CH-CH-C-C(*C*H_3)$_3$), 31.34 (1C, NH-(C=O)-CH_2-*C*H_2-(CH_2)$_2$), 31.25 (2C, 2x(*Ar*)CH-CH-C-*C*H(CH_3)$_2$), 28.7 (1C, NH-(C=O)-*C*H_2-(CH_2)$_3$), 26.4 (1C, NH-(C=O)-(CH_2)$_2$-*C*H_2-CH_2), 23.21 (2C, (*Ar*)CH-CH-C-CH(*C*H_3)$_2$), 23.14 (2C, (*Ar*)CH-CH-C-CH(*C*H_3)$_2$), 18.2 (2C, 2x*C*H_3-(*Ar*)C-CH-CH), 17.4 (2C, 2xBF_2-N-C-C-*C*H_2-CH_3), 15.1 (2C, 2xBF_2-N-C-C-CH_2-*C*H_3), 13.8 (2C, 2xBF_2-N-C-C-*C*H_3), 12.6 (2C, m, 2xBF_2-N-C-*C*H_3).

^{19}F-NMR ($CDCl_3$) δ_C, ppm: -145.87, -146.00 (2F,dt,B*F*$_2$, $^1J_{B,F}$ = 26.1 Hz, $^2J_{F,F}$ = 36.0 Hz).

^{11}B-NMR ($CDCl_3$) δ_C, ppm: 0.66 (1B, t, *B*F_2, $^1J_{B,F}$ = 31.6 Hz).

R_f (CH_2Cl_2/CH_3OH 10:1) = 0.500.

ESI-MS(+):*m/z* found 1340.4575 $[M\text{-}Cl]^+$, calcd. for $C_{70}H_{93}BF_2N_3ORu_2S_3^+$ 1340.4623.

Elemental analysis (%): calcd. for $C_{70}H_{98}BClF_2N_3ORu_2S_3 \cdot 2H_2O \cdot 0.5CH_2Cl_2$ C 58.25, H 6.80, N,

2.89; found C 58.19, H 6.88, N, 2.99.

Synthesis of [(η^6-*p*-MeC$_6$H$_4$Pr^i)$_2$Ru$_2$(μ_2-SCH$_2$C$_6$H$_4$-*p*-Bu^t)$_2$(μ_2-SC$_6$H$_4$-*p*-NH-(CO)R)]Cl (R = 4,4-difluoro-8-(6-hexan-1-yl)-1,3,5,7-tetramethyl-2,6-diethyl-4-bora-3a,4a-diaza-*s*-indacene) (1.2.25)

To a solution of **1.2.11** (0.070 g, 0.162 mmol, 1.3 equiv.) in dry CH_2Cl_2 (20 mL) at r.t., under inert atmosphere (N_2) were added HOBt·H_2O (0.042 g, 0.300 mmol, 2.4 equiv.) and DIPEA (0.05mL, 0.313 mmol, 2.5 equiv.). After 15 min have been added successively EDCI (0.072 g, 0.0.375 mmol, 3 equiv.), **1.2.3** (0.124 g, 0.125 mmol, 1 equiv.) and DIPEA (0.05 mL, 0.313 mmol, 2.5 equiv.). The reaction mixture was stirred at r.t. under inert atmosphere (N_2) for further 72 h and the reaction evolution was verified by TLC (CH_2Cl_2/CH_3OH 10:1 (v/v)). The reaction mixture was concentrated to dryness under reduced pressure and purification by column chromatography using CH_2Cl_2/CH_3OH mixture afforded **1.2.25** as a pink-orange solid (0.115 g, 0.082 mmol, yield 66%).

^{1}H-NMR ($CDCl_3$) δ_H, ppm: 8.18 (2H, d, 2xS-(*Ar*)C-CH-C*H*-C-NH, $^3J_{H,H}$ = 8.7 Hz), 7.56 (2H, d, 2xS-(*Ar*)C-CH-C*H*-C-NH, $^3J_{H,H}$ = 8.7 Hz), 7.39-7.49 (8H, m, 4xCH_2-(*Ar*)C-C*H*-CH-C-C(CH_3)$_3$, 4xCH_2-(*Ar*)C-CH-C*H*-C-C(CH_3)$_3$), 4.98 (2H, d, 2xCH_3-(*Ar*)C-CH-C*H*-C, $^3J_{H,H}$ = 5.8 Hz), 4.87 (2H, d, 2xCH_3-(*Ar*)C-C*H*-CH-C, $^3J_{H,H}$ = 5.7 Hz), 4.68 (2H, d, 2xCH_3-(*Ar*)C-CH-C*H*-C, $^3J_{H,H}$ = 5.8 Hz), 4.61 (2H, d, 2xCH_3-(*Ar*)C-C*H*-CH-C, $^3J_{H,H}$ = 5.7 Hz), 3.54 (2H, s, C*H*$_2$-(*Ar*)C-CH-CH-C-C(CH_3)$_3$), 3.35 (2H, s, C*H*$_2$-(*Ar*)C-CH-CH-C-C(CH_3)$_3$), 2.96-3.00 (2H, m, NH-(C=O)-C*H*$_2$-(CH_2)$_5$), 2.76 (2H, t, NH-(C=O)-(CH_2)$_5$-C*H*$_2$, $^3J_{H,H}$ = 7.4 Hz), 2.47 (6H, s, 2xBF_2-N-C-C*H*$_3$), 2.39 (4H, qvart, 2xBF_2-N-C-C-C*H*$_2$-CH_3, $^3J_{H,H}$ = 7.6 Hz), 2.34 (6H, s, 2xBF_2-N-C-C-C*H*$_3$), 2.00 (2H, sept, 2x(*Ar*)C-CH-CH-C-C*H*(CH_3)$_2$, $^3J_{H,H}$ = 6.9 Hz), 1.79 (2H, qvint, NH-(C=O)-(CH_2)$_4$-C*H*$_2$-CH_2, $^3J_{H,H}$ = 7.2 Hz), 1.66 (6H, s, 2xC*H*$_3$-(*Ar*)C-CH-CH-C), 1.60-1.68 (2H, m, NH-(C=O)-CH_2-C*H*$_2$-(CH_2)$_4$), 1.48-1.60 (4H, m, NH-(C=O)-(CH_2)$_3$-C*H*$_2$-(CH_2)$_2$, NH-(C=O)-(CH_2)$_2$-C*H*$_2$-(CH_2)$_3$,), 1.37 (9H, s, S-CH_2-(*Ar*)C-CH-CH-C-C(C*H*$_3$)$_3$), 1.35 (9H, s, S-CH_2-(*Ar*)C-CH-CH-C-C(C*H*$_3$)$_3$), 1.04 (6H, t, 2xBF_2-N-C-C-CH_2-C*H*$_3$, $^3J_{H,H}$ = 7.5 Hz), 0.99 (6H, d, 2x(*Ar*)C-CH-CH-C-CH(C*H*$_3$)$_2$, $^3J_{H,H}$ = 6.9 Hz), 0.94 (6H, d, 2x(*Ar*)C-CH-CH-C-CH(C*H*$_3$)$_2$, $^3J_{H,H}$ = 6.9 Hz).

^{13}C-NMR ($CDCl_3$) δ_C, ppm: 174.2 (1C, NH-(*C*=O)-CH_2), 152.0 (2C, 2xS-CH_2-(*Ar*)C-CH-CH-*C*-C(CH_3)$_3$), 145.5 (2C, 2xBF_2-N-*C*-CH_3), 145.5 (2C, 2xBF_2-N-*C*-C-CH_3), 141.8 (1C, S-(*Ar*)*C*-CH-CH-C-NH), 136.9 (2C, 2xBF_2-N-C-*C*-CH_3), 136.5, 136.2 (2C, 2xS-CH_2-(*Ar*)*C*-CH-CH-C-C(CH_3)$_3$), 132.6 (2C, 2xS-(*Ar*)C-*C*H-CH-C-NH), 132.5 (2C, 2xBF_2-N-C-*C*-CH_2-CH_3), 131.1 (1C, NH-(C=O)-(CH_2)$_6$-*C*), 129.3, 129.1 (2C, 2xS-CH_2-(*Ar*)C-*C*H-CH-C-C(CH_3)$_3$), 129.9 (1C, S-(*Ar*)C-CH-CH-*C*-NH), 125.72, 125.68 (2C, 2xS-CH_2-(*Ar*)C-CH-*C*H-C-C(CH_3)$_3$), 120.5 (2C, 2xS-(*Ar*)C-CH-*C*H-C-NH), 107.8 (2C, 2xCH_3-(*Ar*)C-CH-CH-*C*), 100.1 (2C, 2xCH_3-(*Ar*)*C*-CH-CH-C), 84.4 (1C, CH_3-(*Ar*)C-*C*H-CH-C), 83.9 (1C, CH_3-(*Ar*)C-CH-*C*H-C), 83.2 (1C, CH_3-(*Ar*)C-CH-*C*H-C), 82.2 (1C, CH_3-(*Ar*)C-*C*H-CH-C), 39.9 (1C, S-*C*H_2-(*Ar*)C-CH-CH-C-C(CH_3)$_3$), 39.2 (1C, S-*C*H_2-(*Ar*)C-CH-CH-C-C(CH_3)$_3$), 37.3 (1C, NH-(C=O)-(CH_2)$_5$-C*H*$_2$), 34.95 (1C, S-CH_2-(*Ar*)C-CH-CH-C-*C*(CH_3)$_3$), 34.93 (1C, S-CH_2-(*Ar*)C-CH-CH-C-*C*(CH_3)$_3$), 31.9 (1C, NH-(C=O)-CH_2-*C*H_2-(CH_2)$_4$), 31.57, 31.55 (6C, 2xS-CH_2-(*Ar*)C-CH-CH-C-C(*C*H_3)$_3$), 31.2 (2C, 2x(*Ar*)CH-CH-C-*C*H(CH_3)$_2$), 30.6 (1C, NH-(C=O)-(CH_2)$_2$-*C*H_2-(CH_2)$_3$), 29.2 (1C, NH-(C=O)-(CH_2)$_3$-*C*H_2-(CH_2)$_2$), 28.8 (1C, NH-(C=O)-*C*H_2-(CH_2)$_5$), 26.0 (1C, NH-(C=O)-(CH_2)$_4$-*C*H_2-CH_2), 23.1 (2C, (*Ar*)CH-CH-C-CH(*C*H_3)$_2$), 23.0 (2C, (*Ar*)CH-CH-C-CH(*C*H_3)$_2$), 18.1 (2C, 2x*C*H_3-(*Ar*)C-CH-CH), 17.3 (2C, 2xBF_2-N-C-C-*C*H_2-CH_3), 15.0 (2C, 2xBF_2-N-C-C-CH_2-*C*H_3), 13.6 (2C, 2xBF_2-N-C-C-*C*H_3), 12.5 (2C, m, 2xBF_2-N-C-*C*H_3).

^{19}F-NMR ($CDCl_3$) δ_C, ppm: -145.93, -146.16 (2F, dt, B*F*$_2$, $^1J_{B,F}$ = 31.7 Hz, $^2J_{F,F}$ = 33.9 Hz).

^{11}B-NMR ($CDCl_3$) δ_C, ppm: 0.64 (1B, t, *B*F_2, $^1J_{B,F}$ = 32.0 Hz),

R_f (CH_2Cl_2/CH_3OH 10:1) = 0.611.

ESI-MS(+): *m/z* found 1368.4966 $[M-Cl]^+$, calcd. for $C_{72}H_{97}BF_2N_3ORu_2S_3^+$ 1368.4936.

Elemental analysis (%): calcd. for $C_{72}H_{97}BClF_2N_3ORu_2S_3 \cdot 1.5CH_2Cl_2$ C 59.05, H 6.74, N 2.81; found C 59.08, H 6.85, N 2.86.

Synthesis of the amide conjugate [(η^6-*p*-MeC$_6$H$_4$Pr^i)$_2$Ru$_2$(μ_2-SCH$_2$C$_6$H$_4$-*p*-Bu^t)$_2$(μ_2-SC$_6$H$_4$-*p*-NH-(CO)R)]Cl (R = 4,4-difluoro-8-(8-octan-1-yl)-1,3,5,7-tetramethyl-2,6-diethyl-4-bora-3a,4a-diaza-*s*-indacene) (1.2.26)

To a solution of **1.2.12** (0.121 g, 0.263 mmol, 1.3 equiv.) in dry CH_2Cl_2 (20 mL) at r.t. under inert atmosphere (N_2) were added HOBt·H_2O (0.067 g, 0.485 mmol, 2.4 equiv.) and DIPEA (0.1mL, 0.505 mmol, 2.5 equiv.). After 15 min have been added successively EDCI (0.116 g, 0.606 mmol, 3 equiv.), **1.2.3** (0.200 g, 0.202 mmol, 1 equiv.) and DIPEA (0.1 mL, 0.505 mmol, 2.5 equiv.). The reaction mixture was stirred at r.t. under inert atmosphere (N_2) for further 72 h and the reaction evolution was verified by TLC (CH_2Cl_2/CH_3OH 10:1 (v/v)). The reaction mixture was concentrated to dryness under reduced pressure and purification by column chromatography using CH_2Cl_2/CH_3OH afforded **1.2.26** as a pink-orange solid (0.063 g, 0.044 mmol, yield 22%).

^{1}H-NMR ($CDCl_3$) δ_H, ppm: 11.00 (1H, N*H*-(C=O)-CH$_2$), 8.13 (2H, d, 2xS-(*Ar*)C-C*H*-CH-C-NH, $^3J_{H,H}$ = 8.7 Hz), 7.56 (2H, d, 2xS-(*Ar*)C-CH-C*H*-C-NH, $^3J_{H,H}$ = 8.7 Hz), 7.39-7.49 (8H, m, 4xCH$_2$-(*Ar*)C-C*H*-CH-C-C(CH$_3$)$_3$, 4xCH$_2$-(*Ar*)C-CH-C*H*-C-C(CH$_3$)$_3$), 4.97 (2H, d, 2xCH$_3$-(*Ar*)C-CH-C*H*-C, $^3J_{H,H}$ = 5.8 Hz), 4.87 (2H, d, 2xCH$_3$-(*Ar*)C-C*H*-CH-C, $^3J_{H,H}$ = 5.8 Hz), 4.68 (2H, d, 2xCH$_3$-(*Ar*)C-CH-C*H*-C, $^3J_{H,H}$ = 5.8 Hz), 4.60 (2H, d, 2xCH$_3$-(*Ar*)C-C*H*-CH-C, $^3J_{H,H}$ = 5.8 Hz), 3.54 (2H, s, C*H$_2$*-(*Ar*)C-CH-CH-C-C(CH$_3$)$_3$), 3.35 (2H, s, C*H$_2$*-(*Ar*)C-CH-CH-C-C(CH$_3$)$_3$), 2.94-2.98 (2H, m, NH-(C=O)-C*H$_2$*-(CH$_2$)$_5$), 2.71 (2H, t, NH-(C=O)-(CH$_2$)$_7$-C*H$_2$*, $^3J_{H,H}$ = 7.5 Hz), 2.48 (6H, s, 2xBF$_2$-N-C-C-C*H$_3$*), 2.39 (4H, qvart, 2xBF$_2$-N-C-C-C*H$_2$*-CH$_3$, $^3J_{H,H}$ = 7.5 Hz), 2.33 (6H, s, 2xBF$_2$-N-C-C*H$_3$*), 2.00 (2H, sept, 2x(*Ar*)C-CH-CH-C-C*H*(CH$_3$)$_2$, $^3J_{H,H}$ = 6.8 Hz), 1.74 (2H, pent., NH-(C=O)-(CH$_2$)$_4$-C*H$_2$*-CH$_2$), 1.66 (6H, s, 2xC*H$_3$*-(*Ar*)C-CH-CH-C), 1.63-1.71 (2H, m, NH-(C=O)-CH$_2$-C*H$_2$*-(CH$_2$)$_4$), 1.53-1.63 (2H, m, NH-(C=O)-(CH$_2$)$_2$-C*H$_2$*-(CH$_2$)$_3$), 1.46-1.54 (2H, m, NH-(C=O)-(CH$_2$)$_3$-C*H$_2$*-(CH$_2$)$_2$), 1.37 (9H, s, S-CH$_2$-(*Ar*)C-CH-CH-C-C(C*H$_3$*)$_3$), 1.34 (9H, s, S-CH$_2$-(*Ar*)C-CH-CH-C-C(C*H$_3$*)$_3$), 1.04 (6H, t, 2xBF$_2$-N-C-C-CH$_2$-C*H$_3$*, $^3J_{H,H}$ = 7.5 Hz), 0.99 (6H, d, (*Ar*)C-CH-CH-C-CH(C*H$_3$*)$_2$, $^3J_{H,H}$ = 6.8 Hz), 0.94 (6H, d, (*Ar*)C-CH-CH-C-CH(C*H$_3$*)$_2$, $^3J_{H,H}$ = 6.8 Hz).

^{13}C-NMR ($CDCl_3$) δ_C, ppm: 174.3 (1C, NH-(*C*=O)-CH$_2$), 152.0 (2C, 2xBF$_2$-N-*C*-CH$_3$), 151.9 (2C, 2xS-CH$_2$-(*Ar*)C-CH-CH-*C*-C(CH$_3$)$_3$), 145.5 (2C, 2xBF$_2$-N-*C*-C-CH$_3$), 141.7 (1C, S-(*Ar*)C-CH-CH-*C*-NH), 136.8, 136.5 (2C, 2xS-CH$_2$-(*Ar*)*C*-CH-CH-C-C(CH$_3$)$_3$), 136.1 (2C, 2xBF$_2$-N-C-*C*-CH$_3$), 132.7 (2C, 2xBF$_2$-N-C-*C*-CH$_2$-CH$_3$), 132.6(2C, 2xS-(*Ar*)C-*C*H-CH-C-NH),132.7 (2C, 2xBF$_2$-N-C-*C*-CH$_2$-CH$_3$), 131.1 (1C, NH-(C=O)-(CH$_2$)$_6$-*C*), 129.1, 129.0 (2C, 2xS-CH$_2$-(*Ar*)C-*C*H-CH-C-C(CH$_3$)$_3$), 125.71, 125.66 (2C, 2xS-CH$_2$-(*Ar*)C-CH-*C*H-C-C(CH$_3$)$_3$), 120.5 (1C, S-(*Ar*)*C*-CH-CH-C-NH), 122.5 (2C, 2xS-(*Ar*)C-CH-*C*H-C-NH), 107.8 (2C, 2xCH$_3$-(*Ar*)C-CH-CH-*C*), 100.1 (2C, 2xCH$_3$-(*Ar*)*C*-CH-CH-C), 84.3 (1C, CH$_3$-(*Ar*)C-CH-*C*H-C), 83.8 (1C, CH$_3$-(*Ar*)C-*C*H-CH-C), 83.2 (1C, CH$_3$-(*Ar*)C-*C*H-CH-C), 82.2 (1C, CH$_3$-(*Ar*)C-CH-*C*H-C), 39.9 (1C, S-*C*H$_2$-(*Ar*)C-CH-CH-C-C(CH$_3$)$_3$), 39.2 (1C, S-*C*H$_2$-(*Ar*)C-CH-CH-C-C(CH$_3$)$_3$), 37.4 (1C, NH-(C=O)-(CH$_2$)$_7$-*C*H$_2$), 34.94 (1C, S-CH$_2$-(*Ar*)C-CH-CH-C-*C*(CH$_3$)$_3$), 34.92 (1C, S-CH$_2$-(*Ar*)C-CH-CH-C-*C*(CH$_3$)$_3$), 34.5 (1C, NH-(C=O)-(CH$_2$)$_5$-*C*H$_2$), 32.0 (3C, S-CH$_2$-(*Ar*)C-CH-CH-C-C(*C*H$_3$)$_3$), 31.56 (3C, S-CH$_2$-(*Ar*)C-CH-CH-C-C(*C*H$_3$)$_3$), 31.54 (1C, NH-(C=O)-CH$_2$-*C*H$_2$-(CH$_2$)$_6$), 31.1 (2C, 2x(*Ar*)CH-CH-C-*C*H(CH$_3$)$_2$), 30.8 (1C, NH-(C=O)-(CH$_2$)$_2$-*C*H$_2$-(CH$_2$)$_5$), 30.6 (1C, NH-(C=O)-(CH$_2$)$_3$-*C*H$_2$-(CH$_2$)$_4$), 29.8 (1C, NH-(C=O)-(CH$_2$)$_4$-*C*H$_2$-(CH$_2$)$_3$), 29.5 (1C, NH-(C=O)-(CH$_2$)$_5$-*C*H$_2$-(CH$_2$)$_2$), 29.4 (1C, NH-(C=O)-(CH$_2$)$_6$-*C*H$_2$-CH$_2$), 29.2 (1C, NH-(C=O)-(CH$_2$)$_7$-*C*H$_2$), 28.7 (1C, NH-(C=O)-*C*H$_2$-(CH$_2$)$_5$), 25.8 (1C, NH-(C=O)-(CH$_2$)$_2$-*C*H$_2$-CH$_2$), 24.9 (1C, NH-(C=O)-(CH$_2$)$_4$-*C*H$_2$-CH$_2$), 23.1 (2C, (*Ar*)CH-CH-C-CH(*C*H$_3$)$_2$), 23.0 (2C, (*Ar*)CH-CH-C-CH(*C*H$_3$)$_2$), 18.1 (2C, 2x*C*H$_3$-(*Ar*)C-CH-CH), 17.3 (2C, 2xBF$_2$-N-C-C-*C*H$_2$-CH$_3$), 15.0 (2C, 2xBF$_2$-N-C-C-CH$_2$-*C*H$_3$) 13.5 (2C, 2xBF$_2$-N-C-*C*H$_3$), 12.5 (2C, t, 2xBF$_2$-N-C-C-*C*H$_3$).

^{19}F-NMR ($CDCl_3$) δ_C, ppm: -145.86, -146.10 (2F, dd,B$\underline{F_2}$, $^1J_{B,F}$ = 32.3 Hz, $^1J_{F,F}$ = 34.1 Hz).
^{11}B-NMR ($CDCl_3$) δ_C, ppm: 0.63 (1B, t, $\underline{B}F_2$, $^1J_{B,F}$ = 32.3 Hz).
R_f(CH_2Cl_2/CH_3OH 10:1) = 0.295.
ESI-MS(+):*m/z* found 1396.5253 $[M\text{-}Cl]^+$, calcd. for $C_{74}H_{100}BF_2N_3ORu_2S_3^+$ 1396.5249.
Elemental analysis (%): calcd. for $C_{74}H_{100}BClF_2N_3ORu_2S_3 \cdot CH_3OH$ C 61.56, H 7.23, N 2.87; found C 61.84, H 7.28, N 2.77.

Synthesis of the ester and amide conjugates BODIPY – dinuclear trithiolato ruthenium(II)-p-cymene complexes 1.2.27 and 1.2.28, 29.

Synthesis of [(η^6-*p*-$MeC_6H_4Pr^i$)$_2$Ru$_2$(μ_2-$SCH_2C_6H_4$-*p*-Bu^t)$_2$(μ_2-SC_6H_4-*p*-CH_2(CO)OR)]Cl (R = 4,4-difluoro-8-(methyl)-1,3,5,7-tetramethyl-2,6-diethyl-4-bora-3a,4a-diaza-*s*-indacene) (1.2.27)
The ester conjugate BODIPY – dinuclear trithiolato ruthenium(II)-*p*-cymene complex was prepared and purified by a adapting literature procedure[174]. To a solution of **1.2.13** (0.084 g, 0.252 mmol, 1.3 equiv.) in dry CH_2Cl_2 (20 mL) at r.t. under inert atmosphere (N_2) were added EDCI (0.056 g, 0.291 mmol, 1.5 equiv.), DMAP (0.006 g, 0.049 mmol, 0.25 equiv.) and **1.2.4** (0.200 g, 0.194 mmol, 1 equiv.). The reaction mixture was stirred at r.t. under inert atmosphere (N_2) for further 72 h and the reaction evolution was verified by TLC (CH_2Cl_2/CH_3OH 10:1 (v/v)). The reaction mixture was concentrated to dryness under reduced pressure and purication by column chromatography using CH_2Cl_2/CH_3OH mixture affording **1.2.27** as a pink-orange solid (0.092 g, 0.068 mmol, yield 35%).
^{1}H-NMR ($CDCl_3$) δ_H, ppm: 7.61 (2H, d, 2xS-(*Ar*)C-CH-C$\underline{H}$-C-CH_2-CO_2H, $^3J_{H,H}$ = 7.8 Hz), 7.38-7.52 (10H, m, 2xS-(*Ar*)C-C$\underline{H}$-CH-C-CH_2-CO_2H, 4xCH_2-(*Ar*)C-C$\underline{H}$-CH-C-C(CH_3)$_3$, 4xCH_2-(*Ar*)C-CH-C$\underline{H}$-C-C(CH_3)$_3$), 5.01 (2H, d, 2xCH_3-(*Ar*)C-CH-C$\underline{H}$-C, $^3J_{H,H}$ = 5.6 Hz), 4.93 (3H, d, HO-C$\underline{H_2}$-C, $^3J_{H,H}$ = 5.4 Hz), 4.89 (2H, d, 2xCH_3-(*Ar*)C-C$\underline{H}$-CH-C, $^3J_{H,H}$ = 5.7 Hz), 4.80 (2H, d, 2xCH_3-(*Ar*)C-CH-C$\underline{H}$-C, $^3J_{H,H}$ = 5.7 Hz), 4.58 (2H, d, 2xCH_3-(*Ar*)C-C$\underline{H}$-CH-C, $^3J_{H,H}$ = 5.7 Hz), 2.49 (6H, s, 2xBF_2-N-C-C$\underline{H_3}$), 2.42 (6H, s, 2xBF_2-N-C-C-C$\underline{H_3}$), 2.40 (4H, qvart, 2xBF_2-N-C-C-C$\underline{H_2}$-CH_3, $^3J_{H,H}$ = 7.6 Hz), 3.93 (2H, s, S-(*Ar*)C-CH-CH-C-C$\underline{H_2}$-CO_2H), 3.57 (2H, s, C$\underline{H_2}$-(*Ar*)C-CH-CH-C-C(CH_3)$_3$), 3.36 (2H, s, C$\underline{H_2}$-(*Ar*)C-CH-CH-C-C(CH_3)$_3$), 1.90 (2H, sept, 2x(*Ar*)C-CH-CH-C-C$\underline{H}$(CH_3)$_2$, $^3J_{H,H}$ = 6.8 Hz), 1.69 (6H, s, 2xC$\underline{H_3}$-(*Ar*)C-CH-CH-C), 1.35 (9H, s, S-CH_2-(*Ar*)C-CH-CH-C-C(C$\underline{H_3}$)$_3$), 1.32 (9H, s, S-CH_2-(*Ar*)C-CH-CH-C-C(C$\underline{H_3}$)$_3$), 1.05 (6H, t, 2xBF_2-N-C-C-CH_2-C$\underline{H_3}$, $^3J_{H,H}$ = 7.6 Hz), 0.94 (6H, d, 2x(*Ar*)C-CH-CH-C-CH(C$\underline{H_3}$)$_2$, $^3J_{H,H}$ = 6.8 Hz), 0.89 (6H, d, 2x(*Ar*)C-CH-CH-C-CH(C$\underline{H_3}$)$_2$, $^3J_{H,H}$ = 6.8 Hz).
^{13}C-NMR ($CDCl_3$) δ_C, ppm: 173.9 (1C, S-(*Ar*)C-CH-CH-C-CH_2-$\underline{C}O_2H$), 154.8 (2C, 2xBF_2-N-$\underline{C}$-CH_3), 151.91, 151.86 (2C, 2xS-CH_2-(*Ar*)C-CH-CH-$\underline{C}$-C(CH_3)$_3$), 137.1 (1C, S-(*Ar*)C-CH-CH-$\underline{C}$-CH_2-CO_2H), 136.8, 136.6 (2C, 2xS-CH_2-(*Ar*)$\underline{C}$-CH-CH-C-C(CH_3)$_3$), 136.6 (2C, 2xBF_2-N-C-$\underline{C}$-CH_3), 136.5 (1C, HO-CH_2-$\underline{C}$), 135.1 (1C, S-(*Ar*)$\underline{C}$-CH-CH-C-CH_2-CO_2H), 133.5 (2C, 2xBF_2-N-C-$\underline{C}$-CH_2-CH_3), 132.3 (2C, 2xS-(*Ar*)C-CH-$\underline{C}$H-C-CH_2-CO_2H), 131.7 (2C, 2xBF_2-N-$\underline{C}$-C-CH_3), 130.8 (2C, 2xS-(*Ar*)C-$\underline{C}$H-CH-C-CH_2-CO_2H), 129.4, 129.1 (2C, 2xS-CH_2-(*Ar*)C-$\underline{C}$H-CH-C-C(CH_3)$_3$), 125.7, 125.6 (2C, 2xS-CH_2-(*Ar*)C-CH-$\underline{C}$H-C-C(CH_3)$_3$), 107.4 (2C, 2xCH_3-(*Ar*)C-CH-CH-$\underline{C}$), 100.7 (2C, 2xCH_3-(*Ar*)$\underline{C}$-CH-CH-C), 83.92 (1C, CH_3-(*Ar*)C-$\underline{C}$H-CH-C), 83.86 (1C, CH_3-(*Ar*)C-CH-$\underline{C}$H-C), 83.6 (1C, CH_3-(*Ar*)C-CH-$\underline{C}$H-C), 82.4 (1C, CH_3-(*Ar*)C-$\underline{C}$H-CH-C), 56.4 (1C, HO-C$\underline{H_2}$-C), 42.33 (1C, S-(*Ar*)C-CH-CH-C-$\underline{C}H_2$-CO_2H), 40.0 (1C, S-$\underline{C}H_2$-(*Ar*)C-CH-CH-C-C(CH_3)$_3$), 39.4 (1C, S-$\underline{C}H_2$-(*Ar*)C-CH-CH-C-C(CH_3)$_3$), 34.91 (1C, S-CH_2-(*Ar*)C-CH-CH-C-$\underline{C}$(CH_3)$_3$), 34.88 (1C, S-CH_2-(*Ar*)C-CH-CH-C-$\underline{C}$(CH_3)$_3$), 31.6 (6C, 2xS-CH_2-(*Ar*)C-CH-CH-C-C($\underline{C}H_3$)$_3$), 1.0 (2C, 2x(*Ar*)CH-CH-C-$\underline{C}$H(CH_3)$_2$), 23.2 (2C, (*Ar*)CH-CH-C-CH($\underline{C}H_3$)$_2$), 22.8 (2C, (*Ar*)CH-CH-C-CH($\underline{C}H_3$)$_2$), 18.2 (2C, 2x$\underline{C}H_3$-(*Ar*)C-CH-CH), 17.3 (2C, 2xBF_2-N-C-C-$\underline{C}H_2$-CH_3), 14.9 (2C, 2xBF_2-N-C-C-CH_2-$\underline{C}H_3$), 12.8 (4C, m, 2xBF_2-N-C-$\underline{C}$H3, 2xBF2-N-C-C-$\underline{C}H_3$).

^{19}F-NMR ($CDCl_3$) δ_C, ppm: -145.97 (2F, dd, B$\underline{F_2}$, $^1J_{B,F}$ = 30.8 Hz, $^2J_{F,F}$ = 33.1 Hz).
^{11}B-NMR ($CDCl_3$) δ_C, ppm: 0.60 (1B, t, $\underline{B}F_2$, $^1J_{B,F}$ = 32.0 Hz).
R_f (CH_2Cl_2/CH_3OH 10:1) = 0.267.
ESI-MS(+):*m/z* found 1313.4132 $[M\text{-}Cl\text{-}H]^+$, calcd. for $C_{68}H_{88}BF_2N_2O_2Ru_2S_3^+$1313.4151;
Elemental analysis (%): calcd. for $C_{68}H_{89}BClF_2N_2O_2Ru_2S_3 \cdot 0.8CH_2Cl_2 \cdot 1.6CH_3OH$ C 57.63, H 6.60, N 1.91; found C 57.61, H 6.60, N, 2.00.

Synthesis of [(η^6-*p*-$MeC_6H_4Pr^i$)$_2$Ru$_2$(μ_2-$SCH_2C_6H_4$-*p*-Bu^t)$_2$(μ_2-SC_6H_4-*p*-CH_2(CO)NHR)]Cl (R = 4,4-difluoro-8-(methyl)-1,3,5,7-tetramethyl-2,6-diethyl-4-bora-3a,4a-diaza-*s*-indacene), (1.2.28)

The amide conjugate BODIPY – dinuclear trithiolato ruthenium(II)-*p*-cymene complex was prepared by adapting a literature procedure[175]. To a solution of **1.2.4** (0.209 g, 0.203 mmol, 1 equiv.) in dry CH_2Cl_2 (20 mL) at r.t. under inert atmosphere (N_2) were added $HOBt \cdot H_2O$ (0.067 g, 0.487 mmol, 2.4 equiv.) and DIPEA (0.1mL, 0.508 mmol, 2.5 equiv.). After 15 min have been added successively EDCI (0.117 g, 0.609 mmol, 3 equiv.), **1.2.15** (0.088 g, 0.264 mmol, 1.3 equiv.) and DIPEA (0.1 mL, 0.508 mmol, 2.5 equiv.). The reaction mixture was stirred at r.t. under inert atmosphere (N_2) for further 72 h and the reaction evolution was verified by TLC (CH_2Cl_2/CH_3OH 10:1 (v/v)). The reaction mixture was concentrated to dryness under reduced pressure and purification by column chromatography using CH_2Cl_2/CH_3OH mixture afforded **1.2.28** as a pink-orange solid (0.142 g, 0.106 mmol, yield 52%).
^{1}H-NMR ($CDCl_3$) δ_H, ppm: 7.68 (2H, d, 2xS-(*Ar*)C-CH-C$\underline{H}$-C-CH_2-CO-NH, $^3J_{H,H}$ = 8.2 Hz), 7.39-7.49 (10H, m, 2xS-(*Ar*)C-C$\underline{H}$-CH-C-CH_2-CO_2H, 4xCH_2-(*Ar*)C-C$\underline{H}$-CH-C-C$(CH_3)_3$, 4xCH_2-(*Ar*)C-CH-C$\underline{H}$-C-C$(CH_3)_3$), 5.06 (2H, d, 2xCH_3-(*Ar*)C-CH-C$\underline{H}$-C, $^3J_{H,H}$ = 5.8 Hz), 4.93 (2H, d, 2xCH_3-(*Ar*)C-C$\underline{H}$-CH-C, $^3J_{H,H}$ = 5.8 Hz), 4.81 (2H, d, 2xCH_3-(*Ar*)C-CH-C$\underline{H}$-C, $^3J_{H,H}$ = 5.8 Hz), 4.68 (2H, d, HN-C$\underline{H_2}$-C, $^3J_{H,H}$ = 4.0 Hz), 4.62 (2H, d, 2xCH_3-(*Ar*)C-C$\underline{H}$-CH-C, $^3J_{H,H}$ = 5.8 Hz), 3.83 (2H, s, S-(*Ar*)C-CH-CH-C-C$\underline{H_2}$-CO-NH), 3.58 (2H, s, C$\underline{H_2}$-(*Ar*)C-CH-CH-C-C$(CH_3)_3$), 3.40 (2H, s, C$\underline{H_2}$-(*Ar*)C-CH-CH-C-C$(CH_3)_3$), 2.45 (6H, s, 2xBF_2-N-C-C$\underline{H_3}$), 2.38 (4H, qvart, 2xBF_2-N-C-C-C$\underline{H_2}$-CH_3, $^3J_{H,H}$ = 7.5 Hz), 2.33 (6H, s, 2xBF_2-N-C-C-C$\underline{H_3}$), 1.96 (2H, sept, 2x(*Ar*)C-CH-CH-C-C$\underline{H}(CH_3)_2$, $^3J_{H,H}$ = 6.9 Hz), 1.61 (6H, s, 2xC$\underline{H_3}$-(*Ar*)C-CH-CH-C), 1.37 (9H, s, S-CH_2-(*Ar*)C-CH-CH-C-C(C$\underline{H_3}$)$_3$), 1.34 (9H, s, S-CH_2-(*Ar*)C-CH-CH-C-C(C$\underline{H_3}$)$_3$), 1.05 (6H, t, 2xBF_2-N-C-C-CH_2-C$\underline{H_3}$, $^3J_{H,H}$ = 7.5 Hz), 0.95 (6H, d, 2x(*Ar*)C-CH-CH-C-CH(C$\underline{H_3}$)$_2$, $^3J_{H,H}$ = 6.9 Hz), 0.90 (6H, d, 2x(*Ar*)C-CH-CH-C-CH(C$\underline{H_3}$)$_2$, $^3J_{H,H}$ = 6.9 Hz).
^{13}C-NMR ($CDCl_3$) δ_C, ppm: 171.3 (1C, S-(*Ar*)C-CH-CH-C-CH_2-($\underline{C}$=O)-NH), 154.2 (2C, 2xBF_2-N-$\underline{C}$-CH_3), 151.9, 151.81 (2C, 2xS-CH_2-(*Ar*)C-CH-CH-$\underline{C}$-C$(CH_3)_3$), 137.0 (2C, 2xBF_2-N-C-$\underline{C}$-CH_3), 136.9 (1C, S-(*Ar*)C-CH-CH-$\underline{C}$-CH_2-(C=O)-NH), 136.8, 136.7 (2C, 2xS-CH_2-(*Ar*)$\underline{C}$-CH-CH-C-C$(CH_3)_3$), 135.9 (1C, S-(*Ar*)$\underline{C}$-CH-CH-C-CH_2-(C=O)-NH), 134.8 (2C, 2xBF_2-N-$\underline{C}$-C-CH_3), 133.3 (2C, 2xBF_2-N-C-$\underline{C}$-CH_2-CH_3), 132.8 (2C, 2xS-(*Ar*)C-CH-$\underline{C}$H-C-CH_2-($\underline{C}$=O)-NH), 132.1 (1C, (C=O)-HN-CH_2-$\underline{C}$), 130.5 (2C, 2xS-(*Ar*)C-$\underline{C}$H-CH-C-CH_2-($\underline{C}$=O)-NH), 129.4, 129.2 (2C, 2xS-CH_2-(*Ar*)C-$\underline{C}$H-CH-C-C$(CH_3)_3$), 125.7, 125.6 (2C, 2xS-CH_2-(*Ar*)C-CH-$\underline{C}$H-C-C$(CH_3)_3$), 107.5 (2C, 2xCH_3-(*Ar*)C-CH-CH-$\underline{C}$), 100.3 (2C, 2xCH_3-(*Ar*)$\underline{C}$-CH-CH-C), 84.2 (1C, CH_3-(*Ar*)C-CH-$\underline{C}$H-C), 83.9 (1C, CH_3-(*Ar*)C-$\underline{C}$H-CH-C), 83.6 (1C, CH_3-(*Ar*)C-CH-$\underline{C}$H-C), 82.4 (1C, CH_3-(*Ar*)C-$\underline{C}$H-CH-C), 42.6 (1C, S-(*Ar*)C-CH-CH-C-$\underline{C}$$H_2$-($\underline{C}$=O)-NH), 40.0 (1C, S-$\underline{C}$$H_2$-(*Ar*)C-CH-CH-C-C$(CH_3)_3$), 39.5 (1C, S-$\underline{C}$$H_2$-(*Ar*)C-CH-CH-C-C$(CH_3)_3$), 37.4 (1C, (C=O)-HN-C$\underline{H_2}$-C), 34.94 (1C, S-$CH_2$-(*Ar*)C-CH-CH-C-$\underline{C}$$(CH_3)_3$), 34.90 (1C, S-$CH_2$-(*Ar*)C-CH-CH-C-$\underline{C}$$(CH_3)_3$), 31.57, 31.54 (6C, 2xS-CH_2-(*Ar*)C-CH-CH-C-C($\underline{C}$$H_3$)$_3$), 31.1 (2C, 2x(*Ar*)CH-CH-C-$\underline{C}$H$(CH_3)_2$), 23.1 (2C, (*Ar*)CH-CH-C-CH($\underline{C}$$H_3$)$_2$), 22.9 (2C, (*Ar*)CH-CH-C-CH($\underline{C}$$H_3$)$_2$), 18.0 (2C, 2x$\underline{C}$$H_3$-(*Ar*)C-CH-CH), 17.4 (2C, 2xBF_2-N-C-C-$\underline{C}$$H_2$-$CH_3$), 15.0 (2C, 2x$BF_2$-N-C-C-$CH_2$-$\underline{C}$$H_3$), 13.0 (2C, 2x$BF_2$-N-C-C-$\underline{C}$$H_3$), 12.7 (2C, m, 2x$BF_2$-N-C-$\underline{C}$$H_3$).

^{19}F-NMR ($CDCl_3$) δ_C, ppm: -145.66 (2F, dt, B$\underline{F_2}$, $^1J_{B,F}$ = 27.6 Hz, $^2J_{F,F}$ = 32.4 Hz).
^{11}B-NMR ($CDCl_3$) δ_C, ppm: 0.57 (1B, t, $\underline{B}F_2$, $^1J_{B,F}$ = 31.2 Hz).
R_f(CH_2Cl_2/CH_3OH 10:1) = 0.472.
ESI-MS(+):*m/z* found 1312.4333 $[M\text{-}Cl]^+$, calcd. for $C_{68}H_{89}BF_2N_3ORu_2S_3^+$ 1312.4310.
Elemental analysis (%): calcd. for $C_{68}H_{89}BClF_2N_3ORu_2S_3 \cdot 3H_2O$ C 58.29, H 6.83, N 3.00; found C 58.29, H 7.26, N 3.02.

Synthesis of [(η^6-*p*-$MeC_6H_4Pr^i$)$_2$Ru$_2$(μ_2-$SCH_2C_6H_4$-*p*-Bu^t)$_2$(μ_2-SC_6H_4-*p*-CH_2(CO)NH-R)]Cl (R = 4,4-difluoro-8-(3-propan-1-yl)-1,3,5,7-tetramethyl-2,6-diethyl-4-bora-3a,4a-diaza-*s*-indacene (1.2.29)

The amide conjugate BODIPY – dinuclear trithiolato ruthenium(II)-*p*-cymene complex was prepared by adapting a literature procedure[175]. To a solution of **1.2.4** (0.300 g, 0.291 mmol, 1 equiv.) in dry CH_2Cl_2 (20 mL) at r.t. under inert atmosphere (N_2) were added HOBt·H_2O (0.096 g, 0.698 mmol, 2.4 equiv.) and DIPEA (0.125 mL, 0.728 mmol, 2.5 equiv.). After 15 min have been added successively EDCI (0.167 g, 0.873 mmol, 3 equiv.), **1.2.16** (0.150 g, 0.378 mmol, 1.3 equiv.) and DIPEA (0.125 mL, 0.728 mmol, 2.5 equiv.). The reaction mixture was stirred at r.t. under inert atmosphere (N_2) for further 72 h and the reaction evolution was verified by TLC (CH_2Cl_2/CH_3OH 10:1 (v/v)). The reaction mixture was concentrated to dryness under reduced pressure and purification by column chromatography using CH_2Cl_2/CH_3OH afforded **1.2.29** as a pink-orange solid (0.208 g, 0.151 mmol, yield 52%).

^{1}H-NMR ($CDCl_3$) δ_H, ppm: 7.63 (2H, d, 2xS-(*Ar*)C-CH-C$\underline{H}$-C-CH_2-CO-NH, $^3J_{H,H}$ = 8.0 Hz), 7,58(2H, d, 2xS-(*Ar*)C-CH-C$\underline{H}$-C-CH_2-CO-NH, $^3J_{H,H}$ = 8.0 Hz), 7.38-7.49 (10H, m, 2xS-(*Ar*)C-C$\underline{H}$-CH-C-CH_2-CO_2H, 4xCH_2-(*Ar*)C-C$\underline{H}$-CH-C-C$(CH_3)_3$, 4xCH_2-(*Ar*)C-CH-C$\underline{H}$-C-C$(CH_3)_3$), 4.97 (2H, d, 2xCH_3-(*Ar*)C-CH-C$\underline{H}$-C, $^3J_{H,H}$ = 5.7 Hz), 4.83 (2H, d, 2xCH_3-(*Ar*)C-C$\underline{H}$-CH-C, $^3J_{H,H}$ = 5.8 Hz), 4.73 (2H, d, 2xCH_3-(*Ar*)C-CH-C$\underline{H}$-C, $^3J_{H,H}$ = 5.7 Hz), 4.57 (2H, d, 2xCH_3-(*Ar*)C-C$\underline{H}$-CH-C, $^3J_{H,H}$ = 5.8 Hz), 3.81 (2H, s, S-(*Ar*)C-CH-CH-C-C$\underline{H_2}$-CO-NH), 3.54 (2H, s, C$\underline{H_2}$-(*Ar*)C-CH-CH-C-C$(CH_3)_3$), 3.41 (2H, qvart, NH-C$\underline{H_2}$-$(CH_2)_2$-C), 3.34 (2H, s, C$\underline{H_2}$-(*Ar*)C-CH-CH-C-C$(CH_3)_3$), 3.01-3.05 (2H, m, NH-CH_2-C$\underline{H_2}$-CH_2), 2.40 (6H, s, 2xBF_2-N-C-C$\underline{H_3}$), 2.39 (6H, s, 2xBF_2-N-C-C-C$\underline{H_3}$), 2.35, (4H, qvart, 2xBF_2-N-C-C-C$\underline{H_2}$-CH_3, $^3J_{H,H}$ = 7.6 Hz), 1.88-1.96 (2H, sept, 2x(*Ar*)C-CH-CH-C-C$\underline{H}(CH_3)_2$, $^3J_{H,H}$ = 6.8 Hz), 1.76-1.85 (4H, m, NH-CH_2-CH_2-C$\underline{H_2}$), 1.60 (6H, s, 2xC$\underline{H_3}$-(*Ar*)C-CH-CH-C), 1.37 (9H, s, S-CH_2-(*Ar*)C-CH-CH-C-C(C$\underline{H_3}$)$_3$), 1.34 (9H, s, S-CH_2-(*Ar*)C-CH-CH-C-C(C$\underline{H_3}$)$_3$), 1.00 (6H, t, 2xBF_2-N-C-C-CH_2-C$\underline{H_3}$, $^3J_{H,H}$ = 7.5 Hz), 0.92 (6H, d, 2x(*Ar*)C-CH-CH-C-CH(C$\underline{H_3}$)$_2$, $^3J_{H,H}$ = 6.8 Hz), 0.88 (6H, d, 2x(*Ar*)C-CH-CH-C-CH(C$\underline{H_3}$)$_2$, $^3J_{H,H}$ = 6.8 Hz).

^{13}C-NMR ($CDCl_3$) δ_C, ppm: 172,0 (1C, S-(*Ar*)C-CH-CH-C-CH_2-(C=O)-NH), 152.0, 151.9 (2C, 2xS-CH_2-(*Ar*)C-CH-CH-C-C$(CH_3)_3$), 151.7 (2C, 2xBF_2-N-C-CH_3), 145.1 (2C, 2xBF_2-N-C-C-CH_3), 139.0 (2C, 2xBF_2-N-C-C-CH_3), 136.7 (1C, S-(*Ar*)C-CH-CH-C-CH_2-(C=O)-NH), 136.6 (2C, 2xS-CH_2-(*Ar*)C-CH-CH-C-C$(CH_3)_3$), 136.5 (2C, 2xBF_2-N-C-C-CH_3), 134.4 (1C, S-(*Ar*)C-CH-CH-C-CH_2-(C=O)-NH), 132.4 (2C, 2xS-(*Ar*)C-CH-CH-C-CH_2-(C=O)-NH), 132.3 (1C, (C=O)-HN-$(CH_2)_3$-C),130.8 (2C, 2xS-(*Ar*)C-CH-CH-C-CH_2-(C=O)-NH), 129.3, 129.1 (2C, 2xS-CH_2-(*Ar*)C-CH-CH-C-C$(CH_3)_3$), 125.7, 125.6 (2C, 2xS-CH_2-(*Ar*)C-CH-CH-C-C$(CH_3)_3$), 107.5 (2C, 2xCH_3-(*Ar*)C-CH-CH-C), 100.5 (2C, 2xCH_3-(*Ar*)C-CH-CH-C), 84.0 (1C, CH_3-(*Ar*)C-CH-CH-C), 83.7 (1C, CH_3-(*Ar*)C-CH-CH-C), 83.6 (1C, CH_3-(*Ar*)C-CH-CH-C), 82.3 (1C, CH_3-(*Ar*)C-CH-CH-C), 43.1 (1C, S-(*Ar*)C-CH-CH-C-CH_2-(C=O)-NH), 40.0 (1C, S-CH_2-(*Ar*)C-CH-CH-C-C$(CH_3)_3$), 39.7 (1C, (C=O)-HN-C$\underline{H_2}$-$(CH_2)_2$-C), 39.3 (1C, S-CH_2-(*Ar*)C-CH-CH-C-C$(CH_3)_3$), 34.94 (1C, S-CH_2-(*Ar*)C-CH-CH-C-C$(CH_3)_3$), 34.91 (1C, S-CH_2-(*Ar*)C-CH-CH-C-C$(CH_3)_3$), 31.55, 31.53 (6C, 2xS-CH_2-(*Ar*)C-CH-CH-C-C(C$H_3)_3$), 31.1 (2C, 2x(*Ar*)CH-CH-C-CH$(CH_3)_2$), 26.4 (1C, (C=O)-HN-CH_2-CH_2-CH_2-C), 23.1 (2C, (*Ar*)CH-CH-C-CH(C$H_3)_2$), 22.8 (2C, (*Ar*)CH-CH-C-CH(C$H_3)_2$), 18.0 (2C, 2xCH_3-(*Ar*)C-CH-CH), 17.3 (2C, 2xBF_2-N-C-C-CH_2-CH_3), 15.0 (2C, 2xBF_2-N-C-C-CH_2-

$\underline{C}H_3$), 13.8 (2C, 2xBF_2-N-C-C-$\underline{C}H_3$), 12.5 (2C, m, 2xBF_2-N-C-$\underline{C}H_3$).
^{19}F-NMR ($CDCl_3$) δ_C, ppm: -145.72 (2F, m, B$\underline{F_2}$).
^{11}B-NMR ($CDCl_3$) δ_C, ppm: 0.59 (1B, t, $\underline{B}F_2$, $^1J_{B,F}$ = 29.7 Hz).
R_f (CH_2Cl_2/CH_3OH 10:1) = 0.267.
ESI-MS(+):*m/z* found 1340.4660 $[M-Cl]^+$, calcd. for $C_{70}H_{93}BF_2N_3ORu_2S_3^+$ 1340.4623;
Elemental analysis (%): calcd. for $C_{70}H_{93}BClF_2N_3ORu_2S_3 \cdot 0.1CH_2Cl_2 \cdot H_2O$ C, 60.07; H, 6.85; N, 3.00; found C, 60.08; H, 6.37; N, 3.06.

Synthesis of the meso-arene BODIPY dyes 30, 31 and 32 functionalized with chloromethylene, hydroxy and carboxy groups.

Synthesis of 4,4-difluoro-8-(4-(chloromethyl)phenyl)-1,3,5,7-tetramethyl-2,6-diethyl-4-bora-3a,4a-diaza-*s*-indacene (1.2.30)
The *meso*-arene BODIPY derivative **1.2.30** was prepared by adapting a literature procedure[395]. To a solution of 4-(chloromethyl)benzoyl chloride (0.368 g, 1.948 mmol, 1 equiv.) in dry CH_2Cl_2 (75 mL) at reflux under inert atmosphere (N_2) was added dropwise 3-ethyl-2,4-dimethylpyrrole (0.500 g, 3.896 mmol, 2 equiv.). The reaction mixture was refluxed for further 3 h, then it was cooled to r.t. and DIPEA (1.4 mL, 9.740 mmol, 5 equiv.) was added. After 30 min, $BF_3 \cdot Et_2O$ (soln. ca. 48% BF_3 in Et_2O, 1.7 mL, 13.636 mmol, 7 equiv.) was added dropwise, then the reaction mixture was heated to reflux for further 2 h. The mixture was concentrated to dryness and purification by column chromatography using EtOAc/Hex afforded **1.2.30** as a pink solid (0.332 g, 0.774 mmol, yield 85%).
^{1}H-NMR ($CDCl_3$) δ_H, ppm: 7.51 (2H, d, Cl-CH_2-C-C$\underline{H}$-CH-C-C, $^3J_{H,H}$ = 8.1 Hz), 7.28 (2H, d, Cl-CH_2-C-CH-C$\underline{H}$-C-C, $^3J_{H,H}$ = 8.1 Hz), 4.67 (2H, s, Cl-C$\underline{H_2}$-Ar), 2.53 (6H, s, 2xBF_2-N-C-C$\underline{H_3}$), 2.29 (4H, qvart, 2xBF_2-N-C-C-C$\underline{H_2}$-CH_3, $^3J_{H,H}$ = 7.6 Hz), 1.28 (6H, s, 2xBF_2-N-C-C-C-C$\underline{H_3}$), 0.97 (6H, t, 2xBF_2-N-C-C-CH_2-C$\underline{H_3}$, $^3J_{H,H}$ = 7.6 Hz).
^{13}C-NMR ($CDCl_3$) δ_C, ppm: 154.1 (2C, 2xBF_2-N-$\underline{C}$-CH_3), 139.5 (2C, 2xBF_2-N-$\underline{C}$-C-CH_3), 138.5 (2C, 2xBF_2-N-C-$\underline{C}$-CH_3), 138.4 (1C, Cl-CH_2-$\underline{C}$-CH-CH-C-C), 136.1(1C, Cl-CH_2-C-CH-CH-$\underline{C}$-C), 133.0 (2C, 2xBF_2-N-C-$\underline{C}$-CH_2-CH_3), 130.8 (1C, 2xBF_2-N-C-$\underline{C}$-Ar), 129.3 (2C, Cl-CH_2-C-$\underline{C}$H-CH-C-C), 128.9 (2C, Cl-CH_2-C-CH-$\underline{C}$H-C-C), 45.8 (1C, Cl-$\underline{C}H_2$-Ar), 17.2 (2C, 2xBF_2-N-C-C-$\underline{C}H_2$-CH_3), 14.7 (2C, 2xBF_2-N-C-C-CH_2-$\underline{C}H_3$), 12.7 (2C, 2xBF_2-N-C-$\underline{C}H_3$), 11.9 (2C, 2xBF_2-N-C-C-$\underline{C}H_3$).
^{19}F-NMR ($CDCl_3$) δ_C, ppm: -145.82 (2F, dd, B$\underline{F_2}$, $^1J_{B,F}$ = 32.79 Hz, $^2J_{F,F}$ =33.55 Hz);
^{11}B-NMR ($CDCl_3$) δ_C, ppm: 0.80 (1B, t, $\underline{B}F_2$, $^1J_{B,F}$ = 32.87 Hz);
R_f(Hex/EtOAc 9:1) = 0.490.
ESI-MS(+):*m/z* found 451.1891 $[M+Na]^+$, calcd. for $C_{24}H_{28}BClF_2N_2Na^+$ 451.1894.
Elemental analysis (%): calcd. for $C_{24}H_{28}BClF_2N_2$ C 67.23, H 6.58, N 6.53; found C 66.56, H 5.91, N 6.81.

Synthesis of 4,4-difluoro-8-(4-(hydroxy)phenyl)-1,3,5,7-tetramethyl-2,6-diethyl-4-bora-3a,4a-diaza-*s*-indacene (1.2.31)
The *meso*-arene BODIPY derivative **1.2.31** was prepared by adapting a literature procedure[179]. To a solution of 4-hydroxybenzaldehyde (0.243 g, 1.948 mmol, 1 equiv.) in dry CH_2Cl_2 (100 mL) at reflux, under inert atmosphere (N_2) was added dropwise 3-ethyl-2,4-dimethylpyrrole (0.500 g, 3.896 mmol, 2 equiv.) and TFA (0.01 mL, 0.097 mmol, 0.05 equiv.). The reaction mixture was refluxed for further 16 h, then DDQ (0.488 g, 1.948 mmol, 1 equiv.) was added. After 30 min, the mixture was cooled to r.t. followed by dropwise addition of TEA (2.74 mL, 19.480 mmol, 10 equiv.) and $BF_3 \cdot Et_2O$ (soln. ca. 48% BF_3 in Et_2O, 2.87 mL, 23.376 mmol, 12 equiv.). After another 30 min

the reaction mixture was filtered, washed with water (3×100 mL), brine (1×100 mL), dried over anhydrous Na_2SO_4, filtered, and concentrated to dryness under reduced pressure. Purification by column chromatography using EtOAc/Hex afforded **1.2.31** as a pink solid (0.217 g, 0.548 mmol, yield 28%).

^{1}H-NMR ($CDCl_3$) δ_H, ppm: 7.12 (2H, d, HO-C-C*H*-CH-C-C, $^3J_{H,H}$ = 8.5 Hz), 6.94 (2H, d, HO-C-CH-C*H*-C-C, $^3J_{H,H}$ = 8.5 Hz), 2.52 (6H, s, 2xBF_2-N-C-C*H*$_3$), 2.30 (4H, qvart, 2xBF_2-N-C-C-C*H*$_2$-CH_3, $^3J_{H,H}$ = 7.6 Hz), 1.34 (6H, s, 2xBF_2-N-C-C-C*H*$_3$), 0.98 (6H, t, 2xBF_2-N-C-C-CH_2-C*H*$_3$, $^3J_{H,H}$ = 7.6 Hz).

^{13}C-NMR ($CDCl_3$) δ_C, ppm: 156,2 (1C, HO-*C*-CH-CH-C-C), 153,7 (2C, 2xBF_2-N-*C*-CH_3), 140,3 (1C, HO-C-CH-CH-*C*-C), 138.6 (2C, 2xBF_2-N-C-*C*-CH_3), 132,8 (2C, 2xBF_2-N-C-*C*-CH_2-CH_3), 131,3 (2C, 2xBF_2-N-*C*-C-CH_3), 129,8 (2C, HO-C-*C*H-CH-C-C), 128,3 (1C, 2xBF_2-N-C-*C*-Ar), 116,2 (2C, HO-C-CH-*C*H-C-C), 17.2 (2C, 2xBF_2-N-C-C-*C*H_2-CH_3), 14.8 (2C, 2xBF_2-N-C-C-CH_2-*C*H_3), 12.6 (2C, 2xBF_2-N-C-*C*H_3), 12.0 (2C, 2xBF_2-N-C-C-*C*H_3).

^{19}F-NMR ($CDCl_3$) δ_F, ppm: -145,68 (2F, dd, B*F*$_2$, $^1J_{B,F}$ = 33.42 Hz, $^2J_{F,F}$ = 33.80 Hz).

^{11}B-NMR ($CDCl_3$) δ_B, ppm: 0.82 (1B, t, *B*F_2, $^1J_{B,F}$ = 33.09 Hz).

R_f(Hex/EtOAc 7:3) = 0.523.

ESI-MS(+):*m/z* found 377.2210 $[M-F]^+$, 397.2271 $[M+H]^+$, 419.2092 $[M+Na]^+$, calcd. for $C_{23}H_{27}BFN_2O^+$ 377.2195, for $C_{23}H_{28}BF_2N_2O^+$ 397.2257, and for $C_{23}H_{27}BF_2N_2NaO^+$ 419.2077.

Elemental analysis (%): calcd. for $C_{23}H_{27}BF_2N_2O \cdot 0.42CH_2Cl_2$ C 65.12, H 6.50, N 6.49; found C 65.12, H 6.48, N 6.21.

Synthesis of 4,4-difluoro-8-(4-(carboxy)phenyl)-1,3,5,7-tetramethyl-2,6-diethyl-4-bora-3a,4a-diaza-*s*-indacene (1.2.32)

BODIPY derivative **1.2.32** was prepared by adapting a literature procedure[179]. To a solution of 4-formylbenzoic acid (0.478 g, 3.117 mmol, 1 equiv.) in dry CH_2Cl_2 (100 mL) at reflux under inert atmosphere (N_2) was added dropwise 3-ethyl-2,4-dimethylpyrrole (0.800 g, 6.234 mmol, 2 equiv.) and TFA (0.01 mL, 0.156 mmol, 0.05 equiv.). The reaction mixture was refluxed for further 16 h, then DDQ (0.722 g, 3.117 mmol, 1 equiv.) was added. The mixture was stirred for another 30 min, then allowed to cool to r.t., followed by dropwise addition of TEA (4.38 mL, 31.170 mmol, 10 equiv.) and $BF_3 \cdot Et_2O$ (soln. ca. 48% BF_3 in Et_2O, 4.60 mL, 37.404 mmol, 12 equiv.). After another 30 min the reaction mixture was filtered, washed with water (3×100 mL), brine (1×100 mL), dried over anhydrous Na_2SO_4, filtered, and concentrated under reduced pressure to dryness. Purification by column chromatography using EtOAc/Hex mixture afforded **1.2.32** as a pink solid (0.337 g, 0.794 mmol, yield 25%).

^{1}H-NMR ($CDCl_3$) δ_H, ppm: 8.25 (2H, d, HO-(C=O)-C-C*H*-CH-C-C, $^3J_{H,H}$ = 8.2 Hz), 7.45 (2H, d, HO-(C=O)-C-CH-C*H*-C-C, $^3J_{H,H}$ = 8.2 Hz), 2.54 (6H, s, 2xBF_2-N-C-C*H*$_3$), 2.30 (4H, qvart, 2xBF_2-N-C-C-C*H*$_2$-CH_3, $^3J_{H,H}$ = 7.5 Hz), 1.27 (6H, s, 2xBF_2-N-C-C-C*H*$_3$), 0.98 (6H, t, 2xBF_2-N-C-C-CH_2-C*H*$_3$, $^3J_{H,H}$ = 7.5 Hz).

^{13}C-NMR ($CDCl_3$) δ_C, ppm: 170.3 (1C, HO-(*C*=O)-Ar), 154.5 (2C, 2xBF_2-N-*C*-CH_3), 141.8 (1C, HO-(C=O)-*C*-CH-CH-C-C), 138.5 (1C, HO-(C=O)-C-CH-CH-*C*-C), 138.2 (2C, 2xBF_2-N-C-*C*-CH_2-CH_3), 133.3 (2C, 2xBF_2-N-C-*C*-CH_3), 131.0 (2C, HO-(C=O)-C-*C*H-CH-C-C), 130.4 (2C, 2xBF_2-N-*C*-C-CH_3), 129.7 (1C, 2xBF_2-N-C-*C*-Ar), 129.1 (2C, HO-(C=O)-C-CH-*C*H-C-C), 17.2 (2C, 2xBF_2-N-C-C-*C*H_2-CH_3), 14.7 (2C, 2xBF_2-N-C-C-CH_2-*C*H_3), 12.7 (2C, t, 2xBF_2-N-C-*C*H_3), 12.0 (2C, 2xBF_2-N-C-C-*C*H_3).

^{19}F-NMR ($CDCl_3$) δ_F, ppm: -145,73 (2F, dd, B*F*$_2$, $^1J_{B,F}$ = 32.95 Hz, $^2J_{F,F}$ = 33.45 Hz).

^{11}B-NMR ($CDCl_3$) δ_B, ppm: 0.79 (1B, t, *B*F_2, $^1J_{B,F}$ = 32.53 Hz).

R_f(CH_2Cl_2/CH_3OH 10:1) = 0.482.

ESI-MS(+):*m/z* found 424.2128 $[M]^+$, 447.3441 $[M+Na]^+$, calcd. for $C_{24}H_{27}BF_2N_2O_2^+$ 424.2128

and $C_{24}H_{27}BF_2N_2NaO_2^+$ 447.2026.
Elemental analysis (%): calcd. $C_{24}H_{27}BF_2N_2O_2 \cdot 0.7EtOAc \cdot 0.6CH_2Cl_2$ C 61.29, H 6.35, N 5.22; found C 61.27, H 6.49, N 5.15.

Synthesis of the amine and ester conjugates BODIPY - dinuclear trithiolato ruthenium(II)-p-cymene complexes 1.2.33 and 1.2.34 containing aryl handles

Synthesis of [(η^6-*p*-MeC$_6$H$_4$Pr^i)$_2$Ru$_2$(μ_2-SCH$_2$C$_6$H$_4$Bu^t)$_2$(μ_2-SC$_6$H$_4$-*p*-NH-CH$_2$R)]Cl (R = 4,4-difluoro-8-(4-phenyl)-1,3,5,7-tetramethyl-2,6-diethyl-4-bora-3a,4a-diaza-*s*-indacene) (1.2.33)
Conjugate **1.2.33** was prepared by adapting a literature procedure [395].To a solution of **1.2.30** (0.156 g, 0.364 mmol, 1.2 equiv.) and KI (0.151 g, 0.909 mmol, 3 equiv.) in dry DMF (10 mL) at reflux, under inert atmosphere were added DIPEA (0.11 mL, 0.606 mmol, 2 equiv.) and a solution of **1.2.3** (0.300 g, 0.303 mmol, 1 equiv.) in dry CH_2Cl_2 (25 mL). The reaction mixture was stirred at reflux under inert atmosphere (N_2) for further 72 h and the reaction evolution was verified by TLC (CH_2Cl_2/CH_3OH 10:1 (v/v)). The reaction mixture was concentrated to dryness under reduced pressure and purification by column chromatography using CH_2Cl_2/CH_3OH afforded **1.2.33** as a pink-orange solid (0.207 g, 0.150 mmol, yield 50%).
^{1}H-NMR ($CDCl_3$) δ_H, ppm: 10.11 (1H, s, S-(*Ar*)C-CH-CH-C-N*H*), 7.54 (2H, d, 2xS-(*Ar*)C-CH-C*H*-C-NH, $^3J_{H,H}$ = 7.9 Hz), 7.39-7.51 (14H, m, NH-CH$_2$-(Ar)C-C*H*-CH-C, 4xCH$_2$-(*Ar*)C-C*H*-CH-C-C(CH$_3$)$_3$, 4xCH$_2$-(*Ar*)C-CH-C*H*-C-C(CH$_3$)$_3$), 7,19(2H, d, 2xS-(*Ar*)C-CH-C*H*-C-NH, $^3J_{H,H}$ = 8.0 Hz), 6.88 (2H, s, NH-CH$_2$-(Ar)C-CH-C*H*-C), 4.99 (2H, d, 2xCH$_3$-(*Ar*)C-CH-C*H*-C, $^3J_{H,H}$ = 5.7 Hz), 4.87 (2H, d, 2xCH$_3$-(*Ar*)C-C*H*-CH-C, $^3J_{H,H}$ = 5.8 Hz), 4.73 (2H, d, 2xCH$_3$-(*Ar*)C-CH-C*H*-C, $^3J_{H,H}$ = 5.7 Hz), 4.57 (4H, d, 2xCH$_3$-(*Ar*)C-C*H*-CH-C, $^3J_{H,H}$ = 5.8 Hz, s, NH-C*H$_2$*-(Ar)C-CH-CH-C), 3.54 (2H, s, C*H$_2$*-(*Ar*)C-CH-CH-C-C(CH$_3$)$_3$), 3.36 (2H, s, C*H$_2$*-(*Ar*)C-CH-CH-C-C(CH$_3$)$_3$), 2.51 (6H, s, 2xBF$_2$-N-C-C*H$_3$*), 2.29, (4H, qvart, 2xBF$_2$-N-C-C-C*H$_2$*-CH$_3$, $^3J_{H,H}$ = 7.6 Hz), 1.94-2.03 (2H, sept, 2x(*Ar*)C-CH-CH-C-C*H*(CH$_3$)$_2$, $^3J_{H,H}$ = 6.8 Hz), 1.69 (6H, s, 2xC*H$_3$*-(*Ar*)C-CH-CH-C), 1.36 (9H, s, S-CH$_2$-(*Ar*)C-CH-CH-C-C(C*H$_3$*)$_3$), 1.34 (9H, s, S-CH$_2$-(*Ar*)C-CH-CH-C-C(C*H$_3$*)$_3$), 1.30 (6H, s, 2xBF$_2$-N-C-C-C*H$_3$*), 0.97 (6H, t, 2xBF$_2$-N-C-C-CH$_2$-C*H$_3$*, $^3J_{H,H}$= 7.4 Hz), 0.97 (6H, d, 2x(*Ar*)C-CH-CH-C-CH(C*H$_3$*)$_2$, $^3J_{H,H}$ = 6.8 Hz), 0.92 (6H, d, 2x(*Ar*)C-CH-CH-C-CH(C*H$_3$*)$_2$, $^3J_{H,H}$ = 6.8 Hz).
^{13}C-NMR ($CDCl_3$) δ_C, ppm: 191,7 (1C, S-(*Ar*)C-CH-CH-C-NH-CH$_2$), 153.7, 151.9 (2C, 2xS-CH$_2$-(*Ar*)C-CH-CH-*C*-C(CH$_3$)$_3$), 151.9 (2C, 2xBF$_2$-N-*C*-CH$_3$), 140.6 (1C, S-(*Ar*)C-CH-CH-*C*-NH), 138.6 (2C, 2xBF$_2$-N-C-*C*-CH$_3$), 137.0 (1C, S-(*Ar*)C-CH-CH-*C*-NH), 136.7 (2C, 2xS-CH$_2$-(*Ar*)*C*-CH-CH-C-C(CH$_3$)$_3$), 133.4 (1C, S-(*Ar*)*C*-CH-CH-C-NH), 132.7 (2C, 2xS-(*Ar*)C-CH-*C*H-C-NH), 131.0 (1C, HN-CH$_2$-*C*), 130.4 (2C, 2xS-(*Ar*)C-*C*H-CH-C-NH), 129.6 (2C, 2xBF$_2$-N-C-*C*-CH$_2$-CH$_3$), 129.3, 129.1 (2C, 2xS-CH$_2$-(*Ar*)C-*C*H-CH-C-C(CH$_3$)$_3$), 125.7, 125.6 (2C, 2xS-CH$_2$-(*Ar*)C-CH-*C*H-C-C(CH$_3$)$_3$), 107.3 (2C, 2xCH$_3$-(*Ar*)C-CH-CH-*C*), 100.3 (2C, 2xCH$_3$-(*Ar*)*C*-CH-CH-C), 84.0 (1C, CH$_3$-(*Ar*)C-CH-*C*H-C), 83.6 (2C, CH$_3$-(*Ar*)C-*C*H-CH-C, 1C, CH$_3$-(*Ar*)C-CH-*C*H-C), 82.2 (1C, CH$_3$-(*Ar*)C-*C*H-CH-C), 39.9 (1C, HN-*C*H$_2$-(CH$_2$)$_2$-C), 39.3 (1C, S-*C*H$_2$-(*Ar*)C-CH-CH-C-C(CH$_3$)$_3$), 34.94 (1C, S-CH$_2$-(*Ar*)C-CH-CH-C-*C*(CH$_3$)$_3$), 34.91 (1C, S-CH$_2$-(*Ar*)C-CH-CH-C-*C*(CH$_3$)$_3$), 31.6 (6C, 2xS-CH$_2$-(*Ar*)C-CH-CH-C-C(*C*H$_3$)$_3$), 31.0 (2C, 2x(*Ar*)CH-CH-C-*C*H(CH$_3$)$_2$), 23.2 (2C, (*Ar*)CH-CH-C-CH(*C*H$_3$)$_2$), 22.9 (2C, (*Ar*)CH-CH-C-CH(*C*H$_3$)$_2$), 20.8 (1C, HN-CH$_2$-*C*H$_2$-CH$_2$), 18.2 (2C, 2x*C*H$_3$-(*Ar*)C-CH-CH), 17.3 (2C, 2xBF$_2$-N-C-C-*C*H$_2$-CH$_3$), 14.8 (1C, HN-CH$_2$-CH$_2$-*C*H$_2$), 14.7 (2C, 2xBF$_2$-N-C-C-CH$_2$-*C*H$_3$), 12.6 (2C, 2xBF$_2$-N-C-C-*C*H$_3$), 12.0 (2C, m, 2xBF$_2$-N-C-*C*H$_3$).
^{19}F-NMR ($CDCl_3$) δ_C, ppm: -145,80 (2F, dd, B*F$_2$*, $^1J_{B,F}$ = 31.40 Hz, $^2J_{F,F}$ = 34.65 Hz).
^{11}B-NMR ($CDCl_3$) δ_C, ppm: 0.82 (1B, t, *B*F$_2$, $^1J_{B,F}$ = 31.30 Hz).
R$_f$(CH_2Cl_2/CH_3OH 10:1) = 0.298.
ESI-MS(+):*m/z* found 1346.4548 $[M-Cl]^+$, calcd. for $C_{72}H_{91}BF_2N_3Ru_2S_3^+$ 1346.4518.

Elemental analysis (%): calcd. for $C_{72}H_{91}BClF_2N_3Ru_2S_3$ C 62.62, H 6.64, N 3.04; found C 62.38, H 6.79, N 3.05.

Synthesis of [(η^6-*p*-MeC$_6$H$_4$Pr^i)$_2$Ru$_2$(μ_2-SCH$_2$C$_6$H$_4$Bu^t)$_2$(μ_2-SC$_6$H$_4$-*p*-CH$_2$(CO)O-R)]Cl (R = 4,4-difluoro-8-(4-phenyl)-1,3,5,7-tetramethyl-2,6-diethyl-4-bora-3a,4a-diaza-*s*-indacene) (1.2.34)

To a solution of **1.2.4** (0.300 g, 0.291 mmol, 1 equiv.) in dry CH_2Cl_2 (50 mL) at r.t. under inert atmosphere (N_2) were added successively EDCI (0.112 g, 0.582 mmol, 2 equiv.), **1.2.31** (0.138 g, 0.349 mmol, 1.2 equiv.) and DMAP (0.018 g, 0.146 mmol, 0.5 equiv.). The reaction mixture was stirred at r.t. under inert atmosphere (N_2) for further 48 h and the reaction evolution was verified by TLC (CH_2Cl_2/CH_3OH 9:1 (v/v)). The reaction mixture was concentrated to dryness under reduced pressure and purification by column chromatography using CH_2Cl_2/CH_3OH, afforded **1.2.34** as a pink-orange solid (0.123 g, 0.087 mmol, yield 30%).

^{1}H-NMR ($CDCl_3$) δ_H, ppm: 7.81 (2H, d, 2xS-(*Ar*)C-CH-C*H*-C-CH$_2$-(C=O), $^3J_{H,H}$ = 7,6 Hz), 7.47 (4H, s, 4xCH$_2$-(*Ar*)C-CH-C*H*-C-C(CH$_3$)$_3$), 7.41 (4H, s, 4xCH$_2$-(*Ar*)C-C*H*-CH-C-C(CH$_3$)$_3$), 7,38(2H, d, 2xS-(*Ar*)C-C*H*-CH-C-CH$_2$-(C=O), $^3J_{H,H}$ = 7,7 Hz), 7.29 (2H, d, (C=O)-O-(*Ar*)C-C*H*-CH-C, $^3J_{H,H}$ = 8.5 Hz), 7.23 (2H, d, (C=O)-O-(*Ar*)C-CH-C*H*-C, $^3J_{H,H}$ = 8.5 Hz), 5.15 (2H, d, 2xCH$_3$-(*Ar*)C-CH-C*H*-C, $^3J_{H,H}$ = 5.3 Hz), 5.02 (2H, d, 2xCH$_3$-(*Ar*)C-C*H*-CH-C, $^3J_{H,H}$ = 5.6 Hz), 4.95 (2H, d, 2xCH$_3$-(*Ar*)C-CH-C*H*-C, $^3J_{H,H}$ = 5.3 Hz), 4.62 (2H, d, 2xCH$_3$-(*Ar*)C-C*H*-CH-C, $^3J_{H,H}$ = 5.3 Hz), 3.93 (2H, s, S-(*Ar*)C-CH-CH-C-C*H$_2$*-(C=O)), 3.62 (2H, s, C*H$_2$*-(*Ar*)C-CH-CH-C-C(CH$_3$)$_3$), 3.44 (2H, s, C*H$_2$*-(*Ar*)C-CH-CH-C-C(CH$_3$)$_3$), 2.51 (6H, s, 2xBF$_2$-N-C-C*H$_3$*), 2.28, (4H, qvart, 2xBF$_2$-N-C-C-C*H$_2$*-CH$_3$, $^3J_{H,H}$ = 7.5 Hz), 1.83-1.94 (2H, sept, 2x(*Ar*)C-CH-CH-C-C*H*(CH$_3$)$_2$, $^3J_{H,H}$ = 6,8 Hz), 1.77 (6H, s, 2xC*H$_3$*-(*Ar*)C-CH-CH-C), 1.36 (9H, s, S-CH$_2$-(*Ar*)C-CH-CH-C-C(C*H$_3$*)$_3$), 1.32 (9H, s, S-CH$_2$-(*Ar*)C-CH-CH-C-C(C*H$_3$*)$_3$), 1.30 (6H, s, 2xBF$_2$-N-C-C-C*H$_3$*), 0.96 (6H, t, 2xBF$_2$-N-C-C-CH$_2$-C*H$_3$*, $^3J_{H,H}$ = 7.5 Hz), 0.91 (6H, d, 2x(*Ar*)C-CH-CH-C-CH(C*H$_3$*)$_2$, $^3J_{H,H}$ = 6.8 Hz), 0.87 (6H, d, 2x(*Ar*)C-CH-CH-C-CH(C*H$_3$*)$_2$, $^3J_{H,H}$ = 6.8 Hz).

^{13}C-NMR ($CDCl_3$) δ_C, ppm: 169.5 (1C, S-(*Ar*)C-CH-CH-C-CH$_2$-(*C*=O)), 154.1 (2C, 2xBF$_2$-N-*C*-CH$_3$), 151.9, 151.8 (2C, 2xS-CH$_2$-(*Ar*)C-CH-CH-*C*-C(CH$_3$)$_3$), 151.2 (1C, (C=O)-O-(*Ar*)*C*-CH-CH-C), 139.1 (2C, 2xBF$_2$-N-C-*C*-CH$_3$), 138.4 (2C, 2xBF$_2$-N-*C*-CH$_2$-CH$_3$), 137.2 (1C, (C=O)-O-(*Ar*)C-CH-CH-*C*), 136.9, 136.8 (2C, 2xS-CH$_2$-(*Ar*)*C*-CH-CH-C-C(CH$_3$)$_3$), 133.6(1C, O-(*Ar*)C-CH-CH-C-*C*), 133.2 (2C, 2xS-(*Ar*)C-CH-*C*H-C-CH$_2$-(C=O)), 130.3 (2C, 2xS-(*Ar*)C-*C*H-CH-C-CH$_2$-(C=O)), 129.7 (2C, (C=O)-O-(*Ar*)C-*C*H-CH-C), 129.4, 129.3 (2C, 2xS-CH$_2$-(*Ar*)C-*C*H-CH-C-C(CH$_3$)$_3$), 125.7, 125.5 (2C, 2xS-CH$_2$-(*Ar*)C-CH-*C*H-C-C(CH$_3$)$_3$), 122.4 (2C, (C=O)-O-(*Ar*)C-CH-*C*H-C), 107.1 (2C, 2xCH$_3$-(*Ar*)C-CH-CH-*C*), 100.7 (2C, 2xCH$_3$-(*Ar*)*C*-CH-CH-C), 84.4 (1C, CH$_3$-(*Ar*)C-CH-*C*H-C), 83.78, 83.75 (1C, CH$_3$-(*Ar*)C-*C*H-CH-C, 1C, CH$_3$-(*Ar*)C-CH-*C*H-C), 82.6 (1C, CH$_3$-(*Ar*)C-*C*H-CH-C), 40.9 (1C, S-(*Ar*)C-CH-CH-C-*C*H$_2$-(C=O)), 40.2 (1C, S-*C*H$_2$-(*Ar*)C-CH-CH-C-C(CH$_3$)$_3$), 39.7 (1C, S-*C*H$_2$-(*Ar*)C-CH-CH-C-C(CH$_3$)$_3$), 34.94 (2C, 2xS-CH$_2$-(*Ar*)C-CH-CH-C-*C*(CH$_3$)$_3$), 34.88 (2C, 2xS-CH$_2$-(*Ar*)C-CH-CH-C-*C*(CH$_3$)$_3$), 31.57, 31.54 (6C, 2xS-CH$_2$-(*Ar*)C-CH-CH-C-C(*C*H$_3$)$_3$), 31.0 (2C, 2x(*Ar*)CH-CH-C-*C*H(CH$_3$)$_2$), 23.2 (2C, (*Ar*)CH-CH-C-CH(*C*H$_3$)$_2$), 22.7 (2C, (*Ar*)CH-CH-C-CH(*C*H$_3$)$_2$), 18.3 (2C, 2x*C*H$_3$-(*Ar*)C-CH-CH), 17.2 (2C, 2xBF$_2$-N-C-C-*C*H$_2$-CH$_3$), 14.7 (2C, 2xBF$_2$-N-C-C-CH$_2$-*C*H$_3$), 12.6 (2C, 2xBF$_2$-N-C-*C*H$_3$), 12.0 (2C, 2xBF$_2$-N-C-C-*C*H$_3$).

^{19}F-NMR ($CDCl_3$) δ_C, ppm: -145,79 (2F, dd, B*F$_2$*, $^1J_{B,F}$ = 33.15 Hz, $^2J_{F,F}$ = 33.44 Hz)

^{11}B-NMR ($CDCl_3$) δ_C, ppm: 0.79 (1B, t, *B*F$_2$, $^1J_{B,F}$ = 32.78 Hz).

R_f(CH_2Cl_2/CH_3OH 10:1) = 0.298.

ESI-MS(+): *m/z* found 1375.4359 [M-Cl]$^+$, calcd. for $C_{73}H_{90}BF_2N_2O_2Ru_2S_3^+$ 1375.4307.

Elemental analysis (%): calcd. for $C_{73}H_{90}BClF_2N_2O_2Ru_2S_3 \cdot 0.25CH_2Cl_2$ C 59.45, H 6.20, N 1.87; found C 59.41, H 6.05, N 1.90.

Synthesis of the ester and amide dyads BODIPY-dinuclear trithiolato ruthenium(II)-p-cymene complexes 1.2.35 and 1.2.36

Synthesis of [(η^6-*p*-MeC$_6$H$_4$Pr^i)$_2$Ru$_2$(μ_2-SCH$_2$C$_6$H$_4$-*p*-Bu^t)$_2$(μ_2-SC$_6$H$_4$-*p*-O(CO)-R)]Cl (R = 4,4-difluoro-8-(4-phenyl)-1,3,5,7-tetramethyl-2,6-diethyl-4-bora-3a,4a-diaza-*s*-indacene) (1.2.35)
To a solution of **1.2.32** (0.100 g, 0.236 mmol, 1.2 equiv.) in dry CH_2Cl_2 (50 mL) at r.t. under inert atmosphere (N_2) were added successively EDCI (0.076 g, 0.394 mmol, 2 equiv.), **1.2.2** (0.195 g, 0.197 mmol, 1 equiv.) and DMAP (0.012 g, 0.099 mmol, 0.5 equiv.). The reaction mixture was stirred at r.t. under inert atmosphere (N_2) for further 72 h and the reaction evolution was verified by TLC (CH_2Cl_2/CH_3OH 9:1 (v/v)). The reaction mixture was concentrated to dryness under reduced pressure and purification by column chromatography using CH_2Cl_2/CH_3OH afforded **1.2.35** as an orange-pink solid (0.069 g, 0.049 mmol, yield 25%).
^{1}H-NMR ($CDCl_3$) δ_H, ppm: 8.33 (2H, d, (C=O)-(*Ar*)C-C*H*-CH-C, $^3J_{H,H}$ = 8.0 Hz), 7.91 (2H, d, 2xS-(*Ar*)C-CH-C*H*-C-O-(C=O), $^3J_{H,H}$ = 8.0 Hz), 7.51 (2H, d, (C=O)-(*Ar*)C-CH-C*H*-C, $^3J_{H,H}$ = 8.0 Hz), 7.48 (4H, s, 4xCH_2-(*Ar*)C-CH-C*H*-C-C(CH_3)$_3$), 7.43 (4H, s, 4xCH_2-(*Ar*)C-C*H*-CH-C-C(CH_3)$_3$), 7,29 (2H, d, 2xS-(*Ar*)C-C*H*-CH-C-O-(C=O), $^3J_{H,H}$ = 8.0 Hz), 5.20 (2H, d, 2xCH_3-(*Ar*)C-CH-C*H*-C, $^3J_{H,H}$ = 5.0 Hz), 5.07 (2H, d, 2xCH_3-(*Ar*)C-C*H*-CH-C, $^3J_{H,H}$ = 5.4 Hz), 5.00 (2H, d, 2xCH_3-(*Ar*)C-CH-C*H*-C, $^3J_{H,H}$ = 5.0 Hz), 4.66 (2H, d, 2xCH_3-(*Ar*)C-C*H*-CH-C, $^3J_{H,H}$ = 5.5 Hz), 3.64 (2H, s, C*H*$_2$-(*Ar*)C-CH-CH-C-C(CH_3)$_3$), 3.47 (2H, s, C*H*$_2$-(*Ar*)C-CH-CH-C-C(CH_3)$_3$), 2.55 (6H, s, 2xBF_2-N-C-C*H*$_3$), 2.32, (4H, qvart, 2xBF_2-N-C-C-C*H*$_2$-CH_3, $^3J_{H,H}$ = 7.4 Hz), 1.91-2.00 (2H, sept, 2x(*Ar*)C-CH-CH-C-C*H*(CH_3)$_2$, $^3J_{H,H}$ = 6.7 Hz), 1.88 (6H, s, 2xC*H*$_3$-(*Ar*)C-CH-CH-C), 1.37 (9H, s, S-CH_2-(*Ar*)C-CH-CH-C-C(C*H*$_3$)$_3$), 1.34 (9H, s, S-CH_2-(*Ar*)C-CH-CH-C-C(C*H*$_3$)$_3$), 1.32 (6H, s, 2xBF_2-N-C-C-C*H*$_3$), 1.00 (6H, t, 2xBF_2-N-C-C-CH_2-C*H*$_3$, $^3J_{H,H}$ = 7.4 Hz), 0.98 (6H, d, 2x(*Ar*)C-CH-CH-C-CH(C*H*$_3$)$_2$, $^3J_{H,H}$ = 6.7 Hz), 0.92 (6H, d, 2x(*Ar*)C-CH-CH-C-CH(C*H*$_3$)$_2$, $^3J_{H,H}$ = 6.7 Hz).
^{13}C-NMR ($CDCl_3$) δ_C, ppm: 169.5 (1C, S-(*Ar*)C-CH-CH-C-O-(*C*=O)), 154.6 (2C, 2xBF_2-N-*C*-CH_3), 151.9, 151.8 (8C, 2xS-CH_2-(*Ar*)C-CH-CH-*C*-C(CH_3)$_3$, 2xS-CH_2-(*Ar*)C-CH-CH-C-*C*(CH_3)$_3$), 151.3 (1C, S-(*Ar*)C-CH-CH-*C*-O), 141.9 (1C, (C=O)-(*Ar*)*C*-CH-CH-C), 138.5 (2C, 2xBF_2-N-C-*C*-CH_2-CH_3), 138.2 (2C, 2xBF_2-N-C-*C*-CH_3), 136.9, 136.8 (2C, 2xS-CH_2-(*Ar*)*C*-CH-CH-C-C(CH_3)$_3$), 135.5 (1C, S-(*Ar*)*C*-CH-CH-C-O), 134.0 (1C, S-(*Ar*)C-CH-*C*H-C-O), 133.4 (2C, 2xBF_2-N-C-*C*-CH_2-CH_3), 131.0 (2C, (C=O)-(*Ar*)*C*-CH-CH-C), 130.4 (2C, (C=O)-(*Ar*)C-CH-CH-*C*), 129.5 (2C, (C=O)-(*Ar*)C-CH-CH-C-*C*), 129.3, 129.2 (2C, 2xS-CH_2-(*Ar*)C-*C*H-CH-C-C(CH_3)$_3$), 125.7, 125.5 (2C, 2xS-CH_2-(*Ar*)C-CH-*C*H-C-C(CH_3)$_3$), 122.6 (1C, S-(*Ar*)C-*C*H-CH-C-O), 107.2 (2C, 2xCH_3-(*Ar*)C-CH-CH-*C*), 100.7 (2C, 2xCH_3-(*Ar*)*C*-CH-CH-C), 84.4 (1C, CH_3-(*Ar*)C-CH-*C*H-C), 83.9, 83.8 (1C, CH_3-(*Ar*)C-*C*H-CH-C, 1C, CH_3-(*Ar*)C-CH-*C*H-C), 82.7 (1C, CH_3-(*Ar*)C-*C*H-CH-C), 40.2 (1C, S-*C*H_2-(*Ar*)C-CH-CH-C-C(CH_3)$_3$), 39.8 (1C, S-*C*H_2-(*Ar*)C-CH-CH-C-C(CH_3)$_3$), 34.95 (2C, 2xS-CH_2-(*Ar*)C-CH-CH-C-*C*(CH_3)$_3$), 34.90 (2C, 2xS-CH_2-(*Ar*)C-CH-CH-C-*C*(CH_3)$_3$), 31.6 (6C, 2xS-CH_2-(*Ar*)C-CH-CH-C-C(*C*H_3)$_3$), 31.0 (2C, 2x(*Ar*)CH-CH-C-*C*H(CH_3)$_2$), 23.3 (2C, (*Ar*)CH-CH-C-CH(*C*H_3)$_2$), 22.8 (2C, (*Ar*)CH-CH-C-CH(*C*H_3)$_2$), 18.4 (2C, 2x*C*H_3-(*Ar*)C-CH-CH), 17.2 (2C, 2xBF_2-N-C-C-*C*H_2-CH_3), 14.7 (2C, 2xBF_2-N-C-C-CH_2-*C*H_3), 12.7 (2C, 2xBF_2-N-C-*C*H_3), 12.1 (2C, 2xBF_2-N-C-C-*C*H_3).
^{19}F-NMR ($CDCl_3$) δ_C, ppm: -145,77 (2F, dd, B*F*$_2$, $^1J_{B,F}$ = 32.11 Hz, $^2J_{F,F}$ = 33.78 Hz).
^{11}B-NMR ($CDCl_3$) δ_C, ppm: 0.80 (1B, t, *B*F_2, $^1J_{B,F}$ = 32.20 Hz).
R_f(CH_2Cl_2/CH_3OH 10:1) = 0.319.
ESI-MS(+):*m/z* found 1361.4181 $[M-Cl]^+$, calcd. for $C_{72}H_{88}BF_2N_2O_2Ru_2S_3^+$ 1361.4151.
Elemental analysis (%): calcd. for $C_{72}H_{88}BClF_2N_2O_2Ru_2S_3 \cdot 0.7CH_3OH$ C 61.56, H 6.45, N 1.97; found C 61.57, H 6.98, N 2.27.

Synthesis of [(η^6-*p*-MeC$_6$H$_4$Pr^i)$_2$Ru$_2$(μ_2-SCH$_2$C$_6$H$_4$-*p*-Bu^t)$_2$(μ_2-SC$_6$H$_4$-*p*-NH(CO)-R)]Cl (R = 4,4-difluoro-8-(4-phenyl)-1,3,5,7-tetramethyl-2,6-diethyl-4-bora-3a,4a-diaza-*s*-indacene) (1.2.36)

To a solution of **1.2.32** (0.103 g, 0.242 mmol, 1.2 equiv.) in dry CH_2Cl_2 (50 mL) at r.t. under inert atmosphere (N_2) were added EDCI (0.116 g, 0.606 mmol, 3 equiv.) and DIPEA (0.1mL, 0.505 mmol, 2.5 equiv.). After 15 min have been added successively HOBt·H_2O (0.067 g, 0.485 mmol, 2.4 equiv.), **1.2.3** (0.200 g, 0.202 mmol, 1 equiv.) and DIPEA (0.1 mL, 0.505 mmol, 2.5 equiv.). The reaction mixture was stirred at r.t. under inert atmosphere (N_2) for further 48 h and the reaction evolution was verified by TLC (CH_2Cl_2/CH_3OH 10:1 (v/v)). The reaction mixture was concentrated to dryness and purification by column chromatography using CH_2Cl_2/CH_3OH afforded **1.2.36** as an orange-pink solid (0.157 g, 0.113 mmol, yield 56%).

^{1}H-NMR ($CDCl_3$) δ_H, ppm: 11.49 (1H, s, S-(*Ar*)C-CH-CH-C-N*H*), 8.71 (2H, d, S-(*Ar*)C-CH-C*H*-C-NH, $^3J_{H,H}$ = 8.2 Hz), 8.56 (2H, d, (C=O)-(*Ar*)C-C*H*-CH-C, $^3J_{H,H}$ = 8.5 Hz), 7.66 (2H, d, (C=O)-(*Ar*)C-CH-C*H*-C, $^3J_{H,H}$ = 8.5 Hz), 7.41-7.51 (10H, m, 4xCH_2-(*Ar*)C-C*H*-CH-C-C$(CH_3)_3$, 4xCH_2-(*Ar*)C-CH-C*H*-C-C$(CH_3)_3$, 2xS-(*Ar*)C-CH-C*H*-C-NH-(C=O)), 5.01 (2H, d, 2xCH_3-(*Ar*)C-CH-C*H*-C, $^3J_{H,H}$ = 5.7 Hz), 4.90 (2H, d, 2xCH_3-(*Ar*)C-C*H*-CH-C, $^3J_{H,H}$ = 5.7 Hz), 4.73 (2H, d, 2xCH_3-(*Ar*)C-CH-C*H*-C, $^3J_{H,H}$ = 5.7 Hz), 4.63 (2H, d, 2xCH_3-(*Ar*)C-C*H*-CH-C, $^3J_{H,H}$ = 5.7 Hz), 3.57 (2H, s, C*H*$_2$-(*Ar*)C-CH-CH-C-C$(CH_3)_3$), 3.37 (2H, s, C*H*$_2$-(*Ar*)C-CH-CH-C-C$(CH_3)_3$), 2.53 (6H, s, 2xBF_2-N-C-C*H*$_3$), 2.29, (4H, qvart, 2xBF_2-N-C-C-C*H*$_2$-CH_3, $^3J_{H,H}$ = 7.5 Hz), 1.97-2.07 (2H, sept, 2x(*Ar*)C-CH-CH-C-C*H*$(CH_3)_2$, $^3J_{H,H}$ = 6.8 Hz), 1.69 (6H, s, 2xC*H*$_3$-(*Ar*)C-CH-CH-C), 1.38 (9H, s, S-CH_2-(*Ar*)C-CH-CH-C-C(C*H*$_3$)$_3$), 1.36 (9H, s, S-CH_2-(*Ar*)C-CH-CH-C-C(C*H*$_3$)$_3$), 1.33 (6H, s, 2xBF_2-N-C-C-C*H*$_3$), 1.00 (6H, d, 2x(*Ar*)C-CH-CH-C-CH(C*H*$_3$)$_2$, $^3J_{H,H}$ = 6.9 Hz), 0.97 (6H, t, 2xBF_2-N-C-C-CH_2-C*H*$_3$, $^3J_{H,H}$ = 7.8 Hz), 0.96 (6H, d, 2x(*Ar*)C-CH-CH-C-CH(C*H*$_3$)$_2$,$^3J_{H,H}$ = 6.8 Hz).

^{13}C-NMR ($CDCl_3$) δ_C, ppm: 166.6 (1C, S-(*Ar*)C-CH-CH-C-NH-(*C*=O)), 153.7 (2C, 2xBF_2-N-*C*-CH_3), 152.1 (2C, 2xS-CH_2-(*Ar*)C-CH-CH-*C*-C$(CH_3)_3$), 141.7 (1C, (C=O)-(*Ar*)C-CH-CH-*C*), 140.2 (2C, 2xS-CH_2-(*Ar*)C-CH-CH-C-*C*$(CH_3)_3$), 139.0 (1C, (C=O)-(*Ar*)*C*-CH-CH-C), 138.9 (2C, 2xBF_2-N-C-*C*-CH_3), 136.9, 136.5 (2C, 2xS-CH_2-(*Ar*)*C*-CH-CH-C-C$(CH_3)_3$), 135.0 (1C, S-(*Ar*)*C*-CH-CH-C-NH), 132.8 (2C, 2xBF_2-N-C-*C*-CH_2-CH_3), 132.6 (2C, (C=O)-(*Ar*)C-CH-*C*H-C), 130.7 (2C, (C=O)-(*Ar*)*C*-CH-CH-C), 130.0 (2C, (C=O)-(*Ar*)C-CH-CH-*C*), 129.96 (2C, S-(*Ar*)C-CH-*C*H-C-NH), 129.3, 129.1 (2C, 2xS-CH_2-(*Ar*)C-*C*H-CH-C-C$(CH_3)_3$), 128.3 (2C, S-(*Ar*)C-*C*H-CH-C-NH), 125.73, 125.69 (2C, 2xS-CH_2-(*Ar*)C-CH-*C*H-C-C$(CH_3)_3$), 122.0 (1C, (C=O)-(*Ar*)C-*C*H-CH-C), 107.8 (2C, 2xCH_3-(*Ar*)C-CH-CH-*C*), 100.2 (2C, 2xCH_3-(*Ar*)*C*-CH-CH-C), 84.3 (1C, CH_3-(*Ar*)C-CH-*C*H-C), 83.9, (1C, CH_3-(*Ar*)C-*C*H-CH-C), 83.3 (1C, CH_3-(*Ar*)C-CH-*C*H-C), 82.2 (1C, CH_3-(*Ar*)C-*C*H-CH-C), 40.0 (1C, S-*C*H_2-(*Ar*)C-CH-CH-C-C$(CH_3)_3$), 39.2 (1C, S-*C*H_2-(*Ar*)C-CH-CH-C-C$(CH_3)_3$), 34.96 (2C, 2xS-CH_2-(*Ar*)C-CH-CH-C-*C*$(CH_3)_3$),34.94 (2C, 2xS-CH_2-(*Ar*)C-CH-CH-C-*C*$(CH_3)_3$), 31.55-31.57 (6C, 2xS-CH_2-(*Ar*)C-CH-CH-C-C(*C*$H_3)_3$), 31.2 (2C, 2x(*Ar*)CH-CH-C-*C*H$(CH_3)_2$), 23.2 (2C, (*Ar*)CH-CH-C-CH(*C*$H_3)_2$), 23.0 (2C, (*Ar*)CH-CH-C-CH(*C*$H_3)_2$), 18.2 (2C, 2x*C*H_3-(*Ar*)C-CH-CH), 17.2 (2C, 2xBF_2-N-C-C-*C*H_2-CH_3), 14.8 (2C, 2xBF_2-N-C-C-CH_2-*C*H_3), 12.6 (2C, 2xBF_2-N-C-*C*H_3), 12.2 (2C, 2xBF_2-N-C-C-*C*H_3).

^{19}F-NMR ($CDCl_3$) δ_C, ppm: -145,69 (2F, dd, B*F*$_2$, $^1J_{B,F}$ = 32.73 Hz, $^2J_{F,F}$ = 33.78 Hz).

^{11}B-NMR ($CDCl_3$) δ_C, ppm: 0.86 (1B, t, *B*F_2, $^1J_{B,F}$ = 32.23 Hz).

R_f(CH_2Cl_2/CH_3OH 10:1) = 0.362.

ESI-MS(+):*m/z* found 1360.4316 $[M\text{-}Cl]^+$, calcd. for $C_{72}H_{89}BF_2N_3ORu_2S_3^+$ 1360.4310.

Elemental analysis (%): calcd. for $C_{72}H_{89}BClF_2N_3ORu_2S_3$·0.5$CH_3OH$ C 61.75, H 6.50, N 2.98; found C 61.75, H 6.50, N 2.94.

1.2.4 Stability in DMSO-d_6

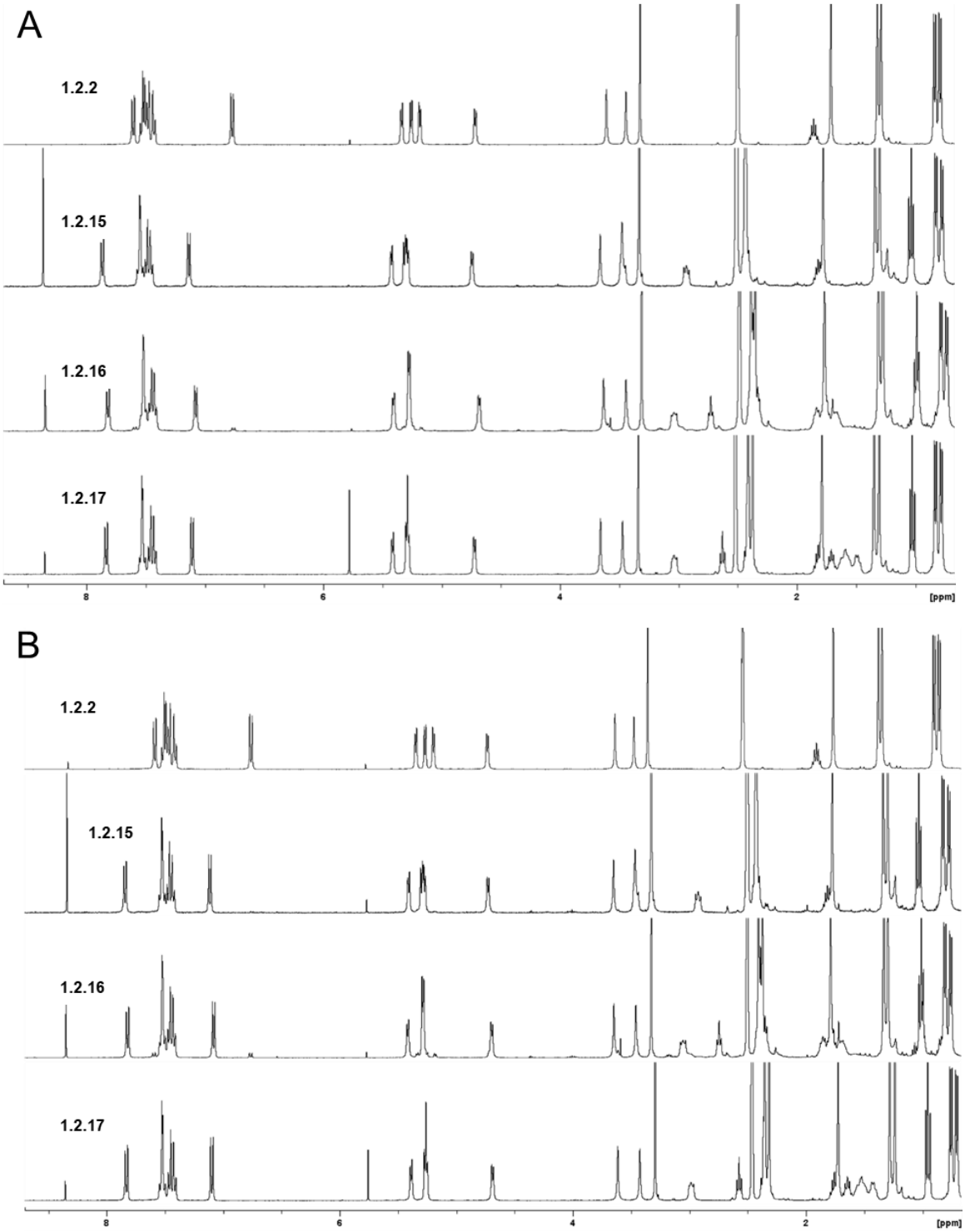

Figure S1.2.5. ^{1}H NMR Spectra of **1.2.2** and **1.2.15**-**1.2.17**recorded in DMSO-d_6 at 25°C; (A) recorded 5 min after sample preparation, and (B) sample after > 30 days storage at 0-5°C in the dark.

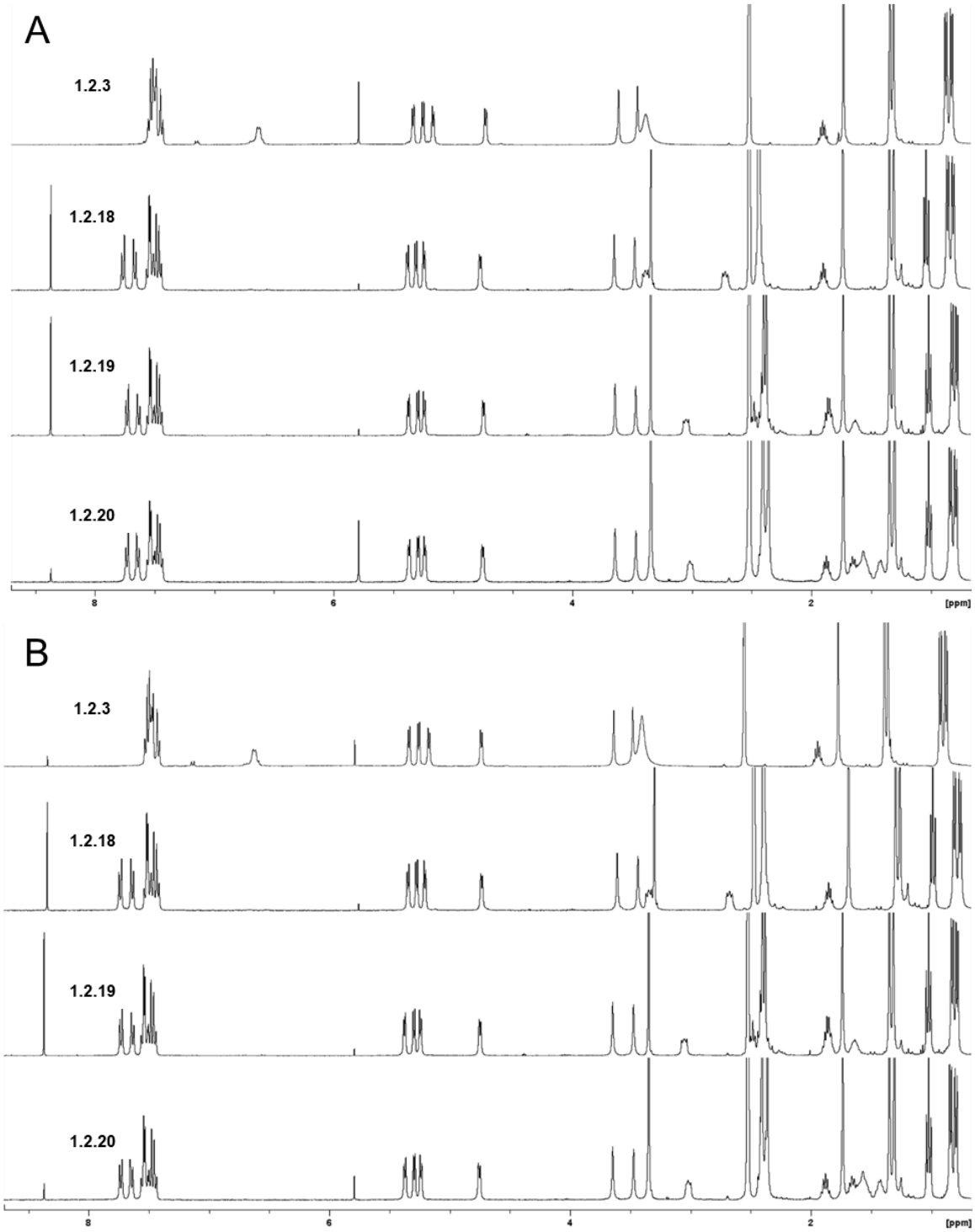

Figure S1.2.6. ^{1}H NMR spectra of **1.2.3** and **1.2.18-1.2.20** recorded in DMSO-d_6 at 25°C; (A) recorded 5 min after sample preparation, and (B) sample after > 30 days storage at 0-5°C in the dark.

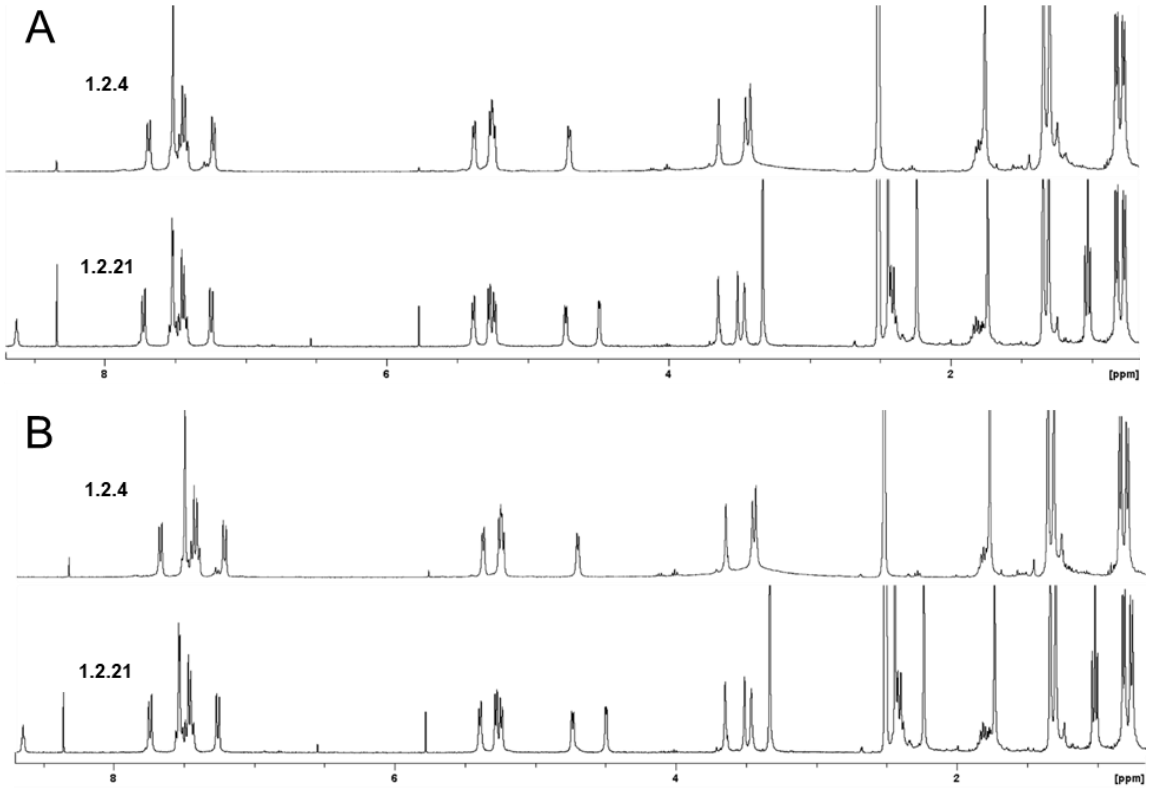

Figure S1.2.7. ^{1}H NMR spectra of **1.2.4** and **1.2.21** recorded in DMSO-d_6 at 25°C; (A) recorded 5 min after sample preparation, and (B) sample after > 30 days storage at 0-5°C in the dark.

The complexes are well soluble in DMSO, solvent used to prepare standard solutions for biological assays. To assess their stability, the compounds were solubilized in DMSO-d_6, and two ^{1}H-NMR spectra were recorded at 25°C 5 min and 28 days after sample preparation. Between the two experiments, the samples were stored at 0°C. For all complexes, there are no significant changes between the spectrum recorded after 5 min and the spectrum recorded after 28 days at 0°C, which indicates a very good stability of the complexes, and makes them suitable for further biological tests.

2.1. Nucleic base-Tagged Dinuclear Trithiolato-Bridged Ruthenium(II)-Arene Complexes[10]

2.1.1. Experimental

Chemistry[11]

General

Chemicals were purchased from Aldrich, Alfa Aesar, Acros Organics, ABCR, and TCI Chemicals and used without further purification. Reactions were performed under inert atmosphere (N_2) using Schlenk techniques with dry solvents (Acros Organics) preserved over molecular sieves. ^{1}H (400.13 MHz) and ^{13}C (100.62 MHz) NMR spectra were recorded on a Bruker Avance II 400 spectrometer at 298 K. The chemical shifts are reported in parts per million (ppm) and referenced to residual solvent peaks[393] ($CDCl_3$, ^{1}H δ 7.26, ^{13}C{^{1}H} δ 77.16 ppm; MeOD-d_4, ^{1}H δ 3.31, ^{13}C{^{1}H} δ 49.00 ppm, DMSO-d_6, ^{1}H δ 2.50, ^{13}C{^{1}H} δ 39.52 ppm,), and coupling constants (*J*) are reported in hertz (Hz). High resolution electrospray ionization mass spectra (ESI-MS) were carried out by the Mass Spectrometry and Protein Analyses Services at DCBP and were obtained on a LTQ Orbitrap XL ESI (Thermo) operated in positive ion mode. Thermal elemental analyses were carried out by the Mass Spectrometry and Protein Analyses Services at DCBP and were obtained on a Flash 2000 Organic Elemental Analyzer (Thermo Scientific). Reactions were monitored by TLC using Merck TLC silica gel coated aluminium sheets 60 F254 and visualized with UV at 254 nm. Compounds were purified by column flash chromatography on silica gel using the elution systems indicated.

***Abbreviations*:**

DIPEA - *N*,*N*-Diisopropylethylamine
DMAP - 4-(Dimethylamino)-pyridine
DMF - Dimethylformamide
EDCI - *N*-(3-Dimethylaminopropyl)-*N'*-ethylcarbodiimide hydrochloride
EtOAc - Ethyl acetate
Hex - *n*-Hexane
HOBt·H₂O - 1-Hydroxybenzotriazole hydrate
MsCl - Methanesulfonyl chloride
^{i}PrOH - 2-Propanol
TEA – Triethylamine

For the description of the NMR spectra: *Ar* – arene, *Tr* – triazole, *Py* - pyridine

Synthesis of the trithiolato-bridged dinuclear ruthenium(II)-arene intermediates

The dithiolato intermediate **2.1.1** ([(η^6-*p*-$MeC_6H_4Pr^i$)$_2$Ru$_2$(μ_2-$SCH_2C_6H_4$-*p*-Bu^t)Cl$_2$]) was prepared and purified by adapting a previously described protocol[53, 131]. Similarly, trithiolato diruthenium amino, carboxy and hydroxy derivatives **2.1.2** ([(η^6-*p*-$MeC_6H_4Pr^i$)$_2$Ru$_2$(μ_2-$SCH_2C_6H_4$-*p*-Bu^t)$_2$(μ_2-SC_6H_4-*p*-NH_2)]Cl), **2.1.3** ([(η^6-*p*-$MeC_6H_4Pr^i$)$_2$Ru$_2$(μ_2-$SCH_2C_6H_4$-*p*-Bu^t)$_2$(μ_2-SC_6H_4-*p*-CH_2CO_2H)]Cl) and **2.1.4** ([(η^6-*p*-$MeC_6H_4Pr^i$)$_2$Ru$_2$(μ_2-$SCH_2C_6H_4$-*p*-Bu^t)$_2$(μ_2-SC_6H_4-*o*-CH_2OH)]Cl) were synthesized following previously reported procedures[30, 131].

[10] This chapter is a draft with title *Synthesis and Antiparasitic Activity of New Nucleic Base-tethered Trithiolato-bridged Dinuclear Ruthenium(II)-Arene Compounds*, which is going to be submitted for publication.
[11] Only syntheses of compounds obtained by the author of this thesis are presented.

Synthesis of [(η^6-*p*-MeC$_6$H$_4$Pr^i)$_2$Ru$_2$(μ_2-SCH$_2$C$_6$H$_4$-*p*-Bu^t)$_2$(μ_2-SC$_6$H$_4$-*p*-CH$_2$-(C=O)-NH-R)]Cl (R = CH$_2$-C≡CH) (2.1.8)

Compound **2.1.8** was synthesized and purified as previously reported[186].

Synthesis of [(η^6-*p*-MeC$_6$H$_4$Pr^i)$_2$Ru$_2$(μ_2-SCH$_2$C$_6$H$_4$-*p*-Bu^t)$_2$(μ_2-SC$_6$H$_4$-*p*-N$_3$)]Cl (2.1.10)

Compound **2.1.10** was prepared by adapting a literature procedure[294]. To a suspension of **2.1.2** (0.300 g, 0.303 mmol, 1 equiv.) in HCl aq. (17%, 10 mL), $NaNO_2$ (0.025 g, 0.364 mmol, 1.2 equiv.) was added at 0°C under inert atmosphere (N_2), and the mixture was further stirred for 1 h. Then NaN_3 (0.024 g, 0.364 mmol, 1.2 equiv.) was added and the reaction mixture was further stirred at 0°C under N_2 for another 5 h, and subsequently at r.t. for 18 h. The reaction evolution was verified by TLC. The reaction mixture was filtered, and precipitate was solubilized in CH_2Cl_2 (30 mL), and the organic solution was washed with H_2O (2x30 mL), with brine (30 mL), dried over anhydrous Na_2SO_4, filtered and concentrated to dryness. Compound **2.1.10** (0.325 g) was recovered as an orange solid still containing traces of the starting amine **2.1.2** and was used in click reactions without further purification. A small quantity was purified by column chromatography to be used for the biological activity assessment.

^{1}H-NMR ($CDCl_3$) δ_H, ppm: 7.87 (2H, d, 2xS-(*Ar*)C-C*H*-CH-C-N$_3$, $^3J_{H,H}$ = 8.3 Hz), 7.41-7.54 (8H, m, 4xS-CH$_2$-(*Ar*)C-C*H*-CH-C-C(CH$_3$)$_3$, 4xS-CH$_2$-(*Ar*)C-CH-C*H*-C-C(CH$_3$)$_3$, $^3J_{H,H}$ = 8.6 Hz), 7.01 (2H, d, 2xS-(*Ar*)C-CH-C*H*-C-N$_3$, $^3J_{H,H}$ = 8.3 Hz), 5.13 (2H, d, 2xCH$_3$-(*Ar*)C-CH-C*H*-C, $^3J_{H,H}$ = 5.6 Hz), 5.05 (2H, d, 2xCH$_3$-(*Ar*)C-CH-C*H*-C, $^3J_{H,H}$ = 5.9 Hz), 4.91 (2H, d, 2xCH$_3$-(*Ar*)C-C*H*-CH-C, $^3J_{H,H}$ = 5.6 Hz), 4.66 (2H, d, 2xCH$_3$-(*Ar*)C-C*H*-CH-C, $^3J_{H,H}$ = 5.7 Hz), 3.67 (2H, s, S-C*H$_2$*-(*Ar*)C-CH-CH-C-C(CH$_3$)$_3$), 3.44 (2H, s, S-C*H$_2$*-(*Ar*)C-CH-CH-C-C(CH$_3$)$_3$), 1.95 (2H, sept, 2x(*Ar*)C-CH-CH-C-C*H*(CH$_3$)$_2$, $^3J_{H,H}$ = 6.8 Hz), 1.75 (6H, s, 2xC*H$_3$*-(*Ar*)C-CH-CH-C), 1.36 (9H, s, S-CH$_2$-(*Ar*)C-CH-CH-C-C(C*H$_3$*)$_3$), 1.34 (9H, s, S-CH$_2$-(*Ar*)C-CH-CH-C-C(C*H$_3$*)$_3$), 0.97 (6H, d, (*Ar*)C-CH-CH-C-CH(C*H$_3$*)$_2$, $^3J_{H,H}$ = 6.8 Hz), 0.92 (6H, d, (*Ar*)C-CH-CH-C-CH(C*H$_3$*)$_2$, $^3J_{H,H}$ = 6.8 Hz).

^{13}C-NMR ($CDCl_3$) δ_H, ppm: 151.82, 151.76 (2C, 2xS-CH$_2$-(*Ar*)C-CH-CH-*C*-C(CH$_3$)$_3$), 140.6 (1C, S-(*Ar*)C-CH-CH-*C*-N$_3$), 136.8 (2C, 2xS-CH$_2$-(*Ar*)*C*-CH-CH-C-C(CH$_3$)$_3$), 134.5 (2C, 2xS-(*Ar*)C-*C*H-CH-C-N$_3$), 134.4 (1C, S-(*Ar*)*C*-CH-CH-C-N$_3$), 129.6, 129.3 (4C, 4xS-CH$_2$-(*Ar*)C-*C*H-CH-C-C(CH$_3$)$_3$), 125.7, 125.6 (4C, 4xS-CH$_2$-(*Ar*)C-CH-*C*H-C-C(CH$_3$)$_3$), 119.6 (2C, 2xS-(*Ar*)C-CH-*C*H-C-N$_3$), 107.3 (2C, 2xCH$_3$-(*Ar*)C-CH-CH-*C*), 100.6 (2C, 2xCH$_3$-(*Ar*)*C*-CH-CH-C), 84.0 (4C, 2xCH$_3$-(*Ar*)C-*C*H-CH-C, 2xCH$_3$-(*Ar*)C-CH-*C*H-C), 83.9 (2C, 2xCH$_3$-(*Ar*)C-CH-*C*H-C), 82.6 (2C, 2xCH$_3$-(*Ar*)C-*C*H-CH-C), 40.2 (1C, S-*C*H$_2$-(*Ar*)C-CH-CH-C-C(CH$_3$)$_3$), 39.8 (1C, S-*C*H$_2$-(*Ar*)C-CH-CH-C-C(CH$_3$)$_3$), 34.92, 34.89 (2C, 2xS-CH$_2$-(*Ar*)C-CH-CH-C-*C*(CH$_3$)$_3$), 31.58, 31.56 (6C, 2xS-CH$_2$-(*Ar*)C-CH-CH-C-C(*C*H$_3$)$_3$), 31.1 (2C, 2x(*Ar*)CH-CH-C-*C*H(CH$_3$)$_2$), 23.2 (2C, (*Ar*)CH-CH-C-CH(*C*H$_3$)$_2$), 22.9 (2C, (*Ar*)CH-CH-C-CH(*C*H$_3$)$_2$), 18.4 (2C, 2x*C*H$_3$-(*Ar*)C-CH-CH).

***R*$_f$** (CH_2Cl_2/CH_3OH 10:1) = 0.327.

ESI-MS(+): *m/z* found 980.2222 $[M-Cl]^+$, calcd. for $C_{48}H_{62}N_3Ru_2S_3^+$ 980.2187.

Elemental analysis (%): calcd. for $C_{48}H_{62}ClN_3Ru_2S_3 \cdot 0.5CH_2Cl_2 \cdot 2CH_3OH$ C 54.09, H 6.38, N 3.75; found: C 54.04, H 6.43, N 3.95.

Synthesis of the compounds constituting family 1

Synthesis of [(η^6-*p*-MeC$_6$H$_4$Pr^i)$_2$Ru$_2$(μ_2-SCH$_2$C$_6$H$_4$-*p*-Bu^t)$_2$(μ_2-SR)]Cl (RSH = 4-aminopyrimidine-2-thiol) (2.1.11)

Compound **2.1.11** was prepared and purified by adapting a literature procedure[53, 62, 131]. To a solution of **2.1.1** (0.300 g, 0.333 mmol, 1 equiv.) in EtOH (200 mL) was added 2-thiocytosine (4-aminopyrimidine-2-thiol) (0.175 g, 1.332 mmol, 4 equiv.), the suspension was heated at reflux for 96 h and the reaction evolution was verified by TLC. The reaction mixture was concentrated to dryness under reduced pressure. Purification by column chromatography (CH_2Cl_2/CH_3OH 9.5:0.5

(v/v)) afforded **2.1.11** as a brown solid (0.044 g, 0.044 mmol, yield 13%).

^{1}H-NMR ($CDCl_3$) δ_H, ppm: 8.02 (1H, d, S-(*Ar*)C-N-C*H*-CH, $^3J_{H,H}$ = 5.4 Hz), 7.37-7.59 (8H, m, 4xS-CH_2-(*Ar*)C-C*H*-CH-C-C$(CH_3)_3$, 4xS-CH_2-(*Ar*)C-CH-C*H*-C-C$(CH_3)_3$), 6.40 (1H, d, S-(*Ar*)C-N-CH-C*H*, $^3J_{H,H}$ = 5.9 Hz), 5.19 (2H, d, 2xCH_3-(*Ar*)C-CH-C*H*-C, $^3J_{H,H}$ = 5.8 Hz), 5.16 (2H, d, 2xCH_3-(*Ar*)C-CH-C*H*-C, $^3J_{H,H}$ = 5.7 Hz), 4.84-4.94 (4H, m br, 4xCH_3-(*Ar*)C-*CH*-CH-C), 3.58 (2H, s br, S-C*H*$_2$-(*Ar*)C-CH-CH-C-C$(CH_3)_3$), 3.49 (2H, s, S-C*H*$_2$-(*Ar*)C-CH-CH-C-C$(CH_3)_3$), 2.46 (2H, sept, 2x(*Ar*)C-CH-CH-C-C*H*$(CH_3)_2$, $^3J_{H,H}$ = 7.0 Hz), 1.95 (6H, s, 2xC*H*$_3$-(*Ar*)C-CH-CH-C), 1.37 (9H, s, S-CH_2-(*Ar*)C-CH-CH-C-C(C*H*$_3$)$_3$), 1.35 (9H, s, S-CH_2-(*Ar*)C-CH-CH-C-C(C*H*$_3$)$_3$), 1.08 (6H, d, (*Ar*)C-CH-CH-C-CH(C*H*$_3$)$_2$, $^3J_{H,H}$ = 6.8 Hz), 0.94-1.04 (6H, m, (*Ar*)C-CH-CH-C-CH(C*H*$_3$)$_2$).

***R*$_f$** (CH_2Cl_2/CH_3OH 10:1) = 0.170.

ESI-MS(+): *m/z* found 956.2179 $[M\text{-}Cl]^+$, calcd. for $C_{46}H_{62}N_3Ru_2S_3^+$ 956.2187.

Elemental analysis (%): calcd. for $C_{46}H_{62}ClN_3Ru_2S_3 \cdot CH_3OH$ C 55.19, H 6.50, N 4.11; found C 55.24, H 6.52, N 4.83.

Synthesis of [(η^6-*p*-$MeC_6H_4Pr^i$)$_2$$Ru_2$($\mu_2$-$SCH_2C_6H_4$-*p*-$Bu^t$)$_2$($\mu_2$-SR)]Cl (RSH = 2-mercapto-1,9-dihydro-6*H*-purin-6-one) (2.1.13)

Compound **2.1.13** was prepared and purified by adapting a literature procedure[53, 62, 131]. To a solution of **2.1.1** (0.300 g, 0.333 mmol, 1 equiv.) in EtOH (50 mL) was added 2-thioxanthine (2-mercapto-1,9-dihydro-6H-purin-6-one) (0.171 g, 0.999 mmol, 3 equiv.), The suspension was heated under reflux for 24 h and the reaction evolution was verified by TLC. The reaction mixture was filtered and the filtrate was concentrated to dryness under reduced pressure. Purification by column chromatography (CH_2Cl_2/CH_3OH 9:1 (v/v)) afforded **2.1.13** as an orange solid (0.152 g, 0.147 mmol, yield 44%).

^{1}H-NMR ($CDCl_3$) δ_H, ppm: 8.11 (1H, s, S-(*Ar*)C-N-C-NH-C*H*-N), 7.40-7.46 (4H, m, 2xS-CH_2-(*Ar*)C-CH-C*H*-C-C$(CH_3)_3$, 2xS-CH_2-(*Ar*)C-C*H*-CH-C-C$(CH_3)_3$), 7.33-7.40 (4H, m, 2xS-CH_2-(*Ar*)C-C*H*-CH-C-C$(CH_3)_3$), 2xS-CH_2-(*Ar*)C-CH-C*H*-C-C$(CH_3)_3$), 5.50 (2H, d, 2xCH_3-(*Ar*)C-CH-C*H*-C, $^3J_{H,H}$ = 5.0 Hz), 5.42 (2H, d, 2xCH_3-(*Ar*)C-CH-C*H*-C, $^3J_{H,H}$ = 5.4 Hz), 5.04 (2H, d, 2xCH_3-(*Ar*)C-C*H*-CH-C, $^3J_{H,H}$ = 5.6 Hz), 4.54 (2H, d, 2xCH_3-(*Ar*)C-C*H*-CH-C, $^3J_{H,H}$ = 4.7 Hz), 3.67 (2H, s, S-C*H*$_2$-(*Ar*)C-CH-CH-C-C$(CH_3)_3$), 3.32 (2H, s, S-C*H*$_2$-(*Ar*)C-CH-CH-C-C$(CH_3)_3$), 2.11 (2H, sept, 2x(*Ar*)C-CH-CH-C-C*H*$(CH_3)_2$, $^3J_{H,H}$ = 6.7 Hz), 1.92 (6H, s, 2xC*H*$_3$-(*Ar*)C-CH-CH-C), 1.32 (9H, s, S-CH_2-(*Ar*)C-CH-CH-C-C(C*H*$_3$)$_3$), 1.27 (9H, s, S-CH_2-(*Ar*)C-CH-CH-C-C(C*H*$_3$)$_3$), 0.84 (6H, d, (*Ar*)C-CH-CH-C-CH(C*H*$_3$)$_2$, $^3J_{H,H}$ = 6.7 Hz), 0.81 (6H, d, (*Ar*)C-CH-CH-C-CH(C*H*$_3$)$_2$, $^3J_{H,H}$ = 6.8 Hz).

^{13}C-NMR ($CDCl_3$) δ_C, ppm: 157.5 (1C, S-(*Ar*)C-NH-*C*=O), 155.2 (1C, S-(*Ar*)C-N-*C*-NH-CH-N), 153.3 (1C, S-(*Ar*)*C*-NH-C=O), 151.84, 151.79 (2C, 2xS-CH_2-(*Ar*)C-CH-CH-*C*-C$(CH_3)_3$), 141.3 (1C, S-(*Ar*)C-N-C-NH-*C*H-N), 137.0, 136.7 (2C, 2xS-CH_2-(*Ar*)*C*-CH-CH-C-C$(CH_3)_3$), 129.3, 129.1 (4C, 4xS-CH_2-(*Ar*)C-*C*H-CH-C-C$(CH_3)_3$), 125.6, 125.5 (4C, 4xS-CH_2-(*Ar*)C-CH-*C*H-C-C$(CH_3)_3$), 118.4 (1C, S-(*Ar*)C-NH-(C=O)-*C*-N), 106.6 (2C, 2xCH_3-(*Ar*)C-CH-CH-*C*), 102.4 (2C, 2xCH_3-(*Ar*)*C*-CH-CH-C), 85.2 (2C, 2xCH_3-(*Ar*)C-CH-*C*H-C), 84.6 (2C, 2xCH_3-(*Ar*)C-*C*H-CH-C), 83.3 (2C, 2xCH_3-(*Ar*)C-*C*H-CH-C), 82.3 (2C, 2xCH_3-(*Ar*)C-CH-*C*H-C), 40.4 (1C, S-*C*H$_2$-(*Ar*)C-CH-CH-C-C$(CH_3)_3$), 40.3 (1C, S-*C*H$_2$-(*Ar*)C-CH-CH-C-C$(CH_3)_3$), 34.8 (2C, 2xS-CH_2-(*Ar*)C-CH-CH-C-*C*$(CH_3)_3$), 31.43, 31.41 (6C, 2xS-CH_2-(*Ar*)C-CH-CH-C-C(*C*H$_3$)$_3$), 31.3 (2C, 2x(*Ar*)CH-CH-C-*C*H$(CH_3)_2$), 23.1 (2C, (*Ar*)CH-CH-C-CH(*C*H$_3$)$_2$), 22.5 (2C, (*Ar*)CH-CH-C-CH(*C*H$_3$)$_2$), 18.5 (2C, 2x*C*H$_3$-(*Ar*)C-CH-CH).

***R*$_f$** (CH_2Cl_2/CH_3OH 10:1) = 0.402.

ESI-MS(+): *m/z* found 997.2109 $[M\text{-}Cl]^+$, calcd. for $C_{47}H_{61}N_4ORu_2S_3^+$ 997.2089.

Elemental analysis (%): calcd. for $C_{47}H_{61}ClN_4ORu_2S_3 \cdot 1.5CH_2Cl_2$ C 50.25, H 5.57, N 4.83; found

C 50.98, H 5.34, N 4.82.

Synthesis of the compounds constituing family 2

Synthesis of [(η^6-*p*-MeC$_6$H$_4$Pr^i)$_2$Ru$_2$(μ_2-SCH$_2$C$_6$H$_4$-p-Bu^t)(μ_2-SC$_6$H$_4$-*p*-CH$_2$CO$_2$R)]Cl (R = 2-(6-amino-9*H*-purin-9-yl)ethyl) (2.1.14)

Compound **2.1.14** was prepared and purified by adapting a literature protocol[131]. To a solution of **2.1.3** (0.300 g, 0.291 mmol, 1 equiv.) in dry CH_2Cl_2 (50 mL) at r.t. under inert atmosphere (N_2) were added successively EDCI (0.112 g, 0.582 mmol, 2 equiv.), 9-(2-hydroxyethyl)adenine (2-(6-amino-9*H*-purin-9-yl)ethan-1-ol) (**2.1.14A**) (0.080 g, 0.437 mmol, 1.5 equiv.) and DMAP (0.018 g, 0.146 mmol, 0.5 equiv.). The reaction mixture was stirred at r.t. under inert atmosphere (N_2) for 72 h and the reaction evolution was verified by TLC. The reaction mixture was concentrated to dryness under reduced pressure. Purification by column chromatography (CH_2Cl_2/CH_3OH 9:1 (v/v)) afforded **2.1.14** as an orange solid (0.148 g, 0.124 mmol, yield 43%).

^{1}H-NMR (MeOD-*d*$_4$) δ_H, ppm: 8.25 (1H, s, N-C*H*-N-C-NH$_2$), 8.19 (1H, s, CH$_2$-N-C*H*-N-C-C-NH$_2$), 7.71 (2H, d, S-(*Ar*)C-CH-C*H*-C-CH$_2$-(C=O)-O, $^3J_{H,H}$ = 8.1 Hz), 7.55 (2H, d, 2xS-CH$_2$-(*Ar*)C-CH-C*H*-C-C(CH$_3$)$_3$, $^3J_{H,H}$ = 8.3 Hz), 7.50 (4H, d, 2xS-CH$_2$-(*Ar*)C-CH-C*H*-C-C(CH$_3$)$_3$, 2xS-CH$_2$-(*Ar*)C-C*H*-CH-C-C(CH$_3$)$_3$, $^3J_{H,H}$ = 8.4 Hz), 7.45 (2H, d, 2xS-CH$_2$-(*Ar*)C-C*H*-CH-C-C(CH$_3$)$_3$, $^3J_{H,H}$ = 8.4 Hz), 7.08 (2H, d, S-(*Ar*)C-C*H*-CH-C-CH$_2$-(C=O)-O, $^3J_{H,H}$ = 8.2 Hz), 5.20 (2H, d, 2xCH$_3$-(*Ar*)C-CH-C*H*-C, $^3J_{H,H}$ = 5.8 Hz), 5.11 (2H, d, 2xCH$_3$-(*Ar*)C-CH-C*H*-C, $^3J_{H,H}$ = 5.9 Hz), 5.04 (2H, d, 2xCH$_3$-(*Ar*)C-C*H*-CH-C, $^3J_{H,H}$ = 5.8 Hz), 4.69 (2H, d, 2xCH$_3$-(*Ar*)C-C*H*-CH-C, $^3J_{H,H}$ = 5.9 Hz), 4.56 (2H, d, (C=O)-O-C*H*$_2$-CH$_2$-N, $^3J_{H,H}$ = 4.9 Hz), 4.48 (2H, d, (C=O)-O-CH$_2$-C*H*$_2$-N, $^3J_{H,H}$ = 4.9 Hz), 3.68 (2H, s, S-C*H*$_2$-(*Ar*)C-CH-CH-C-(CH$_3$)$_3$), 3.61 (2H, s, S-(*Ar*)C-CH-CH-C-C*H*$_2$-(C=O)-O), 3.49 (2H, s, S-C*H*$_2$-(*Ar*)C-CH-CH-C-(CH$_3$)$_3$), 1.80 (2H, sept, 2x(*Ar*)C-CH-CH-C-C*H*(CH$_3$)$_2$, $^3J_{H,H}$ = 6.8 Hz), 1.73 (6H, s, 2xC*H*$_3$-(*Ar*)C-CH-CH-C), 1.39 (9H, s, S-CH$_2$-(*Ar*)C-CH-CH-C-C(C*H*$_3$)$_3$), 1.35 (9H, s, S-CH$_2$-(*Ar*)C-CH-CH-C-C(C*H*$_3$)$_3$), 0.85 (6H, d, 2x(*Ar*)C-CH-CH-C-CH(C*H*$_3$)$_2$, $^3J_{H,H}$ = 6.8 Hz), 0.84 (6H, d, 2x(*Ar*)C-CH-CH-C-CH(C*H*$_3$)$_2$, $^3J_{H,H}$ = 6.9 Hz).

^{13}C-NMR (MeOD-*d*$_4$) δ_C, ppm: 172.3 (1C, S-(*Ar*)C-CH-CH-C-CH$_2$-(*C*=O)-O), 157.4 (1C, N-CH-N-C-*C*-NH$_2$), 153.9 (1C, N-*C*H-N-C-NH$_2$), 152.8, 152.6 (2C, 2xS-CH$_2$-(*Ar*)C-CH-CH-*C*-C(CH$_3$)$_3$), 150.9 (1C, N-*C*-N-(CH$_2$)$_2$), 143.1 (1C, N-*C*H-N-C-C-NH$_2$), 138.6, 138.5 (2C, 2xS-CH$_2$-(*Ar*)*C*-CH-CH-C-C(CH$_3$)$_3$), 138.1 (1C, S-(*Ar*)*C*-CH-CH-C-CH$_2$-(C=O)-O), 135.8 (1C, S-(*Ar*)C-CH-CH-*C*-CH$_2$-(C=O)-O), 134.1 (2C, 2xS-(*Ar*)C-CH-*C*H-C-CH$_2$-(C=O)-O), 130.8, 130.7 (4C, 4xS-CH$_2$-(*Ar*)C-*C*H-CH-C-C(CH$_3$)$_3$), 130.3 (2C, 2xS-(*Ar*)C-*C*H-CH-C-CH$_2$-(C=O)-O), 125.8, 125.6 (4C, 4xS-CH$_2$-(*Ar*)C-CH-*C*H-C-C(CH$_3$)$_3$), 120.1 (1C, N-CH-N-*C*-C-NH$_2$), 107.8 (2C, 2xCH$_3$-(*Ar*)C-CH-CH-*C*), 102.5 (2C, 2xCH$_3$-(*Ar*)*C*-CH-CH-C), 86.1 (2C, 2xCH$_3$-(*Ar*)C-CH-*C*H-C), 84.51 (2C, 2xCH$_3$-(*Ar*)C-*C*H-CH-C), 84.47 (2C, 2xCH$_3$-(*Ar*)C-CH-*C*H-C), 83.9 (2C, 2xCH$_3$-(*Ar*)C-*C*H-CH-C), 64.0 (1C, (C=O)-O-CH$_2$-*C*H$_2$), 44.0 (1C, (C=O)-O-*C*H$_2$-CH$_2$), 41.2 (1C, S-*C*H$_2$-(*Ar*)C-CH-CH-C-C(CH$_3$)$_3$), 41.1 (1C, S-*C*H$_2$-(*Ar*)C-CH-CH-C-C(CH$_3$)$_3$), 40.6 (1C, S-(*Ar*)C-CH-CH-C-*C*H$_2$-(C=O)-O), 35.63, 35.58 (2C, 2xS-CH$_2$-(*Ar*)C-CH-CH-C-*C*(CH$_3$)$_3$), 31.9 (2C, 2x(*Ar*)CH-CH-C-*C*H(CH$_3$)$_2$), 31.84, 31.82 (6C, 2xS-CH$_2$-(*Ar*)C-CH-CH-C-C(*C*H$_3$)$_3$), 23.5 (2C, (*Ar*)CH-CH-C-CH(*C*H$_3$)$_2$), 22.9 (2C, (*Ar*)CH-CH-C-CH(*C*H$_3$)$_2$), 18.2 (2C, 2x*C*H$_3$-(*Ar*)C-CH-CH).

***R*$_f$** (CH_2Cl_2/CH_3OH 10:1) = 0.408.

ESI-MS(+): *m/z* found 1158.2926 [M-Cl]$^+$, calcd. for $C_{57}H_{72}N_5O_2Ru_2S_3^+$ 1158.2930.

Elemental analysis (%): calcd. for $C_{57}H_{72}ClN_5O_2Ru_2S_3 \cdot 0.5CH_2Cl_2 \cdot H_2O$ C 55.10, H 6.03, N 5.59; found C 55.09, H 6.01, N 5.11.

Synthesis of the compounds composing family 3

The nucleic base derivatives **2.1.15-2.1.18** were prepared and purified by adapting literature procedures [298, 299, 396].

Synthesis of 1-propargyl-uracil (1-(prop-2-yn-1-yl)pyrimidine-2,4(1*H*,3*H*)-dione) (2.1.15)

To a solution of uracil (pyrimidine-2,4(1*H*,3*H*)-dione) (0.500 g, 4.371 mmol, 1 equiv.) in dry DMF (20 mL) at 60°C, under inert atmosphere (N_2) was added K_2CO_3 (0.302 g, 2.186 mmol, 0.5 equiv.) followed by dropwise addition of propargyl bromide (0.470 mL, 4.371 mmol, 1 equiv.). The mixture was stirred at 60°C for 48 h and the reaction evolution was verified by TLC. The reaction mixture was allowed to cool at r.t. and was concentrated under reduced pressure. Purification by flash column chromatography (CH_2Cl_2/CH_3OH 10:1 (v/v)) afforded **2.1.15** (0.313 g, 2.085 mmol, yield 48%).

^{1}H-NMR (MeOD-*d*$_4$) δ_H, ppm: 7.69 (1H, d, NH-(C=O)-CH-C*H*, $^3J_{H,H}$ = 7.9 Hz), 5.71 (1H, d, NH-(C=O)-C*H*-CH, $^3J_{H,H}$ = 7.9 Hz), 4.57 (2H, d, NH-(C=O)-N-C*H*$_2$-C≡CH, $^4J_{H,H}$ = 2.5 Hz), 2.91 (1H, t, NH-(C=O)-N-CH$_2$-C≡C*H*, $^4J_{H,H}$ = 2.5 Hz).

^{13}C-NMR (MeOD-*d*$_4$) δ_C, ppm: 166.5 (1C, NH-(*C*=O)-CH-CH), 152.2 (1C, NH-(*C*=O)-N-CH$_2$), 145.7 (1C, NH-(C=O)-CH-*C*H), 102.9 (1C, NH-(C=O)-*C*H-CH), 77.9 (1C, NH-(C=O)-N-CH$_2$-*C*≡CH), 75.6 (1C, NH-(C=O)-N-CH$_2$-C≡*C*H), 37.9 (1C, NH-(C=O)-N-*C*H$_2$-C≡CH).

***R*$_f$** (CH_2Cl_2/CH_3OH 10:1) = 0.496.

ESI-MS(+): *m/z* found 151.0502 $[M+H^+]^+$, 173.0321 $[M+Na^+]^+$, 323.0753 $[2M+Na^+]^+$, 473.1179 $[3M+Na^+]^+$, calcd. for $C_7H_7N_2O_2^+$ 151.0502, $C_7H_6N_2NaO_2^+$ 173.0321, $C_{14}H_{12}N_4NaO_4^+$ 323.0751, $C_{21}H_{18}N_6NaO_6^+$ 473.1180.

Elemental analysis (%): calcd. for $C_7H_6N_2O_2$ C 56.00, H 4.03, N 18.66; found C 56.05, H 3.96, N 18.66.

Synthesis of 1-propargyl-thymine (5-methyl-1-(prop-2-yn-1-yl)pyrimidine-2,4(1*H*,3*H*)-dione) (2.1.16)

To a solution of thymine (2,4-dihydroxy-5-methylpyrimidine) (0.510 g, 3.960 mmol, 1 equiv.) in dry DMF (20 mL) at 60°C under inert atmosphere (N_2) was added K_2CO_3 (0.274 g, 1.980 mmol, 0.5 equiv.) followed by dropwise addition of propargyl bromide (0.43 mL, 3.960 mmol, 1 equiv.). The mixture was stirred at 60°C for 48 h and the reaction evolution was verified by TLC. The reaction mixture was allowed to cool at r.t. and was concentrated under reduced pressure. Purification by flash column chromatography (CH_2Cl_2/CH_3OH 9:1 (v/v)) afforded **2.1.16** (0.280 g, 1.705 mmol, yield 43%).

^{1}H-NMR (MeOD-*d*$_4$) δ_H, ppm: 7.51 (1H, m, NH-(C=O)-N-C*H*, $^4J_{H,H}$ = 1.2 Hz), 4.54 (2H, d, NH-(C=O)-N-C*H*$_2$-C≡CH, $^4J_{H,H}$ = 2.5 Hz), 2.88 (1H, t, NH-(C=O)-N-CH$_2$-C≡C*H*, $^4J_{H,H}$ = 2.5 Hz), 1.88 (3H, d, N-CH-C-C*H*$_3$, $^4J_{H,H}$ = 1.1 Hz).

^{13}C-NMR (MeOD-*d*$_4$) δ_C, ppm: 166.6 (1C, (*C*=O)-NH-(C=O)-N-CH$_2$), 152.3 (1C, (C=O)-NH-(*C*=O)-N-CH$_2$), 141.5 (1C, (C=O)-N-*C*H-C-CH$_3$), 111.9 (1C, (C=O)-N-CH-*C*-CH$_3$), 78.2 (1C, NH-(C=O)-N-CH$_2$-*C*≡CH), 75.3 (1C, NH-(C=O)-N-CH$_2$-C≡*C*H), 37.6 (1C, NH-(C=O)-N-*C*H$_2$-C≡CH), 12.2 (1C, (C=O)-N-CH-C-*C*H$_3$).

***R*$_f$** (CH_2Cl_2/CH_3OH 10:1) = 0.600.

ESI-MS(+): *m/z* found 165.0659 $[M+H]^+$, 187.0478 $[M+Na]^+$, calcd. for $C_8H_9N_2O_2^+$ 165.0659, $C_8H_8N_2NaO_2^+$ 187.0478.

Elemental analysis (%): calcd. for $C_8H_8N_2O_2$ C 58.53, H 4.91, N 17.06; found C 58.56, H 4.93, N 17.04.

Synthesis of [(η^6-*p*-MeC$_6$H$_4$Pr^i)$_2$Ru$_2$(μ_2-SCH$_2$C$_6$H$_4$-*p*-Bu^t)$_2$(μ_2-SC$_6$H$_4$-*p*-R)]Cl (R = 1-((1*H*-1,2,3-triazol-4-yl)methyl)pyrimidine-2,4(1*H*,3*H*)-dione) (2.1.23)

To a solution of **2.1.10** (0.281 g, 0.268 mmol, 1 equiv.) and **2.1.15** (0.048 g, 0.322 mmol, 1.2 equiv.) in dry DMF (10 mL) were added successively $CuSO_4 \cdot 5H_2O$ (0.067 g, 0.268 mmol, 1 equiv.) and sodium ascorbate (0.106 g, 0.536 mmol, 2 equiv.). The reaction mixture was stirred at 60°C under

inert atmosphere (N_2) for further 24 h and the reaction evolution was verified by TLC. The reaction mixture was diluted with EtOAc (100 mL) and washed with H_2O (2×100 mL); the unified aqueous phases were further washed with EtOAc (100 mL). The combined organic phases were washed with brine (100 mL), dried over anhydrous Na_2SO_4, filtered and concentrated to dryness under reduced pressure. Purification by column chromatography (CH_2Cl_2/CH_3OH 9.5:0.5 (v/v)) afforded **2.1.23** as an orange solid (0.054 g, 0.046 mmol, yield 17%).

^{1}H-NMR ($CDCl_3$) δ_H, ppm: 9.40 (1H, s, (*Tr*)N-N=N-C-C*H*), 8.97 (1H, s, CH_2-N-(C=O)-N*H*-(C=O), 8.04 (1H, d, CH_2-N-*C*H-CH-(C=O), $^3J_{H,H}$ = 8.0 Hz), 8.01 (2H, d, 2xS-(*Ar*)C-CH-C*H*-C-(*Tr*)N, $^3J_{H,H}$ = 8.6 Hz), 7.93 (2H, d, 2xS-(*Ar*)C-C*H*-CH-C-(*Tr*)N, $^3J_{H,H}$ = 8.5 Hz), 7.38-7.50 (8H, m, 4xS-CH_2-(*Ar*)C-C*H*-CH-C-C(CH_3)$_3$, 4xS-CH_2-(*Ar*)C-CH-C*H*-C-C(CH_3)$_3$, $^3J_{H,H}$ = 8.5 Hz), 5.74 (1H, dd, CH_2-N-CH-C*H*-(C=O), $^3J_{H,H}$ = 7.8 Hz, $^4J_{H,H}$ = 1.6 Hz), 5.25 (2H, s br, (*Tr*)N-N=N-C-C*H*$_2$-N-(C=O)-NH), 5.10 (2H, d, 2xCH_3-(*Ar*)C-CH-C*H*-C, $^3J_{H,H}$ = 5.7 Hz), 5.01 (2H, d, 2xCH_3-(*Ar*)C-CH-C*H*-C, $^3J_{H,H}$ = 5.8 Hz), 4.89 (2H, d, 2xCH_3-(*Ar*)C-C*H*-CH-C, $^3J_{H,H}$ = 5.7 Hz), 4.67 (2H, d, 2xCH_3-(*Ar*)C-C*H*-CH-C, $^3J_{H,H}$ = 5.8 Hz), 3.61 (2H, s, S-C*H*$_2$-(*Ar*)C-CH-CH-C-C(CH_3)$_3$), 3.40 (2H, s, S-C*H*$_2$-(*Ar*)C-CH-CH-C-C(CH_3)$_3$), 1.98 (2H, sept, 2x(*Ar*)C-CH-CH-C-C*H*(CH_3)$_2$, $^3J_{H,H}$ = 6.8 Hz), 1.73 (6H, s, 2xC*H*$_3$-(*Ar*)C-CH-CH-C), 1.36 (9H, s, S-CH_2-(*Ar*)C-CH-CH-C-C(C*H*$_3$)$_3$), 1.32 (9H, s, S-CH_2-(*Ar*)C-CH-CH-C-C(C*H*$_3$)$_3$), 0.96 (6H, d, (*Ar*)C-CH-CH-C-CH(C*H*$_3$)$_2$, $^3J_{H,H}$ = 6.8 Hz), 0.91 (6H, d, (*Ar*)C-CH-CH-C-CH(C*H*$_3$)$_2$, $^3J_{H,H}$ = 6.9 Hz).

^{13}C-NMR ($CDCl_3$) δ_C, ppm: 163.8 (1C, NH-(*C*=O)-CH-CH), 152.1, 152.0 (2C, 2xS-CH_2-(*Ar*)C-CH-CH-*C*-C(CH_3)$_3$), 151.1 (1C, NH-(*C*=O)-N-CH_2), 145.5 (1C, NH-(C=O)-CH-*C*H), 143.3 (1C, (*Tr*)N-N=N-*C*-CH), 138.5 (1C, S-(*Ar*)C-CH-CH-*C*-(*Tr*)N), 137.1 (1C, S-(*Ar*)*C*-CH-CH-C-(*Tr*)N), 136.6, 136.4 (2C, 2xS-CH_2-(*Ar*)*C*-CH-CH-C-C(CH_3)$_3$), 134.1 (2C, 2xS-(*Ar*)C-*C*H-CH-C-(*Tr*)N), 129.3, 129.1 (4C, 4xS-CH_2-(*Ar*)C-*C*H-CH-C-C(CH_3)$_3$), 125.8, 125.6 (4C, 4xS-CH_2-(*Ar*)C-CH-*C*H-C-C(CH_3)$_3$), 123.7 (1C, (*Tr*)N-N=N-C-*C*H), 120.7 (2C, 2xS-(*Ar*)C-CH-*C*H-C-(*Tr*)N), 107.7 (2C, 2xCH_3-(*Ar*)C-CH-CH-*C*), 102.7 (1C, NH-(C=O)-*C*H-CH), 100.4 (2C, 2xCH_3-(*Ar*)*C*-CH-CH-C), 84.11 (2C, 2xCH_3-(*Ar*)C-CH-*C*H-C), 84.07 (2C, 2xCH_3-(*Ar*)C-*C*H-CH-C), 83.6 (2C, 2xCH_3-(*Ar*)C-CH-*C*H-C), 82.5 (2C, 2xCH_3-(*Ar*)C-*C*H-CH-C), 42.6 (1C, S-(*Ar*)C-CH-CH-C-(*Tr*)N-N=N-C-*C*H_2-N-(C=O)), 40.0 (1C, S-*C*H_2-(*Ar*)C-CH-CH-C-C(CH_3)$_3$), 39.6 (1C, S-*C*H_2-(*Ar*)C-CH-CH-C-C(CH_3)$_3$), 34.91, 34.87 (2C, 2xS-CH_2-(*Ar*)C-CH-CH-C-*C*(CH_3)$_3$), 31.52, 31.50 (6C, 2xS-CH_2-(*Ar*)C-CH-CH-C-C(*C*H_3)$_3$), 31.1 (2C, 2x(*Ar*)CH-CH-C-*C*H(CH_3)$_2$), 23.1 (2C, (*Ar*)CH-CH-C-CH(*C*H_3)$_2$), 22.9 (2C, (*Ar*)CH-CH-C-CH(*C*H_3)$_2$), 18.3 (2C, 2x*C*H_3-(*Ar*)C-CH-CH).

***R*$_f$** (CH_2Cl_2/CH_3OH 10:1) = 0.177.

ESI-MS(+): *m/z* found 1130.2594 $[M\text{-}Cl]^+$, calcd. for $C_{55}H_{68}N_5O_2Ru_2S_3^+$ 1130.2617.

Elemental analysis (%): calcd. for $C_{55}H_{68}ClN_5O_2Ru_2S_3 \cdot 0.1CH_2Cl_2 \cdot 1.7CH_3OH$ C 55.56, H 6.16, N 5.70; found C 55.56, H 6.16, N 5.25.

Synthesis of [(η^6-*p*-$MeC_6H_4Pr^i$)$_2$$Ru_2$($\mu_2$-$SCH_2C_6H_4$-*p*-$Bu^t$)$_2$($\mu_2$-$SC_6H_4$-*p*-R)]Cl (R = 5-methyl-1-((1*H*-1,2,3-triazol-4-yl)methyl)pyrimidine-2,4(1*H*,3*H*)-dione) (2.1.24)

To a solution of **2.1.10** (0.329 g, 0.315 mmol, 1 equiv.), and **2.1.16** (0.062 g, 0.378 mmol, 1.2 equiv.) in dry DMF (10 mL), were added successively $CuSO_4 \cdot 5H_2O$ (0.079 g, 0.315 mmol, 1 equiv.) and sodium ascorbate (0.125 g, 0.630 mmol, 2 equiv.). The reaction mixture was stirred at 60°C under inert atmosphere (N_2) for further 24 h and the reaction evolution was verified by TLC. The reaction mixture was solubilised in EtOAc (100 mL) and washed with H_2O (2×100 mL); the unified aqueous phases were further washed with EtOAc (100 mL). The combined organic phases were washed with brine (100 mL), dried over anhydrous Na_2SO_4, filtered and concentrated to dryness under reduced pressure. Purification by column chromatography (CH_2Cl_2/CH_3OH 9.5:0.5 (v/v)) afforded **2.1.24** as an orange solid (0.112 g, 0.095 mmol, yield 30%).

^{1}H-NMR ($CDCl_3$) δ_H, ppm: 9.41 (1H, s, (*Tr*)N-N=N-C-C*H*), 8.64 (1H, s, CH_2-N-(C=O)-N*H*-(C=O), 8.04 (2H, d, 2xS-(*Ar*)C-CH-C*H*-C-(*Tr*)N, $^3J_{H,H}$ = 8.3 Hz), 7.94 (2H, d, 2xS-(*Ar*)C-C*H*-CH-C-(*Tr*)N, $^3J_{H,H}$ = 8.2 Hz), 7.81 (1H, s, CH_2-N-*C*H-C-CH_3), 7.37-7.50 (8H, m, 4xS-CH_2-(*Ar*)C-C*H*-CH-C-$C(CH_3)_3$, 4xS-CH_2-(*Ar*)C-CH-C*H*-C-$C(CH_3)_3$, $^3J_{H,H}$ = 8.6 Hz), 5.19 (2H, s br, (*Tr*)N-N=N-C-C*H*$_2$-N-(C=O)-NH), 5.10 (2H, d, 2xCH_3-(*Ar*)C-CH-C*H*-C, $^3J_{H,H}$ = 5.7 Hz), 5.01 (2H, d, 2xCH_3-(*Ar*)C-CH-C*H*-C, $^3J_{H,H}$ = 5.8 Hz), 4.89 (2H, d, 2xCH_3-(*Ar*)C-C*H*-CH-C, $^3J_{H,H}$ = 5.6 Hz), 4.67 (2H, d, 2xCH_3-(*Ar*)C-C*H*-CH-C, $^3J_{H,H}$ = 5.8 Hz), 3.61 (2H, s, S-C*H*$_2$-(*Ar*)C-CH-CH-C-$C(CH_3)_3$), 3.40 (2H, s, S-C*H*$_2$-(*Ar*)C-CH-CH-C-$C(CH_3)_3$), 1.99 (2H, sept, 2x(*Ar*)C-CH-CH-C-C*H*$(CH_3)_2$, $^3J_{H,H}$ = 6.9 Hz), 1.95 (3H, s, CH_2-N-CH-C-C*H*$_3$), 1.73 (6H, s, 2xC*H*$_3$-(*Ar*)C-CH-CH-C), 1.36 (9H, s, S-CH_2-(*Ar*)C-CH-CH-C-C(C*H*$_3$)$_3$), 1.32 (9H, s, S-CH_2-(*Ar*)C-CH-CH-C-C(C*H*$_3$)$_3$), 0.96 (6H, d, (*Ar*)C-CH-CH-C-CH(C*H*$_3$)$_2$, $^3J_{H,H}$ = 6.8 Hz), 0.92 (6H, d, (*Ar*)C-CH-CH-C-CH(C*H*$_3$)$_2$, $^3J_{H,H}$ = 6.9 Hz).

^{13}C-NMR ($CDCl_3$) δ_C, ppm: 164.4 (1C, (*C*=O)-NH-(C=O)-N-CH_2), 152.04, 151.96 (2C, 2xS-CH_2-(*Ar*)C-CH-CH-*C*-C$(CH_3)_3$), 151.2 (1C, (C=O)-NH-(*C*=O)-N-CH_2), 143.4 (1C, (*Tr*)N-N=N-*C*-CH), 141.1 (1C, (C=O)-N-*C*H-C-CH_3), 138.5 (1C, S-(*Ar*)C-CH-CH-*C*-(*Tr*)N), 137.0 (1C, S-(*Ar*)*C*-CH-CH-C-(*Tr*)N), 136.6, 136.5 (2C, 2xS-CH_2-(*Ar*)*C*-CH-CH-C-C$(CH_3)_3$), 134.1 (2C, 2xS-(*Ar*)C-*C*H-CH-C-(*Tr*)N), 129.3, 129.1 (4C, 4xS-CH_2-(*Ar*)C-*C*H-CH-C-C$(CH_3)_3$), 125.7, 125.6 (4C, 4xS-CH_2-(*Ar*)C-CH-*C*H-C-C$(CH_3)_3$), 123.5 (1C, (*Tr*)N-N=N-C-*C*H), 120.7 (2C, 2xS-(*Ar*)C-CH-*C*H-C-(*Tr*)N), 111.3 (1C, (C=O)-N-CH-*C*-CH_3), 107.7 (2C, 2xCH_3-(*Ar*)C-CH-CH-*C*), 100.4 (2C, 2xCH_3-(*Ar*)*C*-CH-CH-C), 84.10 (2C, 2xCH_3-(*Ar*)C-CH-*C*H-C), 84.08 (2C, 2xCH_3-(*Ar*)C-*C*H-CH-C), 83.6 (2C, 2xCH_3-(*Ar*)C-CH-*C*H-C), 82.5 (2C, 2xCH_3-(*Ar*)C-*C*H-CH-C), 42.4 (1C, S-(*Ar*)C-CH-CH-C-(*Tr*)N-N=N-C-*C*H$_2$-N-(C=O)), 40.0 (1C, S-*C*H$_2$-(*Ar*)C-CH-CH-C-C$(CH_3)_3$), 39.6 (1C, S-*C*H$_2$-(*Ar*)C-CH-CH-C-C$(CH_3)_3$), 34.90, 34.86 (2C, 2xS-CH_2-(*Ar*)C-CH-CH-C-*C*$(CH_3)_3$), 31.51, 31.49 (6C, 2xS-CH_2-(*Ar*)C-CH-CH-C-C(*C*H$_3$)$_3$), 31.1 (2C, 2x(*Ar*)CH-CH-C-*C*H$(CH_3)_2$), 23.1 (2C, (*Ar*)CH-CH-C-CH(*C*H$_3$)$_2$), 22.9 (2C, (*Ar*)CH-CH-C-CH(*C*H$_3$)$_2$), 18.3 (2C, 2x*C*H$_3$-(*Ar*)C-CH-CH), 12.4 (1C, CH_2-N-CH-C-*C*H$_3$).

***R*$_f$** (CH_2Cl_2/CH_3OH 10:1) = 0.198.

ESI-MS(+): *m/z* found 1144.2745 $[M-Cl]^+$, calcd. for $C_{56}H_{70}N_5O_2Ru_2S_3^+$ 1144.2773.

Elemental analysis (%): calcd. for $C_{56}H_{70}ClN_5O_2Ru_2S_3 \cdot 0.8CH_3OH$ C 56.63, H 6.13, N 5.81; found C 56.63, H 6.37, N 5.18.

Synthesis of [(η^6-*p*-$MeC_6H_4Pr^i$)$_2$$Ru_2$($\mu_2$-$SCH_2C_6H_4$-*p*-$Bu^t$)$_2$($\mu_2$-$SC_6H_4$-*p*-R)]Cl (R = 4-amino-1-((1*H*-1,2,3-triazol-4-yl)methyl)pyrimidin-2(1*H*)-one) (2.1.25)

To a solution of **2.1.10** (0.287 g, 0.275 mmol, 1 equiv.) and **2.1.17** (0.062 g, 0.416 mmol, 1.5 equiv.) in dry DMF (10 mL), were added successively $CuSO_4 \cdot 5H_2O$ (0.069 g, 0.275 mmol, 1 equiv.) and sodium ascorbate (0.109 g, 0.550 mmol, 2 equiv.). The reaction mixture was stirred at 60°C under inert atmosphere (N_2) for 24 h, the reaction evolution being verified by TLC. The reaction mixture was diluted with EtOAc (100 mL) and washed with H_2O (2×100 mL); the unified aqueous phases were further washed with EtOAc (100 mL). The combined organic phases were washed with brine (100 mL), dried over anhydrous Na_2SO_4, filtered and concentrated to dryness under reduced pressure. Purification by column chromatography (CH_2Cl_2/CH_3OH 9:1 (v/v)) afforded **2.1.25** as an orange solid (0.075 g, 0.064 mmol, yield 23%).

^{1}H-NMR ($CDCl_3$) δ_H, ppm: 8.52 (1H, s, (*Tr*)N-N=N-C-C*H*), 7.94 (2H, d, 2xS-(*Ar*)C-CH-C*H*-C-(*Tr*)N, $^3J_{H,H}$ = 8.7 Hz), 7.83 (2H, d, 2xS-(*Ar*)C-C*H*-CH-C-(*Tr*)N, $^3J_{H,H}$ = 8.7 Hz), 7.54 (1H, d, CH_2-N-*C*H-CH-C-NH_2, $^3J_{H,H}$ = 7.4 Hz), 7.38-7.51 (8H, m, 4xS-CH_2-(*Ar*)C-C*H*-CH-C-C$(CH_3)_3$, 4xS-CH_2-(*Ar*)C-CH-C*H*-C-C$(CH_3)_3$, $^3J_{H,H}$ = 8.6 Hz), 6.50 (1H, d, CH_2-N-CH-C*H*-C-NH_2, $^3J_{H,H}$ = 7.3 Hz), 5.13 (2H, d, 2xCH_3-(*Ar*)C-CH-C*H*-C, $^3J_{H,H}$ = 5.2 Hz), 5.12 (2H, s, (*Tr*)N-N=N-C-C*H*$_2$-N-(C=O)-N), 5.03 (2H, d, 2xCH_3-(*Ar*)C-CH-C*H*-C, $^3J_{H,H}$ = 5.9 Hz), 4.90 (2H, d, 2xCH_3-(*Ar*)C-C*H*-

CH-C, $^3J_{H,H}$ = 5.8 Hz), 4.67 (2H, d, 2xCH$_3$-(*Ar*)C-C*H*-CH-C, $^3J_{H,H}$ = 5.8 Hz), 3.62 (2H, s, S-C*H*$_2$-(*Ar*)C-CH-CH-C-C(CH$_3$)$_3$), 3.44 (2H, s, S-C*H*$_2$-(*Ar*)C-CH-CH-C-C(CH$_3$)$_3$), 1.98 (2H, sept, 2x(*Ar*)C-CH-CH-C-C*H*(CH$_3$)$_2$, $^3J_{H,H}$ = 6.8 Hz), 1.74 (6H, s, 2xC*H*$_3$-(*Ar*)C-CH-CH-C), 1.37 (9H, s, S-CH$_2$-(*Ar*)C-CH-CH-C-C(C*H*$_3$)$_3$), 1.33 (9H, s, S-CH$_2$-(*Ar*)C-CH-CH-C-C(C*H*$_3$)$_3$), 0.96 (6H, d, (*Ar*)C-CH-CH-C-CH(C*H*$_3$)$_2$, $^3J_{H,H}$ = 6.8 Hz), 0.92 (6H, d, (*Ar*)C-CH-CH-C-CH(C*H*$_3$)$_2$, $^3J_{H,H}$ = 6.9 Hz).

^{13}C-NMR (CDCl$_3$) δ_C, ppm: 165.7 (1C, N-(C=O)-N-*C*-NH$_2$), 156.0 (1C, N-(*C*=O)-N-CH$_2$), 152.04, 151.96 (2C, 2xS-CH$_2$-(*Ar*)C-CH-CH-*C*-C(CH$_3$)$_3$), 145.0 (1C, N-*C*H-CH-C-NH$_2$), 144.2 (*Tr*)N-N=N-*C*-CH), 138.9 (1C, S-(*Ar*)C-CH-CH-*C*-(*Tr*)N), 136.9 (1C, S-(*Ar*)*C*-CH-CH-C-(*Tr*)N), 136.6 (2C, 2xS-CH$_2$-(*Ar*)*C*-CH-CH-C-C(CH$_3$)$_3$), 134.2 (2C, 2xS-(*Ar*)C-*C*H-CH-C-(*Tr*)N), 129.4, 129.2 (4C, 4xS-CH$_2$-(*Ar*)C-*C*H-CH-C-C(CH$_3$)$_3$), 125.8, 125.6 (4C, 4xS-CH$_2$-(*Ar*)C-CH-*C*H-C-C(CH$_3$)$_3$), 122.5 (1C, (*Tr*)N-N=N-C-*C*H), 120.7 (2C, 2xS-(*Ar*)C-CH-*C*H-C-(*Tr*)N), 107.7 (2C, 2xCH$_3$-(*Ar*)C-CH-CH-*C*), 100.5 (2C, 2xCH$_3$-(*Ar*)*C*-CH-CH-C), 96.6 (1C, N-CH-*C*H-C-NH$_2$), 84.2 (4C, 2xCH$_3$-(*Ar*)C-*C*H-CH-C, 2xCH$_3$-(*Ar*)C-CH-*C*H-C), 83.7 (2C, 2xCH$_3$-(*Ar*)C-CH-*C*H-C), 82.6 (2C, 2xCH$_3$-(*Ar*)C-*C*H-CH-C), 44.9 (1C, S-(*Ar*)C-CH-CH-C-(*Tr*)N-N=N-C-*C*H$_2$-N-(C=O)), 40.2 (1C, S-*C*H$_2$-(*Ar*)C-CH-CH-C-C(CH$_3$)$_3$), 39.7 (1C, S-*C*H$_2$-(*Ar*)C-CH-CH-C-C(CH$_3$)$_3$), 34.9 (2C, 2xS-CH$_2$-(*Ar*)C-CH-CH-C-*C*(CH$_3$)$_3$), 31.6 (6C, 2xS-CH$_2$-(*Ar*)C-CH-CH-C-C(*C*H$_3$)$_3$), 31.1 (2C, 2x(*Ar*)CH-CH-C-*C*H(CH$_3$)$_2$), 23.1 (2C, (*Ar*)CH-CH-C-CH(*C*H$_3$)$_2$), 22.9 (2C, (*Ar*)CH-CH-C-CH(*C*H$_3$)$_2$), 18.3 (2C, 2x*C*H$_3$-(*Ar*)C-CH-CH).

***R*$_f$** (CH$_2$Cl$_2$/CH$_3$OH 9:1) = 0.124.

ESI-MS(+): *m/z* found 1129.2778 [M-Cl]$^+$, calcd. for C$_{55}$H$_{69}$N$_6$ORu$_2$S$_3^+$ 1129.2776.

Elemental analysis (%): calcd. for C$_{55}$H$_{69}$ClN$_6$ORu$_2$S$_3$·0.2CH$_2$Cl$_2$·1.25CH$_3$OH C 55.53, H 6.14, N 6.88; found C 55.57, H 6.14, N 6.71.

Synthesis of [(η^6-*p*-MeC$_6$H$_4$Pr^i)$_2$Ru$_2$(μ_2-SCH$_2$C$_6$H$_4$-*p*-Bu^t)$_2$(μ_2-SC$_6$H$_4$-*p*-R)]Cl (R = 9-((1*H*-1,2,3-triazol-4-yl)methyl)-9*H*-purin-6-amine) (2.1.26)

To a solution of **2.1.10** (0.298 g, 0.285 mmol, 1 equiv.) and **2.1.18** (0.059 g, 0.342 mmol, 1.2 equiv.) in dry DMF (10 mL), were added successively CuSO$_4$·5H$_2$O (0.071 g, 0.285 mmol, 1 equiv.) and sodium ascorbate (0.113 g, 0.570 mmol, 2 equiv.). The reaction mixture was stirred at 60°C under inert atmosphere (N$_2$) for further 24 h and the reaction evolution was verified by TLC. The reaction mixture was diluted with EtOAc (100 mL) and washed with H$_2$O (2×100 mL); the unified aqueous phases were further washed with EtOAc (100 mL). The combined organic phases were washed with brine (100 mL), dried over anhydrous Na$_2$SO$_4$, filtered and concentrated to dryness under reduced pressure. Purification by column chromatography (CH$_2$Cl$_2$/CH$_3$OH 10:1 (v/v)) afforded **2.1.26** as an orange solid (0.091 g, 0.077 mmol, yield 27%).

^{1}H-NMR (CDCl$_3$) δ_H, ppm: 9.16 (1H, s br, (*Tr*)N-N=N-C-C*H*), 8.36 (1H, s br, N-C*H*-N-C-NH$_2$), 8.29 (1H, s br, CH$_2$-N-C*H*-NH-C-C-NH$_2$), 7.95 (2H, d, 2xS-(*Ar*)C-CH-C*H*-C-(*Tr*)N, $^3J_{H,H}$ = 8.9 Hz), 7.91 (2H, d, 2xS-(*Ar*)C-C*H*-CH-C-(*Tr*)N, $^3J_{H,H}$ = 8.9 Hz), 7.36-7.48 (8H, m, 4xS-CH$_2$-(*Ar*)C-C*H*-CH-C-C(CH$_3$)$_3$, 4xS-CH$_2$-(*Ar*)C-CH-C*H*-C-C(CH$_3$)$_3$, $^3J_{H,H}$ = 8.5 Hz), 6.20 (2H, s br, N-CH-N-C-C-N*H*$_2$), 5.66 (2H, s, (*Tr*)N-N=N-C-C*H*$_2$-N-CH-N), 5.07 (2H, d, 2xCH$_3$-(*Ar*)C-CH-C*H*-C, $^3J_{H,H}$ = 5.8 Hz), 4.98 (2H, d, 2xCH$_3$-(*Ar*)C-CH-C*H*-C, $^3J_{H,H}$ = 5.8 Hz), 4.89 (2H, d, 2xCH$_3$-(*Ar*)C-C*H*-CH-C, $^3J_{H,H}$ = 5.8 Hz), 4.63 (2H, d, 2xCH$_3$-(*Ar*)C-C*H*-CH-C, $^3J_{H,H}$ = 5.8 Hz), 3.58 (2H, s, S-C*H*$_2$-(*Ar*)C-CH-CH-C-C(CH$_3$)$_3$), 3.38 (2H, s, S-C*H*$_2$-(*Ar*)C-CH-CH-C-C(CH$_3$)$_3$), 1.95 (2H, sept, 2x(*Ar*)C-CH-CH-C-C*H*(CH$_3$)$_2$, $^3J_{H,H}$ = 6.8 Hz), 1.70 (6H, s, 2xC*H*$_3$-(*Ar*)C-CH-CH-C), 1.33 (9H, s, S-CH$_2$-(*Ar*)C-CH-CH-C-C(C*H*$_3$)$_3$), 1.29 (9H, s, S-CH$_2$-(*Ar*)C-CH-CH-C-C(C*H*$_3$)$_3$), 0.92 (6H, d, (*Ar*)C-CH-CH-C-CH(C*H*$_3$)$_2$, $^3J_{H,H}$ = 6.8 Hz), 0.87 (6H, d, (*Ar*)C-CH-CH-C-CH(C*H*$_3$)$_2$, $^3J_{H,H}$ = 6.9 Hz).

^{13}C-NMR ($CDCl_3$) δ_C, ppm: 155.5 (1C, N-CH-N-C-<u>C</u>-NH_2), 152.9 (1C, N-<u>C</u>H-N-C-NH_2), 152.0, 151.9 (2C, 2xS-CH_2-(*Ar*)C-CH-CH-<u>C</u>-C$(CH_3)_3$), 150.0 (1C, N-<u>C</u>-N-CH_2-(*Tr*)C), 143.6 (*Tr*)N-N=N-<u>C</u>-CH), 141.2 (1C, N-<u>C</u>H-N-C-C-NH_2), 138.6 (1C, S-(*Ar*)C-CH-CH-<u>C</u>-(*Tr*)N), 136.9 (1C, S-(*Ar*)<u>C</u>-CH-CH-C-(*Tr*)N), 136.6, 136.5 (2C, 2xS-CH_2-(*Ar*)<u>C</u>-CH-CH-C-C$(CH_3)_3$), 134.1 (2C, 2xS-(*Ar*)C-<u>C</u>H-CH-C-(*Tr*)N), 129.3, 129.1 (4C, 4xS-CH_2-(*Ar*)C-<u>C</u>H-CH-C-C$(CH_3)_3$), 125.7, 125.6 (4C, 4xS-CH_2-(*Ar*)C-CH-<u>C</u>H-C-C$(CH_3)_3$), 122.8 (1C, (*Tr*)N-N=N-C-<u>C</u>H), 120.7 (2C, 2xS-(*Ar*)C-CH-<u>C</u>H-C-(*Tr*)N), 119.4 (1C, N-CH-N-<u>C</u>-C-NH_2), 107.5 (2C, 2xCH_3-(*Ar*)C-CH-CH-<u>C</u>), 100.4 (2C, 2xCH_3-(*Ar*)<u>C</u>-CH-CH-C), 84.0 (4C, 2xCH_3-(*Ar*)C-<u>C</u>H-CH-C, 2xCH_3-(*Ar*)C-CH-<u>C</u>H-C), 83.7 (2C, 2xCH_3-(*Ar*)C-CH-<u>C</u>H-C), 82.4 (2C, 2xCH_3-(*Ar*)C-<u>C</u>H-CH-C), 40.0 (1C, S-<u>C</u>H_2-(*Ar*)C-CH-CH-C-C$(CH_3)_3$), 39.6 (1C, S-<u>C</u>H_2-(*Ar*)C-CH-CH-C-C$(CH_3)_3$), 38.5 (1C, S-(*Ar*)C-CH-CH-C-(*Tr*)N-N=N-C-<u>C</u>H_2-N-C-N), 34.85, 34.81 (2C, 2xS-CH_2-(*Ar*)C-CH-CH-C-<u>C</u>$(CH_3)_3$), 31.48, 31.45 (6C, 2xS-CH_2-(*Ar*)C-CH-CH-C-C(<u>C</u>$H_3)_3$), 31.1 (2C, 2x(*Ar*)CH-CH-C-<u>C</u>H$(CH_3)_2$), 23.0 (2C, (*Ar*)CH-CH-C-CH(<u>C</u>$H_3)_2$), 22.8 (2C, (*Ar*)CH-CH-C-CH(<u>C</u>$H_3)_2$), 18.2 (2C, 2x<u>C</u>H_3-(*Ar*)C-CH-CH).
R_f (CH_2Cl_2/CH_3OH 10:1) = 0.156.
ESI-MS(+): *m/z* found 1153.2896 $[M\text{-}Cl]^+$, calcd. for $C_{56}H_{69}N_8Ru_2S_3^+$ 1053.2889.
Elemental analysis (%): calcd. for $C_{56}H_{69}ClN_8Ru_2S_3 \cdot 0.7CH_2Cl_2$ C 54.59, H 5.69, N 8.98; found C 54.65, H 5.68, N 8.51.

Synthesis of the compounds constituting family 4

Synthesis of 6-(azidomethyl)uracil (6-(azidomethyl)pyrimidine-2,4(1*H*,3*H*)-dione) (2.1.27)

Compound **2.1.27** was prepared by adapting a previously reported procedure[397]. To a solution 6-(chloromethyl)uracil (6-(chloromethyl)pyrimidine-2,4(1*H*,3*H*)-dione) (0.600 g, 3.662 mmol, 1 equiv.) in dry DMF (10 mL) at 50°C under inert atmosphere (N_2) was added NaN_3 (0.476 g, 7.324 mmol, 2 equiv.) and the mixture was stirred overnight. The reaction mixture was allowed to cool to r.t., filtered and washed with CH_2Cl_2. The filtrate was concentrated under reduced pressure affording **2.1.27** as white solid (0.133 g, 0.796 mmol, yield 22%).
^{1}H-NMR (DMSO-d_6) δ_H, ppm: 10.86 (2H, m br, 2xNH), 5.53 (1H, s, NH-(C=O)-C<u>H</u>-C-CH_2-N_3), 4.23 (2H, s, NH-(C=O)-CH-C-C<u>H_2</u>-N_3).
^{13}C-NMR (DMSO-d_6) δ_C, ppm: 163.9 (1C, NH-(<u>C</u>=O)-CH-C-CH_2-N_3), 151.4 (1C, NH-(C=O)-CH-<u>C</u>-CH_2-N_3), 150.5 (1C, NH-(<u>C</u>=O)-NH), 98.7 (1C, NH-(C=O)-<u>C</u>H-C-CH_2-N_3), 49.4 (1C, NH-(C=O)-CH-C-<u>C</u>H_2-N_3).
R_f (CH_2Cl_2/CH_3OH 10:1) = 0.244.
ESI-MS(+): *m/z* found 199.0705 $[M+CH_3OH]^+$, calcd. for $C_6H_9N_5O_3$ 199.0705.
Elemental analysis (%): calcd. for $C_5H_5N_5O_2 \cdot 0.3CH_2Cl_2 \cdot 0.2CH_3OH$ C 33.19, H 3.24, N 35.19; found C 33.22, H 2.74, N 35.18.

Synthesis of [(η^6-*p*-$MeC_6H_4Pr^i$)$_2$$Ru_2$($\mu_2$-$SCH_2C_6H_4$-*p*-$Bu^t$)$_2$($\mu_2$-$SC_6H_4$-*p*-$CH_2$-(C=O)-NH-R]Cl (R = 6-((4-(methylamino)-1*H*-1,2,3-triazol-1-yl)methyl)pyrimidine-2,4(1*H*,3*H*)-dione) (2.1.31)

To a solution of **2.1.8** (0.300 g, 0.280 mmol, 1 equiv.) in mixture of CH_3CN/H_2O 1:1 v/v (40 mL) under inert atmosphere (N_2) at r.t were added successively **2.1.27** (0.056 g, 0.336 mmol, 1.2 equiv.), $Cu_2SO_4 \cdot 5H_2O$ (0.070 g, 0.280 mmol, 1 equiv.) and sodium ascorbate (0.111 g, 0.560 mmol, 2 equiv.). The mixture was stirred at 50°C overnight and the reaction evolution was verified by TLC. The reaction mixture was cooled to r.t., filtered and diluted with EtOAc (2x30 mL). The organic phase was successively washed with H_2O (2x30 mL), dried over anhydrous Na_2SO_4, filtered and concentrated under reduced pressure. Purification by flash column chromatography (CH_2Cl_2/CH_3OH 9:1 (v/v)) afforded **2.1.31** as an orange solid (0.111 g, 0.090 mmol, yield 32%).
^{1}H-NMR (MeOD-d_4) δ_H, ppm: 8.04 (1H, s, (*Tr*)C-N=N-N-C<u>H</u>), 7.79 (2H, d, 2xS-(*Ar*)C-CH-C<u>H</u>-C-CH_2-(C=O)-NH, $^3J_{H,H}$ = 8.2 Hz), 7.53 (4H, m, 4xS-CH_2-(*Ar*)C-CH-C<u>H</u>-C-C$(CH_3)_3$, $^3J_{H,H}$ = 8.4

Hz), 7.47 (4H, m, 4xS-CH_2-(*Ar*)C-C*H*-CH-C-C(CH_3)$_3$, $^3J_{H,H}$ = 8.4 Hz), 7.27 (2H, d, 2xS-(*Ar*)C-C*H*-CH-C-CH_2-(C=O)-NH, $^3J_{H,H}$ = 8.2 Hz), 5.42 (2H, s, (C=O)-NH-CH_2-(*Tr*)C-N=N-N-C*H*$_2$), 5.26 (2H, d, 2xCH_3-(*Ar*)C-CH-C*H*-C, $^3J_{H,H}$ = 5.7 Hz), 5.19 (1H, s, NH-(C=O)-NH-(C=O)-C*H*-C), 5.12 (2H, d, 2xCH_3-(*Ar*)C-CH-C*H*-C, $^3J_{H,H}$ = 5.8 Hz), 5.05 (2H, d, 2xCH_3-(*Ar*)C-C*H*-CH-C, $^3J_{H,H}$ = 5.7 Hz), 4.73 (2H, d, 2xCH_3-(*Ar*)C-C*H*-CH-C, $^3J_{H,H}$ = 5.8 Hz), 4.48 (2H, s, (C=O)-NH-C*H*$_2$-(*Tr*)C-N=N-N-CH_2), 3.69 (2H, s, S-C*H*$_2$-(*Ar*)C-CH-CH-C-(CH_3)$_3$), 3.55 (2H, s, S-(*Ar*)C-CH-CH-C-C*H*$_2$-(C=O)-NH), 3.50 (2H, s, S-C*H*$_2$-(*Ar*)C-CH-CH-C-(CH_3)$_3$), 1.87 (2H, sept, 2x(*Ar*)C-CH-CH-C-C*H*(CH_3)$_2$, $^3J_{H,H}$ = 6.9 Hz), 1.76 (6H s, 2xC*H*$_3$-(*Ar*)C-CH-CH-C), 1.38 (9H, s, S-CH_2-(*Ar*)C-CH-CH-C-C(C*H*$_3$)$_3$), 1.35 (9H, s, S-CH_2-(*Ar*)C-CH-CH-C-C(C*H*$_3$)$_3$), 0.91 (6H, d, 2x(*Ar*)C-CH-CH-C-CH(C*H*$_3$)$_2$, $^3J_{H,H}$ = 6.9 Hz), 0.88 (6H, d, 2x(*Ar*)C-CH-CH-C-CH(C*H*$_3$)$_2$, $^3J_{H,H}$ = 6.9 Hz).

^{13}C-NMR (MeOD-*d*$_4$) δ$_C$, ppm: 173.4 (1C, S-(*Ar*)C-CH-CH-C-CH_2-(*C*=O)-NH), 166.5 (1C, NH-(C=O)-NH-(*C*=O)-CH-C), 153.2 (1C, NH-(C=O)-NH-(C=O)-CH-*C*), 152.7, 152.6 (2C, 2xS-CH_2-(*Ar*)C-CH-CH-*C*-C(CH_3)$_3$), 152.4 (1C, NH-(*C*=O)-NH-(C=O)-CH-C), 146.6 (1C, (*Tr*)*C*-N=N-N-CH), 138.6, 138.5 (2C, 2xS-CH_2-(*Ar*)*C*-CH-CH-C-C(CH_3)$_3$), 137.8 (1C, S-(*Ar*)*C*-CH-CH-C-CH_2-(C=O)-NH), 137.3 (1C, S-(*Ar*)C-CH-CH-*C*-CH_2-(C=O)-NH), 134.3 (2C, 2xS-(*Ar*)C-CH-*C*H-C-CH_2-(C=O)-NH), 130.7 (2C, 2xS-(*Ar*)C-*C*H-CH-C-CH_2-(C=O)-NH), 130.5, 130.3 (4C, 4xS-CH_2-(*Ar*)C-*C*H-CH-C-C(CH_3)$_3$), 126.7, 126.6 (4C, 4xS-CH_2-(*Ar*)C-CH-*C*H-C-C(CH_3)$_3$), 125.5 (1C, (*Tr*)C-N=N-N-*C*H), 107.9 (2C, 2xCH_3-(*Ar*)C-CH-CH-*C*), 102.5 (2C, 2xCH_3-(*Ar*)*C*-CH-CH-C), 100.2 (1C, NH-(C=O)-NH-(C=O)-*C*H-C), 86.0 (2C, 2xCH_3-(*Ar*)C-CH-*C*H-C), 84.55 (2C, 2xCH_3-(*Ar*)C-*C*H-CH-C), 84.52 (2C, 2xCH_3-(*Ar*)C-CH-*C*H-C), 83.9 (2C, 2xCH_3-(*Ar*)C-*C*H-CH-C), 50.5 (1C, (C=O)-NH-CH_2-(*Tr*)C-N=N-N-*C*H$_2$), 43.2 (1C, S-(*Ar*)C-CH-CH-C-*C*H$_2$-(C=O)-NH), 41.2 (1C, S-*C*H$_2$-(*Ar*)C-CH-CH-C-C(CH_3)$_3$), 40.7 (1C, S-*C*H$_2$-(*Ar*)C-CH-CH-C-C(CH_3)$_3$), 35.8 (1C, (C=O)-NH-*C*H$_2$-(*Tr*)C-N=N-N-CH_2), 35.62, 35.57 (2C, 2xS-CH_2-(*Ar*)C-CH-CH-C-*C*(CH_3)$_3$), 32.0 (2C, 2x(*Ar*)CH-CH-C-*C*H(CH_3)$_2$), 31.85, 31.82 (6C, 2xS-CH_2-(*Ar*)C-CH-CH-C-C(*C*H$_3$)$_3$), 23.6 (2C, (*Ar*)CH-CH-C-CH(*C*H$_3$)$_2$), 22.9 (2C, (*Ar*)CH-CH-C-CH(*C*H$_3$)$_2$), 18.2 (2C, 2x*C*H$_3$-(*Ar*)C-CH-CH).

***R*$_f$** (CH_2Cl_2/CH_3OH 10:1) = 0.268.

ESI-MS(+): *m/z* found 1201.2973 $[M-Cl]^+$, calcd. for $C_{58}H_{73}N_6O_3Ru_2S_3^+$ 1201.2988.

Elemental analysis (%): calcd. for $C_{58}H_{73}ClN_6O_3Ru_2S_3 \cdot 7.5CH_2Cl_2 \cdot 15H_2O$ C 36.71, H 5.55, N 3.92; found: C 36.35, H 5.01, N 4.08.

Synthesis of 9-(2-methanesulfonate ethyl)adenine (2-(6-amino-9*H*-purin-9-yl)ethyl methanesulfonate) (2.1.32A) and 9-(2-azidoethyl)adenine (9-(2-azidoethyl)-9*H*-purin-6-amine) (2.1.32)

To a solution of 9-(2-hydroxyethyl)adenine (2-(6-amino-9*H*-purin-9-yl)ethan-1-ol) (0.200 g, 1.116 mmol, 1 equiv.) in dry DMF (50 mL) at 0°C under inert atmosphere (N_2), were added successively MsCl (0.22 mL, 2.790 mmol, 2.5 equiv.), and TEA (0.39 mL, 2.790 mmol, 2.5 equiv.). The mixture was further stirred at 0°C for 3 h and then at r.t. overnight. The reaction evolution was verified by TLC, the mixture was concentrated under reduced pressure. The obtained mesylate **2.1.32A** was solubilized in dry DMF (20 mL) under inert atmosphere (N_2), NaN_3 (0.145 g, 2.232 mmol, 2 equiv.) was added and the mixture was stirred at 60°C for 48 h. A second portion of NaN_3 (0.145 g, 2.232 mmol, 2 equiv.) was added and the reaction mixture was further stirred for 72 h. The reaction evolution was verified by TLC; the mixture was filtrated and the filtrate was diluted with CH_3OH (5 mL) and hexane (5 mL) and concentrated under reduced pressure. The residue was suspended in CH_2Cl_2 (30 mL) and filtered. The precipitate was solubilized in CH_3OH (30 mL) and concentrated under reduced pressure to afford **2.1.32** as a white solid (0.214 g, 1.046 mmol, yield 94%) which was used without further purification.

2.1.32A

^{1}H-NMR (MeOD-*d*$_4$) δ$_H$, ppm: 8.24 (1H, s, N-C*H*-N-C-NH$_2$), 8.16 (1H, s, N-C*H*-N-C-C-NH$_2$), 4.34 (2H, t, N-C*H*$_2$-CH$_2$-O-(SO$_2$)-CH$_3$, $^3J_{H,H}$ = 5.4 Hz), 3.90 (2H, t, N-CH$_2$-C*H*$_2$-O-(SO$_2$)-CH$_3$, $^3J_{H,H}$ = 5.4 Hz), 2.86 (3H, s, N-CH$_2$-CH$_2$-O-(SO$_2$)-C*H*$_3$).
ESI-MS(+): *m/z* found 258.0662 [M+H]$^+$, calcd. for $C_8H_{12}N_5O_3S^+$ 258.0655.

2.1.32
^{1}H-NMR (MeOD-*d*$_4$) δ$_H$, ppm: 8.22 (1H, s, N-C*H*-N-C-NH$_2$), 8.16 (1H, s, N-C*H*-N-C-C-NH$_2$), 4.42 (2H, t, N-C*H*$_2$-CH$_2$-N$_3$, $^3J_{H,H}$ = 5.8 Hz), 3.80 (2H, t, N-CH$_2$-C*H*$_2$-N$_3$, $^3J_{H,H}$ = 5.8 Hz).
^{13}C-NMR (MeOD-*d*$_4$) δ$_C$, ppm: 157.5 (1C, N-CH-N-C-*C*-NH$_2$), 153.7 (1C, N-*C*H-N-C-NH$_2$), 150.8 (1C, N-*C*-N-CH$_2$-CH$_2$-N$_3$), 143.0 (1C, CH$_2$-N-*C*H-N-C-C-NH$_2$), 120.2 (1C, N-CH-N-*C*-C-NH$_2$), 51.4 (1C, N-C-N-*C*H$_2$-CH$_2$-N$_3$), 44.3 (1C, N-C-N-CH$_2$-*C*H$_2$-N$_3$).
***R*$_f$** (CH$_2$Cl$_2$/CH$_3$OH 10:1) = 0.260.
ESI-MS(+): *m/z* found 205.0944 [M+H]$^+$, calcd. for $C_7H_9N_8^+$ 205.0945.

Synthesis of [(*η*^{6}-*p*-MeC$_6$H$_4$Pr^i)$_2$Ru$_2$(*μ*$_2$-SCH$_2$C$_6$H$_4$-*p*-Bu^t)$_2$(*μ*$_2$-SC$_6$H$_4$-*p*-CH$_2$-(C=O)-NH-R)]Cl (R = 9-(2-(4-(methylamino)-1*H*-1,2,3-triazol-1-yl)ethyl)-9*H*-purin-6-amine) (2.1.33)
To a solution of **2.1.8** (0.228 g, 0.213 mmol, 1 equiv.) and **2.1.31** (0.130 g, 0.639 mmol, 3 equiv.) in dry DMF (10 mL), were added successively CuSO$_4$·5H$_2$O (0.053 g, 0.213 mmol, 1 equiv.) and sodium ascorbate (0.084 g, 0.426 mmol, 2 equiv.). The reaction mixture was stirred at 60°C under inert atmosphere (N$_2$) for further 24 h and the reaction evolution was verified by TLC. The reaction mixture was solubilized in EtOAc (100 mL) and washed with H$_2$O (2×100 mL); the unified aqueous phases were further washed with EtOAc (100 mL). The combined organic phases were washed with brine (100 mL), dried over anhydrous Na$_2$SO$_4$, filtered and concentrated to dryness under reduced pressure. Purification by column chromatography (CH$_2$Cl$_2$/CH$_3$OH 9:1 (v/v)) afforded **2.1.33** as an orange solid (0.035 g, 0.027 mmol, yield 13%).
^{1}H-NMR (DMSO-*d*$_6$) δ$_H$, ppm: 8.55 (1H, t, S-(*Ar*)C-CH-CH-C-CH$_2$-(C=O)-N*H*, $^3J_{H,H}$ = 5.6 Hz), 8.13 (1H, s, N-C*H*-N-C-NH$_2$), 7.89 (1H, s, N-C*H*-N-C-C-NH$_2$), 7.82 (1H, s, (*Tr*)C-N=N-N-C*H*), 7.69 (2H, d, 2xS-(*Ar*)C-CH-C*H*-C-CH$_2$-(C=O)-NH, $^3J_{H,H}$ = 8.1 Hz), 7.50 (4H, m, 4xS-CH$_2$-(*Ar*)C-CH-C*H*-C-C(CH$_3$)$_3$, $^3J_{H,H}$ = 8.7 Hz), 7.42 (4H, m, 4xS-CH$_2$-(*Ar*)C-C*H*-CH-C-C(CH$_3$)$_3$, $^3J_{H,H}$ = 8.4 Hz), 7.22 (2H, d, 2xS-(*Ar*)C-C*H*-CH-C-CH$_2$-(C=O)-NH, $^3J_{H,H}$ = 7.1 Hz), 7.21 (2H, s br, N-CH-N-C-N*H*$_2$), 5.36 (2H, d, 2xCH$_3$-(*Ar*)C-CH-C*H*-C, $^3J_{H,H}$ = 5.7 Hz), 5.24 (4H, d, 2xCH$_3$-(*Ar*)C-C*H*-CH-C, 2xCH$_3$-(*Ar*)C-CH-C*H*-C, $^3J_{H,H}$ = 6.1 Hz), 4.84 (2H, t, (*Tr*)C-N=N-N-C*H*$_2$-CH$_2$-N, $^3J_{H,H}$ = 5.6 Hz), 4.68 (2H, d, 2xCH$_3$-(*Ar*)C-C*H*-CH-C, $^3J_{H,H}$ = 5.8 Hz), 4.63 (2H, t, (*Tr*)C-N=N-N-CH$_2$-C*H*$_2$-N, $^3J_{H,H}$ = 5.7 Hz), 4.24 (2H, d, (C=O)-NH-C*H*$_2$-(*Tr*)C-N=N-N-CH$_2$, $^3J_{H,H}$ = 5.5 Hz), 3.63 (2H, s, S-C*H*$_2$-(*Ar*)C-CH-CH-C-(CH$_3$)$_3$), 3.44 (2H, s, S-C*H*$_2$-(*Ar*)C-CH-CH-C-(CH$_3$)$_3$), 3.42 (2H, s, S-(*Ar*)C-CH-CH-C-C*H*$_2$-(C=O)-NH), 1.71-1.79 (2H, m, 2x(*Ar*)C-CH-CH-C-C*H*(CH$_3$)$_2$), 1.75 (6H s, 2xC*H*$_3$-(*Ar*)C-CH-CH-C), 1.33 (9H, s, S-CH$_2$-(*Ar*)C-CH-CH-C-C(C*H*$_3$)$_3$), 1.29 (9H, s, S-CH$_2$-(*Ar*)C-CH-CH-C-C(C*H*$_3$)$_3$), 0.78 (6H, d, 2x(*Ar*)C-CH-CH-C-CH(C*H*$_3$)$_2$, $^3J_{H,H}$ = 6.8 Hz), 0.74 (6H, d, 2x(*Ar*)C-CH-CH-C-CH(C*H*$_3$)$_2$, $^3J_{H,H}$ = 6.8 Hz).
^{13}C-NMR (DMSO-*d*$_6$) δ$_C$, ppm: 169.6 (1C, S-(*Ar*)C-CH-CH-C-CH$_2$-(*C*=O)-NH), 155.9 (1C, N-CH-N-C-*C*-NH$_2$), 152.5 (1C, N-*C*H-N-C-NH$_2$), 150.5, 150.4 (2C, 2xS-CH$_2$-(*Ar*)C-CH-CH-*C*-C(CH$_3$)$_3$), 149.5 (1C, (*Tr*)N-N=N-(CH$_2$)$_2$-N-*C*-N)), 144.7 (1C, (*Tr*)*C*-N=N-N-CH), 140.5 (1C, N-*C*H-N-C-C-NH$_2$), 137.0, 136.8 (2C, 2xS-CH$_2$-(*Ar*)*C*-CH-CH-C-C(CH$_3$)$_3$), 136.1 (1C, S-(*Ar*)*C*-CH-CH-C-CH$_2$-(C=O)-NH), 135.2 (1C, S-(*Ar*)C-CH-CH-*C*-CH$_2$-(C=O)-NH), 132.2 (2C, 2xS-(*Ar*)C-CH-*C*H-C-CH$_2$-(C=O)-NH), 129.29, 129.24 (4C, 4xS-CH$_2$-(*Ar*)C-CH-*C*H-C-C(CH$_3$)$_3$), 128.9 (2C, 2xS-(*Ar*)C-*C*H-CH-C-CH$_2$-(C=O)-NH), 125.2, 125.0 (4C, 4xS-CH$_2$-(*Ar*)C-*C*H-CH-C-C(CH$_3$)$_3$), 123.1 (1C, (*Tr*)C-N=N-N-*C*H), 118.6 (1C, N-CH-N-*C*-C-NH$_2$), 105.2 (2C, 2xCH$_3$-(*Ar*)C-CH-CH-*C*), 101.4 (2C, 2xCH$_3$-(*Ar*)*C*-CH-CH-C), 85.2 (2C, 2xCH$_3$-(*Ar*)C-CH-*C*H-C, 82.6 (2C, 2xCH$_3$-

(*Ar*)C-*C*H-CH-C), 82.4 (2C, 2xCH$_3$-(*Ar*)C-CH-*C*H-C), 82.3 (2C, 2xCH$_3$-(*Ar*)C-*C*H-CH-C), 48.4 (1C, (C=O)-NH-CH$_2$-(*Tr*)C-N=N-N-CH$_2$-*C*H$_2$), 42.9 (1C, (C=O)-NH-CH$_2$-(*Tr*)C-N=N-N-*C*H$_2$-CH$_2$), 41.6 (1C, S-(*Ar*)C-CH-CH-C-*C*H$_2$-(C=O)-NH), 39.5 (1C, S-*C*H$_2$-(*Ar*)C-CH-CH-C-C(CH$_3$)$_3$), 39.3 (1C, S-*C*H$_2$-(*Ar*)C-CH-CH-C-C(CH$_3$)$_3$), 34.40, 34.34 (2C, 2xS-CH$_2$-(*Ar*)C-CH-CH-C-*C*(CH$_3$)$_3$), 34.2 (1C, (C=O)-NH-*C*H$_2$-(*Tr*)C-N=N-N-CH$_2$), 31.15, 31.13 (6C, 2xS-CH$_2$-(*Ar*)C-CH-CH-C-C(*C*H$_3$)$_3$), 29.9 (2C, 2x(*Ar*)CH-CH-C-*C*H(CH$_3$)$_2$), 23.0 (2C, (*Ar*)CH-CH-C-CH(*C*H$_3$)$_2$), 21.7 (2C, (*Ar*)CH-CH-C-CH(*C*H$_3$)$_2$), 17.5 (2C, 2x*C*H$_3$-(*Ar*)C-CH-CH).

***R*$_f$** (CH$_2$Cl$_2$/CH$_3$OH 9:1) = 0.088.

ESI-MS(+): *m/z* found 1238.3424 [M-Cl]$^+$, calcd. for $C_{60}H_{76}N_9ORu_2S_3^+$ 1238.3416.

Elemental analysis (%): calcd. for $C_{60}H_{76}ClN_9ORu_2S_3 \cdot 0.1CH_2Cl_2 \cdot 1.5CH_3OH$ C 55.64, H 6.23, N 9.48; found C 55.65, H 6.21, N 9.28.

Synthesis of the compounds constituting family 5

Synthesis of [(η^6-*p*-MeC$_6$H$_4$Pr^i)$_2$Ru$_2$(μ_2-SCH$_2$C$_6$H$_4$-*p*-Bu^t)$_2$(μ_2-SC$_6$H$_4$-*p*-R) (R = 4-phenyl-1*H*-1,2,3-triazole) (2.1.37)

To a solution of **2.1.10** (0.246 g, 0.235 mmol, 1 equiv.) and ethynylbenzene (0.03 mL, 0.282 mmol, 1.2 equiv.) in dry DMF (10 mL), were added successively CuSO$_4 \cdot 5H_2O$ (0.059 g, 0.235 mmol, 1 equiv.) and sodium ascorbate (0.093 g, 0.470 mmol, 2 equiv.). The reaction mixture was stirred at r.t. under inert atmosphere (N$_2$) for further 24 h and the reaction evolution was verified by TLC. The reaction mixture was filtered and the filtrate was diluted with EtOAc (100 mL), washed with H$_2$O (2×100 mL), with brine (100 mL), dried over anhydrous Na$_2$SO$_4$, filtered and concentrated to dryness under reduced pressure. Purification by column chromatography (CH$_2$Cl$_2$/CH$_3$OH 10:1 (v/v)) afforded **2.1.37** as an orange solid (0.193 g, 0.186 mmol, yield 79%).

^{1}H-NMR (CDCl$_3$) δ_H, ppm: 9.21 (1H, s, (*Tr*)N-N=N-C-C*H*), 8.16 (2H, d, 2xS-(*Ar*)C-CH-C*H*-C-(*Tr*)N, $^3J_{H,H}$ = 8.7 Hz), 8.08 (2H, d, 2x(*Tr*)N-N=N-C-(*Ar*)C-C*H*-CH-CH, $^3J_{H,H}$ = 7.1 Hz), 8.01 (2H, d, 2xS-(*Ar*)C-C*H*-CH-C-(*Tr*)N, $^3J_{H,H}$ = 8.6 Hz), 7.39-7.51 (10H, m, 4xS-CH$_2$-(*Ar*)C-C*H*-CH-C-C(CH$_3$)$_3$, 4xS-CH$_2$-(*Ar*)C-CH-C*H*-C-C(CH$_3$)$_3$, 2x(*Tr*)N-N=N-C-(*Ar*)C-CH-C*H*-CH, $^3J_{H,H}$ = 8.6 Hz), 7.33 (1H, m, (*Tr*)N-N=N-C-(*Ar*)C-CH-CH-C*H*, $^3J_{H,H}$ = 7.4 Hz), 5.13 (2H, d, 2xCH$_3$-(*Ar*)C-CH-C*H*-C, $^3J_{H,H}$ = 5.7 Hz), 5.03 (2H, d, 2xCH$_3$-(*Ar*)C-CH-C*H*-C, $^3J_{H,H}$ = 5.8 Hz), 4.96 (2H, d, 2xCH$_3$-(*Ar*)C-C*H*-CH-C, $^3J_{H,H}$ = 5.8 Hz), 4.65 (2H, d, 2xCH$_3$-(*Ar*)C-C*H*-CH-C, $^3J_{H,H}$ = 5.9 Hz), 3.61 (2H, s, S-C*H*$_2$-(*Ar*)C-CH-CH-C-C(CH$_3$)$_3$), 3.41 (2H, s, S-C*H*$_2$-(*Ar*)C-CH-CH-C-C(CH$_3$)$_3$), 1.99 (2H, sept, 2x(*Ar*)C-CH-CH-C-C*H*(CH$_3$)$_2$, $^3J_{H,H}$ = 6.9 Hz), 1.75 (6H, s, 2xC*H*$_3$-(*Ar*)C-CH-CH-C), 1.37 (9H, s, S-CH$_2$-(*Ar*)C-CH-CH-C-C(C*H*$_3$)$_3$), 1.33 (9H, s, S-CH$_2$-(*Ar*)C-CH-CH-C-C(C*H*$_3$)$_3$), 0.95 (6H, d, (*Ar*)C-CH-CH-C-CH(C*H*$_3$)$_2$, $^3J_{H,H}$ = 6.9 Hz), 0.91 (6H, d, (*Ar*)C-CH-CH-C-CH(C*H*$_3$)$_2$, $^3J_{H,H}$ = 6.9 Hz).

^{13}C-NMR (CDCl$_3$) δ_C, ppm: 152.0, 151.9 (2C, 2xS-CH$_2$-(*Ar*)C-CH-CH-*C*-C(CH$_3$)$_3$), 148.8 (1C, (*Tr*)N-N=N-*C*-CH), 138.0 (1C, S-(*Ar*)C-CH-CH-*C*-(*Tr*)N), 137.2 (1C, S-(*Ar*)*C*-CH-CH-C-(*Tr*)N), 136.73, 136.65 (2C, 2xS-CH$_2$-(*Ar*)*C*-CH-CH-C-C(CH$_3$)$_3$), 134.3 (2C, 2xS-(*Ar*)C-*C*H-CH-C-(*Tr*)N), 130.5 (1C, (*Tr*)N-N=N-C-(*Ar*)*C*-CH-CH-CH), 129.4, 129.2 (4C, 4xS-CH$_2$-(*Ar*)C-*C*H-CH-C-C(CH$_3$)$_3$), 129.0 (2C, 2x(*Tr*)N-N=N-C-(*Ar*)C-CH-*C*H-CH), 128.3 (1C, (*Tr*)N-N=N-C-(*Ar*)C-CH-CH-*C*H), 126.2 (2C, 2x(*Tr*)N-N=N-C-(*Ar*)C-*C*H-CH-CH), 125.7, 125.6 (4C, 4xS-CH$_2$-(*Ar*)C-CH-*C*H-C-C(CH$_3$)$_3$), 120.7 (2C, 2xS-(*Ar*)C-CH-*C*H-C-(*Tr*)N), 119.2 (1C, (*Tr*)N-N=N-C-*C*H), 107.5 (2C, 2xCH$_3$-(*Ar*)C-CH-CH-*C*), 100.6 (2C, 2xCH$_3$-(*Ar*)*C*-CH-CH-C), 84.07 (2C, 2xCH$_3$-(*Ar*)C-CH-*C*H-C), 84.04 (2C, 2xCH$_3$-(*Ar*)C-*C*H-CH-C), 83.95 (2C, 2xCH$_3$-(*Ar*)C-CH-*C*H-C), 82.5 (2C, 2xCH$_3$-(*Ar*)C-*C*H-CH-C), 40.0 (1C, S-*C*H$_2$-(*Ar*)C-CH-CH-C-C(CH$_3$)$_3$), 39.6 (1C, S-*C*H$_2$-(*Ar*)C-CH-CH-C-C(CH$_3$)$_3$), 34.93, 34.88 (2C, 2xS-CH$_2$-(*Ar*)C-CH-CH-C-*C*(CH$_3$)$_3$), 31.55, 31.53 (6C, 2xS-CH$_2$-(*Ar*)C-CH-CH-C-C(*C*H$_3$)$_3$), 31.1 (2C, 2x(*Ar*)CH-CH-C-*C*H(CH$_3$)$_2$), 23.1 (2C, (*Ar*)CH-CH-C-CH(*C*H$_3$)$_2$), 22.9 (2C, (*Ar*)CH-CH-C-CH(*C*H$_3$)$_2$), 18.3 (2C, 2x*C*H$_3$-(*Ar*)C-CH-CH).

R_f (CH_2Cl_2/CH_3OH 10:1) = 0.314.
ESI-MS(+): *m/z* found 1082.2664 $[M\text{-}Cl]^+$, calcd. for $C_{56}H_{68}N_3Ru_2S_3^+$ 1082.2657.
Elemental analysis (%): calcd. for $C_{56}H_{68}ClN_3Ru_2S_3 \cdot 0.1CH_2Cl_2 \cdot 2CH3OH$ C 58.67, H 6.46, N 3.53; found C 58.67, H 6.48, N 3.14.

Synthesis of [(η^6-*p*-$MeC_6H_4Pr^i$)$_2$$Ru_2$($\mu_2$-$SCH_2C_6H_4$-*p*-$Bu^t$)$_2$($\mu_2$-$SC_6H_4$-*p*-R) (R = (1*H*-1,2,3-triazol-4-yl)methanol) (2.1.38)
To a solution of **2.1.10** (0.300 g, 0.287 mmol, 1 equiv.) and propargyl alcohol (0.02 mL, 0.344 mmol, 1.2 equiv.) in dry DMF (10 mL) were added successively $CuSO_4 \cdot 5H_2O$ (0.072 g, 0.287 mmol, 1 equiv.) and sodium ascorbate (0.114 g, 0.574 mmol, 2 equiv.). The reaction mixture was stirred at r.t. under inert atmosphere (N_2) for further 24 h and the reaction evolution was verified by TLC. The reaction mixture was concentrated to dryness under reduced pressure and purification by column chromatography (CH_2Cl_2/CH_3OH 10:1 (v/v)) afforded **2.1.38** as an orange solid (0.081 g, 0.076 mmol, yield 26%).
^{1}H-NMR ($CDCl_3$) δ_H, ppm: 8.98 (1H, s, (*Tr*)N-N=N-C-C*H*), 7.88-7.95 (4H, m, 2xS-(*Ar*)C-C*H*-CH-C-(*Tr*)N, 2xS-(*Ar*)C-CH-C*H*-C-(*Tr*)N), 7.39-7.52 (8H, m, 4xS-CH_2-(*Ar*)C-C*H*-CH-C-$C(CH_3)_3$, 4xS-CH_2-(*Ar*)C-CH-C*H*-C-$C(CH_3)_3$, $^3J_{H,H}$ = 8.3 Hz), 5.10 (2H, d, 2xCH_3-(*Ar*)C-CH-C*H*-C, $^3J_{H,H}$ = 5.5 Hz), 5.00 (2H, d, 2xCH_3-(*Ar*)C-CH-C*H*-C, $^3J_{H,H}$ = 5.7 Hz), 4.96 (2H, s, S-(*Ar*)C-CH-CH-C-(*Tr*)N-N=N-C-CH_2-OH), 4.89 (2H, d, 2xCH_3-(*Ar*)C-C*H*-CH-C, $^3J_{H,H}$ = 5.5 Hz), 4.67 (2H, d, 2xCH_3-(*Ar*)C-C*H*-CH-C, $^3J_{H,H}$ = 5.6 Hz), 3.62 (2H, s, S-CH_2-(*Ar*)C-CH-CH-C-$C(CH_3)_3$), 3.42 (2H, s, S-CH_2-(*Ar*)C-CH-CH-C-$C(CH_3)_3$), 1.98 (2H, sept, 2x(*Ar*)C-CH-CH-C-C*H*$(CH_3)_2$, $^3J_{H,H}$ = 6.8 Hz), 1.75 (6H, s, 2xCH_3-(*Ar*)C-CH-CH-C), 1.37 (9H, s, S-CH_2-(*Ar*)C-CH-CH-C-C(CH_3)$_3$), 1.33 (9H, s, S-CH_2-(*Ar*)C-CH-CH-C-C(CH_3)$_3$), 0.97 (6H, d, (*Ar*)C-CH-CH-C-CH(CH_3)$_2$, $^3J_{H,H}$ = 6.8 Hz), 0.92 (6H, d, (*Ar*)C-CH-CH-C-CH(CH_3)$_2$, $^3J_{H,H}$ = 6.8 Hz).
^{13}C-NMR ($CDCl_3$) δ_C, ppm: 152.1, 152.0 (2C, 2xS-CH_2-(*Ar*)C-CH-CH-*C*-C$(CH_3)_3$), 150.8 (1C, (*Tr*)N-N=N-*C*-CH), 138.0 (1C, S-(*Ar*)C-CH-CH-*C*-(*Tr*)N), 137.5 (1C, S-(*Ar*)*C*-CH-CH-C-(*Tr*)N), 136.7, 136.5 (2C, 2xS-CH_2-(*Ar*)*C*-CH-CH-C-$C(CH_3)_3$), 134.0 (2C, S-(*Ar*)C-*C*H-CH-C-(*Tr*)N), 129.4, 129.2 (4C, 4xS-CH_2-(*Ar*)C-*C*H-CH-C-$C(CH_3)_3$), 125.8, 125.7 (4C, 4xS-CH_2-(*Ar*)C-CH-*C*H-C-$C(CH_3)_3$), 122.0 (1C, (*Tr*)N-N=N-C-*C*H), 120.7 (2C, 2xS-(*Ar*)C-CH-*C*H-C-(*Tr*)N), 107.7 (2C, 2xCH_3-(*Ar*)C-CH-CH-*C*), 100.5 (2C, 2xCH_3-(*Ar*)*C*-CH-CH-C), 84.10 (2C, 2xCH_3-(*Ar*)C-CH-*C*H-C), 84.05 (2C, 2xCH_3-(*Ar*)C-*C*H-CH-C), 83.7 (2C, 2xCH_3-(*Ar*)C-CH-*C*H-C), 82.5 (2C, 2xCH_3-(*Ar*)C-*C*H-CH-C), 56.7 (1C, S-(*Ar*)C-CH-CH-C-(*Tr*)N-N=N-C-*C*H_2-OH), 40.1 (1C, S-*C*H_2-(*Ar*)C-CH-CH-C-$C(CH_3)_3$), 39.6 (1C, S-*C*H_2-(*Ar*)C-CH-CH-C-$C(CH_3)_3$), 34.96, 34.92 (2C, 2xS-CH_2-(*Ar*)C-CH-CH-C-*C*$(CH_3)_3$), 31.57, 31.54 (6C, 2xS-CH_2-(*Ar*)C-CH-CH-C-C(*C*H_3)$_3$), 31.2 (2C, 2x(*Ar*)CH-CH-C-*C*H$(CH_3)_2$), 23.1 (2C, (*Ar*)CH-CH-C-CH(*C*H_3)$_2$), 22.9 (2C, (*Ar*)CH-CH-C-CH(*C*H_3)$_2$), 18.3 (2C, 2x*C*H_3-(*Ar*)C-CH-CH).
R_f (CH_2Cl_2/CH_3OH 10:1) = 0.196.
ESI-MS(+): *m/z* found 1036.2462 $[M\text{-}Cl]^+$, calcd. for $C_{51}H_{66}N_3ORu_2S_3^+$ 1036.2450.
Elemental analysis (%): calcd. for $C_{51}H_{66}ClN_3ORu_2S_3 \cdot 0.4CH_2Cl_2$ C 55.88, H 6.09, N 3.80; found C 55.87, H 6.19, N 3.32.

Synthesis of [(η^6-*p*-$MeC_6H_4Pr^i$)$_2$$Ru_2$($\mu_2$-$SCH_2C_6H_4$-*p*-$Bu^t$)$_2$($\mu_2$-$SC_6H_4$-*p*-R) (R = 2-(1*H*-1,2,3-triazol-4-yl)pyridine) (2.1.39)
To a solution of **2.1.10** (0.306 g, 0.293 mmol, 1 equiv.) and 2-ethynylpyridine (0.04 mL, 0.352 mmol, 1.2 equiv.) in dry DMF (10 mL) were added successively $CuSO_4 \cdot 5H_2O$ (0.073 g, 0.293 mmol, 1 equiv.) and sodium ascorbate (0.116 g, 0.586 mmol, 2 equiv.). The reaction mixture was stirred at r.t. under inert atmosphere (N_2) for further 24 h and the reaction evolution was verified by TLC. The reaction mixture was diluted with EtOAc (100 mL) and washed with H_2O (2×100 mL);

the unified aqueous phases were further washed with EtOAc (100 mL). The combined organic phases were washed with brine (100 mL), dried over anhydrous Na_2SO_4, filtered and concentrated to dryness under reduced pressure. Purification by column chromatography (CH_2Cl_2/CH_3OH 10:1 (v/v)) afforded **2.1.39** as an orange solid (0.030 g, 0.027 mmol, yield 9%).

^{1}H-NMR (DMSO-*d*$_6$) δ_H, ppm: 9.41 (1H, s, (*Tr*)N-N=N-C-C*H*), 8.68 (1H, m, (*Tr*)N-N=N-C-(*Py*)C-N-C*H*-CH, $^3J_{H,H}$ = 4.2 Hz), 8.14 (1H, d, (*Tr*)N-N=N-C-(*Py*)C-N-CH-CH-CH-C*H*, $^3J_{H,H}$ = 7.9 Hz), 7.97-8.03 (4H, m, 2xS-(*Ar*)C-CH-C*H*-C-(*Tr*)N, 2xS-(*Ar*)C-C*H*-CH-C-(*Tr*)N), 7.97 (1H, td, (*Tr*)N-N=N-C-(*Py*)C-N-CH-CH-C*H*, $^3J_{H,H}$ = 7.7 Hz, $^4J_{H,H}$ = 1.7 Hz), 7.41-7.53 (9H, m, 4xS-CH_2-(*Ar*)C-C*H*-CH-C-C(CH_3)$_3$, 4xS-CH_2-(*Ar*)C-CH-C*H*-C-C(CH_3)$_3$), (*Tr*)N-N=N-C-(*Py*)C-N-CH-C*H*), 5.44 (2H, d, 2xCH_3-(*Ar*)C-CH-C*H*-C, $^3J_{H,H}$ = 5.6 Hz), 5.30-5.34 (4H, m, 2xCH_3-(*Ar*)C-C*H*-CH-C, 2xCH_3-(*Ar*)C-CH-C*H*-C, $^3J_{H,H}$ = 6.5 Hz), 4.77 (2H, d, 2xCH_3-(*Ar*)C-C*H*-CH-C, $^3J_{H,H}$ = 5.7 Hz), 3.68 (2H, s, S-C*H*$_2$-(*Ar*)C-CH-CH-C-C(CH_3)$_3$), 3.49 (2H, s, S-C*H*$_2$-(*Ar*)C-CH-CH-C-C(CH_3)$_3$), 1.90 (2H, sept, 2x(*Ar*)C-CH-CH-C-C*H*(CH_3)$_2$, $^3J_{H,H}$ = 6.8 Hz), 1.80 (6H, s, 2xC*H*$_3$-(*Ar*)C-CH-CH-C), 1.34 (9H, s, S-CH_2-(*Ar*)C-CH-CH-C-C(C*H*$_3$)$_3$), 1.30 (9H, s, S-CH_2-(*Ar*)C-CH-CH-C-C(C*H*$_3$)$_3$), 0.84 (6H, d, (*Ar*)C-CH-CH-C-CH(C*H*$_3$)$_2$, $^3J_{H,H}$ = 6.8 Hz), 0.80 (6H, d, (*Ar*)C-CH-CH-C-CH(C*H*$_3$)$_2$, $^3J_{H,H}$ = 6.8 Hz).

^{13}C-NMR (DMSO-*d*$_6$) δ_C, ppm: 150.6, 150.4 (2C, 2xS-CH_2-(*Ar*)C-CH-CH-*C*-C(CH_3)$_3$), 149.7 (1C, (*Tr*)N-N=N-C-(*Py*)C-N-*C*H-CH), 149.4 (1C, (*Tr*)N-N=N-C-(*Py*)*C*-N-CH-CH), 148.4 (1C, (*Tr*)N-N=N-*C*-CH), 138.8 (1C, S-(*Ar*)C-CH-CH-*C*-(*Tr*)N), 137.4 (1C, (*Tr*)N-N=N-C-(*Py*)C-N-CH-CH-*C*H), 136.9, 136.8 (2C, 2xS-CH_2-(*Ar*)*C*-CH-CH-C-C(CH_3)$_3$), 135.8 (1C, S-(*Ar*)*C*-CH-CH-C-(*Tr*)N), 134.0 (2C, 2xS-(*Ar*)C-*C*H-CH-C-(*Tr*)N), 129.3, 129.0 (4C, 4xS-CH_2-(*Ar*)C-*C*H-CH-C-C(CH_3)$_3$), 125.3, 125.1 (4C, 4xS-CH_2-(*Ar*)C-CH-*C*H-C-C(CH_3)$_3$), 123.5 (1C, (*Tr*)N-N=N-C-(*Py*)C-N-CH-*C*H), 121.1 (1C, (*Tr*)N-N=N-C-*C*H), 120.0 (2C, 2xS-(*Ar*)C-CH-*C*H-C-(*Tr*)N), 119.9 (1C, (*Tr*)N-N=N-C-(*Py*)C-N-CH-CH-CH-*C*H), 105.7 (2C, 2xCH_3-(*Ar*)C-CH-CH-*C*), 101.4 (2C, 2xCH_3-(*Ar*)*C*-CH-CH-C), 84.8 (2C, 2xCH_3-(*Ar*)C-CH-*C*H-C), 83.0 (2C, 2xCH_3-(*Ar*)C-*C*H-CH-C, 82.7 (2C, 2xCH_3-(*Ar*)C-CH-*C*H-C), 82.3 (2C, 2xCH_3-(*Ar*)C-*C*H-CH-C), 39.7 (1C, S-*C*H$_2$-(*Ar*)C-CH-CH-C-C(CH_3)$_3$), 39.5 (1C, S-*C*H$_2$-(*Ar*)C-CH-CH-C-C(CH_3)$_3$), 34.43, 34.38 (2C, 2xS-CH_2-(*Ar*)C-CH-CH-C-*C*(CH_3)$_3$), 31.2 (6C, 2xS-CH_2-(*Ar*)C-CH-CH-C-C(*C*H$_3$)$_3$), 29.0 (2C, 2x(*Ar*)CH-CH-C-*C*H(CH_3)$_2$), 22.9 (2C, (*Ar*)CH-CH-C-CH(*C*H$_3$)$_2$), 21.9 (2C, (*Ar*)CH-CH-C-CH(*C*H$_3$)$_2$), 17.6 (2C, 2x*C*H$_3$-(*Ar*)C-CH-CH).

***R*$_f$** (CH_2Cl_2/CH_3OH 10:1) = 0.240.

ESI-MS(+): *m/z* found 1083.2722 $[M-Cl]^+$, calcd. for $C_{55}H_{67}N_4Ru_2S_3^+$ 1083.2609.

Elemental analysis (%): calcd. for $C_{55}H_{67}ClN_4Ru_2S_3 \cdot CH_3OH$ C 58.49, H 6.22, N 4.87; found C 58.46, H 6.47, N 4.38.

2.1.2. Stability in DMSO-d_6

The conjugates are well soluble in DMSO, solvent used to prepare standard solutions for biological assays.

The NMR spectra of conjugates **2.1.28**, **2.1.33** and **2.1.39** were measured in DMSO-d_6.

Further stability studies in this solvent were realized for compounds **2.1.28**, **2.1.33** and **2.1.39**. Figure S2.1.1 present the ^{1}H NMR spectra of conjugates **2.1.28**, **2.1.33** and **2.1.39** registered at r.t. 5 min and more than 120 days after sample preparation (the samples were stored at 0-5°C).

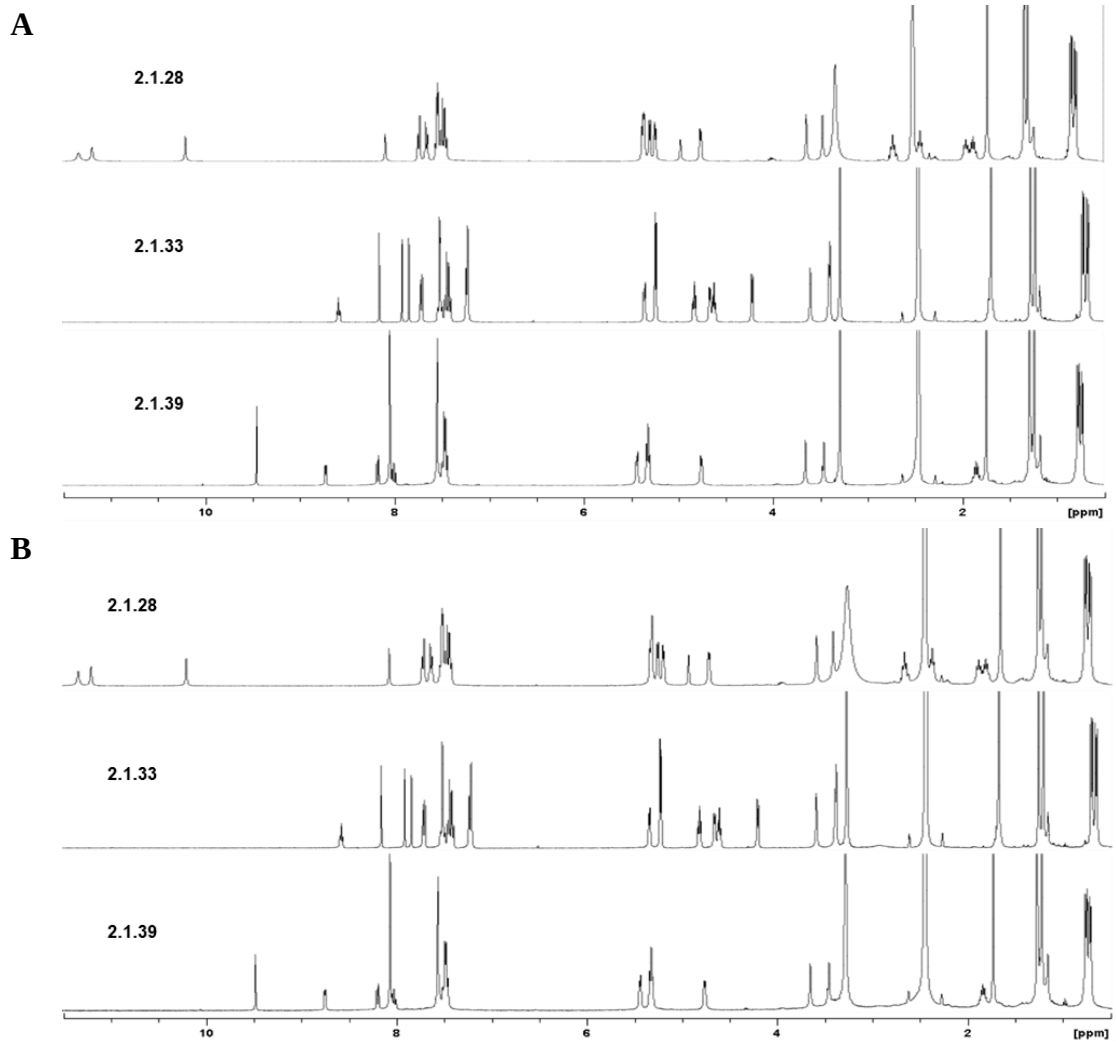

Figure S2.1.1. ^{1}H NMR spectra of **2.1.28**, **2.1.33** and **2.1.39** recorded in DMSO-d_6 at 25°C; (A) recorded 5 min after sample preparation, and (B) sample after > 120 days storage at 0-5°C in the dark.

To assess their stability, compounds **2.1.28**, **2.1.33** and **2.1.39** were dissolved in DMSO-d_6, and two ^{1}H-NMR spectra were recorded at 25°C 5 min and at least 120 days after sample preparation. Between the two experiments, the samples were stored at 0°C. For all complexes, there are no significant changes between the spectrum recorded after 5

min and the spectrum recorded after at least 120 days at 0°C, which indicates a very good stability of the complexes, and makes them suitable for further biological tests.

Also, conjugates **2.1.23**, **2.1.24**, **2.1.25** and **2.1.26** were used as solutions in DMSO-d_6 for the ^{1}H NMR studies aiming to identify interactions with complementary nucleobases.

The ability of nucleobase-diruthenium conjugates **2.1.23**-**2.1.26** to form pairs with complementary nucleobases *via* hydrogen bond interactions was investigated using ^{1}H NMR experiments. The spectra were recorded on a Bruker Avance II 400 (400.13 MHz) spectrometer at 298 K. The diruthenium conjugate (ca. 5 mg) was solubilized in 0.5 mL of DMSO-d_6. A sample of the complementary nucleobase in DMSO-d_6 was prepared in parallel. ^{1}H NMR spectra were recorded for both starting solutions. The solution of the complementary nucleobase was added in small aliquots (titrated) to the solution of diruthenium conjugate to achieve the molar ratio 1:1 and ^{1}H NMR spectra were recorded for each mixture at 5 min after sample preparation.

The most dramatic changes were observed at the addition of guanine to cytosine conjugate **2.1.25** (relative molar proportion 1:1, Figure S2.1.2, possible interaction *via* three H-bonds). In this case the signals corresponding to guanine at 6.04, 6.25 10.45 and 10.63 ppm were slightly broadened and correspondingly downfield shifted to 6.08, 6.30, 10.52 and 10.69 ppm (Figure S2.1.2). Also, upon addition of guanine, the cytosine signals in conjugate **2.1.25** at 7.02 and 7.15 ppm shifted to 7.03 and 7.14 ppm, respectively (Figure S2.1.2).

The changes were less noticeable/striking for adenine-uracil and adenine-thymine interactions (only two H-bonds). Thus, upon addition of adenine to uracil conjugate **2.1.23** (relative molar proportion 1:1, Figure S2.1.3), the adenine signal at 7.09 ppm is slightly upfield shifted to 7.07 ppm, while the signal at 12.79 ppm is downfield shifted to 12.82 ppm (Figure S2.1.3). Concomitantly, the uracil signal at 11.35 ppm in conjugate **2.1.23** became broader. A similar pattern was observed in case of thymine conjugate **2.1.24** and adenine (Figure S2.1.4).

At the addition of uracil to adenine conjugate **2.1.26** only the uracil signal at 10.80 ppm was downfield shifted to 10.82 ppm (Figure S2.1.5).

The addition of thymine to adenine conjugate **2.1.26** (relative molar proportion 1:1), led only to slight shifts of the thymine signals from 10.57 and 10.98 ppm to 10.59 and 10.99 ppm, while the adenine signal in conjugate **2.1.26** was downfield shifted to from 7.51 to 7.53 ppm (Figure S2.1.6).

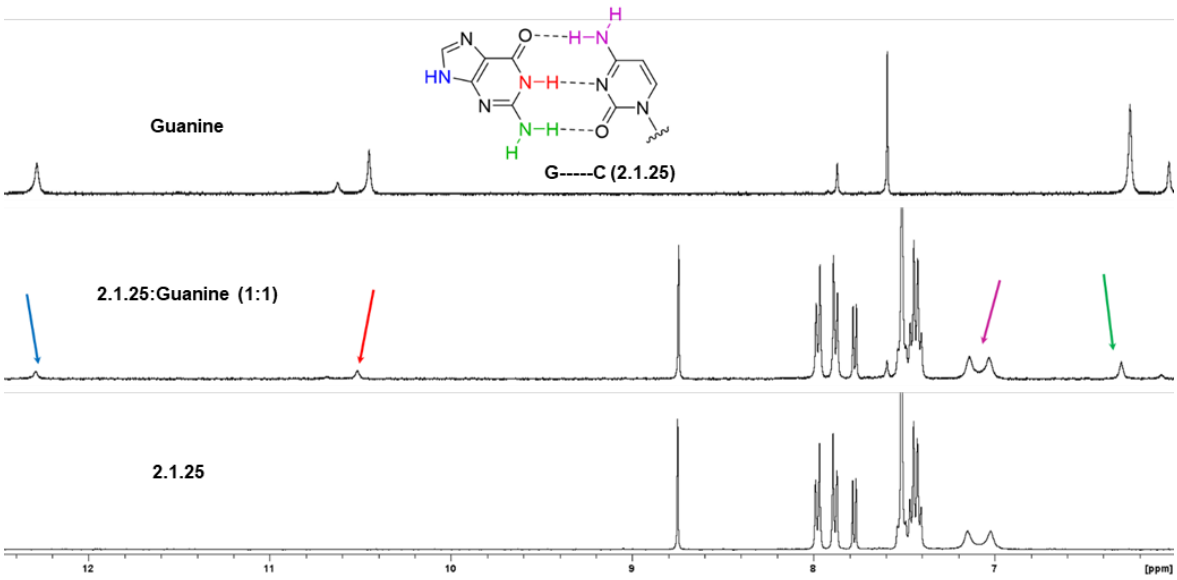

Figure S2.1.2. Study of H-bond interactions with complementary nucleobases by ^{1}H NMR at r.t. for cytosine conjugate **2.1.25** and guanine.

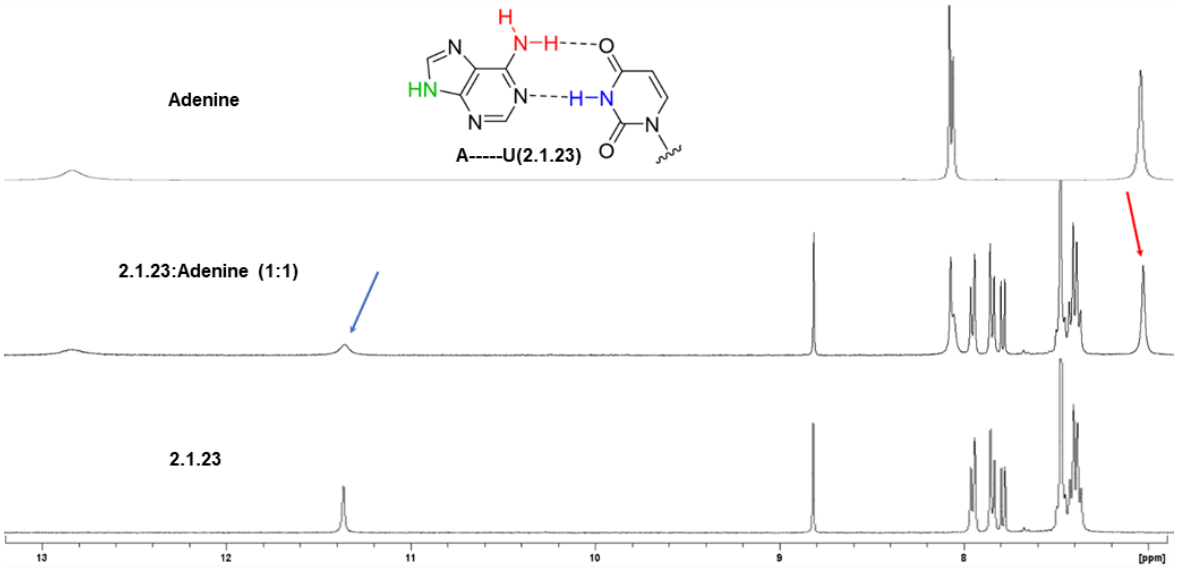

Figure S2.1.3. Study of H-bond interactions with complementary nucleobases by ^{1}H NMR for uracil conjugate **2.1.23** and adenine.

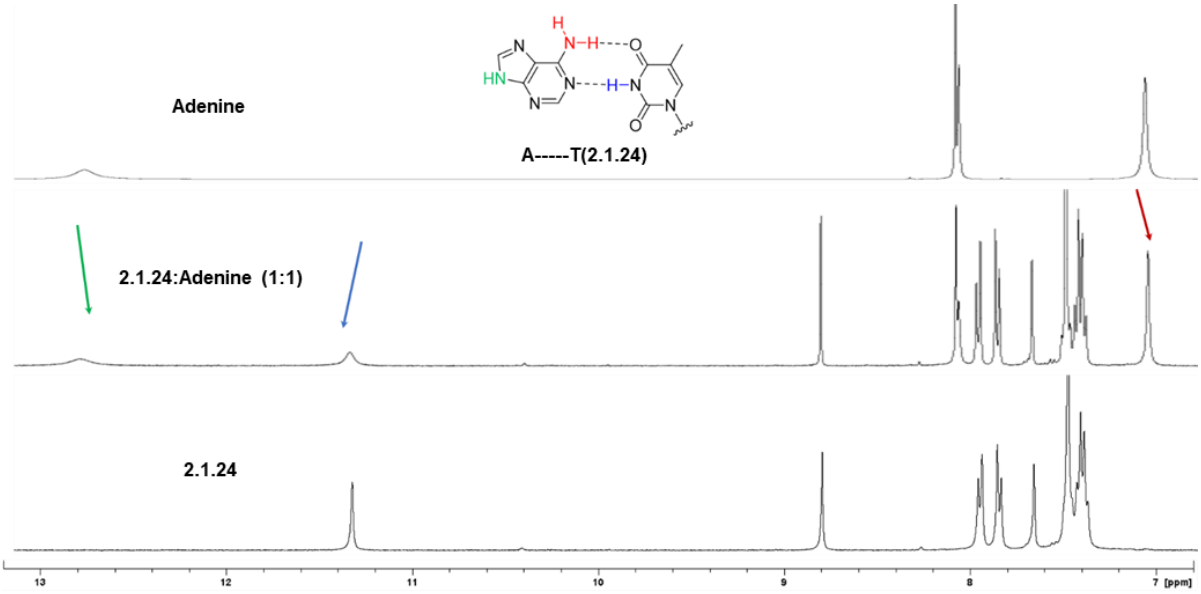

Figure S2.1.4. Study of H-bond interactions with complementary nucleobases by ^{1}H NMR at r.t. for thymine conjugate **2.1.24** and adenine.

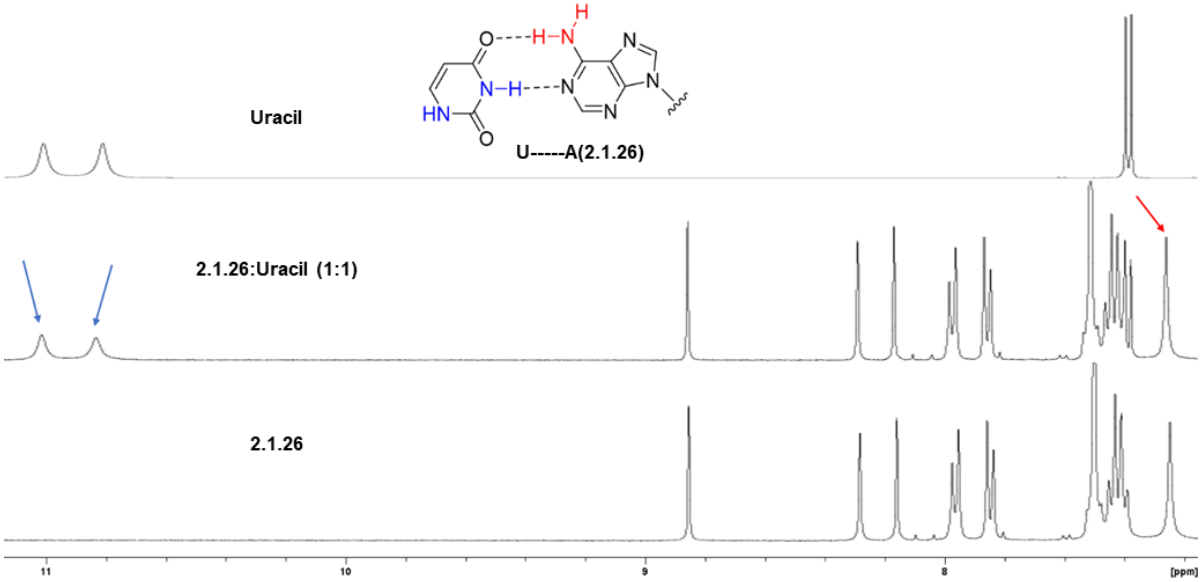

Figure S2.1.5. Study of H-bond interactions with complementary nucleobases by ^{1}H NMR for adenine conjugate **2.1.26** and uracil.

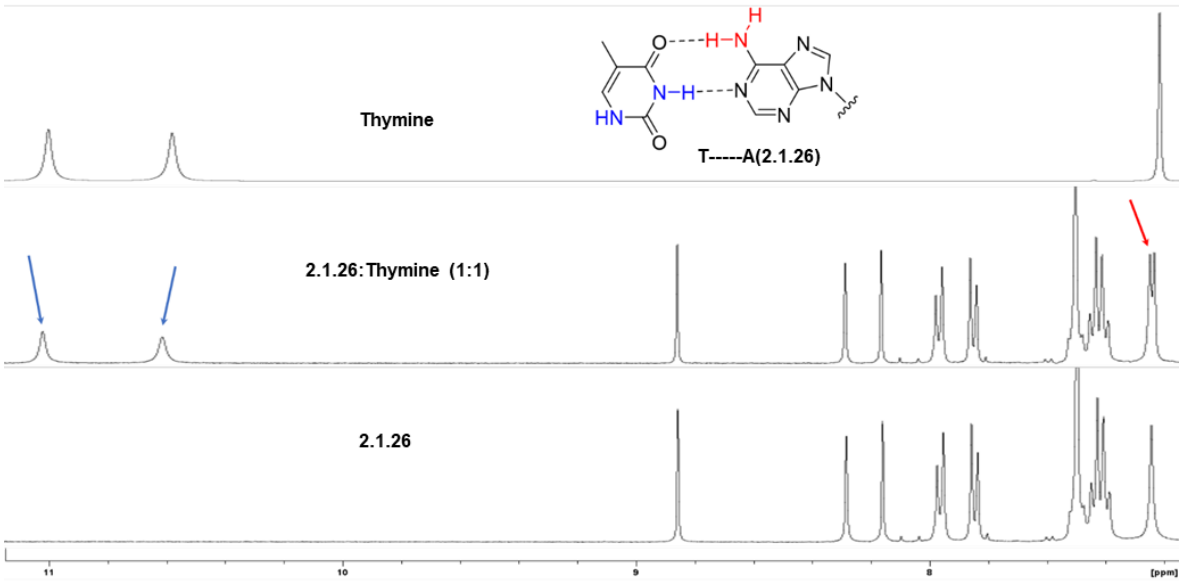

Figure S2.1.6. Study of H-bond interactions with complementary nucleobases by ^{1}H NMR for adenine conjugate **2.1.26** and thymine.

2.2. Trithiolato-Bridged Ruthenium(II)-Arene Complexes Bearing Lipophilic Moiety[12]

2.2.1. Biological activity

Table S2.2.1. Primary efficacy/cytotoxicity screening of the lipophilic compounds in non-infected HFF cultures and *T. gondii* β-gal tachyzoites cultured in HFF.

Lipophilic compound	Compound	HFF viability (%)		*T. gondii* β-gal growth (%)	
		0.1 µM	1 µM	0.1 µM	1 µM
Geraniol	**2.2.4**	102 ± 2	88 ± 3	86 ± 2	89 ± 1
Farnesol	**2.2.5**	98 ± 3	94 ± 1	96 ± 6	117 ± 3
Geranylgeraniol	**2.2.6**	100 ± 1	94 ± 5	305 ± 5	149 ± 2
Ethanol	**2.2.7**	-	-	-	-
Butanol	**2.2.8**	105 ± 5	104 ± 2	141 ± 23	91 ± 11
Lipoic acid	**2.2.9**	101 ± 1	99 ± 2	91 ± 6	99 ± 3
Acetic acid	**2.2.10**	-	-	-	-
Butyric acid	**2.2.11**	104 ± 5	94 ± 7	240 ± 12	197 ± 10
Hexanoic acid	**2.2.12**	100 ±1	103 ± 1	185 ± 12	172 ± 7
Decanoic acid	**2.2.13**	102 ± 8	103 ± 1	181 ± 7	148 ± 13
Myristic acid	**2.2.14**	111 ± 5	106 ± 3	190 ± 5	144 ± 9
Stearic acid	**2.2.15**	112 ± 2	105 ± 2	233 ± 9	159 ± 6
Oleic acid	**2.2.16**	114 ± 3	104 ± 13	302 ± 12	279 ± 13
Elaidic acid	**2.2.17**	98 ± 6	101 ± 4	204 ± 10	151 ± 9
Linoleic acid	**2.2.18**	111 ± 5	107 ± 3	217 ± 3	159 ± 6
α-Linolenic acid	**2.2.19**	95 ± 11	84 ± 5	128 ± 12	101 ± 5
γ-Linolenic acid	**2.2.20**	98 ± 3	89 ± 2	113 ± 1	118 ± 5

[12] This chapter is a draft with title *Lipophilic trithiolato-bridged dinuclear ruthenium(II)-arene conjugates*, which is going to be submitted for publication.

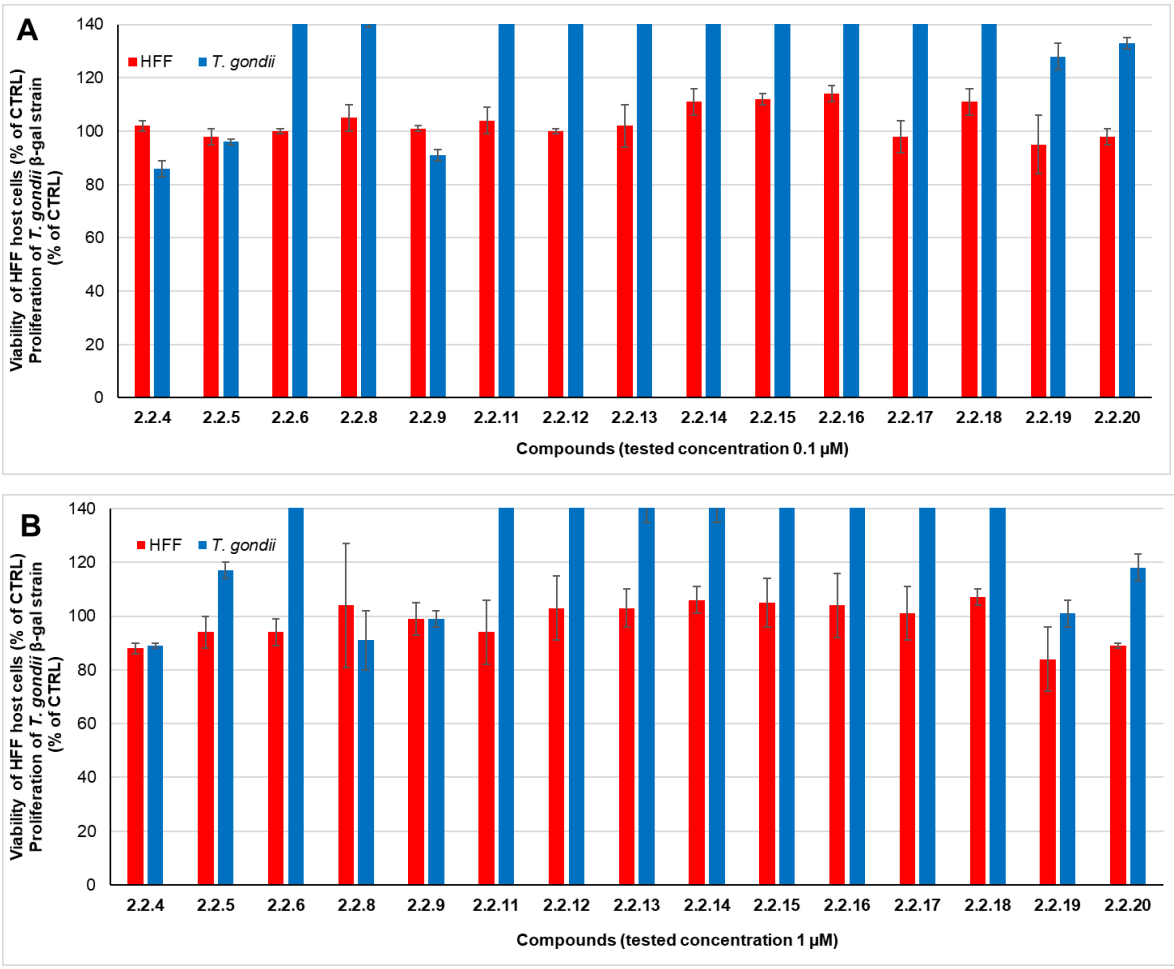

Figure S2.2.1. Clustered column chart showing the *in vitro* activities at 0.1 (A) and 1 (B) µM of the 15 lipophilic compounds on HFF viability and *T. gondii* β-gal proliferation. Non-infected HFF monolayers treated only with 0.1% DMSO exhibited 100% viability and 100% proliferation was attributed to *T. gondii* β-gal tachyzoites treated with 0.1% DMSO only. For each assay, standard deviations were calculated from triplicates.

2.2.2. Experimental

Chemistry[13]

General

Chemicals were purchased from Aldrich, Alfa Aesar, Acros Organics, ABCR, and TCI Chemicals and used without further purification. Reactions were performed under inert atmosphere (N_2) using Schlenk techniques with dry solvents (Acros Organics) preserved over molecular sieves. ^{1}H (400.13 MHz) and ^{13}C (100.62 MHz) NMR spectra were recorded on a Bruker Avance II 400 spectrometer at 298 K. The chemical shifts are reported in parts per million (ppm) and referenced to residual solvent peaks[393] ($CDCl_3$, ^{1}H δ 7.26, $^{13}C\{^{1}H\}$ δ 77.16 ppm), and coupling constants (J) are reported in hertz (Hz). High resolution electrospray ionization mass spectra (ESI-MS) were carried out by the Mass Spectrometry and Protein Analyses Services at DCBP and were obtained on a LTQ Orbitrap XL ESI (Thermo) operated in positive ion mode. Thermal elemental analyses were carried out by the Mass Spectrometry and Protein Analyses Services at DCBP and were obtained on a Flash 2000 Organic Elemental Analyzer (Thermo Scientific). Reactions were monitored by TLC using Merck TLC silica gel coated aluminium sheets 60 F254 and visualized with UV at 254 nm.

[13] Only syntheses of compounds obtained by the author of this thesis are presented.

Compounds were purified by column flash chromatography on silica gel using the elution systems indicated.

Abbreviations:
DIPEA - *N*,*N*-Diisopropylethylamine
DMAP - 4-(Dimethylamino)-pyridine
EDCI - *N*-(3-Dimethylaminopropyl)-*N'*-ethylcarbodiimide hydrochloride
HOBt·H₂O - 1-Hydroxybenzotriazole hydrate

For the description of the NMR spectra: *Ar* – arene.

The synthesis of the carboxy ([(η^6-*p*-MeC$_6$H$_4$Pr^i)$_2$Ru$_2$(μ_2-SCH$_2$C$_6$H$_4$-*p*-Bu^t)$_2$(μ_2-SC$_6$H$_4$-*p*-CH$_2$CO$_2$H)]Cl), hydroxy ([(η^6-*p*-MeC$_6$H$_4$Pr^i)$_2$Ru$_2$(μ_2-SCH$_2$C$_6$H$_4$-*p*-Bu^t)$_2$(μ_2-SC$_6$H$_4$-*p*-OH)]Cl),and amino ([(η^6-*p*-MeC$_6$H$_4$Pr^i)$_2$Ru$_2$(μ_2-SCH$_2$C$_6$H$_4$-*p*-Bu^t)$_2$(μ_2-SC$_6$H$_4$-*p*-NH$_2$)]Cl) diruthenium intermediates **2.2.1**-**2.2.3**, and that of the respective ethyl ester **2.2.7** ([(η^6-*p*-MeC$_6$H$_4$Pr^i)$_2$Ru$_2$(μ_2-SCH$_2$C$_6$H$_4$-*p*-Bu^t)$_2$(μ_2-SC$_6$H$_4$-*p*-CH$_2$COEt)]Cl), and of the acetic acid ester **2.2.10a** ([(η^6-*p*-MeC$_6$H$_4$Pr^i)$_2$Ru$_2$(μ_2-SCH$_2$C$_6$H$_4$-*p*-Bu^t)$_2$(μ_2-SC$_6$H$_4$-*p*-OAc)]Cl) and amide **2.2.10b** ([(η^6-*p*-MeC$_6$H$_4$Pr^i)$_2$Ru$_2$(μ_2-SCH$_2$C$_6$H$_4$-*p*-Bu^t)$_2$(μ_2-SC$_6$H$_4$-*p*-NHAc)]Cl) were reported previously[30, 62, 131].

General procedure A - obtainment of the first series of ester conjugates 2.2.4a-2.2.7a and 2.2.8a
To a solution of **2.2.1** (1 equiv.) in dry CH_2Cl_2 (50 mL) at room temperature under inert atmosphere (N_2), were added EDCI (2 equiv.), alcohol derivative (1.2-1.5 equiv.), and DMAP (0.5 equiv.). The reaction mixture was stirred at room temperature for 24 h, the reaction evolution was verified by ^{1}H NMR ($CDCl_3$) and TLC and then the mixture was concentrated to dryness under reduced pressure. Purification by column chromatography using a CH_2Cl_2/MeOH mixture as eluent afforded the product as an orange solid.

General procedure B - obtainment of the second of ester conjugates 2.2.9a and 2.2.11a-2.2.17a
To a solution of fatty acid (1.1-1.5 equiv.) in dry CH_2Cl_2 (50 mL) at room temperature under inert atmosphere (N_2), were added EDCI (1.1-2 equiv.), **2.2.2** (1 equiv.), and DMAP (0.25-0.5 equiv.). The reaction mixture was stirred at room temperature for 24 h, the reaction evolution was verified by ^{1}H NMR ($CDCl_3$) and TLC and then the mixture was concentrated to dryness under reduced pressure. Purification by column chromatography using a CH_2Cl_2/MeOH mixture as eluent afforded the product as an orange solid.

General procedure C - obtainment of the amide conjugates 2.2.9b and 2.2.11b-2.2.20b
To a solution of fatty acid (1.5 equiv.) in dry CH_2Cl_2 (50 mL) at room temperature under inert atmosphere (N_2), were added HOBt·H_2O (2.4 equiv.) and DIPEA (2.5 equiv.). After 10 min were added successively EDCI (3 equiv.), **2.2.3** (1 equiv.)., and DIPEA (2.5 equiv.). The reaction mixture was stirred at room temperature for 24 h, the reaction evolution was verified by ^{1}H NMR ($CDCl_3$) and TLC and then the mixture was concentrated to dryness under reduced pressure. Purification by column chromatography using a CH_2Cl_2/MeOH mixture as eluent afforded the product as an orange solid.

Synthesis of the first series of ester conjugates 2.2.4a-2.2.7a and 2.2.8a

Synthesis of [(η^6-*p*-MeC$_6$H$_4$Pr^i)$_2$Ru$_2$(μ_2-SCH$_2$C$_6$H$_4$-*p*-Bu^t)$_2$(μ_2-SC$_6$H$_4$-*p*-CH$_2$CO$_2$R)]Cl (R = (*E*)-3,7-dimethylocta-2,6-dien-1-yl), 2.2.4a

2.2.1 (0.200 g, 0.194 mmol, 1 equiv.), EDCI (0.074 g, 0.388 mmol, 2 equiv.), geraniol (0.036 g, 0.233 mmol, 1.2 equiv.) and DMAP (0.012 g, 0.097 mmol, 0.5 equiv.); isolated product **2.2.4a** (0.139 g, 0.119 mmol, yield 61%).

^{1}H-NMR (CDCl$_3$) δ_H, ppm: 7.56 (2H, d, 2xS-(*Ar*)C-CH-C*H*-C-CH$_2$-(C=O)-O-CH$_2$, $^3J_{H,H}$ = 8.1 Hz), 7.26-7.34 (8H, m, 4xCH$_2$-(*Ar*)C-C*H*-CH-C-C(CH$_3$)$_3$, 4xCH$_2$-(*Ar*)C-CH-C*H*-C-C(CH$_3$)$_3$), 7.07 (2H, d, 2xS-(*Ar*)C-CH-C*H*-C-O-(C=O)-CH$_2$, $^3J_{H,H}$ = 8.1 Hz), 5.19 (1H, td, (C=O)-O-CH$_2$-C*H*), 5.96 (2H, d, 2xCH$_3$-(*Ar*)C-CH-C*H*-C, $^3J_{H,H}$ = 5.8 Hz), 4.93 (1H, td, CH$_2$-C*H*=C(CH$_3$)$_2$), 4.85 (2H, d, 2xCH$_3$-(*Ar*)C-C*H*-CH-C, $^3J_{H,H}$ = 5.8 Hz), 4.76 (2H, d, 2xCH$_3$-(*Ar*)C-CH-C*H*-C, $^3J_{H,H}$ = 5.8 Hz), 4.46 (4H, m, 2xCH$_3$-(*Ar*)C-C*H*-CH-C, (C=O)-O-C*H*$_2$-CH), 3.47 (2H, s, (*Ar*)C-C*H*$_2$-(C=O)-O), 3.46 (2H, s, C*H*$_2$-(*Ar*)C-CH-CH-C-C(CH$_3$)$_3$), 3.28 (2H, s, C*H*$_2$-(*Ar*)C-CH-CH-C-C(CH$_3$)$_3$), 1.92-1.99 (m, 2H, (C=O)-O-CH$_2$-CH=C-C*H*$_2$-CH$_2$), 1.87-1.92 (m, 2H, (C=O)-O-CH$_2$-CH=C-CH$_2$-C*H*$_2$), 1.72 (2H, sept, 2x(*Ar*)C-CH-CH-C-C*H*(CH$_3$)$_2$, $^3J_{H,H}$ = 6.8 Hz), 1.60 (6H, s, 2xC*H*$_3$-(*Ar*)C-CH-CH-C), 1.55 (3H, s, (C=O)-O-CH$_2$-CH=C-C*H*$_3$), 1.53 (3H, s, CH=C-C*H*$_3$), 1.45 (3H, s, CH=C-C*H*$_3$), 1.21 (9H, s, S-CH$_2$-(*Ar*)C-CH-CH-C-C(C*H*$_3$)$_3$), 1.18 (9H, s, S-CH$_2$-(*Ar*)C-CH-CH-C-C(C*H*$_3$)$_3$), 0.77 (6H, d, (*Ar*)C-CH-CH-C-CH(C*H*$_3$)$_2$, $^3J_{H,H}$ = 6.8 Hz), 0.72 (6H, d, (*Ar*)C-CH-CH-C-CH(C*H*$_3$)$_2$, $^3J_{H,H}$ = 6.9 Hz).

^{13}C-NMR (CDCl$_3$) δ_C, ppm: 171.2 (1C, (*Ar*)C-CH$_2$-(*C*=O)-O-CH$_2$), 151.9, 151.7 (2C, 2xS-CH$_2$-(*Ar*)C-CH-CH-*C*-C(CH$_3$)$_3$), 142.7 (1C, S-(*Ar*)C-CH-CH-*C*-CH$_2$-(C=O)-O-CH$_2$), 136.81, 136.77 (2C, 2xS-CH$_2$-(*Ar*)*C*-CH-CH-C-C(CH$_3$)$_3$), 136.6 (1C, S-(*Ar*)*C*-CH-CH-C-CH$_2$-(C=O)-O-CH$_2$), 134.9 (1C, (C=O)-O-CH$_2$-CH=*C*), 132.8 (2C, 2xS-(*Ar*)C-CH-*C*H-C-CH$_2$-(C=O)-O-CH$_2$), 132.0 (1C, *C*(CH$_3$)$_2$), 130.1 (2C, 2xS-(*Ar*)C-*C*H-CH-C-CH$_2$-(C=O)-O-CH$_2$), 129.4, 129.2 (2C, 2xS-CH$_2$-(*Ar*)C-*C*H-CH-C-C(CH$_3$)$_3$), 125.7, 125.5 (2C, 2xS-CH$_2$-(*Ar*)C-CH-*C*H-C-C(CH$_3$)$_3$), 123.8 (1C, *C*H=C(CH$_3$)$_2$), 118.2 (1C, (C=O)-O-CH$_2$-*C*H), 107.1 (2C, 2xCH$_3$-(*Ar*)C-CH-CH-*C*), 100.6 (2C, 2xCH$_3$-(*Ar*)*C*-CH-CH-C), 84.3 (2C, 2xCH$_3$-(*Ar*)C-CH-*C*H-C), 83.7 (4C, 2xCH$_3$-(*Ar*)C-*C*H-CH-C, 2xCH$_3$-(*Ar*)C-CH-*C*H-C), 82.6 (2C, 2xCH$_3$-(*Ar*)C-*C*H-CH-C), 62.1 (1C, (C=O)-O-*C*H$_2$), 40.9 (1C, (*Ar*)C-*C*H$_2$-(C=O)), 40.1 (1C, S-*C*H$_2$-(*Ar*)C-CH-CH-C-C(CH$_3$)$_3$), 39.7 (1C, C*H*$_2$-CH=C(CH$_3$)$_2$), 39.6 (1C, S-*C*H$_2$-(*Ar*)C-CH-CH-C-C(CH$_3$)$_3$), 34.91 (1C, S-CH$_2$-(*Ar*)C-CH-CH-C-*C*(CH$_3$)$_3$), 34.86 (1C, S-CH$_2$-(*Ar*)C-CH-CH-C-*C*(CH$_3$)$_3$), 31.55 (3C, S-CH$_2$-(*Ar*)C-CH-CH-C-C(*C*H$_3$)$_3$), 31.53 (3C, S-CH$_2$-(*Ar*)C-CH-CH-C-C(*C*H$_3$)$_3$), 30.9 (2C, 2x(*Ar*)CH-CH-C-*C*H(CH$_3$)$_2$), 26.4 (1C, C*H*$_2$-CH$_2$-CH=C(CH$_3$)$_3$), 25.8 (1C, CH=C-*C*H$_3$), 23.2 (2C, (*Ar*)CH-CH-C-CH(*C*H$_3$)$_2$), 22.7 (2C, (*Ar*)CH-CH-C-CH(*C*H$_3$)$_2$), 18.3 (2C, 2x*C*H$_3$-(*Ar*)C-CH-CH), 17.9 (1C, CH=C-*C*H$_3$), 16.6 (1C, (C=O)-O-CH$_2$-CH=C-C*H*$_3$).

***R*$_f$** (CH$_2$Cl$_2$/CH$_3$OH 10:1 (v/v)) = 0.333.

ESI-MS(+): *m/z* found 1133.3471 [M-Cl]$^+$, calcd. for C$_{60}$H$_{81}$O$_2$Ru$_2$S$_3^+$ 1133.3480.

Elemental analysis (%): calcd. for C$_{60}$H$_{81}$ClO$_2$Ru$_2$S$_3$·1.75CH$_3$OH C 60.59, H 7.25; found C 60.57, H 7.39.

Synthesis of ([(η^6-*p*-MeC$_6$H$_4$Pr^i)$_2$Ru$_2$(μ_2-SCH$_2$C$_6$H$_4$-*p*-Bu^t)$_2$(μ_2-SC$_6$H$_4$-*p*-CH$_2$CO$_2$R)]Cl (R = (2*E*,6*E*)-3,7,11-trimethyldodeca-2,6,10-trien-1-yl), 2.2.5a

2.2.1 (0.300 g, 0.291 mmol, 1 equiv.), EDCI (0.112 g, 0.582 mmol, 2 equiv.), farnesol (0.100 g, 0.437 mmol, 1.5 equiv.) and DMAP (0.018 g, 0.146 mmol, 0.5 equiv.); isolated product **2.2.5a** (0.179 g, 0.145 mmol, yield 50%).

^{1}H-NMR (CDCl$_3$) δ_H, ppm: 7.72 (2H, d, 2xS-(*Ar*)C-CH-C*H*-C-CH$_2$-(C=O)-O-CH$_2$, $^3J_{H,H}$ = 8.1 Hz), 7.41-7.49 (8H, m, 4xCH$_2$-(*Ar*)C-C*H*-CH-C-C(CH$_3$)$_3$, 4xCH$_2$-(*Ar*)C-CH-C*H*-C-C(CH$_3$)$_3$), 7.23 (2H, d, 2xS-(*Ar*)C-CH-C*H*-C-O-(C=O)-CH$_2$, $^3J_{H,H}$ = 8.1 Hz), 5.35 (1H, t, (C=O)-O-CH$_2$-C*H*, $^3J_{H,H}$

= 6.2 Hz), 5.96 (4H, m, 2xCH$_3$-(*Ar*)C-CH-C*H*-C, CH$_2$-C*H*=C(CH$_3$)-CH$_2$, CH$_2$-C*H*=C(CH$_3$)$_2$), 5.08 (2H, d, 2xCH$_3$-(*Ar*)C-C*H*-CH-C, $^3J_{H,H}$ = 5.8 Hz), 5.01 (2H, d, 2xCH$_3$-(*Ar*)C-CH-C*H*-C, $^3J_{H,H}$ = 5.7 Hz), 4.61-4.63 (4H, m, 2xCH$_3$-(*Ar*)C-C*H*-CH-C, (C=O)-O-C*H*$_2$-CH), 3.62 (2H, s, (*Ar*)C-C*H*$_2$-(C=O)-O), 3.61 (2H, s, C*H*$_2$-(*Ar*)C-CH-CH-C-C(CH$_3$)$_3$), 3.44 (2H, s, C*H*$_2$-(*Ar*)C-CH-CH-C-C(CH$_3$)$_3$), 2.04-2.15 (m, 2H, (C=O)-O-CH$_2$-CH=C-C*H*$_2$-CH$_2$), 1.96-2.00 (m, 2H, (C=O)-O-CH$_2$-CH=C-CH$_2$-C*H*$_2$), 1.88 (2H, sept, 2x(*Ar*)C-CH-CH-C-C*H*(CH$_3$)$_2$, $^3J_{H,H}$ = 6.8 Hz), 1.76 (6H, s, 2xC*H*$_3$-(*Ar*)C-CH-CH-C), 1.71 (6H, s, (C=O)-O-CH$_2$-CH=C-C*H*$_3$, CH$_2$-CH-C(C*H*$_3$)-CH$_2$), 1.67 (3H, s, CH=C-C*H*$_3$), 1.60 (3H, s, CH=C-C*H*$_3$), 1.37 (9H, s, S-CH$_2$-(*Ar*)C-CH-CH-C-C(C*H*$_3$)$_3$), 1.33 (9H, s, S-CH$_2$-(*Ar*)C-CH-CH-C-C(C*H*$_3$)$_3$), 0.92 (6H, d, (*Ar*)C-CH-CH-C-CH(C*H*$_3$)$_2$, $^3J_{H,H}$ = 6.8 Hz), 0.88 (6H, d, (*Ar*)C-CH-CH-C-CH(C*H*$_3$)$_2$, $^3J_{H,H}$ = 6.8 Hz).

^{13}C-NMR (CDCl$_3$) δ$_C$, ppm: 171.3 (1C, (*Ar*)C-CH$_2$-(*C*=O)-O-CH$_2$), 151.9, 151.7 (2C, 2xS-CH$_2$-(*Ar*)C-CH-CH-*C*-C(CH$_3$)$_3$), 142.7 (1C, S-(*Ar*)C-CH-CH-*C*-CH$_2$-(C=O)-O-CH$_2$), 136.86, 136.81 (2C, 2xS-CH$_2$-(*Ar*)*C*-CH-CH-C-C(CH$_3$)$_3$), 136.7 (1C, S-(*Ar*)*C*-CH-CH-C-CH$_2$-(C=O)-O-CH$_2$), 135.7 (1C, C(CH$_3$)-(CH$_2$)$_2$-CH=*C*(CH$_3$)), 134.9 (1C, (C=O)-O-CH$_2$-CH=*C*(CH$_3$)), 132.8 (2C, 2xS-(*Ar*)C-*C*H-CH-C-CH$_2$-(C=O)-O-CH$_2$), 131.5 (1C, *C*(CH$_3$)$_2$), 130.1 (2C, 2xS-(*Ar*)C-CH-*C*H-C-CH$_2$-(C=O)-O-CH$_2$), 129.4, 129.2 (2C, 2xS-CH$_2$-(*Ar*)C-*C*H-CH-C-C(CH$_3$)$_3$), 125.7, 125.5 (2C, 2xS-CH$_2$-(*Ar*)C-CH-*C*H-C-C(CH$_3$)$_3$), 124.4 (1C, *C*H=C(CH$_3$)$_2$), 123.7 (1C, C(CH$_3$)-(CH$_2$)$_2$-*C*H=C(CH$_3$)), 118.2 (1C, (C=O)-O-CH$_2$-*C*H), 107.1 (2C, 2xCH$_3$-(*Ar*)C-CH-CH-*C*), 100.6 (2C, 2xCH$_3$-(*Ar*)*C*-CH-CH-C), 84.3 (2C, 2xCH$_3$-(*Ar*)C-CH-*C*H-C), 83.8 (4C, 2xCH$_3$-(*Ar*)C-*C*H-CH-C, 2xCH$_3$-(*Ar*)C-CH-*C*H-C), 82.6 (2C, 2xCH$_3$-(*Ar*)C-*C*H-CH-C), 40.9 (1C, (*Ar*)C-*C*H$_2$-(C=O)), 40.2 (1C, C*H*$_2$-CH=C(CH$_3$)$_2$), 39.84 (1C, S-*C*H$_2$-(*Ar*)C-CH-CH-C-C(CH$_3$)$_3$), 39.71 (1C, S-*C*H$_2$-(*Ar*)C-CH-CH-C-C(CH$_3$)$_3$), 39.65 (1C, (C=O)-O-*C*H$_2$), 34.93 (1C, S-CH$_2$-(*Ar*)C-CH-CH-C-*C*(CH$_3$)$_3$), 34.88 (1C, S-CH$_2$-(*Ar*)C-CH-CH-C-*C*(CH$_3$)$_3$), 31.57 (3C, S-CH$_2$-(*Ar*)C-CH-CH-C-C(*C*H$_3$)$_3$), 31.55 (3C, S-CH$_2$-(*Ar*)C-CH-CH-C-C(*C*H$_3$)$_3$), 30.9 (2C, 2x(*Ar*)CH-CH-C-*C*H(CH$_3$)$_2$), 26.9 (1C, C*H*$_2$-CH$_2$-CH=C(CH$_3$)$_3$), 26.4 (1C, CH$_2$-C*H*$_2$-CH=C(CH$_3$)$_3$), 25.9 (1C, O-CH$_2$-CH=C-*C*H$_3$), 23.2 (2C, (*Ar*)CH-CH-C-CH(*C*H$_3$)$_2$), 22.7 (2C, (*Ar*)CH-CH-C-CH(*C*H$_3$)$_2$), 18.3 (2C, 2x*C*H$_3$-(*Ar*)C-CH-CH), 17.9 (1C, C(*C*H$_3$)-(CH$_2$)$_2$-CH=C(CH$_3$)$_2$), 16.7 (1C, CH=C-*C*H$_3$), 16.2 (1C, CH=C-*C*H$_3$).

***R*$_f$** (CH$_2$Cl$_2$/CH$_3$OH 10:1 (v/v)) = 0.429.

ESI-MS(+): *m/z* found 1201.4089 [M-Cl]$^+$, calcd. for C$_{65}$H$_{89}$O$_2$Ru$_2$S$_3^+$ 1201.4106.

Elemental analysis (%): calcd. for C$_{65}$H$_{89}$ClO$_2$Ru$_2$S$_3$·0.25CH$_2$Cl$_2$·0.5CH$_3$OH C 62.01, H 7.24; found C 62.09, H 7.14.

Synthesis of [(*η*^{6}-*p*-MeC$_6$H$_4$Pr^i)$_2$Ru$_2$(*μ*$_2$-SCH$_2$C$_6$H$_4$-*p*-Bu^t)$_2$(*μ*$_2$-SC$_6$H$_4$-*p*-CH$_2$CO$_2$R)]Cl (R = (2*E*,6*E*,10*E*)-3,7,11,15-tetramethylhexadeca-2,6,10,14-tetraen-1-yl), 2.2.6a

2.2.1 (0.190 g, 0.184 mmol, 1 equiv.), EDCI (0.071 g, 0.368 mmol, 2 equiv.), geranylgeraniol (0.094 g, 0.276 mmol, 1.5 equiv.) and DMAP (0.011 g, 0.092 mmol, 0.5 equiv.); isolated product **2.2.6a** (0.091 g, 0.070 mmol, yield 38%).

^{1}H-NMR (CDCl$_3$) δ$_H$, ppm: 7.72 (2H, d, 2xS-(*Ar*)C-CH-C*H*-C-CH$_2$-(C=O)-O-CH$_2$, $^3J_{H,H}$ = 8.0 Hz), 7.41-7.49 (8H, m, 4xCH$_2$-(*Ar*)C-C*H*-CH-C-C(CH$_3$)$_3$, 4xCH$_2$-(*Ar*)C-CH-C*H*-C-C(CH$_3$)$_3$), 7.23 (2H, d, 2xS-(*Ar*)C-CH-C*H*-C-O-(C=O)-CH$_2$, $^3J_{H,H}$ = 8.1 Hz), 5.36 (1H, t, (C=O)-O-CH$_2$-C*H*, $^3J_{H,H}$ = 6.6 Hz), 5.08-5.14 (4H, m, 2xCH$_3$-(*Ar*)C-CH-C*H*-C, CH$_2$-C*H*=C(CH$_3$)-CH$_2$, CH$_2$-C*H*=C(CH$_3$)$_2$), 5.02 (2H, d, 2xCH$_3$-(*Ar*)C-C*H*-CH-C, $^3J_{H,H}$ = 5.8 Hz), 4.93 (2H, d, 2xCH$_3$-(*Ar*)C-CH-C*H*-C, $^3J_{H,H}$ = 5.7 Hz), 4.62-4.64 (4H, m, 2xCH$_3$-(*Ar*)C-C*H*-CH-C, (C=O)-O-C*H*$_2$-CH), 3.62 (2H, s, C*H*$_2$-(*Ar*)C-CH-CH-C-C(CH$_3$)$_3$, (*Ar*)C-C*H*$_2$-(C=O)-O), 3.45 (2H, s, C*H*$_2$-(*Ar*)C-CH-CH-C-C(CH$_3$)$_3$), 2.03-2.16 (m, 2H, (C=O)-O-CH$_2$-CH=C-C*H*$_2$-CH$_2$), 1.95-2.02 (m, 2H, (C=O)-O-CH$_2$-CH=C-CH$_2$-C*H*$_2$), 1.88 (2H, sept, 2x(*Ar*)C-CH-CH-C-C*H*(CH$_3$)$_2$, $^3J_{H,H}$ = 6.8 Hz), 1.76 (6H, s, 2xC*H*$_3$-(*Ar*)C-CH-CH-C), 1.72 (6H, s, (C=O)-O-CH$_2$-CH=C-C*H*$_3$, CH$_2$-CH-C(C*H*$_3$)-CH$_2$), 1.68 (3H, s, CH$_2$-CH-C(C*H*$_3$)-CH$_2$), 1.61 (3H, s, CH=C-C*H*$_3$), 1.60 (3H, s, CH=C-C*H*$_3$), 1.37 (9H, s, S-CH$_2$-(*Ar*)C-CH-CH-C-

C(C<u>*H*₃</u>)$_3$), 1.33 (9H, s, S-CH$_2$-(*Ar*)C-CH-CH-C-C(C<u>*H*₃</u>)$_3$), 0.93 (6H, d, (*Ar*)C-CH-CH-C-CH(C<u>*H*₃</u>)$_2$, $^3J_{H,H}$ = 6.8 Hz), 0.88 (6H, d, (*Ar*)C-CH-CH-C-CH(C<u>*H*₃</u>)$_2$, $^3J_{H,H}$ = 6.8 Hz).

^{13}C-NMR (CDCl$_3$) δ_C, ppm: 171.3 (1C, (*Ar*)C-CH$_2$-(<u>*C*</u>=O)-O-CH$_2$), 151.9, 151.7 (2C, 2xS-CH$_2$-(*Ar*)C-CH-CH-<u>*C*</u>-C(CH$_3$)$_3$), 142.8 (1C, S-(*Ar*)C-CH-CH-<u>*C*</u>-CH$_2$-(C=O)-O-CH$_2$), 136.89, 136.83 (2C, 2xS-CH$_2$-(*Ar*)<u>*C*</u>-CH-CH-C-C(CH$_3$)$_3$), 136.7 (1C, S-(*Ar*)<u>*C*</u>-CH-CH-C-CH$_2$-(C=O)-O-CH$_2$), 135.8 (1C, CH$_2$-CH=<u>*C*</u>(CH$_3$)), 135.2 (1C, CH$_2$-CH=<u>*C*</u>(CH$_3$)), 134.9 (1C, (C=O)-O-CH$_2$-CH=<u>*C*</u>), 132.9 (2C, 2xS-(*Ar*)C-CH-<u>*C*</u>H-C-CH$_2$-(C=O)-O-CH$_2$), 131.4 (1C, <u>*C*</u>(CH$_3$)$_2$), 130.1 (2C, 2xS-(*Ar*)C-<u>*C*</u>H-CH-C-CH$_2$-(C=O)-O-CH$_2$), 129.5, 129.3 (2C, 2xS-CH$_2$-(*Ar*)C-<u>*C*</u>H-CH-C-C(CH$_3$)$_3$), 125.7, 125.5 (2C, 2xS-CH$_2$-(*Ar*)C-CH-<u>*C*</u>H-C-C(CH$_3$)$_3$), 124.5 (1C, <u>*C*</u>H=C(CH$_3$)$_2$), 124.3 (1C, <u>*C*</u>H=C(CH$_3$)), 123.7 (1C, <u>*C*</u>H=C(CH$_3$)), 118.2 (1C, (C=O)-O-CH$_2$-<u>*C*</u>H), 107.1 (2C, 2xCH$_3$-(*Ar*)C-CH-CH-<u>*C*</u>), 100.6 (2C, 2xCH$_3$-(*Ar*)<u>*C*</u>-CH-CH-C), 84.3 (2C, 2xCH$_3$-(*Ar*)C-CH-<u>*C*</u>H-C), 83.8 (4C, 2xCH$_3$-(*Ar*)C-<u>*C*</u>H-CH-C, 2xCH$_3$-(*Ar*)C-CH-<u>*C*</u>H-C), 82.6 (2C, 2xCH$_3$-(*Ar*)C-<u>*C*</u>H-CH-C), 40.9 (1C, (*Ar*)C-<u>*C*</u>H$_2$-(C=O)), 40.2 (1C, <u>*C*</u>H$_2$-CH=C(CH$_3$)), 39.84 (1C, S-<u>*C*</u>H$_2$-(*Ar*)C-CH-CH-C-C(CH$_3$)$_3$), 39.71 (1C, S-<u>*C*</u>H$_2$-(*Ar*)C-CH-CH-C-C(CH$_3$)$_3$), 39.65 (1C, (C=O)-O-<u>*C*</u>H$_2$), 34.94 (1C, S-CH$_2$-(*Ar*)C-CH-CH-C-<u>*C*</u>(CH$_3$)$_3$), 34.89 (1C, S-CH$_2$-(*Ar*)C-CH-CH-C-<u>*C*</u>(CH$_3$)$_3$), 31.58 (3C, S-CH$_2$-(*Ar*)C-CH-CH-C-C(<u>*C*</u>H$_3$)$_3$), 31.56 (3C, S-CH$_2$-(*Ar*)C-CH-CH-C-C(<u>*C*</u>H$_3$)$_3$), 30.9 (2C, 2x(*Ar*)CH-CH-C-<u>*C*</u>H(CH$_3$)$_2$), 26.9 (1C, CH$_2$-<u>*C*</u>H$_2$-CH=C(CH$_3$)), 26.8 (1C, <u>*C*</u>H$_2$-CH$_2$-CH=C(CH$_3$)$_2$), 26.4 (1C, CH$_2$-<u>*C*</u>H$_2$-CH=C(CH$_3$)$_2$), 25.9 (1C, 1C, O-CH$_2$-CH=C(<u>*C*</u>H$_3$)), 23.2 (2C, (*Ar*)CH-CH-C-CH(<u>*C*</u>H$_3$)$_2$), 22.7 (2C, (*Ar*)CH-CH-C-CH(<u>*C*</u>H$_3$)$_2$), 18.3 (2C, 2x<u>*C*</u>H$_3$-(*Ar*)C-CH-CH), 17.8 (1C, CH$_2$-CH=C(<u>*C*</u>H$_3$)-CH$_2$), 16.7 (1C, CH$_2$-CH=C(<u>*C*</u>H$_3$)-CH$_2$), 16.22 (1C, CH=C-<u>*C*</u>H$_3$), 16.17 (1C, CH=C-<u>*C*</u>H$_3$).

***R*$_f$** (CH$_2$Cl$_2$/CH$_3$OH 10:1 (v/v)) = 0.430.

ESI-MS(+): *m/z* found 1269.4743 [M-Cl]$^+$, calcd. for C$_{70}$H$_{97}$O$_2$Ru$_2$S$_3^+$ 1269.4732.

Elemental analysis (%): calcd. for C$_{70}$H$_{97}$ClO$_2$Ru$_2$S$_3$·0.75CH$_3$OH C 63.97, H 7.59; found C 64.00, H 7.86.

Synthesis of [(η^6-*p*-MeC$_6$H$_4$Pr^i)$_2$Ru$_2$(μ_2-SCH$_2$C$_6$H$_4$-*p*-Bu^t)$_2$(μ_2-SC$_6$H$_4$-*p*-CH$_2$CO$_2$R)]Cl (R = butyl), 2.2.8a

2.2.1 (0.200 g, 0.194 mmol, 1 equiv.), EDCI (0.074 g, 0.388 mmol, 2 equiv.), *n*-butanol (0.017 g, 0.233 mmol, 1.2 equiv.) and DMAP (0.012 g, 0.097 mmol, 0.5 equiv.); isolated product **2.2.8a** (0.077 g, 0.069 mmol, yield 36%).

^{1}H-NMR (CDCl$_3$) δ_H, ppm: 7.70 (2H, d, 2xS-(*Ar*)C-CH-C<u>*H*</u>-C-CH$_2$-(C=O)-O-CH$_2$, $^3J_{H,H}$ = 8.2 Hz), 7.40-7.47 (8H, m, 4xCH$_2$-(*Ar*)C-C<u>*H*</u>-CH-C-C(CH$_3$)$_3$, 4xCH$_2$-(*Ar*)C-CH-C<u>*H*</u>-C-C(CH$_3$)$_3$), 7.21 (2H, d, 2xS-(*Ar*)C-CH-C<u>*H*</u>-C-CH$_2$-(C=O)-O-CH$_2$, $^3J_{H,H}$ = 8.2 Hz), 5.09 (2H, d, 2xCH$_3$-(*Ar*)C-CH-C<u>*H*</u>-C, $^3J_{H,H}$ = 5.7 Hz), 4,98 (2H, d, 2xCH$_3$-(*Ar*)C-C<u>*H*</u>-CH-C, $^3J_{H,H}$ = 5.8 Hz), 4.88 (2H, d, 2xCH$_3$-(*Ar*)C-CH-C<u>*H*</u>-C, $^3J_{H,H}$ = 5.7 Hz), 4.59 (2H, d, 2xCH$_3$-(*Ar*)C-C<u>*H*</u>-CH-C, $^3J_{H,H}$ = 5.7 Hz), 4,08 (2H, t, (C=O)-O-C<u>*H*₂</u>-CH$_2$, $^3J_{H,H}$ = 6.7 Hz), 3.59 (4H, m, C<u>*H*₂</u>-(*Ar*)C-CH-CH-C-C(CH$_3$)$_3$, S-(*Ar*)C-CH-CH-C-C<u>*H*₂</u>-(C=O)), 3.41 (2H, s, C<u>*H*₂</u>-(*Ar*)C-CH-CH-C-C(CH$_3$)$_3$), 1.87 (2H, sept, 2x(*Ar*)C-CH-CH-C-C<u>*H*</u>(CH$_3$)$_2$, $^3J_{H,H}$ = 6.8 Hz), 1.73 (6H, s, 2xC<u>*H*₃</u>-(*Ar*)C-CH-CH-C), 1.74 (2H, quint, (C=O)-O-CH$_2$-C<u>*H*₂</u>-CH$_2$, $^3J_{H,H}$ = 6.8 Hz), 1.29-1.40 (2H, m, (C=O)-O-(CH$_2$)$_2$-C<u>*H*₂</u>), 1.34 (9H, s, S-CH$_2$-(*Ar*)C-CH-CH-C-C(C<u>*H*₃</u>)$_3$), 1.31 (9H, s, S-CH$_2$-(*Ar*)C-CH-CH-C-C(C<u>*H*₃</u>)$_3$), 0.91 (3H, t, CH$_2$-C<u>*H*₃</u>, $^3J_{H,H}$ = 7.2 Hz), 0.90 (6H, d, (*Ar*)C-CH-CH-C-CH(C<u>*H*₃</u>)$_2$, $^3J_{H,H}$ = 6.9 Hz), 0.86 (6H, d, (*Ar*)C-CH-CH-C-CH(C<u>*H*₃</u>)$_2$, $^3J_{H,H}$ = 6.9 Hz).

^{13}C-NMR (CDCl$_3$) δ_C, ppm: 172.3 (1C, (*Ar*)C-CH$_2$-(<u>*C*</u>=O)-O-CH$_2$), 151.8, 151.7 (2C, 2xS-CH$_2$-(*Ar*)C-CH-CH-<u>*C*</u>-C(CH$_3$)$_3$), 136.75, 136.72 (2C, 2xS-CH$_2$-(*Ar*)<u>*C*</u>-CH-CH-C-C(CH$_3$)$_3$), 136.6 (1C, S-(*Ar*)<u>*C*</u>-CH-CH-C-CH$_2$-(C=O)-O-CH$_2$), 134.9 (1C, S-(*Ar*)C-CH-CH-<u>*C*</u>-CH$_2$-(C=O)-O-CH$_2$), 132.8 (2C, 2xS-(*Ar*)C-CH-<u>*C*</u>H-C-CH$_2$-(C=O)-O-CH$_2$), 130.0 (2C, 2xS-(*Ar*)C-<u>*C*</u>H-CH-C-CH$_2$-(C=O)-O-CH$_2$), 129.4, 129.2 (2C, 2xS-CH$_2$-(*Ar*)C-<u>*C*</u>H-CH-C-C(CH$_3$)$_3$), 125.7, 125.5 (2C, 2xS-CH$_2$-(*Ar*)C-CH-<u>*C*</u>H-C-C(CH$_3$)$_3$), 107.1 (2C, 2xCH$_3$-(*Ar*)C-CH-CH-<u>*C*</u>), 100.6 (2C, 2xCH$_3$-(*Ar*)<u>*C*</u>-

CH-CH-C), 84.2 (2C, 2xCH$_3$-(*Ar*)C-CH-*C*H-C), 83.71 (2C, 2xCH$_3$-(*Ar*)C-*C*H-CH-C), 83.67 (2C, 2xCH$_3$-(*Ar*)C-CH-*C*H-C), 82.5 (2C, 2xCH$_3$-(*Ar*)C-*C*H-CH-C), 65.0 (1C, (C=O)-O-*C*H$_2$), 40.9 (1C, CH$_2$-(C=O)-O), 40.1 (1C, S-*C*H$_2$-(*Ar*)C-CH-CH-C-C(CH$_3$)$_3$), 39.6 (1C, S-*C*H$_2$-(*Ar*)C-CH-CH-C-C(CH$_3$)$_3$), 34.87 (1C, S-CH$_2$-(*Ar*)C-CH-CH-C-*C*(CH$_3$)$_3$), 34.82 (1C, S-CH$_2$-(*Ar*)C-CH-CH-C-*C*(CH$_3$)$_3$), 31.51 (3C, S-CH$_2$-(*Ar*)C-CH-CH-C-C(*C*H$_3$)$_3$), 31.49 (3C, S-CH$_2$-(*Ar*)C-CH-CH-C-C(*C*H$_3$)$_3$), 30.8 (2C, 2x(*Ar*)CH-CH-C-*C*H(CH$_3$)$_2$), 30.7 (1C, *C*H$_2$-CH$_2$-CH$_3$), 23.1 (2C, (*Ar*)CH-CH-C-CH(*C*H$_3$)$_2$), 22.7 (2C, (*Ar*)CH-CH-C-CH(*C*H$_3$)$_2$), 19.2 (1C, *C*H$_2$-CH$_3$), 18.2 (2C, 2x*C*H$_3$-(*Ar*)C-CH-CH), 13.8 (1C, CH$_2$-*C*H$_3$).

***R*$_f$** (CH$_2$Cl$_2$/CH$_3$OH 10:1 (v/v)) = 0.313.

ESI-MS(+): *m/z* found 1053.2828 [M-Cl]$^+$, calcd. for C$_{54}$H$_{73}$O$_2$Ru$_2$S$_3^+$ 1053.2854.

Elemental analysis (%): calcd. for C$_{54}$H$_{73}$ClO$_2$Ru$_2$S$_3$ C 59.62, H, 6.76; found C 60.10, H 6.73.

Synthesis of the second of ester conjugates 2.2.9a and 2.2.11a-2.2.17a

Synthesis of [(η^6-*p*-MeC$_6$H$_4$Pr^i)$_2$Ru$_2$(μ_2-SCH$_2$C$_6$H$_4$-*p*-Bu^t)$_2$(μ_2-SC$_6$H$_4$-*p*-O(CO)R)]Cl (R = (*R*)-4-(1,2-dithiolan-3-yl)butan-1-yl), 2.2.9a

α-Lipoic acid (0.096 g, 0.455 mmol, 1.5 equiv.), EDCI (0.116 g, 0.606 mmol, 2 equiv.), **2.2.2** (0.300 g, 0.303 mmol, 1 equiv.) and DMAP (0.019 g, 0.152 mmol, 0.5 equiv.); isolated product **2.2.9a** (0.267 g, 0.227 mmol, yield 75%).

^{1}H-NMR (CDCl$_3$) δ_H, ppm: 7.80 (2H, d, 2xS-(*Ar*)C-C*H*-CH-C-O-(C=O)-CH$_2$, $^3J_{H,H}$ = 8.6 Hz), 7.49-7.44 (8H, m, 4xCH$_2$-(*Ar*)C-C*H*-CH-C-C(CH$_3$)$_3$, 4xCH$_2$-(*Ar*)C-CH-C*H*-C-C(CH$_3$)$_3$), 7.05 (2H, d, 2xS-(*Ar*)C-CH-C*H*-C-O-(C=O)-CH$_2$, $^3J_{H,H}$ = 8.6 Hz), 5.14 (2H, d, 2xCH$_3$-(*Ar*)C-CH-C*H*-C, $^3J_{H,H}$ = 5.8 Hz), 5.02 (2H, d, 2xCH$_3$-(*Ar*)C-C*H*-CH-C, $^3J_{H,H}$ = 5.9 Hz), 4.94 (2H, d, 2xCH$_3$-(*Ar*)C-CH-C*H*-C, $^3J_{H,H}$ = 5.8 Hz), 4.63 (2H, d, 2xCH$_3$-(*Ar*)C-C*H*-CH-C, $^3J_{H,H}$ = 5.8 Hz), 3.59-3.66 (1H, m, (C=O)-(CH$_2$)$_4$-C*H*), 3.61 (2H, s, C*H*$_2$-(*Ar*)C-CH-CH-C-C(CH$_3$)$_3$), 3.44 (2H, s, C*H*$_2$-(*Ar*)C-CH-CH-C-C(CH$_3$)$_3$), 3.11-3.24 (2H, m, (C=O)-(CH$_2$)$_4$-CH-CH$_2$-C*H*$_2$), 2.60 (2H, t, (C=O)-C*H*$_2$-CH$_2$, $^3J_{H,H}$ = 7.4 Hz), 2.47-2.55 (1H, sext, (C=O)-(CH$_2$)$_4$-CH-C*H*$_2$-CH$_2$, $^3J_{H,H}$ = 6.6 Hz), 1.84-1.99 (3H, m, 2x(*Ar*)C-CH-CH-C-C*H*(CH$_3$)$_2$, $^3J_{H,H}$ = 6.9 Hz, (C=O)-(CH$_2$)$_4$-CH-C*H*$_2$-CH$_2$, $^3J_{H,H}$ = 6.9 Hz), 1.72-1.83 (4H, m, (C=O)-CH$_2$-C*H*$_2$-CH$_2$-CH$_2$-CH, (C=O)-CH$_2$-CH$_2$-CH$_2$-C*H*$_2$-CH), 1.77 (6H, s, 2xC*H*$_3$-(*Ar*)C-CH-CH-C), 1.52-1.65 (2H, m, (C=O)-CH$_2$-CH$_2$-C*H*$_2$-CH$_2$-CH), 1.36 (9H, s, S-CH$_2$-(*Ar*)C-CH-CH-C-C(C*H*$_3$)$_3$), 1.33 (9H, s, S-CH$_2$-(*Ar*)C-CH-CH-C-C(C*H*$_3$)$_3$), 0.94 (6H, d, (*Ar*)C-CH-CH-C-CH(C*H*$_3$)$_2$, $^3J_{H,H}$ = 6.9 Hz), 0.89 (6H, d, (*Ar*)C-CH-CH-C-CH(C*H*$_3$)$_2$, $^3J_{H,H}$ = 6.9 Hz).

^{13}C-NMR (CDCl$_3$) δ_C, ppm: 171.9 (1C, (*Ar*)C-O-(*C*=O)-CH$_2$), 152.0, 151.9 (2C, 2xS-CH$_2$-(*Ar*)C-CH-CH-*C*-C(CH$_3$)$_3$), 151.3 (1C, S-(*Ar*)C-CH-CH-*C*-O-(C=O)-CH$_2$), 136.90, 136.88 (2C, 2xS-CH$_2$-(*Ar*)*C*-CH-CH-C-C(CH$_3$)$_3$), 135.2 (1C, S-(*Ar*)*C*-CH-CH-C-O-(C=O)-CH$_2$), 133.8 (2C, 2xS-(*Ar*)C-*C*H-CH-C-O-(C=O)-CH$_2$), 129.5, 129.3 (2C, 2xS-CH$_2$-(*Ar*)C-*C*H-CH-C-C(CH$_3$)$_3$), 125.8, 125.6 (2C, 2xS-CH$_2$-(*Ar*)C-CH-*C*H-C-C(CH$_3$)$_3$), 122.6 (2C, 2xS-(*Ar*)C-CH-*C*H-C-O-(C=O)-CH$_2$), 107.3 (2C, 2xCH$_3$-(*Ar*)C-CH-CH-*C*), 100.8 (2C, 2xCH$_3$-(*Ar*)*C*-CH-CH-C), 84.4 (2C, 2xCH$_3$-(*Ar*)C-CH-*C*H-C), 83.9 (4C, 2xCH$_3$-(*Ar*)C-*C*H-CH-C, 2xCH$_3$-(*Ar*)C-CH-*C*H-C), 82.8 (2C, 2xCH$_3$-(*Ar*)C-*C*H-CH-C), 56.6 (1C, (C=O)-(CH$_2$)$_4$-*C*H), 40.6 (1C, CH-*C*H$_2$-CH$_2$), 40.3 (1C, S-*C*H$_2$-(*Ar*)C-CH-CH-C-C(CH$_3$)$_3$), 39.8 (1C, S-*C*H$_2$-(*Ar*)C-CH-CH-C-C(CH$_3$)$_3$), 38.8 (1C, CH-CH$_2$-*C*H$_2$), 35.03 (1C, S-CH$_2$-(*Ar*)C-CH-CH-C-*C*(CH$_3$)$_3$), 34.99 (1C, S-CH$_2$-(*Ar*)C-CH-CH-C-*C*(CH$_3$)$_3$), 34.8 (1C, (C=O)-CH$_2$-*C*H$_2$), 34.4 (1C, (C=O)-*C*H$_2$), 31.67 (3C, S-CH$_2$-(*Ar*)C-CH-CH-C-C(*C*H$_3$)$_3$), 31.65 (3C, S-CH$_2$-(*Ar*)C-CH-CH-C-C(*C*H$_3$)$_3$), 31.1 (2C, 2x(*Ar*)CH-CH-C-*C*H(CH$_3$)$_2$), 29.0 (1C, (C=O)-(CH$_2$)$_2$-*C*H$_2$), 24.8 (1C, (C=O)-(CH$_2$)$_3$-*C*H$_2$), 23.3 (1C, (*Ar*)CH-CH-C-CH(*C*H$_3$)$_2$), 22.8 (1C, (*Ar*)CH-CH-C-CH(*C*H$_3$)$_2$), 18.4 (2C, 2x*C*H$_3$-(*Ar*)C-CH-CH).

***R*$_f$** (CH$_2$Cl$_2$/CH$_3$OH 10:1 (v/v)) = 0.429.

ESI-MS(+): *m/z* found 1143.2350 [M-Cl]$^+$, calcd. for C$_{56}$H$_{75}$O$_2$Ru$_2$S$_5^+$ 1143.2452.

Elemental analysis (%): calcd. for $C_{56}H_{75}ClO_2Ru_2S_5 \cdot H_2O$ C 56.23, H 6.49; found C 56.27, H, 6.38.

Synthesis of [(η^6-*p*-MeC$_6$H$_4$Pr^i)$_2$Ru$_2$(μ_2-SCH$_2$C$_6$H$_4$-*p*-Bu^t)$_2$(μ_2-SC$_6$H$_4$-*p*-O(CO)R)]Cl (R = propyl), 2.2.11a

Butyric acid (0.021 g, 0.242 mmol, 1.2 equiv.), EDCI (0.077 g, 0.404 mmol, 2 equiv.), **2.2.2** (0.200 g, 0.202 mmol, 1 equiv.) and DMAP (0.012 g, 0.101 mmol, 0.5 equiv.); isolated product **2.2.11a** (0.125 g, 0.118 mmol, yield 58%).

^{1}H-NMR ($CDCl_3$) δ_H, ppm: 7.78 (2H, d, 2xS-(*Ar*)C-CH-C*H*-C-O-(C=O)-CH$_2$, $^3J_{H,H}$ = 8.6 Hz), 7.39-7.48 (8H, m, 4xCH$_2$-(*Ar*)C-C*H*-CH-C-C(CH$_3$)$_3$, 4xCH$_2$-(*Ar*)C-CH-C*H*-C-C(CH$_3$)$_3$), 7.04 (2H, d, 2xS-(*Ar*)C-C*H*-CH-C-O-(C=O)-CH$_2$, $^3J_{H,H}$ = 8.6 Hz), 5.12 (2H, d, 2xCH$_3$-(*Ar*)C-CH-C*H*-C, $^3J_{H,H}$ = 5.7 Hz), 5.01 (2H, d, 2xCH$_3$-(*Ar*)C-C*H*-CH-C, $^3J_{H,H}$ = 5.8 Hz), 4.91 (2H, d, 2xCH$_3$-(*Ar*)C-CH-C*H*-C, $^3J_{H,H}$ = 5.7 Hz), 4.62 (2H, d, 2xCH$_3$-(*Ar*)C-C*H*-CH-C, $^3J_{H,H}$ = 5.8 Hz), 3.61 (2H, s, C*H*$_2$-(*Ar*)C-CH-CH-C-C(CH$_3$)$_3$), 3.43 (2H, s, C*H*$_2$-(*Ar*)C-CH-CH-C-C(CH$_3$)$_3$), 2.55 (2H, t, (C=O)-C*H*$_2$-CH$_2$, $^3J_{H,H}$ = 7.4 Hz), 1.89 (2H, sept, 2x(*Ar*)C-CH-CH-C-C*H*(CH$_3$)$_2$, $^3J_{H,H}$ = 7.1 Hz), 1.77 (6H, s, 2xC*H*$_3$-(*Ar*)C-CH-CH-C), 1.74-1.83 (2H, sext, (C=O)-CH$_2$-C*H*$_2$-CH$_2$, $^3J_{H,H}$ = 7.4 Hz), 1.36 (9H, s, S-CH$_2$-(*Ar*)C-CH-CH-C-C(C*H*$_3$)$_3$), 1.32 (9H, s, S-CH$_2$-(*Ar*)C-CH-CH-C-C(C*H*$_3$)$_3$), 1.05 (3H, t, CH$_2$-C*H*$_3$, $^3J_{H,H}$ = 7.4 Hz), 0.94 (6H, d, (*Ar*)C-CH-CH-C-CH(C*H*$_3$)$_2$, $^3J_{H,H}$ = 6.8 Hz), 0.89 (6H, d, (*Ar*)C-CH-CH-C-CH(C*H*$_3$)$_2$, $^3J_{H,H}$ = 6.9 Hz).

^{13}C-NMR ($CDCl_3$) δ_C, ppm: 172.0 (1C, (*Ar*)C-O-(*C*=O)-CH$_2$), 151.9, 151.8 (2C, 2xS-CH$_2$-(*Ar*)C-CH-CH-*C*-C(CH$_3$)$_3$), 151.2 (1C, S-(*Ar*)C-CH-CH-*C*-O-(C=O)-CH$_2$), 136.79, 136.77 (2C, 2xS-CH$_2$-(*Ar*)*C*-CH-CH-C-C(CH$_3$)$_3$), 135.0 (1C, S-(*Ar*)*C*-CH-CH-C-O-(C=O)-CH$_2$), 133.7 (2C, 2xS-(*Ar*)C-CH-*C*H-C-O-(C=O)-CH$_2$), 129.4, 129.2 (2C, 2xS-CH$_2$-(*Ar*)C-*C*H-CH-C-C(CH$_3$)$_3$), 125.7, 125.5 (2C, 2xS-CH$_2$-(*Ar*)C-CH-*C*H-C-C(CH$_3$)$_3$), 122.5 (2C, 2xS-(*Ar*)C-*C*H-CH-C-O-(C=O)-CH$_2$), 107.2 (2C, 2xCH$_3$-(*Ar*)C-CH-CH-*C*), 100.7 (2C, 2xCH$_3$-(*Ar*)*C*-CH-CH-C), 84.3 (2C, 2xCH$_3$-(*Ar*)C-CH-*C*H-C), 83.8 (4C, 2xCH$_3$-(*Ar*)C-*C*H-CH-C, 2xCH$_3$-(*Ar*)C-CH-*C*H-C), 82.7 (2C, 2xCH$_3$-(*Ar*)C-*C*H-CH-C), 40.2 (1C, S-*C*H$_2$-(*Ar*)C-CH-CH-C-C(CH$_3$)$_3$), 39.7 (1C, S-*C*H$_2$-(*Ar*)C-CH-CH-C-C(CH$_3$)$_3$), 36.3 (1C, (C=O)-*C*H$_2$), 34.92 (1C, S-CH$_2$-(*Ar*)C-CH-CH-C-*C*(CH$_3$)$_3$), 34.87 (1C, S-CH$_2$-(*Ar*)C-CH-CH-C-*C*(CH$_3$)$_3$), 31.56 (3C, S-CH$_2$-(*Ar*)C-CH-CH-C-C(*C*H$_3$)$_3$), 31.54 (3C, S-CH$_2$-(*Ar*)C-CH-CH-C-C(*C*H$_3$)$_3$), 31.0 (2C, 2x(*Ar*)CH-CH-C-*C*H(CH$_3$)$_2$), 23.2 (2C, (*Ar*)CH-CH-C-CH(*C*H$_3$)$_2$), 22.7 (2C, (*Ar*)CH-CH-C-CH(*C*H$_3$)$_2$), 18.5 (1C, *C*H$_2$-CH$_3$), 18.3 (2C, 2x*C*H$_3$-(*Ar*)C-CH-CH), 13.8 (1C, CH$_2$-*C*H$_3$).

***R*$_f$** (CH_2Cl_2/CH_3OH 10:1 (v/v)) = 0.285.

ESI-MS(+): *m/z* found 1025.2512 [M-Cl]$^+$, calcd. for $C_{52}H_{69}O_2Ru_2S_3^+$ 1025.2541.

Elemental analysis (%): calcd. for $C_{52}H_{69}ClO_2Ru_2S_3 \cdot 0.5CH_3OH$ C 58.61, H 6.65; found C 58.64, H 6.91.

Synthesis of [(η^6-*p*-MeC$_6$H$_4$Pr^i)$_2$Ru$_2$(μ_2-SCH$_2$C$_6$H$_4$-*p*-Bu^t)$_2$(μ_2-SC$_6$H$_4$-*p*-O(CO)R)]Cl (R = pentyl), 2.2.12a

Hexanoic acid (0.029 g, 0.242 mmol, 1.2 equiv.), EDCI (0.077 g, 0.404 mmol, 2 equiv.), **2.2.2** (0.200 g, 0.202 mmol, 1 equiv.), and DMAP (0.012 g, 0.101 mmol, 0.5 equiv.); isolated product **2.2.12a** (0.194 g, 0.178 mmol, yield 88%).

^{1}H-NMR ($CDCl_3$) δ_H, ppm: 7.77 (2H, d, 2xS-(*Ar*)C-CH-C*H*-C-O-(C=O)-CH$_2$, $^3J_{H,H}$ = 8.6 Hz), 7.45 (4H, m, 4xCH$_2$-(*Ar*)C-C*H*-CH-C-C(CH$_3$)$_3$), 7.40 (4H, s, 4xCH$_2$-(*Ar*)C-CH-C*H*-C-C(CH$_3$)$_3$), 7.04 (2H, d, 2xS-(*Ar*)C-C*H*-CH-C-O-(C=O)-CH$_2$, $^3J_{H,H}$ = 8.6 Hz), 5.12 (2H, d, 2xCH$_3$-(*Ar*)C-CH-C*H*-C, $^3J_{H,H}$ = 5.7 Hz), 5.00 (2H, d, 2xCH$_3$-(*Ar*)C-C*H*-CH-C, $^3J_{H,H}$ = 5.8 Hz), 4.91 (2H, d, 2xCH$_3$-(*Ar*)C-CH-C*H*-C, $^3J_{H,H}$ = 5.8 Hz), 4.61 (2H, d, 2xCH$_3$-(*Ar*)C-C*H*-CH-C, $^3J_{H,H}$ = 5.8 Hz), 3.60 (2H, s, C*H*$_2$-(*Ar*)C-CH-CH-C-C(CH$_3$)$_3$), 3.42 (2H, s, C*H*$_2$-(*Ar*)C-CH-CH-C-C(CH$_3$)$_3$), 2.56 (2H, t,

(C=O)-C<u>*H*</u>$_2$-CH$_2$, $^3J_{H,H}$ = 7.5 Hz), 1.88 (2H, sept, 2x(*Ar*)C-CH-CH-C-C<u>*H*</u>(CH$_3$)$_2$, $^3J_{H,H}$ = 6.9 Hz), 1.76 (6H, s, 2xC<u>*H*</u>$_3$-(*Ar*)C-CH-CH-C), 1.71-1.78 (2H, m, (C=O)-CH$_2$-C<u>*H*</u>$_2$-CH$_2$), 1.30-1.41 (4H, m, (C=O)-(CH$_2$)$_2$-C<u>*H*</u>$_2$, (C=O)-(CH$_2$)$_3$-C<u>*H*</u>$_2$), 1.35 (9H, s, S-CH$_2$-(*Ar*)C-CH-CH-C-C(C<u>*H*</u>$_3$)$_3$), 1.31 (9H, s, S-CH$_2$-(*Ar*)C-CH-CH-C-C(C<u>*H*</u>$_3$)$_3$), 0.93 (3H, t, CH$_2$-C<u>*H*</u>$_3$, $^3J_{H,H}$ = 6.9 Hz), 0.93 (6H, d, (*Ar*)C-CH-CH-C-CH(C<u>*H*</u>$_3$)$_2$, $^3J_{H,H}$ = 6.9 Hz), 0.87 (6H, d, (*Ar*)C-CH-CH-C-CH(C<u>*H*</u>$_3$)$_2$, $^3J_{H,H}$ = 6.9 Hz).

^{13}C-NMR (CDCl$_3$) δ$_C$, ppm: 172.1 (1C, (*Ar*)C-O-(<u>*C*</u>=O)-CH$_2$), 151.9, 151.7 (2C, 2xS-CH$_2$-(*Ar*)C-CH-CH-<u>*C*</u>-C(CH$_3$)$_3$), 151.2 (1C, S-(*Ar*)C-CH-CH-<u>*C*</u>-O-(C=O)-CH$_2$), 136.8 (2C, 2xS-CH$_2$-(*Ar*)<u>*C*</u>-CH-CH-C-C(CH$_3$)$_3$), 135.0 (1C, S-(*Ar*)<u>*C*</u>-CH-CH-C-O-(C=O)-CH$_2$), 133.6 (2C, 2xS-(*Ar*)C-CH-<u>*C*</u>H-C-O-(C=O)-CH$_2$), 129.4, 129.2 (2C, 2xS-CH$_2$-(*Ar*)C-<u>*C*</u>H-CH-C-C(CH$_3$)$_3$), 125.7, 125.5 (2C, 2xS-CH$_2$-(*Ar*)C-CH-<u>*C*</u>H-C-C(CH$_3$)$_3$), 122.4 (2C, 2xS-(*Ar*)C-<u>*C*</u>H-CH-C-O-(C=O)-CH$_2$), 107.2 (2C, 2xCH$_3$-(*Ar*)C-CH-CH-<u>*C*</u>), 100.7 (2C, 2xCH$_3$-(*Ar*)<u>*C*</u>-CH-CH-C), 84.3 (2C, 2xCH$_3$-(*Ar*)C-CH-<u>*C*</u>H-C), 83.7 (4C, 2xCH$_3$-(*Ar*)C-<u>*C*</u>H-CH-C, 2xCH$_3$-(*Ar*)C-CH-<u>*C*</u>H-C), 82.6 (2C, 2xCH$_3$-(*Ar*)C-<u>*C*</u>H-CH-C), 40.1 (1C, S-<u>*C*</u>H$_2$-(*Ar*)C-CH-CH-C-C(CH$_3$)$_3$), 39.7 (1C, S-<u>*C*</u>H$_2$-(*Ar*)C-CH-CH-C-C(CH$_3$)$_3$), 34.89 (1C, S-CH$_2$-(*Ar*)C-CH-CH-C-<u>*C*</u>(CH$_3$)$_3$), 34.84 (1C, S-CH$_2$-(*Ar*)C-CH-CH-C-<u>*C*</u>(CH$_3$)$_3$), 34.4 (1C, (C=O)-<u>*C*</u>H$_2$), 31.53 (3C, S-CH$_2$-(*Ar*)C-CH-CH-C-C(<u>*C*</u>H$_3$)$_3$), 31.51 (3C, S-CH$_2$-(*Ar*)C-CH-CH-C-C(<u>*C*</u>H$_3$)$_3$), 31.4 (1C, <u>*C*</u>H$_2$-CH$_2$-CH$_3$), 30.9 (2C, 2x(*Ar*)CH-CH-C-<u>*C*</u>H(CH$_3$)$_2$), 24.6 (1C, (C=O)-CH$_2$-<u>*C*</u>H$_2$), 23.2 (2C, (*Ar*)CH-CH-C-CH(<u>*C*</u>H$_3$)$_2$), 22.7 (2C, (*Ar*)CH-CH-C-CH(<u>*C*</u>H$_3$)$_2$), 22.4 (1C, <u>*C*</u>H$_2$-CH$_3$), 18.3 (2C, 2x<u>*C*</u>H$_3$-(*Ar*)C-CH-CH), 14.0 (1C, CH$_2$-<u>*C*</u>H$_3$).

***R*$_f$** (CH$_2$Cl$_2$/CH$_3$OH 10:1 (v/v)) = 0.277.

ESI-MS(+): *m/z* found 1053.2840 [M-Cl]$^+$, calcd. for C$_{54}$H$_{73}$O$_2$Ru$_2$S$_3^+$ 1053.2854.

Elemental analysis (%): calcd. for C$_{54}$H$_{73}$ClO$_2$Ru$_2$S$_3$·CH$_3$OH C 58.98, H 6.93; found C 58.95, H 6.90.

Synthesis of ([(*η*^{6}-*p*-MeC$_6$H$_4$Pr^i)$_2$Ru$_2$(*μ*$_2$-SCH$_2$C$_6$H$_4$-*p*-Bu^t)$_2$(*μ*$_2$-SC$_6$H$_4$-*p*-O(CO)R)]Cl (R = nonyl), 2.2.13a

Decanoic acid (0.043 g, 0.242 mmol, 1.2 equiv.), EDCI (0.077 g, 0.404 mmol, 2 equiv.), **2.2.2** (0.200 g, 0.202 mmol, 1 equiv.) and DMAP (0.012 g, 0.101 mmol, 0.5 equiv.); isolated product **2.2.13a** (0.183 g, 0.160 mmol, yield 79%).

^{1}H-NMR (CDCl$_3$) δ$_H$, ppm: 7.79 (2H, d, 2xS-(*Ar*)C-CH-C<u>*H*</u>-C-O-(C=O)-CH$_2$, $^3J_{H,H}$ = 8.4 Hz), 7.38-7.49 (8H, m, 4xCH$_2$-(*Ar*)C-C<u>*H*</u>-CH-C-C(CH$_3$)$_3$, 4xCH$_2$-(*Ar*)C-CH-C<u>*H*</u>-C-C(CH$_3$)$_3$), 7.04 (2H, d, 2xS-(*Ar*)C-CH-C<u>*H*</u>-C-O-(C=O)-CH$_2$, $^3J_{H,H}$ = 8.4 Hz), 5.14 (2H, d, 2xCH$_3$-(*Ar*)C-CH-C<u>*H*</u>-C, $^3J_{H,H}$ = 5.6 Hz), 5.02 (2H, d, 2xCH$_3$-(*Ar*)C-C<u>*H*</u>-CH-C, $^3J_{H,H}$ = 5.7 Hz), 4.93 (2H, d, 2xCH$_3$-(*Ar*)C-CH-C<u>*H*</u>-C, $^3J_{H,H}$ = 5.6 Hz), 4.63 (2H, d, 2xCH$_3$-(*Ar*)C-C<u>*H*</u>-CH-C, $^3J_{H,H}$ = 5.7 Hz), 3.61 (2H, s, C<u>*H*</u>$_2$-(*Ar*)C-CH-CH-C-C(CH$_3$)$_3$), 3.44 (2H, s, C<u>*H*</u>$_2$-(*Ar*)C-CH-CH-C-C(CH$_3$)$_3$), 2.57 (2H, t, (C=O)-C<u>*H*</u>$_2$-CH$_2$, $^3J_{H,H}$ = 7.5 Hz), 1.89 (2H, sept, 2x(*Ar*)C-CH-CH-C-C<u>*H*</u>(CH$_3$)$_2$, $^3J_{H,H}$ = 6.8 Hz), 1.77 (6H, s, 2xC<u>*H*</u>$_3$-(*Ar*)C-CH-CH-C), 1.71-1-84 (2H, m., (C=O)-CH$_2$-C<u>*H*</u>$_2$-CH$_2$, ^{3}J$_{H,H}$ = 7.7 Hz), 1.36 (9H, s, S-CH$_2$-(*Ar*)C-CH-CH-C-C(C<u>*H*</u>$_3$)$_3$), 1.33 (9H, s, S-CH$_2$-(*Ar*)C-CH-CH-C-C(C<u>*H*</u>$_3$)$_3$), 1.20-1.46 (12H, m, (C=O)-(CH$_2$)$_2$-C<u>*H*</u>$_2$, (C=O)-(CH$_2$)$_3$-C<u>*H*</u>$_2$, (C=O)-(CH$_2$)$_4$-C<u>*H*</u>$_2$, (C=O)-(CH$_2$)$_5$-C<u>*H*</u>$_2$, (C=O)-(CH$_2$)$_6$-C<u>*H*</u>$_2$, (C=O)-(CH$_2$)$_7$-C<u>*H*</u>$_2$,), 0.94 (6H, d, (*Ar*)C-CH-CH-C-CH(C<u>*H*</u>$_3$)$_2$, $^3J_{H,H}$ = 6.8 Hz), 0.89 (6H, d, (*Ar*)C-CH-CH-C-CH(C<u>*H*</u>$_3$)$_2$, $^3J_{H,H}$ = 6.8 Hz), 0.88 (3H, t, CH$_2$-C<u>*H*</u>$_3$, $^3J_{H,H}$ = 6.9 Hz).

^{13}C-NMR (CDCl$_3$) δ$_C$, ppm: 172.2 (1C, (*Ar*)C-O-(<u>*C*</u>=O)-CH$_2$), 151.9, 151.7 (2C, 2xS-CH$_2$-(*Ar*)C-CH-CH-<u>*C*</u>-C(CH$_3$)$_3$), 151.2 (1C, S-(*Ar*)C-CH-CH-<u>*C*</u>-O-(C=O)-CH$_2$), 136.83, 136.80 (2C, 2xS-CH$_2$-(*Ar*)<u>*C*</u>-CH-CH-C-C(CH$_3$)$_3$), 135.1 (1C, S-(*Ar*)<u>*C*</u>-CH-CH-C-O-(C=O)-CH$_2$), 133.7 (2C, 2xS-(*Ar*)C-CH-<u>*C*</u>H-C-O-(C=O)-CH$_2$), 129.4, 129.2 (2C, 2xS-CH$_2$-(*Ar*)C-<u>*C*</u>H-CH-C-C(CH$_3$)$_3$), 125.7, 125.5 (2C, 2xS-CH$_2$-(*Ar*)C-CH-<u>*C*</u>H-C-C(CH$_3$)$_3$), 122.5 (2C, 2xS-(*Ar*)C-<u>*C*</u>H-CH-C-O-(C=O)-CH$_2$), 107.2 (2C, 2xCH$_3$-(*Ar*)C-CH-CH-<u>*C*</u>), 100.7 (2C, 2xCH$_3$-(*Ar*)<u>*C*</u>-CH-CH-C), 84.3 (2C, 2xCH$_3$-(*Ar*)C-CH-<u>*C*</u>H-C), 83.8 (4C, 2xCH$_3$-(*Ar*)C-<u>*C*</u>H-CH-C, 2xCH$_3$-(*Ar*)C-CH-<u>*C*</u>H-C), 82.7 (2C, 2xCH$_3$-(*Ar*)C-<u>*C*</u>H-CH-C), 40.2 (1C, S-<u>*C*</u>H$_2$-(*Ar*)C-CH-CH-C-C(CH$_3$)$_3$), 39.7 (1C, S-<u>*C*</u>H$_2$-(*Ar*)C-CH-CH-

C-C(CH_3)$_3$), 34.92 (1C, S-CH_2-(*Ar*)C-CH-CH-C-<u>C</u>(CH_3)$_3$), 34.87 (1C, S-CH_2-(*Ar*)C-CH-CH-C-<u>C</u>(CH_3)$_3$), 34.5 (1C, (C=O)-<u>C</u>H_2), 32.0 (1C, (C=O)-(CH_2)$_2$-<u>C</u>H_2), 31.57 (3C, S-CH_2-(*Ar*)C-CH-CH-C-C(<u>C</u>H_3)$_3$),31.54 (3C, S-CH_2-(*Ar*)C-CH-CH-C-C(<u>C</u>H_3)$_3$), 31.0 (2C, 2x(*Ar*)CH-CH-C-<u>C</u>H(CH_3)$_2$), 29.2-29.5 (8C, (C=O)-(CH_2)$_3$-<u>C</u>H_2, (C=O)-(CH_2)$_4$-<u>C</u>H, (C=O)-(CH_2)$_5$-<u>C</u>H_2, (C=O)-(CH_2)$_6$-<u>C</u>H_2), 25.0 (1C, (C=O)-CH_2-<u>C</u>H_2), 23.2 (2C, (*Ar*)CH-CH-C-CH(<u>C</u>H_3)$_2$), 22.8 (1C, <u>C</u>H_2-CH_3), 22.7 (2C, (*Ar*)CH-CH-C-CH(<u>C</u>H_3)$_2$), 18.3 (2C, 2x<u>C</u>H_3-(*Ar*)C-CH-CH), 14.2 (1C, CH_2-<u>C</u>H_3).
***R*$_f$** (CH_2Cl_2/CH_3OH 10:1 (v/v)) = 0.380.
ESI-MS(+): *m/z* found 1109.3482 [M-Cl]$^+$, calcd. for $C_{58}H_{81}O_2Ru_2S_3^+$ 1109.3480.
Elemental analysis (%): calcd. for $C_{58}H_{81}ClO_2Ru_2S_3 \cdot 1.15H_2O$ C 59.81, H 7.21; found C 59.81, H 7.22.

Synthesis of [(η^6-*p*-$MeC_6H_4Pr^i$)$_2$$Ru_2$($\mu_2$-$SCH_2C_6H_4$-*p*-$Bu^t$)$_2$($\mu_2$-$SC_6H_4$-*p*-O(CO)R)]Cl (R = tridecyl), 2.2.14a
Myristic acid (0.055 g, 0.242 mmol, 1.2 equiv.), EDCI (0.077 g, 0.404 mmol, 2 equiv.), **2.2.2** (0.200 g, 0.202 mmol, 1 equiv.) and DMAP (0.012 g, 0.101 mmol, 0.5 equiv.); isolated product **2.2.14a** (0.188 g, 0.157 mmol, yield 78%).
^{1}H-NMR ($CDCl_3$) δ_H, ppm: 7.79 (2H, d, 2xS-(*Ar*)C-CH-C<u>H</u>-C-O-(C=O)-CH_2, $^3J_{H,H}$ = 8.5 Hz), 7.47 (4H, s, 4xCH_2-(*Ar*)C-C<u>H</u>-CH-C-C(CH_3)$_3$), 7.41 (4H, s, 4xCH_2-(*Ar*)C-CH-C<u>H</u>-C-C(CH_3)$_3$), 7.04 (2H, d, 2xS-(*Ar*)C-CH-C<u>H</u>-C-O-(C=O)-CH_2, $^3J_{H,H}$ = 8.5 Hz), 5.14 (2H, d, 2xCH_3-(*Ar*)C-CH-C<u>H</u>-C, $^3J_{H,H}$ = 5.7 Hz), 5.02 (2H, d, 2xCH_3-(*Ar*)C-C<u>H</u>-CH-C, $^3J_{H,H}$ = 5.8 Hz), 4.93 (2H, d, 2xCH_3-(*Ar*)C-CH-C<u>H</u>-C, $^3J_{H,H}$ = 5.7 Hz), 4.63 (2H, d, 2xCH_3-(*Ar*)C-C<u>H</u>-CH-C, $^3J_{H,H}$ = 5.8 Hz), 3.62 (2H, s, C<u>H$_2$</u>-(*Ar*)C-CH-CH-C-C(CH_3)$_3$), 3.45 (2H, s, C<u>H$_2$</u>-(*Ar*)C-CH-CH-C-C(CH_3)$_3$), 2.57 (2H, t, (C=O)-C<u>H$_2$</u>-CH_2, $^3J_{H,H}$ = 7.4 Hz), 1.89 (2H, sept, 2x(*Ar*)C-CH-CH-C-C<u>H</u>(CH_3)$_2$, $^3J_{H,H}$ = 6.9 Hz), 1.77 (6H, s, 2xC<u>H$_3$</u>-(*Ar*)C-CH-CH-C), 1.66-1.80 (2H, m, (C=O)-CH_2-C<u>H$_2$</u>-CH_2), 1.36 (9H, s, S-CH_2-(*Ar*)C-CH-CH-C-C(C<u>H$_3$</u>)$_3$), 1.33 (9H, s, S-CH_2-(*Ar*)C-CH-CH-C-C(C<u>H$_3$</u>)$_3$), 1.21-1.45 (26H, m, (C=O)-(CH_2)$_2$-C<u>H$_2$</u>, (C=O)-(CH_2)$_3$-C<u>H$_2$</u>, (C=O)-(CH_2)$_4$-C<u>H$_2$</u>, (C=O)-(CH_2)$_5$-C<u>H$_2$</u>, (C=O)-(CH_2)$_6$-C<u>H$_2$</u>, (C=O)-(CH_2)$_7$-C<u>H$_2$</u>, (C=O)-(CH_2)$_8$-C<u>H$_2$</u>, (C=O)-(CH_2)$_9$-C<u>H$_2$</u>, (C=O)-(CH_2)$_{10}$-C<u>H$_2$</u>, (C=O)-(CH_2)$_{11}$-C<u>H$_2$</u>), 0.94 (6H, d, (*Ar*)C-CH-CH-C-CH(C<u>H$_3$</u>)$_2$, $^3J_{H,H}$ = 6.8 Hz), 0.89 (6H, d, (*Ar*)C-CH-CH-C-CH(C<u>H$_3$</u>)$_2$, $^3J_{H,H}$ = 6.9 Hz), 0.88 (3H, t, CH_2-C<u>H$_3$</u>, $^3J_{H,H}$ = 7.0 Hz).
^{13}C-NMR ($CDCl_3$) δ_C, ppm: 172.1 (1C, (*Ar*)C-O-(<u>C</u>=O)-CH_2), 151.9, 151.7 (2C, 2xS-CH_2-(*Ar*)C-CH-CH-<u>C</u>-C(CH_3)$_3$), 151.2 (1C, S-(*Ar*)C-CH-CH-<u>C</u>-O-(C=O)-CH_2), 136.75, 136.73 (2C, 2xS-CH_2-(*Ar*)<u>C</u>-CH-CH-C-C(CH_3)$_3$), 135.0 (1C, S-(*Ar*)<u>C</u>-CH-CH-C-O-(C=O)-CH_2), 133.6 (2C, 2xS-(*Ar*)C-CH-<u>C</u>H-C-O-(C=O)-CH_2), 129.4, 129.2 (2C, 2xS-CH_2-(*Ar*)C-<u>C</u>H-CH-C-C(CH_3)$_3$), 125.7, 125.5 (2C, 2xS-CH_2-(*Ar*)C-CH-<u>C</u>H-C-C(CH_3)$_3$), 122.4 (2C, 2xS-(*Ar*)C-<u>C</u>H-CH-C-O-(C=O)-CH_2), 107.2 (2C, 2xCH_3-(*Ar*)C-CH-CH-<u>C</u>), 100.7 (2C, 2xCH_3-(*Ar*)<u>C</u>-CH-CH-C), 84.3 (2C, 2xCH_3-(*Ar*)C-CH-<u>C</u>H-C), 83.7 (4C, 2xCH_3-(*Ar*)C-<u>C</u>H-CH-C, 2xCH_3-(*Ar*)C-CH-<u>C</u>H-C), 2.6 (2C, 2xCH_3-(*Ar*)C-<u>C</u>H-CH-C), 40.1 (1C, S-<u>C</u>H_2-(*Ar*)C-CH-CH-C-C(CH_3)$_3$), 39.7 (1C, S-<u>C</u>H_2-(*Ar*)C-CH-CH-C-C(CH_3)$_3$), 34.89 (1C, S-CH_2-(*Ar*)C-CH-CH-C-<u>C</u>(CH_3)$_3$), 34.84 (1C, S-CH_2-(*Ar*)C-CH-CH-C-<u>C</u>(CH_3)$_3$), 34.5 (1C, (C=O)-<u>C</u>H_2), 32.0 (1C, <u>C</u>H_2-CH_2-CH_3), 31.53 (3C, S-CH_2-(*Ar*)C-CH-CH-C-C(<u>C</u>H_3)$_3$), 31.51 (3C, S-CH_2-(*Ar*)C-CH-CH-C-C(<u>C</u>H_3)$_3$), 30.9 (2C, 2x(*Ar*)CH-CH-C-<u>C</u>H(CH_3)$_2$), 27.7-29.8 (8C, (C=O)-(CH_2)$_5$-<u>C</u>H_2, (C=O)-(CH_2)$_6$-<u>C</u>H, (C=O)-(CH_2)$_7$-<u>C</u>H_2, (C=O)-(CH_2)$_8$-<u>C</u>H_2, (C=O)-(CH_2)$_9$-<u>C</u>H_2, (C=O)-(CH_2)$_{10}$-<u>C</u>H_2, (C=O)-(CH_2)$_{11}$-<u>C</u>H_2, (C=O)-(CH_2)$_{12}$-<u>C</u>H_2), 29.6 (1C, (C=O)-(CH_2)$_4$-<u>C</u>H_2), 29.5 (1C, (C=O)-(CH_2)$_{13}$-<u>C</u>H_2), 29.4 (1C, (C=O)-(CH_2)$_3$-<u>C</u>H_2), 29.3 (1C, (C=O)-(CH_2)$_2$-<u>C</u>H_2), 24.9 (1C, (C=O)-CH_2-<u>C</u>H_2), 23.2 (2C, (*Ar*)CH-CH-C-CH(<u>C</u>H_3)$_2$), 22.8 (1C, <u>C</u>H_2-CH_3), 22.7 (2C, (*Ar*)CH-CH-C-CH(<u>C</u>H_3)$_2$), 18.3 (2C, 2x<u>C</u>H_3-(*Ar*)C-CH-CH), 14.2 (1C, CH_2-<u>C</u>H_3).
***R*$_f$** (CH_2Cl_2/CH_3OH 10:1 (v/v)) = 0.400.
ESI-MS(+): *m/z* found 1165.4112 [M-Cl]$^+$, calcd. for $C_{62}H_{89}O_2Ru_2S_3^+$ 1165.4106.

Elemental analysis (%): calcd. for $C_{62}H_{89}ClO_2Ru_2S_3 \cdot H_2O$ C 61.13, H 7.53; found C 61.12, H 7.53.

Synthesis of the amide conjugates 2.2.9b and 2.2.11b-2.2.20b

Synthesis of [(η^6-*p*-MeC$_6$H$_4$Pr^i)$_2$Ru$_2$(μ_2-SCH$_2$C$_6$H$_4$-*p*-Bu^t)$_2$(μ_2-SC$_6$H$_4$-*p*-NH(CO)R)]Cl (R = (*R*)-4-(1,2-dithiolan-3-yl)butan-1-yl), 2.2.9b

α-Lipoic acid (0.096 g, 0.455 mmol, 1.5 equiv.), HOBt·H$_2$O (0.098 g, 0.727 mmol, 2.4 equiv.), DIPEA (0.196 g, 1.515 mmol, 5 equiv.), EDCI (0.196 g, 1.022 mmol, 3.37 equiv.), and **2.2.3** (0.300 g, 0.303 mmol, 1 equiv.); isolated product **2.2.9b** (0.326 g, 0.277 mmol, yield 91%).

^{1}H-NMR (CDCl$_3$) δ_H, ppm: 8.15 (2H, d, 2xS-(*Ar*)C-C*H*-CH-C-NH-(C=O)-CH$_2$, $^3J_{H,H}$ = 8.7 Hz), 7.56 (2H, d, 2xS-(*Ar*)C-CH-C*H*-C-NH-(C=O)-CH$_2$, $^3J_{H,H}$ = 8.7 Hz), 7.38-7.49 (8H, m, 4xCH$_2$-(*Ar*)C-C*H*-CH-C-C(CH$_3$)$_3$, 4xCH$_2$-(*Ar*)C-CH-C*H*-C-C(CH$_3$)$_3$), 4.97 (2H, d, 2xCH$_3$-(*Ar*)C-CH-C*H*-C, $^3J_{H,H}$ = 5.7 Hz), 4.87 (2H, d, 2xCH$_3$-(*Ar*)C-C*H*-CH-C, $^3J_{H,H}$ = 5.8 Hz), 4.68 (2H, d, 2xCH$_3$-(*Ar*)C-CH-C*H*-C, $^3J_{H,H}$ = 5.8 Hz), 4.60 (2H, d, 2xCH$_3$-(*Ar*)C-C*H*-CH-C, $^3J_{H,H}$ = 5.8 Hz), 3.57-3.64 (1H, sept, (C=O)-(CH$_2$)$_4$-C*H*, $^3J_{H,H}$ = 6.6 Hz), 3.54 (2H, s, C*H$_2$*-(*Ar*)C-CH-CH-C-C(CH$_3$)$_3$), 3.35 (2H, s, C*H$_2$*-(*Ar*)C-CH-CH-C-C(CH$_3$)$_3$), 3.06-3.20 (2H, m, (C=O)-(CH$_2$)$_4$-CH-CH$_2$-C*H$_2$*), 2.73 (2H, t, (C=O)-C*H$_2$*-CH$_2$, $^3J_{H,H}$ = 7.3 Hz), 2.44-2.52 (1H, sext, (C=O)-(CH$_2$)$_4$-CH-C*H$_2$*-CH$_2$, $^3J_{H,H}$ = 6.4 Hz), 1.90-2.05 (3H, m, 2x(*Ar*)C-CH-CH-C-C*H*(CH$_3$)$_2$, $^3J_{H,H}$ = 6.9 Hz, (C=O)-(CH$_2$)$_4$-CH-C*H$_2$*-CH$_2$, $^3J_{H,H}$ = 6.9 Hz), 1.69-1.87 (5H, m, (C=O)-CH$_2$-C*H$_2$*-CH$_2$-CH$_2$-CH, (C=O)-CH$_2$-CH$_2$-CH$_2$-C*H$_2$*-CH), 1.66 (6H, s, 2xC*H$_3$*-(*Ar*)C-CH-CH-C), 1.50-1.60 (2H, m, (C=O)-CH$_2$-CH$_2$-C*H$_2$*-CH$_2$-CH), 1.36 (9H, s, S-CH$_2$-(*Ar*)C-CH-CH-C-C(C*H$_3$*)$_3$), 1.34 (9H, s, S-CH$_2$-(*Ar*)C-CH-CH-C-C(C*H$_3$*)$_3$), 0.99 (6H, d, (*Ar*)C-CH-CH-C-CH(C*H$_3$*)$_2$, $^3J_{H,H}$ = 6.9 Hz), 0.94 (6H, d, (*Ar*)C-CH-CH-C-CH(C*H$_3$*)$_2$, $^3J_{H,H}$ = 6.9 Hz).

^{13}C-NMR (CDCl$_3$) δ_C, ppm: 173.9 (1C, (*Ar*)C-NH-(*C*=O)-CH$_2$), 152.00, 151.98 (2C, 2xS-CH$_2$-(*Ar*)C-CH-CH-*C*-C(CH$_3$)$_3$), 141.7 (1C, S-(*Ar*)C-CH-CH-*C*-NH-(C=O)-CH$_2$), 136.84, 136.52 (2C, 2xS-CH$_2$-(*Ar*)*C*-CH-CH-C-C(CH$_3$)$_3$), 135.2 (1C, S-(*Ar*)*C*-CH-CH-C-O-(C=O)-CH$_2$), 132.6 (2C, 2xS-(*Ar*)C-*C*H-CH-C-NH-(C=O)-CH$_2$), 129.3, 129.0 (2C, 2xS-CH$_2$-(*Ar*)C-*C*H-CH-C-C(CH$_3$)$_3$), 125.70, 125.65 (2C, 2xS-CH$_2$-(*Ar*)C-CH-*C*H-C-C(CH$_3$)$_3$), 120.4 (2C, 2xS-(*Ar*)C-CH-*C*H-C-NH-(C=O)-CH$_2$), 107.8 (2C, 2xCH$_3$-(*Ar*)C-CH-CH-*C*), 100.1 (2C, 2xCH$_3$-(*Ar*)*C*-CH-CH-C), 84.3 (2C, 2xCH$_3$-(*Ar*)C-CH-*C*H-C), 83.8 (2C, 2xCH$_3$-(*Ar*)C-*C*H-CH-C), 83.2 (2C, 2xCH$_3$-(*Ar*)C-CH-*C*H-C), 82.2 (2C, 2xCH$_3$-(*Ar*)C-*C*H-CH-C), 56.7 (1C, (C=O)-(CH$_2$)$_4$-*C*H), 40.3 (1C, CH-*C*H$_2$-CH$_2$), 39.9 (1C, S-*C*H$_2$-(*Ar*)C-CH-CH-C-C(CH$_3$)$_3$), 39.2 (1C, S-*C*H$_2$-(*Ar*)C-CH-CH-C-C(CH$_3$)$_3$), 38.6 (1C, CH-CH$_2$-*C*H$_2$), 37.1 (1C, (C=O)-*C*H$_2$), 34.94 (1C, S-CH$_2$-(*Ar*)C-CH-CH-C-*C*(CH$_3$)$_3$), 34.91 (1C, S-CH$_2$-(*Ar*)C-CH-CH-C-*C*(CH$_3$)$_3$), 34.8 (1C, (C=O)-CH$_2$-*C*H$_2$), 31.55 (3C, S-CH$_2$-(*Ar*)C-CH-CH-C-C(*C*H$_3$)$_3$), 31.54 (3C, S-CH$_2$-(*Ar*)C-CH-CH-C-C(*C*H$_3$)$_3$), 31.1 (2C, 2x(*Ar*)CH-CH-C-*C*H(CH$_3$)$_2$), 28.9 (1C, (C=O)-(CH$_2$)$_3$-*C*H$_2$), 25.5 (1C, (C=O)-(CH$_2$)$_2$-*C*H$_2$), 23.1 (1C, (*Ar*)CH-CH-C-CH(*C*H$_3$)$_2$), 23.0 (1C, (*Ar*)CH-CH-C-CH(*C*H$_3$)$_2$), 18.1 (2C, 2x*C*H$_3$-(*Ar*)C-CH-CH).

***R*$_f$** (CH$_2$Cl$_2$/CH$_3$OH 10:1 (v/v)) = 0.439.

ESI-MS(+): *m/z* found 1142.2512 [M-Cl]$^+$, calcd. for $C_{56}H_{76}NORu_2S_5^+$ 1142.2612.

Elemental analysis (%): calcd. for $C_{56}H_{75}ClNORu_2S_5 \cdot H_2O$ C 56.28, H 6.58, N 1.17; found C 56.29, H 6.50, N 1.15.

Synthesis of [(η^6-*p*-MeC$_6$H$_4$Pr^i)$_2$Ru$_2$(μ_2-SCH$_2$C$_6$H$_4$-*p*-Bu^t)$_2$(μ_2-SC$_6$H$_4$-*p*-NH(CO)R)]Cl (R = propyl), 2.2.11b

Butyric acid (0.027 g, 0.303 mmol, 1.5 equiv.), HOBt·H$_2$O (0.067 g, 0.485 mmol, 2.4 equiv.), DIPEA (0.131 g, 1.010 mmol, 5 equiv.), EDCI (0.116 g, 0.606 mmol, 3 equiv.), and **2.2.3** (0.200 g, 0.202 mmol, 1 equiv.); isolated product **2.2.11b** (0.103 g, 0.097 mmol, yield 48%).

^{1}H-NMR ($CDCl_3$) δ_H, ppm: 11.06 (1H, (*Ar*)C-N*H*-(C=O)), 8.14 (2H, d, 2xS-(*Ar*)C-CH-C*H*-C-NH-(C=O)-CH_2, $^3J_{H,H}$ = 8.7 Hz), 7.56 (2H, d, 2xS-(*Ar*)C-C*H*-CH-C-NH-(C=O)-CH_2, $^3J_{H,H}$ = 8.7 Hz), 7.39-7.49 (8H, m, 4xCH_2-(*Ar*)C-C*H*-CH-C-$C(CH_3)_3$, 4xCH_2-(*Ar*)C-CH-C*H*-C-$C(CH_3)_3$), 4.98 (2H, d, 2xCH_3-(*Ar*)C-CH-C*H*-C, $^3J_{H,H}$ = 5.8 Hz), 4.87 (2H, d, 2xCH_3-(*Ar*)C-C*H*-CH-C, $^3J_{H,H}$ = 5.8 Hz), 4.69 (2H, d, 2xCH_3-(*Ar*)C-CH-C*H*-C, $^3J_{H,H}$ = 5.8 Hz), 4.60 (2H, d, 2xCH_3-(*Ar*)C-C*H*-CH-C, $^3J_{H,H}$ = 5.8 Hz), 3.55 (2H, s, C*H*$_2$-(*Ar*)C-CH-CH-C-$C(CH_3)_3$), 3.36 (2H, s, C*H*$_2$-(*Ar*)C-CH-CH-C-$C(CH_3)_3$), 2.69 (2H, t, (C=O)-C*H*$_2$-CH_2, $^3J_{H,H}$ = 7.4 Hz), 2.00 (2H, sept, 2x(*Ar*)C-CH-CH-C-C*H*$(CH_3)_2$, $^3J_{H,H}$ = 7.0 Hz), 1.78 (2H, sext, (C=O)-CH_2-C*H*$_2$-CH_2, $^3J_{H,H}$ = 7.4 Hz), 1.66 (6H, s, 2xC*H*$_3$-(*Ar*)C-CH-CH-C), 1.37 (9H, s, S-CH_2-(*Ar*)C-CH-CH-C-C(C*H*$_3$)$_3$), 1.35 (9H, s, S-CH_2-(*Ar*)C-CH-CH-C-C(C*H*$_3$)$_3$), 1.02 (3H, t, CH_2-C*H*$_3$, $^3J_{H,H}$ = 7.4 Hz), 0.99 (6H, d, (*Ar*)C-CH-CH-C-CH(C*H*$_3$)$_2$, $^3J_{H,H}$ = 6.9 Hz), 0.94 (6H, d, (*Ar*)C-CH-CH-C-CH(C*H*$_3$)$_2$, $^3J_{H,H}$ = 6.9 Hz).

^{13}C-NMR ($CDCl_3$) δ_C, ppm: 174.2 (1C, (*Ar*)C-NH-(*C*=O)-CH_2), 152.01, 151.99 (2C, 2xS-CH_2-(*Ar*)C-CH-CH-*C*-$C(CH_3)_3$), 141.7 (1C, S-(*Ar*)C-CH-CH-*C*-NH-(C=O)-CH_2), 136.9, 136.5 (2C, 2xS-CH_2-(*Ar*)*C*-CH-CH-C-$C(CH_3)_3$), 132.7 (2C, 2xS-(*Ar*)C-*C*H-CH-C-NH-(C=O)-CH_2), 129.3 (1C, S-(*Ar*)*C*-CH-CH-C-NH-(C=O)-CH_2), 129.1, 129.0 (2C, 2xS-CH_2-(*Ar*)C-*C*H-CH-C-$C(CH_3)_3$), 125.71, 125.66 (2C, 2xS-CH_2-(*Ar*)C-CH-*C*H-C-$C(CH_3)_3$), 120.5 (2C, 2xS-(*Ar*)C-CH-*C*H-C-NH-(C=O)-CH_2), 107.8 (2C, 2xCH_3-(*Ar*)C-CH-CH-*C*), 100.2 (2C, 2xCH_3-(*Ar*)*C*-CH-CH-C), 84.3 (2C, 2xCH_3-(*Ar*)C-CH-*C*H-C), 83.8 (4C, 2xCH_3-(*Ar*)C-*C*H-CH-C), 83.2 (2C, 2xCH_3-(*Ar*)C-CH-*C*H-C), 82.2 (2C, 2xCH_3-(*Ar*)C-*C*H-CH-C), 39.9 (1C, S-*C*H_2-(*Ar*)C-CH-CH-C-C$(CH_3)_3$), 39.3 (1C, (C=O)-*C*H_2), 39.2 (1C, S-*C*H_2-(*Ar*)C-CH-CH-C-C$(CH_3)_3$), 34.94 (1C, S-CH_2-(*Ar*)C-CH-CH-C-*C*$(CH_3)_3$), 34.92 (1C, S-CH_2-(*Ar*)C-CH-CH-C-*C*$(CH_3)_3$), 31.57 (3C, S-CH_2-(*Ar*)C-CH-CH-C-C(*C*$H_3)_3$), 31.55 (3C, S-CH_2-(*Ar*)C-CH-CH-C-C(*C*$H_3)_3$), 31.1 (2C, 2x(*Ar*)CH-CH-C-*C*H$(CH_3)_2$), 23.1 (2C, (*Ar*)CH-CH-C-CH(*C*$H_3)_2$), 23.0 (2C, (*Ar*)CH-CH-C-CH(*C*$H_3)_2$), 19.2 (1C, *C*H_2-CH_3), 18.1 (2C, 2x*C*H_3-(*Ar*)C-CH-CH), 14.0 (1C, CH_2-*C*H_3).

R_f (CH_2Cl_2/CH_3OH 10:1 (v/v)) = 0.255.

ESI-MS(+): *m/z* found 1024.2682 $[M-Cl]^+$, calcd. for $C_{52}H_{70}NORu_2S_3^+$ 1024.2701.

Elemental analysis (%): calcd. for $C_{52}H_{70}ClNORu_2S_3$ C 58.98, H 6.66, N 1.32; found C 61.44, H 7.47, N 1.19.

Synthesis of [(η^6-*p*-$MeC_6H_4Pr^i$)$_2$$Ru_2$($\mu_2$-$SCH_2C_6H_4$-*p*-$Bu^t$)$_2$($\mu_2$-$SC_6H_4$-*p*-NH(CO)R)]Cl (R = pentyl), 2.2.12b

Hexanoic acid (0.036 g, 0.303 mmol, 1.5 equiv.), HOBt·H_2O (0.67 g, 0.485 mmol, 2.4 equiv.), DIPEA (0.131 g, 1.010 mmol, 5 equiv.), EDCI (0.116 g, 0.606 mmol, 3 equiv.), and **2.2.3** (0.200 g, 0.202 mmol, 1 equiv.); isolated product **2.2.12b** (0.109 g, 0.100 mmol, yield 50%).

^{1}H-NMR ($CDCl_3$) δ_H, ppm: 11.12 (1H, s, (*Ar*)C-N*H*-(C=O)), 8.15 (2H, d, 2xS-(*Ar*)C-CH-C*H*-C-NH-(C=O)-CH_2, $^3J_{H,H}$ = 8.2 Hz), 7.04 (2H, d, 2xS-(*Ar*)C-C*H*-CH-C-NH-(C=O)-CH_2, $^3J_{H,H}$ = 8.7 Hz), 7.38-7.48 (8H, m, 4xCH_2-(*Ar*)C-C*H*-CH-C-$C(CH_3)_3$, 4xCH_2-(*Ar*)C-CH-C*H*-C-$C(CH_3)_3$),4.97 (2H, d, 2xCH_3-(*Ar*)C-CH-C*H*-C, $^3J_{H,H}$ = 5.8 Hz), 4.87 (2H, d, 2xCH_3-(*Ar*)C-C*H*-CH-C, $^3J_{H,H}$ = 5.8 Hz), 4.69 (2H, d, 2xCH_3-(*Ar*)C-CH-C*H*-C, $^3J_{H,H}$ = 5.8 Hz), 4.60 (2H, d, 2xCH_3-(*Ar*)C-C*H*-CH-C, $^3J_{H,H}$ = 5.8 Hz), 3.54 (2H, s, C*H*$_2$-(*Ar*)C-CH-CH-C-$C(CH_3)_3$), 3.35 (2H, s, C*H*$_2$-(*Ar*)C-CH-CH-C-$C(CH_3)_3$), 2.70 (2H, t, (C=O)-C*H*$_2$-CH_2, $^3J_{H,H}$ = 7.5 Hz), 1.99 (2H, sept, 2x(*Ar*)C-CH-CH-C-C*H*$(CH_3)_2$, $^3J_{H,H}$ = 6.9 Hz), 1.74 (2H, pent., (C=O)-CH_2-C*H*$_2$-CH_2), 1.66 (6H, s, 2xC*H*$_3$-(*Ar*)C-CH-CH-C), 1.30-1.43 (4H, m, (C=O)-$(CH_2)_2$-C*H*$_2$, (C=O)-$(CH_2)_3$-C*H*$_2$), 1.36 (9H, s, S-CH_2-(*Ar*)C-CH-CH-C-C(C*H*$_3$)$_3$), 1.34 (9H, s, S-CH_2-(*Ar*)C-CH-CH-C-C(C*H*$_3$)$_3$), 0.98 (6H, d, (*Ar*)C-CH-CH-C-CH(C*H*$_3$)$_2$, $^3J_{H,H}$ = 6.8 Hz), 0.93 (6H, d, (*Ar*)C-CH-CH-C-CH(C*H*$_3$)$_2$, $^3J_{H,H}$ = 6.9 Hz), 0.87 (3H, t, CH_2-C*H*$_3$, $^3J_{H,H}$ = 7.0 Hz).

^{13}C-NMR ($CDCl_3$) δ_C, ppm: 174.3 (1C, (*Ar*)C-NH-(*C*=O)-CH_2), 151.98, 151.94 (2C, 2xS-CH_2-(*Ar*)C-CH-CH-*C*-$C(CH_3)_3$), 141.7 (1C, S-(*Ar*)C-CH-CH-*C*-NH-(C=O)-CH_2), 136.8, 136.5 (2C,

2xS-CH_2-(*Ar*)<u>*C*</u>-CH-CH-C-C(CH_3)$_3$), 132.6 (2C, 2xS-(*Ar*)C-<u>*C*</u>H-CH-C-NH-(C=O)-CH_2), 129.3, 129.04 (2C, 2xS-CH_2-(*Ar*)C-<u>*C*</u>H-CH-C-C(CH_3)$_3$), 129.00 (1C, S-(*Ar*)<u>*C*</u>-CH-CH-C-NH-(C=O)-CH_2), 125.7, 125.6 (2C, 2xS-CH_2-(*Ar*)C-CH-<u>*C*</u>H-C-C(CH_3)$_3$), 120.4 (2C, 2xS-(*Ar*)C-CH-<u>*C*</u>H-C-NH-(C=O)-CH_2), 107.7 (2C, 2xCH_3-(*Ar*)C-CH-CH-<u>*C*</u>), 100.1 (2C, 2xCH_3-(*Ar*)<u>*C*</u>-CH-CH-C), 84.3 (2C, 2xCH_3-(*Ar*)C-CH-<u>*C*</u>H-C), 83.8 (2C, 2xCH_3-(*Ar*)C-<u>*C*</u>H-CH-C), 83.2 (2C, 2xCH_3-(*Ar*)C-CH-<u>*C*</u>H-C), 82.2 (2C, 2xCH_3-(*Ar*)C-<u>*C*</u>H-CH-C), 39.9 (1C, S-<u>*C*</u>H_2-(*Ar*)C-CH-CH-C-C(CH_3)$_3$), 39.2 (1C, S-<u>*C*</u>H_2-(*Ar*)C-CH-CH-C-C(CH_3)$_3$), 37.4 (1C, (C=O)-<u>*C*</u>H_2), 34.91 (1C, S-CH_2-(*Ar*)C-CH-CH-C-<u>*C*</u>(CH_3)$_3$), 34.89 (1C, S-CH_2-(*Ar*)C-CH-CH-C-<u>*C*</u>(CH_3)$_3$), 31.6 (1C, <u>*C*</u>H_2-CH_2-CH_3), 31.53 (3C, S-CH_2-(*Ar*)C-CH-CH-C-C(<u>*C*</u>H_3)$_3$), 31.52 (3C, S-CH_2-(*Ar*)C-CH-CH-C-C(<u>*C*</u>H_3)<u>$_3$</u>), 31.1 (2C, 2x(*Ar*)CH-CH-C-<u>*C*</u>H(CH_3)$_2$), 25.5 (1C, (C=O)-CH_2-<u>*C*</u>H_2), 23.1 (2C, (*Ar*)CH-CH-C-CH(<u>*C*</u>H_3)<u>$_2$</u>), 23.0 (2C, (*Ar*)CH-CH-C-CH(<u>*C*</u>H_3)<u>$_2$</u>), 22.8 (1C, <u>*C*</u>H_2-CH_3), 18.1 (2C, 2x<u>*C*</u>H_3-(*Ar*)C-CH-CH), 14.2 (1C, CH_2-<u>*C*</u>H_3).

***R*$_f$** (CH_2Cl_2/CH_3OH 10:1 (v/v)) = 0.234.

ESI-MS(+): *m/z* found 1052.3014 $[M-Cl]^+$, calcd. for $C_{54}H_{74}NORu_2S_3^+$ 1052.3014.

Elemental analysis (%): calcd. for $C_{54}H_{74}ClNORu_2S_3 \cdot 0.5CH_3OH$ C 59.35, H 6.95, N 1.28; found C 59.40, H 7.06, N 1.28.

Synthesis of [(η^6-*p*-$MeC_6H_4Pr^i$)$_2$Ru$_2$(μ_2-$SCH_2C_6H_4$-*p*-Bu^t)$_2$(μ_2-SC_6H_4-*p*-NH(CO)R)]Cl (R = nonyl), 2.2.13b

Decanoic acid (0.053 g, 0.303 mmol, 1.5 equiv.), HOBt·H_2O (0.067 g, 0.485 mmol, 2.4 equiv.), DIPEA (0.131 g, 1.010 mmol, 5 equiv.), EDCI (0.116 g, 0.606 mmol, 3 equiv.), and **2.2.3** (0.200 g, 0.202 mmol, 1 equiv.); isolated product **2.2.13b** (0.205 g, 0.179 mmol, yield 89%).

^{1}H-NMR ($CDCl_3$) δ_H, ppm: 11.11 (1H, s, N<u>*H*</u>-(C=O)), 8.15 (2H, d, 2xS-(*Ar*)C-CH-C<u>*H*</u>-C-NH-(C=O)-CH_2, $^3J_{H,H}$ = 8.3 Hz), 7.56 (2H, d, 2xS-(*Ar*)C-CH-C<u>*H*</u>-C-NH-(C=O)-CH_2, $^3J_{H,H}$ = 8.5 Hz), 7.39-7.48 (8H, m, 4xCH_2-(*Ar*)C-C<u>*H*</u>-CH-C-C(CH_3)$_3$, 4xCH_2-(*Ar*)C-CH-C<u>*H*</u>-C-C(CH_3)$_3$), 4.97 (2H, d, 2xCH_3-(*Ar*)C-CH-C<u>*H*</u>-C, $^3J_{H,H}$ = 5.7 Hz), 4.87 (2H, d, 2xCH_3-(*Ar*)C-C<u>*H*</u>-CH-C, $^3J_{H,H}$ = 5.8 Hz), 4.69 (2H, d, 2xCH_3-(*Ar*)C-CH-C<u>*H*</u>-C, $^3J_{H,H}$ = 5.7 Hz), 4.60 (2H, d, 2xCH_3-(*Ar*)C-C<u>*H*</u>-CH-C, $^3J_{H,H}$ = 5.8 Hz), 3.54 (2H, s, C<u>*H*$_2$</u>-(*Ar*)C-CH-CH-C-C(CH_3)$_3$), 3.35 (2H, s, C<u>*H*$_2$</u>-(*Ar*)C-CH-CH-C-C(CH_3)$_3$), 2.70 (2H, t, (C=O)-C<u>*H*$_2$</u>-CH_2, $^3J_{H,H}$ = 7.4 Hz), 1.99 (2H, sept, 2x(*Ar*)C-CH-CH-C-C<u>*H*</u>(CH_3)$_2$, $^3J_{H,H}$ = 6.8 Hz), 1.69-1.81 (2H, m, (C=O)-CH_2-C<u>*H*$_2$</u>-CH_2, $^3J_{H,H}$ = 7.6 Hz), 1.66 (6H, s, 2xC<u>*H*$_3$</u>-(*Ar*)C-CH-CH-C), 1.36 (9H, s, S-CH_2-(*Ar*)C-CH-CH-C-C(C<u>*H*$_3$</u>)$_3$), 1.34 (9H, s, S-CH_2-(*Ar*)C-CH-CH-C-C(C<u>*H*$_3$</u>)$_3$), 1.19-1.44 (12H, m, (C=O)-$(CH_2)_2$-C<u>*H*$_2$</u>, (C=O)-$(CH_2)_3$-C<u>*H*$_2$</u>, (C=O)-$(CH_2)_4$-C<u>*H*$_2$</u>, (C=O)-$(CH_2)_5$-C<u>*H*$_2$</u>, (C=O)-$(CH_2)_6$-C<u>*H*$_2$</u>, (C=O)-$(CH_2)_7$-C<u>*H*$_2$</u>), 0.98 (6H, d, (*Ar*)C-CH-CH-C-CH(C<u>*H*$_3$</u>)$_2$, $^3J_{H,H}$ = 6.8 Hz), 0.93 (6H, d, (*Ar*)C-CH-CH-C-CH(C<u>*H*$_3$</u>)$_2$, $^3J_{H,H}$ = 6.8 Hz), 0.86 (3H, t, CH_2-C<u>*H*$_3$</u>, $^3J_{H,H}$ = 6.9 Hz).

^{13}C-NMR ($CDCl_3$) δ_C, ppm: 174.4 (1C, (*Ar*)C-NH-(<u>*C*</u>=O)-CH_2), 151.99, 151.96 (2C, 2xS-CH_2-(*Ar*)C-CH-CH-<u>*C*</u>-C(CH_3)$_3$), 141.8 (1C, S-(*Ar*)C-CH-CH-<u>*C*</u>-NH-(C=O)-CH_2), 136.85, 136.54 (2C, 2xS-CH_2-(*Ar*)<u>*C*</u>-CH-CH-C-C(CH_3)$_3$), 132.6 (2C, 2xS-(*Ar*)C-<u>*C*</u>H-CH-C-NH-(C=O)-CH_2), 129.3, 129.1 (2C, 2xS-CH_2-(*Ar*)C-<u>*C*</u>H-CH-C-C(CH_3)$_3$), 129.0 (1C, S-(*Ar*)<u>*C*</u>-CH-CH-C-NH-(C=O)-CH_2), 125.7, 125.6 (2C, 2xS-CH_2-(*Ar*)C-CH-<u>*C*</u>H-C-C(CH_3)$_3$), 120.4 (2C, 2xS-(*Ar*)C-CH-<u>*C*</u>H-C-NH-(C=O)-CH_2), 107.8 (2C, 2xCH_3-(*Ar*)C-CH-CH-<u>*C*</u>), 100.1 (2C, 2xCH_3-(*Ar*)<u>*C*</u>-CH-CH-C), 84.3 (2C, 2xCH_3-(*Ar*)C-CH-<u>*C*</u>H-C), 83.8 (2C, 2xCH_3-(*Ar*)C-<u>*C*</u>H-CH-C, 83.2 (2C, 2xCH_3-(*Ar*)C-CH-<u>*C*</u>H-C), 82.2 (2C, 2xCH_3-(*Ar*)C-<u>*C*</u>H-CH-C), 39.9 (1C, S-<u>*C*</u>H_2-(*Ar*)C-CH-CH-C-C(CH_3)$_3$), 39.2 (1C, S-<u>*C*</u>H_2-(*Ar*)C-CH-CH-C-C(CH_3)$_3$), 37.5 (1C, (C=O)-<u>*C*</u>H_2), 34.93 (1C, S-CH_2-(*Ar*)C-CH-CH-C-<u>*C*</u>(CH_3)$_3$), 34.90 (1C, S-CH_2-(*Ar*)C-CH-CH-C-<u>*C*</u>(CH_3)$_3$), 32.1 (1C, <u>*C*</u>H_2-CH_2-CH_3), 31.55 (3C, S-CH_2-(*Ar*)C-CH-CH-C-C(<u>*C*</u>H_3)$_3$), 31.54 (3C, S-CH_2-(*Ar*)C-CH-CH-C-C(<u>*C*</u>H_3)$_3$), 31.1 (2C, 2x(*Ar*)CH-CH-C-<u>*C*</u>H(CH_3)$_2$), 29.8 (1C, (C=O)-$(CH_2)_5$-<u>*C*</u>H_2), 29.7 (1C, (C=O)-$(CH_2)_4$-<u>*C*</u>H_2), 29.51 (1C, (C=O)-$(CH_2)_3$-<u>*C*</u>H_2), 29.49 (1C, (C=O)-$(CH_2)_2$-<u>*C*</u>H_2), 25.9 (1C, (C=O)-CH_2-<u>*C*</u>H_2), 23.1 (2C, (*Ar*)CH-CH-

C-CH($\underline{C}H_3$)$_2$), 23.0 (2C, (*Ar*)CH-CH-C-CH($\underline{C}H_3$)$_2$), 22.8 (1C, $\underline{C}H_2$-CH_3), 18.1 (2C, 2x$\underline{C}H_3$-(*Ar*)C-CH-CH), 14.3 (1C, CH_2-$\underline{C}H_3$).
R_f (CH_2Cl_2/CH_3OH 10:1 (v/v)) = 0.380.
ESI-MS(+): *m/z* found 1108.3690 $[M-Cl]^+$, calcd. for $C_{58}H_{82}NORu_2S_3^+$ 1108.3640.
Elemental analysis (%): calcd. for $C_{58}H_{82}ClNORu_2S_3$ C 60.94, H 7.23, N 1.23; found C 61.05, H 7.58, N 1.23.

Synthesis of [(η^6-*p*-MeC$_6$H$_4$Pr^i)$_2$Ru$_2$(μ_2-SCH$_2$C$_6$H$_4$-*p*-Bu^t)$_2$(μ_2-SC$_6$H$_4$-*p*-NH(CO)R)]Cl (R = tridecyl), 2.2.14b
Myristic acid (0.069 g, 0.303 mmol, 1.5 equiv.), HOBt·H_2O (0.067 g, 0.485 mmol, 2.4 equiv.), DIPEA (0.131 g, 1.010 mmol, 5 equiv.), EDCI (0.116 g, 0.606 mmol, 3 equiv.), and **2.2.3** (0.200 g, 0.202 mmol, 1 equiv.); isolated product **2.2.14b** (0.126 g, 0.105 mmol, yield 52%).
^{1}H-NMR ($CDCl_3$) δ_H, ppm: 11.08 (1H, s, N$\underline{H}$-(C=O)), 8.15 (2H, d, 2xS-(*Ar*)C-CH-C$\underline{H}$-C-NH-(C=O)-CH_2, $^3J_{H,H}$ = 8.5 Hz), 7.56 (2H, d, 2xS-(*Ar*)C-C$\underline{H}$-CH-C-NH-(C=O)-CH_2, $^3J_{H,H}$ = 8.5 Hz), 7.39-7.49 (8H, m, 4xCH_2-(*Ar*)C-C$\underline{H}$-CH-C-C(CH_3)$_3$, 4xCH_2-(*Ar*)C-CH-C$\underline{H}$-C-C(CH_3)$_3$), 4.98 (2H, d, 2xCH_3-(*Ar*)C-CH-C$\underline{H}$-C, $^3J_{H,H}$ = 5.8 Hz), 4.87 (2H, d, 2xCH_3-(*Ar*)C-C$\underline{H}$-CH-C, $^3J_{H,H}$ = 5.8 Hz), 4.69 (2H, d, 2xCH_3-(*Ar*)C-CH-C$\underline{H}$-C, $^3J_{H,H}$ = 5.8 Hz), 4.60 (2H, d, 2xCH_3-(*Ar*)C-C$\underline{H}$-CH-C, $^3J_{H,H}$ = 5.8 Hz), 3.54 (2H, s, C$\underline{H_2}$-(*Ar*)C-CH-CH-C-C(CH_3)$_3$), 3.35 (2H, s, C$\underline{H_2}$-(*Ar*)C-CH-CH-C-C(CH_3)$_3$), 2.69 (2H, t, (C=O)-C$\underline{H_2}$-CH_2, $^3J_{H,H}$ = 7.5 Hz), 2.00 (2H, sept, 2x(*Ar*)C-CH-CH-C-C$\underline{H}$(CH_3)$_2$, $^3J_{H,H}$ = 6.9 Hz), 1.69-1.77 (2H, m, (C=O)-CH_2-C$\underline{H_2}$-CH_2), 1.66 (6H, s, 2xC$\underline{H_3}$-(*Ar*)C-CH-CH-C), 1.37 (9H, s, S-CH_2-(*Ar*)C-CH-CH-C-C(C$\underline{H_3}$)$_3$), 1.35 (9H, s, S-CH_2-(*Ar*)C-CH-CH-C-C(C$\underline{H_3}$)$_3$), 1.20-1.44 (20H, m, (C=O)-(CH_2)$_2$-C$\underline{H_2}$, (C=O)-(CH_2)$_3$-C$\underline{H_2}$, (C=O)-(CH_2)$_4$-C$\underline{H_2}$, (C=O)-(CH_2)$_5$-C$\underline{H_2}$, (C=O)-(CH_2)$_6$-C$\underline{H_2}$, (C=O)-(CH_2)$_7$-C$\underline{H_2}$, (C=O)-(CH_2)$_8$-C$\underline{H_2}$, (C=O)-(CH_2)$_9$-C$\underline{H_2}$, (C=O)-(CH_2)$_{10}$-C$\underline{H_2}$, (C=O)-(CH_2)$_{11}$-C$\underline{H_2}$, (C=O)-(CH_2)$_{12}$-C$\underline{H_2}$), 0.98 (6H, d, (*Ar*)C-CH-CH-C-CH(C$\underline{H_3}$)$_2$, $^3J_{H,H}$ = 6.8 Hz), 0.94 (6H, d, (*Ar*)C-CH-CH-C-CH(C$\underline{H_3}$)$_2$, $^3J_{H,H}$ = 6.9 Hz), 0.87 (3H, t, CH_2-C$\underline{H_3}$, $^3J_{H,H}$ = 6.9 Hz).
^{13}C-NMR ($CDCl_3$) δ_C, ppm: 174.4 (1C, (*Ar*)C-NH-(C=O)-CH_2), 152.00, 151.97 (2C, 2xS-CH_2-(*Ar*)C-CH-CH-C-C(CH_3)$_3$), 141.8 (1C, S-(*Ar*)C-CH-CH-C-NH-(C=O)-CH_2), 136.9, 136.6 (2C, 2xS-CH_2-(*Ar*)C-CH-CH-C-C(CH_3)$_3$), 132.6 (2C, 2xS-(*Ar*)C-CH-CH-C-NH-(C=O)-CH_2), 129.3, 129.1 (2C, 2xS-CH_2-(*Ar*)C-CH-CH-C-C(CH_3)$_3$), 129.0 (1C, S-(*Ar*)C-CH-CH-C-NH-(C=O)-CH_2), 125.70, 125.65 (2C, 2xS-CH_2-(*Ar*)C-CH-CH-C-C(CH_3)$_3$), 120.5 (2C, 2xS-(*Ar*)C-CH-CH-C-NH-(C=O)-CH_2), 107.8 (2C, 2xCH_3-(*Ar*)C-CH-CH-C), 100.1 (2C, 2xCH_3-(*Ar*)C-CH-CH-C), 84.3 (2C, 2xCH_3-(*Ar*)C-CH-CH-C), 83.8 (2C, 2xCH_3-(*Ar*)C-CH-CH-C), 83.2 (2C, 2xCH_3-(*Ar*)C-CH-CH-C), 82.2 (2C, 2xCH_3-(*Ar*)C-CH-CH-C), 39.9 (1C, S-$\underline{C}H_2$-(*Ar*)C-CH-CH-C-C(CH_3)$_3$), 39.2 (1C, S-$\underline{C}H_2$-(*Ar*)C-CH-CH-C-C(CH_3)$_3$), 37.5 (1C, (C=O)-$\underline{C}H_2$), 34.94 (1C, S-CH_2-(*Ar*)C-CH-CH-C-$\underline{C}$(CH_3)$_3$), 34.91 (1C, S-CH_2-(*Ar*)C-CH-CH-C-$\underline{C}$(CH_3)$_3$), 32.1 (1C, $\underline{C}H_2$-CH_2-CH_3), 31.56 (3C, S-CH_2-(*Ar*)C-CH-CH-C-C($\underline{C}H_3$)$_3$), 31.54 (3C, S-CH_2-(*Ar*)C-CH-CH-C-C($\underline{C}H_3$)$_3$), 31.1 (2C, 2x(*Ar*)CH-CH-C-$\underline{C}$H(CH_3)$_2$), 29.5-29.7 (8C, (C=O)-(CH_2)$_2$-$\underline{C}H_2$, (C=O)-(CH_2)$_3$-$\underline{C}H_2$, (C=O)-(CH_2)$_4$-$\underline{C}H_2$, (C=O)-(CH_2)$_5$-$\underline{C}H_2$, (C=O)-(CH_2)$_6$-$\underline{C}$H, (C=O)-(CH_2)$_7$-$\underline{C}H_2$, (C=O)-(CH_2)$_8$-$\underline{C}H_2$, (C=O)-(CH_2)$_9$-$\underline{C}H_2$, (C=O)-(CH_2)$_{10}$-$\underline{C}H_2$), 25.0 (1C, (C=O)-CH_2-$\underline{C}H_2$),23.1 (2C, (*Ar*)CH-CH-C-CH($\underline{C}H_3$)$_2$), 23.0 (2C, (*Ar*)CH-CH-C-CH($\underline{C}H_3$)$_2$), 22.8 (1C, $\underline{C}H_2$-CH_3), 18.1 (2C, 2x$\underline{C}H_3$-(*Ar*)C-CH-CH), 14.3 (1C, CH_2-$\underline{C}H_3$).
R_f (CH_2Cl_2/CH_3OH 10:1 (v/v)) = 0.360.
ESI-MS(+): *m/z* found 1164.4317 $[M-Cl]^+$, calcd. for $C_{62}H_{90}NORu_2S_3^+$ 1164.4266.
Elemental analysis (%): calcd. for $C_{62}H_{90}ClNORu_2S_3$: C 62.15, H 7.57, N 1.17; found C 62.08, H 7.82, 1.19.

3. Trithiolato-Bridged Ruthenium(II)-Arene Complexes Bearing an Organic Drug[14]

3.1. Biological activity

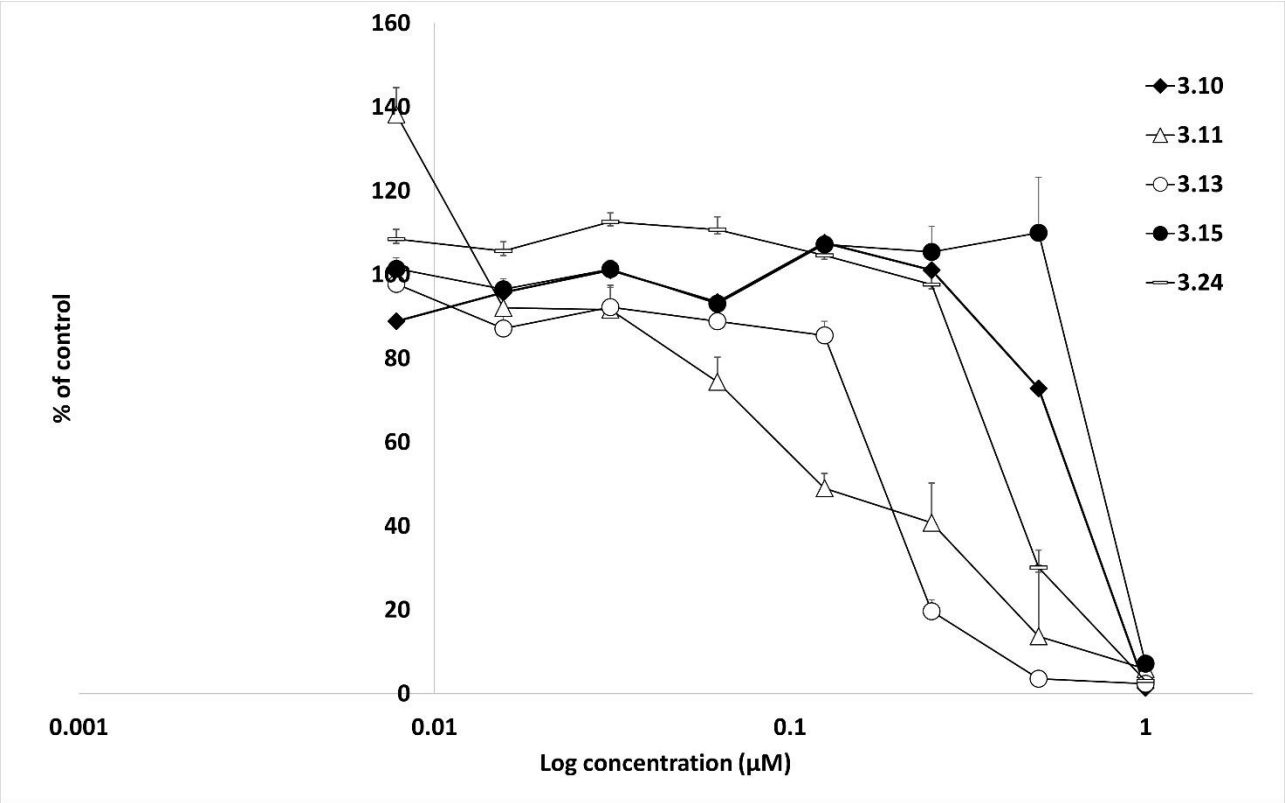

Figure S3.1. Dose response curves for compounds **3.10**, **3.11**, **3.13**, **3.15** and **3.24** as inhibitors of *T. gondii* β-gal tachyzoites proliferation. Vertical bars represent standard deviation for each tested concentration. Eight concentrations between 1 and 0.007 µM were used, each point being the average of six independent replicates.

3.2. Experimental

Chemistry[15]

General

The chemicals were purchased from Aldrich, Alfa Aesar, Acros Organics, ABCR, and TCI Chemicals and used without further purification. Reactions were performed under inert atmosphere (N_2) using Schlenk techniques with dry solvents (Acros Organics) preserved over molecular sieves. Reactions were monitored by TLC using Macherey-Nagel TLC silica gel coated aluminium sheets Alugram® Xtra SIL G/UV_{254} and visualised with UV at 254 nm and $KMnO_4$ stain. Compounds were purified by column flash chromatography on silica gel (Aldrich, 40-60 mesh) using the elution systems indicated. ^{1}H (300.13 and 400.13 MHz), ^{13}C (100.62 MHz) and ^{19}F (282.40 MHz) NMR spectra were recorded on a AVANCE III HD 300 and on a Bruker Avance II 400 spectrometers at 298 K. The chemical shifts are reported in parts per million (ppm) and referenced to residual solvent peaks ($CDCl_3$, ^{1}H δ 7.26, ^{13}C δ 77.16 ppm; MeOD-d_4, ^{1}H δ 3.31, ^{13}C δ 49.00 ppm; DMSO-d_6 ^{1}H δ

[14] This chapter was published as Synthesis and Antiparasitic Activity of New Conjugates—Organic Drugs Tethered to Trithiolato-Bridged Dinuclear Ruthenium(II)–Arene Complexes, Inorganics, 2021, 9, 59. https://doi.org/10.3390/inorganics9080059. This article is licensed under a Creative Commons Attribution International License (CC BY 4.0).

[15] Only syntheses of compounds obtained by the author of this thesis are presented.

2.50 ^{13}C δ 39.52 ppm [393]), and coupling constants (*J*) are reported in hertz (Hz). High resolution electrospray ionization mass spectra (ESI-MS) were carried out by the Mass Spectrometry and Protein Analyses Services at DCBP and were obtained on a LTQ Orbitrap XL ESI (Thermo) operated in positive ion mode. Thermal elemental analyses were carried out by the Mass Spectrometry and Protein Analyses Services at DCBP and were obtained on a Flash 2000 Organic Elemental Analyzer (Thermo Scientific).

Abbreviations:

Ciprofloxacin - 1-Cyclopropyl-6-fluoro-4-oxo-7-(piperazin-1-yl)-1,4-dihydroquinoline-3-carboxylic acid
Dapsone - 4,4'-sulfonyldianiline
DIPEA - *N*,*N*-Diisopropylethylamine
DMAP - *N*,*N*-Dimethyl-4-aminopyridine
DMF – Dimethylformamide
HBTU – 2-(1 H -benzotriazol-1-yl)-1,1,3,3-tetramethyluronium hexafluorophosphate
HOBt·H₂O – 1-Hydroxybenzotriazole hydrate
EDCI – *N*-(3-Dimethylaminopropyl)-*N*′-ethylcarbodiimide hydrochloride
Menadione - 2-methylnaphthalene-1,4-dione
Metronidazole - 2-(2-methyl-5-nitro-1*H*-imidazol-1-yl)ethan-1-ol
MsCl - methanesulfonyl chloride
Sulfadiazine - 4-amino-*N*-(pyrimidin-2-yl)benzenesulfonamide
Sulfadoxine - 4-amino-*N*-(5,6-dimethoxypyrimidin-4-yl)benzenesulfonamide
Sulfamethoxazole - 4-amino-*N*-(5-methylisoxazol-3-yl)benzenesulfonamide
TEA – triethylamine
TFA – Trifluoroacetic acid
Triclosan - 5-chloro-2-(2,4-dichlorophenoxy)phenol
For the description of the NMR spectra: *Ar* – arene, *Cipro* – ciprofloxacin, *Im* – imidazole, *Napht* – naphthalen, *Tr* – triazole.

Synthesis of the diruthenium intermediates

The synthesis of the dithiolato intermediate **3.1**[53, 131] ([(η^6-*p*-$MeC_6H_4Pr^i$)$_2$$Ru_2$($\mu_2$-$SCH_2C_6H_4$-*p*-$Bu^t$)$Cl_2$]), of the mixed trithiolato compounds **3.2**[131] ([(η^6-*p*-$MeC_6H_4Pr^i$)$_2$$Ru_2$($\mu_2$-$SCH_2C_6H_4$-*p*-$Bu^t$)$_2$($\mu_2$-$SC_6H_4$-*p*-$CH_2CO_2H$)]Cl), **3.3**[53, 131] ([(η^6-*p*-$MeC_6H_4Pr^i$)$_2$$Ru_2$($\mu_2$-$SCH_2C_6H_4$-*p*-$Bu^t$)$_2$($\mu_2$-$SC_6H_4$-*p*-OH)]Cl) and **3.4**[131] ([(η^6-*p*-$MeC_6H_4Pr^i$)$_2$$Ru_2$($\mu_2$-$SCH_2C_6H_4$-*p*-$Bu^t$)$_2$($\mu_2$-$SC_6H_4$-*p*-$NH_2$)]Cl), and of the symmetric trithiolato compounds **3.5** ([(η^6-*p*-$MeC_6H_4Pr^i$)$_2$$Ru_2$($\mu_2$-$SC_6H_4$-*p*-$OH)_3$]Cl)[131] and **3.6** ([(η^6-*p*-$MeC_6H_4Pr^i$)$_2$$Ru_2$($\mu_2$-$SC_6H_4$-*p*-$NH_2$)]Cl)[30] were described previously.

Synthesis of [(η^6-*p*-$MeC_6H_4Pr^i$)$_2$$Ru_2$($\mu_2$-$SCH_2C_6H_4$-*p*-$Bu^t$)$_2$($\mu_2$-$SC_6H_4$-*p*-$CH_2$-(C=O)-NH-R)]Cl (R = CH_2-C≡CH) (3.7)

To a solution of **3.2** (1.00 g, 0.969 mmol, 1 equiv.) in dry CH_2Cl_2 (50 mL) at r.t. under inert atmosphere (N_2) were added successively EDCI (0.557 g, 2.907 mmol, 3 equiv.) and DIPEA (0.42 mL, 2.423 mmol, 2.5 equiv.). After 15 min were added HOBt·H_2O (0.320 g, 2.326 mmol, 2.4 equiv.), propargylamine (0.163 g, 2.907 mmol, 3 equiv.) and DIPEA (0.42 mL, 2.423 mmol, 2.5 equiv.). The reaction mixture was stirred at r.t. under inert atmosphere (N_2) for further 24 h and the reaction evolution was verified by TLC (CH_2Cl_2/CH_3OH 10:1 (v/v)). The reaction mixture was concentrated to dryness under reduced pressure and purified by column chromatography using CH_2Cl_2/CH_3OH mixture afforded **3.7** as an orange solid (0.861 g, 0.805 mmol, yield 83%).

^{1}H-NMR ($CDCl_3$) δ_H, ppm: 9.37 (1H, m br, S-(*Ar*)C-CH-CH-C-CH_2-(C=O)-N*H*), 7.53-7.62 (4H, m, 2xS-(*Ar*)C-CH-C*H*-C-CH_2-(C=O)-NH, 2xS-(*Ar*)C-C*H*-CH-C-CH_2-(C=O)-NH, $^3J_{H,H}$ = 8.1 Hz), 7.37-7.50 (8H, m, 4xCH_2-(*Ar*)C-C*H*-CH-C-C$(CH_3)_3$, 4xCH_2-(*Ar*)C-CH-C*H*-C-C$(CH_3)_3$, $^3J_{H,H}$ = 8.3 Hz), 5.00 (2H, d, 2xCH_3-(*Ar*)C-CH-C*H*-C, $^3J_{H,H}$ = 5.7 Hz), 4.89 (2H, d, 2xCH_3-(*Ar*)C-CH-C*H*-C, $^3J_{H,H}$ = 5.8 Hz), 4.77 (2H, d, 2xCH_3-(*Ar*)C-C*H*-CH-C, $^3J_{H,H}$ = 5.7 Hz), 4.59 (2H, d, 2xCH_3-(*Ar*)C-C*H*-CH-C, $^3J_{H,H}$ = 5.8 Hz), 3.98-4.02 (2H, m, (*Ar*)C-CH_2-(C=O)-NH-CH_2-C≡CH, $^4J_{H,H}$ = 1.9 Hz), 3.82 (2H, s, S-(*Ar*)C-CH-CH-C-CH_2-(C=O)-NH), 3.56 (2H, s, CH_2-(*Ar*)C-CH-CH-C-C$(CH_3)_3$), 3.36 (2H, s, CH_2-(*Ar*)C-CH-CH-C-C$(CH_3)_3$), 2.03-2.05 (1H, t br, (*Ar*)C-CH_2-(C=O)-NH-CH_2-C≡C*H*, $^4J_{H,H}$ = 2.1 Hz), 1.92 (2H, sept, 2x(*Ar*)C-CH-CH-C-C*H*$(CH_3)_2$, $^3J_{H,H}$ = 6.8 Hz), 1.68 (6H, s, 2xCH_3-(*Ar*)C-CH-CH-C), 1.36 (9H, s, S-CH_2-(*Ar*)C-CH-CH-C-C(CH_3)$_3$), 1.33 (9H, s, S-CH_2-(*Ar*)C-CH-CH-C-C(CH_3)$_3$), 0.94 (6H, d, 2x(*Ar*)C-CH-CH-C-CH(CH_3)$_2$, $^3J_{H,H}$ = 6.8 Hz), 0.90 (6H, d, 2x(*Ar*)C-CH-CH-C-CH(CH_3)$_2$, $^3J_{H,H}$ = 6.9 Hz).

^{13}C-NMR ($CDCl_3$) δ_C, ppm: 171.5 (1C, S-(*Ar*)C-CH-CH-C-CH_2-(*C*=O)-NH), 152.01, 151.95 (2C, 2xS-CH_2-(*Ar*)C-CH-CH-*C*-C$(CH_3)_3$), 138.3 (1C, S-(*Ar*)*C*-CH-CH-C-CH_2-(C=O)-NH), 136.8, 136.5 (2C, 2xS-CH_2-(*Ar*)*C*-CH-CH-C-C$(CH_3)_3$), 134.7 (1C, S-(*Ar*)C-CH-CH-*C*-CH_2-(C=O)-NH), 132.3 (2C, 2xS-(*Ar*)C-*C*H-CH-C-CH_2-(C=O)-NH), 130.8 (2C, 2xS-(*Ar*)C-CH-*C*H-C-CH_2-(C=O)-NH), 129.3, 129.1 (2C, 2xS-CH_2-(*Ar*)C-*C*H-CH-C-C$(CH_3)_3$), 125.7, 125.6 (2C, 2xS-CH_2-(*Ar*)C-CH-*C*H-C-C$(CH_3)_3$), 107.5 (2C, 2xCH_3-(*Ar*)C-CH-CH-*C*), 100.5 (2C, 2xCH_3-(*Ar*)*C*-CH-CH-C), 84.0 (2C, 2xCH_3-(*Ar*)C-CH-*C*H-C), 83.72 (2C, 2xCH_3-(*Ar*)C-*C*H-CH-C), 83.69 (2C, 2xCH_3-(*Ar*)C-CH-*C*H-C), 82.4 (2C, 2xCH_3-(*Ar*)C-*C*H-CH-C), 81.0 (1C, (*Ar*)C-CH_2-(C=O)-NH-CH_2-*C*≡CH), 70.0 (1C, (*Ar*)C-CH_2-(C=O)-NH-CH_2-C≡*C*H), 42.7 (1C, S-(*Ar*)C-CH-CH-C-*C*H_2-(C=O)-NH), 40.0 (1C, S-*C*H_2-(*Ar*)C-CH-CH-C-C$(CH_3)_3$), 39.4 (1C, S-*C*H_2-(*Ar*)C-CH-CH-C-C$(CH_3)_3$), 34.93 (1C, S-CH_2-(*Ar*)C-CH-CH-C-*C*$(CH_3)_3$), 34.90 (1C, S-CH_2-(*Ar*)C-CH-CH-C-*C*$(CH_3)_3$), 31.55, 31.53 (6C, 2xS-CH_2-(*Ar*)C-CH-CH-C-C(*C*H_3)$_3$), 31.0 (2C, 2x(*Ar*)CH-CH-C-*C*H$(CH_3)_2$), 29.1 (1C, (*Ar*)C-CH_2-(C=O)-NH-*C*H_2-C≡CH), 23.2 (2C, (*Ar*)CH-CH-C-CH(*C*H_3)$_2$), 22.9 (2C, (*Ar*)CH-CH-C-CH(*C*H_3)$_2$), 18.2 (2C, 2x*C*H_3-(*Ar*)C-CH-CH).

R_f (CH_2Cl_2/CH_3OH 10:1) = 0.282.

ESI-MS(+): *m/z* found 1034.2565 $[M\text{-}Cl]^+$, calcd. for $C_{53}H_{68}NORu_2S_3^+$ 1034.2545.

Elemental analysis (%): calcd. for $C_{53}H_{68}ClNORu_2S_3 \cdot CH_2Cl_2$ C 56.12, H 6.12, N 1.21; found C 56.58, H 6.06, N 1.23.

Synthesis of the conjugates with sulfa-drugs (dapsone, sulfamethoxazole, sulfadiazine, sulfadoxine)

Synthesis of [(η^6-*p*-$MeC_6H_4Pr^i$)$_2$$Ru_2$($\mu_2$-$SCH_2C_6H_4$-*p*-$Bu^t$)($\mu_2$-$SC_6H_4$-*p*-$CH_2$-(C=O)-NH-R)]Cl (R = 4-((4-aminophenyl)sulfonyl)-*N*-aniline) (3.8)

To a solution of **3.2** (0.200 g, 0.194 mmol, 1 equiv.) in dry CH_3CN (50 mL) at r.t. under inert atmosphere (N_2), were added successively HOBt (0.064 g, 0.466 mmol, 2.4 equiv.), EDCI (0.112 g, 0.582 mmol, 3 equiv.), dapsone (0.074 g, 0.291 mmol, 1.5 equiv.) and DIPEA (0.17 mL, 0.970 mmol, 5 equiv.). The reaction mixture was stirred at r.t. under inert atmosphere (N_2) for further 24 h and the reaction evolution was verified by TLC (CH_2Cl_2/CH_3OH 9:1 (v/v)). The reaction mixture was filtered and concentrated to dryness under reduced pressure. Purification by column chromatography using CH_2Cl_2/CH_3OH mixture afforded **3.8** as an orange solid (0.072 g, 0.057 mmol, yield 29%).

^{1}H-NMR ($CDCl_3$) δ_H, ppm: 11.57 (1H, m br, S-(*Ar*)C-CH-CH-C-CH_2-(C=O)-N*H*), 8.13 (2H, d, 2x(C=O)-NH-(*Ar*)C-CH-C*H*-C-(SO_2), $^3J_{H,H}$ = 8.9 Hz), 7.73 (2H, d, 2x(C=O)-NH-(*Ar*)C-C*H*-CH-C-(SO_2), $^3J_{H,H}$ = 8.8 Hz), 7.56-7.66 (6H, m, 2xS-(*Ar*)C-CH-C*H*-C-CH_2-(C=O)-NH, 2xS-(*Ar*)C-C*H*-CH-C-CH_2-(C=O)-NH, 2x(SO_2)-(*Ar*)C-C*H*-CH-C-NH_2), 7.35-7.50 (8H, m, 4xCH_2-(*Ar*)C-C*H*-CH-C-C$(CH_3)_3$, 4xCH_2-(*Ar*)C-CH-C*H*-C-C$(CH_3)_3$, $^3J_{H,H}$ = 8.4 Hz), 6.81 (2H, d br, 2x(SO_2)-(*Ar*)C-CH-

C*H*-C-NH$_2$, $^3J_{H,H}$ = 7.0 Hz), 5.00 (2H, d, 2xCH$_3$-(*Ar*)C-CH-C*H*-C, $^3J_{H,H}$ = 5.6 Hz), 4.86 (2H, d, 2xCH$_3$-(*Ar*)C-CH-C*H*-C, $^3J_{H,H}$ = 5.7 Hz), 4.78 (2H, d, 2xCH$_3$-(*Ar*)C-C*H*-CH-C, $^3J_{H,H}$ = 5.6 Hz), 4.56 (2H, d, 2xCH$_3$-(*Ar*)C-C*H*-CH-C, $^3J_{H,H}$ = 5.7 Hz), 4.00 (2H, s, S-(*Ar*)C-CH-CH-C-C*H*$_2$-(C=O)-NH), 3.56 (2H, s, C*H*$_2$-(*Ar*)C-CH-CH-C-C(CH$_3$)$_3$), 3.35 (2H, s, C*H*$_2$-(*Ar*)C-CH-CH-C-C(CH$_3$)$_3$), 1.85 (2H, sept, 2x(*Ar*)C-CH-CH-C-C*H*(CH$_3$)$_2$, $^3J_{H,H}$ = 6.8 Hz), 1.67 (6H, s, 2xC*H*$_3$-(*Ar*)C-CH-CH-C), 1.36 (9H, s, S-CH$_2$-(*Ar*)C-CH-CH-C-C(C*H*$_3$)$_3$), 1.34 (9H, s, S-CH$_2$-(*Ar*)C-CH-CH-C-C(C*H*$_3$)$_3$), 0.87 (6H, d, 2x(*Ar*)C-CH-CH-C-CH(C*H*$_3$)$_2$, $^3J_{H,H}$ = 6.9 Hz), 0.85 (6H, d, 2x(*Ar*)C-CH-CH-C-CH(C*H*$_3$)$_2$, $^3J_{H,H}$ = 6.9 Hz).

^{13}C-NMR (CDCl$_3$) δ$_C$, ppm: 171.0 (1C, S-(*Ar*)C-CH-CH-C-CH$_2$-(*C*=O)-NH), 152.00, 151.97 (2C, 2xS-CH$_2$-(*Ar*)C-CH-CH-*C*-C(CH$_3$)$_3$), 148.6 (1C, (SO$_2$)-(*Ar*)C-CH-CH-*C*-NH$_2$), 144.2 (1C, (C=O)-NH-(*Ar*)*C*-CH-CH-C-(SO$_2$)), 137.9 (1C, S-(*Ar*)C-CH-CH-*C*-CH$_2$-(C=O)-NH), 136.8, 136.5 (2C, 2xS-CH$_2$-(*Ar*)*C*-CH-CH-C-C(CH$_3$)$_3$), 135.8 (1C, (C=O)-NH-(*Ar*)C-CH-CH-*C*-(SO$_2$)), 135.2 (1C, S-(*Ar*)*C*-CH-CH-C-CH$_2$-(C=O)-NH), 132.5 (1C, (SO$_2$)-(*Ar*)*C*-CH-CH-C-NH$_2$), 132.4 (2C, 2xS-(*Ar*)C-*C*H-CH-C-CH$_2$-(C=O)-NH), 130.7 (2C, 2xS-(*Ar*)C-CH-*C*H-C-CH$_2$-(C=O)-NH), 129.42, 129.35 (2C, 2xS-CH$_2$-(*Ar*)C-*C*H-CH-C-C(CH$_3$)$_3$), 129.1 (2C, 2x(SO$_2$)-(*Ar*)C-*C*H-CH-C-NH$_2$), 128.1 (2C, 2x(C=O)-NH-(*Ar*)C-C*H*-CH-C-(SO$_2$)), 125.74, 125.65 (2C, 2xS-CH$_2$-(*Ar*)C-CH-*C*H-C-C(CH$_3$)$_3$), 120.1 (2C, 2x(C=O)-NH-(*Ar*)C-CH-C*H*-C-(SO$_2$)), 116.0 (2C, 2x(SO$_2$)-(*Ar*)C-CH-*C*H-C-NH$_2$), 107.3 (2C, 2xCH$_3$-(*Ar*)C-CH-CH-*C*), 100.7 (2C, 2xCH$_3$-(*Ar*)*C*-CH-CH-C), 84.1 (2C, 2xCH$_3$-(*Ar*)C-CH-*C*H-C), 83.7 (2C, 2xCH$_3$-(*Ar*)C-*C*H-CH-C), 83.5 (2C, 2xCH$_3$-(*Ar*)C-CH-*C*H-C), 82.5 (2C, 2xCH$_3$-(*Ar*)C-*C*H-CH-C), 44.1 (1C, S-(*Ar*)C-CH-CH-C-*C*H$_2$-(C=O)-NH), 40.0 (1C, S-*C*H$_2$-(*Ar*)C-CH-CH-C-C(CH$_3$)$_3$), 39.4 (1C, S-*C*H$_2$-(*Ar*)C-CH-CH-C-C(CH$_3$)$_3$), 34.9 (2C, 2xS-CH$_2$-(*Ar*)C-CH-CH-C-*C*(CH$_3$)$_3$), 31.6 (6C, 2xS-CH$_2$-(*Ar*)C-CH-CH-C-C(*C*H$_3$)$_3$), 31.0 (2C, 2x(*Ar*)CH-CH-C-*C*H(CH$_3$)$_2$), 23.2 (2C, (*Ar*)CH-CH-C-CH(*C*H$_3$)$_2$), 22.7 (2C, (*Ar*)CH-CH-C-CH(*C*H$_3$)$_2$), 18.2 (2C, 2x*C*H$_3$-(*Ar*)C-CH-CH).

R$_f$ (CH$_2$Cl$_2$/CH$_3$OH 10:1) = 0.216.

ESI-MS(+): *m/z* found 1227.2786 [M-Cl]$^+$, calcd. for C$_{62}$H$_{75}$N$_2$O$_3$Ru$_2$S$_4^+$ 1227.2742.

Elemental analysis (%): calcd. for C$_{62}$H$_{75}$ClN$_2$O$_3$Ru$_2$S$_4$·1.2CH$_3$OH C 58.37, H 6.18, N 2.15; found C 58.37, H 6.14, N 2.20.

Synthesis of [(η^6-*p*-MeC$_6$H$_4$Pr^i)$_2$Ru$_2$(μ$_2$-SCH$_2$C$_6$H$_4$-*p*-Bu^t)(μ$_2$-SC$_6$H$_4$-*p*-CH$_2$-(C=O)-NH-R)]Cl (R = 4-amino-*N*-(pyrimidin-2-yl)benzenesulfonamide) (3.10)

To a solution of **3.2** (0.300 g, 0.291 mmol, 1 equiv.) in dry DMF (10 mL) at r.t. under inert atmosphere (N$_2$) were added EDCI (0.167 g, 0.873 mmol, 3 equiv.) and DIPEA (0.13 mL, 0.728 mmol, 2.5 equiv.). After 5 min HOBt (0.096 g, 0.698 mmol, 2.4 equiv.), sulfadiazine (0.087 g, 0.349 mmol, 1.2 equiv.) and DIPEA (0.13 mL, 0.728 mmol, 2.5 equiv.), were successively added. The reaction mixture was stirred at r.t. under inert atmosphere (N$_2$) for further 48 h and the reaction evolution was verified by TLC (CH$_2$Cl$_2$/CH$_3$OH 9.5:0.5 (v/v)). The reaction mixture was filtered and the filtrate concentrated to dryness under reduced pressure. Purification by column chromatography using CH$_2$Cl$_2$/CH$_3$OH mixture afforded **3.10** as an orange solid (0.088 g, 0.070 mmol, yield 24%).

^{1}H-NMR (CDCl$_3$) δ$_H$, ppm: 11.44 (1H, s br, (S=O)$_2$-N*H*-(*Ar*)C-N-CH), 8.94 (1H, s, S-(*Ar*)C-CH-CH-C-CH$_2$-(C=O)-N*H*), 8.60 (2H, d, (S=O)$_2$-NH-(*Ar*)C-N-C*H*-CH-C*H*, $^3J_{H,H}$ = 4.9 Hz), 7.89 (2H, d, 2xNH-(*Ar*)C-CH-C*H*-C-(S=O)$_2$, $^3J_{H,H}$ = 9.0 Hz), 7.84 (2H, d, 2xNH-(*Ar*)C-C*H*-CH-C-(S=O)$_2$, $^3J_{H,H}$ = 9.0 Hz), 7.66 (2H, d, 2xS-(*Ar*)C-CH-C*H*-C-CH$_2$-(C=O)-NH, $^3J_{H,H}$ = 7.8 Hz), 7.36-7.48 (10H, m, 4xCH$_2$-(*Ar*)C-C*H*-CH-C-C(CH$_3$)$_3$, 4xCH$_2$-(*Ar*)C-CH-C*H*-C-C(CH$_3$)$_3$, 2xS-(*Ar*)C-C*H*-CH-C-CH$_2$-(C=O)-NH, $^3J_{H,H}$ = 8.3 Hz), 6.93 (1H, t, (S=O)$_2$-NH-(*Ar*)C-N-CH-C*H*-CH, $^3J_{H,H}$ = 4.9 Hz), 5.02 (2H, d, 2xCH$_3$-(*Ar*)C-CH-C*H*-C, $^3J_{H,H}$ = 5.6 Hz), 4.89 (2H, d, 2xCH$_3$-(*Ar*)C-C*H*-CH-C, $^3J_{H,H}$ = 5.8 Hz), 4.80 (2H, d, 2xCH$_3$-(*Ar*)C-CH-C*H*-C, $^3J_{H,H}$ = 5.6 Hz), 4.56 (2H, d, 2xCH$_3$-(*Ar*)C-C*H*-

CH-C, $^{3}J_{H,H}$ = 5.7 Hz), 3.79 (2H, s, S-(*Ar*)C-CH-CH-C-C$\underline{H_2}$-(C=O)-NH), 3.57 (2H, s, C$\underline{H_2}$-(*Ar*)C-CH-CH-C-C$(CH_3)_3$), 3.36 (2H, s, C$\underline{H_2}$-(*Ar*)C-CH-CH-C-C$(CH_3)_3$), 1.86 (2H, sept, 2x(*Ar*)C-CH-CH-C-C$\underline{H}(CH_3)_2$, $^{3}J_{H,H}$ = 6.8 Hz), 1.69 (6H, s, 2xC$\underline{H_3}$-(*Ar*)C-CH-CH-C), 1.36 (9H, s, S-CH_2-(*Ar*)C-CH-CH-C-C(C$\underline{H_3}$)$_3$), 1.33 (9H, s, S-CH_2-(*Ar*)C-CH-CH-C-C(C$\underline{H_3}$)$_3$), 0.88 (6H, d, 2x(*Ar*)C-CH-CH-C-CH(C$\underline{H_3}$)$_2$, $^{3}J_{H,H}$ = 6.8 Hz), 0.85 (6H, d, 2x(*Ar*)C-CH-CH-C-CH(C$\underline{H_3}$)$_2$, $^{3}J_{H,H}$ = 6.9 Hz).

^{13}C-NMR ($CDCl_3$) δ_C, ppm: 170.3 (1C, S-(*Ar*)C-CH-CH-C-CH_2-(C=O)-NH), 158.8 (2C, $(S=O)_2$-NH-(*Ar*)C-N-CH-CH-CH), 156.9 (1C, $(S=O)_2$-NH-(*Ar*)C-N-CH-CH-CH), 151.93, 151.90 (2C, 2xS-CH_2-(*Ar*)C-CH-CH-C-C$(CH_3)_3$), 143.5 (1C, NH-(*Ar*)C-CH-CH-C-$(S=O)_2$), 136.8, 136.6 (2C, 2xS-CH_2-(*Ar*)C-CH-CH-C-C$(CH_3)_3$), 136.3 (1C, S-(*Ar*)C-CH-CH-C-CH_2-(C=O)-NH), 136.1 (1C, S-(*Ar*)C-CH-CH-C-CH_2-(C=O)-NH), 133.4 (1C, NH-(*Ar*)C-CH-CH-C-$(S=O)_2$), 132.7 (2C, 2xS-(*Ar*)C-CH-CH-C-CH_2-(C=O)-NH), 130.2 (2C, 2xS-(*Ar*)C-CH-CH-C-CH_2-(C=O)-NH), 129.5, 129.4 (2C, 2xS-CH_2-(*Ar*)C-CH-CH-C-C$(CH_3)_3$), 129.1 (2C, 2xNH-(*Ar*)C-CH-CH-C-$(S=O)_2$), 125.7, 125.6 (2C, 2xS-CH_2-(*Ar*)C-CH-CH-C-C$(CH_3)_3$), 119.2 (2C, 2xNH-(*Ar*)C-CH-CH-C-$(S=O)_2$), 116.0 (1C, $(S=O)_2$-NH-(*Ar*)C-N-CH-CH-CH), 107.3 (2C, 2xCH_3-(*Ar*)C-CH-CH-C), 100.7 (2C, 2xCH_3-(*Ar*)C-CH-CH-C), 84.1 (2C, 2xCH_3-(*Ar*)C-CH-CH-C), 83.7 (2C, 2xCH_3-(*Ar*)C-CH-CH-C), 83.5 (2C, 2xCH_3-(*Ar*)C-CH-CH-C), 82.5 (2C, 2xCH_3-(*Ar*)C-CH-CH-C), 44.0 (1C, S-(*Ar*)C-CH-CH-C-CH_2-(C=O)-NH), 40.0 (1C, S-CH_2-(*Ar*)C-CH-CH-C-C$(CH_3)_3$), 39.5 (1C, S-CH_2-(*Ar*)C-CH-CH-C-C$(CH_3)_3$), 34.92 (1C, S-CH_2-(*Ar*)C-CH-CH-C-C$(CH_3)_3$), 34.89 (1C, S-CH_2-(*Ar*)C-CH-CH-C-C$(CH_3)_3$), 31.6 (6C, 2xS-CH_2-(*Ar*)C-CH-CH-C-C$(CH_3)_3$), 31.0 (2C, 2x(*Ar*)CH-CH-C-CH$(CH_3)_2$), 23.2 (2C, (*Ar*)CH-CH-C-CH$(CH_3)_2$), 22.7 (2C, (*Ar*)CH-CH-C-CH$(CH_3)_2$), 18.2 (2C, 2xCH_3-(*Ar*)C-CH-CH).

R_f (CH_2Cl_2/CH_3OH 10:1) = 0.284.

ESI-MS(+): *m/z* found 1229.2645 $[M\text{-}Cl]^+$, calcd. for $C_{60}H_{73}N_4O_3Ru_2S_4^+$ 1229.2647.

Elemental analysis (%): calcd. for $C_{60}H_{73}ClN_4O_3Ru_2S_4 \cdot 0.2CH_2Cl_2 \cdot 0.5CH_3OH$ C 56.21, H 5.86, N 4.32; found C 56.25, H 5.84, N 4.03.

Synthesis of the conjugates with triclosan and with metronidazole

Synthesis of [(η^6-*p*-$MeC_6H_4Pr^i$)$_2$$Ru_2$($\mu_2$-$SCH_2C_6H_4$-*p*-$Bu^t$)$_2$($\mu_2$-$SC_6H_4$-*p*-$CH_2$-(C=O)-O-R)]Cl (R = 5-chloro-2-(2,4-dichlorophenoxy)phenoxy) (3.12)

To a solution of **3.2** (0.200 g, 0.194 mmol, 1 equiv.) in dry CH_2Cl_2 (50 mL) at r.t. under inert atmosphere (N_2), were added successively EDCI (0.074 g, 0.388 mmol, 2 equiv.), triclosan (0.067 g, 0.233 mmol, 1.2 equiv.) and DMAP (0.012 g, 0.097 mmol, 0.5 equiv.). The reaction mixture was stirred at r.t. under inert atmosphere (N_2) for further 24 h and the reaction evolution was verified by TLC (CH_2Cl_2/CH_3OH 9:1 (v/v)). The reaction mixture was filtered and concentrated to dryness under reduced pressure. Purification by column chromatography using CH_2Cl_2/CH_3OH mixture afforded **3.12** as an orange solid (0.102 g, 0.078 mmol, yield 40%).

^{1}H-NMR ($CDCl_3$) δ_H, ppm: 7.72 (2H, d, S-(*Ar*)C-CH-C$\underline{H}$-C-CH_2-(C=O)-O, $^{3}J_{H,H}$ = 8.2 Hz), 7.50 (1H, CH_2-(C=O)-O-(*Ar*)C-C$\underline{H}$-C(Cl)-CH-CH, $^{4}J_{H,H}$ = 2.5 Hz), 7.39-7.49 (8H, m, 4xS-CH_2-(*Ar*)C-C$\underline{H}$-CH-C-C$(CH_3)_3$, 4xS-CH_2-(*Ar*)C-CH-C$\underline{H}$-C-C$(CH_3)_3$, $^{3}J_{H,H}$ = 8.7 Hz), 7.23 (2H, d, S-(*Ar*)C-C$\underline{H}$-CH-C-CH_2-(C=O)-O, $^{3}J_{H,H}$ = 8.2 Hz), 7.19 (1H, dd, CH_2-(C=O)-O-(*Ar*)C-CH-C(Cl)-C$\underline{H}$-CH, $^{3}J_{H,H}$ = 8.7 Hz, $^{4}J_{H,H}$ = 2.5 Hz), 7.18 (1H, d, O-(*Ar*)C-C(Cl)-C$\underline{H}$-C(Cl)-CH-CH, $^{4}J_{H,H}$ = 2.4 Hz), 7.17 (1H, dd, O-(*Ar*)C-C(Cl)-CH-C(Cl)-C$\underline{H}$-CH, $^{3}J_{H,H}$ = 7.1 Hz, $^{4}J_{H,H}$ = 2.5 Hz), 6.89 (1H, d, CH_2-(C=O)-O-(*Ar*)C-CH-C(Cl)-CH-C$\underline{H}$, $^{3}J_{H,H}$ = 8.8 Hz), 6.84 (1H, d, O-(*Ar*)C-C(Cl)-CH-C(Cl)-CH-C$\underline{H}$, $^{3}J_{H,H}$ = 9.4 Hz), 5.09 (2H, d, 2xCH_3-(*Ar*)C-CH-C$\underline{H}$-C, $^{3}J_{H,H}$ = 5.8 Hz), 4.98 (2H, d, 2xCH_3-(*Ar*)C-CH-C$\underline{H}$-C, $^{3}J_{H,H}$ = 5.8 Hz), 4.88 (2H, d, 2xCH_3-(*Ar*)C-C$\underline{H}$-CH-C, $^{3}J_{H,H}$ = 5.8 Hz), 4.60 (2H, d, 2xCH_3-(*Ar*)C-C$\underline{H}$-CH-C, $^{3}J_{H,H}$ = 5.8 Hz), 3.81 (2H, s, S-(*Ar*)C-CH-CH-C-C$\underline{H_2}$-(C=O)-O), 3.60 (2H, s, S-C$\underline{H_2}$-(*Ar*)C-CH-CH-C-$(CH_3)_3$, 3.42 (2H, s, S-C$\underline{H_2}$-(*Ar*)C-CH-CH-C-$(CH_3)_3$, 1.88 (2H, sept, 2x(*Ar*)C-CH-CH-C-C$\underline{H}(CH_3)_2$, $^{3}J_{H,H}$ = 6.9 Hz), 1.71 (6H, s, 2xC$\underline{H_3}$-(*Ar*)C-CH-CH-C), 1.35 (9H, s, S-CH_2-

(*Ar*)C-CH-CH-C-C(C*H*$_3$)$_3$), 1.32 (9H, s, S-CH$_2$-(*Ar*)C-CH-CH-C-C(C*H*$_3$)$_3$), 0.90 (6H, d, 2x(*Ar*)C-CH-CH-C-CH(C*H*$_3$)$_2$, $^3J_{H,H}$ = 6.9 Hz), 0.86 (6H, d, 2x(*Ar*)C-CH-CH-C-CH(C*H*$_3$)$_2$, $^3J_{H,H}$ = 6.9 Hz).

^{13}C-NMR ($CDCl_3$) δ_C, ppm: 168.7 (1C, S-(*Ar*)C-CH-CH-C-CH$_2$-(*C*=O)-O), 151.9, 151.7 (2C, 2xS-CH$_2$-(*Ar*)C-CH-CH-*C*-C(CH$_3$)$_3$), 151.1 (1C, CH$_2$-(C=O)-O-(*Ar*)C-CH-C(Cl)-CH-CH-*C*-O), 146.7 (1C, CH$_2$-(C=O)-O-(*Ar*)*C*-CH-C(Cl)-CH-CH), 141.8 (1C, O-(*Ar*)*C*-C(Cl)-CH-C(Cl)-CH-CH), 137.2 (1C, S-(*Ar*)*C*-CH-CH-C-CH$_2$-(C=O)-O), 136.80, 136.76 (2C, 2xS-CH$_2$-(*Ar*)*C*-CH-CH-C-C(CH$_3$)$_3$), 133.5 (1C, S-(*Ar*)C-CH-CH-*C*-CH$_2$-(C=O)-O), 133.0 (2C, 2xS-(*Ar*)C-CH-*C*H-C-CH$_2$-(C=O)-O), 130.6 (1C, CH$_2$-(C=O)-O-(*Ar*)C-*C*H-C(Cl)-CH-CH), 130.1 (2C, 2xS-(*Ar*)C-*C*H-CH-C-CH$_2$-(C=O)-O), 129.7 (1C, CH$_2$-(C=O)-O-(*Ar*)C-CH-*C*(Cl)-CH-CH), 129.5 (1C, O-(*Ar*)C-C(Cl)-CH-*C*(Cl)-CH-CH), 129.4, 129.2 (4C, 4xS-CH$_2$-(*Ar*)C-*C*H-CH-C-C(CH$_3$)$_3$), 128.4 (1C, CH$_2$-(C=O)-O-(*Ar*)C-CH-C(Cl)-*C*H-CH), 127.3 (1C, O-(*Ar*)C-C(Cl)-CH-C(Cl)-*C*H-CH), 125.9 (1C, O-(*Ar*)C-*C*(Cl)-CH-C(Cl)-CH-CH), 125.7, 125.5 (4C, 4xS-CH$_2$-(*Ar*)C-CH-*C*H-C-C(CH$_3$)$_3$), 124.4 (1C, O-(*Ar*)C-C(Cl)-*C*H-C(Cl)-CH-CH), 120.6 (1C, CH$_2$-(C=O)-O-(*Ar*)C-CH-C(Cl)-CH-*C*H), 120.3 (1C, O-(*Ar*)C-C(Cl)-CH-C(Cl)-CH-*C*H), 107.2 (2C, 2xCH$_3$-(*Ar*)C-CH-CH-*C*), 100.6 (2C, 2xCH$_3$-(*Ar*)*C*-CH-CH-C), 84.1 (2C, 2xCH$_3$-(*Ar*)C-CH-*C*H-C), 83.84 (2C, 2xCH$_3$-(*Ar*)C-*C*H-CH-C), 83.80 (2C, 2xCH$_3$-(*Ar*)C-CH-*C*H-C), 82.5 (2C, 2xCH$_3$-(*Ar*)C-*C*H-CH-C), 40.1 (2C, S-*C*H$_2$-(*Ar*)C-CH-CH-C-C(CH$_3$)$_3$, S-(*Ar*)C-CH-CH-C-*C*H$_2$-(C=O)-O), 39.6 (1C, S-*C*H$_2$-(*Ar*)C-CH-CH-C-C(CH$_3$)$_3$), 34.91, 34.86 (2C, 2xS-CH$_2$-(*Ar*)C-CH-CH-C-*C*(CH$_3$)$_3$), 31.53, 31.55 (6C, 2xS-CH$_2$-(*Ar*)C-CH-CH-C-C(*C*H$_3$)$_3$), 30.9 (2C, 2x(*Ar*)CH-CH-C-*C*H(CH$_3$)$_2$), 23.1 (2C, (*Ar*)CH-CH-C-CH(*C*H$_3$)$_2$), 22.8 (2C, (*Ar*)CH-CH-C-CH(*C*H$_3$)$_2$), 18.2 (2C, 2x*C*H$_3$-(*Ar*)C-CH-CH).

R_f (CH_2Cl_2/CH_3OH 10:1) = 0.324.

ESI-MS(+): *m/z* found 1267.1651 $[M\text{-}Cl]^+$, calcd. for $C_{62}H_{70}Cl_3O_3Ru_2S_3^+$ 1267.1634.

Elemental analysis (%): calcd. for $C_{62}H_{70}Cl_4O_3Ru_2S_3 \cdot 2.5CH_3OH$ C 56.00, H 5.83; found C 55.97, H 5.87.

Synthesis of [(η^6-*p*-MeC$_6$H$_4$Pr^i)$_2$Ru$_2$(μ_2-SCH$_2$C$_6$H$_4$-*p*-Bu^t)$_2$(μ_2-SC$_6$H$_4$-*p*-CH$_2$-(C=O)-O-R)]Cl (R = 2-(2-methyl-5-nitro-1*H*-imidazol-1-yl)ethan-1-oate) (3.13)

To a solution of **3.2** (0.200 g, 0.194 mmol, 1 equiv.) in dry CH_2Cl_2 (50 mL) at r.t. under inert atmosphere (N_2) were added successively EDCI (0.074 g, 0.388 mmol, 2 equiv.), metronidazole (0.040 g, 0.233 mmol, 1.2 equiv.) and DMAP (0.012 g, 0.097 mmol, 0.5 equiv.). The reaction mixture was stirred at r.t. under inert atmosphere (N_2) for further 24 h and the reaction evolution was verified by TLC (CH_2Cl_2/CH_3OH 9:1 (v/v)). The reaction mixture was concentrated to dryness under reduced pressure and purified by column chromatography followed by purification on analytical TLCs using CH_2Cl_2/CH_3OH mixture afforded **3.13** as an orange solid (0.117 g, 0.099 mmol, yield 51%).

^{1}H-NMR ($CDCl_3$) δ_H, ppm: 7.98 (1H, s, CH$_3$-(*Im*)C-N-C*H*-C-(NO$_2$), 7.72 (2H, d, S-(*Ar*)C-CH-C*H*-C-CH$_2$-(C=O)-O, $^3J_{H,H}$ = 7.5 Hz), 7.38-7.51 (8H, m, 4xS-CH$_2$-(*Ar*)C-C*H*-CH-C-C(CH$_3$)$_3$, 4xS-CH$_2$-(*Ar*)C-CH-C*H*-C-C(CH$_3$)$_3$, $^3J_{H,H}$ = 8.4 Hz), 7.17 (2H, d, S-(*Ar*)C-C*H*-CH-C-CH$_2$-(C=O)-O, $^3J_{H,H}$ = 7.5 Hz), 5.10 (2H, d, 2xCH$_3$-(*Ar*)C-CH-C*H*-C, $^3J_{H,H}$ = 5.3 Hz), 4.98 (2H, d, 2xCH$_3$-(*Ar*)C-CH-C*H*-C, $^3J_{H,H}$ = 5.6 Hz), 4.93 (2H, d, 2xCH$_3$-(*Ar*)C-C*H*-CH-C, $^3J_{H,H}$ = 5.2 Hz), 4.77 (2H, t, (*Im*)N-CH$_2$-C*H*$_2$-O, $^3J_{H,H}$ = 4.7 Hz), 4.61 (2H, d, 2xCH$_3$-(*Ar*)C-C*H*-CH-C, $^3J_{H,H}$ = 5.7 Hz), 4.48 (2H, t, (*Im*)N-C*H*$_2$-CH$_2$-O, $^3J_{H,H}$ = 4.7 Hz), 3.60 (2H, s, S-C*H*$_2$-(*Ar*)C-CH-CH-C-(CH$_3$)$_3$, 3.59 (2H, s, S-(*Ar*)C-CH-CH-C-C*H*$_2$-(C=O)-O), 3.41 (2H, s, S-C*H*$_2$-(*Ar*)C-CH-CH-C-(CH$_3$)$_3$, 2.62 (3H, s, C*H*$_3$-(*Im*)C-N-CH-C-(NO$_2$), 1.89 (2H, sept, 2x(*Ar*)C-CH-CH-C-C*H*(CH$_3$)$_2$, $^3J_{H,H}$ = 6.8 Hz), 1.73 (6H, s, 2xC*H*$_3$-(*Ar*)C-CH-CH-C), 1.37 (9H, s, S-CH$_2$-(*Ar*)C-CH-CH-C-C(C*H*$_3$)$_3$), 1.34 (9H, s, S-CH$_2$-(*Ar*)C-CH-CH-C-C(C*H*$_3$)$_3$), 0.93 (6H, d, 2x(*Ar*)C-CH-CH-C-CH(C*H*$_3$)$_2$, $^3J_{H,H}$ = 6.8 Hz), 0.88 (6H, d, 2x(*Ar*)C-CH-CH-C-CH(C*H*$_3$)$_2$, $^3J_{H,H}$ = 6.8 Hz).

^{13}C-NMR ($CDCl_3$) δ_C, ppm: 170.6 (1C, S-(*Ar*)C-CH-CH-C-CH_2-(C=O)-O), 152.0, 151.90 (2C, 2xS-CH_2-(*Ar*)C-CH-CH-*C*-C$(CH_3)_3$), 151.87 (1C, CH_3-(*Im*)*C*-N-CH-C-NO_2), 138.8 (1C, CH_3-(*Im*)C-N-CH-*C*-NO_2), 136.9 (1C, S-(*Ar*)*C*-CH-CH-C-CH_2-(C=O)-O), 136.7 (2C, 2xS-CH_2-(*Ar*)*C*-CH-CH-C-C$(CH_3)_3$), 134.0 (1C, S-(*Ar*)C-CH-CH-*C*-CH_2-(C=O)-O), 133.0 (2C, 2xS-(*Ar*)C-CH-*C*H-C-CH_2-(C=O)-O), 132.7 (1C, CH_3-(*Im*)C-N-*C*H-C-NO_2), 130.2 (2C, 2xS-(*Ar*)C-*C*H-CH-C-CH_2-(C=O)-O), 129.4, 129.2 (4C, 4xS-CH_2-(*Ar*)C-*C*H-CH-C-C$(CH_3)_3$), 125.8, 125.6 (4C, 4xS-CH_2-(*Ar*)C-CH-*C*H-C-C$(CH_3)_3$), 107.2 (2C, 2xCH_3-(*Ar*)C-CH-CH-*C*), 100.7 (2C, 2xCH_3-(*Ar*)*C*-CH-CH-C), 84.2 (2C, 2xCH_3-(*Ar*)C-CH-*C*H-C), 83.82 (2C, 2xCH_3-(*Ar*)C-*C*H-CH-C), 83.78 (2C, 2xCH_3-(*Ar*)C-CH-*C*H-C), 82.6 (2C, 2xCH_3-(*Ar*)C-*C*H-CH-C), 63.2 (1C, (*Im*)N-CH_2-*C*H_2-O-(C=O)), 45.4 (1C, (*Im*)N-*C*H_2-CH_2-O-(C=O)), 40.5 (1C, S-(*Ar*)C-CH-CH-C-*C*H_2-(C=O)-O), 40.1 (1C, S-*C*H_2-(*Ar*)C-CH-CH-C-C$(CH_3)_3$), 39.6 (1C, S-*C*H_2-(*Ar*)C-CH-CH-C-C$(CH_3)_3$), 34.94, 34.90 (2C, 2xS-CH_2-(*Ar*)C-CH-CH-C-*C*$(CH_3)_3$), 31.57, 31.55 (6C, 2xS-CH_2-(*Ar*)C-CH-CH-C-C(*C*$H_3)_3$), 31.0 (2C, 2x(*Ar*)CH-CH-C-*C*H$(CH_3)_2$), 23.2 (2C, (*Ar*)CH-CH-C-CH(*C*$H_3)_2$), 22.8 (2C, (*Ar*)CH-CH-C-CH(*C*$H_3)_2$), 18.3 (2C, 2x*C*H_3-(*Ar*)C-CH-CH), 14.8 (1C, *C*H_3-(*Im*)C-N-CH-C-NO_2).
R_f (CH_2Cl_2/CH_3OH 10:1) = 0.235.
ESI-MS(+): *m/z* found 1150.2798 $[M\text{-}Cl]^+$, calcd. for $C_{56}H_{72}N_3O_4Ru_2S_3^+$ 1150.2766.
Elemental analysis (%): calcd. for $C_{56}H_{72}ClN_3O_4Ru_2S_3 \cdot 1.2CH_3OH$ C 56.16, H 6.33, N 3.43; found C 56.18, H 6.32 N 3.40.

Synthesis of 2-(2-methyl-5-nitro-1*H*-imidazol-1-yl)ethyl methanesulfonate (3.14a)
To a solution of metronidazole (0.500 g, 2.921 mmol, 1 equiv.) in dry CH_2Cl_2 (50 mL) at 0°C under inert atmosphere (N_2) were added dropwise MsCl (0.27 mL, 3.505 mmol, 1.2 equiv.) and TEA (0.61 mL, 4.382 mmol, 1.5 equiv.). The reaction mixture was stirred at 0°C under inert atmosphere (N_2) for further 2 h and the reaction evolution was verified by TLC (CH_2Cl_2/CH_3OH 10:1 (v/v)). The reaction was quenched with water (50 mL). The isolated aqueous phase was further extracted with CH_2Cl_2 (2×30 mL). The combined organic phases were washed with brine (50 mL), dried over anhydrous Na_2SO_4, filtered and concentrated to dryness under reduced pressure. The product **3.14a** isolated as a white solid (0.444 g, 1.781 mmol, yield 61%) was used in next step without further purification.
^{1}H-NMR (DMSO-d_6) δ_H, ppm: 8.09 (1H, s, CH_3-(*Im*)C-N-C*H*-C-(NO_2), 4.66 (2H, t, (*Im*)N-C*H*$_2$-CH_2-O-(S=O)-CH_3, $^3J_{H,H}$ = 5.1 Hz), 4.55 (2H, t, (*Im*)N-CH_2-C*H*$_2$-O-(S=O)-CH_3, $^3J_{H,H}$ = 5.1 Hz), 3.15 (3H, s, (*Im*)N-CH_2-CH_2-O-(S=O)-C*H*$_3$), 2.47 (3H, s, C*H*$_3$-(*Im*)C-N-CH-C-(NO_2).
^{13}C-NMR (DMSO-d_6) δ_C, ppm: 151.7 (1C, CH_3-(*Im*)*C*-N-CH-C-NO_2), 138.4 (1C, CH_3-(*Im*)C-N-CH-*C*-NO_2), 132.8 (1C, CH_3-(*Im*)C-N-*C*H-C-NO_2), 68.4 (1C, (*Im*)N-CH_2-*C*H_2-O-(S=O)-CH_3), 45.1 (1C, (*Im*)N-*C*H_2-CH_2-O-(S=O)-CH_3), 36.7 (1C, (*Im*)N-CH_2-CH_2-O-(S=O)-*C*H_3), 14.0 (1C, *C*H_3-(*Im*)C-N-CH-C-NO_2).
R_f (CH_2Cl_2/CH_3OH 10:1) = 0.624.
ESI-MS(+): *m/z* found 250.0495 $[M+H]^+$, calcd. for $C_7H_{12}N_3O_5S^+$ 250.0492.
Elemental analysis (%): calcd. for $C_7H_{11}N_3O_5S \cdot 0.2CH_2Cl_2 \cdot 0.4H_2O$ C 31.63, H 4.50, N 15.37; found C 31.61, H 4.55, N 15.39.

Synthesis of 1-(2-azidoethyl)-2-methyl-5-nitro-1*H*-imidazole (3.14)
To a solution of **3.14a** (0.444 g, 1.781 mmol, 1 equiv.) in dry DMF (5 mL) was added NaN_3 (0.232 mL, 3.562 mmol, 2 equiv.) and the reaction mixture was heated at 60°C under inert atmosphere (N_2) for 24 h. The mixture was allowed to cool to r.t., Et_2O (150 mL) was added and the mixture was washed with H_2O (2×200 mL). The organic phase was washed with brine (100 mL), dried over anhydrous Na_2SO_4, filtered and concentrated to dryness under reduced pressure. **3.14** was isolated as a white solid (0.165 g, 0.841 mmol, yield 47%) and was used in next step without further

purification.
^{1}H-NMR ($CDCl_3$) δ_H, ppm: 8.00 (1H, s, CH_3-(*Im*)C-N-C*H*-C-NO_2), 4.44 (2H, t, (*Im*)N-C*H*$_2$-CH_2-N_3, $^{3}J_{H,H}$ = 5.6 Hz), 3.79 (2H, t, (*Im*)N-CH_2-C*H*$_2$-N_3, $^{3}J_{H,H}$ = 5.6 Hz), 2.56 (3H, s, C*H*$_3$-(*Im*)C-N-CH-C-NO_2).
^{13}C-NMR ($CDCl_3$) δ_C, ppm: 151.4 (1C, CH_3-(*Im*)*C*-N-CH-C-NO_2), 138.4 (1C, CH_3-(*Im*)C-N-CH-*C*-NO_2), 133.4 (1C, CH_3-(*Im*)C-N-*C*H-C-NO_2), 51.1 (1C, (*Im*)N-CH_2-*C*H_2-N_3), 45.7 (1C, (*Im*)N-*C*H_2-CH_2-N_3), 14.7 (1C, *C*H_3-(*Im*)C-N-CH-C-NO_2).
R_f (CH_2Cl_2/CH_3OH 10:1) = 0.699.
ESI-MS(+): *m/z* found 197.0787 $[M+H]^+$, calcd. for $C_6H_9N_6O_2^+$ 197.0781.
Elemental analysis (%): calcd. for $C_6H_8N_6O_2$ C 36.74, H 4.11, N 42.84; found C 38.43, H 4.45, N 40.47.

Synthesis of [(η^6-*p*-$MeC_6H_4Pr^i$)$_2$$Ru_2$($\mu_2$-$SCH_2C_6H_4$-*p*-$Bu^t$)$_2$($\mu_2$-$SC_6H_4$-*p*-$CH_2$-(C=O)-NH-R)]Cl (R = *N*-((1-(2-(2-methyl-5-nitro-1*H*-imidazol-1-yl)ethyl)-1*H*-1,2,3-triazol-4-yl)methyl)amine) (3.15)
To a solution of **3.7** (0.200 g, 0.187 mmol, 1 equiv.) in dry DMF (10 mL) at r.t. under inert atmosphere (N_2) were successively added **3.14** (0.044 g, 0.224 mmol, 1.2 equiv.), $CuSO_4 \cdot 5H_2O$ (0.047 g, 0.187 mmol, 1 equiv.) and sodium L-ascorbate (0.074 g, 0.374 mmol, 2 equiv.). The reaction mixture was stirred at r.t. under inert atmosphere (N_2) for 48 h and the reaction evolution was verified by TLC (CH_2Cl_2/CH_3OH 10:1 (v/v)). The reaction mixture was filtered, solubilized in EtOAc (100 mL) and washed with H_2O (3×100 mL). The unified aqueous phases were extracted with EtOAc (100 mL) and the combined organic phases were further washed with brine (100 mL), dried over anhydrous Na_2SO_4, filtered and concentrated to dryness under reduced pressure. Purification by column chromatography using CH_2Cl_2/CH_3OH mixture afforded **3.15** as an orange solid (0.078 g, 0.061 mmol, yield 33%).
^{1}H-NMR (DMSO-d_6) δ_H, ppm: 8.64 (1H, t br, S-(*Ar*)C-CH-CH-C-CH_2-(C=O)-N*H*), 8.18 (1H, s br, (*Tr*)C-N=N-N-C*H*), 7.88 (1H, s, CH_3-(*Im*)C-N-C*H*-C-NO_2), 7.69 (2H, d, 2xS-(*Ar*)C-CH-C*H*-C-CH_2-(C=O)-NH, $^{3}J_{H,H}$ = 7.9 Hz), 7.47-7.52 (4H, m, 4xS-CH_2-(*Ar*)C-CH-C*H*-C-C$(CH_3)_3$, $^{3}J_{H,H}$ = 8.6 Hz), 7.37-7.45 (4H, m, 4xS-CH_2-(*Ar*)C-C*H*-CH-C-C$(CH_3)_3$, $^{3}J_{H,H}$ = 8.3 Hz), 7.21 (2H, d, 2xS-(*Ar*)C-C*H*-CH-C-CH_2-(C=O)-NH, $^{3}J_{H,H}$ = 8.0 Hz), 5.37 (2H, d, 2xCH_3-(*Ar*)C-CH-C*H*-C, $^{3}J_{H,H}$ = 5.3 Hz), 5.25 (4H, d, 2xCH_3-(*Ar*)C-CH-C*H*-C, 2xCH_3-(*Ar*)C-C*H*-CH-C, $^{3}J_{H,H}$ = 5.8 Hz), 4.78-4.84 (2H, t br, (*Im*)N-C*H*$_2$-CH_2-(*Tr*)N), 4.66-4.75 (4H, m, (*Im*)N-CH_2-C*H*$_2$-(*Tr*)N, 2xCH_3-(*Ar*)C-C*H*-CH-C), 4.25 (2H, d, (C=O)-NH-C*H*$_2$-(*Tr*)C-N=N-N-CH_2, $^{3}J_{H,H}$ = 5.2 Hz), 3.63 (2H, s, S-C*H*$_2$-(*Ar*)C-CH-CH-C-$(CH_3)_3$), 3.43 (4H, s, S-(*Ar*)C-CH-CH-C-C*H*$_2$-(C=O)-NH, S-C*H*$_2$-(*Ar*)C-CH-CH-C-$(CH_3)_3$), 1.86 (3H, s, C*H*$_3$-(*Im*)C-N-CH-C-NO_2), 1.72-1.81 (2H, m, 2x(*Ar*)C-CH-CH-C-C*H*$(CH_3)_2$), 1.75 (6H s, 2xC*H*$_3$-(*Ar*)C-CH-CH-C), 1.33 (9H, s, S-CH_2-(*Ar*)C-CH-CH-C-C(C*H*$_3$)$_3$), 1.29 (9H, s, S-CH_2-(*Ar*)C-CH-CH-C-C(C*H*$_3$)$_3$), 0.79 (6H, d, 2x(*Ar*)C-CH-CH-C-CH(C*H*$_3$)$_2$, $^{3}J_{H,H}$ = 6.8 Hz), 0.74 (6H, d, 2x(*Ar*)C-CH-CH-C-CH(C*H*$_3$)$_2$, $^{3}J_{H,H}$ = 6.7 Hz).
^{13}C-NMR (DMSO-d_6) δ_C, ppm: 169.6 (1C, S-(*Ar*)C-CH-CH-C-CH_2-(*C*=O)-NH), 150.5, 150.3 (2C, 2xS-CH_2-(*Ar*)C-CH-CH-*C*-C$(CH_3)_3$), 145.2 (2C, (*Tr*)*C*-N=N-N-CH, CH_3-(*Im*)*C*-N-CH-C-NO_2), 137.0, 136.8 (2C, 2xS-CH_2-(*Ar*)*C*-CH-CH-C-C$(CH_3)_3$), 136.1 (1C, S-(*Ar*)*C*-CH-CH-C-CH_2-(C=O)-NH), 135.2 (1C, S-(*Ar*)C-CH-CH-*C*-CH_2-(C=O)-NH), 133.2 (1C, s, CH_3-(*Im*)C-N-CH-*C*-NO_2), 132.2 (2C, 2xS-(*Ar*)C-CH-*C*H-C-CH_2-(C=O)-NH), 129.29 (2C, 2xS-(*Ar*)C-*C*H-CH-C-CH_2-(C=O)-NH), 129.25, 128.9 (4C, 4xS-CH_2-(*Ar*)C-*C*H-CH-C-C$(CH_3)_3$), 125.2, 125.0 (4C, 4xS-CH_2-(*Ar*)C-CH-*C*H-C-C$(CH_3)_3$), 123.8 (2C, (*Tr*)C-N=N-N-*C*H, CH_3-(*Im*)C-N-C*H*-C-NO_2), 105.2 (2C, 2xCH_3-(*Ar*)C-CH-CH-*C*), 101.3 (2C, 2xCH_3-(*Ar*)*C*-CH-CH-C), 85.1 (2C, 2xCH_3-(*Ar*)C-CH-*C*H-C), 82.6 (2C, 2xCH_3-(*Ar*)C-*C*H-CH-C), 82.4 (2C, 2xCH_3-(*Ar*)C-CH-*C*H-C), 82.3 (2C, 2xCH_3-(*Ar*)C-*C*H-CH-C), 48.6 (2H, m, (*Im*)N-CH_2-*C*H_2-(*Tr*)N), 46.3 (2H, m, (*Im*)N-*C*H_2-CH_2-(*Tr*)N),

41.6 (1C, S-(*Ar*)C-CH-CH-C-<u>C</u>H$_2$-(C=O)-NH), 39.7 (1C, S-<u>C</u>H$_2$-(*Ar*)C-CH-CH-C-C(CH$_3$)$_3$), 39.5 (1C, S-<u>C</u>H$_2$-(*Ar*)C-CH-CH-C-C(CH$_3$)$_3$), 34.39, 34.34 (2C, 2xS-CH$_2$-(*Ar*)C-CH-CH-C-<u>C</u>(CH$_3$)$_3$), 34.1 (1C, (C=O)-NH-<u>C</u>H$_2$-(*Tr*)C-N=N-N-CH$_2$), 31.2, 31.1 (6C, 2xS-CH$_2$-(*Ar*)C-CH-CH-C-C(<u>C</u>H$_3$)$_3$), 29.9 (2C, 2x(*Ar*)CH-CH-C-<u>C</u>H(CH$_3$)$_2$), 23.0 (2C, (*Ar*)CH-CH-C-CH(<u>C</u>H$_3$)$_2$), 21.8 (2C, (*Ar*)CH-CH-C-CH(<u>C</u>H$_3$)$_2$), 17.5 (2C, 2x<u>C</u>H$_3$-(*Ar*)C-CH-CH), 12.9 (1C, <u>C</u>H$_3$-(*Im*)C-N-CH-C-NO$_2$).
R$_f$ (CH$_2$Cl$_2$/CH$_3$OH 10:1) = 0.117.
ESI-MS(+): *m/z* found 1231.3262 [M-Cl]$^+$, calcd. for C$_{59}$H$_{75}$N$_6$O$_4$Ru$_2$S$_3^+$ 1231.3093.
Elemental analysis (%): calcd. for C$_{59}$H$_{75}$ClN$_6$O$_4$Ru$_2$S$_3$·CH$_2$Cl$_2$·1.8H$_2$O C 52.09, H 5.87, N 6.07; found C 52.04, H 5.95, N 6.56.

References

1. Montoya, J.G. and O. Liesenfeld, *Toxoplasmosis.* Lancet, 2004. **363**(9425): p. 1965-76.
2. Robert-Gangneux, F. and M.L. Darde, *Epidemiology of and diagnostic strategies for toxoplasmosis.* Clin Microbiol Rev, 2012. **25**(2): p. 264-96.
3. Pappas, G., N. Roussos, and M.E. Falagas, *Toxoplasmosis snapshots: global status of Toxoplasma gondii seroprevalence and implications for pregnancy and congenital toxoplasmosis.* Int J Parasitol, 2009. **39**(12): p. 1385-94.
4. Paris, L., *106 - Toxoplasmosis*, in *Hunter's Tropical Medicine and Emerging Infectious Diseases (Tenth Edition)*, D.R.H. Edward T. Ryan, Tom Solomon, Naomi E. Aronson, Timothy P. Endy, Editor. 2020, Elsevier. p. 803-813.
5. Halonen, S.K. and L.M. Weiss, *Toxoplasmosis.* Handb Clin Neurol, 2013. **114**: p. 125-45.
6. Sibley, L.D., et al., *Genetic diversity of Toxoplasma gondii in animals and humans.* Philos Trans R Soc Lond B Biol Sci, 2009. **364**(1530): p. 2749-61.
7. Dubey, J.P., D.S. Lindsay, and C.A. Speer, *Structures of Toxoplasma gondii tachyzoites, bradyzoites, and sporozoites and biology and development of tissue cysts.* Clin Microbiol Rev, 1998. **11**(2): p. 267-99.
8. Milne, G., J.P. Webster, and M. Walker, *Toxoplasma gondii: AnUnderestimated Threat?* Trends Parasitol, 2020. **36**(12): p. 959-969.
9. Al Malki, J.S., N.A. Hussien, and F. Al Malki, *Maternal toxoplasmosis and the risk of childhood autism: serological and molecular small-scale studies.* BMC Pediatr, 2021. **21**(1): p. 133.
10. Massie, G.N., et al., *Uptake and transmission of Toxoplasma gondii oocysts by migratory, filter-feeding fish.* Vet Parasitol, 2010. **169**(3-4): p. 296-303.
11. Lindsay, D.S. and J.P. Dubey, *Long-term survival of Toxoplasma gondii sporulated oocysts in seawater.* J Parasitol, 2009. **95**(4): p. 1019-20.
12. Jones, J., A. Lopez, and M. Wilson, *Congenital toxoplasmosis.* Am Fam Physician, 2003. **67**(10): p. 2131-8.
13. Ahmed, M., A. Sood, and J. Gupta, *Toxoplasmosis in pregnancy.* Eur J Obstet Gynecol Reprod Biol, 2020. **255**: p. 44-50.
14. Smith, N.C., et al., *Control of human toxoplasmosis.* Int. J. Parasitol., 2021. **51**(2-3): p. 95-121.
15. Abo-Al-Ela, H.G., *Toxoplasmosis and Psychiatric and Neurological Disorders: A Step toward Understanding Parasite Pathogenesis.* ACS Chem Neurosci, 2020. **11**(16): p. 2393-2406.
16. Johnson, S.K. and P.T.J. Johnson, *Toxoplasmosis: Recent Advances in Understanding the Link Between Infection and Host Behavior.* Annu Rev Anim Biosci, 2021. **9**: p. 249-264.
17. Dunay, I.R., et al., *Treatment of Toxoplasmosis: Historical Perspective, Animal Models, and Current Clinical Practice.* Clin. Microbiol. Rev., 2018. **31**(4): p. pii: e00057-17.
18. Antczak, M., K. Dzitko, and H. Dlugonska, *Human toxoplasmosis-Searching for novel chemotherapeutics.* Biomed Pharmacother, 2016. **82**: p. 677-84.
19. Montazeri, M., et al., *Drug Resistance in Toxoplasma gondii.* Front Microbiol, 2018. **9**: p. 2587.
20. Deng, Y., et al., *Recent progress on anti-Toxoplasma drugs discovery: Design, synthesis and screening.* Eur J Med Chem, 2019. **183**: p. 111711.
21. Andrade, R.M., et al., *Auranofin is highly efficacious against Toxoplasma gondii in vitro and in an in vivo experimental model of acute toxoplasmosis.* PLoS Negl Trop Dis, 2014. **8**(7): p. e2973.
22. Carradori, S., et al., *Synthesis and biological evaluation of anti-Toxoplasma gondii activity of a novel scaffold of thiazolidinone derivatives.* J Enzyme Inhib Med Chem, 2017. **32**(1): p. 746-758.
23. Baramee, A., et al., *Synthesis and in vitro activities of ferrocenic aminohydroxynaphthoquinones against Toxoplasma gondii and Plasmodium falciparum.* Bioorg Med Chem, 2006. **14**(5): p. 1294-302.

24. Portes, J.A., et al., *Reduction of Toxoplasma gondii Development Due to Inhibition of Parasite Antioxidant Enzymes by a Dinuclear Iron(III) Compound.* Antimicrob Agents Chemother, 2015. **59**(12): p. 7374-86.
25. Portes, J.A., et al., *A new iron(III) complex-containing sulfadiazine inhibits the proliferation and induces cystogenesis of Toxoplasma gondii.* Parasitol Res, 2018. **117**(9): p. 2795-2805.
26. Portes, J.A., et al., *In vitro treatment of Toxoplasma gondii with copper(II) complexes induces apoptosis-like and cellular division alterations.* Vet Parasitol, 2017. **245**: p. 141-152.
27. Batista, L.C., et al., *Antiproliferative activity and conversion of tachyzoite to bradyzoite of Toxoplasma gondii promoted by new zinc complexes containing sulfadiazine.* RSC Advances, 2015. **5**(122): p. 100606-100617.
28. Barna, F., et al., *In Vitro Effects of Novel Ruthenium Complexes in Neospora caninum and Toxoplasma gondii Tachyzoites.* Antimicrob. Agents Chemother., 2013. **57**(11): p. 5747-5754.
29. Basto, A.P., et al., *Characterization of the Activities of Dinuclear Thiolato-Bridged Arene Ruthenium Complexes against Toxoplasma gondii.* Antimicrob. Agents Chemother., 2017. **61**(9).
30. Paunescu, E., et al., *The quest of the best - A SAR study of trithiolato-bridged dinuclear Ruthenium(II)-Arene compounds presenting antiparasitic properties.* Eur. J. Med. Chem., 2021. **222**: p. 113610.
31. Meneceur, P., et al., *In vitro susceptibility of various genotypic strains of Toxoplasma gondii to pyrimethamine, sulfadiazine, and atovaquone.* Antimicrob Agents Chemother, 2008. **52**(4): p. 1269-77.
32. Biot, C., et al., *Synthesis and antimalarial activity in vitro and in vivo of a new ferrocene-chloroquine analogue.* J Med Chem, 1997. **40**(23): p. 3715-8.
33. Basto, A.P., et al., *Targeting of the mitochondrion by dinuclear thiolato-bridged arene ruthenium complexes in cancer cells and in the apicomplexan parasite Neospora caninum.* Metallomics, 2019. **11**(2): p. 462-474.
34. Hans T. Schacht, R.C.H., and M. Rakowski DuBois, *Structural characterization of 1:2 tris(.mu.-benzenethiolato)bis[(hexamethylbenzeneruthenium] chloride-chloroform.* Inorganic Chemistry 1992. **31 (9)**: p. 1728-1730.
35. Kazushi, M., M. Aki, and N. Akira, *Preparation and Structural Characterization of Cationic Dinuclear Ruthenium(II) — Thiolate Complexes, [Ru2(SPh)3(η6-p-cymene)2]Y (Y = Cl and PF6).* Chemistry Letters, 1992. **21**(9): p. 1795-1798.
36. Cherioux, F., et al., *Specific reactivity of SH versus OH functions towards dinuclear arene ruthenium units: synthesis of cationic complexes of the type [(arene)(2)Ru(2)(SR)(3)](+).* Polyhedron, 2003. **22**(4): p. 543-548.
37. Gras, M., et al., *Thiophenolato-bridged dinuclear areneruthenium complexes: a new family of highly cytotoxic anticancer agents.* Dalton Trans., 2010. **39**: p. 10305-10313.
38. Giannini, F., et al., *Highly cytotoxic trithiophenolatodiruthenium complexes of the type [(eta(6)-p-MeC6H4Pr (i))(2)Ru-2(SC6H4-p-X)(3)](+): synthesis, molecular structure, electrochemistry, cytotoxicity, and glutathione oxidation potential.* J. Biol. Inorg. Chem., 2012. **17**(6): p. 951-960.
39. Cherioux, F., B. Therrien, and G. Suss-Fink, *First Star-Like Oligophenylene Molecules Containing a Dinuclear Organometallic Core.* Eur. J. Inorg. Chem., 2003: p. 1043-1047.
40. Giannini, F., et al., *Highly cytotoxic diruthenium trithiolato complexes of the type [(eta(6)-p-MeC6H4Pri)(2)Ru-2(mu(2)-SR)(3)](+): synthesis, characterization, molecular structure and in vitro anticancer activity.* New J. Chem., 2013. **37**(11): p. 3503-3511.
41. Giannini, F., et al., *Tuning the in vitro cell cytotoxicity of dinuclear arene ruthenium trithiolato complexes: Influence of the arene ligand.* J. Organomet. Chem., 2015. **783**: p. 40-45.
42. Gupta, G., et al., *Highly water soluble trithiolato-bridged dinuclear arene ruthenium complexes.* Inorganica Chimica Acta, 2014. **423**: p. 524-529.

43. Chérioux, F., B. Therrien, and G. Süss-Fink, *Synthesis and structural characterisation of new cationic dinuclear ruthenium(II) thiolato complexes of the type [Ru2(η6-arene)2(μ-p-S–C6H4–Br)3]+*. Inorganica Chimica Acta, 2004. **357**(3): p. 834-838.
44. Trondl, R., et al., *NKP-1339, the first ruthenium-based anticancer drug on the edge to clinical application.* Chem. Sci., 2014. **5**: p. 2925-2932.
45. Alessio, E. and L. Messori, *NAMI-A and KP1019/1339, Two Iconic Ruthenium Anticancer Drug Candidates Face-to-Face: A Case Story in Medicinal Inorganic Chemistry.* Molecules, 2019. **24**(10): p. DOI: 10.3390/molecules24101995.
46. Coverdale, J.P.C., T. Laroiya-McCarron, and I. Romero-Canelón, *Designing Ruthenium Anticancer Drugs: What Have We Learnt from the Key Drug Candidates?* . Inorganics, 2019. **7**(3): p. 31. DOI: 10.3390/inorganics7030031.
47. Alessio, E., *Thirty years of the drug candidate NAMI-A and the myths in the field of ruthenium anticancer compounds: a personal perspective.* Eur. J. Inorg. Chem., 2016. **2017**(12): p. 1549-1560.
48. Berndsen, R.H., et al., *Combination of ruthenium(II)-arene complex [Ru(eta(6)-p-cymene)Cl2(pta)] (RAPTA-C) and the epidermal growth factor receptor inhibitor erlotinib results in efficient angiostatic and antitumor activity.* Sci. Rep., 2017. **7**: p. 43005.
49. Weiss, A., et al., *In vivo anti-tumor activity of the organometallic ruthenium(II)-arene complex [Ru(η6-p-cymene)Cl2(pta)] (RAPTA-C) in human ovarian and colorectal carcinomas.* Chem. Sci., 2014. **5**: p. 4742-4748.
50. Murray, B.S., et al., *The development of RAPTA compounds for the treatment of tumors.* Coord. Chem. Rev., 2016. **306**(Part 1): p. 86-114.
51. Bergamo, A., et al., *In vivo tumour and metastasis reduction and in vitro effects on invasion assays of the ruthenium RM175 and osmium AFAP51 organometallics in the mammary cancer model.* J. Inorg. Biochem., 2010. **104**(1): p. 79-86.
52. Aird, R.E., et al., *In vitro and in vivo activity and cross resistance profiles of novel ruthenium (II) organometallic arene complexes in human ovarian cancer.* Br. J. Cancer, 2002. **86**(10): p. 1652-1657.
53. Giannini, F., et al., *Synthesis, characterization and in vitro anticancer activity of highly cytotoxic trithiolato diruthenium complexes of the type [(eta(6)-p-(MeC6H4Pr)-Pr-i)(2)Ru-2(mu(2)-SR1)(2)(mu(2)-SR2)](+) containing different thiolato bridges.* J. Organomet. Chem., 2013. **744**: p. 41-48.
54. Meier, S.M., et al., *Identification of the structural determinants for anticancer activity of a ruthenium arene peptide conjugate.* Chemistry, 2013. **19**(28): p. 9297-307.
55. Ang, W.H., et al., *Rational design of an organometallic glutathione transferase inhibitor.* Angew Chem Int Ed Engl, 2009. **48**(21): p. 3854-7.
56. Nazarov, A.A., et al., *Protein ruthenation and DNA alkylation: chlorambucil-functionalized RAPTA complexes and their anticancer activity.* Dalton Trans, 2015. **44**(8): p. 3614-23.
57. Yang, M. and U. Bierbach, *Metal-containing pharmacophores in molecularly targeted anticancer therapies and diagnostics.* Eur. J. Inorg. Chem. , 2017. **12**: p. 1561-1572.
58. Wang, X. and Z. Guo, *Targeting and delivery of platinum-based anticancer drugs.* Chem. Soc. Rev., 2013. **42**(1): p. 202-224.
59. Wang, X., X. Wang, and Z. Guo, *Functionalization of platinum complexes for biomedical applications.* Acc. Chem. Res., 2015. **48**(9): p. 2622-2631.
60. Giannini, F., et al., *Cytotoxic peptide conjugates of dinuclear arene ruthenium trithiolato complexes.* MedChemComm, 2015. **6**(2): p. 347-350.
61. Stibal, D., et al., *Chlorambucil conjugates of dinuclear p-cymene ruthenium trithiolato complexes: synthesis, characterization and cytotoxicity study in vitro and in vivo.* J. Biol. Inorg. Chem., 2016. **21**(4): p. 443-452.
62. Studer, V., et al., *Conjugates containing two and three trithiolato-bridged dinuclear ruthenium(II)-arene units as in vitro antiparasitic and anticancer agents.* Pharmaceuticals, 2020. **13**(12): p. 471.
63. Jelk, J., et al., *Anti-parasitic dinuclear thiolato-bridged arene ruthenium complexes alter the mitochondrial ultrastructure and membrane potential in Trypanosoma brucei*

bloodstream forms. Exp. Parasitol., 2019. **205**(107753): p. doi: 10.1016/j.exppara.2019.107753.
64. Furrer, J. and G. Suss-Fink, *Thiolato-bridged dinuclear arene ruthenium complexes and their potential as anticancer drugs.* Coord. Chem. Rev., 2016. **309**: p. 36-50.
65. Giannini, F., G. Suss-Fink, and J. Furrer, *Efficient Oxidation of Cysteine and Glutathione Catalyzed by a Dinuclear Areneruthenium Trithiolato Anticancer Complex.* Inorg. Chem., 2011. **50**(21): p. 10552-10554.
66. Thota, S., et al., *Ru(II) Compounds: Next-Generation Anticancer Metallotherapeutics?* J. Med. Chem., 2018. **61**(14): p. 5805-5821.
67. Meier-Menches, S.M., et al., *Structure-activity relationships for ruthenium and osmium anticancer agents - towards clinical development.* Chem. Soc. Rev., 2018. **47**(3): p. 909-928.
68. Adams, M., M. Hanif, and C.G. Hartinger, *Ruthenium Anticancer Agents - From Cisplatin Analogues to Rational Drug Design. Encyclopedia of Inorganic and Bioinorganic Chemistry*, in *Encyclopedia of Inorganic and Bioinorganic Chemistry*. 2017, John Wiley & Sons, Ltd. . p. 1-21. DOI: 10.1002/9781119951438.eibc250.
69. Gambino, D. and L. Otero, *Perspectives on what ruthenium-based compounds could offer in the development of potential antiparasitic drugs.* Inorg. Chim. Acta, 2012. **393**: p. 103-114.
70. Brown, R.W. and C.J.T. Hyland, *Medicinal organometallic chemistry - an emerging strategy for the treatment of neglected tropical diseases.* MedChemComm, 2015. **6**(7): p. 1230-1243.
71. Gambino, D. and L. Otero, *Design of prospective antiparasitic metal-based compounds including selected organometallic cores.* Inorg. Chim. Acta, 2018. **472**: p. 58-75.
72. Ong, Y.C., et al., *Metal Compounds against Neglected Tropical Diseases.* Chem. Rev., 2019. **119**(2): p. 730-796.
73. Kuster, T., et al., *A New Promising Application for Highly Cytotoxic Metal Compounds: eta(6)-Areneruthenium(II) Phosphite Complexes for the Treatment of Alveolar Echinococcosis.* J. Med. Chem., 2012. **55**(9): p. 4178-4188.
74. Demoro, B., et al., *New organoruthenium complexes with bioactive thiosemicarbazones as co-ligands: potential anti-trypanosomal agents.* Dalton Trans., 2012. **41**(5): p. 1534-1543.
75. Rajapakse, C.S.K., et al., *Synthesis, Characterization, and in vitro Antimalarial and Antitumor Activity of New Ruthenium(II) Complexes of Chloroquine.* Inorg. Chem., 2009. **48**(3): p. 1122-1131.
76. Yildirim, H., et al., *Ruthenium (II) complexes of thiosemicarbazone: Synthesis, biosensor applications and evaluation as antimicrobial agents.* Mater. Sci. Eng. C, 2014. **44**: p. 1-8.
77. Lapasam, A., et al., *Antimicrobial selectivity of ruthenium, rhodium, and iridium half sandwich complexes containing phenyl hydrazone Schiff base ligands towards B. thuringiensis and P. aeruginosa bacteria.* Inorg. Chim. Acta, 2019. **484**: p. 255-263.
78. Ude, Z., et al., *A novel dual-functioning ruthenium(II)-arene complex of an anti-microbial ciprofloxacin derivative - Anti-proliferative and anti-microbial activity.* J. Inorg. Biochem., 2016. **160**: p. 210-217.
79. Laurent, Q., L.K. Batchelor, and P.J. Dyson, *Applying a Trojan Horse Strategy to Ruthenium Complexes in the Pursuit of Novel Antibacterial Agents.* Organometallics, 2018. **37**(6): p. 915-923.
80. Bodio, E., et al., *Development of Trackable Anticancer Agents Based on Metal Complexes.* Adv. Inorg. Chem., 2016. **68**: p. 253-299.
81. Bertrand, B., et al., *Development of trackable metal-based drugs: new generation of therapeutic agents.* Dalton Trans., 2016. **45**(33): p. 13005-13011.
82. Ali, M., et al., *Anticancer Agents: Does a Phosphonium Behave Like a Gold(I) Phosphine Complex? Let a "Smart" Probe Answer!* J. Med. Chem., 2015. **58**(11): p. 4521-4528.
83. Tasan, S., et al., *BODIPY-phosphane as a versatile tool for easy access to new metal-based theranostics.* Dalton Trans., 2013. **42**(17): p. 6102-6109.
84. Doulain, P.E., et al., *Towards the elaboration of new gold-based optical theranostics.* Dalton Trans., 2015. **44**(11): p. 4874-4883.

85. Gupta, G., et al., *Mitochondrial Localization of Highly Fluorescent and Photostable BODIPY-Based Ruthenium(II), Rhodium(III), and Iridium(III) Metal Complexes.* Inorg. Chem., 2019. **58**(13): p. 8587-8595.
86. Zhao, J., et al., *Anticancer Activity of Bifunctional Organometallic Ru(II) Arene Complexes Containing a 7-Hydroxycoumarin Group.* Organometallics, 2018. **37**(3): p. 441-447.
87. Ma, W.L., et al., *Potential anticancer agent for selective damage to mitochondria or lysosomes: Naphthalimide-modified fluorescent biomarker half-sandwich iridium (III) and ruthenium (II) complexes.* Eur. J. Med. Chem., 2019. **181**.
88. Sameiro, M. and T. Goncalves, *Fluorescent Labeling of Biomolecules with Organic Probes.* Chem. Rev., 2009. **109**(1): p. 190-212.
89. Lavis, L.D. and R.T. Raines, *Bright ideas for chemical biology.* ACS Chem. Biol., 2008. **3**(3): p. 142-155.
90. Thakur, A., R. Singla, and V. Jaitak, *Coumarins as anticancer agents: A review on synthetic strategies, mechanism of action and SAR studies.* Eur. J. Med. Chem., 2015. **101**: p. 476-495.
91. Emami, S. and S. Dadashpour, *Current developments of coumarin-based anti-cancer agents in medicinal chemistry.* Eur. J. Med. Chem., 2015. **102**: p. 611-630.
92. Srikrishna, D., C. Godugu, and P.K. Dubey, *A Review on Pharmacological Properties of Coumarins.* Mini-Rev. Med. Chem., 2018. **18**(2): p. 113-141.
93. Pereira, T.M., et al., *Coumarin Compounds in Medicinal Chemistry: Some Important Examples from the Last Years.* Curr. Topics Med. Chem., 2018. **18**(2): p. 124-148.
94. Balcioglu, S., et al., *Therapeutic potential of coumarin bearing metal complexes: Where are we headed?* Bioorg. Med. Chem. Lett., 2020. **30**(2).
95. New, E.J., et al., *Investigations using fluorescent ligands to monitor platinum(IV) reduction and platinum(II) reactions in cancer cells.* Dalton Trans., 2009(16): p. 3092-3101.
96. Skoczynska, A., et al., *Synthesis, structural analysis, redox properties and in vitro antitumor evaluation of half-sandwich complexes of Ru(II) with aminocoumarins.* Polyhedron, 2017. **127**: p. 307-314.
97. Ndinguri, M.W., et al., *Exploring water-soluble Pt(II) complexes of diethylenetriamine derivatives functionalized at the central nitrogen. Synthesis, characterization, and reaction with 5 '-GMP.* Inorg. Chim. Acta, 2010. **363**(8): p. 1796-1804.
98. Hua, W.Y., et al., *Combination of 7-hydroxycoumarin in a platinum(IV) complex derived from cisplatin enhanced cytotoxicity with multiple mechanisms of action.* J. Inorg. Biochem., 2018. **186**: p. 17-23.
99. Wedlock, L.E. and S.J. Berners-Price, *Recent Advances in Mapping the Sub-cellular Distribution of Metal-Based Anticancer Drugs.* Aust. J. Chem., 2011. **64**(6): p. 692-704.
100. Qin, X.D., et al., *Theranostic Pt(IV) Conjugate with Target Selectivity for Androgen Receptor.* Inorg. Chem., 2018. **57**(9): p. 5019-5029.
101. Bertrand, B., et al., *New Gold(I) Organometallic Compounds with Biological Activity in Cancer Cells.* Eur. J. Inorg. Chem., 2014(27): p. 4532-4536.
102. Ye, R.R., et al., *Coumarin-appended phosphorescent cyclometalated iridium(III) complexes as mitochondria-targeted theranostic anticancer agents.* Dalton Trans., 2016. **45**(33): p. 13042-13051.
103. Trommenschlager, A., et al., *Gold(I)-Coumarin-Caffeine-Based Complexes as New Potential Anti-Inflammatory and Anticancer Trackable Agents.* ChemMedChem, 2018. **13**(22): p. 2408-2414.
104. Demelo, J.S.S., R.S. Becker, and A.L. Macanita, *Photophysical Behavior of Coumarins as a Function of Substitution and Solvent - Experimental-Evidence for the Existence of a Lowest Lying (1)(Eta,Pi(Asterisk)) State.* J. Phys. Chem., 1994. **98**(24): p. 6054-6058.
105. Chaurasia, C.S. and J.M. Kauffman, *Synthesis and Fluorescent Properties of a New Photostable Thiol Reagent Bacm.* J. Heterocycl. Chem., 1990. **27**(3): p. 727-733.
106. Webb, M.R. and J.E.T. Corrie, *Fluorescent coumarin-labeled nucleotides to measure ADP release from actomyosin.* Biophys. J., 2001. **81**(3): p. 1562-1569.

107. Reisfeld, R., et al., *The Spectroscopic Behavior of Rhodamine 6g in Polar and Non-Polar Solvents and in Thin Glass and Pmma Films.* Chem. Phys. Lett., 1988. **147**(2-3): p. 142-147.
108. Dubey, J.P., *Toxoplasmosis of Animals and Humans*. 2nd ed. 2009 CRC Press
109. Kaye, A., *Toxoplasmosis: Diagnosis, Treatment, and Prevention in Congenitally Exposed Infants.* J. Pediatr. Health Care, 2011. **25**(6): p. 355-364.
110. Fichera, M.E. and D.S. Roos, *A plastid organelle as a drug target in apicomplexan parasites.* Nature, 1997. **390**(6658): p. 407-409.
111. Oxford Diffraction, CrysAlisPro (Version 1.171.40.37a). Oxford Diffraction Ltd., Yarnton, Oxfordshire, UK.
112. Macchi, P., et al., *Low-energy contamination of Mo microsource X-ray radiation: analysis and solution of the problem.* J. Appl. Crystallogr., 2011. **44**: p. 763-771.
113. Sheldrick, G.M., *SHELXT - Integrated space-group and crystal-structure determination.* Acta Crystallogr., Sect. A: Found. Adv., 2015. **71**: p. 3-8.
114. Sheldrick, G.M., *Crystal structure refinement with SHELXL.* Acta Crystallographica Section C-Structural Chemistry, 2015. **71**: p. 3-8.
115. Dolomanov, O.V., et al., *OLEX2: a complete structure solution, refinement and analysis program.* J. Appl. Crystallogr., 2009. **42**: p. 339-341.
116. Fischer, M. and J. Georges, *Fluorescence quantum yield of rhodamine 6G in ethanol as a function of concentration using thermal lens spectrometry.* Chem. Phys. Lett., 1996. **260**(1-2): p. 115-118.
117. McFadden, D.C., F. Seeber, and J.C. Boothroyd, *Use of Toxoplasma gondii expressing beta-galactosidase for colorimetric assessment of drug activity in vitro.* Antimicrob. Agents Chemother., 1997. **41**(9): p. 1849-1853.
118. Muller, J., et al., *Buparvaquone is active against Neospora caninum in vitro and in experimentally infected mice.* Int. J. Parasitol. Drugs - Drug Resist., 2015. **5**(1): p. 16-25.
119. Bertrand, B., et al., *Metal-based BODIPY derivatives as multimodal tools for life sciences.* Coord. Chem. Rev., 2018. **358**: p. 108-124.
120. Timerbaev, A.R., *Application of ICP-MS to the development of metal-based drugs and diagnostic agents: where do we stand?* Journal of Analytical Atomic Spectrometry, 2021. **36**(2): p. 254-266.
121. Paitandi, R.P., et al., *Pyrazole appended quinoline-BODIPY based arene ruthenium complexes: their anticancer activity and potential applications in cellular imaging.* Dalton Trans, 2018. **47**(48): p. 17500-17514.
122. Gupta, G., et al., *Novel BODIPY-based Ru(II) and Ir(III) metalla-rectangles: cellular localization of compounds and their antiproliferative activities.* Chem Commun (Camb), 2016. **52**(23): p. 4274-7.
123. Jagodinsky, J.C., et al., *Evaluation of fluorophore-tethered platinum complexes to monitor the fate of cisplatin analogs.* J. Biol. Inorg. Chem., 2015. **20**(7): p. 1081-1095.
124. Raza, M.K., et al., *Monofunctional BODIPY-appended imidazoplatin for cellular imaging and mitochondria-targeted photocytotoxicity.* Inorg. Chem. , 2017. **56**: p. 11019−11029.
125. Suss-Fink, G., *Arene ruthenium complexes as anticancer agents.* Dalton Trans., 2010. **39**(7): p. 1673-1688.
126. Nazarov, A.A., et al., *Anthracene-tethered ruthenium(II) arene complexes as tools to visualize the cellular localization of putative organometallic anticancer compounds.* Inorg. Chem. , 2012. **51**(6): p. 3633–3639.
127. Kumara, R.R., R. Ramesha, and J.G. Małeckib, *Synthesis and structure of arene ruthenium(II) benzhydrazone complexes: Antiproliferative activity, apoptosis induction and cell cycle analysis.* J. Organomet. Chem., 2018. **862**: p. 95-104.
128. Dondaine, L., et al., *Coumarin-phosphine-based smart probes for tracking biologically relevant metal complexes: from theoretical to biological investigations.* Eur. J. Inorg. Chem., 2016(4): p. 545-553.
129. Ma, W., et al., *Rhodamine-modified fluorescent half-sandwich iridium and ruthenium complexes: potential application as bioimaging and anticancer agents.* Dalton Trans., 2019. **48**(15): p. 4788-4793.

130. Harvey, P.D., et al., *Ruthenium and osmium complexes of phosphine-porphyrin derivatives as potential bimetallic theranostics: photophysical studies.* Organometallics, 2015. **34**(7): p. 1218–1227.
131. Desiatkina, O., et al., *Coumarin-tagged dinuclear trithiolato-bridged ruthenium(II)arene complexes: photophysical properties and antiparasitic activity.* ChemBioChem, 2020. **21**(19): p. 2818-2835.
132. Ulrich, G., R. Ziessel, and A. Harriman, *The chemistry of fluorescent BODPY dyes: versatility unsurpassed.* Angew. Chem., Int. Ed. , 2008. **47**(7): p. 1184−1201.
133. Yang, L., et al., *Some observations relating to the stability of the BODIPY fluorophore under acidic and basic conditions.* Dyes Pigm., 2011. **91**(2): p. 264-267.
134. Rumyantsev, E.V., S.N. Alyoshin, and Y.S. Marfin, *Kinetic study of Bodipy resistance to acids and alkalis: Stability ranges in aqueous and non-aqueous solutions.* Inorg. Chim. Acta, 2013. **408**: p. 181-185.
135. Boens, N., V. Leen, and W. Dehaen, *Fluorescent indicators based on BODIPY.* Chem. Soc. Rev., 2012. **41**(3): p. 1130-1172.
136. Goncalves, M.S., *Fluorescent labeling of biomolecules with organic probes.* Chem. Rev., 2009. **109**(1): p. 190-212.
137. Loudet, A. and K. Burgess, *BODIPY dyes and their derivatives: syntheses and spectroscopic properties* Chem. Rev., 2007. **107**(11): p. 4891−4932.
138. Alford, R., et al., *Toxicity of organic fluorophores used in molecular imaging: literature review.* Mol. Imaging, 2009. **8**(6): p. 341-354.
139. Zhang, S., et al., *A BODIPY-based fluorescent dye for mitochondria in living cells, with low cytotoxicity and high photostability.* Org. Biomol. Chem., 2013. **11**(4): p. 555-558.
140. Kowada, T., H. Maeda, and K. Kikuchi, *BODIPY-based probes for the fluorescence imaging of biomolecules in living cells.* Chem. Soc. Rev. , 2015. **44**: p. 4953−4972.
141. Raza, M.K., et al., *Pyriplatin-Boron-Dipyrromethene Conjugates for Imaging and Mitochondria-Targeted Photodynamic Therapy.* Inorg Chem, 2018. **57**(22): p. 14374-14385.
142. Mitra, K., et al., *BODIPY-Appended 2-(2-Pyridyl)benzimidazole Platinum(II) Catecholates for Mitochondria-Targeted Photocytotoxicity.* ChemMedChem, 2016. **11**(17): p. 1956-67.
143. Liu, Y., et al., *Near infrared BODIPY-platinum conjugates for imaging, photodynamic therapy and chemotherapy.* Dyes Pigm., 2017. **141**: p. 5-12.
144. Caffaro, C.E. and J.C. Boothroyd, *Evidence for host cells as the major contributor of lipids in the intravacuolar network of Toxoplasma-infected cells.* Eukaryot. Cell, 2011. **10**(8): p. 1095-1099.
145. Charron, A.J. and L.D. Sibley, *Host cells: mobilizable lipid resources for the intracellular parasite Toxoplasma gondii.* J Cell Sci, 2002. **115**(Pt 15): p. 3049-59.
146. Nolan, S.J., J.D. Romano, and I. Coppens, *Host lipid droplets: An important source of lipids salvaged by the intracellular parasite Toxoplasma gondii.* PLoS Pathog., 2017. **13**(6): p. e1006362.
147. Hu, X., D. Binns, and M.L. Reese, *The coccidian parasites Toxoplasma and Neospora dysregulate mammalian lipid droplet biogenesis.* J. Biol. Chem., 2017. **292**(26): p. 11009-11020.
148. Gomes, A.F., et al., *Toxoplasma gondii-skeletal muscle cells interaction increases lipid droplet biogenesis and positively modulates the production of IL-12, IFN-g and PGE2.* Parasit Vectors, 2014. **7**: p. 47.
149. Klein, A.V. and T.W. Hambley, *Platinum drug distribution in cancer cells and tumors.* Chem. Rev., 2009. **109**(10): p. 4911-4920.
150. Baruah, H., C.G. Barry, and U. Bierbach, *Platinum-intercalator conjugates: from DNA-targeted cisplatin derivatives to adenine binding complexes as potential modulators of gene regulation.* Curr Top Med Chem, 2004. **4**(15): p. 1537-1549.
151. Miller, M.A., et al., *Platinum compounds for high-resolution in vivo cancer imaging.* ChemMedChem, 2014. **9**: p. 1131−1135.

152. Zhou, Q.X., et al., *BODIPY-modified Ru(II) arene complex--a new ligand dissociation mechanism and a novel strategy to red shift the photoactivation wavelength of anticancer metallodrugs.* Dalton Trans., 2013. **42**(8): p. 2786-2791.
153. Bodio, E., et al., *Advances in Inorganic Chemistry, Chapter Six - Development of Trackable Anticancer Agents Based on Metal Complexes*, in *Insights from Imaging in Bioinorganic Chemistry*, R. van Eldik and C.D. Hubbard, Editors. 2016, Academic Press. p. 253-299.
154. Liu, Z., et al., *The potent oxidant anticancer activity of organoiridium catalysts.* Angew Chem Int Ed Engl, 2014. **53**(15): p. 3941-6.
155. Trommenschlager, A., et al., *Gold(I)-BODIPY-imidazole bimetallic complexes as new potential anti-inflammatory and anticancer trackable agents.* Dalton Trans. , 2017. **46**(25): p. 8051-8056.
156. Flores, O., et al., *In vitro and in vivo trackable titanocene-based complexes using optical imaging or SPECT.* Dalton Trans, 2017. **46**(42): p. 14548-14555.
157. Bhattacharyya, A., et al., *BODIPY appended copper(ii) complexes for cellular imaging and singlet oxygen mediated anticancer activity in visible light.* RSC Advances, 2016. **6**(106): p. 104474-104482.
158. Sun, T., et al., *Mitochondrial-localized fluorescent BODIPY-platinum conjugate.* ACS Med. Chem. Lett. , 2015. **6**: p. 430−433.
159. Ulrich, G. and R. Ziessel, *Convenient and efficient synthesis of functionalized oligopyridine ligands bearing accessory pyrromethene-BF2 fluorophores.* J. Org. Chem., 2004. **69**(6): p. 2070-2083.
160. Olmsted, J., *Calorimetric determinations of absolute fluorescence quantum yields.* J. Phys. Chem. , 1979. **83**(20): p. 2581–2584.
161. Madhu, S., et al., *Synthesis, X-ray structure, spectral and electrochemical properties of a b-meso covalently linked BODIPY–Ru(II) dipyrrin complex.* New J. Chem., 2014. **38**: p. 5551-5558.
162. Paitandi, R.P., et al., *Pyrazole appended quinoline-BODIPY based arene ruthenium complexes: their anticancer activity and potential applications in cellular imaging.* Dalton Trans., 2018. **47**(48): p. 17500-17514.
163. Wang, T.J., et al., *Two novel BODIPY-Ru(II) arene dyads enabling effective photo-inactivation against cancer cells.* Dalton Trans., 2015. **44**(28): p. 12726-12734.
164. Zimbron, J.M., et al., *Synthesis, photophysical properties, and living cell imaging of theranostic half-sandwich iridium−4,4-Difluoro-4-bora-3a,4a-diaza-s-indacene (BODIPY) dyads.* Organometallics, 2017. **36**: p. 3435−3442.
165. Paitandi, R.P., et al., *Anticancer activity of iridium(III) complexes based on a pyrazole-appended quinoline-based BODIPY.* Inorg. Chem., 2017. **56**(20): p. 12232-12247.
166. Juris, A., et al., *Ru(II) polypyridine complexes: photophysics, photochemistry, eletrochemistry, and chemiluminescence.* Coord. Chem. Rev., 1988. **84**: p. 85–277.
167. Galletta, M., et al., *Absorption spectra, photophysical properties, and redox behavior of ruthenium(II) polypyridine complexes containing accessory dipyrromethene−BF2 chromophores.* J. Phys. Chem. A, 2006. **110**(13): p. 4348–4358.
168. Bennett, M.A. and A.K. Smith, *Arene Ruthenium(Ii) Complexes Formed by Dehydrogenation of Cyclohexadienes with Ruthenium(Iii) Trichloride.* J. Chem. Soc. Dalton Trans., 1974(2): p. 233-241.
169. Wood, T.E. and A. Thompson, *Advances in the chemistry of dipyrrins and their complexes.* Chem Rev, 2007. **107**(5): p. 1831-61.
170. Krumova, K. and G. Cosa, *Bodipy dyes with tunable redox potentials and functional groups for further tethering: preparation, electrochemical, and spectroscopic characterization.* J. Am. Chem. Soc., 2010. **132**(49): p. 17560-17569.
171. Omel'kov, A.V., et al., *Depth-dependent investigation of the apolar zone of lipid membranes using a series of fluorescent probes, Me-4-BODIPY-8-labeled phosphatidylcholines.* Russ. J. Bioorg. Chem., 2007. **33**(5): p. 505-510.
172. Boldyrev, I.A. and J.G. Molotkovsky, *A synthesis and properties of new 4,4-difluoro-3a,4a-diaza-s-indacene (BODIPY)-labeled lipids.* Russ. J. Bioorg. Chem., 2006. **32**(1): p. 78-83.

173. Boldyrev, I.A., et al., *New BODIPY lipid probes for fluorescence studies of membranes.* J. Lipid Res., 2007. **48**(7): p. 1518-1532.
174. Paunescu, E., et al., *Varying the metal to ethacrynic acid ratio in ruthenium(ii)/osmium(ii)-p-cymene conjugates.* J. Inorg. Biochem., 2017. **175**: p. 198-207.
175. Hanessian, S., et al., *Synthesis of chemically functionalized superparamagnetic nanoparticles as delivery vectors for chemotherapeutic drugs.* Bioorg. Med. Chem., 2008. **16**(6): p. 2921-2931.
176. Ceulemans, M., et al., *Gadolinium(III)-DOTA complex functionalized with BODIPY as a potential bimodal contrast agent for MRI and optical imaging.* Inorganics, 2015. **3**(4): p. 516-533.
177. Sohail, A., et al., *The environment shapes the inner vestibule of LeuT.* Plos Comput. Biol., 2016. **12**(11): p. e1005197.
178. Kue, C.S., et al., *Recent strategies to improve boron dipyrromethene (BODIPY) for photodynamic cancer therapy: an updated review.* Photochem Photobiol Sci, 2018. **17**(11): p. 1691-1708.
179. Cui, A., et al., *Synthesis, spectral properties and photostability of novel boron–dipyrromethene dyes.* J. Photochem. Photobiol. A, 2007. **186**(1): p. 85–92.
180. Wagner, R.W. and J.S. Lindsey, *A molecular photonic wire.* J. Am. Chem. Soc., 1994. **116**(21): p. 9759–9760.
181. Brückner, C., et al., *Synthesis of meso-phenyl-4,6-dipyrrins, preparation of their Cu(II), Ni(II), and Zn(II) chelates, and structural characterization of bis[meso-phenyl-4,6-dipyrrinato]Ni(II).* Can. J. Chem., 1996. **74**: p. 2182-2193.
182. Pakhomov, A.A., et al., *Synthesis, crystal structure and optical properties of a new meso-acrylate BODIPY dye.* Mendeleev Commun., 2016. **26**(3): p. 196-198.
183. Shi, W.-J., et al., *A BODIPY-based "OFF-ON" fluorescent probe for fast and selective detection of hypochlorite in living cells.* Dyes Pigm., 2019. **170**: p. 107566.
184. Matarranz, B., et al., *Self-Assembly of a Carboxyl-Functionalized BODIPY Dye via Hydrogen Bonding.* Crystals, 2018. **8**(11): p. 436.
185. Marfin, Y.S., et al., *Effects of Concentration on Aggregation of BODIPY-Based Fluorescent Dyes Solution.* J Fluoresc, 2020. **30**(6): p. 1611-1621.
186. Desiatkina, O., et al., *Synthesis and antiparasitic activity of new conjugates - organic drugs tethered to trithiolato-bridged dinuclear ruthenium(II)–arene complexes.* Inorganics, 2021. **9**(8): p. 59.
187. Erxleben, A., *Mitochondria-Targeting Anticancer Metal Complexes.* Curr Med Chem, 2019. **26**(4): p. 694-728.
188. Guan, R., et al., *Metal complexes for mitochondrial bioimaging.* J. Inorg. Biochem., 2020. **204**: p. 110985.
189. Torgerson, P.R., et al., *World Health Organization estimates of the global and regional disease burden of 11 foodborne parasitic diseases, 2010: A data synthesis.* PLoS Med., 2015. **12**(12): p. e1001920.
190. Meireles, L.R., et al., *Human toxoplasmosis outbreaks and the agent infecting form. Findings from a systematic review.* Rev. Inst. Med. Trop. Sao Paulo, 2015. **57**(5): p. 369-376.
191. Kamerkar, S. and P.H. Davis, *Toxoplasma on the brain: understanding host-pathogen interactions in chronic CNS infection.* J. Parasitol. Res., 2012. **2012**: p. 589295.
192. Neville, A.J., et al., *Clinically available medicines demonstrating anti-toxoplasma activity.* Antimicrob. Agents Chemother., 2015. **59**(12): p. 7161-7169.
193. Vargas-Villavicencio, J.A., A. Besne-Merida, and D. Correa, *Vertical transmission and fetal damage in animal models of congenital toxoplasmosis: A systematic review.* Vet. Parasitol., 2016. **223**: p. 195-204.
194. Alday, P.H. and J.S. Doggett, *Drugs in development for toxoplasmosis: advances, challenges, and current status.* Drug Des., Dev. Ther., 2017. **11**: p. 273-293.
195. Konstantinovic, N., et al., *Treatment of toxoplasmosis: Current options and future perspectives.* Food Waterborne Parasitol., 2019. **15**: p. e00036.

196. Eyles, D.E., *The present status of the chemotherapy of toxoplasmosis.* Am. J. Trop. Med. Hyg., 1953. **2**(3): p. 429-444.
197. Montazeri, M., et al., *A systematic review of In vitro and In vivo activities of anti-toxoplasma drugs and compounds (2006-2016).* Front. Microbiol., 2017. **8**: p. 25.
198. Dittmar, A.J., A.A. Drozda, and I.J. Blader, *Drug repurposing screening identifies novel compounds that effectively inhibit Toxoplasma gondii growth.* mSphere, 2016. **1**(2).
199. Radke, J.B., et al., *Evaluation of current and emerging antimalarial medicines for Inhibition of Toxoplasma gondii growth in vitro.* ACS Infect. Dis., 2018. **4**(8): p. 1264-1274.
200. Sibley, L.D., *Toxoplasma gondii: perfecting an intracellular life style.* Traffic, 2003. **4**(9): p. 581-586.
201. Coppens, I., *Exploitation of auxotrophies and metabolic defects in Toxoplasma as therapeutic approaches.* Int. J. Parasitol., 2014. **44**(2): p. 109-120.
202. Hammarton, T.C., J.C. Mottram, and C. Doerig, *The cell cycle of parasitic protozoa: potential for chemotherapeutic exploitation.* Prog. Cell. Cycle Res., 2003. **5**: p. 91-101.
203. Suprabhat Mukherjee, N.M., Prajna Gayen, Priya Roy, Santi P Sinha Babu, *Metabolic inhibitors as antiparasitic drugs: Pharmacological, biochemical and molecular perspectives* Curr. Drug. Metab., 2016. **17**(10): p. 937-970.
204. de Koning, H.P., D.J. Bridges, and R.J. Burchmore, *Purine and pyrimidine transport in pathogenic protozoa: from biology to therapy.* FEMS Microbiol. Rev., 2005. **29**(5): p. 987-1020.
205. Berg, M., et al., *Inhibitors of the purine salvage pathway: A valuable approach for antiprotozoal chemotherapy?* Curr. Med. Chem., 2010. **17**(23): p. 2456-2481.
206. Datta, A.K., R. Datta, and B. Sen, *Antiparasitic chemotherapy: tinkering with the purine salvage pathway.* Adv. Exp. Med. Biol., 2008. **625**: p. 116-132.
207. el Kouni, M.H., *Potential chemotherapeutic targets in the purine metabolism of parasites.* Pharmacol. Ther., 2003. **99**(3): p. 283-309.
208. Chaudhary, K., B.A. Fox, and D.J. Bzik, *Comparative Aspects of Nucleotide and Amino Acid Metabolism in Toxoplasma gondii and Other Apicomplexa*, in *Toxoplasma Gondii. The Model Apicomplexan - Perspectives and Methods*, L.M. Weiss and K. Kim, Editors. 2014, Academic Press. p. 663-706.
209. el Kouni, M.H., *Adenosine metabolism in Toxoplasma gondii: potential targets for chemotherapy.* Curr. Pharm. Des., 2007. **13**(6): p. 581-597.
210. Kim, Y.A., et al., *Synthesis, biological evaluation and molecular modeling studies of N6-benzyladenosine analogues as potential anti-toxoplasma agents.* Biochem. Pharmacol., 2007. **73**(10): p. 1558-1572.
211. Iltzsch, M.H., et al., *Structure-activity relationship for the binding of nucleoside ligands to adenosine kinase from Toxoplasma gondii.* Biochem. Pharmacol., 1995. **49**(10): p. 1501-1512.
212. Kim, Y.A., et al., *Structure-activity relationships of carbocyclic 6-benzylthioinosine analogues as subversive substrates of Toxoplasma gondii adenosine kinase.* Bioorg. Med. Chem., 2010. **18**(10): p. 3403-3412.
213. Al Safarjalani, O.N., F.N. Naguib, and M.H. El Kouni, *Uptake of nitrobenzylthioinosine and purine beta-L-nucleosides by intracellular Toxoplasma gondii.* Antimicrob. Agents Chemother., 2003. **47**(10): p. 3247-3251.
214. Sullivan, W.J., Jr., et al., *IMP dehydrogenase from the protozoan parasite Toxoplasma gondii.* Antimicrob. Agents Chemother., 2005. **49**(6): p. 2172-2179.
215. Luft, B.J., *Potent in vivo activity of arprinocid, a purine analogue, against murine toxoplasmosis.* J. Infect. Dis., 1986. **154**(4): p. 692-694.
216. Gherardi, A. and M.E. Sarciron, *Molecules targeting the purine salvage pathway in apicomplexan parasites.* Trends Parasitol., 2007. **23**(8): p. 384-389.
217. Wang, Y., et al., *3-Methyladenine blocks Toxoplasma gondii division prior to centrosome replication.* Mol. Biochem. Parasitol., 2010. **173**(2): p. 142-153.
218. Krug, E.C., J.J. Marr, and R.L. Berens, *Purine metabolism in Toxoplasma gondii.* J. Biol. Chem., 1989. **264**(18): p. 10601-10607.

219. Chaudhary, K., et al., *Purine salvage pathways in the apicomplexan parasite Toxoplasma gondii.* J. Biol. Chem., 2004. **279**(30): p. 31221-31227.
220. Perrotto, J., D.B. Keister, and A.H. Gelderman, *Incorporation of precursors into Toxoplasma DNA.* J. Protozool., 1971. **18**(3): p. 470-473.
221. Fox, B.A. and D.J. Bzik, *The Model Apicomplexan - Perspectives and Methods. Chapter 9 - Biochemistry and metabolism of Toxoplasma gondii: purine and pyrimidine acquisition in Toxoplasma gondii and other Apicomplexa*, in *Toxoplasma gondii (Third Edition)*. 2020. p. 397-449.
222. Fox, B.A. and D.J. Bzik, *De novo pyrimidine biosynthesis is required for virulence of Toxoplasma gondii.* Nature, 2002. **415**(6874): p. 926-929.
223. Fox, B.A. and D.J. Bzik, *Avirulent uracil auxotrophs based on disruption of orotidine-5'-monophosphate decarboxylase elicit protective immunity to Toxoplasma gondii.* Infect. Immun., 2010. **78**(9): p. 3744-3752.
224. Schwartzman, J.D. and E.R. Pfefferkorn, *Pyrimidine synthesis by intracellular Toxoplasma gondii.* J. Parasitol., 1981. **67**(2): p. 150-158.
225. Iltzsch, M.H., *Pyrimidine salvage pathways in Toxoplasma gondii.* J. Eukaryot Microbiol., 1993. **40**(1): p. 24-28.
226. Luengo, A., D.Y. Gui, and M.G. Vander Heiden, *Targeting Metabolism for Cancer Therapy.* Cell Chem. Biol., 2017. **24**(9): p. 1161-1180.
227. Seley-Radtke, K.L. and M.K. Yates, *The evolution of nucleoside analogue antivirals: A review for chemists and non-chemists. Part 1: Early structural modifications to the nucleoside scaffold.* Antiviral Res., 2018. **154**: p. 66–86.
228. Yates, M.K. and K.L. Seley-Radtke, *The evolution of antiviral nucleoside analogues: A review for chemists and non-chemists. Part II: Complex modifications to the nucleoside scaffold.* Antiviral Res., 2019. **162**: p. 5-21.
229. Azzouz, S. and P. Lawton, *In vitro effects of purine and pyrimidine analogues on Leishmania donovani and Leishmania infantum promastigotes and intracellular amastigotes.* Acta Parasitol., 2017. **62**(3): p. 582-588.
230. Al Safarjalani, O.N., et al., *Carbocyclic 6-benzylthioinosine analogues as subversive substrates of Toxoplasma gondii adenosine kinase: biological activities and selective toxicities.* Biochem Pharmacol, 2010. **80**(7): p. 955-63.
231. Donaldson, T.M., et al., *Inhibition and structure of Toxoplasma gondii purine nucleoside phosphorylase.* Eukaryot Cell, 2014. **13**(5): p. 572-9.
232. Anthony, E.J., et al., *Metallodrugs are unique: Opportunities and challenges of discovery and development* Chem. Sci., 2020. **11**: p. 12888-12917.
233. Loginova, N.V., et al., *Metal complexes as promising agents for biomedical applications.* Curr. Med. Chem. , 2020. **27**(31): p. 5213-5249.
234. Ong, Y.C. and G. Gasser, *Organometallic compounds in drug discovery: Past, present and future.* Drug Discovery Today: Technol., 2019. In Press, Corrected Proof.
235. Konkankit, C.C., et al., *Anticancer activity of complexes of the third row transition metals, rhenium, osmium, and iridium.* Dalton Trans., 2018. **47**(30): p. 9934-9974.
236. Simpson, P.V., et al., *Metal-based antitumor compounds: beyond cisplatin.* Future Med. Chem., 2019. **11**(2): p. 119-135.
237. Gasser, G., I. Ott, and N. Metzler-Nolte, *Organometallic anticancer compounds.* J. Med. Chem., 2011. **54**(1): p. 3-25.
238. Frei, A., et al., *Metal complexes as a promising source for new antibiotics.* Chem. Sci., 2020. **11**: p. 2627-2639.
239. Frei, A., *Metal complexes, an untapped source of antibiotic potential?* Antibiotics, 2020. **9**(2): p. 90.
240. Sierra, M.A., L. Casarrubios, and M.C. de la Torre, *Bio-organometallic derivatives of antibacterial drugs.* Chem. Eur. J., 2019. **25**(30): p. 7232-7242.
241. Sousa, E.H.S., et al., *Potential therapeutic approaches for a sleeping pathogen: tuberculosis a case for bioinorganic chemistry.* J. Biol. Inorg. Chem., 2020. **25**: p. 685–704.

242. Sovari, S.N. and F. Zobi, *Recent studies on the antimicrobial activity of transition metal complexes of groups 6–12.* Chemistry, 2020. **2**(2): p. 418-452.
243. Li, F., J.G. Collins, and F.R. Keene, *Ruthenium complexes as antimicrobial agents.* Chem. Soc. Rev., 2015. **44**: p. 2529-2542.
244. Mbaba, M., T.M. Golding, and G.S. Smith, *Recent advances in the biological investigation of organometallic platinum-group metal (Ir, Ru, Rh, Os, Pd, Pt) complexes as antimalarial agents.* Molecules, 2020. **25**(22): p. 5276.
245. Navarro, M., et al., *Metallodrugs for the treatment of Trypanosomatid diseases: recent advances and new insights.* Curr. Pharm. Des., 2021. **27**(15): p. 1763-1789.
246. Adams, M., et al., *The synthesis and antiparasitic activity of aryl- and ferrocenyl-derived thiosemicarbazone ruthenium(II)-arene complexes.* Dalton Trans., 2013. **42**(13): p. 4677-4685.
247. Fernandez, M., et al., *Novel ruthenium(II) cyclopentadienyl thiosemicarbazone compounds with antiproliferative activity on pathogenic trypanosomatid parasites.* J. Inorg. Biochem., 2015. **153**: p. 306-314.
248. Kenny, R.G. and C.J. Marmion, *Toward multi-targeted platinum and ruthenium drugs - A new paradigm in cancer drug treatment regimens?* Chem. Rev., 2019. **119**(2): p. 1058-1137.
249. Zhao, Y., et al., *Medicinal Chemistry, Edited by Peter J. Sadler, Rudi van Eldik, Chapter Eight - Pharmacophore conjugation strategy for multi-targeting metal-based anticancer complexes.* Advances in Inorganic Chemistry, 2020. **75**: p. 257-285.
250. Lynam, J.M., *Nucleobase-containing transition metal complexes as building blocks for biological markers and supramolecular structures* Dalton Trans., 2008: p. 4067-4078.
251. Kowalski, K., *Organometallic nucleosides - Synthesis, transformations, and applications* Coord. Chem. Rev., 2021. **432**: p. 213705
252. Kowalski, K., *Ferrocenyl-nucleobase complexes: Synthesis, chemistry and applications.* Coord. Chem. Rev., 2016. **317**: p. 132-156.
253. Sce, F., et al., *Supramolecular architectures based on p-cymene/ruthenium complexes functionalized with nucleobases.* CrystEngComm, 2017. **19**: p. 6039-6048
254. Singh, A., et al., *Ferrocene-appended pharmacophores: an exciting approach for modulating the biological potential of organic scaffolds.* Dalton Trans., 2019. **48**(9): p. 2840-2860.
255. Daniluk, M., et al., *Ferrocene amino acid ester uracil conjugates: synthesis, structure, electrochemistry and antimicrobial evaluation.* ChemistrySelect, 2019. **4**(37): p. 11130-11135.
256. James, P., et al., *Enantioselective synthesis of ferrocenyl nucleoside analogues with apoptosis-inducing activity.* Org. Lett., 2006. **8**(13): p. 2763-2766.
257. Florindo, P.R., et al., *Organoruthenium(II) nucleoside conjugates as colon cytotoxic agents.* New J. Chem., 2019. **43**: p. 1195-1205.
258. Leitao, M.I.P.S., F. Herrera, and A. Petronilho, *N-Heterocyclic Carbenes Derived from Guanosine: Synthesis and Evidences of Their Antiproliferative Activity.* ACS Omega, 2018. **3**(11): p. 15653-15656.
259. Collado, A., M. Gómez-Gallego, and M.A. Sierra, *Nucleobases Having M–C Bonds: An Emerging Bio-Organometallic Field.* Eur. J. Org. Chem., 2018. **2018**(14): p. 1617–1623.
260. Kaczmarek, R., et al., *Organometallic nucleosides: Synthesis and biological evaluation of substituted dicobalt hexacarbonyl 2'-deoxy-5-oxopropynyluridines.* ChemistryOpen, 2018. **7**(3): p. 237-247.
261. Nguyen, H.V., et al., *Organometallic nucleoside analogues with ferrocenyl linker groups: synthesis and cancer cell line studies.* J. Med. Chem., 2014. **57**(13): p. 5817-5822.
262. Ismail, M.K., et al., *Effect of regiochemistry and methylation on the anticancer activity of a ferrocene-containing organometallic nucleoside analogue.* ChemBioChem, 2020. **21**(17): p. 2487-2494.
263. Skiba, J., et al., *Metallocene-uracil conjugates: Synthesis and biological evaluation of novel mono-, di- and tri-nuclear systems.* J. Organomet. Chem., 2015. **782**: p. 52-61.

264. Singh, A., et al., *1H-1,2,3-triazole-tethered uracil-ferrocene and uracil-ferrocenylchalcone conjugates: Synthesis and antitubercular evaluation.* Chem. Biol. Drug Des., 2017. **89**(6): p. 856-861.
265. Rep, V., et al., *Purine and purine isostere derivatives of ferrocene: An evaluation of ADME, antitumor and electrochemical properties.* Molecules, 2020. **25**(7): p. 1570.
266. Djaković, S., et al., *Synthesis and biological evaluations of mono- and bis-ferrocene uracil derivatives.* Appl. Organomet. Chem., 2020. **35**(1).
267. Kowalski, K., et al., *Cymantrene, cyrhetrene and ferrocene nucleobase conjugates: Synthesis, structure, computational study, electrochemistry and antitrypanosomal activity.* ChemPlusChem, 2017. **82**(2): p. 303-314.
268. Gramni, L., et al., *Anticancer evaluation of ruthenium(III) complexes with N-donor ligands tethered to coumarin or uracil moieties.* Inorg. Chim. Acta, 2015. **492**: p. 98-107.
269. Riccardi, C., et al., *RuIII complexes for anticancer therapy: The importance of being nucleolipidic* Eur. J. Org. Chem., 2017. **2017**(7): p. 1100-1119.
270. Correa, R.S., et al., *Ru(II) complexes containing uracil nucleobase analogs with cytotoxicity against tumor cells.* J. Inorg. Biochem., 2019. **198**: p. 110751.
271. Bomfim, L.M., et al., *Ruthenium(II) complexes with 6-methyl-2-thiouracil selectively reduce cell proliferation, cause DNA double-strand break and trigger caspase-mediated apoptosis through JNK/p38 pathways in human acute promyelocytic leukemia cells.* Sci. Rep., 2019. **9**(1): p. 11483.
272. Silva, V.R., et al., *A ruthenium-based 5-fluorouracil complex with enhanced cytotoxicity and apoptosis induction action in HCT116 cells.* Sci. Rep., 2018. **8**(1): p. 288.
273. Liu, K.-G., et al., *Arene-ruthenium(II) complexes containing 5-fluorouracil-1-methyl isonicotinate: Synthesis and characterization of their anticancer activity.* Inorg. Chim. Acta, 2012. **388**: p. 78-83.
274. Li, Z.J., et al., *Two half-sandwiched ruthenium (II) compounds containing 5-fluorouracil derivatives: synthesis and study of DNA intercalation.* PLoS One, 2015. **10**(3): p. e0120211.
275. Gonchar, M.R., et al., *Ruthenium(II)–arene and triruthenium-carbonyl cluster complexes with new water-soluble phopsphites based on glucose: Synthesis, characterization and antiproliferative activity.* J. Organomet. Chem., 2020. **919**: p. 121312.
276. Florindo, P.R., et al., *New [(η5-C5H5)Ru(N–N)(PPh3)][PF6] compounds: colon anticancer activity and GLUT-mediated cellular uptake of carbohydrate-appended complexes.* Dalton Trans., 2016. **45**: p. 11926–11930.
277. Lee, S.Y., C.Y. Kim, and T.G. Nam, *Ruthenium complexes as anticancer agents: a brief history and perspectives.* Drug Des., Dev. Ther., 2020. **14**: p. 5375-5392.
278. Farrer, N.J. and D.M. Griffith, *Exploiting azide-alkyne click chemistry in the synthesis, tracking and targeting of platinum anticancer complexes.* Curr. Opin. Chem. Biol., 2020. **55**: p. 59-68.
279. Kroll, A., et al., *A luminescent ruthenium azide complex as a substrate for copper-catalyzed click reactions.* Eur. J. Inorg. Chem., 2014(22): p. 3462-3466.
280. Mede, T., M. Jager, and U.S. Schubert, *"Chemistry-on-the-complex": functional Ru(II) polypyridyl-type sensitizers as divergent building blocks.* Chem. Soc. Rev., 2018. **47**(20): p. 7577-7627.
281. Cisnetti, F., C. Gibard, and A. Gautier, *Post-functionalization of metal–NHC complexes: A useful toolbox for bioorganometallic chemistry (and beyond)?* J. Organomet. Chem., 2015. **782**: p. 22-30.
282. Liang, L. and D. Astruc, *The copper(I)-catalyzed alkyne-azide cycloaddition (CuAAC) "click" reaction and its applications. An overview.* Coord. Chem. Rev., 2011. **255**(23–24): p. 2933-2945.
283. Meldal, M. and C.W. Tornoe, *Cu-catalyzed azide-alkyne cycloaddition.* Chem. Rev., 2008. **108**(8): p. 2952-3015.
284. Kolb, H.C. and K.B. Sharpless, *The growing impact of click chemistry on drug discovery.* Drug Discov. Today, 2003. **8**(24): p. 1128-1137.

285. Zhang, W.Y., et al., *Strategies for conjugating iridium(III) anticancer complexes to targeting peptides via copper-free click chemistry.* Inorg. Chim. Acta, 2020. **503**: p. 119396.
286. Zabarska, N., A. Stumper, and S. Rau, *CuAAC click reactions for the design of multifunctional luminescent ruthenium complexes.* Dalton Trans., 2016. **45**(6): p. 2338-2351.
287. Wang, X., et al., *Imaging of a clickable anticancer iridium catalyst.* J. Inorg. Biochem., 2018. **180**: p. 179-185.
288. Ganesh, V., et al., *10 years of click chemistry: synthesis and applications of ferrocene-derived triazoles.* Chem. Asian J., 2011. **6**(10): p. 2670-2694.
289. Singh, G., et al., *A strategic approach to the synthesis of ferrocene appended chalcone linked triazole allied organosilatranes: Antibacterial, antifungal, antiparasitic and antioxidant studies.* Bioorg. Med. Chem., 2019. **27**(1): p. 188-195.
290. Kumar, K., et al., *Azide-alkyne cycloaddition en route towards 1H-1,2,3-triazole-tethered beta-lactam-ferrocene and beta-lactam-ferrocenylchalcone conjugates: synthesis and in vitro anti-tubercular evaluation.* Dalton Trans., 2013. **42**(5): p. 1492-1500.
291. Singh, A., et al., *Azide-alkyne cycloaddition en route to 4-aminoquinoline-ferrocenylchalcone conjugates: synthesis and anti-TB evaluation.* Future Med. Chem., 2017. **9**(15): p. 1701-1708.
292. Karmis, R.E., et al., *Luminescent iridium(III) complexes of N-heterocyclic carbene ligands prepared using the 'click reaction'.* Dalton Trans., 2019. **48**(27): p. 9998-10010.
293. Mandal, S., et al., *Synthesis of a sugar-functionalized iridium complex and its application as a fluorescent lectin sensor.* Tetrahedron Lett., 2012. **53**(30): p. 3915-3918.
294. Păunescu, E., et al., *A versatile access to new halogenated 7-azidocoumarins for photoaffinity labeling: Synthesis and photophysical properties.* Dyes Pigm., 2011. **91**(3): p. 427-434.
295. Kitamura, M., et al., *A reagent for safe and efficient diazo-transfer to primary amines: 2-azido-1,3-dimethylimidazolinium hexafluorophosphate.* Org. Biomol. Chem., 2014. **12**(25): p. 4397-4406.
296. Beckmann, H.S. and V. Wittmann, *One-pot procedure for diazo transfer and azide-alkyne cycloaddition: triazole linkages from amines.* Org. Lett., 2007. **9**(1): p. 1-4.
297. Roy, B., et al., *Design, synthesis and RNase A inhibition activity of catechin and epicatechin and nucleobase chimeric molecules.* Bioorg. Med. Chem. Lett., 2008. **18**(20): p. 5411-4.
298. Vo, D.D. and M. Duca, *Drug Target miRNA: Methods and Protocols*. 2017, New York: Springer 137–154.
299. Krim, J., M. Taourirte, and J.W. Engels, *Synthesis of 1,4-disubstituted mono and bis-triazolocarbo-acyclonucleoside analogues of 9-(4-hydroxybutyl)guanine by Cu(I)-catalyzed click azide-alkyne cycloaddition.* Molecules, 2011. **17**(1): p. 179-190.
300. Blume, M. and F. Seeber, *Metabolic interactions between Toxoplasma gondii and its host.* F1000Res., 2018. **Faculty Rev-1719**(7).
301. Pernas, L., et al., *Mitochondria restrict growth of the intracellular parasite Toxoplasma gondii by limiting its uptake of fatty acids.* Cell Metab., 2018. **27**(4): p. 886-897.e4.
302. Nolan, S.J., et al., *Novel approaches to kill Toxoplasma gondii by exploiting the uncontrolled uptake of unsaturated fatty acids and vulnerability to lipid storage inhibition of the parasite.* Antimicrob. Agents Chemother., 2018. **62**(10).
303. Mazumdar, J., et al., *Apicoplast fatty acid synthesis is essential for organelle biogenesis and parasite survival in Toxoplasma gondii.* Proc. Natl. Acad. Sci., 2006. **103**(35): p. 13192-13197.
304. Coppens, I., *Contribution of host lipids to Toxoplasma pathogenesis.* Cell Microbiol., 2006. **8**(1): p. 1-9.
305. Bisanz, C., et al., *Toxoplasma gondii acyl-lipid metabolism: de novo synthesis from apicoplast-generated fatty acids versus scavenging of host cell precursors.* Biochem. J., 2006. **394**(Pt 1): p. 197-205.

306. Ramakrishnan, S., et al., *The intracellular parasite Toxoplasma gondii depends on the synthesis of long-chain and very long-chain unsaturated fatty acids not supplied by the host cell.* Mol. Microbiol., 2015. **97**(1): p. 64-76.
307. Liang, X., et al., *Acquisition of exogenous fatty acids renders apicoplast-based biosynthesis dispensable in tachyzoites of Toxoplasma.* J. Biol. Chem., 2020. **295**(22): p. 7743-7752.
308. Kim, J., et al., *Polymeric biomaterials for the delivery of platinum-based anticancer drugs.* Biomater. Sci., 2015. **3**(7): p. 1002-1017.
309. Stathopoulos, G.P. and T. Boulikas, *Lipoplatin formulation review article.* J. Drug Deliv., 2012. **2012**: p. 581363.
310. Boulikas, T., *Clinical overview on Lipoplatin: a successful liposomal formulation of cisplatin.* Expert Opin. Investig. Drugs, 2009. **18**(8): p. 1197-1218.
311. Dragovich, T., et al., *A Phase 2 trial of the liposomal DACH platinum L-NDDP in patients with therapy-refractory advanced colorectal cancer.* Cancer Chemother. Pharmacol., 2006. **58**(6): p. 759-764.
312. Duan, X., et al., *Nanoparticle formulations of cisplatin for cancer therapy.* Wiley Interdiscip. Rev.: Nanomed. Nanobiotechnol., 2016. **8**(5): p. 776-791.
313. Najjar, A., N. Rajabi, and R. Karaman, *Recent Approaches to Platinum(IV) Prodrugs: A Variety of Strategies for Enhanced Delivery and Efficacy.* Curr. Pharm. Des., 2017. **23**(16): p. 2366-2376.
314. Deo, K.M., et al., *Synthesis, characterisation and influence of lipophilicity on cellular accumulation and cytotoxicity of unconventional platinum(iv) prodrugs as potent anticancer agents.* Dalton Trans., 2019. **48**(46): p. 17228-17240.
315. Jayawardhana, A., et al., *Fatty acid-like Pt(IV) prodrugs overcome cisplatin resistance in ovarian cancer by harnessing CD36.* Chem. Commun., 2020. **56**(73): p. 10706-10709.
316. Ratzon, E., et al., *Platinum(IV)-fatty acid conjugates overcome inherently and acquired Cisplatin resistant cancer cell lines: an in-vitro study.* BMC Cancer, 2016. **16**: p. 140.
317. Chen, Q., et al., *Platinum(IV) prodrugs with long lipid chains for drug delivery and overcoming cisplatin resistance.* Chem. Commun., 2018. **54**(42): p. 5369-5372.
318. Stilgenbauer, M., et al., *A spermine-conjugated lipophilic Pt(IV) prodrug designed to eliminate cancer stem cells in ovarian cancer.* Chem. Commun., 2019. **55**(43): p. 6106-6109.
319. Gabano, E., et al., *An unsymmetric cisplatin-based Pt(IV) derivative containing 2-(2-propynyl)octanoate: a very efficient multi-action antitumor prodrug candidate.* Dalton Trans., 2017. **46**(41): p. 14174-14185.
320. Fujiyama, S., et al., *Phase I clinical study of a novel lipophilic platinum complex (SM-11355) in patients with hepatocellular carcinoma refractory to cisplatin/lipiodol.* Br. J. Cancer, 2003. **89**(9): p. 1614-1619.
321. Okusaka, T., H. Kasugai, and H. Ishii, *A randomized phase II trial of intra-arterial chemotherapy using a novel lipophilic platinum derivative (SM-11355) in comparison with Zinostatin Stimalamer in patients with hepatocellular carcinoma.* J. Clin. Oncol., 2009. **27**(15S): p. 4583.
322. Okusaka, T., et al., *A randomized phase II trial of intra-arterial chemotherapy using SM-11355 (Miriplatin) for hepatocellular carcinoma.* Invest. New Drugs, 2012. **30**(5): p. 2015–2025.
323. Zheng, Y.R., et al., *Pt(IV) prodrugs designed to bind non-covalently to human serum albumin for drug delivery.* J. Am. Chem. Soc., 2014. **136**(24): p. 8790-8798.
324. Novohradsky, V., et al., *Epigenetic and antitumor effects of platinum(IV)-octanoato conjugates.* Sci. Rep., 2017. **7**: p. 3751.
325. Clavel, C.M., et al., *Thermoresponsive organometallic arene ruthenium complexes for tumour targeting.* Chem. Sci., 2014. **5**: p. 1097-1101.
326. Paunescu, E., et al., *Anticancer organometallic osmium(II)-p-cymene complexes.* ChemMedChem, 2015. **10**(9): p. 1539-1547.
327. Kilpin, K.J., et al., *Ruthenium(II) and osmium(II) 1,2,3-triazolylidene organometallics: a preliminary investigation into the biological activity of 'click' carbene complexes.* Dalton Trans., 2014. **43**(3): p. 1443-1448.

328. Süss-Fink, G., et al., *Synthesis and anticancer activity of long-chain isonicotinic ester ligand-containing arene ruthenium complexes and nanoparticles.* J. Clust. Sci., 2010. **21**: p. 313–324.
329. Stíbal, D., et al., *Dinuclear arene ruthenium thiolato complexes with fluorous side-chains.* Inorg. Chim. Acta, 2016. **444**: p. 51-55.
330. Savino, S., et al., *Multi-acting mitochondria-targeted platinum(IV) prodrugs of kiteplatin with alpha-Lipoic Acid in the axial positions.* Int. J. Mol. Sci., 2018. **19**(7): p. 2050.
331. Wang, M.-M., et al., *Unveiling the anti-cancer mechanism for half sandwich and cyclometalated Ir(III)-based complexes with functionalized a-lipoic acid.* RSC Adv., 2020. **10**: p. 5392-5398
332. Riccardi, C., et al., *"Dressing up" an Old Drug: An Aminoacyl Lipid for the Functionalization of Ru(III)-Based Anticancer Agents.* ACS Biomater. Sci. Eng., 2018. **4**(1): p. 163-174.
333. Vaccaro, M., et al., *Lipid based nanovectors containing ruthenium complexes: a potential route in cancer therapy.* Chem. Commun., 2009(11): p. 1404-1406.
334. Hartinger, C.G., N. Metzler-Nolte, and P.J. Dyson, *Challenges and opportunities in the development of organometallic anticancer drugs.* Organometallics, 2012. **31**(16): p. 5677–5685.
335. Lin, K., et al., *Applications of ruthenium complex in tumor diagnosis and therapy.* Front. Pharmacol., 2018. **9**: p. 1323.
336. Lazarević, T., A. Rilak, and Ž.D. Bugarčić, *Platinum, palladium, gold and ruthenium complexes as anticancer agents: Current clinical uses, cytotoxicity studies and future perspectives.* Eur. J. Med. Chem., 2017. **142**: p. 8-31.
337. Zhang, P. and P.J. Sadler, *Advances in the design of organometallic anticancer complexes.* J. Organomet. Chem., 2017. **839**: p. 5-14.
338. Golbaghi, G. and A. Castonguay, *Rationally designed ruthenium complexes for breast cancer therapy.* Molecules, 2020. **25**(2): p. 265.
339. Dkhar, L., et al., *Cp and indenyl ruthenium complexes containing dithione derivatives: Synthesis, antibacterial and antifungal study.* J. Organomet. Chem., 2020. **923**: p. 121418.
340. Su, W., Z. Tang, and P. Li, *Development of arene ruthenium antitumor complexes.* Mini. Rev. Med. Chem., 2016. **16**(10): p. 787-795.
341. Cherioux, F., et al., *Dendritic systems based on dinuclear ruthenium or rhodium units generating peripheral catalytic sites.* Chem. Eur. J., 2002. **8**(19): p. 4377-4382.
342. Muthna, D., et al., *In-vitro and in-vivo evaluation of the anticancer activity of diruthenium-2, a new trithiolato arene ruthenium complex [(eta6-p-MeC6H4Pri)2Ru2(mu-S-p-C6H4OH)3]Cl.* Anticancer Drugs, 2016. **27**(7): p. 643-650.
343. Tomšík, P., et al., *[(p-MeC6H4Pri)2Ru2(SC6H4-p-But)3]Cl (diruthenium-1), a dinuclear arene ruthenium compound with very high anticancer activity: An in vitro and in vivo study.* J. Organomet. Chem., 2015. **782**: p. 42-51.
344. Chellan, P. and P.J. Sadler, *Enhancing the activity of drugs by conjugation to organometallic fragments.* Chem. Eur. J., 2020. **26**(40): p. 8676-8688.
345. Wei, H.X., et al., *A systematic review and meta-analysis of the efficacy of anti-Toxoplasma gondii medicines in humans.* PLoS One, 2015. **10**(9): p. e0138204.
346. Shammaa, A.M., T.G. Powell, and I. Benmerzouga, *Adverse outcomes associated with the treatment of Toxoplasma infections.* Sci. Rep., 2021. **11**(1): p. 1035.
347. Mansour, A.M. and K. Radacki, *Experimental and DFT studies of sulfadiazine 'piano-stool' Ru(II) and Rh(III) complexes.* RSC Adv., 2020. **10**: p. 10673-10680.
348. Chellan, P., et al., *Organometallic conjugates of the drug sulfadoxine for combatting antimicrobial resistance.* Chem. Eur. J., 2018. **24**(40): p. 10078-10090.
349. Kotzé, T.J., et al., *Synthesis and antimicrobial study of organoiridium amido-sulfadoxine complexes.* Inorg. Chim. Acta, 2020. **517**: p. 120175.
350. McLeod, R., et al., *Triclosan inhibits the growth of Plasmodium falciparum and Toxoplasma gondii by inhibition of apicomplexan Fab I.* Int. J. Parasitol., 2001. **31**(2): p. 109-113.

351. Martins-Duarte, E.S., et al., *Apicoplast fatty acid synthesis is essential for pellicle formation at the end of cytokinesis in Toxoplasma gondii.* J. Cell. Sci. , 2016. **129**(17): p. 3320–3331.
352. Muench, S.P., et al., *Development of a triclosan scaffold which allows for adaptations on both the A- and B-ring for transport peptides.* Bioorg. Med. Chem. Lett., 2013. **23**(12): p. 3551-3555.
353. Cheng, G., et al., *Design, synthesis, and biological activity of diaryl ether inhibitors of Toxoplasma gondii enoyl reductase.* Bioorg. Med. Chem. Lett., 2013. **23**(7): p. 2035-2043.
354. Stec, J., et al., *Modification of triclosan scaffold in search of improved inhibitors for enoyl-acyl carrier protein (ACP) reductase in Toxoplasma gondii.* ChemMedChem, 2013. **8**(7): p. 1138-1160.
355. Samuel, B.U., et al., *Delivery of antimicrobials into parasites.* Proc. Natl. Acad. Sci. U. S. A., 2003. **100**(24): p. 14281-14286.
356. El-Zawawy, L.A., et al., *Triclosan and triclosan-loaded liposomal nanoparticles in the treatment of acute experimental toxoplasmosis.* Exp. Parasitol., 2015. **149**: p. 54-64.
357. El-Zawawy, L.A., et al., *Preventive prospective of triclosan and triclosan-liposomal nanoparticles against experimental infection with a cystogenic ME49 strain of Toxoplasma gondii.* Acta Trop., 2015. **141**(Pt A): p. 103-11.
358. Dingsdag, S.A. and N. Hunter, *Metronidazole: an update on metabolism, structure-cytotoxicity and resistance mechanisms.* J. Antimicrob. Chemother., 2018. **73**(2): p. 265-279.
359. Hernandez Ceruelos, A., et al., *Therapeutic uses of metronidazole and its side effects: an update.* Eur. Rev. Med. Pharmacol. Sci., 2019. **23**(1): p. 397-401.
360. Chew, W.K., et al., *Significant reduction of brain cysts caused by Toxoplasma gondii after treatment with spiramycin coadministered with metronidazole in a mouse model of chronic toxoplasmosis.* Antimicrob. Agents Chemother., 2012. **56**(4): p. 1762-1768.
361. Dale, L.D., et al., *Studies on DNA damage and induction of SOS repair by novel multifunctional bioreducible compounds. II. A metronidazole adduct of a ruthenium-arene compound.* Anti-Cancer Drug Des., 1992. **7**(1): p. 3-14.
362. Martins-Duarte, E.S., et al., *Ciprofloxacin derivatives affect parasite cell division and increase the survival of mice infected with Toxoplasma gondii.* PLos One, 2015. **10**(5): p. e0125705.
363. Dubar, F., et al., *Ester prodrugs of ciprofloxacin as DNA-gyrase inhibitors: synthesis, antiparasitic evaluation and docking studies.* MedChemComm, 2011. **2**(5): p. 430-435.
364. Koloczek, P., et al., *Polymeric micelle-mediated delivery of half-sandwich ruthenium(II) complexes with phosphanes derived from fluoroloquinolones for lung adenocarcinoma treatment.* Eur. J. Pharm. Biopharm., 2018. **128**: p. 69-81.
365. Turel, I., et al., *First ruthenium organometallic complex of antibacterial agent ofloxacin. Crystal structure and interactions with DNA.* Inorg. Chem., 2010. **49**(23): p. 10750-10752.
366. Scholer, N., et al., *Atovaquone nanosuspensions show excellent therapeutic effect in a new murine model of reactivated toxoplasmosis.* Antimicrob. Agents Chemother., 2001. **45**(6): p. 1771-1779.
367. Muller, J., et al., *Development of a murine vertical transmission model for Toxoplasma gondii oocyst infection and studies on the efficacy of bumped kinase inhibitor (BKI)-1294 and the naphthoquinone buparvaquone against congenital toxoplasmosis.* J. Antimicrob. Chemother., 2017. **72**(8): p. 2334-2341.
368. Ferreira, R.A., et al., *Activity of natural and synthetic naphthoquinones against Toxoplasma gondii, in vitro and in murine models of infection.* Parasite, 2002. **9**(3): p. 261-269.
369. Gormley, P.D., et al., *Effects of drug therapy on Toxoplasma cysts in an animal model of acute and chronic disease.* Invest. Ophthalmol. Visual Sci., 1998. **39**(7): p. 1171-1175.
370. Srivastava, I.K., H. Rottenberg, and A.B. Vaidya, *Atovaquone, a broad spectrum antiparasitic drug, collapses mitochondrial membrane potential in a malarial parasite.* J. Biol. Chem., 1997. **272**(7): p. 3961-3966.

371. Spoerlein-Guettler, C., et al., *Ferrocene and (arene)ruthenium(II) complexes of the natural anticancer naphthoquinone plumbagin with enhanced efficacy against resistant cancer cells and a genuine mode of action.* J. Inorg. Biochem., 2014. **138**: p. 64-72.
372. Tabrizi, L. and H. Chiniforoshan, *Ruthenium(II) p-cymene complexes of naphthoquinone derivatives as antitumor agents: A structure-activity relationship study.* J. Organomet. Chem., 2016. **822**: p. 211-220.
373. Kubanik, M., et al., *Towards targeting anticancer drugs: ruthenium(II)-arene complexes with biologically active naphthoquinone-derived ligand systems.* Dalton Trans., 2016. **45**(33): p. 13091-13103.
374. Kandioller, W., et al., *Organometallic anticancer complexes of lapachol: metal centre-dependent formation of reactive oxygen species and correlation with cytotoxicity.* Chem. Commun., 2013. **49**(32): p. 3348-3350.
375. Hackl, C.M., et al., *Synthesis and in vivo anticancer evaluation of poly(organo) phosphazene-based metallodrug conjugates.* Dalton Trans., 2017. **46**(36): p. 12114-12124.
376. Fedorowicz, J. and J. Saczewski, *Modifications of quinolones and fluoroquinolones: hybrid compounds and dual-action molecules.* Monatsh. Chem., 2018. **149**(7): p. 1199-1245.
377. Schmidt, M., et al., *Conjugation of ciprofloxacin with poly(2-oxazoline)s and polyethylene glycol via end groups.* Bioconjugate Chem., 2015. **26**(9): p. 1950-1962.
378. Cilibrizzi, A., et al., *A tri-functional vanadium(iv) complex to detect cysteine oxidation.* Dalton Trans., 2017. **46**(21): p. 6994-7004.
379. Srinivasan, N., A. Yurek-George, and A. Ganesan, *Rapid deprotection of N-Boc amines by TFA combined with freebase generation using basic ion-exchange resins.* Mol. Diversity, 2005. **9**(4): p. 291-293.
380. Kongkathip, N., et al., *Potent antitumor activity of synthetic 1,2-naphthoquinones and 1,4-naphthoquinones.* Bioorg. Med. Chem., 2003. **11**(14): p. 3179-3191.
381. Wang, S.H., et al., *Synthesis and biological evaluation of lipophilic 1,4-naphthoquinone derivatives against human cancer cell lines.* Molecules, 2015. **20**(7): p. 11994-12015.
382. Kumar, B.S., et al., *Synthesis of pharmacologically important naphthoquinones and anticancer activity of 2-benzyllawsone through DNA topoisomerase-II inhibition.* Bioorg. Med. Chem., 2017. **25**(4): p. 1364-1373.
383. Salmon-Chemin, L., et al., *2-and 3-Substituted 1,4-naphthoquinone derivatives as subversive substrates of trypanothione reductase and lipoamide dehydrogenase from Trypanosoma cruzi: Synthesis and correlation between redox cycling activities and in vitro cytotoxicity.* J. Med. Chem., 2001. **44**(4): p. 548-565.
384. Davioud-Charvet, E., et al., *A prodrug form of a Plasmodium falciparum glutathione reductase inhibitor conjugated with a 4-anilinoquinoline.* J. Med. Chem., 2001. **44**(24): p. 4268-4276.
385. Biot, C., et al., *5-Substituted tetrazoles as bioisosteres of carboxylic acids. Bioisosterism and mechanistic studies on glutathione reductase inhibitors as antimalarials.* J. Med. Chem., 2004. **47**(24): p. 5972-5983.
386. Biot, C., et al., *Double-drug development against antioxidant enzymes from Plasmodium falciparum.* Redox Rep., 2003. **8**(5): p. 280-283.
387. Paunescu, E., et al., *Nonsteroidal anti-inflammatory-organometallic anticancer compounds.* Inorg. Chem., 2016. **55**(4): p. 1788-1808.
388. Stibal, D., G. Suss-Fink, and B. Therrien, *Crystal structure of (μ-4-hy-droxy-benzene-thiol-ato-κ(2) S:S)bis-(μ-phenyl-methane-thiol-ato-κ(2) S:S)bis-[(η(6)-1-isopropyl-4-methyl-benzene)-ruthenium(II)] tetra-fluorido-borate* Acta Crystallogr., Sect. E: Crystallogr. Commun., 2015. **71 (Pt 10)**: p. 1174-1176.
389. Bell, D.J., et al., *Sulfadoxine-pyrimethamine-based combinations for malaria: a randomised blinded trial to compare efficacy, safety and selection of resistance in Malawi.* PLoS One, 2008. **3**(2): p. e1578.
390. Terlouw, D.J., et al., *Sulfadoxine-pyrimethamine in treatment of malaria in Western Kenya: increasing resistance and underdosing.* Antimicrob. Agents Chemother., 2003. **47**(9): p. 2929-2932.

391. Peters, P.J., et al., *Safety and toxicity of sulfadoxine/pyrimethamine: implications for malaria prevention in pregnancy using intermittent preventive treatment.* Drug Saf., 2007. **30**(6): p. 481-501.
392. Deloron, P., et al., *Sulfadoxine/pyrimethamine intermittent preventive treatment for malaria during pregnancy.* Emerg. Infect. Dis., 2010. **16**(11): p. 1666-1670.
393. Fulmer, G.R., et al., *NMR Chemical Shifts of Trace Impurities: Common Laboratory Solvents, Organics, and Gases in Deuterated Solvents Relevant to the Organometallic Chemist.* Organometallics, 2010. **29**(9): p. 2176-2179.
394. Ibao, A.F., et al., *Thiolato-Bridged Arene-Ruthenium Complexes: Synthesis, Molecular Structure, Reactivity, and Anticancer Activity of the Dinuclear Complexes (arene)2Ru2(SR)2Cl2.* European Journal of Inorganic Chemistry, 2012(9): p. 1531-1535.
395. Kursunlu, A.N., et al., *A symmetric and selective fluorescent Cu(II) sensor based on bodipy and s-triazine.* J. Lumin., 2014. **149**: p. 215-220.
396. Lolk, L., et al., *A click chemistry approach to pleuromutilin conjugates with nucleosides or acyclic nucleoside derivatives and their binding to the bacterial ribosome.* J. Med. Chem., 2008. **51**(16): p. 4957-4967.
397. Jansa, P., et al., *Efficient one-pot synthesis of polysubstituted 6-[(1H-1,2,3-triazol-1-yl)methyl]uracils through the "click" protocol.* Collect. Czech. Chem. Commun., 2011. **76**: p. 1121-1131.

List of Structures

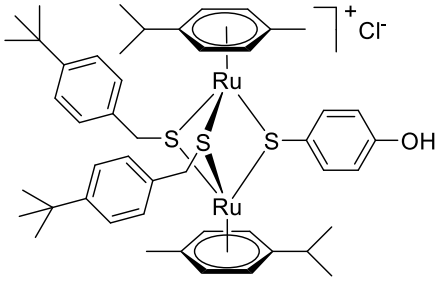

1.1.2a; 1.2.2; 2.2.2; 3.3

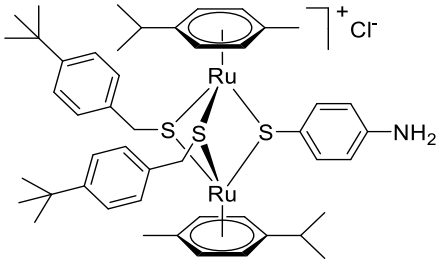

1.1.3a; 1.2.3; 2.1.2; 2.2.3; 3.4

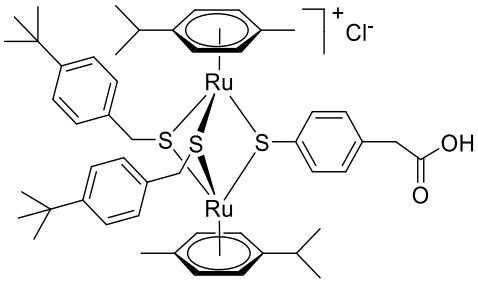

1.1.4a; 1.2.4; 2.1.3; 2.2.1; 3.2

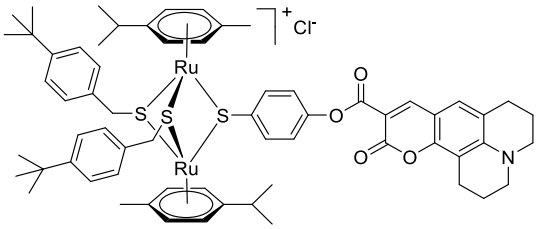

1.1.12a

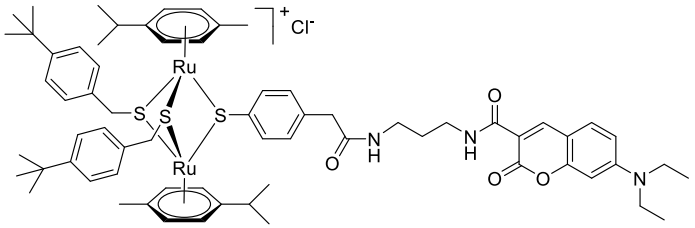

1.1.15

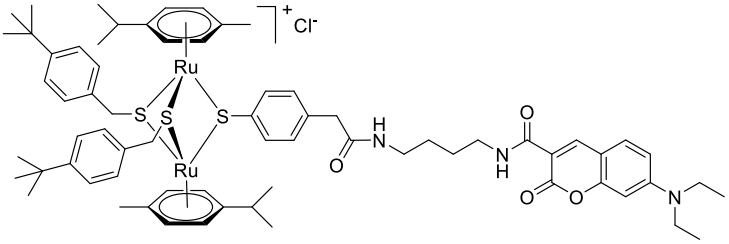

1.1.16a

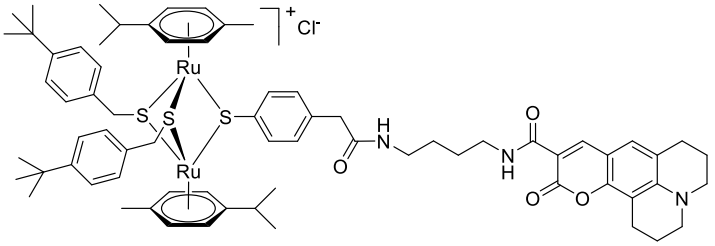

1.1.17a

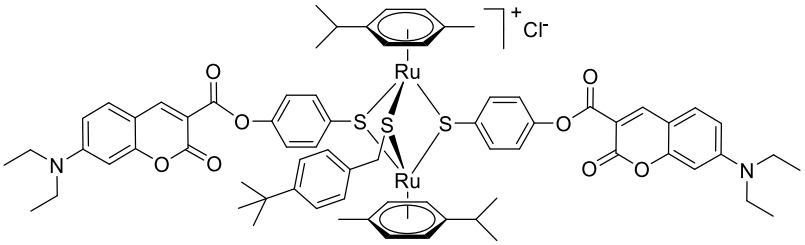

1.1.20

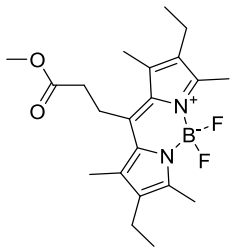

1.2.5

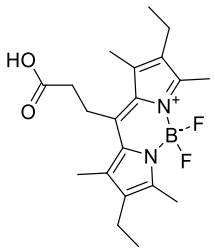

1.2.9

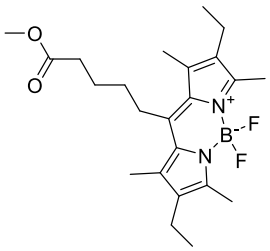

1.2.6

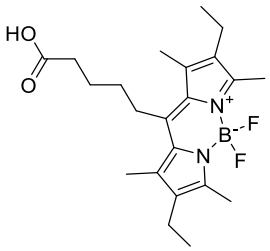

1.2.10

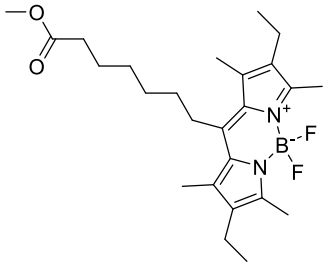

1.2.7

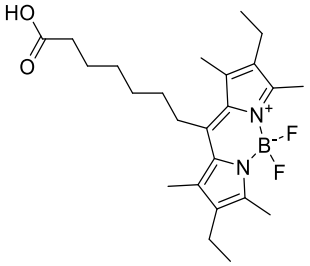

1.2.11

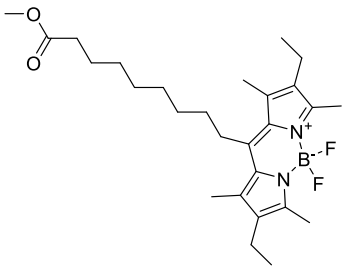

1.2.8

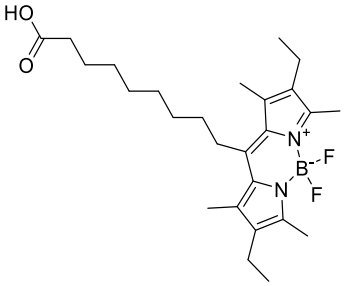

1.2.12

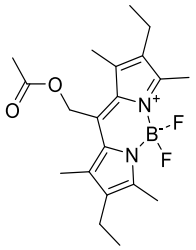

1.2.13

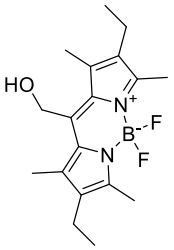

1.2.14

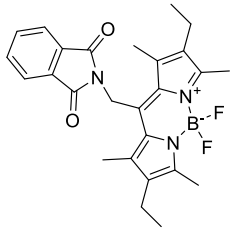

1.2.15

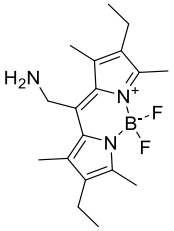

1.2.17

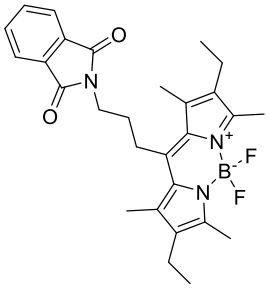

1.2.16

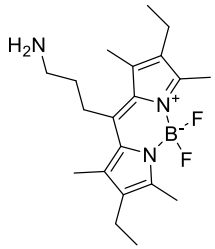

1.2.18

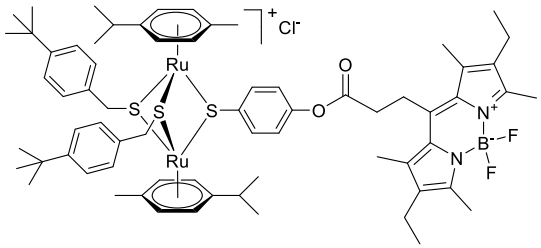

1.2.19

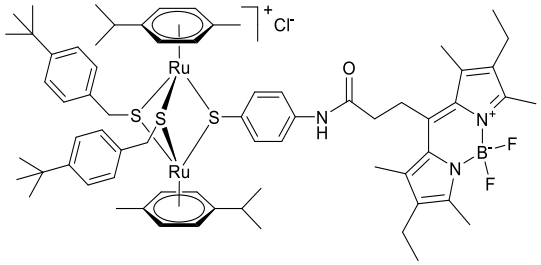

1.2.23

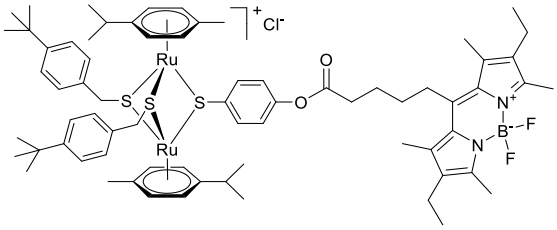

1.2.20

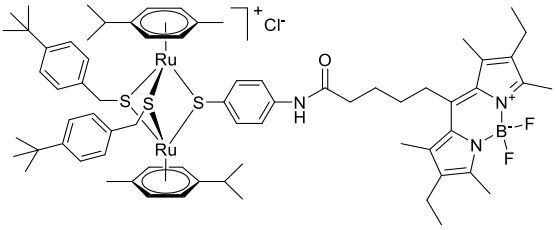

1.2.24

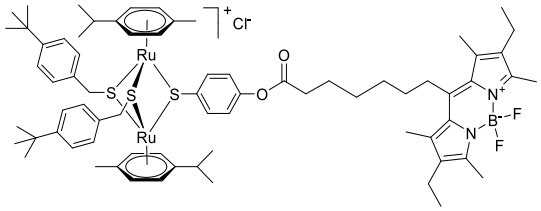

1.2.21

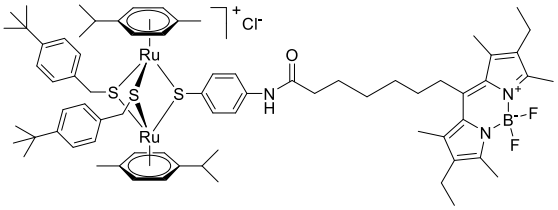

1.2.25

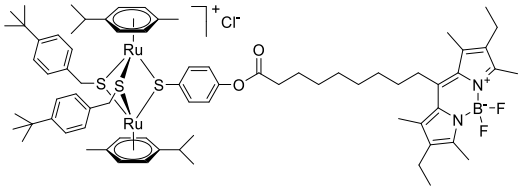

1.2.22

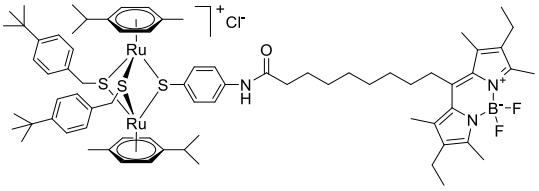

1.2.26

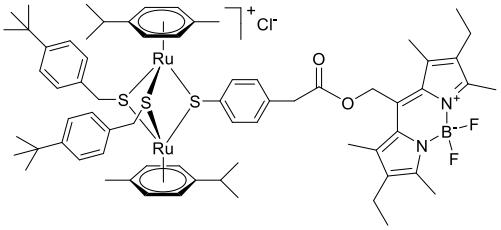

1.2.27

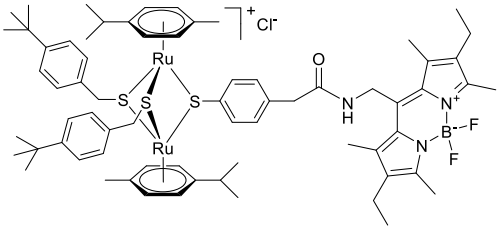

1.2.28

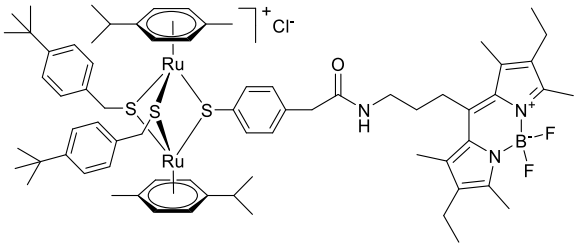

1.2.29

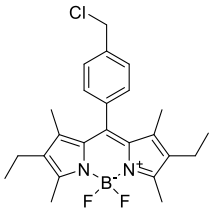

1.2.30

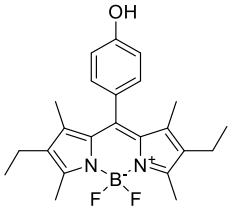

1.2.31

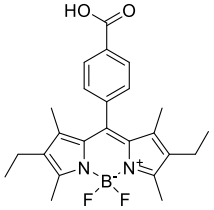

1.2.32

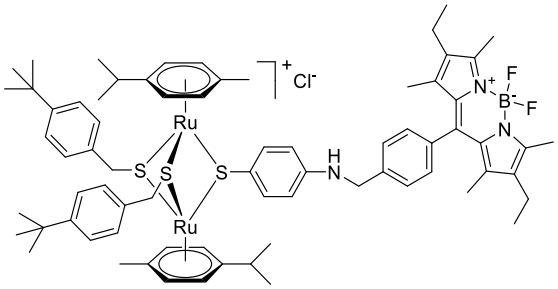

1.2.33

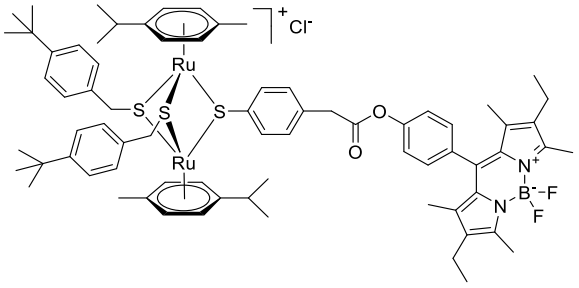

1.2.34

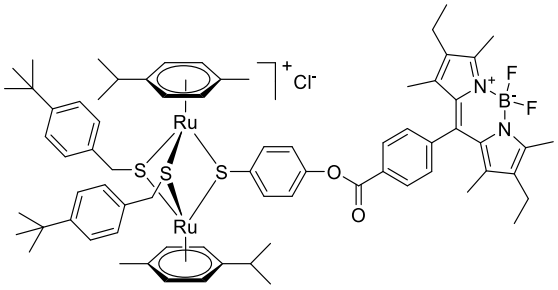

1.2.35

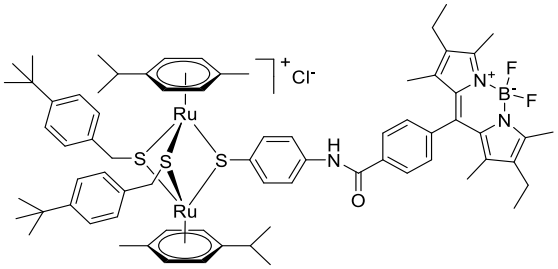

1.2.36

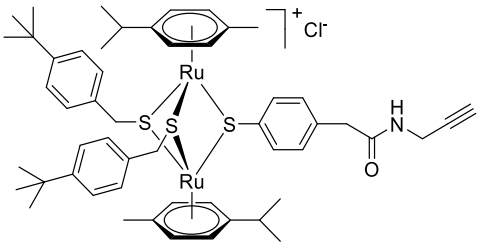

2.1.8; 3.7

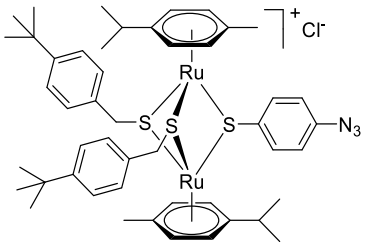

2.1.10

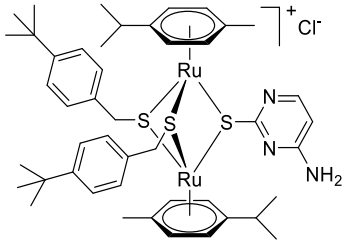

2.1.11

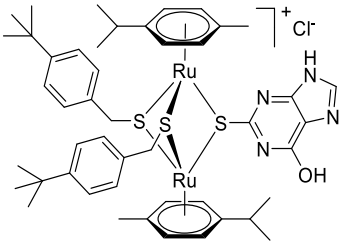

2.1.13

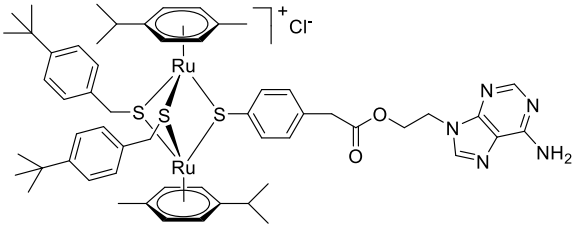

2.1.14

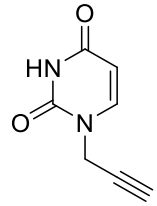

2.1.15

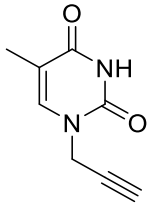

2.1.16

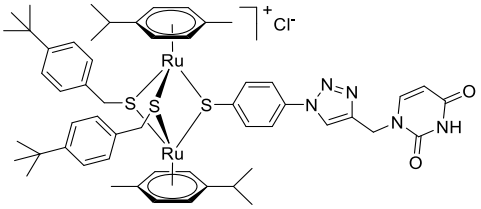

2.1.23

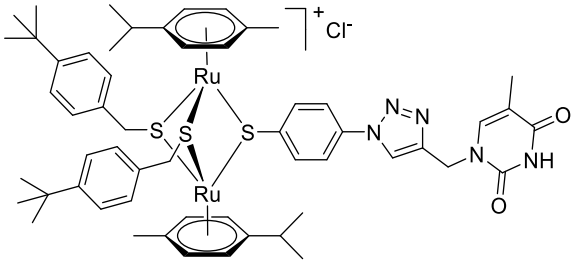

2.1.24

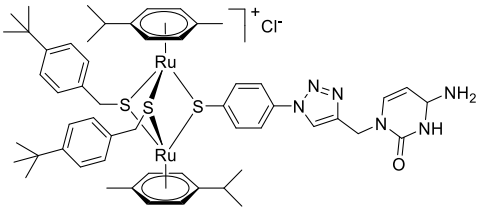

2.1.25

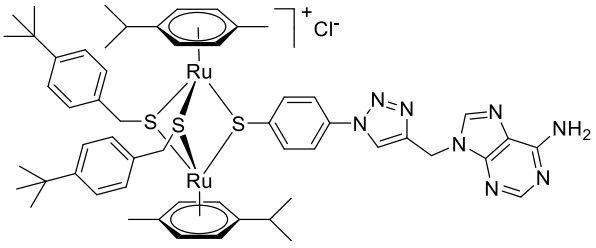

2.1.26

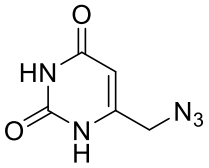

2.1.27

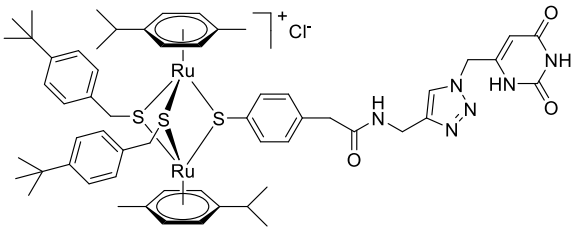

2.1.31

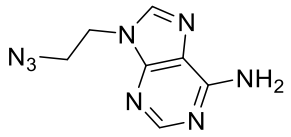

2.1.32

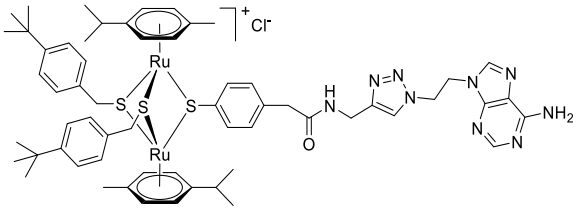

2.1.33

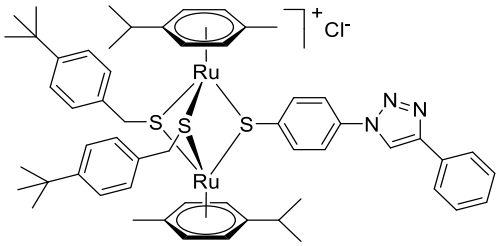

2.1.37

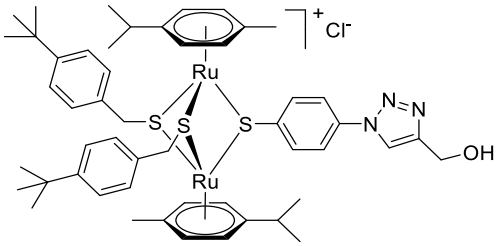

2.1.38

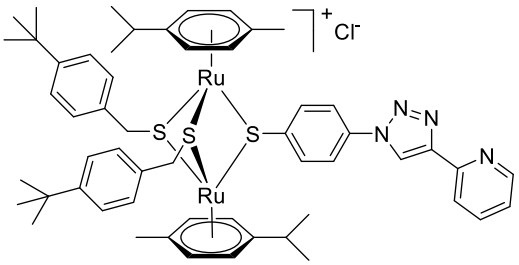

2.1.39

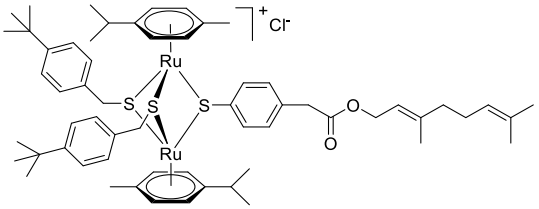

2.2.4a

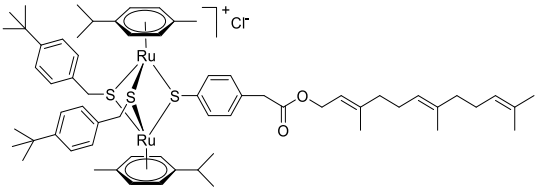

2.2.5a

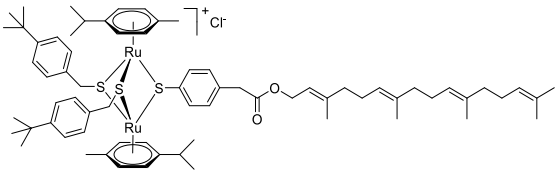

2.2.6a

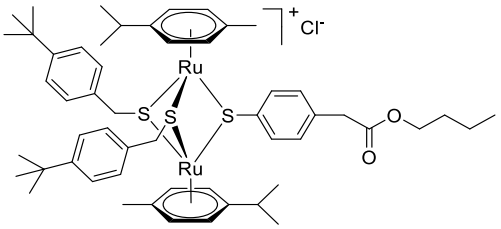

2.2.8a

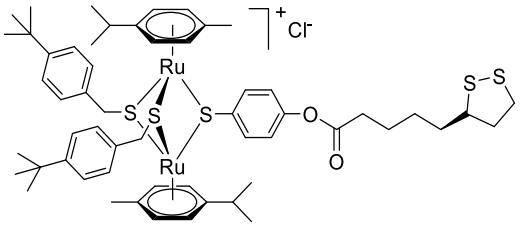

2.2.9a

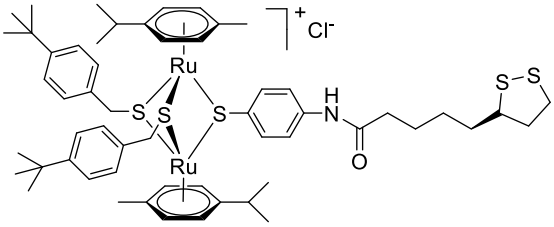

2.2.9b

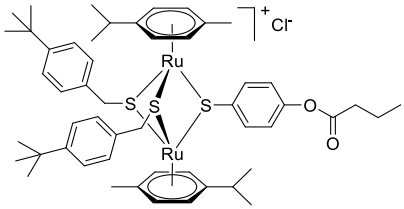

2.2.11a

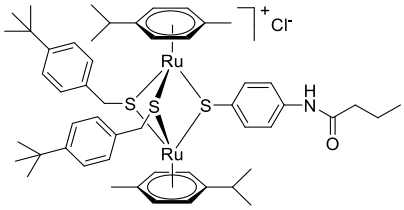

2.2.11b

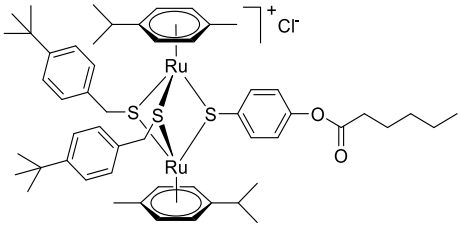

2.2.12a

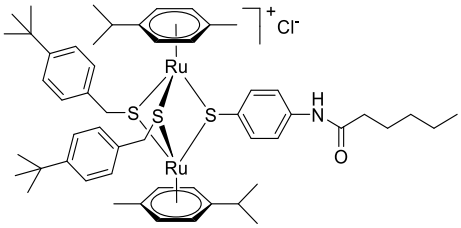

2.2.12b

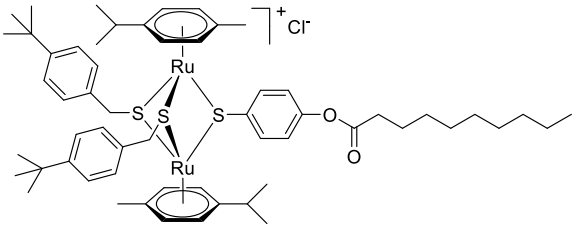

2.2.13a

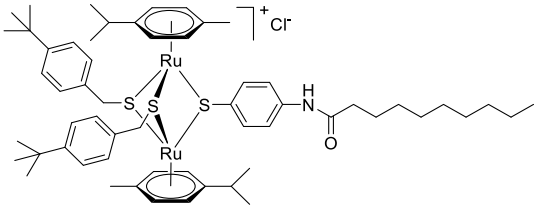

2.2.13b

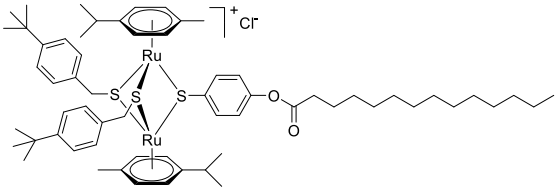

2.2.14a

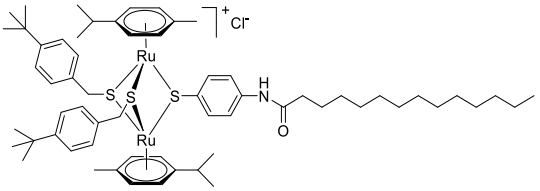

2.2.14b

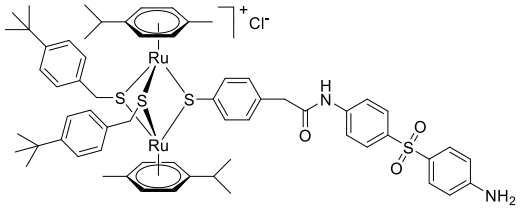

3.8

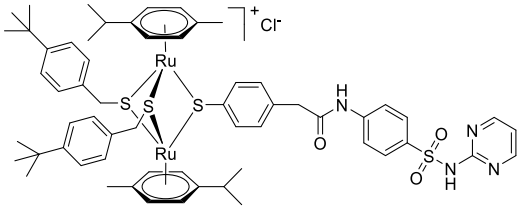

3.10

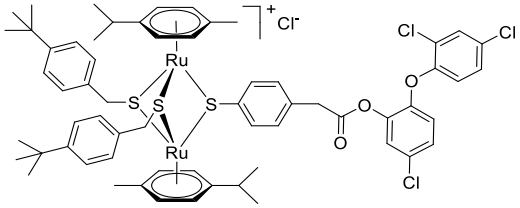

3.12

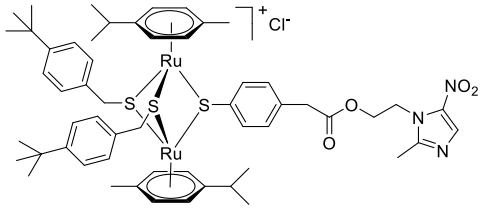

3.13

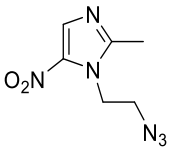

3.14

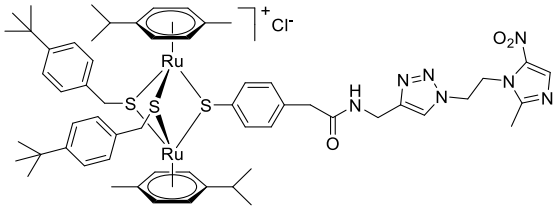

3.15

Abbreviations

A24 – human lung adenocarcinoma, wild type
(D-)A24cisPt8.0 – human lung adenocarcinoma, cisplatin resistant
A2780 – human ovarian cancer cells
A2780cisR – human ovarian cancer cells, cisplatin resistant
AIDS – acquired immunodeficiency syndrome
AR – androgen receptor
$BF_3{\cdot}Et_2O$ – boron trifluoride diethyl etherate
BODIPY – 4,4-difluoro-4-bora-3a,4a-diaza-*s*-indacene fluorescent markers
BrdU – 5-bromo-2'-deoxy-uridine
CI – confidence interval
Ciprofloxacin – 1-cyclopropyl-6-fluoro-4-oxo-7-(piperazin-1-yl)-1,4-dihydroquinoline-3-carboxylic acid
CNS – central nervous system
ConA – concanavalin A
CPRG – chlorophenol red-β-D-galactopyranoside
CTR – controls
CuAAC – Copper-catalysed azide-alkyne [3 + 2] cycloaddition
Cys – cysteine
Cyt c – cytochrome c
Dapsone – 4,4'-sulfonyldianiline
DDQ – 2,3-dichloro-5,6-dicyano-*p*-benzoquinone
DIPEA – *N*,*N*-diisopropylethylamine
DMAP – 4-(dimethylamino)-pyridine
DMEM - Dulbecco's Modified Eagle's Medium
DMF – dimethylformamide
DMSO – dimethylsulfoxide
Dye1-CO_2H – 7-(diethylamino)-2-oxo-2*H*-chromene-3-carboxylic acid
Dye2-CO_2H – 11-oxo-2,3,6,7-tetrahydro-1*H*,5*H*,11*H*-pyrano[2,3-*f*]pyrido[3,2,1-*ij*]quinoline-10-carboxylic acid (coumarin 343)
EDCI – *N*-(3-dimethylaminopropyl)-*N'*-ethylcarbodiimide hydrochloride
ESI-MS – Electrospray ionization mass spectrometry
EtOAc – ethyl acetate
Φ_F – fluorescence quantum yield
FCS – fetal calf serum
GSH – glutathione
GSSG – glutathione-disulfide
HBTU – 2-(1 H -benzotriazol-1-yl)-1,1,3,3-tetramethyluronium hexafluorophosphate
HCT116 – human colon cancer cells
HEK293 – human embryonic kidney cells
Hex – n-hexane
HFF – human foreskin fibroblasts
HIV – human immunodeficiency viruses
$HOBt{\cdot}H_2O$ – 1-hydroxybenzotriazole hydrate
HR ESI-MS – high resolution electrospray ionization mass spectrometry
HsA – human serum albumin
IC_{50} – half maximal inhibitory concentration

ICP-MS – inductively coupled plasma mass spectrometry
ISC – inter-system-crossing
KP-1339 - sodium *trans*-[tetrachloridobis(1*H*-indazole)ruthenate(III)]
LI – limit inferior
LNCaP (AR+) cells – androgen-sensitive human prostate adenocarcinoma cells overexpressing androgen receptor
LPS – lipopolysaccharide
LS – limit superior
LSCM – laser scanning confocal microscope
Mb – myoglobin
MDA-MB-231 – human breast adenocarcinoma
Menadione – 2-methylnaphthalene-1,4-dione
Metronidazole – 2-(2-methyl-5-nitro-1*H*-imidazol-1-yl)ethan-1-ol
MsCl – methanesulfonyl chloride
NAMI-A – Imidazolium [*trans*-[tetrachlorido(*S*-dimethylsulfoxide)-(1*H*-imidazole)ruthenate(III)]
NMR – nuclear magnetic resonance
PBS – phosphate-buffered saline
PDT – photo dynamic therapy
PET - photoinduced electron transfer
^{i}*PrOH* – 2-propanol
PV – parasitophorous vacuole
PVM – parasitophorous vacuole membrane
RAPTA-C - [Ru(II)(η^6-*p*-$MeC_6H_4Pr^i$)Cl_2(PTA)], PTA = 1,3,5-triaza-7-phosphoadamantane
RF24 – immortalized human endothelial cells
RM175 – [Ru(II)(η^6-biphenyl)Cl(en)]PF_6, en = 1,2-ethylenediamine
ROS – reactive oxygen species
SAR – structure-activity relationship
SD - standard deviation
SE – standard error
Sulfadiazine – 4-amino-*N*-(pyrimidin-2-yl)benzenesulfonamide
Sulfadoxine – 4-amino-*N*-(5,6-dimethoxypyrimidin-4-yl)benzenesulfonamide
Sulfamethoxazole – 4-amino-*N*-(5-methylisoxazol-3-yl)benzenesulfonamide
TD_{50} – the median toxic dose at which toxicity occurs in 50% of cases
TEA – triethylamine
TEM – transmission electron microscopy
Tf – transferrin
TFA – trifluoroacetic acid
T. gondii β-gal – *Toxoplasma gondii* RH strain tachyzoites expressing β-galactosidase
THF – tetrahydrofuran
TLC – thin layer chromatography
Triclosan – 5-chloro-2-(2,4-dichlorophenoxy)phenol
Ub – ubiquitin

List of Publications and Conference Contributions

Articles:

2021 — N. Anghel, J. Müller, M. Serricchio, J. Jelk, P. Bütikofer, G. Boubaker, D. Imhof, J. Ramseier, **O. Desiatkina**, E. Păunescu, S. Braga-Lagache, M. Heller, J. Furrer, A. Hemphill, **Cellular and Molecular Targets of a Nucleotide-Tagged Trithiolato-Bridged Arene Ruthenium Complexes in the Protozoan Parasites *Toxoplasma gondii* and *Trypanosoma brucei***, *Int. J. Mol. Sci.* (2021), 22, 10787.

2021 — **O. Desiatkina**, S. K. Johns, N. Anghel, G. Boubaker, A. Hemphill, J. Furrer, E. Păunescu, **Synthesis and Antiparasitic Activity of New Conjugates—Organic Drugs Tethered to Trithiolato-Bridged Dinuclear Ruthenium(II)–Arene Complexes**, *Inorganics* (2021), 9, 59.

2021 — E. Păunescu, G. Boubaker, **O. Desiatkina**, N. Anghel, Y. Amdouni, A.Hemphill, J. Furrer, **The quest of the best e A SAR study of trithiolato-bridged dinuclear Ruthenium(II)-Arene compounds presenting antiparasitic properties**, *Eur. J. Med. Chem.* (2021), 222, 113610.

2020 — V. Studer, N. Anghel, **O. Desiatkina**, T. Felder, G. Boubaker, Y. Amdouni, J. Ramseier, M. Hungerbühler, C. Kempf, J. T. Heverhagen, A. Hemphill, N. Ruprecht, J. Furrer, E. Paunescu, **Conjugates Containing Two and Three Trithiolato-Bridged Dinuclear Ruthenium(II)-ArenenUnits as In Vitro Antiparasitic and Anticancer Agents**, *Pharmaceuticals* (2020), 13, 471.

2020 — **O. Desiatkina**, E. Păunescu, M. Mösching, N. Anghel, G. Boubaker, Y. Amdouni, A. Hemphill, J. Furrer, **Coumarin-Tagged Dinuclear Trithiolato-Bridged Ruthenium(II)·Arene Complexes: Photophysical Properties and Antiparasitic Activity**, ChemBioChem. (2020) 21(19) 2818–2835.

Conferences:

29 August-2 September 2021 — **O. Desiatkina**, M. Mösching, E. Păunescu, J. Furrer, N. Anghel, G. Boubaker, Y. Amdouni, A. Hemphill, **Synthesis and Biological activity of Trithiolato-Bridged Dinuclear Ruthenium(II)-Arene Complexes with Nucleic bases,** XXVI EFMC International Symposium on Medicinal Chemistry (EFMC-ISMC 2021)

15 October 2020 — **O. Desiatkina**, E. Păunescu, J. Furrer, N. Anghel, G. Boubaker, Y. Amdouni, A. Hemphill, **Development of Ruthenium Complexes as Antiparasitic Agents**, ApicoWplexa wirtual meeting: Drugs and drug targets.

4 February 2020 — **O. Desiatkina**, E. Păunescu, N. Anghel, G. Boubaker, Y. Amdouni, A. Hemphill, J. Furrer, **BODIPY-Tagged Dinuclear Trithiolato-Bridged Ruthenium(II)-Arene Complexes – Photophysical Properties and Bioactivity**, 2nd Anglo-Swiss Symposium 2020, Basel, Switzerland.

14-15 November 2019 — **O. Desiatkina**, E. Păunescu, J. Furrer, N. Anghel, G. Boubaker, Y. Amdouni, A. Hemphill, **Photophysical Properties and Antiparasitic Activity of Dinuclear Trithiolato-Bridged Ruthenium(II)-Arene Complexes tagged with Coumarin Dyes**, 1st Workshop on Metals in Medicine, Paris, France.

6 September 2019	**O. Desiatkina**, E. Păunescu, J. Furrer, **Synthesis and Photophysical Properties of BODIPY-Tethered Trithiolato-Bridged Dinuclear Ruthenium(II)-Arene Compounds**, Swiss Chemical Society Fall Meeting 2019, Zürich, Switzerland.
5-6 September 2019	**O. Desiatkina**, E. Păunescu, J. Furrer, N. Anghel, G. Boubaker, Y. Amdouni, A. Hemphill, **Photophysical Properties and Antiparasitic Activity of BODIPY-Tethered Dinuclear Trithiolato-Bridged Ruthenium(II)-Arene Complexes**, 6th European Federation for Medicinal Chemistry Young Medicinal Chemist Symposium (EFMS-YMCS), Athens, Greece.
11-16 August 2019	**O. Desiatkina**, E. Păunescu, J. Furrer, N. Anghel, G. Boubaker, Y. Amdouni, A. Hemphill, **Coumarin-Tagged Dinuclear Trithiolato-Bridged Ruthenium(II)-Arene Complexes – Photophysical Properties and Antiparasitic Activity**, 19th International Conference on Biological Inorganic Chemistry (ICBIC-19), Interlaken, Switzerland.
7 September 2018	**O. Desiatkina**, E. Păunescu, J. Furrer, **Coumarin-labeled Dinuclear Trithiolato-Bridged Ruthenium(II) Arene Complexes - Synthesis, Characterization and Spectral Properties**, Swiss Chemical Society Fall Meeting 2018, Lausanne, Switzerland.
26-30 August 2018	**O. Desiatkina**, E. Păunescu, J. Furrer, **Synthesis, Spectral Properties and Biological Evaluation of New Conjugates BODIPY – Dinuclear Trithiolato-Bridged Ruthenium Arene Complexes**, 14th European Biological Inorganic Chemistry Conference EuroBIC 14, Birmingham, UK.

Declaration of consent

on the basis of Article 18 of the PromR Phil.-nat. 19

Name/First Name: Desiatkina Oksana

Registration Number: 17-125-345

Study program: Doctoral Degree Program in Chemistry and Molecular Sciences

Bachelor ☐ Master ☐ Dissertation ☑

Title of the thesis: Ruthenium complexes for the treatment of protozoan diseases of medical and veterinary importance

Supervisor: Prof. Dr. Julien Furrer

I declare herewith that this thesis is my own work and that I have not used any sources other than those stated. I have indicated the adoption of quotations as well as thoughts taken from other authors as such in the thesis. I am aware that the Senate pursuant to Article 36 paragraph 1 litera r of the University Act of September 5th, 1996 and Article 69 of the University Statute of June 7th, 2011 is authorized to revoke the doctoral degree awarded on the basis of this thesis.
For the purposes of evaluation and verification of compliance with the declaration of originality and the regulations governing plagiarism, I hereby grant the University of Bern the right to process my personal data and to perform the acts of use this requires, in particular, to reproduce the written thesis and to store it permanently in a database, and to use said database, or to make said database available, to enable comparison with theses submitted by others.

Bern, 4.10.2021

Place/Date

Signature